



do more
feel better
live longer

Chemoselective C–H Functionalisation of Aliphatic Azacycles – Utilisation of Electrophilic Iodine as a Mild Oxidant.

Robert Joseph Griffiths

A report submitted for the Degree of Doctor of Philosophy

University of Strathclyde

Department of Pure and Applied Chemistry

and GlaxoSmithKline

2018

This thesis is the result of the author's original research. It has been composed by the author and has not been previously submitted for examination which has led to the award of a degree, except where otherwise indicated in Section 4.2.

The copyright of this thesis belongs to the author under the terms of the United Kingdom Copyright Acts as qualified by University of Strathclyde Regulation 3.50. Due acknowledgement must always be made of the use of any material contained in, or derived from, this thesis.

Signed:

Date: March 2018

Science without religion is lame, religion without science is blind.

Albert Einstein

Imagination is more important than knowledge.

Albert Einstein

Abstract

Over half of the small molecules approved for use in the U.S.A. by the FDA in 2012 contained at least one nitrogen heterocycle. Of these, 11% contained a piperidine motif, emphasising the importance of saturated nitrogen-containing heterocycles in drug discovery. As such, rapid, step-efficient and reliable diversification strategies of this functional group are highly desirable.

Late-stage C–H functionalisation of high value scaffolds is a powerful tool that has potentially wide application in the pharmaceutical industry. The underlying principle is to use the subtle difference in reactivity of C–H bonds to carry out selective and efficient functionalisation of a complex late-stage intermediate or final compound. This strategy could be harnessed to expedite the exploration of the medicinal chemistry properties of biologically active small molecules. There are a wide array of methods at the disposal of synthetic chemists to carry out selective C–H functionalisation, which are discussed within this thesis, but a number of these are not applicable to the late-stage functionalisation of modern drug molecules. This can be due to functional groups being incompatible with the reaction conditions, the inconvenience of installing an appropriate directing group, or the functionalisation not being sufficiently selective.

This body of work provides an introduction to the field of late-stage C–H functionalisation. Chapter two describes the development and consolidation of a C–H functionalisation protocol for the α -C–H oxidation of cyclic amines to lactams using molecular iodine as the oxidant. This transition metal-free process, carried out under ambient reaction conditions, was then applied to the late-stage oxidation of a selection of high value small molecules with relevance to the pharmaceutical and agrochemical sectors. The impact of this work within a medicinal chemistry application is also discussed.

With an understanding of this process in hand, diversification of this oxidative platform is explored in chapter three, which describes the discovery of a β -C–H trifluoroacylation protocol. Chapter four describes how these findings were refined and consolidated into the development of a robust methodology to carry out oxidative C–H sulfonylation of saturated nitrogen heterocycles at the β -position. The functionality installed into resulting enaminyll sulfone scaffolds was then exploited to provide access to a wide array of highly functionalised azacyclic scaffolds. Iodine-mediated oxidation is demonstrated to provide access to either α or β -functionalised products, which have been showcased to have application for medicinal and synthetic chemistry.

Acknowledgements

Firstly I would like to thank Dr Eric Talbot, my industrial supervisor throughout the first three years of my PhD. Your support, education and guidance has helped me to become a confident and adept synthetic organic chemist, and your interesting views on varying issues have certainly led to some stimulating discussions in the lab. You have helped me to overcome the issues I faced early on in my studies and to achieve a great deal in a relatively short space of time, and I genuinely hope that we get the opportunity to work together again in the future. My thanks also go to Dr Matt Campbell for the help and advice that you offered to me following Eric's departure; your diligence and attention to detail has helped my thesis to reach a standard that I am proud of.

I also want to acknowledge the contribution of Dr Glenn Burley to my PhD studies; your crisis management and provision of a fresh pair of eyes has helped to progress my research well, and has enabled me to achieve a high standard of work throughout my PhD. Thanks also to all the members of the Burley group for inviting me up for social gatherings and, of course, Craggan retreats – long live the unicorn!

Next, I would like to thank Joe, Jonny and Matt for all the fun and games we've had over my three and a half years at GSK. It's been a pleasure to get to know you, and I know that we shall continue to be friends long after I finish my PhD. I also have to thank Leon for your hard work and contributions on the sulfonylation work, and I hope you remember us when you're off making your millions. I also want to acknowledge my fellow students within the PhD program and my colleagues within RRI DPU, both past and present. Your friendship and advice has been invaluable to me during my PhD, and I have learned things that I shall take with me throughout my career.

I extend a big thank you to Steve Richards, who has so patiently, diligently and enthusiastically helped me to solve some pretty baffling NMR problems, and thanks

also to Sean Lynn and Richard Upton for your additional NMR support when it has been required. I also want to thank Graham Inglis for your selfless helpfulness with the mTOR work, and for your willingness to engage my work within a GSK medicinal chemistry project. I hope that the findings from that work can help to progress the project, and aid in the development of an effective medicine one day.

I would like to offer a huge thank you to Prof. Harry Kelly and Prof. William Kerr for organising the PhD program, and for accepting me onto it. Looking back on my PhD, I can honestly say that I have had a truly fantastic experience, and it is one I would wholly recommend to anyone. You have both provided with me with support and advice throughout my studies, and challenged me to constantly evolve and improve as a chemist. Thanks also go to Andrea Malley for your help and assistance, without which the PhD program would undoubtedly run significantly less smoothly. I also thank GSK for the financial support of this research through the GSK/University of Strathclyde Centre for Doctoral Training in Synthetic and Medicinal Chemistry.

I am also thankful to my parents, Martin and Gill, and my brother Michael. You have offered me a great deal of support (both emotional and financial!) throughout my education, and I will embrace the advice that you have given me as I begin my career in earnest. You have been a great inspiration to me, and I hope that I can continue to do you proud in the years to come.

Finally, the biggest thanks of all go to my amazing wife, Emily. You have been my rock during my PhD, and I couldn't have achieved what I have without you. Thanks for tolerating me on the worse days, when I've come home in a foul mood. Thanks for supporting me, keeping me in check, and helping me to put things in perspective and see what is truly important. I have done a lot these past few years, but nothing compares to the pride I have in marrying you in 2016, which is by far and away the highlight this time. I know that going forwards you will continue to be a massive

support to me throughout my career, and know that I will always do everything I can for you.

Contents

Abstract	ii
Acknowledgements	iv
Contents	vii
Abbreviations	x
Chapter 1. Introduction	1
1.1 Azacycles in Pharmaceuticals	1
1.2 Scope of Existing Methods of Late-Stage Functionalisation	5
1.3 C–H Oxidation	16
1.4 C–H Oxidation of Aliphatic Azacycles	37
1.5 Hypothesis to be Tested	49
1.6 Aims	50
Chapter 2. Transition-Metal-Free Amine Oxidation: a Chemoselective Strategy for the Late-Stage Formation of Lactams	52
2.1 Discovery and Optimisation of C–H Oxidation Methodology	52
2.2 Substrate Scope of the Iodine-Mediated C–H Oxidation of Azacycles	58
2.3 Mechanistic Investigations of Lactam Formation	63
2.4 Late-Stage C–H Oxidation of Bioactive Small Molecules	71
2.5 Application for Drug Discovery	77
2.6 Developing a Predictive Model for the Iodine-Mediated C–H Oxidation of Azacycles	84
2.7 Summary	92
2.8 Experimental	94
General Experimental	94
Synthetic Procedures	98

Appendix 1	158
Appendix 2	159
Assay Protocols	160
Chapter 3. Elaboration of Iodine-Mediated Azacycle C–H Oxidation	165
3.1 Deviations from Anticipated Lactam Formation	165
3.2 Proposed Nucleophilic Trapping of Iminium Intermediate	171
3.3 Electrophilic Trapping of an Enamine Intermediate	180
3.4 Summary	186
3.5 Experimental	188
General Experimental	188
Synthetic Procedures	192
Chapter 4. Oxidative β -Sulfonylation of Azacycles	206
4.1 Rationale and Precedent for Oxidative β -Sulfonylation	206
4.2 Reaction Optimisation and Substrate Scope	210
4.3 Mechanistic Investigations	217
4.4 Synthetic Diversification of the Enaminyll Sulfone Scaffold	221
4.5 Summary	241
4.6 Experimental	242
General Experimental	242
Synthetic Procedures	246
Appendix 3	278
Overall Conclusions	310
Future Work	312
Bibliography	320
Appendix 4. Publications List	347

Abbreviations

<i>%rsm</i>	Percentage of remaining starting material
°	Degrees
2D	Two-dimensional
3D	Three-dimensional
5-HT _{2A}	Serotonin _{2A}
Å	Angstrom
Ac	Acetyl
AcOH	Acetic acid
ADC	Antibody-Drug Conjugate
AQ	Aminoquinoline
aq.	Aqueous
ATP	Adenosine Triphosphate
ATR	Ataxia telangiectasia and Rad3 related
BEH	Ethylene Bridged Hybrid
BHT	2,6-Di- <i>tert</i> -butyl-4-methylphenol
BM	Bacillus megaterium
BMS	Bristol-Myers-Squibb
Bn	Benzyl
Boc	<i>tert</i> -Butyloxycarbonyl
BOX	Bisoxazoline
Bpy	2,2'-bipyridine
BQ	Benzoquinone
br.	Broad

Bu	Butyl
Bu	Butyl
Bz	Benzoyl
C	Celsius
Cbz	Carboxybenzyl
CF ₃ -PDP	(2 <i>R</i> ,2' <i>R</i>)-1,1'- <i>bis</i> -((5-(2,6- <i>bis</i> -(trifluoromethyl)phenyl)pyridin-2-yl)methyl)-2,2'-bipyrrolidine
<i>c</i> logP	Log ₁₀ (calculated partition coefficient between <i>n</i> -octanol and water)
cm	Centimetres
cm ⁻¹	Wavenumbers
CNS	Central Nervous System
COD	1,5-Cyclooctadiene
CYP	Cytochrome P450
d	Doublet
δ	Chemical shift
D	Deuterium
D ₂	Dopamine ₂
Da	Daltons
dba	Dibenzylideneacetone
DBU	1,8-Diazabicyclo[5.4.0]undec-7-ene
DCE	1,2-Dichloroethane
DCM	Dichloromethane
dd	Doublet of doublets
ddd	Doublet of doublets of doublets

dddd	Doublet of doublet of doublet of doublets
ddt	Doublet of doublet of triplets
DIPEA	<i>N,N</i> -Diisopropylethylamine
DMA	<i>N,N</i> -dimethylaniline
DMAP	4-Dimethylaminopyridine
DMF	<i>N,N</i> -Dimethylformamide
dq	Doublet of quartets
dquin	Doublet of quintets
dr	Diastereomeric ratio
dt	Doublet of triplets
dtbpy	4,4'-Di- <i>tert</i> -butyl-2,2'-dipyridyl
dtd	Doublet of triplet of doublets
dtdd	Doublet of triplet of doublet of doublets
E ₂	Bimolecular elimination
EDG	Electron-Donating Group
EDTA	Ethylenediaminetetraacetic acid
ee	Enantiomeric excess
E _i	Intramolecular elimination
eq.	Equivalents
ES	Electrospray
ESI	Electrospray Ionisation
Et	Ethyl
EtOAc	Ethyl acetate
EtOH	Ethanol

EWG	Electron-Withdrawing Group
FAD	Flavin Adenine Dinucleotide
FaSSIF	Fasted State Simulated Intestinal Fluid
FDA	Food and Drug Administration
FeSSIF	Fed State Simulated Intestinal Fluid
fXA	Coagulation factor Xa
g	Grams
<i>g</i>	Earth's gravitational force; 9.8 ms ⁻²
GC	Gas Chromatography
GDH	Glutamate Dehydrogenase
GPCR	G-Protein coupled receptor
GSK	GlaxoSmithKline
h	Hours
HAT	Hydrogen Atom Transfer
hERG	Human ether-a-go-go related gene
HFIP	1,1,1,3,3,3-hexafluoroisopropanol
hNK-1	Human neurokinin 1
HOMO	Highest Occupied Molecular Orbital
HPLC	High-Performance Liquid Chromatography
HRMS	High-Resolution Mass Spectrometry
Hz	Hertz
IC ₅₀	Half maximal inhibitory concentration
ID ₅₀	Half maximal concentration of differentiation
IL-8	Interleukin-8

IR	Infrared
<i>J</i>	Coupling constant
K	Kelvin
kcal	Kilocalorie
KIE	Kinetic Isotope Effect
LC	Liquid Chromatography
LCMS	Liquid Chromatography-Mass Spectrometry
M	Molar
m	Multiplet
M	Molecular mass
<i>m</i> -cpba	<i>meta</i> -Chloroperbenzoic acid
M.pt	Melting point
<i>m/z</i>	Mass to charge ratio
MBP-RebF	Maltose-Binding Protein-Rebeccamycin Flavin Reductase
MDAP	Mass-Directed Automated Preparative
Me	Methyl
Me	Methyl
MeCN	Acetonitrile
mg	Milligrams
MHz	Megahertz
min	Minutes
mL	Millilitres
mM	Millimolar
mm	Millimetres

mmol	Millimoles
mol	Moles
mol%	Percentage by moles
MS	Molecular Sieves
MS	Mass Spectroscopy
mTOR	Mammalian target of rapamycin
<i>n</i>	Linear
NADPH	Nicotinamide Adenine Dinucleotide Phosphate
NADPH	Nicotinamide Adenine Dinucleotide
NCS	<i>N</i> -Chlorosuccinimide
NIS	<i>N</i> -Iodosuccinimide
nm	Nanometres
nM	Nanomolar
NMR	Nuclear Magnetic Resonance
nr	No reaction
Ns	4-nitrophenylsulfonyl
PDP	(2 <i>S</i> ,2' <i>S</i>)-1,1'- <i>bis</i> -(pyridin-2-ylmethyl)-2,2'-bipyrrolidine
PET	Positive Emission Tomography
Ph	Phenyl
pH	Potential of hydrogen
phen	1,10-Phenanthroline
PI3K	Phosphoinositide-3-kinase
<i>pIC</i> ₅₀	-Log ₁₀ (IC ₅₀)
pin	Pinacol

PIP ₂	Phosphatidylinositol-(4,5)-triphosphate
PIP ₃	Phosphatidylinositol-(3,4,5)-triphosphate
Piv	Pivaloyl
pM	Picomolar
PMB	<i>para</i> -Methoxybenzyl
ppm	Parts per million
Pr	Propyl
PSA	Polar Surface Area
q	Quartet
qd	Quartet of doublets
qt	Quartet of triplets
quin	Quintet
quind	Quintet of doublets
RAR	Retinoic Acid Receptor
RebH	Rebeccamycin halogenase
ROR γ	RAR-Related orphan receptor- γ
RRI DPU	Respiratory Refractory and Inflammation Discovery Performance Unit
RT	Room temperature, 25 °C
R _t	Retention time
s	Singlet
SAR	Structure-Activity Relationship
<i>sec</i>	Secondary
SET	Single-Electron Transfer
S _N Ar	Nucleophilic aromatic substitution

Su	Succinimide
sxt	Sextet
T	Temperature
t	Triplet
TBHP	<i>tert</i> -Butylhydroperoxide
TBME	<i>tert</i> -Butyl methyl ether
tdd	Triplet of doublets of doublets
TEMPO	(2,2,6,6-Tetramethylpiperidin-1-yl)oxyl radical
<i>tert</i>	Tertiary
Tf	Trifluoromethylsulfonyl
TFA	Trifluoroacetic acid
TFDO	Methyl(trifluoromethyl)dioxirane
THF	Tetrahydrofuran
TLC	Thin Layer Chromatography
Tof	Time-of-Flight
Tol	<i>para</i> -Tolyl
TR-FRET	Time-Resolved Fluorescence Energy Transfer
Ts	<i>para</i> -Toluenesulfonyl
tt	Triplet of triplets
U	Units of activity; μmolmin^{-1}
U.S.A	United States of America
UV	Ultraviolet
v/v	Volume/volume
v_{max}	Absorption maxima

vol%	Percentage by volume
Vps	Vacuolar protein sorting 34
W	Watts
w/v	Weight/volume
wt%	Percentage by weight
λ	Wavelength
μL	Microlitres
μM	Micromolar
μm	Micrometres
μmol	Micromoles

Chapter 1. Introduction

1.1 Azacycles in Pharmaceuticals

Through to 2012 there have been 1994 pharmaceutical agents approved for use in the U.S.A. by the Food and Drug Administration (FDA) (Figure 1); 1086 of these were small molecules.¹

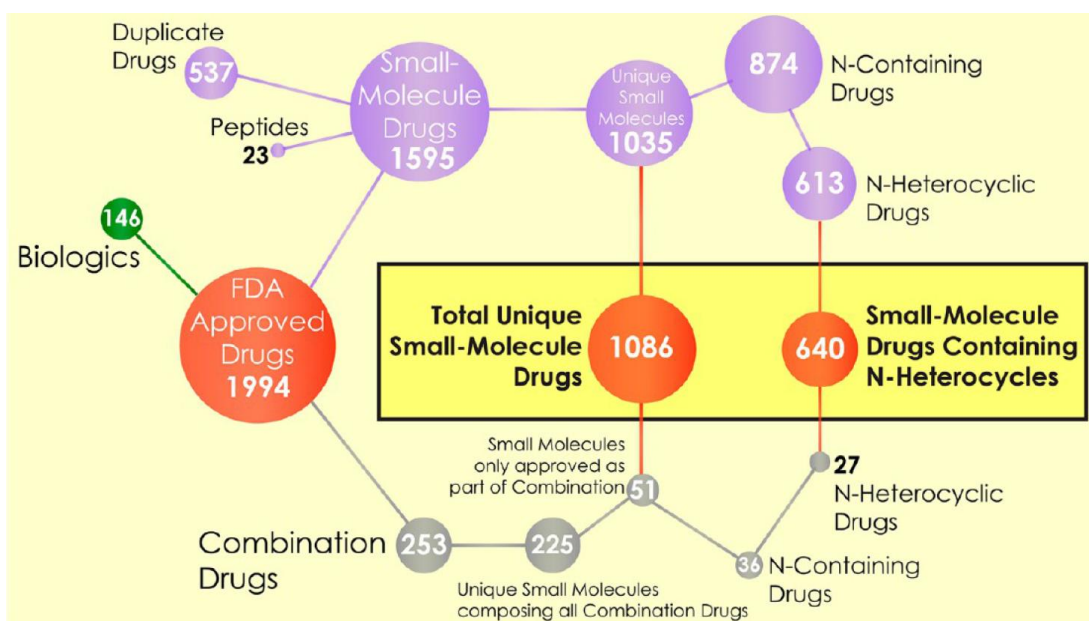


Figure 1. Breakdown of U.S.A. FDA approved drugs²

Some 59% of these small molecules contained at least one nitrogen heterocycle,^{1,3} and of these the piperidine motif is the most prevalent, accounting for 11% of the drugs that contain a nitrogen heterocycle.⁴⁻⁶ This highlights the importance of aliphatic nitrogen-containing heterocycles (azacycles) as motifs in drug discovery, and is exemplified in the top-selling blockbuster drugs paroxetine, **1.1.1**, and sildenafil, **1.1.2** (Figure 2).

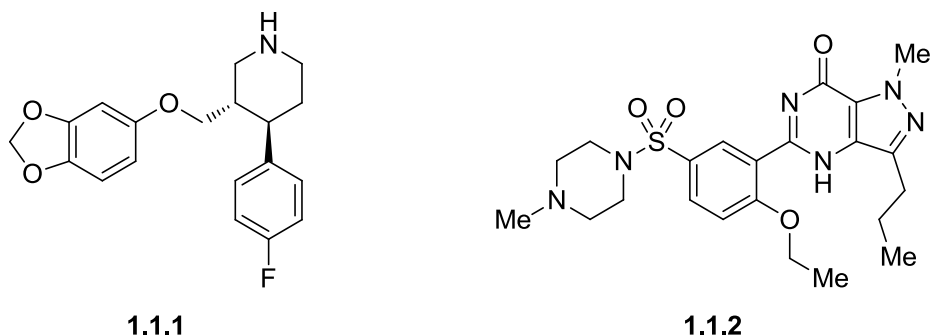


Figure 2. Blockbuster drugs containing an aliphatic nitrogen heterocycle.

Given the prominence of azacycles within pharmaceuticals discovery, rapid, step-efficient and reliable diversification strategies of this functional group are highly desirable.

Late-stage C–H functionalisation is a powerful tool that has potentially wide application in the pharmaceutical industry.⁷ The underlying principle is to use the subtle difference in reactivity of C–H bonds to carry out selective and efficient functionalisation of a complex late-stage intermediate or final compound. This would allow step and atom-efficient tuning of the efficacy and physicochemical properties of biologically active small molecules. This approach has the potential to expedite the process of identifying structure-activity relationships (SARs) by allowing rapid access to molecular diversity,^{8,9} thereby providing a molecular map of the regions and functional groups of the small molecule that are important for improved properties (Figure 3).

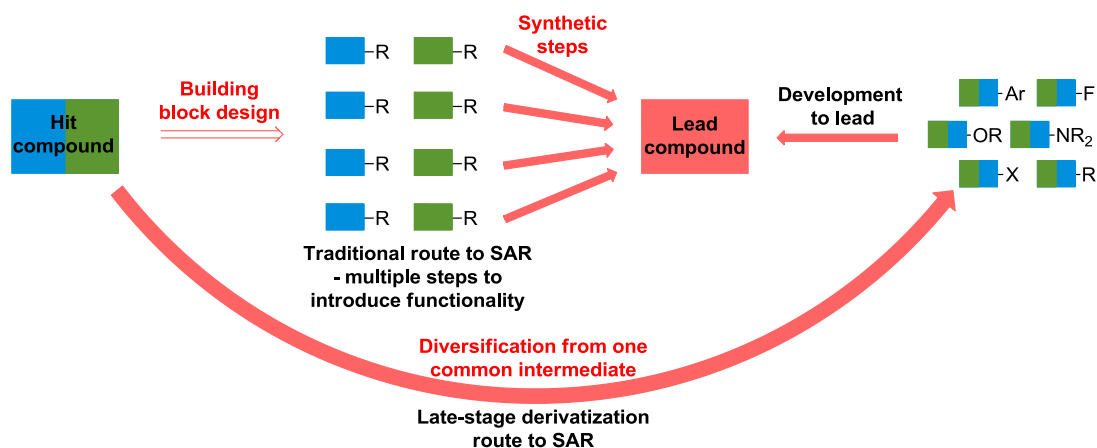


Figure 3. Potential application of late-stage functionalisation as a tool for medicinal chemistry to speed up the development of lead compounds.

Drug design requires a fine balance of physical and biological properties to achieve potency for the desired target, while maintaining high selectivity over other biological systems, high aqueous solubility, metabolic stability and permeability.^{10,11} Seemingly subtle and cosmetic changes to the molecular structure, such as replacement of a C–H with a C–F or C–Me, can often be all that is needed to turn a molecule from a failed candidate into a viable medicine. During the discovery of the human neurokinin 1 (hNK-1) receptor antagonist aprepitant, **1.1.4**, compound **1.1.3** was developed as an advanced lead (Figure 4a), but was prevented from entering clinical trials owing to poor metabolic stability *in vivo*.¹² It was hypothesised that debenzilation could be slowed by incorporation of a methyl group onto the benzylic position, as this would provide steric hindrance to metabolising enzymes.¹³ Additionally, fluorine-substitution of the phenyl ring was proposed as a method to mitigate against oxidative metabolism, due to the strength of the C–F bond,¹⁴ and the electronegativity of fluorine will make the aryl group less electron-rich, reducing the propensity for oxidation. As a result, iterative molecular changes were investigated to try to block the sites of metabolism, eventually leading to **1.1.4**.¹⁵ Aprepitant retained the affinity of **1.1.3**, but the changes to the scaffold blocked metabolic weak points in **1.1.3**, resulting in prolonged central duration of action, indicating slower clearance from the central nervous system (CNS).

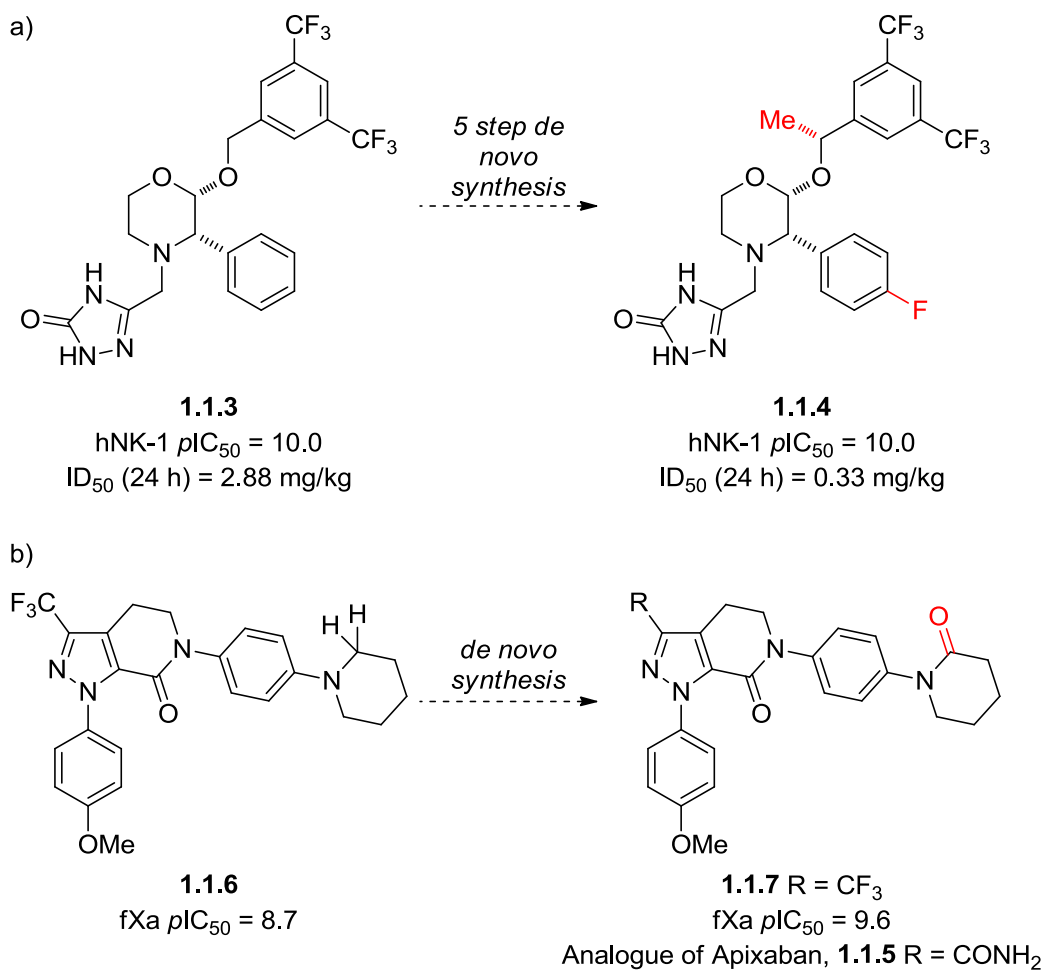


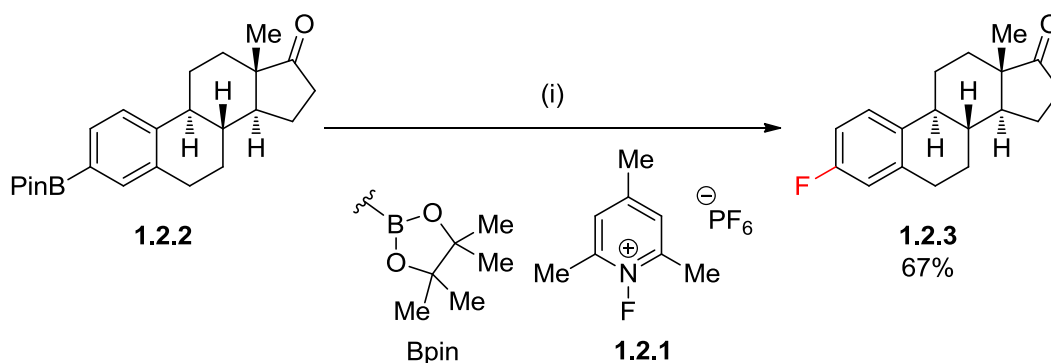
Figure 4. a) Compound **1.1.3** was identified as a lead compound for hNK-1 inhibition. Late-stage C–H functionalisation may have sped up the development of **1.1.3** into **1.1.4**. b) Piperidine **1.1.6** was found to be a potent inhibitor of fXa, but increasing planarity to **1.1.7** resulted in an increase in potency. pIC_{50} = $-\log_{10}$ (half maximal inhibitory concentration); ID_{50} = half maximal concentration of differentiation.

Late-stage C–H bond functionalisation was not used in this campaign, with several *de novo* syntheses required to make the ten reported final compounds during the optimisation of the structure of **1.1.3**. Unfortunately, methodologies were not available that would have facilitated late-stage conversion of the appropriate C–H bonds into C–Me and C–F bonds. It is, however, highly apparent how such an approach would have accelerated the discovery of **1.1.4**, particularly since the fluorine group had to be installed in the first step of the five-step syntheses. Another example of how late-stage functionalisation may have expedited drug development is in the discovery of Apixaban **1.1.5** (Figure 4b) as an inhibitor of coagulation factor Xa (fXa).¹⁶ Aryl piperidine **1.1.6** was found to be a potent antagonist against fXa, but

planarity of the pendant amine group was found to have an important contribution to potent inhibition of fXa. However, the more potent lactam **1.1.7** was prepared *via* a low-yielding (20%) Ullman coupling from the corresponding aryl iodide. Late-stage C–H oxidation of **1.1.6** may have helped realise this discovery sooner.

1.2 Scope of Existing Methods of Late-Stage Functionalisation

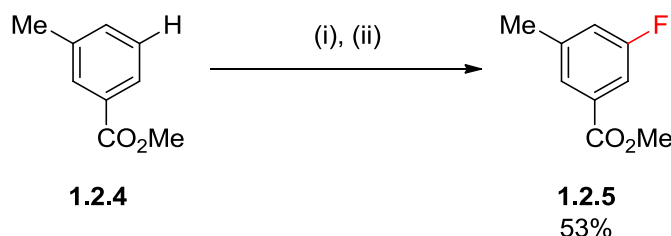
Late-stage functionalisation is a broad and varied field, and one that will continue to grow as interest from drug discovery groups develops. The incorporation of fluorine onto drug scaffolds is widely used as a way of modulating the metabolic and physicochemical parameters, while minimising any conformational changes to the drug compound.¹⁷ As such, the introduction of fluorine substituents into a molecule at a later stage allows for more rapid screening of these parameters. A range of methods are now available to facilitate late-stage fluorination, but most typically require a pre-installed functional group as a coupling partner.^{18–29} Hartwig *et al.* have recently reported a copper-mediated process for the conversion of arylboronic esters to the corresponding aryl fluoride with the use of the *N*-fluoropyridinium reagent **1.2.1** (Scheme 1).¹⁸ The protocol was subsequently applied in the late-stage fluorination of steroid derivative **1.2.2** to the fluorinated product **1.2.3**.



Scheme 1. Cu(I)/Cu(III)-mediated late-stage fluorination of the steroid derivative **1.2.2**. Conditions: (i) (*tert*-BuCN)₂CuOTf (2.0 eq.), **1.2.1** (3.0 eq.), AgF (2.0 eq.), THF, 50 °C, 18 h.

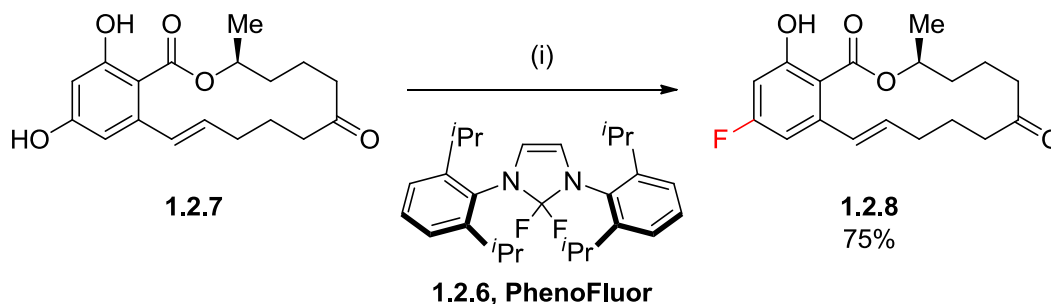
While the requirement for a boronic ester group to be already installed is not ideal, examples of two-step, one-pot C–H borylation/C–B fluorination are also reported, for

example on aryl ester **1.2.4** (Scheme 2), which widens the scope of application for late-stage fluorination.



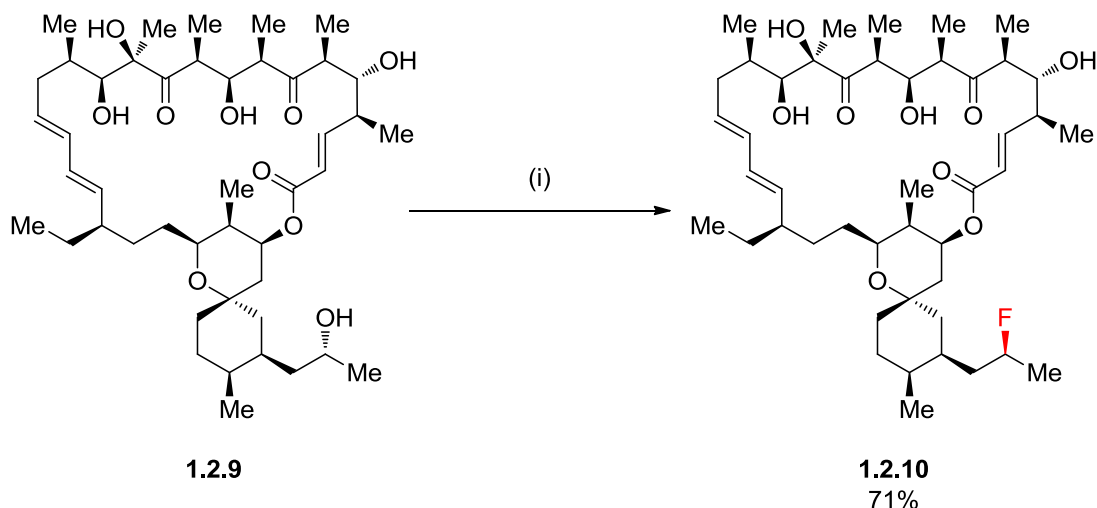
Scheme 2. Formal C–H fluorination – Ir-catalysed C–H borylation of 1.2.4, followed by Cu-mediated C–B fluorination. Conditions: (i) [(COD)IrOMe]₂ (0.1 mol%), dtbpy (0.2 mol%), B₂Pin₂ (0.75 eq.), THF, 80 °C, 18 h; (ii) (*tert*-BuCN)₂CuOTf (2.0 eq.), **1.2.1** (3.0 eq.), AgF (2.0 eq.), THF, 50 °C, 18 h.

Alcohols can also be used as a functional handle for selective late-stage fluorination. Ritter *et al.* have reported the deoxyfluorination of phenols using PhenoFluor **1.2.6** (Scheme 3) to enable the selective conversion of phenol **1.2.7** into aryl fluoride **1.2.8**, proceeding *via* a S_NAr process.¹⁹



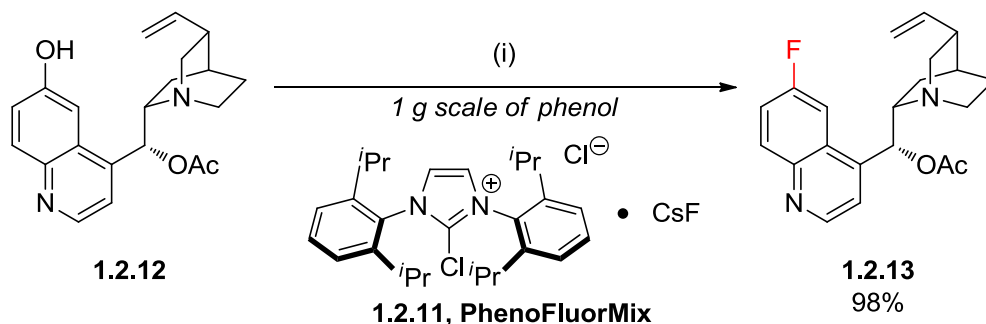
Scheme 3. Deoxyfluorination of 1.2.7 with PhenoFluor. Conditions (i) **1.2.6** (1.2 eq.), CsF (3.0 eq.), toluene, 110 °C, 20 h.

Modification of the reaction conditions allows for the deoxyfluorination of aliphatic alcohols;²⁹ these conditions are much more functional group tolerant than traditional methods for conversion of alcohols into fluorides.^{30–33} Under these modified reaction parameters, highly selective deoxyfluorination of oligomycin A, **1.2.9**, can be carried out to give the corresponding fluorinated derivative **1.2.10** in a stereoinvertive process (Scheme 4).²⁹



Scheme 4. Deoxyfluorination of 1.2.9 with PhenoFluor. Conditions (i) **1.2.6** (4.0 eq.), DIPEA (3.0 eq.), DCM, RT – 0 °C, 16 h.

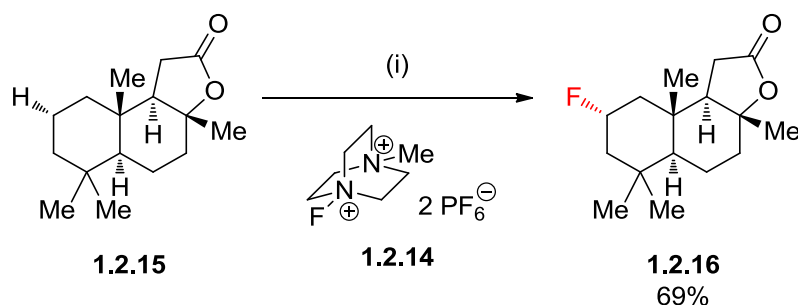
However, the moisture sensitivity of **1.2.6** means that it needs to be stored under strictly anhydrous conditions, such as in a glovebox, which limits the practical application of this reagent in medicinal chemistry research laboratories. Subsequent modification of the structure of **1.2.6** led to the development of PhenoFluorMix, **1.2.11** (Scheme 5), which does not hydrolyse and can be dried prior to deoxyfluorination.²⁰



Scheme 5. Elaborated late-stage deoxyfluorination using PhenoFluorMix. Conditions: **1.2.11** (3.6 eq.), toluene, 110 °C, 24 h.

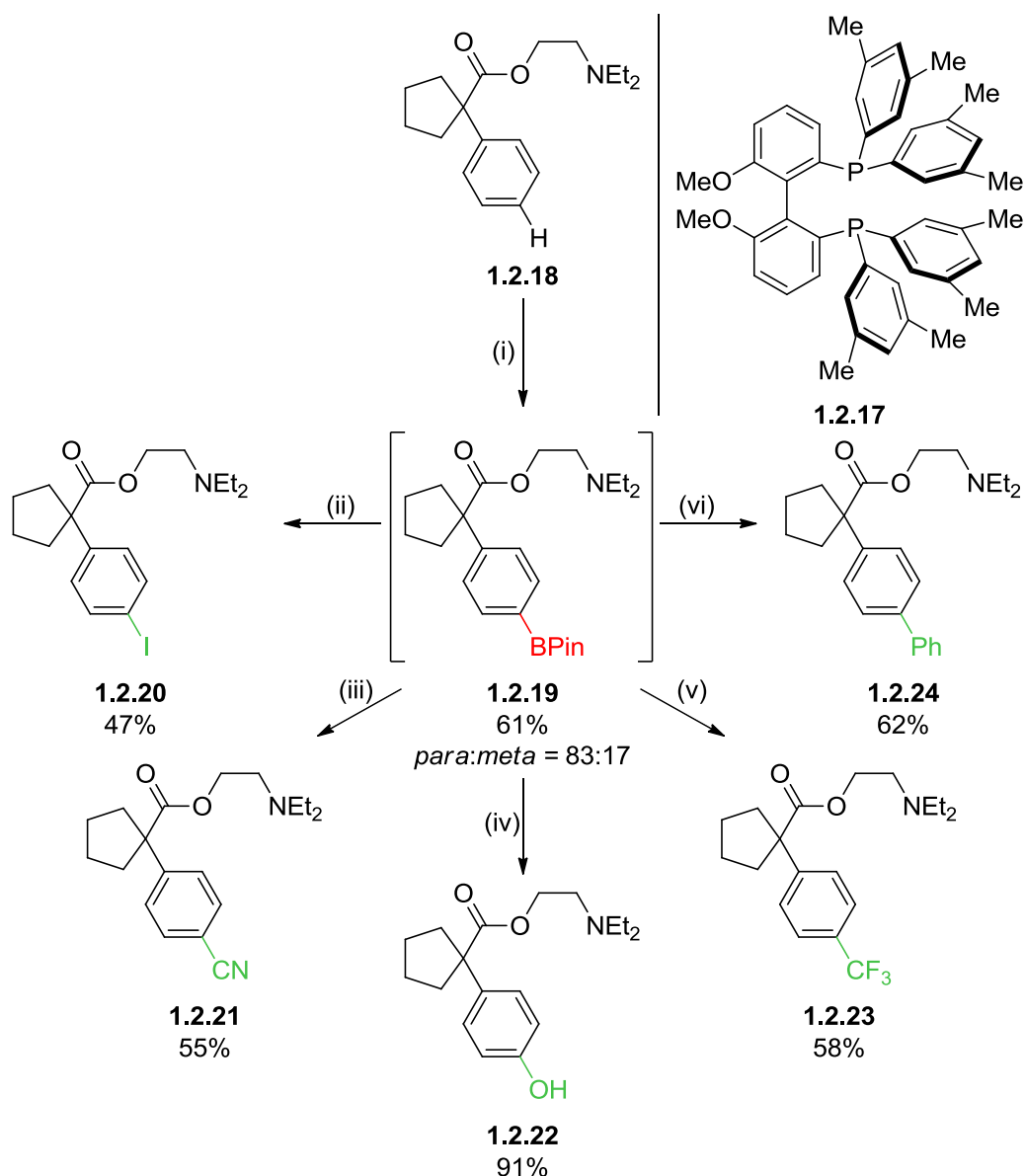
This can then be utilised for late-stage deoxyfluorination on a preparative scale,²⁰ as well as for the installation of ¹⁸F radiotracer labels that have application in positive emission tomography (PET) scanning.²¹

Transition-metal-free C–H fluorination can also be carried in an oxidative procedure using potassium persulfate as the oxidant and Selectfluor II (PF₆), **1.2.14**, as the source of fluorine (Scheme 6).³⁴ This was applied to the late-stage fluorination of sclareolide **1.2.15**, with regioselectivity observed for methine and methylene units remote from electron-withdrawing groups, and stereoselectivity driven through release of strain induced by the proximal axial methyl groups.³⁵ While some examples in this work require the use of large excesses of the oxidant or substrate, the high functional group tolerance and lack of dependency on directing groups or coupling partners gives this strategy good potential for application to medicinal chemistry projects.



Scheme 6. Transition-metal-free oxidative C–H fluorination of 1.2.15. Conditions: (i) K₂S₂O₈ (1.0 eq.), **1.2.14** (2.5 eq.), MeCN/H₂O, 50 °C, 69%.

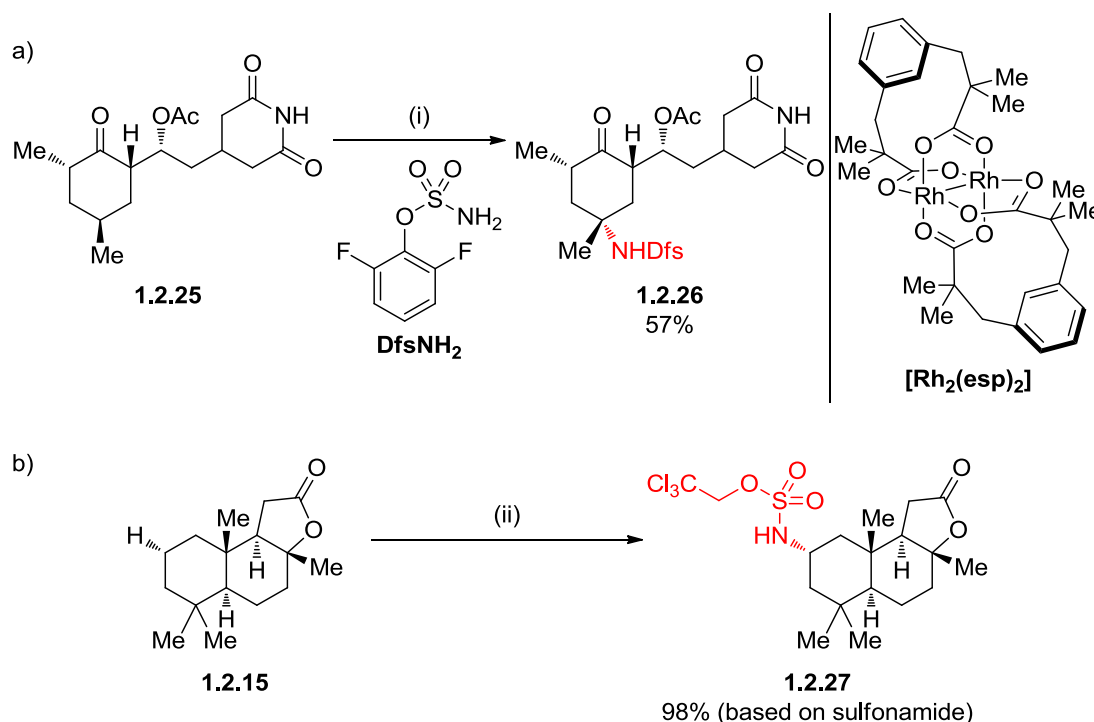
Selective C–H borylation of late-stage intermediates is also a highly desirable process due to the vast array of transformations that boronic acids and their derivatives can undergo,^{36–38} and as a result a great deal of research has been dedicated to the development of metal-catalysed C–H borylation procedures.³⁹ The reaction most commonly occurs at sterically accessible sp² C–H positions, which can lead to mixtures of *meta*- and *para*-substituted products. Using highly sterically hindered ligand **1.2.17** (Scheme 7), Itami *et al.* have developed conditions to favour *para*-selectivity for iridium-catalysed C–H borylation.⁴⁰



Scheme 7. Late-stage *para*-selective C–H borylation of caramiphen, and subsequent diversification to a range of analogues. Conditions: (i) B_2pin_2 (1.0 eq.), $[Ir(COD)OH]_2$ (1.5 mol%), **1.2.17** (3.0 mol%), hexane, 85 °C, 20 h; (ii) CuI (10 mol%), 1,10-phenanthroline·H₂O (20 mol%), KI (3.0 eq.), MeOH/H₂O, 80 °C, 12 h; (iii) $Cu(NO_3)_2 \cdot H_2O$ (2.0 eq.), $Zn(CN)_2$ (3.0 eq.), CsF (1.3 eq.), MeOH/H₂O, 100 °C, 6 h; (iv) *aq.* NaOH (1.0 eq.), *aq.* H₂O₂ (2.3 eq.), THF, RT, 3 h; (v) $[Cu(phen)CF_3]$ (1.2 eq.), KF (1.0 eq.), DMF, 50 °C, air, 2 h; (vi) PhI (1.5 eq.) $Pd(PPh_3)_4$ (6.3 mol%), K₂CO₃ (2.0 eq.), toluene/H₂O, 80 °C, 36 h.

They demonstrated the application of this methodology as a tool for the late-stage diversification of caramiphen, **1.2.18**, used in the treatment of Parkinson's disease.⁴¹ C–H borylation selectively at the *para*-position gave intermediate **1.2.19**, which enabled the formation of a diverse subset of compounds **1.2.20-1.2.24**, *via* iodination, cyanation, oxidation, trifluoromethylation, and arylation of the boronic ester.

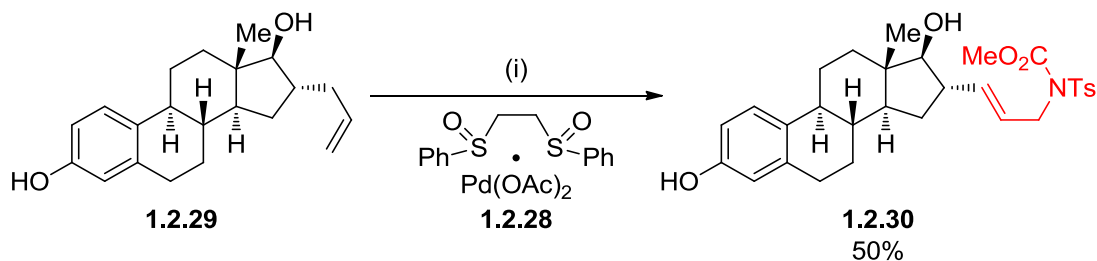
The importance and ubiquitous nature of the carbon-nitrogen bond in pharmaceuticals and biologically active compounds means that there has been great interest in introducing C–N bonds into complex substrates.⁴² Metal-catalysed nitrene insertion into C–H bonds has developed into a robust field to facilitate this C–N bond formation *via* a C–H amination strategy.^{43–51} This has more recently been applied in a late-stage functionalisation strategy for the amination of natural products, such as acylated cycloheximide **1.2.25** (Scheme 8a)⁴⁷ and **1.2.15** (Scheme 8b).³⁵



Scheme 8. Late-stage C–H amination *via* Rh-catalysed nitrene insertion. Conditions: (i) $[\text{Rh}_2(\text{esp})_2]$ (1 mol%), DfsNH_2 (1.2 eq.), $\text{PhI}(\text{OAc})_2$ (2.0 eq.), $\text{PhMe}_2\text{CCO}_2\text{H}$ (0.5 eq.), MgO (2.0 eq.), 5 Å MS, *iso*-PrOAc, RT, 12 h; (ii) **1.2.15** (5.0 eq.), $[\text{Rh}_2(\text{esp})_2]$ (5 mol%), $\text{PhI}(\text{O}t\text{-Bu})_2$ (2.0 eq.), $\text{NH}_2\text{SO}_2\text{OCH}_2\text{CCl}_3$ (1.0 eq.), C_6H_6 .

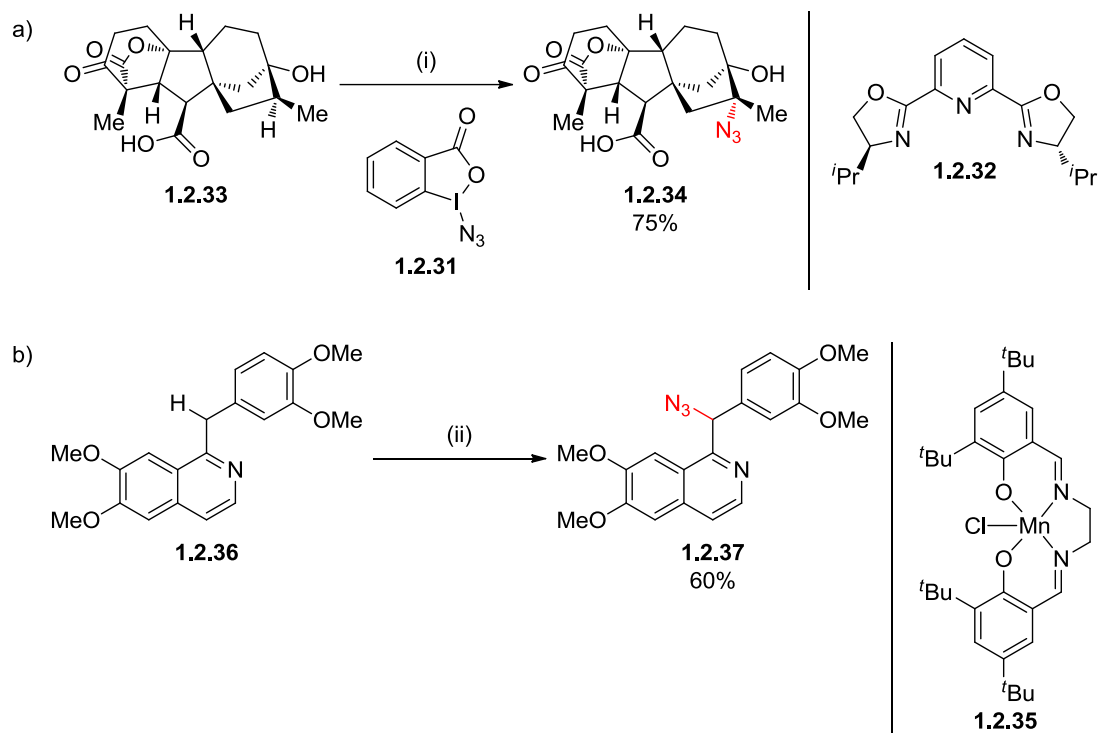
The use of sterically bulky rhodium catalysts, such as $[\text{Rh}_2(\text{esp})_2]$ means that this type of C–H functionalisation is highly susceptible to steric hindrance, and selectivity is typically driven by stereoelectronic parameters toward methylene and methine units distal from electron-withdrawing groups, and through the release of steric clashes.³⁵

Allylic C–H amination is possible using the palladium catalyst-ligand complex **1.2.28** in an oxidative process,^{52–56} and has been applied to the late-stage amination of the estrone derivative **1.2.29** (Scheme 9).⁵⁶



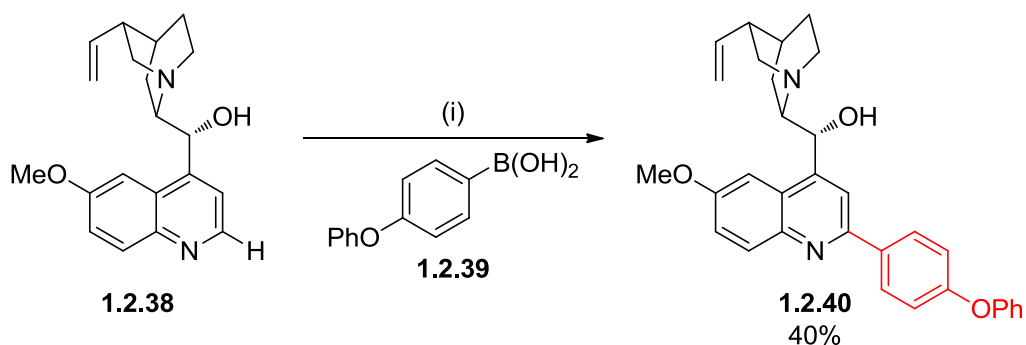
Scheme 9. Pd-catalysed allylic C–H amination of steroid derivative 1.2.29. Conditions: (i) **1.2.28** (5 mol%), TsNHCO₂Me (1.5 eq.), 2,5-dimethylbenzoquinone (1 eq.), TBME. Ts = *para*-toluenesulfonyl.

Alternatively, C–H bonds can be functionalised *via* an azidation strategy to install C–N functionality, which offers several potential pathways for further derivatisation.^{57–60} Hartwig *et al.* reported the use of an iron catalyst and azidation reagent **1.2.31**, in the presence of pybox ligand **1.2.32**, to carry out a C–H azidation transformation (Scheme 10a).⁶¹ High selectivity for tertiary C–H bonds remote from electron-withdrawing groups is observed, and the selectivity and functional group tolerance is utilised to facilitate a late-stage azidation of a derivative of tetrahydrogibberellic acid **1.2.33**. Manganese can also be used to catalyse C–H azidation reactions; Groves *et al.* have expanded on their C–H fluorination work^{62,63} to report the use of Mn-salen catalyst **1.2.35** to carry out late-stage C–H azidation on a suite of biologically relevant molecules, such as papaverine (**1.2.36**, Scheme 10b).⁶⁴



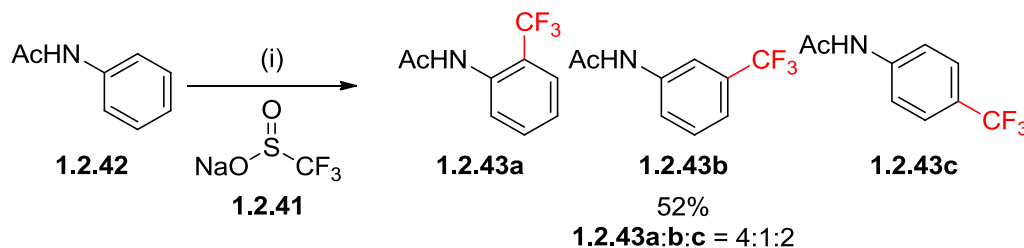
Scheme 10. Late-stage C–H azidation of biologically active compounds 1.2.33 and 1.2.36. Conditions: (i) $\text{Fe}(\text{OAc})_2$ (10 mol%), **1.2.32** (11 mol%), **1.2.31** (2.0 eq.), MeCN, RT; (ii) **1.2.35** (5 mol%), NaN_3 (4 eq.), PhIO (3 to 6 eq.), EtOAc, RT.

Late-stage C–C bond formation is another important area of late-stage C–H functionalisation.⁶⁵ Aryl boronic acids can be used for the arylation of heterocycles in Minisci-type reactions *via* the transition-metal-free oxidative formation of aryl radicals. An exemplar of this is the late-stage arylation of quinine **1.2.38** (Scheme 11), offering efficient elaboration of this anti-malarial agent.⁶⁶



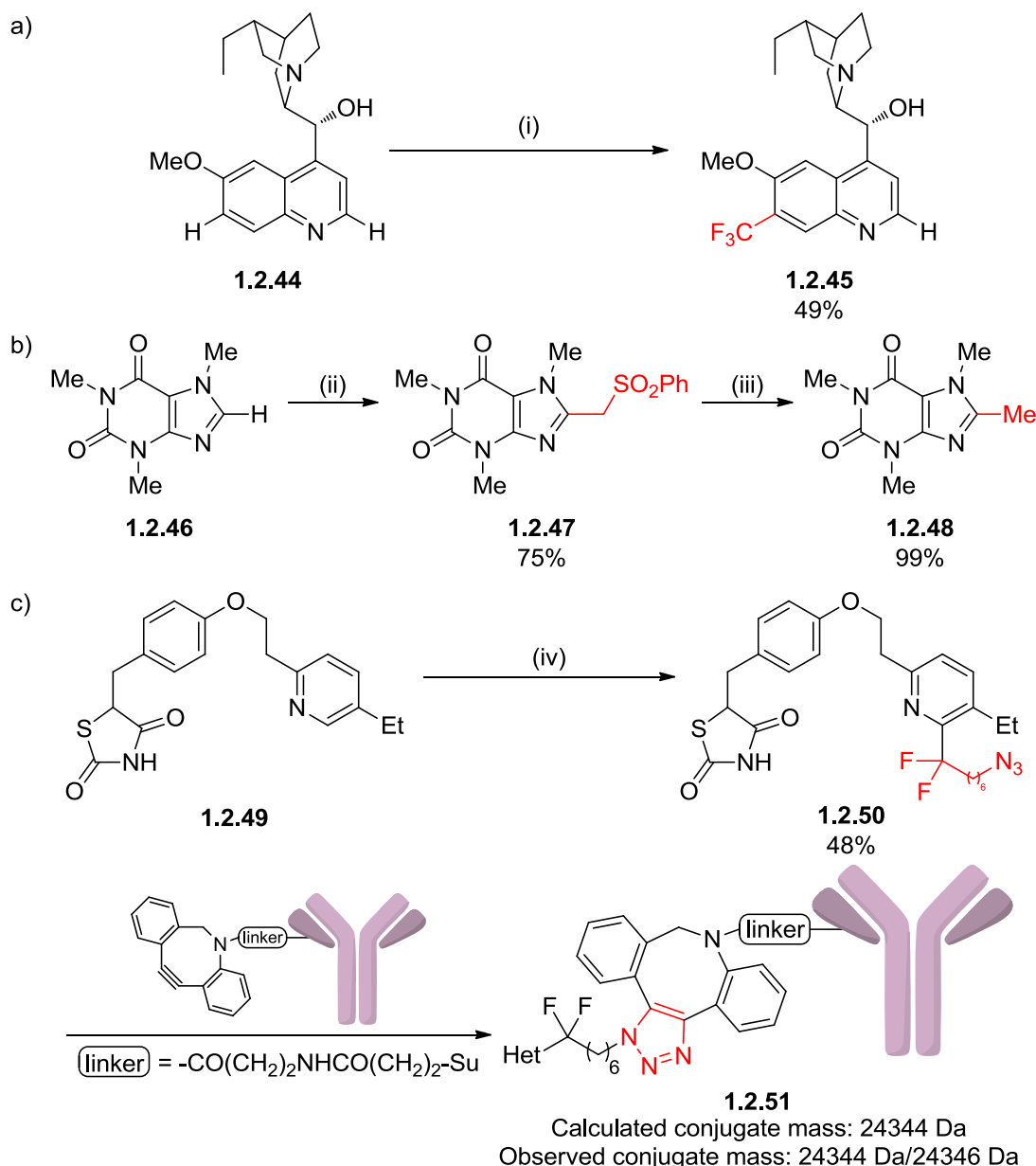
Scheme 11. Late-stage borono-Minisci arylation of quinine. Conditions: (i) **1.2.39** (3.0 eq.), TFA (3.0 eq.), AgNO_3 (0.2 eq.), $\text{K}_2\text{S}_2\text{O}_8$ (2.0 eq.), DCM/ H_2O , RT.

More recently the process of C-centred radical addition to heterocycles has been expanded to allow for addition of alkyl groups, provided the radical generated can be stabilised, through the use of alkylsulfinate salts based on the Langlois reagent, **1.2.41** (Scheme 12).⁶⁷ The seminal report by Langlois *et al.* describes the C–H trifluoromethylation of a small selection of electron-rich arenes, however the selectivities of trifluoromethylation are generally low.



Scheme 12. Initial report of the use of **1.2.41** for the C–H trifluoromethylation of aromatic rings. Conditions: (i) **1.2.41** (4.0 eq.), *tert*-BuOOH (7.0 eq.), Cu(OTf)₂ (10 mol%), MeCN/H₂O, RT.

The Baran group have since pioneered the field of using alkyl sulfinate salts for the late-stage diversification of biologically-relevant molecules with a suite of functionalities.^{68–73} The use of **1.2.41** under oxidative conditions facilitates the selective transition-metal free trifluoromethylation of dihydroquinine **1.2.44**, to give **1.2.45** (Scheme 13a).⁶⁸ Caffeine, **1.2.46**, can be reacted with a sulfone sulfinate to form **1.2.47** (Scheme 13b), which can then undergo a reductive cleavage of the sulfone to facilitate a formal C–H methylation of the heterocycle.⁷³ This method of C–H alkylation can also be used to install tagging groups onto pharmaceutical molecules, such as the antidiabetic pioglitazone, **1.2.49**. The pioglitazone derivative **1.2.50** can then be conjugated to antibodies *via* a copper-free azide-alkyne cycloaddition⁷⁴ to facilitate the preparation of antibody-drug conjugates (ADCs) (Scheme 13c).^{75,76} Bioconjugation of medicinal agents is very important as it can lead to improvements in the selectivity of a pharmaceutical by hijacking the antigen-selectivity of the biologic, and can also provide insight the mode of therapeutic action.^{77,78} This result is also a unique exemplar of how late-stage functionalisation can be used to not just adjust the properties of the small molecule itself, but also be used to explore different types of therapeutic approaches for the drug.

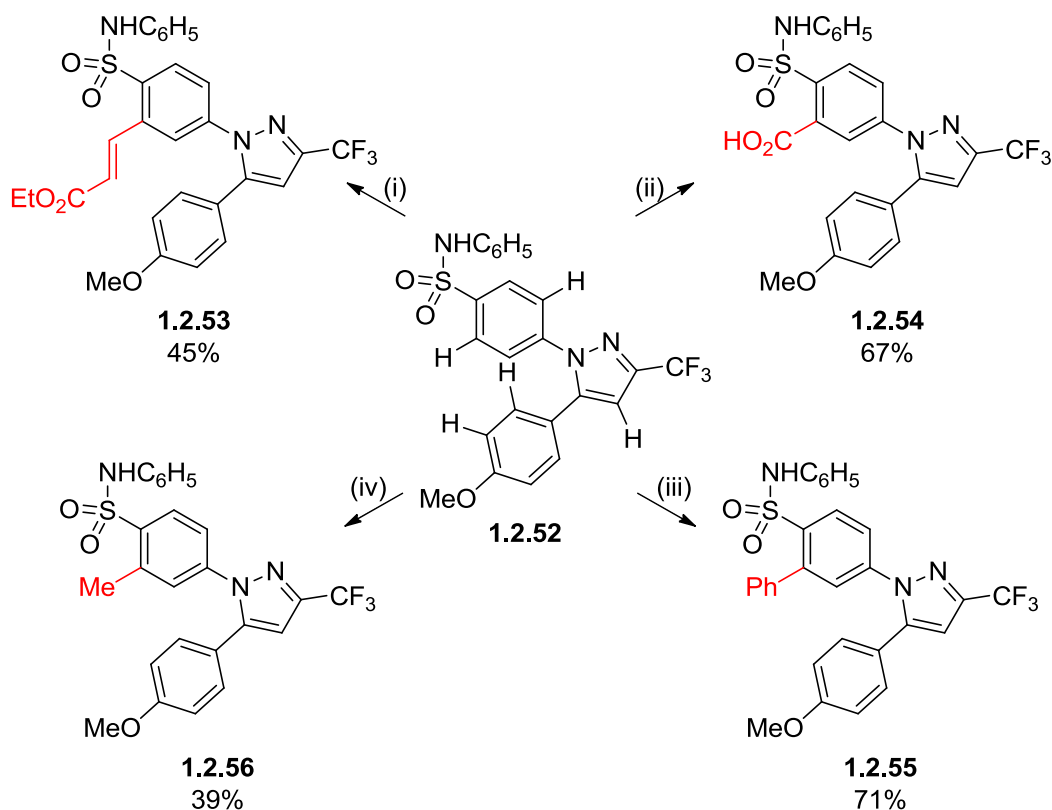


Scheme 13. Late-stage alkylation of heterocycles via the generation of alkyl radicals from alkylsulfinate salts. Conditions: (i) **1.2.41** (3.0 eq.), *tert*-BuOOH (5.0 eq.), DCM/H₂O, RT, 24 h; (ii) (PhSO₂CH₂SO₂)₂Zn (3.0 eq.), *tert*-BuOOH (5.0 eq.), PhCF₃/H₂O, RT, 24 h; (iii) SmI₂ (4 eq.), H₂O (50 eq.), THF, RT, 30 min; (iv) N₃(CH₂)₆CF₂SO₂Na (3.0 eq.), ZnCl₂ (1.5 eq.), TFA (1.0 eq.), *tert*-BuOOH (5.0 eq.), DMSO/H₂O, 50 °C, 11 h. Su = succinimide.

The reactivity and site-selectivity observed in this type of C–H functionalisation typically relies on the innate oxidative susceptibility of the substrate, meaning that formation of mixtures of regioisomers can be possible. Although this is beneficial if wide scaffold diversity is desired, it can become a problem when trying to screen

functionality along a specific vector in a precious intermediate, or when investigating functionalisation away from the innately reactive C–H position. This issue, however, can be circumvented effectively through the use of a directing group.

The Yu group have pioneered the field of palladium- and copper-catalysed directed C–H activation,^{79–83} and have reported several examples of late-stage functionalisation. Compound **1.2.52**, an analogue of anti-inflammatory celecoxib, can be diversified to compounds **1.2.53–1.2.56** through a series of Pd-catalysed C–H activation procedures, directed by the pendant pentafluorophenyl sulfonamide (Scheme 14).⁸⁴



Scheme 14. Pd-catalysed late-stage derivatisation of a celecoxib directed by a sulfonamide.

Conditions: (i) Pd(OAc)₂ (20 mol%), Ac-Leu-OH (40 mol%), AgOAc (4.0 eq.), ethyl acrylate (4.0 eq.), DMF (10.0 eq.), AcOH (2.0 eq.), DCM, 100 °C, 48 h; (ii) Pd(OAc)₂ (20 mol%), AgOAc (2.0 eq.), (2,2,6,6-Tetramethylpiperidin-1-yl)oxyl radical (TEMPO) (2.0 eq.), KH₂PO₄ (2.0 eq.), *n*-C₆H₁₄, CO (1 atm), 130 °C, 24 h; (iii) Pd(OAc)₂ (20 mol%), benzoquinone (BQ) (20 mol%), PhBpin (2.0 eq.), K₂HPO₄ (1.0 eq.), Ag₂CO₃ (2.0 eq.), *tert*-AmylOH, 110 °C, 24 h; (iv) Pd(OAc)₂ (20 mol%), BQ (20 mol%), MeB(OH)₂ (2.0 eq.), K₂HPO₄ (1.0 eq.), Ag₂CO₃ (2.0 eq.), *tert*-AmylOH, 110 °C, 24 h.

These transformations are interesting from a medicinal chemistry point of view owing to the diverse application of the products. Olefin **1.2.53** contains a Michael acceptor that could be used as a site for covalent inhibition.⁸⁵ Carboxylation to **1.2.54** would be useful for increasing the number of hydrogen bond donors and acceptors. Introduction of the carboxylic acid would also serve to lower lipophilicity, while on the other hand arylation and methylation products **1.2.55** and **1.2.56** would see increases in lipophilicity, which could lead to increased permeability.

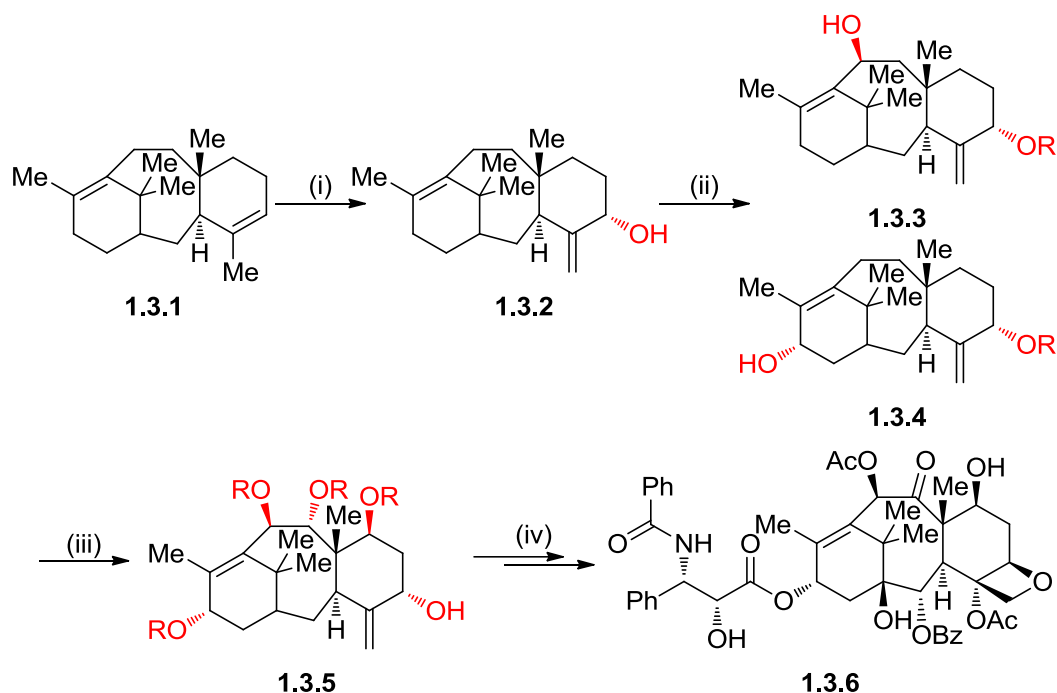
Directing groups offer many benefits in terms of regioselectivity, but installation and removal of directing groups adds steps to the synthetic protocol. This can sometimes be challenging to carry out,⁸⁶ and so, if directing groups are a necessity, it is much better if a functionality that is already present in the late-stage intermediate can be used to guide the functionalisation.

1.3 C–H Oxidation

Attrition of small molecules remains at a high rate at any stage of drug development, despite improved understanding of drug-target interactions, drug distribution and drug metabolism.^{87,88} As such, the average cost of discovery and development of a new molecular entity for a typical large pharmaceutical company was estimated to be \$1.8 billion in 2010.⁸⁹ Traditionally, drug failure has resulted from low efficacy, toxic side-effects, poor pharmacokinetic properties or poor bioavailability, and sub-optimal physicochemical properties have been found to be a common source of drug attrition.⁹⁰ Hence, a subtle balance of lipophilicity and polarity is needed to secure a drug candidate's positive future; techniques to screen the physicochemical parameters of a drug molecule and the synthesis of metabolites through selective oxidation of C–H bonds would therefore be a valuable tool for drug development.^{91,92}

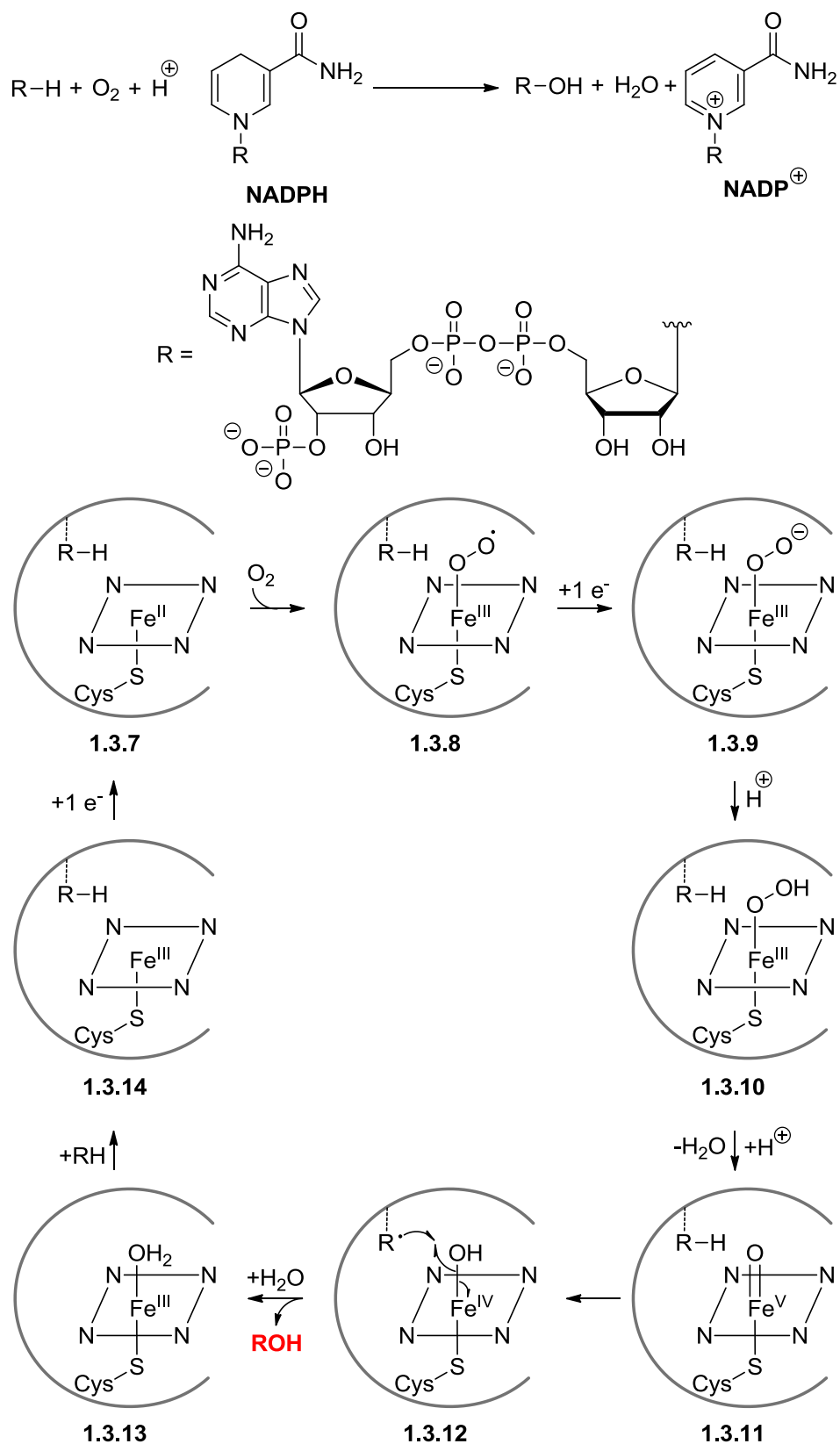
Nature, of course, is an expert in the selective oxidation of C–H bonds through the use of cytochrome p450 (CYP) monooxygenase enzymes.⁹³ For example, during the

biosynthesis of taxol, **1.3.6** (Scheme 15), CYP-dependent hydroxylase enzymes mediate the oxygenation of the scaffold of the diiterpene taxadiene **1.3.1**, which are subsequently modified into carbonyl, ester or ether links to form **1.3.6**.⁹⁴⁻⁹⁹



Scheme 15. Biosynthesis of taxol (1.3.6) from taxadiene (1.3.1). Conditions: (i) CYP taxadiene 5 α -hydroxylase;⁹⁴ (ii) CYP taxane 10 β -hydroxylase⁹⁵ or CYP taxane 13 α -hydroxylase,⁹⁶ R = H or Ac; (iii) CYP taxoid 7 β -hydroxylase,⁹⁷ R = H or Ac; (iv) multiple steps, several of which remain undefined.

The active site of CYPs possess a haem-iron centre, **1.3.7**, which is a co-factor consisting of a ferrous ion contained within a porphyrin macrocycle, and this ion is tethered to the protein *via* a cysteine thiolate ligand (Scheme 16).



Scheme 16. Mechanism of oxygenation reactions catalysed by cytochrome p450 enzymes. Full structure of haem porphyrin omitted for clarity.

The oxygenation process is facilitated by molecular oxygen, utilising nicotinamide adenine dinucleotide phosphate (NADPH) co-factor as a reductant.¹⁰⁰ As the substrate enters the active site, and is held in proximity to the haem centre, **1.3.7**, molecular oxygen coordinates to the ferrous centre, oxidising it to ferric haem complex **1.3.8**, which is then reduced to peroxide **1.3.9** by NADPH. Protonation to **1.3.10** is followed by dehydration to generate the iron(V)-oxo species **1.3.11**, which can then abstract a hydrogen atom from the substrate. The hydroxyl group and the substrate radical recombine to give **1.3.12**, and ejection of the monooxygenated product leaves ferric haem complex **1.3.13**. A new molecule of substrate then enters the active site, **1.3.14**, and reduction by NADPH reforms **1.3.7**.

In such biotransformations, the substrate is held in the active site in a specific conformation, enabling high levels of selectivity for oxidation. This process can be mimicked with directing groups and bulky catalyst ligands, but most chemical oxidation selectivity is driven by the innate reactivity of the substrate; this can be influenced by three main factors: inductive effects, hyperconjugation, and sterics.¹⁰¹ An understanding of these factors is critical to be able to predict reactivity for late-stage oxidation processes. An overview of some observed patterns of innate reactivity in C–H oxidation is detailed in Figure 5, which describes general trends that can help predict the most likely site of oxidation. Typically, oxidation will preferentially occur at the most electron-rich C–H bond. Due to inductive donation of electron density through hyperconjugative effects, this means that for non-metal insertion pathways the reactivity trend for C–H insertion is (highest to lowest): tertiary > secondary > primary > methyl. This is reflected in the bond dissociation energies for these different orders of C–H bond (Table 1), with the methyl C–H bond strength being approximately 8 kcalmol⁻¹ more than a tertiary a C–H bond.¹⁰²

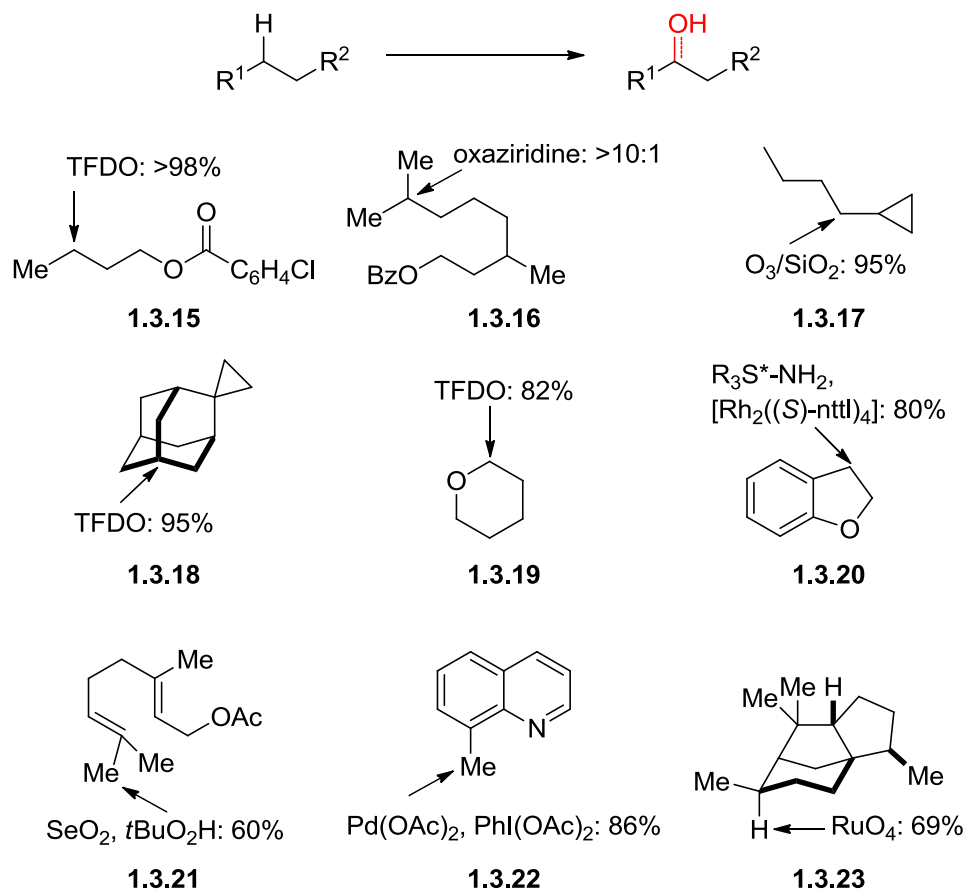


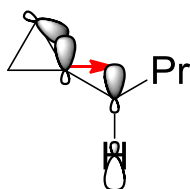
Figure 5. Observed selectivities for innate C–H oxidation due to inductive, hyperconjugative and steric effects. Positions where oxidation occurs are indicated by arrows, along with the reagents used to affect these oxidations.

Bond Order	Me-H	MeCH ₂ -H	Me ₂ CH-H	Me ₃ C-H
Bond Strength/ kcalmol ⁻¹	105	101	99	97

Table 1. The strength of the C–H bond decreases with increasing substitution on the carbon atom.

This trend accounts for the selective oxidation of **1.3.15** by methyl(trifluoromethyl)dioxirane (TFDO) at the methylene group that is most distal from the ester group, thus resulting in the indicated position being more electron-rich than the other methylene units, and still more reactive than the primary C–H bonds at the end of the carbon chain.¹⁰³ Similarly, **1.3.16** contains two tertiary C–H bonds, and it is the site furthest from the benzoyl ester that is selectively oxidised by an oxaziridine organocatalyst, though typical tertiary > secondary reactivity is observed.¹⁰⁴

Compound **1.3.17** deviates from this expected reactivity with most non-metal electrophilic oxidants, as the methylene vicinal to the cyclopropyl group is selectively oxidised by ozone/silicon dioxide.¹⁰⁵ This is a result of hyperconjugation between the C–C σ -bonding orbital of the cyclopropane and the neighbouring C–H σ^* -antibonding orbital, activating this C–H bond to oxidation (Figure 6).¹⁰⁶



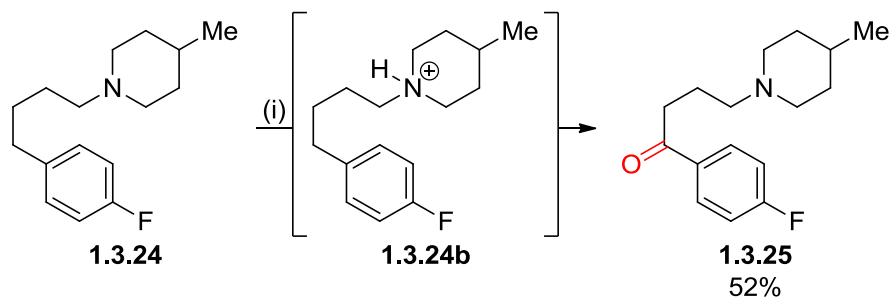
1.3.17

Figure 6. The ‘bent’ bonds of the cyclopropyl ring means that donation from the C–C σ -bonding orbital into the adjacent C–H σ^* orbital is possible, activating this position to oxidation.

Delocalisation of electron density from the bent cyclopropyl bonds to the neighbouring C–H antibonding orbital makes an oxidation event at this position with an electrophilic oxidant more facile.¹⁰⁷ This arises because the cyclopropane σ -bonding orbital has considerable π -character, and is approximately sp^2 in nature; this means that the cyclopropane highest occupied molecular orbital (HOMO) is high in energy and is a good electron donor.^{106,108} The strict orbital necessities of hyperconjugation are illustrated by cyclopropyl-substituted **1.3.18**, where the appropriate orbital overlap for activation of the vicinal position by cyclopropane is not possible, and so this position is now disfavoured due to steric hindrance.^{109,110} Hyperconjugative effects also lead to activation of C–H bonds adjacent to heteroatoms; despite oxygen being inductively electron-withdrawing due to its electronegativity, the nonbonding electrons of the ethereal oxygen lone pair in **1.3.19** can donate electron density to adjacent C–H bonds *via* hyperconjugation, activating this position to oxidation.^{111–114} This effect is reduced through conjugation of the lone pair, and is why nitrenoid insertion occurs selectively at the benzylic position for **1.3.20**.¹¹⁵ In a similar manner to cyclopropyl rings, alkenes and aromatic rings can activate allylic and benzylic C–H bonds through hyperconjugation between the π bonding orbital and the C–H σ^* -antibonding orbital. This is showcased with **1.3.21**¹¹⁶ and **1.3.22**,¹¹⁷ respectively, where oxidation occurs

at the most electron-rich C–H bond. Finally, a reduced rate of oxidation is often observed for hindered C–H bonds, exemplified in the ruthenium-mediated oxidation of cedrane **1.3.23**.¹¹⁸ Despite having four tertiary C–H sites, high selectivity for the indicated position is observed, which is attributed to the significant steric crowding around the other three.

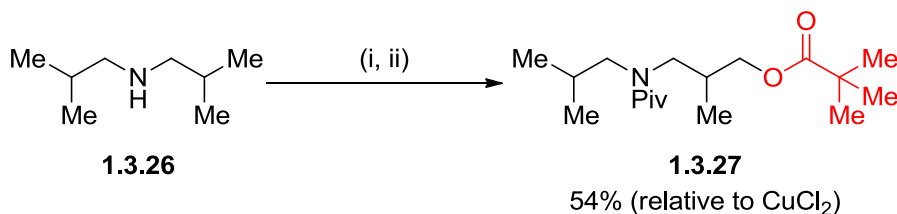
Using these reactivity trends, it is possible to implement C–H oxidation protocols onto late-stage intermediates and bioactive compounds in a predictive manner. Sanford *et al.* reported an iron-catalysed C–H oxidation process selective for benzylic sites remote from the heteroatom, wherein selectivity was greatly improved on addition of trifluoroacetic acid (TFA) to the reaction system.¹¹⁹ This likely arose due to protonation of the nitrogen lessening the hyperconjugative effect of the lone pair, and thus increasing the inductive electron-withdrawing effect. As a result, the more remote C–H bonds become more electron-rich, as illustrated in the synthesis of melperone, **1.3.25**, from **1.3.24** via ammonium intermediate **1.3.24b** (Scheme 17); high levels of selectivity are observed for benzylic oxidation over positions adjacent to the heteroatom and tertiary C–H bonds.



Scheme 17. Remote, benzylic Fe-catalysed late-stage C–H oxidation of aliphatic amine 1.3.24. Conditions: (i) TFA (1.1. eq.), FeCl₃ (5 mol%), picolinic acid (13 mol%), *tert*-BuOOH (70 wt% in H₂O, 18.0 eq.), pyridine/MeCN, RT, 48 h.

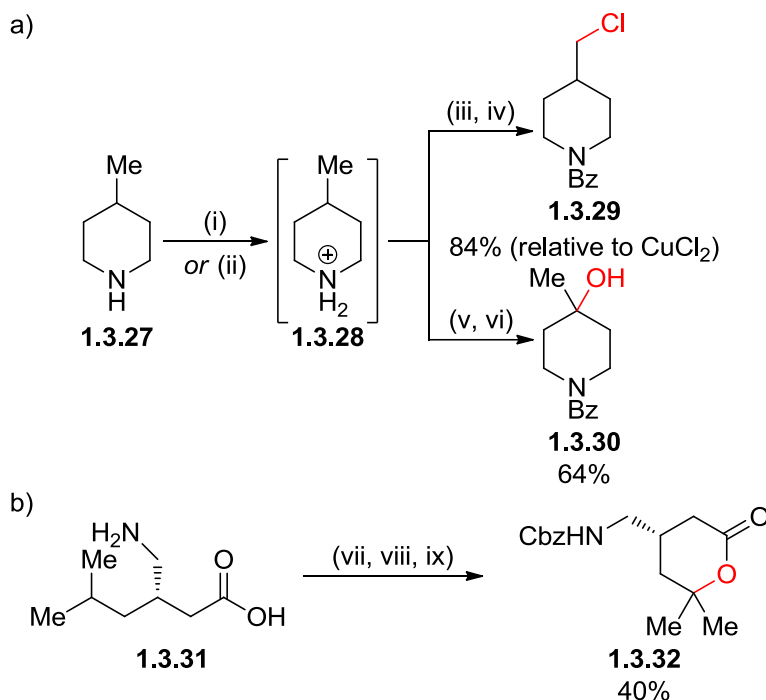
Similar principles are used in the platinum-catalysed remote C–H oxidation of aliphatic amines, where strongly acidic conditions induce changes to the electronic influence the heteroatom has on the molecule (Scheme 18).¹²⁰ The protonated amine

1.3.26 undergoes a remote C–H chlorination, which is then displaced by the aqueous solvent to give an alcohol that is then protected by pivaloyl chloride to give **1.3.27**.



Scheme 18. Platinum-catalysed remote C–H oxidation aliphatic amines. Conditions: (i) K₂PtCl₄ (1 mol%), CuCl₂ (1.0 eq.), **1.3.26** (5.0 eq.), aq. H₂SO₄ (5.5 eq.), 150 °C, 48 h; (ii) PivCl (3.0 eq.), DCM/Et₃N, RT, 3 h.

While the use of a platinum catalyst is a novel addition to the field of C–H functionalisation, and the low catalyst loading is an attractive prospect, the copper(II) chloride oxidant is the limiting reagent. This need for super-stoichiometric amounts of the amine substrate, in addition to elevated reaction temperature and time, currently limits the application of this methodology for late-stage oxidation. A complementary transition-metal-free process has subsequently been developed using potassium persulfate as an oxidant.¹²¹ Here, despite the reaction running under acidic conditions, the selectivity of oxidation is different to the Pt-catalysed process, with tertiary C–H oxidation strongly preferred. A direct comparison to the previously described Pt-catalysed process is discussed on amine **1.3.27** (Scheme 19a). Under the Pt-catalysed conditions, oxidation of the acidified intermediate **1.3.28** occurs selectively at the most remote, primary C–H bond, affording alkyl chloride **1.3.29**, whereas the potassium persulfate method produced tertiary alcohol **1.3.30** selectively.

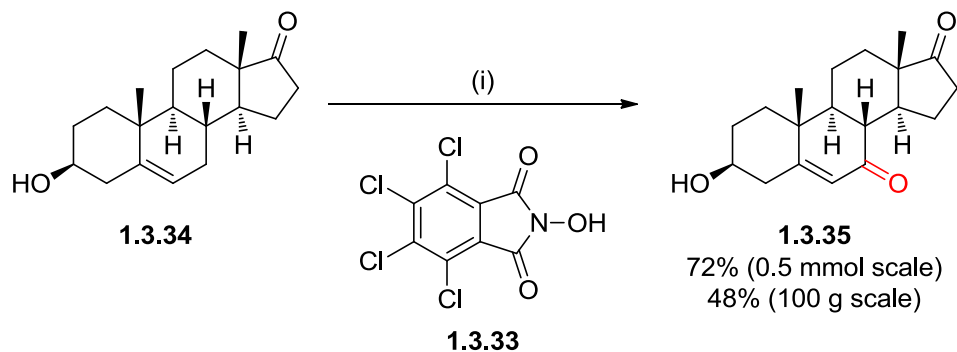


Scheme 19. a) Complementary remote C–H oxidation with high selectivity for tertiary C–H bonds; b) Oxidation applied to bioactive compound pregabalin. Conditions: (i) aq. H₂SO₄ (1.1 eq.); (ii) aq. H₂SO₄ (2.2 eq.); (iii) K₂PtCl₄ (1.0 mol%), CuCl₂ (1.0 eq.), **1.3.28** (10.0 eq.), 150 °C, 12 h; (iv) BzCl (3.0 eq.), DCM/Et₃N, RT, 3 h; (v) K₂S₂O₈ (2.0 eq.), H₂O, 80 °C, 4 h; (vi) BzCl (3.0 eq.), Et₃N (10.0 eq.), MeCN, RT, 12 h; (vii) aq. H₂SO₄ (2.2 eq.), (viii) K₂S₂O₈ (2.0 eq.), H₂O, 80 °C, 4 h; (ix) CbzCl (1.5 eq.), aq. NaOH (8.0 eq.), THF 0 °C to RT, 36 h.

This protocol was then applied to a selection of simple bioactive small molecules; oxidation of pregabalin **1.3.31** (Scheme 19b) resulted in cyclisation to amino lactone **1.3.32**. While the scope of substrates is limited in terms of functional group variability for this work, it does offer a selective oxidation using an inexpensive and safe oxidant in aqueous solvent.

Another example of hyperconjugation effects controlling selectivity of oxidation in complex molecules is allylic C–H oxidation, which has been used as a late-stage manipulation in a number of natural product syntheses,¹²² but the majority of transformations still use highly toxic or expensive reagents.¹²³ Electrochemistry offers an attractive alternative to traditional reagents, particularly for large scale application, owing to the higher sustainability of the process.¹²⁴ Using **1.3.33** as a mediator and *tert*-butylhydroperoxide (TBHP) as a co-oxidant, Baran *et al.* have recently reported

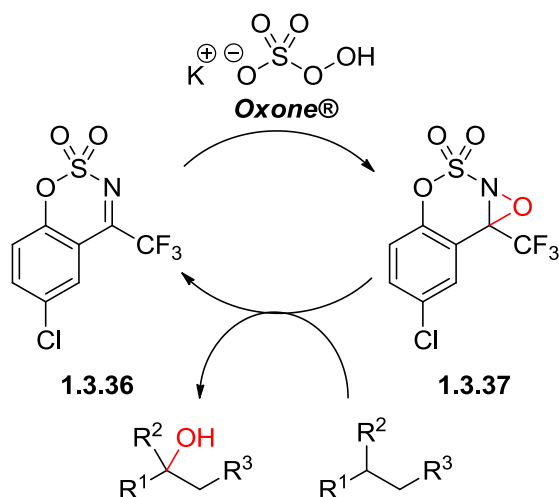
the application of electrochemical conditions to carry out highly selective C–H oxidation at the allylic position of a suite of small molecules (Scheme 20).¹²⁵ They also applied the protocol to a series of bioactive molecules, including the steroid dehydroepiandrosterone **1.3.34**.



Scheme 20. Late-stage allylic C–H oxidation of steroid 1.3.34 under electrochemical conditions. Conditions: (i) **1.3.33** (20 mol%), pyridine (20 mol%), *tert*-BuOOH (1.5 eq.), LiClO₄ (60 mol%), acetone, 10 mA mmol⁻¹, RT.

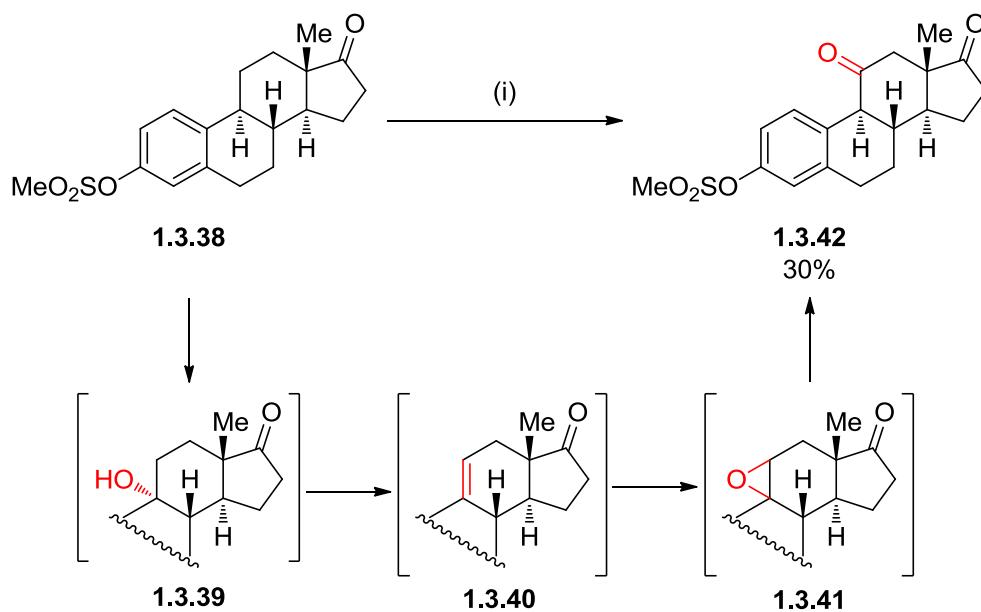
On small scale (0.5 mmol substrate) protocols, yields were in general very comparable to *prior art* for allylic oxidation – for example 81% for cobalt-mediated oxidation,¹²⁶ and 51% for chromium-mediated oxidation.¹²⁶ They also demonstrate the straightforward scalability of this method *via* a 100 gram-scale preparation of **1.3.35**, at 48% yield. From the perspective of process chemistry, the use of inexpensive carbon electrodes with minimal by-products is much more sustainable than the use of expensive and/or toxic oxidants.

While the use of more sustainable reagents is a benefit, transition-metal free oxidation can often require the use of high stoichiometries of expensive and/or hazardous oxidants. As such, organocatalytic methods of C–H oxidation are also desirable, as this potentially increases the sustainability of this transformation. One such example is reported by Du Bois *et al.*, which employs the oxaziridine organocatalyst **1.3.37** (Scheme 21), prepared *in situ* from benzoxathiazine **1.3.36** in the presence of a co-oxidant, such as Oxone®.^{127,128}



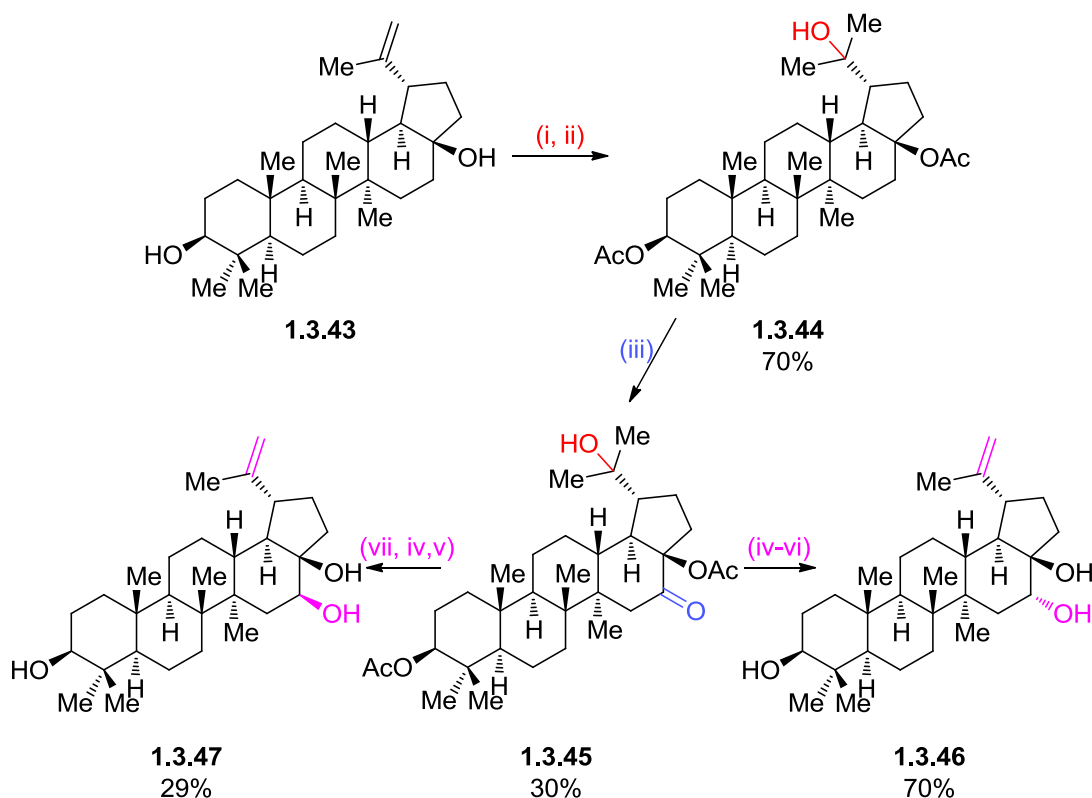
Scheme 21. Organocatalysed tertiary C–H oxidation of aliphatic C–H bonds, catalysed by 1.3.37.

Initial reports required the use of up to eight equivalents of hydrogen peroxide to promote modest yields of alcohol products.¹²⁷ However, following extensive studies of the decomposition of **1.3.37** in a variety of solvents at the reaction temperature, it was found that the rate of conversion of **1.3.37** back to **1.3.36** was significantly slowed down in fluorinated solvent, and Oxone® was found to be the optimal oxidant in the formation of **1.3.37**.¹²⁹ In general, substrate scope was limited and yields were modest, though in cases of low product yield, high recovery of starting material was possible, which is an important factor in the functionalisation of precious late-stage compounds. Across the suite of small molecules examined, oxidation occurred, as expected, at the tertiary C–H position selectively, however, when the conditions were applied to estrone derivative **1.3.38**, oxidation to ketone **1.3.42** was observed (Scheme 22). Tertiary benzylic C–H oxidation is proposed to occur to give alcohol **1.3.39**, which is then setup to undergo an elimination to alkene **1.3.40**.¹³⁰ Oxidation of this putative alkene to **1.3.41** can then occur, followed by a 1,2-shift to produce the ketone product.



Scheme 22. Late-stage C–H oxidation of estrone derivative 1.3.38, proposed to undergo elimination, re-oxidation and migration to ketone 1.3.42. Conditions: (i) **1.3.36** (20 mol%), Oxone® (2.5 eq.), 9:1 H₂O:(CF₃)₂CHOH, 70 °C, 12 h.

With a potential application of late-stage oxidation being the manipulation of physicochemical properties, Baran *et al.* have reported a study into the effect a series of late-stage oxidative transformations of the lupane natural product betulin, **1.3.43**, has on solubility.¹³¹ One particularly interesting example is oxidation with TFDO, which, following protection of the oxidatively susceptible functional groups in **1.3.43**, yielded ketone **1.3.45** as the major oxidation product (Scheme 23).



Scheme 23. Late-stage C–H oxidation of betulin in a study of the effect this approach can have on the solubility of complex bioactive molecules. Conditions: (i) sodium-*bis*-[*N*-salicylidene-2-aminoisobutyrate]-cobaltate(III) (10 mol%), PhSiH₃ (8.0 eq.), EtOH, O₂, RT, 10 h; (ii) Ac₂O (4.0 eq.), DMAP (10 mol%), pyridine, RT, 2 h; (iii) TFDO (2.0 eq.), DCM, 0 °C, 2 h; (iv) LiAlH₄ (1.5 eq.), THF, -95 °C – RT, 16 h; (v) HCl (50.0 eq.), DCM, 0 °C, 1 h; (vi) aq. NaOH, THF, MeOH, RT, 12 h; (vii) Zn(BH₄)₂ (2.0 eq.), toluene, RT, 1 h.

Several oxidants were screened, including precedented chromium oxide conditions,^{132,133} but TFDO was the only one to give any selectivity of oxidation; this is remarkable as the ¹³C NMR demonstrates that this methylene unit is not the most electron rich site, and results from the oxidised methylene unit being the most sterically accessible. The trifluoromethyl group of TFDO adds extra steric bulk to the reactive oxidant, clashing with the methyl groups on the framework of **1.3.44**. Computational studies on the activation energies of the scaffold C–H bonds agree with the observed selectivity, and predict abstraction of the equatorial C–H bond to occur first. This bond is more reactive due to a combination of higher steric accessibility and the strain-release effect.^{35,134} Selective reductions of ketone **1.3.45**, followed by alcohol elimination and ester hydrolysis afforded alcohols **1.3.46** and **1.3.47** using lithium aluminium hydride and zinc borohydride, respectively.

The solubility of each of the alcohols **1.3.46** and **1.3.47** was then tested in simulated intestinal fluid, in both fasted and fed states,¹³⁵ and compared to the values for **1.3.43** (Table 2).

Entry	Substrate	Relative Solubility Enhancement (FaSSIF) ^[a]	Relative Solubility Enhancement (FeSSIF) ^[b]
1	1.3.46	274-fold	no change
2	1.3.47	8-fold	0.08-fold

Table 2. Relative solubility enhancement of alcohols 1.3.43 and 1.3.44. [a] Solubility ratio of substrate to **1.3.43** in the fasted state simulated intestinal fluid; [b] Solubility ratio of substrate to **1.3.43** in the fed state simulated intestinal fluid.

The key difference between the two is that the fed state was not only at a lower pH than the fasted state, but also contained a higher concentration of sodium taurochlorate and egg lethicin additives, resulting in a higher ionic strength. Alcohol **1.3.46** saw a greatly increased solubility in the fasted state simulated intestinal fluid (FaSSIF) in comparison to **1.3.43**, while **1.3.47** had a much smaller increase. Interestingly, in the fed state simulated intestinal fluid (FeSSIF) assay, **1.3.46** had no change compared to **1.3.43**, and **1.3.47** had diminished solubility. This highlights the challenge of predicting the effect that skeletal oxidation will have on solubility, but more importantly the compounds were prepared rapidly, and thus the screening data was collected very quickly due to the implementation of a late-stage strategy. Medicinal chemistry decisions as to future compound design therefore can be made more efficiently.

An additional way of functionalising regio- and chemoselectively without the use of a directing group is to use a sterically-hindered catalyst system to limit the orientation that a substrate can approach the catalyst with. White *et al.* have reported the use of the Fe(PDP) catalyst-ligand system **1.3.48** (Figure 7) as a sterically hindered catalyst to facilitate iron-catalysed aliphatic C–H oxidation.¹³⁶

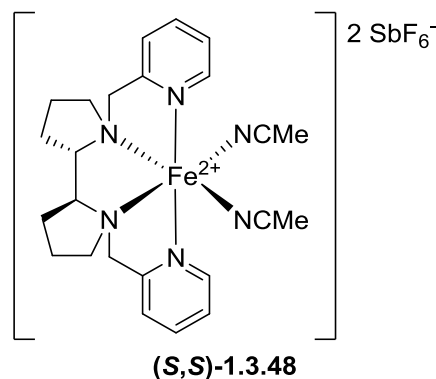
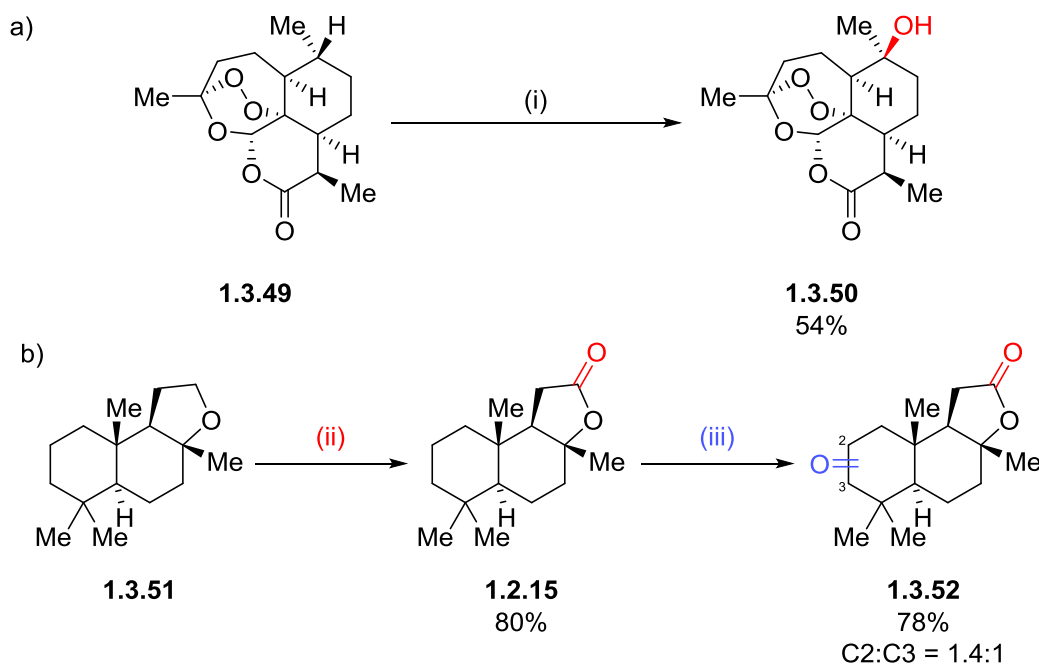


Figure 7. Fe(*S,S*-PDP) catalyst – the bulky ligand allows for control of site-selectivity in iron-catalysed C–H oxidation. PDP = (*2S,2'S*)-1,1'-*bis*-(pyridin-2-ylmethyl)-2,2'-bipyrrolidine. Both enantiomers of the ligand were used interchangeably, and gave identical results.

An example of the stereoelectronic control that the catalyst enables is the oxidation of artemisinin, **1.3.49**, to alcohol **1.3.50** (Scheme 24a). Compound **1.3.49** contains five tertiary C–H bonds, and oxidation is selective for the one that is most remote from the electron-withdrawing groups. It should be noted that to achieve the yield of 54%, the starting material had to be isolated and re-submitted to the reaction conditions, however, this serves to highlight the selectivity and cleanliness of the reaction that the substrate can be recovered with sufficient purity. In contrast, ambroxide, **1.3.51**, which contains two tertiary C–H sites is oxidised at the ethereal position to form the lactone sclareolide, **1.2.15** (Scheme 24b), which in turn can be oxidised at the two methylenic sites remote from the lactone, with slight bias towards the less sterically hindered site. This selectivity arises due to inductive effects deactivating the tertiary position β to the ethereal oxygen, and steric hindrance blocking oxidation of the more distal tertiary C–H bond on the ring junction. The oxidation proceeds with an element of innate reactivity from the substrate, with electron-rich positions reacting faster than electron-poor positions. But due to the steric bulk of the ligand, selectivity of oxidation occurs due to a combination of steric and electronic parameters, and can be highly susceptible to seemingly subtle steric hindrance within the substrate. Accordingly, predicting sites of oxidation can vary from substrate to substrate, depending on how much crowding there is around the more electron-rich C–H bonds.^{136,137}



Scheme 24. Late-stage aliphatic C–H oxidation under stereoelectronic control using iron catalyst 1.3.48. Conditions: (i) (*S,S*)-**1.3.48** (15 mol%), AcOH (1.5 eq.), H₂O₂ (3.6 eq.), MeCN, RT, 30 min; (ii) (*R,R*)-**1.3.48** (15 mol%), AcOH (1.5 eq.), H₂O₂ (3.6 eq.), MeCN, RT, 30 min; (iii) (*R,R*)-**1.3.48** (25 mol%), AcOH (0.5 eq.), H₂O₂ (5.0 eq.), MeCN, RT, 30 min.

Catalyst **1.3.48** was subsequently derivatised to reduce the cone angle of approach towards to iron centre, leading to catalyst Fe(CF₃-PDP), **1.3.53** (Figure 8).¹³⁸

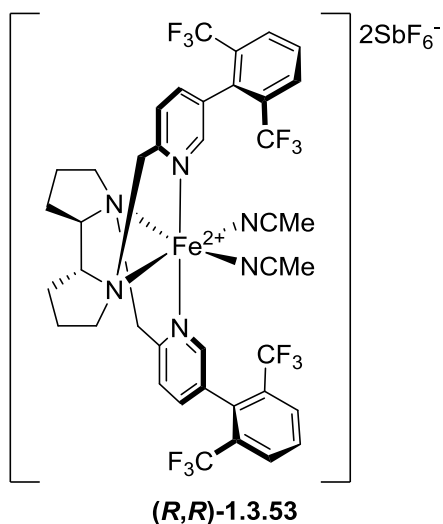
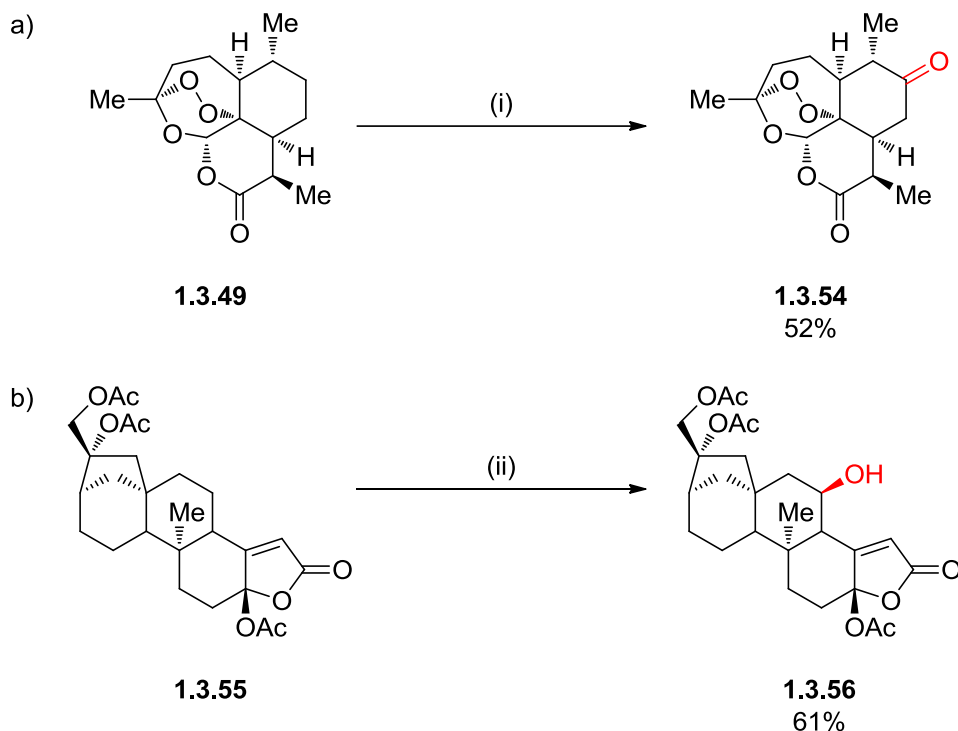


Figure 8. Fe(*R,R*-CF₃-PDP) catalyst – reducing the cone angle of approach trajectory for incoming substrates increases the steric control of oxidation. CF₃-PDP = (*2R,2'R*)-1,1'-bis-((5-(2,6-bis-(trifluoromethyl)phenyl)pyridin-2-yl)methyl)-2,2'-bipyrrrolidine. Both enantiomers of the ligand were used interchangeably, and gave identical results.

The two additional *bis*-trifluoromethylphenyl rings reduce the maximum available approach trajectory for incoming substrates from 145° down to 76°. This has the effect of increasing the selectivity of oxidation in favour of steric factors, and provides a greater level of catalyst control in predicting the site of oxidation. This is illustrated in the oxidation of **1.3.49** (Scheme 25a), which occurs with high selectivity on the remote methylene, to afford ketone **1.3.54**.

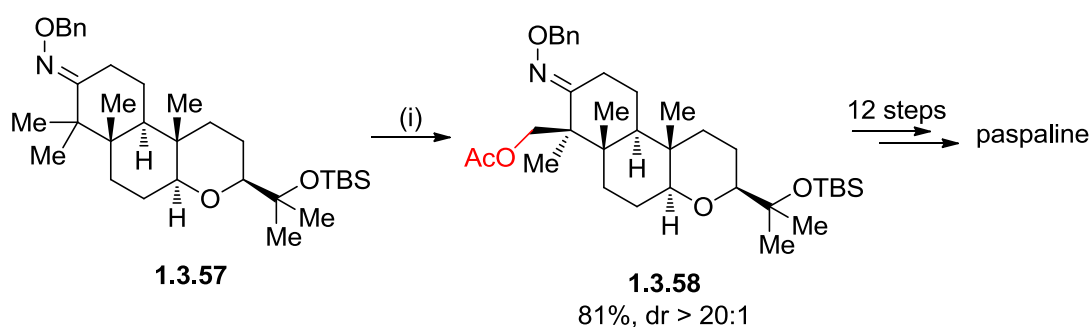


Scheme 25. Catalyst-controlled late-stage oxidation using catalyst **1.3.53.** Conditions: (i) (*S,S*)-**1.3.53** (15 mol%), AcOH (1.5 eq.), H₂O₂ (3.6 eq.), MeCN, RT, 30 min, 52%; (ii) (*R,R*)-**1.3.53** (15 mol%), AcOH (1.5 eq.), H₂O₂ (3.6 eq.), MeCN, RT, 30 min.

Due to the steric constraints of the ligand, the catalytic centre cannot reach the more reactive tertiary C–H bond, and so oxidation occurs at the most electron-rich and sterically accessible methylene; this highlights the difference in chemoselectivity that can be achieved between the two catalysts. Another example of the difference that this catalyst-controlled protocol introduces is in the oxidation of *tri*-acetoxytricalysiolide B, **1.3.55**, which affords alcohol **1.3.56** with high selectivity (Scheme 25b).

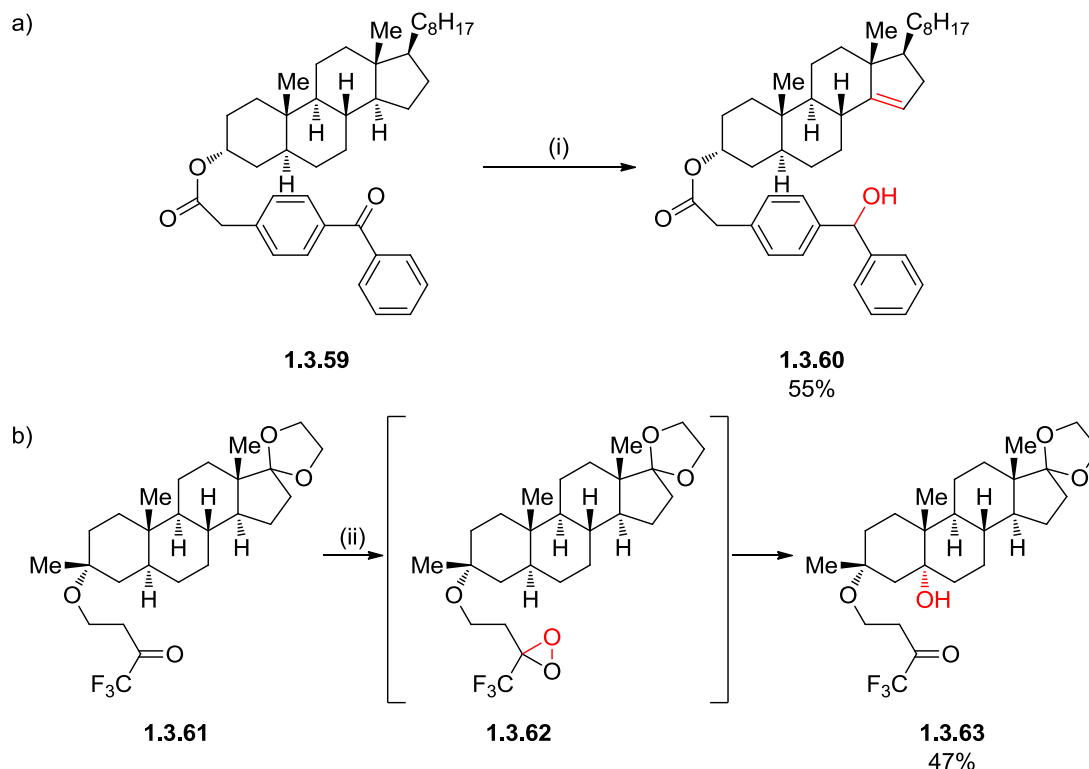
The regioselectivity and yield with this catalyst are superior to catalyst **1.3.48**, and the chemoselectivity to stop at the alcohol is also remarkable. Normally, the C–H bond adjacent to the alcohol would be more reactive to oxidation than the starting substrate due to hyperconjugative activation. In this case, however, the product alcohol creates sufficient steric hindrance to be blocked from accessing the catalytic active site, and hence mono-oxidation is observed as the major oxidation product.

While high regioselectivity can be achieved through careful ligand design, restricting the approach of a substrate to the catalyst, or harnessing the innate reactivity of the substrate, predicting the site of oxidation can vary from substrate to substrate. Installation of a directing group can avoid this issue, because the oxidant is guided into the site of oxidation, restricted by where the directing group is designed to reach. Among others, carboxylate, oxazoline, oxime and pyridine-type functional groups have all been used as directing groups to direct metal-catalysed C–H oxidation reactions.^{80,139–142} Johnson *et al.* have reported the application a palladium-catalysed C–H acetoxylation in their synthesis of the indole diterpenoid paspaline.¹⁴³ They describe the use of an *O*-benzyloxime as a traceless directing group to carry out guided oxidation of the primary C–H bond on the nearby equatorial methyl group of intermediate **1.3.57** (Scheme 26). This example illustrates the power of directed C–H functionalisation, because oxidation occurs where the catalyst is guided to, and so primary C–H bond activation is achievable.



Scheme 26. Late-stage Pd-catalysed C–H oxidation of a terpenoid scaffold in the synthesis of the natural product paspaline. Conditions: (i) Pd(OAc)₂ (15 mol%), PhI(OAc)₂ (1.5 eq.), AcOH/Ac₂O, 100 °C, 1 h.

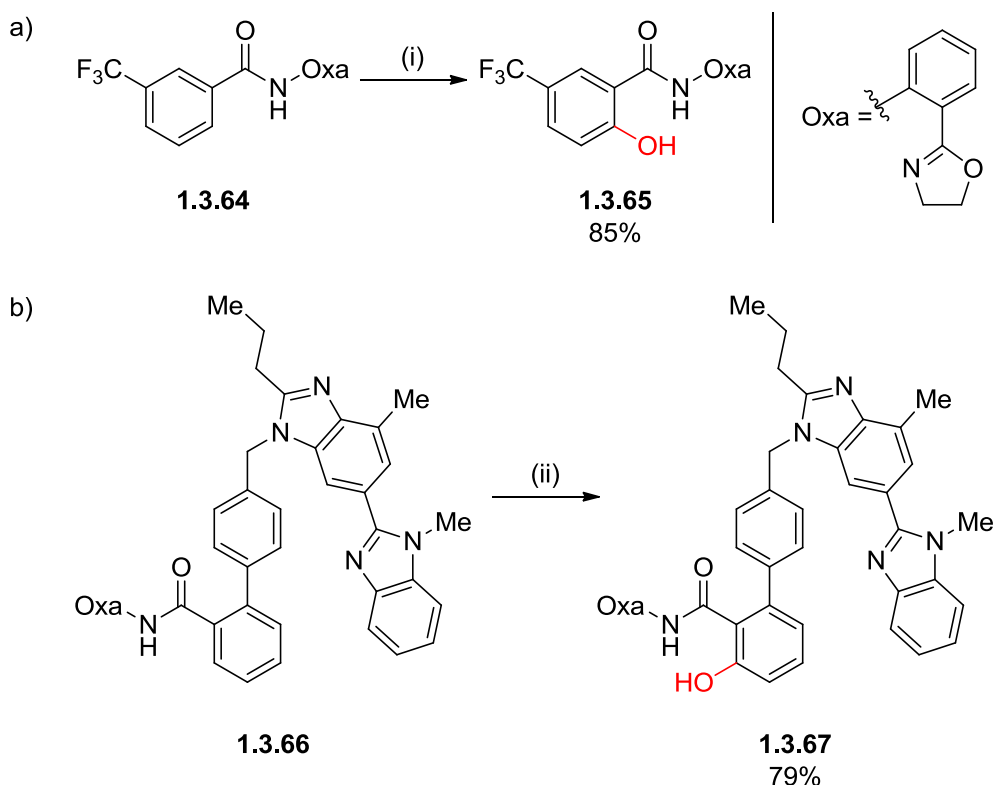
Directed oxidation can also be carried out under transition-metal free conditions. Breslow, widely considered as the pioneer of “designer” directing groups, has reported several accounts of steroid halogenation using a tethered directing group.^{144–146} Work from this laboratory has also described the use of a tethered benzophenone group to carry out a photochemical oxidation of the C/D ring junction in steroid derivative **1.3.59** via a Norrish type II reaction (Scheme 27a).^{147,148}



Scheme 27. Transition-metal free directed C–H oxidation. Conditions: (i) 450 W UV lamp, RT, 75 min; (ii) Oxone® (5.0eq.), NaHCO₃ (15.0 eq.), *tert*-BuOH/aq. Na₂EDTA, RT, 24 h.

Photochemical excitation of **1.3.59** leads to abstraction of the hydrogen on the C/D ring junction, and abstraction of the adjacent hydrogen leads to formation of alkene **1.3.60** through transfer of hydrogen to the ketone tether. More recently the Inoue group have reported the selective hydroxylation of steroidal C–H bonds directed by a tethered trifluoromethyl ketone (Scheme 27b).¹⁴⁹ Oxone® is used to oxidise ketone **1.3.61** to the intermediary dioxirane **1.3.62**, which can then oxidatively insert into the axial tertiary C–H bond on the A/B ring junction, affording alcohol **1.3.63**.

Directing groups have additionally been used to facilitate the oxidation of aryl C–H bonds.^{65,150–152} The Yu group reported the seminal example of palladium-catalysed *ortho*-hydroxylation of benzoic acid derivatives, with oxygen insertion originating from atmospheric oxygen.¹⁵³ The basis of this transformation was subsequently used in the development of a copper-catalysed oxidation under an oxygen atmosphere, using the oxazoline group on amide **1.3.64** as a directing group (Scheme 28a).^{154,155}

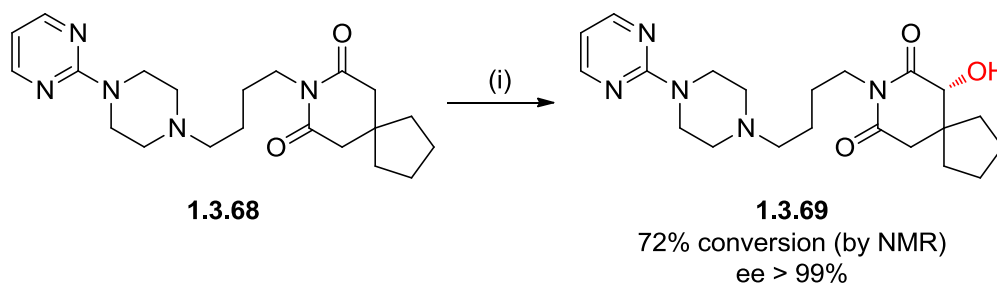


Scheme 28. Cu-catalysed C–H hydroxylation using an oxazoline directing group. Conditions: (i) Cu(OAc)₂ (1.0 eq.), Na₂CO₃ (1.0 eq.), H₂O (20.0 eq.), DMSO, 80 °C, O₂, 6 h; (ii) Cu(OAc)₂ (1.2 eq.), Na₂CO₃ (1.0 eq.), H₂O (20.0 eq.), DMSO, 80 °C, O₂, 6 h.

This methodology was then combined with other work for oxazoline-directed copper-catalysed C–H activation to report the late-stage diversification of **1.3.66**, a derivative of marketed hypertension treatment telmisartan, including hydroxylation to phenol **1.3.67** (Scheme 28b).⁸³ Directing groups offer numerous advantages in terms of chemo- and regioselectivity, and enable functionalisation of positions that are not the most innately reactive centre. On the other hand, the requirement to install and remove

these groups adds steps into a synthetic sequence, and certain directing groups that facilitate a desired transformation may not be compatible with the late-stage substrate.

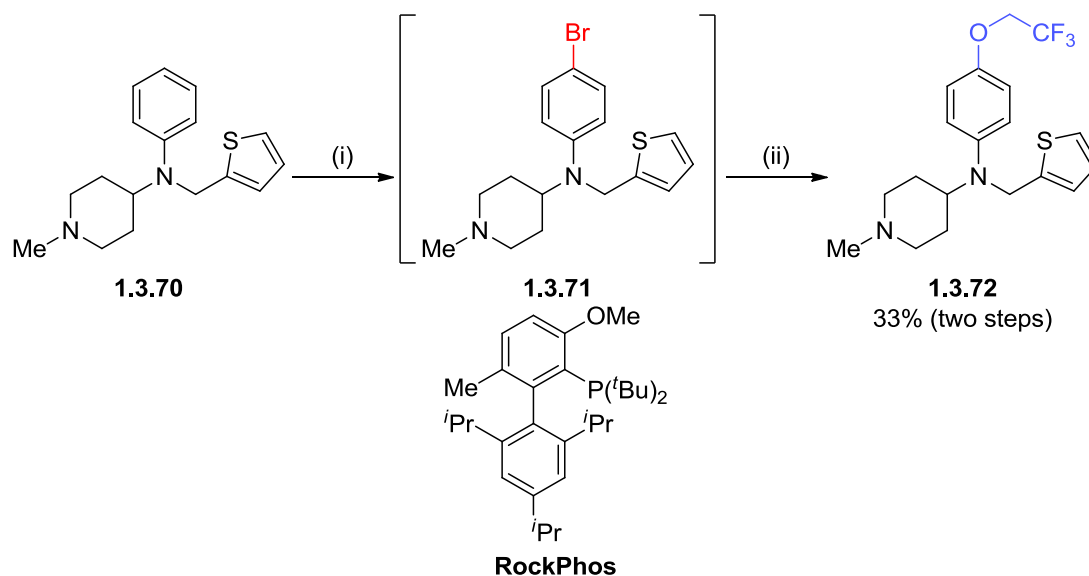
Enzymatic C–H oxidation^{156,157} is another strategy that can be used to carry out highly selective late-stage oxidation of complex molecules. Utilising the ability of enzymes to facilitate C–H oxidative transformations is particularly important for understanding the metabolic pathways of pharmaceutical compounds. Through rational design and directed evolution approaches, Arnold *et al.* were able to carry out efficient and enantioselective C–H hydroxylation of buspirone, **1.3.68**, (Scheme 29) using a variant of the *Bacillus megaterium*-encoded monooxygenase CYP BM-3.¹⁵⁸



Scheme 29. Enzyme-catalysed late-stage C–H oxidation of buspirone. Conditions: (i) **1.3.68** (2.0 mM), CYP BM-3 9-10A-F₈₇A monooxygenase (0.5 μM), isocitrate dehydrogenase (1.0 U/mL), NADP⁺ (0.05 mM), isocitrate (25.0 mM), Epps buffer (pH 8.2, 100 mM (with 1.0% (v/v) DMSO, 1.0% (v/v) acetone, 0.5% (v/v) DMF) 15 mL), RT, 7 h.

Compound **1.3.68** is a known substrate of human CYP3A4, and metabolite **1.3.69** is known to be pharmacologically active, so reliable and sustainable synthesis of enantiopure material is very important for further pharmacological and toxicological profiling.

Non-CYP enzymes can also be used to carry out C–H oxidation reactions. Lewis *et al.* report the use of engineered variants of rebeccamycin halogenase (RebH) to carry out selective C–H bromination of thenalidine, **1.3.70** (Scheme 30).¹⁵⁹ The crude brominated species **1.3.71** could then be used in an array of palladium-catalysed cross coupling reactions, including alkoxylation to afford **1.3.72**.



Scheme 30. Enzyme-catalysed late-stage C–H bromination of thenalidine, followed by a Buchwald-Hartwig etherification – a one-pot formal C–H alkoxylation. Conditions: (i) RebH 4-V (5 mol%), maltose-binding protein-rebeccamycin flavin reductase (MBP-RebF) (0.05 mol%), glutamate dehydrogenase (GDH) (9.0 U/mL), catalase (35.0 U/mL), NaBr (20.0 eq.), glucose (40.0), nicotinamide adenine dinucleotide (NAD) (0.2 eq.), flavin adenine dinucleotide (FAD) (0.2 eq.), phosphate buffer (pH 8.0, 25 mM (with 3.5% (v/v) *iso*-PrOH), RT, 16 h; (ii) [(allyl)PdCl]₂ (0.5 mol%), RockPhos (1.5 mol%), CF₃CH₂OH (2.0 eq.), Cs₂CO₃ (2.0 eq.), toluene, 90 °C, 14 h.

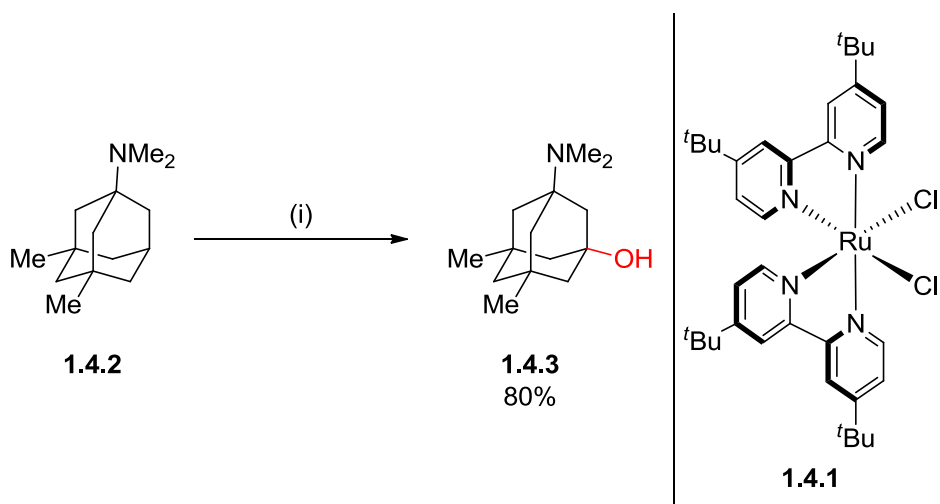
Enzymatic transformations offer great advantage in terms of regio- and enantioselectivity of C–H oxidation, although product yields can be low if the substrate does not fit the enzyme active site well. This means that laborious and systematic re-evolution of the protein can often be required, which can take a long time to optimise.

Several examples of late-stage oxidation have been highlighted here, but examples in the literature on substrates containing aliphatic azacycles are somewhat lacking. This is despite the prevalence of azacycles in modern small molecule pharmaceuticals, meaning that application of these protocols to industrial medicinal chemistry is limited.

1.4 C–H Oxidation of Aliphatic Azacycles

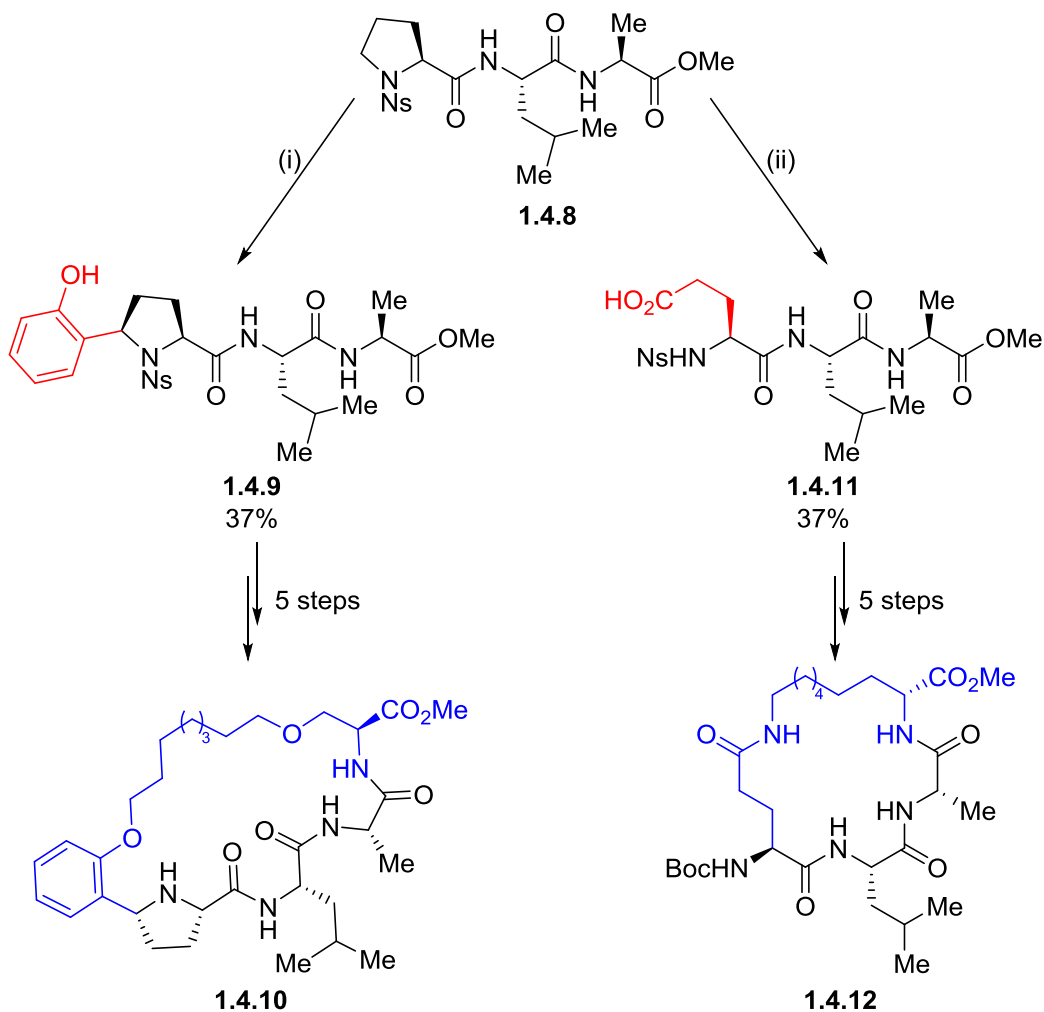
Oxidation of inert C–H bonds under reaction conditions that tolerate electron-rich nitrogen functionality is a significant challenge in the field of C–H functionalisation. Regular issues that arise are nitrogen chelation to the catalyst, forming a strong

nitrogen-metal bond that leads to catalyst deactivation, and direct oxidation of nitrogen to afford *N*-oxides. Additionally, common electronic deactivation methods for amines (such as acylation) do not overcome the effects of hyperconjugative activation of C–H bonds adjacent to the nitrogen atom. One method to circumvent these problems is to temporarily block the reactive nitrogen centre with Lewis or Brønsted acid additives.^{119,121,160–162} Limitations of current methods include the need to use excess starting substrate, high loadings of oxidant, and the necessity to recycle recovered unreacted starting material in order to achieve acceptable product yields. The Du Bois group have recently reported work that goes some way to address these issues, through the use of sterically hindered ruthenium catalyst **1.4.1** (Scheme 31).¹⁶³



Scheme 31. Ru-catalysed late-stage C–H oxidation of amine-substituted bioactive molecule 1.4.2. Conditions: (i) **1.4.1** (5 mol%), H₅IO₆ (2.0 eq.), CF₃SO₃H (6.0 eq.), AcOH/H₂O, RT, 4 h.

They used trifluoromethane sulfonic (triflic) acid as a Brønsted acid additive to transiently block the activating effects of the amine nitrogen atom. This enabled the C–H hydroxylation of a selection of small molecules containing basic amine functionality, including **1.4.2**, a derivative of the antiparkinsonian amantadine. Given the wealth of amine-containing pharmaceuticals and natural products, the application to more complex small molecules with amine functionality is limited; this may be as a result of the high stoichiometry of triflic acid required, limiting application in the presence of acid-sensitive functional groups.



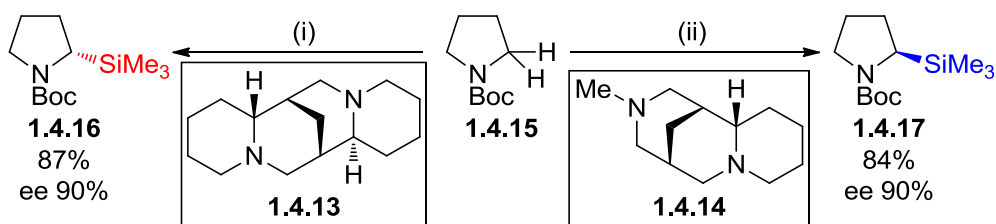
Scheme 33. Oxidative diversification of tripeptide 1.4.8 for the preparation of macrocyclic scaffolds. Conditions: (i) (*S,S*)-**1.3.48** (15 mol%), AcOH (1.5 eq.), H₂O₂ (5.7 eq.), MeCN, 0 °C, 30 min, then PhOH (2.0 eq.), BF₃•OEt₂ (4.0eq.), DCM, -78 to 0 °C, 3 h; (ii) (*S,S*)-**1.3.48** (25 mol%), AcOH (0.5 eq.), H₂O₂ (5.0 eq.), MeCN, RT, 75 min.

A C–H oxidation/ α -arylation strategy was used to generate the arylated peptide **1.4.9**, which was then converted into macrocycle **1.4.10** in five steps. In addition, **1.4.8** could be oxidatively ring-opened to give tripeptide **1.4.11**, formally constituting a remarkable conversion of a proline residue into a glutamic acid residue. This new tripeptide was then used to prepare macrocycle **1.4.12** in a five step sequence.

This illustrates the power to construct a diverse set of molecules from one common late-stage intermediate through a relatively short number of steps by the use of selective C–H functionalisation strategies. However, the requirement of the nosyl protecting group to be used to prevent catalyst deactivation slightly limits the

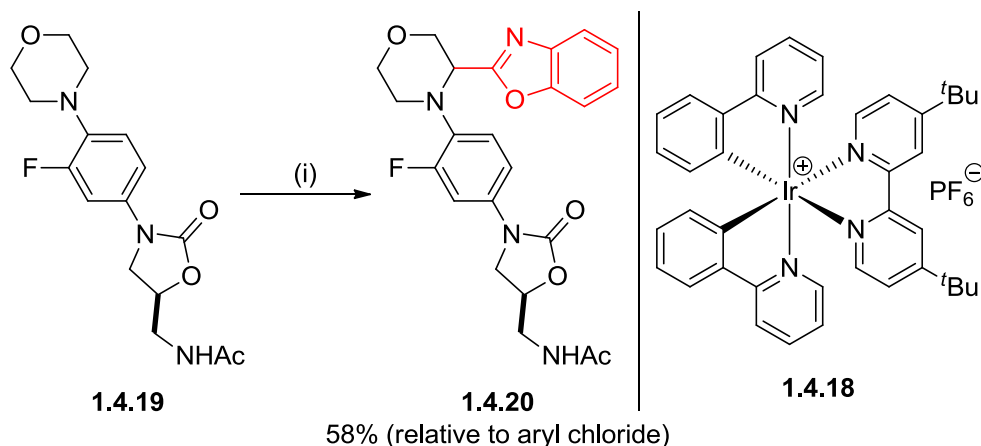
application of this methodology for late-stage application in medicinal chemistry, as extra steps are required for its introduction and removal.

On the other hand, if the protecting group can be harnessed as a directing group, then value is added to its role in the synthetic process. α -Lithiation directed by acyl-type protecting groups is a well-established strategy for α -functionalisation of simple aliphatic azacycles. This can be carried out with high enantioselectivity using either the naturally occurring alkaloid (–)-sparteine, **1.4.13**,^{165,166} or the (+)-sparteine surrogate **1.4.14**, developed by O'Brien *et al.*,^{167–169} as chiral ligands (Scheme 34). The need to use a strong base such as *sec*-butyllithium, however, rules out this method from the majority of late-stage azacycle C–H functionalisation strategies.



Scheme 34. Enantioselective α -lithiation strategy for α -C–H functionalisation of azacycles. Conditions: (i) *sec*-BuLi (1.3 eq.), **1.4.13** (1.3 eq.), Et₂O, -78 °C, 5 h, then Me₃SiCl (1.5 eq.), RT, 16 h; (ii) *sec*-BuLi (1.3 eq.), **1.4.14** (1.3 eq.), Et₂O, -78 °C, 5 h, then Me₃SiCl (1.5 eq.), RT, 16 h.

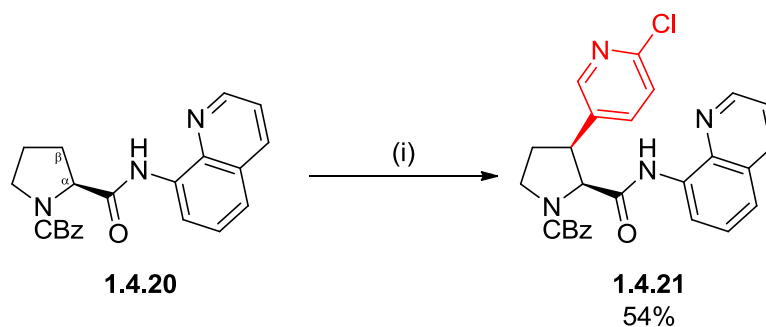
Nevertheless, the work of Beak, Hoppe and O'Brien in the field of α -lithiation chemistry has laid the groundwork for research focussed on C–H functionalisation of aliphatic azacycles at positions adjacent to the heteroatom, including palladium-mediated C–H bond activation, photoredox functionalisation and carbenoid insertion.^{170–174} For example, MacMillan *et al.* have used photoredox catalyst **1.4.18** to catalyse a late-stage C–H arylation of the antibiotic linezolid, **1.4.19** (Scheme 35).¹⁷⁵ This proceeds *via* abstraction of an electron from the morpholino-nitrogen lone pair, oxidatively generating an α -amino radical, which can then react with the arene coupling partner in a radical-radical coupling, forming **1.4.20** following loss of a chloride anion.



Scheme 35. Photoredox-catalysed α -arylation of linezolid. Conditions: (i) **1.4.18** (1 mol%), 26 W light bulb, 2-chlorobenzoxazole (1.0 eq.), NaOAc (2.0 eq.), **1.4.19** (3.0 eq.), *N,N*-dimethylaniline (DMA), RT, 12 h.

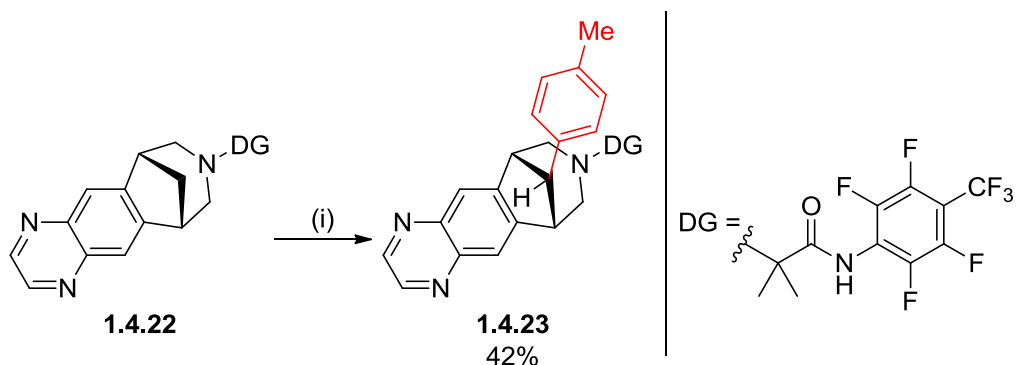
While this is a very useful addition to the field of azacycle C–H functionalisation, the fact that the reaction requires excess stoichiometry of the precious pharmaceutical amine somewhat limits the wider application of this protocol to late-stage functionalisation.

Methods for more remote C–H functionalisation at β and γ positions of aliphatic azacycles are less well-established. The Bull group have reported a palladium-catalysed C–H arylation at the β -position of a selection of proline derivatives, such as **1.4.20** (Scheme 36).¹⁷⁶ The aminoquinoline (AQ) group masking the proline carboxylate directs the catalyst towards the C-3 position, enacting insertion into the C–H bond. This leads to formation of the β -arylated products, such as **1.4.21**. While the stereospecificity of this reaction is widely applicable, the scope of functionality in the aryl group is somewhat limited. Additionally, the fact that the directing group has to be attached *via* an amide bond to the proline carboxylate limits the procedure to proline-based systems, excluding other pyrrolidine variants.



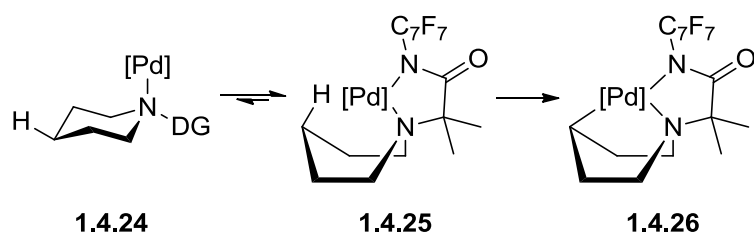
Scheme 36. Stereospecific β -C–H arylation of proline derivatives using an aminoquinoline directing group. Conditions: (i) Pd(OAc)₂ (5 mol%), 2-chloro-5-iodopyridine (1.8 eq.), AgOAc (1.8 eq.), 110 °C.

Sanford *et al.* have recently disclosed an elegant process for the palladium-catalysed transannular C–H arylation of piperidines, providing γ -functionalised products. This was applied to a suite of systems pre-organised into a boat conformation, and also for a selection of piperidine ring systems, including the varenicline derivative **1.4.22** (Scheme 37).¹⁷⁷



Scheme 37. Transannular C–H arylation of a derivative of varenicline. Conditions: (i) Pd(OAc)₂ (10 mol%), *para*-iodotoluene (30.0 eq.), CsOPiv (3.0 eq.), 150 °C, 18 h, air.

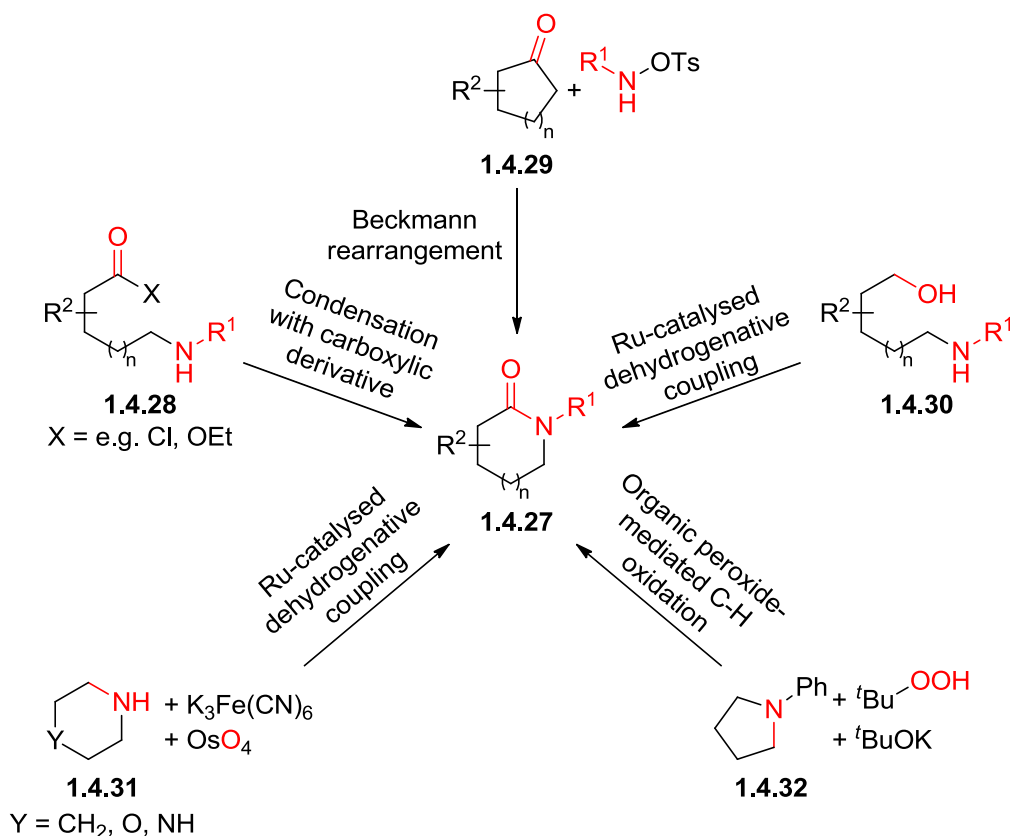
By using a carefully designed directing group, double coordination of the palladium catalyst enables access to the less-populated boat conformation **1.4.25** (Scheme 38), which is required to achieve the desired transannular functionalisation. The steric effects of the geminal dimethyl group increase the proportion of this conformation present in the reaction and, once in this conformation, chelation from both nitrogen atoms to the catalyst allows for activation of the transannular C–H bond to form palladacycle **1.4.26**, which can then undergo arylation with the aryl iodide.



Scheme 38. The amide directing group is able to facilitate double coordination of the Pd-catalyst and steric effects promote a chair conformation, allowing transannular C–H arylation to take place.

At this stage, the scope of this transformation is limited, and the reaction conditions are not ideal from an industrial application perspective, particularly regarding high excess of aryl iodide, high temperature and lengthy reaction time. Nevertheless, this seminal piece of work marks the first example of directed aliphatic C–H activation at a remote site, and undoubtedly will be developed into a very powerful addition to the field of C–H activation in the future.

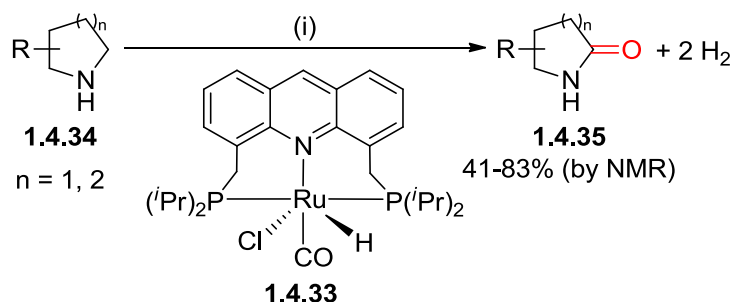
Due to the ubiquity of aliphatic azacycles in bioactive small molecules, methods to oxidise azacycles to the corresponding lactam would be desirable for widening library scope and assessing metabolic liability. Lactams are also found across a wide range of medicinal agents and natural products.^{178–181} The majority of current preparative methods of lactams, such as **1.4.27** (Scheme 39), involve condensation of amines with an activated carboxylic acid derivative **1.4.28**,¹⁸² Beckmann rearrangement from a cyclic ketone **1.4.29**,¹⁸³ or intramolecular dehydrogenative coupling of amines **1.4.30** with alcohols.^{184,185}



Scheme 39. Scope of traditional methods for the preparation of lactams from pre-activated starting materials, or *via* C–H oxidation of amines.

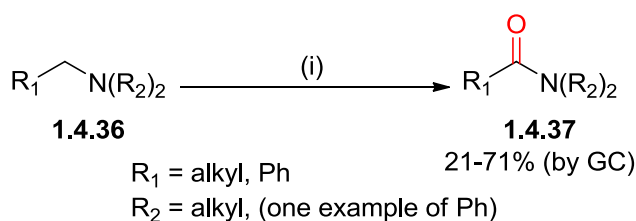
A comparative process to this latter example is to directly form the lactam moiety *via* chemoselective oxidation of cyclic amines such as **1.4.31** and **1.4.32**. This has traditionally required the use of expensive and toxic transition-metal catalysts, such as osmium¹⁸⁶ and mercury complexes,¹⁸⁷ or forcing oxidative conditions, such as organic peroxides^{188–190} and ruthenium oxides,^{191–193} which can have poor functional group tolerance, and can result in over-oxidation to the corresponding imide.

Recent work by Milstein *et al.* has involved the development of the acridine-based ruthenium pincer complex **1.4.33**^{194–196} to catalyse the dehydrogenative conversion of cyclic amines such as **1.4.34** to the corresponding lactams (Scheme 40).¹⁹⁷



Scheme 40. Ru-catalysed oxidation of cyclic amines to lactams. Conditions: (i) **1.4.33** (1 to 5 mol%), NaOH (1.5 to 5 mol%), 1,4-dioxane/H₂O, 150 °C, 48-89 h.

The catalytic nature of this oxidation is an attractive aspect, alongside water being the oxygen source, and hydrogen gas being the only by-product. The efficiency of this process is limited somewhat, however, by the need to heat the reaction to a very high reaction temperature of 150 °C for at least two days, in order for the expensive, air-sensitive catalyst to mediate oxidation. Although an interesting selectivity for secondary amines over tertiary amines is observed, the scope of the substrates surveyed is limited in terms of functionality, with only very simple cyclic amines examined, and aromatisable heterocycles, such as indoline and 3-(*N,N*-dimethylamino)pyrrolidine, forming the corresponding indole and pyrrole selectively. Ferric chloride offers a cheap alternative to ruthenium catalysis (Scheme 41), as reported by Emmert *et al.* for the oxidation of a selection of amines such as **1.4.36** to the corresponding amides **1.4.37**.¹⁹⁸

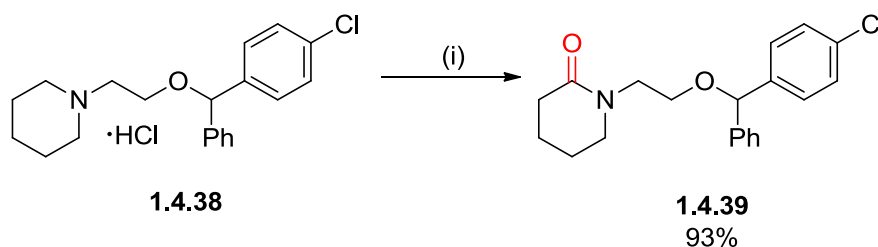


Scheme 41. Fe-catalysed oxidation of amines to amides, using a peroxide oxidant. Conditions: (i) FeCl₃•6H₂O (5.0 mol%), 2-picolinic acid (5.0 mol%), PhCO₃*tert*-Bu (3.0 eq.), H₂O (1.0-30.0 eq.), 50 °C, 2-48 h.

Milder reaction conditions enable reasonable conversions from amine substrates to the corresponding amides, though the report focusses principally on tertiary alkylamines, with no cyclic substrates examined. Additionally, yields were significantly diminished

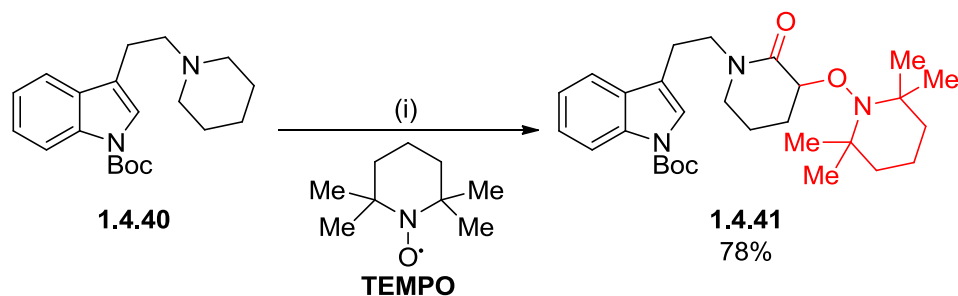
for unsymmetrical substrates, and the substrate scope is currently limited by the requirement of a strong peroxide oxidant.

Mizuno *et al.* have shown that gold nanoparticles, supported on alumina, offer an excellent alternative to these procedures.¹⁹⁹ They demonstrate that chemoselective oxidation of a selection of secondary and tertiary amines to the corresponding amides and lactams under mild conditions is possible. The Au/Al₂O₃ catalyst is reusable, and the functional group tolerance of the procedure is fairly broad, exemplified by selective late-stage oxidation of cloperastine hydrochloride (**1.4.38**) to lactam **1.4.39** (Scheme 42). The scope of substrates was limited to symmetrical amines, however, and the procedure is complicated by the multistep process required to prepare the colloidal catalyst.



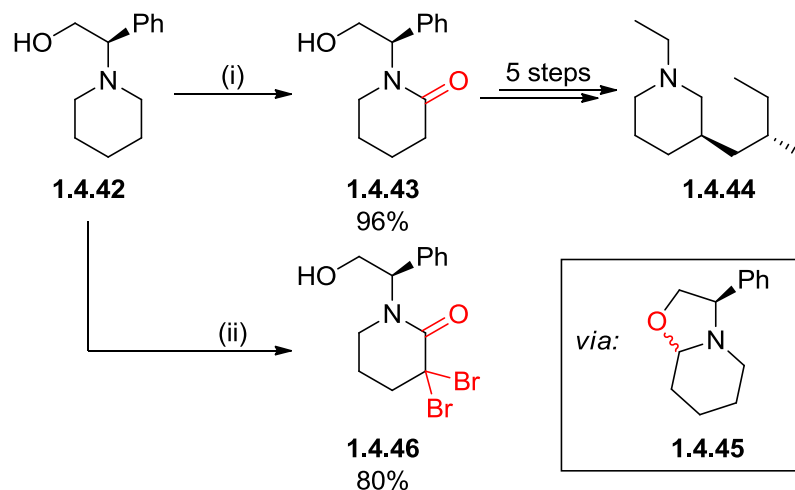
Scheme 42. Au-catalysed oxidation of cyclic amines to lactams. Conditions: (i) Au/Al₂O₃ (4 mol%), H₂O, O₂ (1 atm), 80 °C, 24 h.

Transition metal free processes for the α -C–H oxidation of amines to lactams are somewhat less well-precedented. In trying to carry out tandem allylic and alkene oxidation to generate glycidic amides,²⁰⁰ Sartillo-Piscil *et al.* found that a sodium chlorite/TEMPO oxidation system resulted in selectivity for endocyclic oxidation to prepare 3-alkoxyamine lactams.²⁰¹ Oxidation of a small selection of piperidine and pyrrolidine motifs yielded the TEMPO-derived alkoxyamine lactams, such as **1.4.41** (Scheme 43) prepared from tryptamine derivative **1.4.40**.



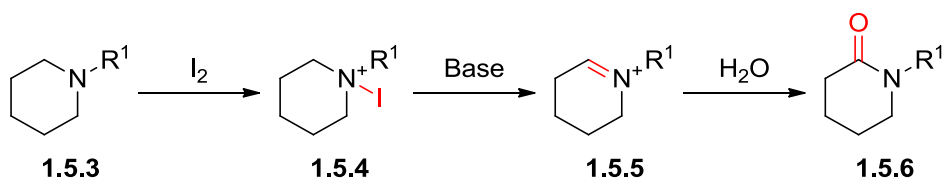
Scheme 43. NaClO₂/TEMPO mediated C–H oxidation of cyclic amine **1.4.40**. Conditions: (i) NaClO₂ (2.0 eq.), TEMPO (1.5 eq.), NaOCl (1.5 eq.), MeCN, 0 °C to RT, 3 h. Boc = *tert*-butyloxycarbonyl.

This is an interesting case where the reaction provides both α - and β -functionalisation, providing two functional handles along different vectors that could be manipulated further. The use of sodium chlorite here demonstrates the oxidising ability of the halogens. Fluorine, being the most electronegative halogen atom, has long been known as an effective oxidant, but electrophilic sources of fluorine are often expensive, sensitive and highly reactive reagents.^{202–204} In contrast, bromine has been used by Juarez *et al.* to carry out α -oxidation of a piperidine scaffold as an intermediate in the synthesis of the natural product stenusine, **1.4.44** (Scheme 44).²⁰⁵



Scheme 44. Use of elemental bromine to oxidise a piperidine scaffold to the corresponding lactam. Conditions: (i) Br₂ (3.0 eq.), AcOH/water, 0 °C, 3 h, then aq. NaOH, 90 °C, 1 h, 96%; (ii) Br₂ (10.0 eq.), AcOH/water, 0 °C to reflux, 3 h, then K₂CO₃, 0 °C, 80%.

Inspired by this, and the aforementioned isolated cases of natural product oxidation, the working hypothesis of this thesis is that C–H oxidation of aliphatic azacycles is accessible through the use of an electrophilic source of iodine, and that this mild oxidant could be used for the chemoselective late-stage oxidative functionalisation of high value azacyclic scaffolds (Scheme 45).



Scheme 45. General approach for the iodine-mediated C–H oxidation of azacycles.

1.6 Aims

The specific aims of this thesis are:

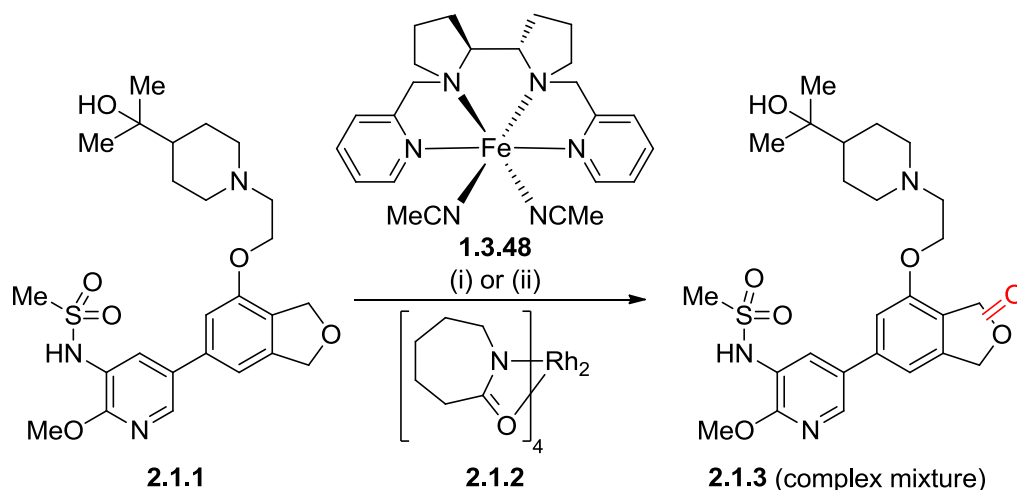
- The use of molecular iodine as a mediator of the C–H oxidation of aliphatic azacycles shall be tested and optimised for a range of model substrates to probe substrate scope. The application to late-stage oxidation will be tested by using the developed methodology to chemoselectively oxidise a suite of high value bioactive small molecules.
- The impact that this oxidative transformation has on biological and physicochemical properties shall be explored for some examples.
- The reaction shall be examined in detail in order to gain more mechanistic understanding, and offer rationale for selectivities observed. This understanding of oxidation shall then be used to elaborate the conditions toward a more general α -C–H functionalisation method.
- Through understanding and interception of intermediates in the oxidation to lactams, a strategy for the β -selective C–H oxidative functionalisation of azacycles shall be designed. The installation of functionality at this position

shall be exploited by diversification of the azacycle scaffold through a series of chemical transformations.

Entry	Conditions	Predicted oxidation
1	Fe(PDP), H ₂ O ₂ ^{136,137}	Methylene (c, d)
2	Rh ^I catalyst, TBHP ²²⁰	Ring-open piperidine
3	I ₂ , base ^{211,212}	Piperidine ring (c)
4	CuI, O ₂ ⁹¹	Piperidine ring (b, c)
5	RuO ₄ ^{191–193}	Piperidine ring (c)
6	Organocatalyst, Oxone® ¹²⁸	3° C-H (a)
7	TFDO ¹⁰¹	Least electron-deficient methylene (d)
8	SeO ₂ ²²¹	Benzylic position (d)

Table 3. Proposed conditions and selectivities for C–H oxidation screen of compound 2.1.1a. Fe(PDP) = **1.3.48**; TFDO = methyl(trifluoromethyl)dioxirane.

The ability to selectively oxidise different C–H bonds at different sites, within a molecule in a targeted manner using complementary chemical and/or enzymatic methods, would undoubtedly be very useful to medicinal chemistry groups. Iron-catalysed C–H oxidation using catalyst **1.3.48**, as reported by White *et al.*,^{136,137} and oxidation using rhodium catalyst **2.1.2**²²⁰ were investigated, but this resulted in complex mixtures of oxidative products **2.1.3** being formed (Scheme 46).



Scheme 46. C–H oxidation of 2.1.1 using iron and rhodium catalysis. Conditions: (i) (*S,S*)-**1.3.48** (15 mol%), AcOH, 1.5 eq., H₂O₂ (3.6 eq.), MeCN, RT, 30 min; (ii) **2.1.2** (10 mol%), *tert*-BuOOH (10 eq.), DCE, 40 °C, 16 h.

In light of the complexity of the crude reaction mixture using **1.3.48** and **2.1.2**, products were not isolated, although benzylic oxidation, such as at position *e* in Figure 10, appeared to be a primary site of oxidation based on crude ^1H NMR analysis. The next set of conditions explored was the use of molecular iodine as an oxidant, which has been described for the C–H oxidation of a piperidine ring contained within a number of natural products to the corresponding lactams **2.1.4** to **2.1.6** (Figure 11), oxidation product sites highlighted in red).^{211,213,215}

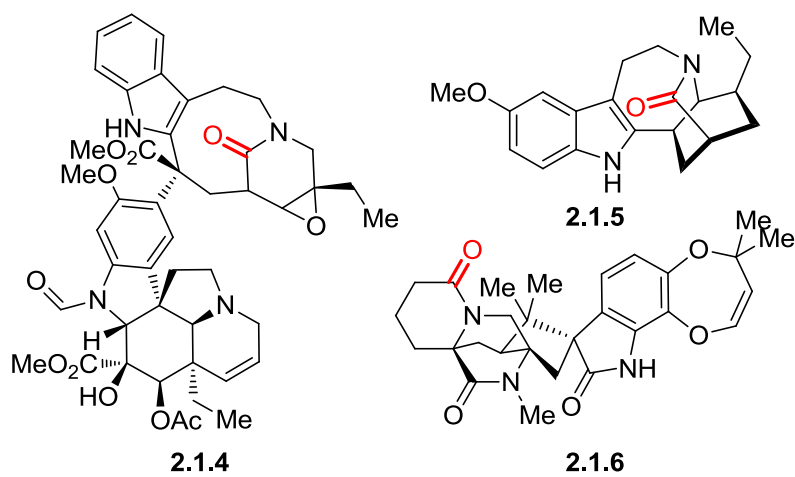
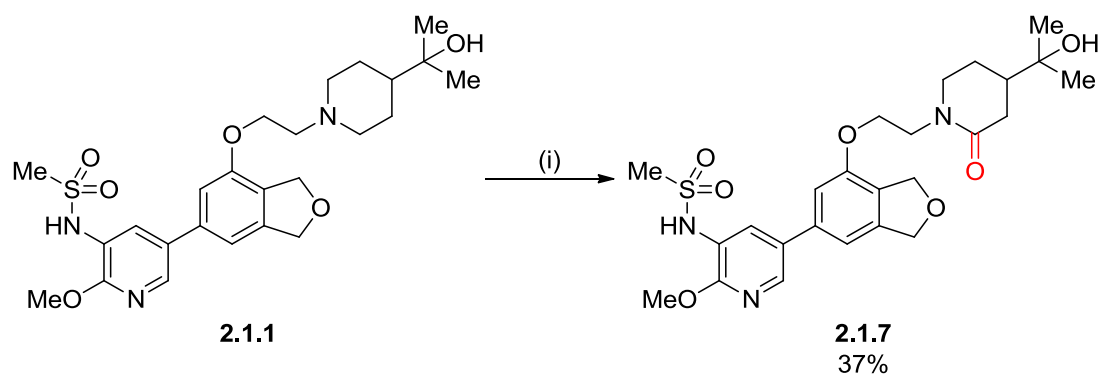


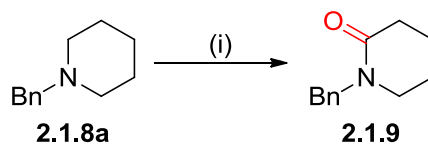
Figure 11. Lactam functionality installed *via* iodine-mediated C–H oxidation of piperidine ring systems within alkaloidal natural products.

Accordingly, oxidation of **2.1.1** with iodine and sodium bicarbonate²¹¹ afforded highly selective oxidation to lactam **2.1.7** (Scheme 47).



Scheme 47. C–H oxidation of **2.1.1** by molecular iodine under basic conditions. Conditions: (i) I_2 (2.5 eq.), NaHCO_3 (10.0 eq.), THF:H₂O (2.5:1, 10.0 mM), 16 h, RT.

The exquisite chemoselectivity of this reaction in the presence of other oxidatively susceptible positions prompted further study into the detail of this transformation. 1-Benzylpiperidine **2.1.8a** was selected as a model substrate in the optimisation of this reaction procedure (Table 4).



Entry	Eq. of I ₂	Solvent system	Concentration of 2.1.8a / M	Conversion ^[a] to 2.1.9 (%)
1	10	Toluene:H ₂ O (2.5:1)	0.025	No reaction (nr)
2	10	DCM:H ₂ O (2.5:1)	0.025	nr
3	10	MeOH:H ₂ O (2.5:1)	0.025	5
4	10	HFIP ^[b] :H ₂ O (2.5:1)	0.025	2
5	10	H ₂ O	0.025	6
6	10	MeCN:H ₂ O (2.5:1)	0.025	6
7	10	THF:H ₂ O (2.5:1)	0.025	91
8	10	DMSO:H ₂ O (2.5:1)	0.025	90
9	10	THF:H ₂ O (2.5:1)	0.1	59
10	10	THF:H ₂ O (2.5:1)	0.05	57
11	1.1	THF:H ₂ O (2.5:1)	0.025	15
12	2.5	THF:H ₂ O (2.5:1)	0.025	31
13	5.0	THF:H ₂ O (2.5:1)	0.025	68
14	7.5	THF:H₂O (2.5:1)	0.025	96^[c]
15	7.5 ^[d]	THF:H ₂ O (2.5:1)	0.025	62
16 ^[e]	7.5	THF:H ₂ O (2.5:1)	0.025	nr
17	7.5	THF	0.025	nr
18 ^[f]	7.5	THF:H ₂ O (2.5:1)	0.025	No change in reaction by LCMS

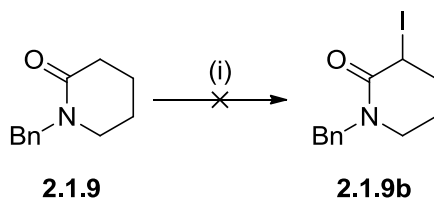
Table 4. Optimization of iodine-mediated C–H oxidation of 2.1.8a to lactam 2.1.9. Conditions: (i) **2.1.8a** (1.0 eq.), NaHCO₃ (10.0 eq.), I₂ (1.1 – 10.0 eq.) in solvent stirred at room temperature for 4 h. [a] Conversion determined by ¹H NMR analysis of crude material against an internal standard. [b] HFIP = 1,1,1,3,3,3-hexafluoroisopropanol. [c] Isolated yield. [d] NIS used as the iodine source instead of I₂. [e] No NaHCO₃ present. [f] Reaction carried out under a nitrogen atmosphere; conversion not measured.

It was also observed that the ratio of formation of **2.1.9b** relative to **2.1.9** was proportional to the concentration of **2.1.8a** (Table 5), although selectivity could not be switched to favour formation of **2.1.9b** using the conditions that were screened.

Concentration of 2.1.8a (M)	2.1.9:2.1.9b ^[a]
0.2	3:1
0.1	9:1
0.05	18:1
0.025	>20:1

Table 5. Effect of concentration of 2.1.8a on ratio of 2.1.9 to 2.1.9b. Conditions: I₂ (7.5 eq.), NaHCO₃ (10.0 eq.), THF:H₂O (2.5:1), 4 h, RT. [a] Ratios determined by ¹H NMR analysis of the crude material.

To clarify that **2.1.9b** was indeed formed during the course of the reaction, and not *via* iodination of the lactam product, **2.1.9** was re-submitted to the reaction conditions (Scheme 49). No reaction was observed, which suggests that **2.1.9b** is forming in a competitive side-reaction pathway; this shall be discussed in more detail later in this chapter as part of the mechanistic proposal for this reaction.



Scheme 49. Resubmission of 2.1.9 to the oxidation conditions to confirm that 2.1.9b does not form by iodination of 2.1.9. Conditions: (i) I₂ (7.5 eq.), NaHCO₃ (10.0 eq.), THF:H₂O (2.5:1, 0.05 M), 4 h, RT. Unreacted **2.1.9** was not isolated from the reaction mixture.

In summary, by studying the parameters of solvent, concentration, stoichiometry of iodine and iodine source, it was found that the stoichiometry of iodine and concentration of the substrate were critical factors for high yields of product. A dilute reaction concentration of 0.025 M and 7.5 equivalents of iodine were necessary for high and selective conversion to **2.1.9**, but the protocol is operationally simple, runs at room temperature for just a few hours, and does not require an inert atmosphere.

2.2 Substrate Scope of the Iodine-Mediated C–H Oxidation of Azacycles

With the optimised conditions in hand, the substrate scope for the C–H oxidation of amines **2.1.8a-n** was explored (Table 6).

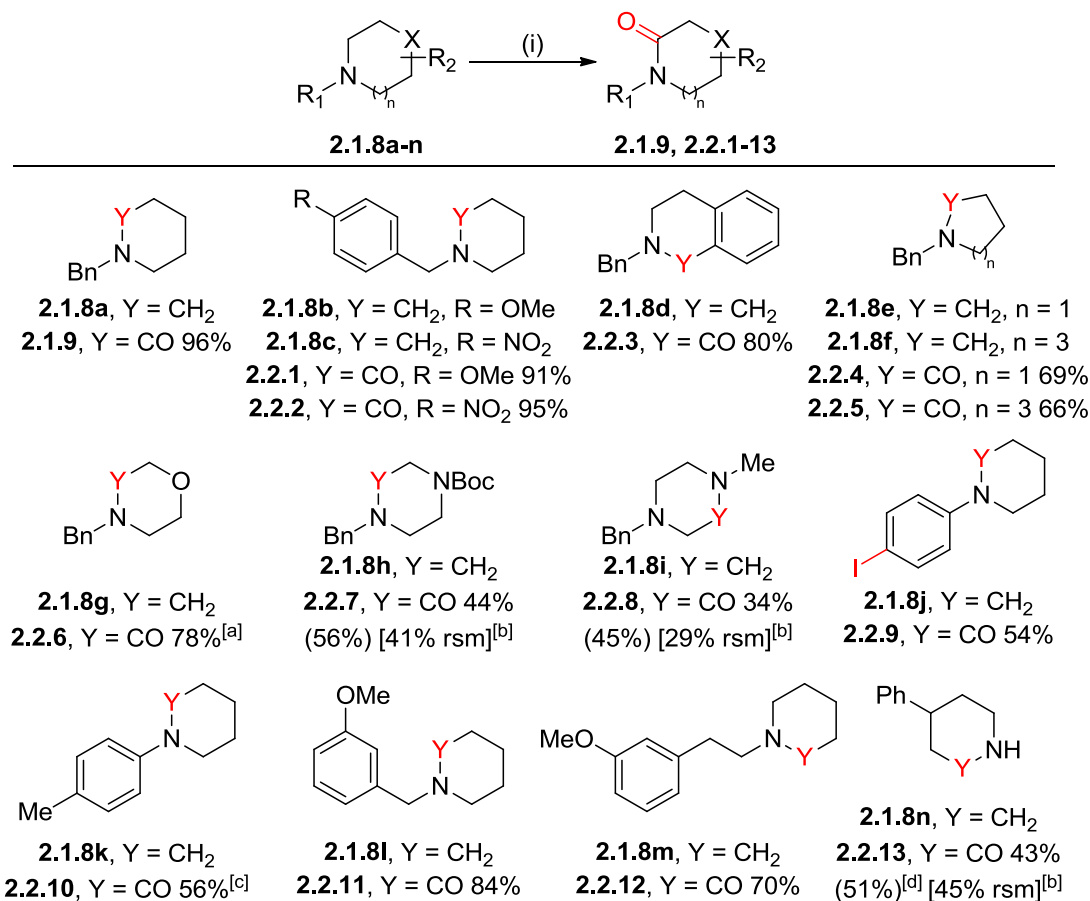


Table 6. Model substrate scope of chemoselective C–H oxidation of cyclic amines 2.1.8a-n. Conditions: (i) I₂ (7.5 eq.), NaHCO₃ (10.0 eq.), THF:H₂O (2.5:1, 0.025 M), RT, 4 h. Isolated yields shown; values in parentheses show conversion to product determined by ¹H NMR analysis of the crude material against an internal standard. Bn = benzyl. Boc = *tert*-butyloxycarbonyl. PMB = *para*-methoxybenzyl. [a] Reaction run in 2.5:1 DMSO/H₂O solvent system. [b] % rsm = percentage of remaining starting material observed by crude ¹H NMR. [c] I₂ was added in three portions of 2.5 eq. each hour. [d] Reaction stirred for 20 h.

Under these conditions, no exocyclic benzylic oxidation was observed despite both electron-releasing and electron-withdrawing substituents on the aromatic ring, affording lactams **2.2.1** and **2.2.2**, respectively, in 91% and 95% yield, respectively. The regioselectivity of endocyclic benzylic oxidation over the non-benzylic position

was observed in the formation of tetrahydroisoquinolinone product **2.2.3**. Oxidation also proceeded well for different ring sizes, with γ -lactam **2.2.4** and ϵ -lactam **2.2.5** prepared in 69% and 66% yields, respectively.

Other aliphatic azacyclic systems were tolerated, with morpholinone **2.2.6** prepared in 78% yield. Interestingly, stalling of the reaction at 42% conversion to **2.2.6** was observed by NMR in the formation of **2.2.6**, which was alleviated by changing the solvent from THF/water to DMSO/water. Unfortunately, the use of DMSO/water as the solvent did not improve yields for the oxidation of piperazine motifs, and hence THF/water was used as the reaction solvent. Lactam **2.2.7** was prepared in 44% yield, though complete selectivity was observed for oxidation of the methylene group adjacent to the more electron-rich nitrogen. When the *tert*-butyloxycarbonyl (Boc) group was replaced with a methyl group, regioselectivity was switched to the oxidation of the methylene unit in the β -position to the *N*-benzyl group, to afford **2.2.8** in 45% conversion. Switching to a DMSO/water solvent system had no change in the reactivity of **2.1.8h**, while for **2.1.8i** a mixture of singly and doubly oxidised products were observed, so the THF/water solvent system was preferred on the grounds of improved selectivity of oxidation. The reasons for these observed solvent effects are not well understood. The morpholine and piperazine substrates **2.1.8g-i** are more polar than the piperidine analogue **2.1.8a**, hence it is possible that they are able to adopt a more reactive conformation in DMSO, which has a higher dielectric constant than THF.^{222,223} This effect may not be as strong for **2.1.8h**, because the *tert*-butyl group on the Boc group increases lipophilicity, and will add steric bulk that may hinder the reaction.

For the anilinic substrate **2.1.8j**, concomitant *para*-iodination and lactamisation was observed in the formation of **2.2.9**, resulting from the high mesomeric donation of electron density into the aromatic ring. When the *para*-position was blocked with a methyl group in **2.1.8k**, some trace iodination was observed, though the by-product could be eliminated by modifying the reaction setup such that iodine was added portionwise, affording **2.2.10** in 56% yield. Controlled C–H oxidation in the presence

of electron-rich aromatics was possible however: lactams **2.2.11** and **2.2.12** prepared from **2.1.8l** and **2.1.8m**, respectively, in 84% and 70% yields, respectively. Slower conversion to secondary lactam **2.2.13** was seen, along with reaction stalling, which is possibly attributable to lower nucleophilicity of the secondary amine.

The effects of substituents on the azacyclic ring were also explored with substrates **2.1.8o-u** (Table 7).

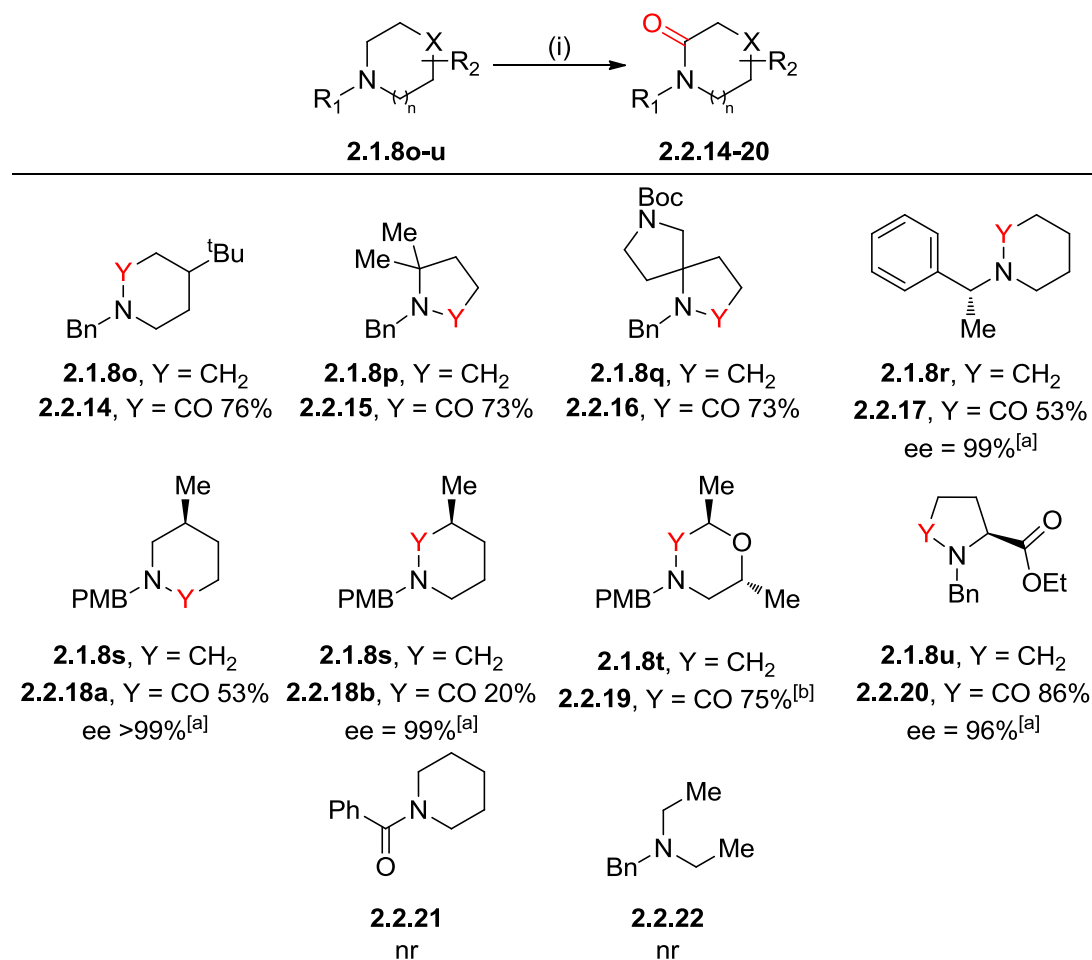


Table 7. Further substrate scope of chemoselective C–H oxidation of cyclic amines 2.1.8o-u, examining the effects of ring-substitution on the azacycle. Conditions: (i) I₂ (7.5 eq.), NaHCO₃ (10.0 eq.), THF:H₂O (2.5:1, 0.025 M), RT, 4 h. Isolated yields shown; values in parentheses show conversion to product determined by ¹H NMR analysis of the crude material against an internal standard. [a] ee determined by chiral HPLC analysis against the corresponding racemates **2.8.2**, **2.8.4a**, **2.8.4b** and **2.8.5**, respectively (see experimental section). [b] Reaction run in 2.5:1 DMSO/H₂O solvent system. Bn = benzyl. Boc = *tert*-butyloxycarbonyl. PMB = *para*-methoxybenzyl.

Oxidation of **2.1.8o** to **2.2.14** proceeded efficiently in the presence of a *tert*-butyl group in the γ -position, despite the ring-locking effect that this group may have imparted. Steric hindrance adjacent to the nitrogen atom was also tolerated well; lactam **2.2.15** isolated in 73% yield from **2.1.8p** despite the steric hindrance that the proximal geminal dimethyl group would impart. A by-product from the formation of **2.2.15** was iodolactam **2.2.15b** in 12% yield (Figure 12).

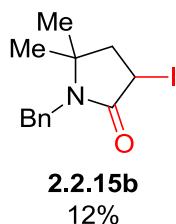


Figure 12. Iodolactam by-product generated during the formation of lactam **2.2.15**.

The ratio of **2.2.15** to **2.2.15b** (*ca.* 7:1) was lower than the ratio of **2.1.9** to **2.1.9b** (>20:1, Table 5, entry 5), possibly because the geminal dimethyl group of **2.1.8p** imparted a Thorpe-Ingold effect on the substrate.^{224–227} Steric repulsion could increase the angle between the two methyl groups compared to hydrogen atoms in a methylene unit. This would have the effect of decreasing the bond angle on the quaternary carbon of the intermediary iminium species **2.2.15c** (Figure 12).

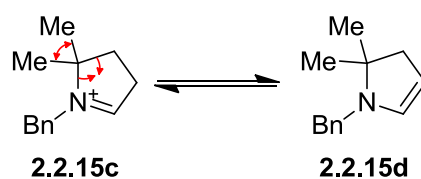


Figure 13. The geminal dimethyl group possibly creates a Thorpe-Ingold effect, slightly destabilising the iminium intermediate to increase the propensity for tautomerism to enamine **2.2.15d**.

This would then increase the steric strain in the iminium ring slightly since the double bond is adjacent to the contracted bond angle, and this could slightly increase the propensity for tautomerism to enamine **2.2.15d**, which can then be iodinated and oxidised to afford **2.2.15b**.

Iodination was not observed in the formation of spirocyclic lactam **2.2.16**, which was prepared in 73% yield. This suggests that the Boc-pyrrolidine ring system invokes less of a Thorpe-Ingold effect due to imparting less ring-strain on the ring being oxidised. Spirocyclic scaffolds are finding increasing importance in drug discovery as bioisosteres, for introducing conformational restriction and for accessing novel vectors for molecular growth.²²⁸ Therefore, the ability to selectively functionalise one side of spirocyclic fragment from commercially available reagents has high value for medicinal chemistry, and the expedient expansion of compound libraries.

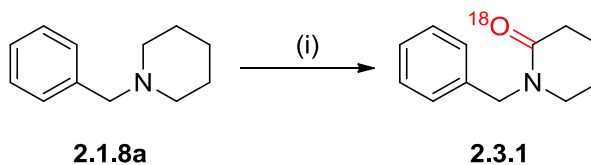
The high endocyclic selectivity for oxidation is reflected by the retention of the exocyclic benzylic stereogenic centre in **2.2.17**. Additionally, the β -stereocentres in **2.2.18a**, **2.2.18b** and morpholinone **2.2.19** were retained, illustrating how this methodology can be applied to more complex, chiral drug-like substrates. Compounds **2.2.18a** and **2.2.18b** were formed from **2.1.8s** in a ratio of almost 3:1, suggesting that where there is a regioselectivity issue oxidation will occur preferentially at the less sterically-hindered position. The retention of the β -stereochemical information indicates that the reaction mechanism is perhaps more complex; if the lactam arises *via* water addition into an iminium ion generated by oxidation, then this iminium ion does not tautomerise to an enamine easily, otherwise racemisation would be observed. Further mechanistic investigations shall be discussed in a later section. Finally, the proline-derivative **2.1.8u** was oxidised selectively to lactam **2.2.20**, and this also occurred with retention of the α -stereocentre. This is consistent with the observation that regioselectivity of oxidation is directed by steric hindrance, with oxidation occurring at the less sterically hindered position adjacent to the nitrogen, rather than at the site with the more acidic proton.

Benzoyl-protected piperidine **2.2.21** showed no reactivity under these reaction conditions. The nitrogen atom of **2.2.21** is less nucleophilic than the azacyclic nitrogen atoms in previous examples due to conjugation of the *N*-lone pair into the amide carbonyl. This highlights the importance of the nucleophilicity of the nitrogen atom

for oxidation to occur, and accounts for why oxidation of the lactam products to the corresponding imide is not observed. This is in contrast to some other ruthenium and copper-mediated procedures where over-oxidation can be observed.^{229–232} Acyclic substrate **2.2.22** also showed no reactivity towards oxidation to the corresponding amide, which indicates that a rigid ring system is required for oxidation to occur. While this limits the substrate scope, it can also be seen as advantageous chemoselectivity of cyclic amines over acyclic amines, which is of high importance if this methodology is to be used in a late-stage application. Before discussing the application of the iodine-mediated C–H oxidation as a tool for late-stage oxidation, it was felt that the further investigation into the possible mechanism of this process would be beneficial. This would then allow for better understanding and a more logical selection of drug substrates to test the applicability to late-stage functionalisation.

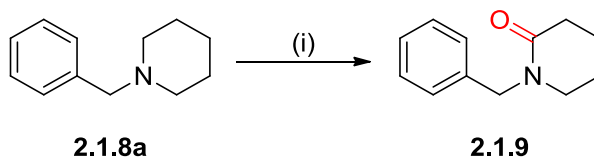
2.3 Mechanistic Investigations of Lactam Formation

Isotopic labelling studies were carried out by exchanging water in the solvent for ¹⁸O-labelled water. This afforded lactam **2.3.1**, which showed full incorporation of the ¹⁸O-label.



Scheme 50. ¹⁸O-incorporation into the lactam product **2.3.1** when ¹⁸O-labelled water was used in the solvent. Conditions (i) I₂ (7.5 eq.), NaHCO₃ (10.0 eq.), THF:H₂¹⁸O (2.5:1, 0.025 M), RT, 4 h, >99%.

However, exchange of oxygen atoms between the base and water may occur, so this did not rule out the base as the source of oxygen atom in the lactam product. Since ¹⁸O-labelled sodium bicarbonate could not be sourced commercially, the use of alternative bases that could be labelled (such as sodium acetate), or would remove the presence of oxygen completely (such as triethylamine) was investigated.



Entry	Base	Conversion ^[a] to 2.1.9 (%)
1	NaOAc	57
2	Et ₃ N	0
3	DBU ^[b]	0

Table 8. Alternative bases screened for the oxidation to 2.1.9. Conditions: (i) I₂ (7.5 eq.), Base (10.0 eq.), THF:H₂O (2.5:1, 0.025 M), RT, 4 h. [a] Conversion determined by ¹H NMR analysis of crude material against an internal standard. [b] DBU = 1,8-diazabicyclo[5.4.0]undec-7-ene.

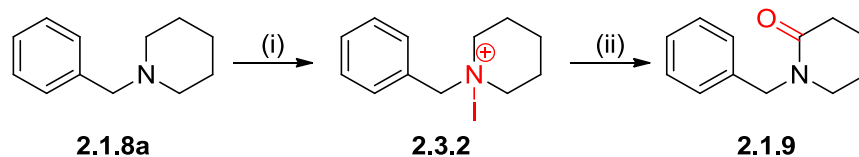
Amine bases triethylamine and 1,8-diazabicyclo[5.4.0]undec-7-ene (DBU) were ineffective replacements for sodium bicarbonate, with no reaction observed. Sodium acetate was a competent surrogate, however, with desired lactam **2.1.9** generated in 57% conversion. This was useful for the isotopic labelling investigations as ¹⁸O-labelled sodium acetate is commercially available, and as such more detailed labelling studies could be carried out (Table 9).

Entry	Base/Solvent Partner	[M+H] ⁺ of Lactam Peak ^[a]
1	NaOAc/H ₂ O	190.1 (100%): 2.1.9
2	Na ¹⁸ OAc/H ₂ O	190.1 (100%): 2.1.9
3	Na ¹⁸ OAc/H ₂ ¹⁸ O	192.1 (100%): 2.3.1 (¹⁸ O incorporation)

Table 9. ¹⁸O-incorporation studies using labelled and unlabelled variants of sodium acetate and water. [a] [M+H]⁺ peak from mass spectrometry (MS) spectrum of the peak attributed to the lactam product at 0.86 minutes in the high pH liquid chromatography (LC) of the reaction mixture.

These data indicate that the oxygen atom incorporated into the lactam product derives from the water in the solvent mixture, and not from the base, at least in the case of sodium acetate. Furthermore, during optimisation studies, running the reaction under an atmosphere of nitrogen showed no change in the reaction profile, hence it is unlikely that oxygen is derived from the atmosphere.

Studies of reactive intermediates were also carried out, by analysis of the progress of the reaction by ^1H NMR (Table 10).



Entry	Eq. NaHCO_3	Time/min	2.1.8a:2.3.2:2.1.9 ^[a]
1	0.0	0	0:1:0
2	1.0	30	0:1:0
3	2.0	60	0:1.53:1
4	3.0	90	0:0.56:1
5	5.0	120	0:0:1
6	8.0	240	0:0:1
7	10.0	360	0:0:1

Table 10. NMR studies into mechanism of oxidation *via* monitoring reaction progress by NMR. Conditions: (i) I_2 (7.5 eq.), d^8 -THF (0.2 M), RT, 1.5 h; (ii) NaHCO_3 (x eq.), d^8 -THF: D_2O (0.025 M), RT. [a] Ratios based on ^1H NMR analysis of aliquots of the reaction mixture, and comparison of integrals of the benzylic CH_2 chemical shifts.

Pre-mixing **2.1.8a** with iodine in deuterated THF showed consumption of **2.1.8a** and conversion to an intermediate, proposed to be *N*-iodoammonium intermediate **2.3.2** by ^1H NMR. Addition of deuterated water and sequential addition of sodium bicarbonate resulted in full conversion of **2.3.2** to lactam **2.1.9**. A change in chemical shift of the benzylic 2H signal of **2.1.8a** from 3.48 ppm to 4.31 ppm is observed on mixing **2.1.8a** with molecular iodine (Figure 14). This significant difference in chemical shift is typical of that observed between a tertiary amine and a quaternary ammonium salt due to greater deshielding,^{233,234} hence the structure of **2.3.2** was proposed to be an *N*-iodoammonium intermediate. Subsequently, consumption of this intermediate and formation of **2.1.9** was observed on sequential addition of sodium bicarbonate and deuterated water.

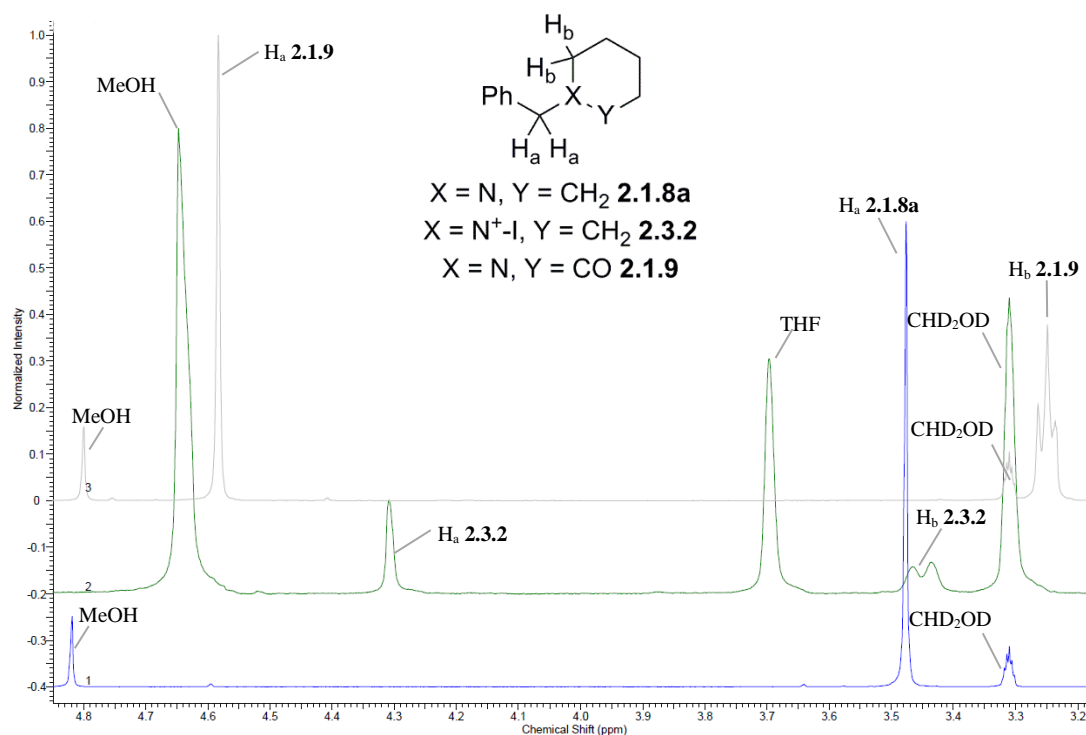
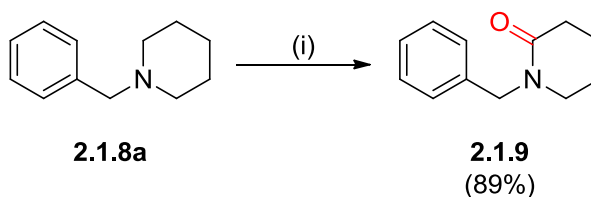


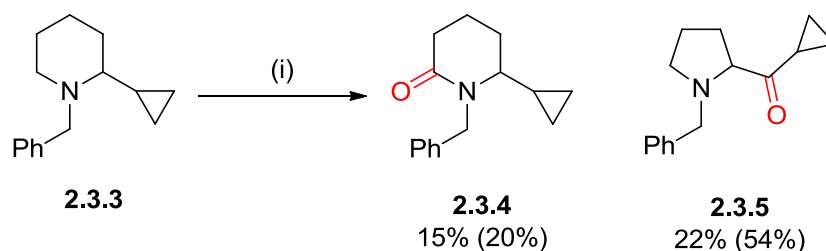
Figure 14. Overlays of ^1H NMR spectra of **2.1.8a** (blue), **2.3.2** (green) and **2.1.9** (grey) to show the conversion of **2.1.8a** into **2.1.9**, via **2.3.2**.

Petride *et al.* have reported the dimerization and oxidative cleavage of *N*-benzyl aziridine to piperazines via an electron transfer and hydrogen atom transfer (HAT) mechanism using electrochemical oxidation conditions.²³⁵ Subsequently, they observed the formation of the same piperazine products while investigating the use of molecular iodine to carry out *N*-dealkylation.²³⁶ This raised the possibility of a radical-based mechanism for the iodine-mediated C–H oxidation conditions that had been developed. This was probed by the addition of TEMPO to the reaction mixture during the conversion of **2.1.8a** to **2.1.9** using the optimised oxidation conditions (Scheme 51). No significant inhibition of the formation of **2.1.9** was observed, so the reaction is more likely to be proceeding through an ionic pathway rather than a HAT or radical mechanism.



Scheme 51. TEMPO does not inhibit the oxidation of 2.1.8a to 2.1.9. Conditions (i) I₂ (7.5 eq.), NaHCO₃ (10.0 eq.), TEMPO (1.0 eq.), THF:H₂O (2.5:1, 0.025 M), RT, 4 h. Value in parentheses shows conversion to product determined by ¹H NMR analysis of the crude material against an internal standard.

A radical-clock test was carried out to confirm this result. Radical-clock reactions involve competition between a unimolecular radical process with a known rate constant (the clock) and a bimolecular reaction with a trapping agent, giving a mixture of rearranged and unrearranged products.^{237,238} For example, a radical formed next to a cyclopropyl ring would be anticipated to exhibit ring-opening of the cyclopropane, with a rate constant of $1.3 \times 10^8 \text{ s}^{-1}$ at 25°C.²³⁹ As such, cyclopropyl-substituted substrate **2.3.3** was subjected to the oxidation conditions (Scheme 52).

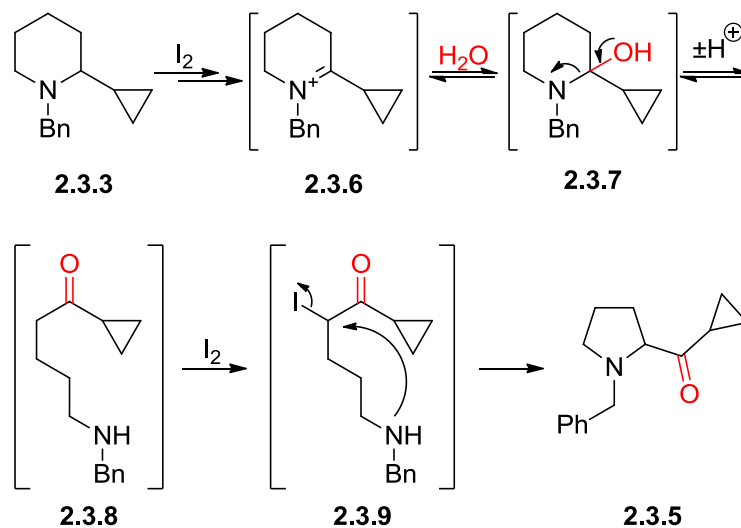


Scheme 52. Radical-clock investigation using 2.3.3. Conditions: (i) I₂ (7.5 eq.), NaHCO₃ (10.0 eq.), THF:H₂O (2.5:1, 0.025 M), RT, 1 h. Isolated yields shown; values in parentheses show conversion to product determined by ¹H NMR analysis of the crude material against an internal standard.

Lactam **2.3.4** and ketone **2.3.5** were formed in the reaction, with no evidence of ring opening observed. This observation, in conjunction with the result of the TEMPO experiment (Scheme 51), supported the likelihood of an ionic mechanism rather than a radical mechanism for the oxidation.

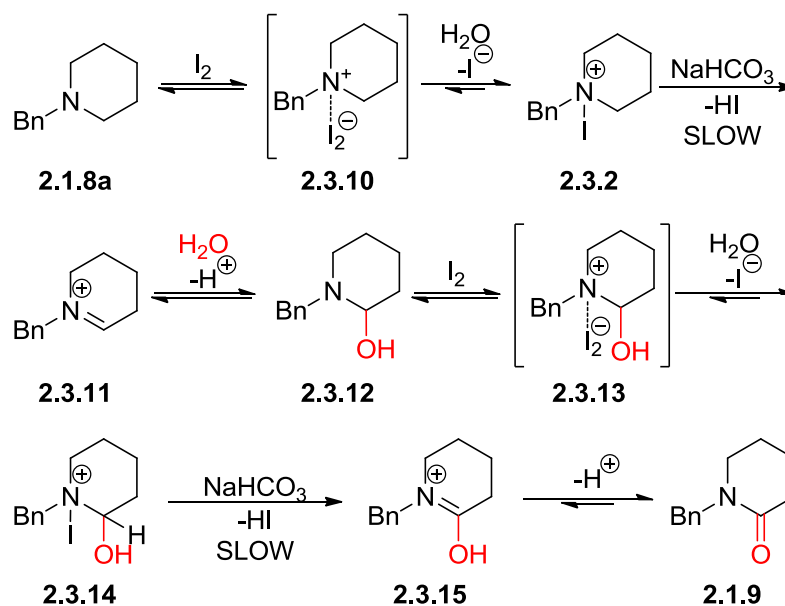
A possible mechanism for the formation of **2.3.5** involved initial iodine-mediated oxidation to iminium **2.3.6** adjacent the cyclopropyl group (Scheme 53). Nucleophilic attack of the iminium ion by water affords intermediate **2.3.7**, which can then lead to

ring-opening to form ketone **2.3.8**. Iodination of the enolisable position leads to α -iodoketone **2.3.9**, which can then undergo an intramolecular substitution from the amine to afford **2.3.5**.



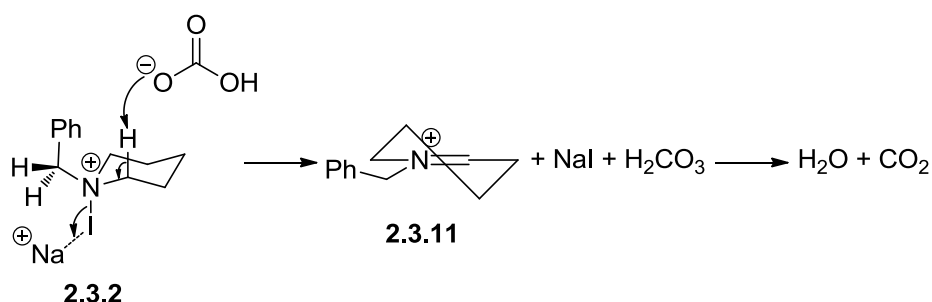
Scheme 53. Proposed mechanism for the formation of rearrangement product 2.3.5.

Nagakura *et al.* have described the formation of charge transfer complexes between aliphatic amines, such as triethylamine, and molecular iodine, which degrade to iodoammonium species in presence of moisture.²¹⁶⁻²¹⁸ As such, it was proposed that **2.1.8a** and iodine interact to form the charge-transfer complex **2.3.10** (Scheme 54), which quickly degrades to **2.3.2** due to the aqueous solvent.



Scheme 54. Proposed reaction mechanism of the iodine-mediated C–H oxidation of cyclic amines to lactams.

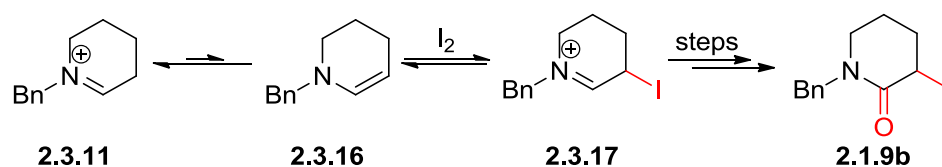
Sodium bicarbonate is a weak base, so full deprotonation of the methylene group adjacent to the nitrogen of **2.3.2** is unlikely. This is corroborated by the fact that no exocyclic oxidation is observed, nor is racemisation of the α -stereocentre in **2.1.8u**, despite the fact that these positions are both more acidic than the observed oxidised positions. The fact that oxidation occurs selectively at the endocyclic position indicates that pK_a is not the sole driver and, therefore, it is proposed that chemoselectivity for endocyclic oxidation comes from a fixed chair conformation of **2.3.2** (Scheme 55).



Scheme 55. Fixed chair conformation and entropic gain driving endocyclic deprotonation.

The exocyclic methylene unit can freely rotate, and therefore an antiperiplanar arrangement of the benzylic hydrogens and the N–I bond is only transient. There will be a larger distribution of conformational states whereby the benzyl group will adopt a *trans* configuration relative to the large iodine atom as a result of steric repulsion. This means that the benzylic hydrogens are more likely to adopt a dihedral angle of about 60° in relation to the iodine atom, and thus would not be in the correct conformation for elimination of the iodide. In contrast, the endocyclic α -C–H bond and N–I bond are forced into an antiperiplanar arrangement by the chair conformation of the ring, which is preorganised for deprotonation and elimination to occur. This is assisted by coordination of the sodium cation as a Lewis acid to the iodide leaving group, which may explain why no reactivity was observed with non-ionic bases. Owing to the low basicity of sodium bicarbonate, deprotonation is slow, hence why a large excess of the base is required for oxidation to reach completion. There is also the possibility of an enthalpic driving force through formation of strongly bonded sodium iodide salt, and an entropic gain by formation of carbonic acid, which is unstable and rapidly decomposes to water and carbon dioxide.^{240,241}

The resultant iminium ion **2.3.11** (Scheme 54) is susceptible to nucleophilic attack by water to form hydroxy-amine **2.3.12**, which can subsequently form a second charge-transfer species **2.3.13** with iodine. Degradation occurs to *N*-iodoammonium intermediate **2.3.14**, which can then be deprotonated to hydroxyiminium species **2.3.15**, and this can then tautomerise to the lactam product **2.1.9**. Alternatively, **2.3.11** could tautomerise to the enamine form **2.3.16** (Scheme 56), which would then be susceptible to iodination β to the nitrogen to form **2.3.17**, ultimately leading to formation of iodolactam **2.1.9b**.



Scheme 56. Tautomerism of iminium 2.3.11 to enamine 2.3.16, leading to formation of iodolactam by-product 2.1.9b.

With the model substrate scope of the reaction established, and a more thorough understanding of the mechanism of the oxidation methodology, the utility of this protocol as a tool for late-stage oxidation was tested.

2.4 Late-Stage C–H Oxidation of Bioactive Small Molecules

The tolerance of a series of high value bioactive small molecules **2.4.1a-g** from the pharmaceutical and agrochemical industries to iodine-mediate C–H oxidation of azacycles was investigated (Table 11).

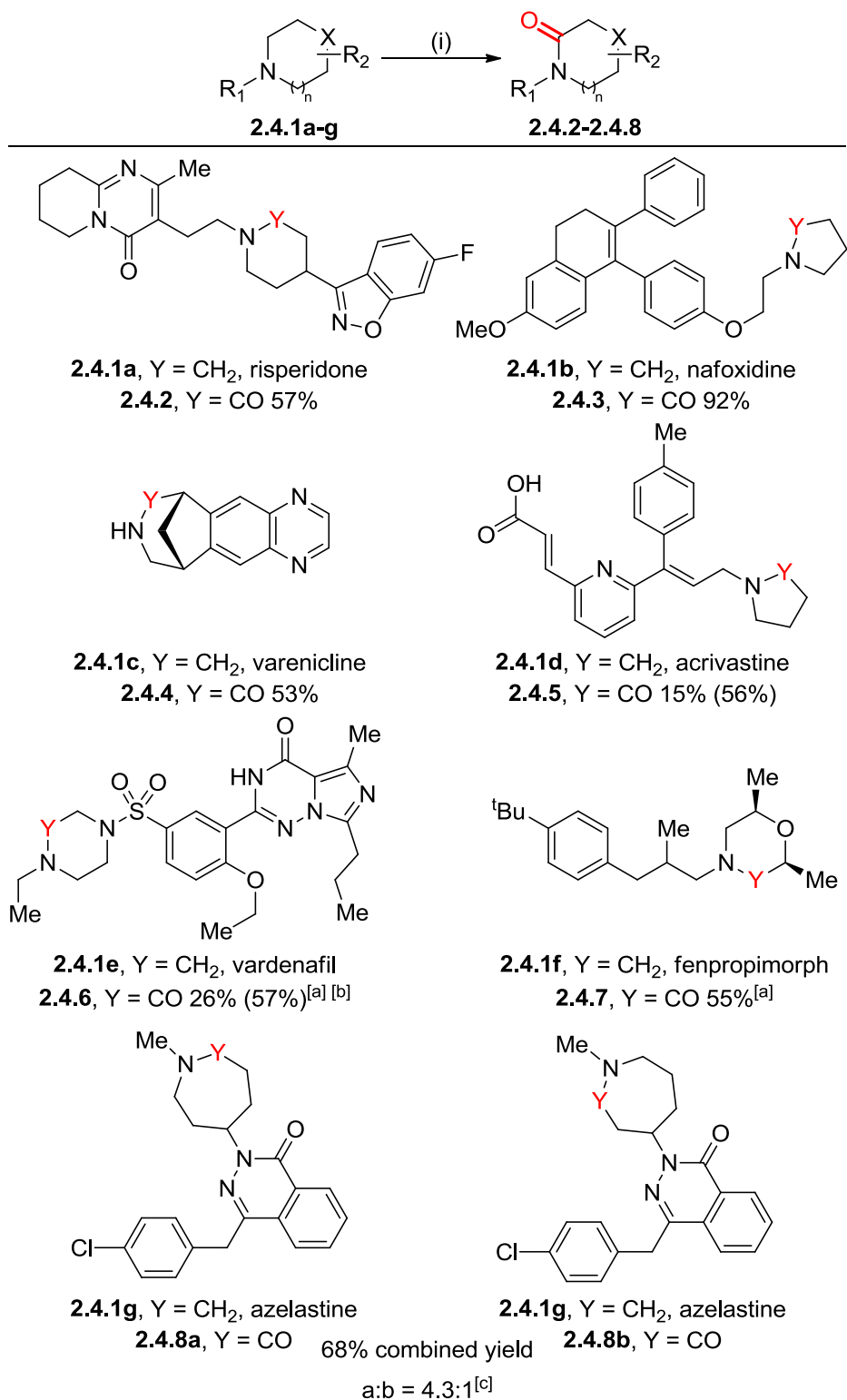


Table 11. Substrate scope of late-stage C–H oxidation of industrially relevant scaffolds 2.4.1a-g. Conditions: (i) I₂ (7.5 eq.), NaHCO₃ (10.0 eq.), THF:H₂O (2.5:1, 0.025 M), RT, 4 h. Isolated yields shown; values in parentheses show conversion to product determined by ¹H NMR analysis of the crude material against an internal standard. [a] Reaction run in 2.5:1 DMSO/H₂O solvent system. [b] LCMS analysis of reaction mixture showed a *ca.* 3:1 ratio of **2.4.6** to unreacted **2.4.1e**. [c] Ratio of products determined by ¹H NMR analysis prior to separation.

Lactams **2.4.2** – **2.4.4** were prepared from **2.4.1a-c** in 53-92% yields. Azacycles **2.4.1d** and **2.4.1e** were converted to lactams **2.4.5** and **2.4.6**, respectively, in yields of 15% and 26%, despite conversion to product by ¹H NMR being 56% and 57%, respectively. The low isolated yield of **2.4.5** and **2.4.6** was attributed partly to the challenging purification, which required the use of reverse phase HPLC. These examples demonstrate that chemoselective C–H oxidation can be achieved using this oxidation protocol in the presence of alkenes, electron-rich aromatic rings, aromatic heterocycles, allylic positions, carboxylic acids and sulfonamides. Morpholinone **2.4.7** was prepared from **2.4.1f** as an inseparable mixture of two diastereomers, with full retention of the *cis*-orientation of the ring methyl groups, highlighting the applicability to late-stage chiral intermediates. Oxidation of the asymmetrical azepane ring in azelastine, **2.4.1g**, resulted in regioselective formation of the lactam on the less-hindered side of the ring, with lactams **2.4.8a** and **2.4.8b** formed in 68% combined yields, and in a ratio of over 4:1 by ¹H NMR analysis. Computational modelling of the lowest energy conformation of the proposed iminium intermediates in the formation of lactams **2.4.8a** and **2.4.8b** led to a rationale for the observed regioselectivity. For iminium **2.4.9a** (Figure 15), the 4-chlorophenyl group is orientated perpendicular to the heteroaromatic core. This results in the iminium moiety (iminium carbon highlighted in pink) being readily accessible for nucleophilic attack by water. In contrast, for iminium **2.4.9b** the 4-chlorophenyl group is positioned underneath the iminium (Figure 16). This potentially has the effect of slowing down the rate of water addition for this regioisomer as one side of the iminium is blocked from nucleophilic attack. This reduced rate of water addition could account for the regioselectivity observed.

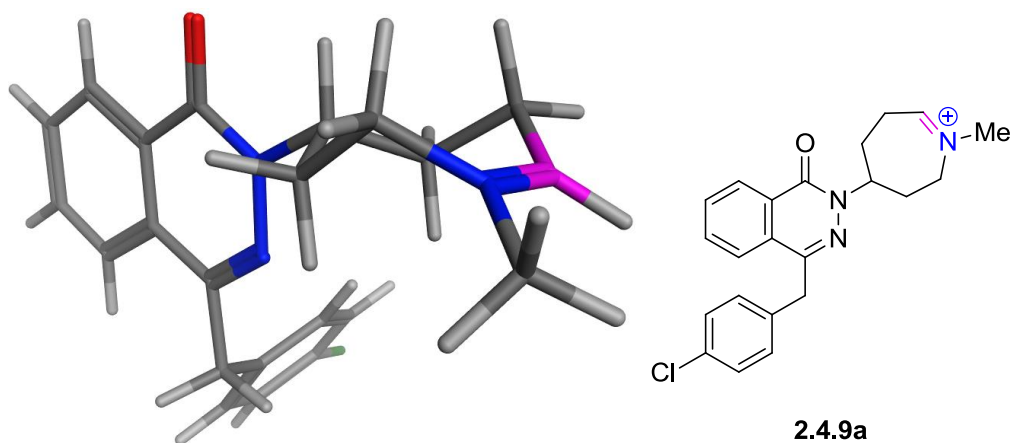


Figure 15. Lowest energy conformation of iminium intermediate **2.4.9a**.²⁴²

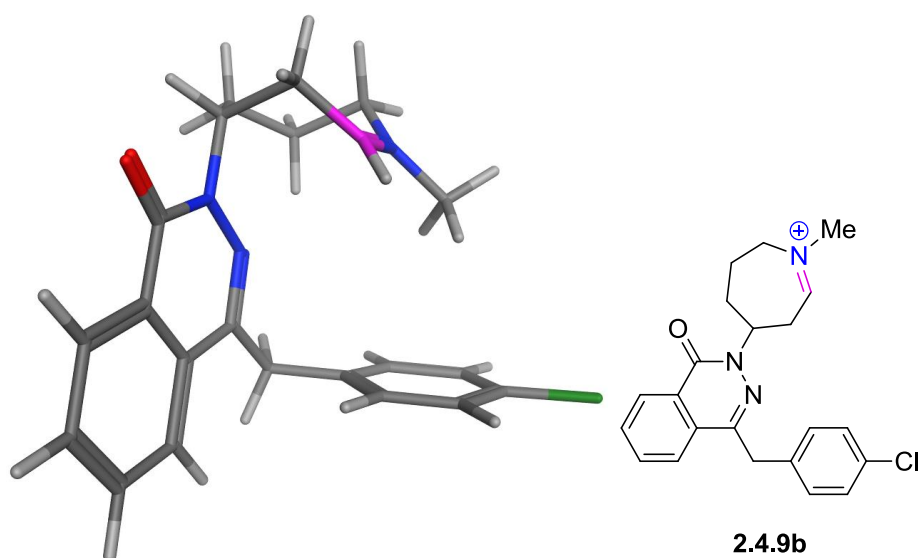
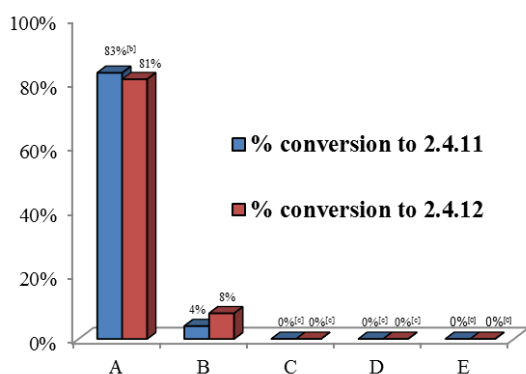
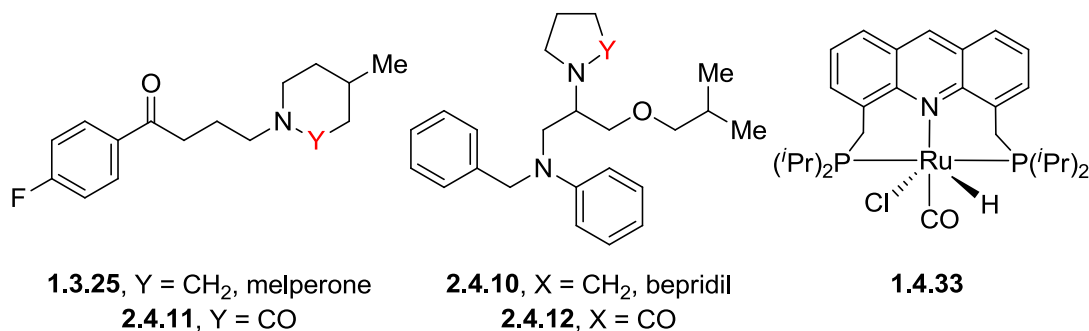


Figure 16. Lowest energy conformation of iminium intermediate **2.4.9b**.²⁴²

In general, chemoselective oxidation was achieved with late-stage substrates **2.4.1a-g**, and full consumption of these substrates was observed. Unreacted starting material was only seen in the formation of piperazinone **2.4.6** and the morpholinone **2.4.7**, which is consistent with the observations in the model substrate scope. Additionally, where low conversion to the desired lactam product occurred, formation of oxidative by-products was observed by mass spectrometry in small amounts, though none of these species were isolable. These results demonstrate the general chemoselectivity

of this operationally straightforward methodology for the oxidation of cyclic amines within complex small molecules.

The direct C–H oxidation of amines to amides is not a novel transformation, and several reported methods have already been discussed earlier.^{191,197–199,201} However, the reported examples have, in general, shown limited substrate scope, particularly in terms of application to drug-like molecules. As such, a direct comparison of the developed iodine-mediated methodology with literature precedent for the oxidation of amines was carried out, with a focus on the competency to oxidise marketed drug compounds melperone, **1.3.25**, and bepridil, **2.4.10** (Figure 17).

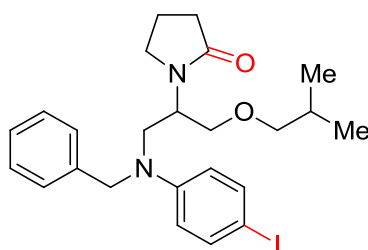


Entry	Conditions ^[a]
A	I ₂ /NaHCO ₃
B	1.4.33 /NaOH ¹⁹⁷
C	FeCl ₃ ·6H ₂ O (5 mol%), 2-picolinic acid (5 mol%), PhCO ₃ <i>tert</i> -Bu (3.0 eq.), H ₂ O, 50 °C, 24 h
D	RuO ₂ /NaIO ₄ ¹⁹³
E	PhI(OAc) ₂ ²⁴³

Figure 17. Comparative analysis of late-stage C–H oxidation of amines conditions using drug compounds **1.3.25 and **2.4.10** as exemplars.** [a] General conditions: A: I₂ (7.5 eq.), NaHCO₃ (10.0 eq.), RT, 4 h; B: **1.4.33** (1 mol%), NaOH, 150 °C, 48 h; C: FeCl₃·6H₂O (5 mol%), 2-picolinic acid (5 mol%), PhCO₃*tert*-Bu (3.0 eq.), H₂O, 50 °C, 24 h; D: RuO₂ (10 mol%), NaIO₄ (6.3 eq.), RT, 64 h; E: PhI(OAc)₂ (2.2 eq.), H₂O, RT, 16 h. Values shown describe conversion to product determined by ¹H NMR analysis of the crude material against an internal standard. For more detailed reaction conditions, see the experimental section, page 153. [b] Isolated yield. [c] Complex mixture of oxidative by-products.

The developed iodine-mediated oxidative method offered substantially higher yielding chemoselective oxidation to lactams **2.4.11** and **2.4.12** than the literature precedent tested. Melperone **1.3.25** was oxidised to the corresponding lactam **2.4.11** in 83% yield, while lactam **2.4.12** was formed in 81% conversion from **2.4.10**. In contrast, the conditions reported by Milstein *et al.*¹⁹⁷ that used ruthenium catalyst **1.4.33** at high reaction temperature (entry B) afforded a reaction profile with few observable by-products by ¹H NMR for either substrate, but the oxidation was very slow, with only 4% and 8% conversion to **2.4.11** and **2.4.12**, respectively, after 48 hours at 150 °C. This rate of reaction is far too slow for this procedure to be a viable tool for use in medicinal chemistry laboratories, as it will not serve to speed up the iterative SAR process. Reaction conditions C-E all showed no trace of the desired lactams, with only complex mixtures of oxidative by-products observed. This was expected given the highly oxidising nature of the reagents that were used in these reaction conditions, and the potential oxidative susceptibility of these drugs.

While the conversion to **2.4.12** was 81% by ¹H NMR, this product could only be recovered in 30% isolated yield. The disparity between isolated yield and conversion was because a second HPLC purification of **2.4.12** was required to separate it from iodinated by-product **2.4.12b** (Figure 18), which co-eluted during chromatography.



2.4.12b
5% (17%)

Figure 18. Iodinated aniline generated as a by-product during oxidation of **2.4.10** to **2.4.12**. Isolated yield shown, value in parentheses shows conversion to product determined by ¹H NMR analysis of the crude material against an internal standard.

This minor by-product was formed in 17% conversion during the course of the reaction. While this was not ideal, it was a minor impurity, and offers an additional vector to functionalise, which could be useful for early-phase medicinal chemistry. Additionally, complete chemoselectivity for oxidation of the cyclic amine over the acyclic amine was observed, demonstrating the utility that this protocol offers by selectively oxidised cyclic amines over acyclic amines.

The applicability of this iodine-mediated C–H oxidation methodology as a synthetic tool for late-stage oxidation has been validated. Accordingly, an assessment of the direct implication of this methodology on medicinal chemistry properties of drug-like molecules was investigated.

2.5 Application for Drug Discovery

The underlying principle underpinning late-stage functionalisation chemistry is to be able to derivatize compounds that are medically important, and examine the effects that these changes have on the biological properties of the molecule.^{7,131} As such, the influence that this methodology could have on medicinal chemistry projects was studied by analysis of some properties of oxidative products. One application that was explored was the late-stage oxidation of compounds that block the human ether-a-go-go related gene (hERG) potassium ion channel. Blocking of the hERG channel has been linked to QT prolongation, leading to arrhythmias, and can therefore make a compound toxic to the cardiovascular system, depending on the required dose and therapeutic window.^{244–246} Lipophilic basic amines are typically toxicophores for hERG,²⁴⁷ and so the possibility of using this methodology to carry out late-stage reduction in hERG activity was investigated. Risperidone, **2.4.1a** (Table 12), is an antagonist of serotonin (5-HT_{2A}) and dopamine (D₂) receptors, and is a marketed treatment for schizophrenia.²⁴⁸ It is also known to inhibit the hERG ion channel,²⁴⁹ with a *p*IC₅₀ value in the hERG antagonist Barracuda assay of 5.9 (Table 12). This is reflected by the calculated *p*K_{aH} of 8.8²⁵⁰ and a calculated partition coefficient (*clogP*)²⁵¹ of 2.7 imparted by the flanking lipophilic aryl groups.

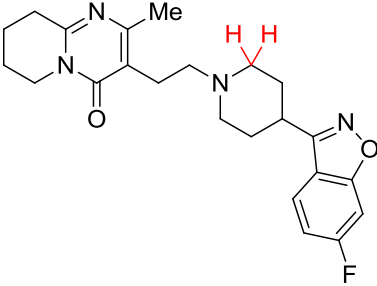
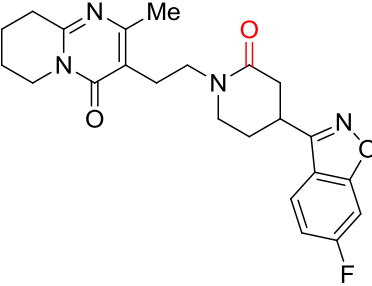
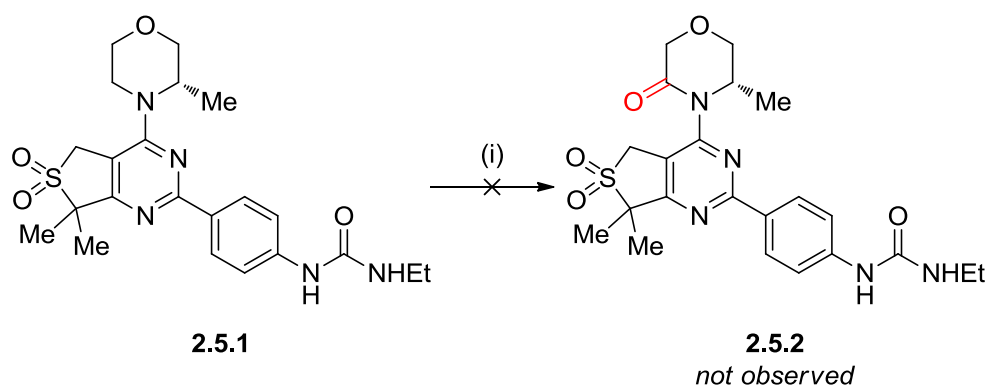
Compound		
	2.4.1a	2.4.2
hERG pIC_{50} (n)	5.9 (5)	4.7 (3)
$clogP^{251}$	2.7	1.6
PSA²⁵² (Å)	64.2	81.2
5-HT_{2A} pIC_{50} (n)	>8.5 (131)	4.7 (4)
D₂ pIC_{50} (n)	8.1 (95)	<4.0 (1)

Table 12. Changing medicinal chemistry properties via oxidation of 2.4.1a to lactam 2.4.2. n = number of times the assay was run for that compound. $clogP$ = logarithm (base 10) of the calculated partition coefficient between *n*-octanol and water. PSA = polar surface area. 5-HT_{2A} = serotonin_{2A}. D₂ = dopamine₂.

Oxidation of the basic piperidine core of **2.4.1a** to lactam **2.4.2** had the desired effect of significantly lowering the affinity for hERG, with a pIC_{50} 4.7 measured for **2.4.2**, as opposed to the much higher pIC_{50} of 5.9 for **2.4.1a**. Additionally, a drop in $clogP$ from 2.7 to 1.6, and an increase in the polar surface area (PSA) from 64.2 to 81.2 was observed, owing to the addition of a polar, electronegative oxygen atom. A loss of affinity for both 5-HT_{2A} and D₂ inhibition was observed, with decreases from greater than 8.5 to 4.7 for 5-HT_{2A} and from 8.1 to less than 4.0 for D₂ from **2.4.1a** to **2.4.2**, respectively. This is perhaps unsurprising, because the basicity of the piperidine in **2.4.1a** is important for binding to both receptors, with basic amines the natural ligands in both cases. The basicity is subsequently lost on oxidation to **2.4.2**, which led to the reduced ability of **2.4.2** to inhibit either receptor. Despite this negative result, the negation of hERG activity demonstrated that late-stage C–H oxidation could be used to rapidly decrease off-target toxicological effects, thereby potentially reducing rates of attrition in drug discovery. Evidently, this modification should be considered if basicity is not a major factor in interactions between the substrate and the biological target. In this way, promising compounds that exhibit higher than desired levels of

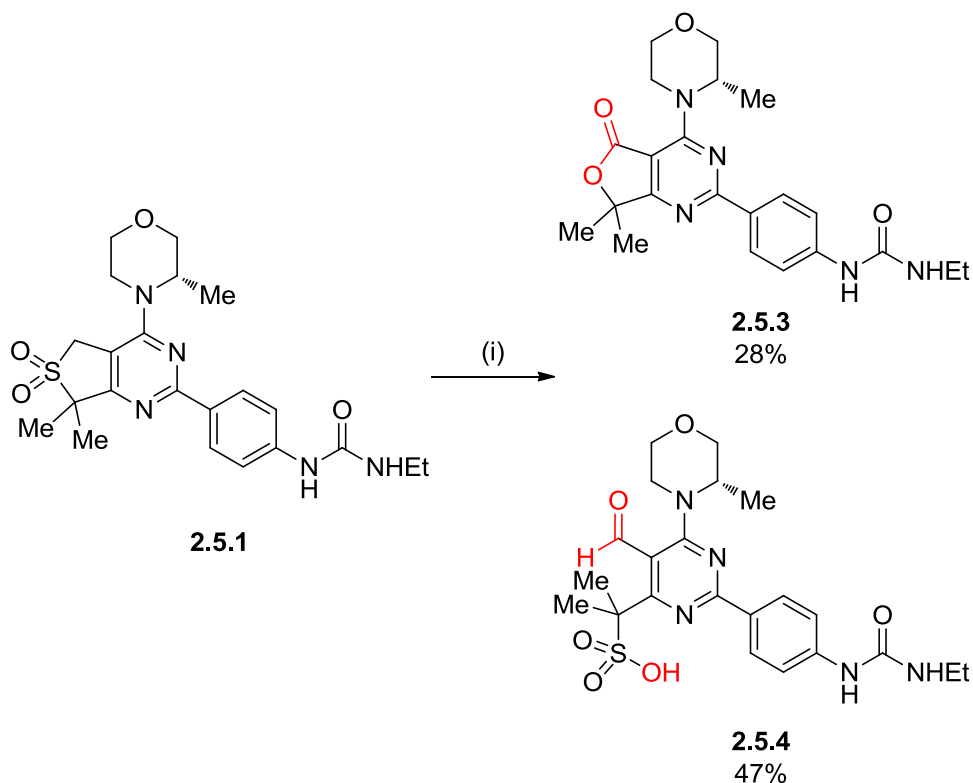
*h*ERG activity may be saved from termination by rapidly examining the effects that reducing the basicity has on the bioactivity with the target and with *h*ERG.

Application of the developed C–H oxidation methodology for the preparation of novel inhibitors against a biological target was also explored. Compound **2.5.1** (Scheme 57) is an inhibitor of the mammalian target of rapamycin (mTOR) kinase,²⁵³ and the potential to oxidise **2.5.1** was tested under the developed iodine-mediated C–H oxidation conditions.



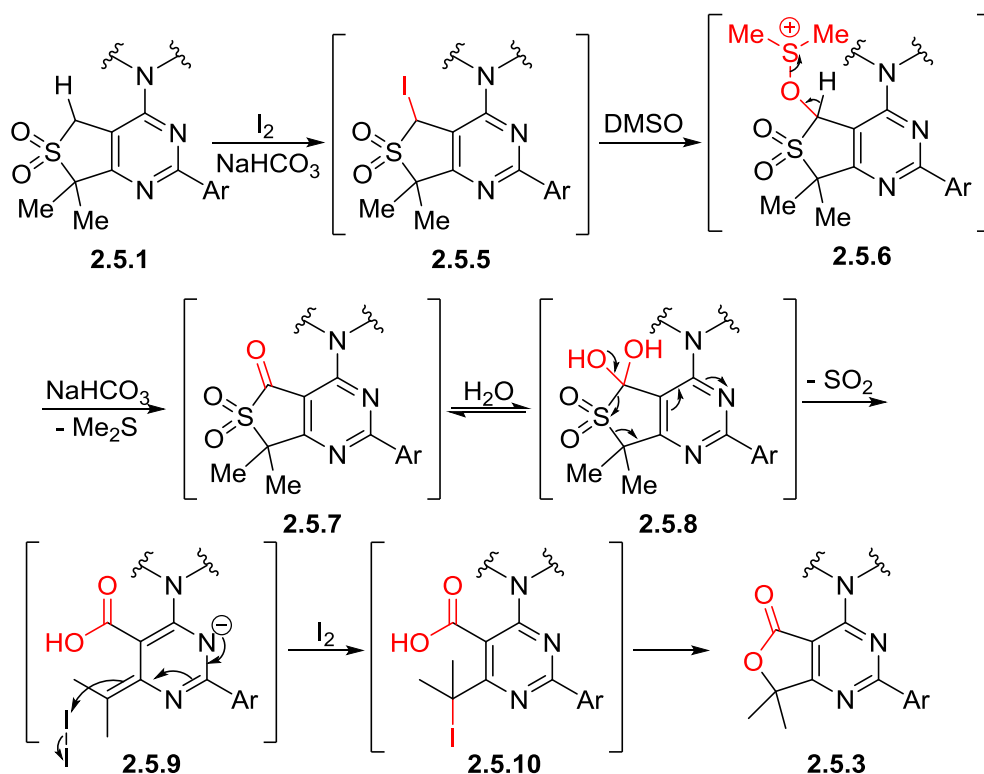
Scheme 57. Morpholine 2.5.1 showed no reaction under the standard oxidation conditions. Conditions: (i) I₂ (7.5 eq.), NaHCO₃ (10.0 eq.), DMSO:H₂O (2.5:1, 0.025 M), 4 h, RT, nr.

Under the standard conditions at room temperature, no reaction of **2.5.1** was observed. On increasing the reaction temperature, gradual consumption of the starting material occurred, but the expected lactam product **2.5.2** was not formed. Instead, lactone **2.5.3** and sulfonic acid **2.5.4** (Scheme 58) were formed unexpectedly in 28% and 47% yield, respectively, and were each isolated from two different reaction runs.



Scheme 58. Unexpected oxidation products 2.5.3 and 2.5.4 were isolated from the reaction of 2.5.1 under iodine-mediated oxidative conditions at elevated temperature. Conditions: (i) I₂ (7.5 eq.), NaHCO₃ (10.0 eq.), DMSO:H₂O (2.5:1, 0.025 M), 100 °C, 48 h.

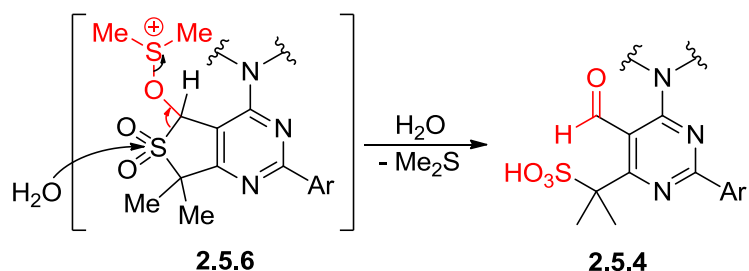
These unusual transformations were unexpected, and it was proposed that the anticipated lactam **2.5.2** was not made because the morpholino-nitrogen lone pair is less available for *N*-iodination, due to conjugation into the electron-deficient pyrimidine core of **2.5.1**. Deuteration studies of **2.5.1** have indicated that the hydrogen atoms adjacent to the sulfone are moderately acidic, since deuterium exchange was observed at this position in deuterated basic aqueous media over a 24 hour timescale. A hypothesis for the mechanism through which **2.5.3** might form is detailed in Scheme 59.



Scheme 59. Postulated mechanism for the formation of 2.5.3. Structures have been simplified for clarity.

Iodination adjacent to the sulfone was thought to be feasible under the basic reaction conditions to afford **2.5.5**. Subsequent Kornblum oxidation *via* DMSO ligated intermediate **2.5.6** would afford ketone **2.5.7**,^{254,255} which could exist in the hydrate form **2.5.8** under the aqueous reaction conditions. Extrusion of sulfur dioxide gas from **2.5.8** promoted by the high reaction temperature and the electron-deficient pyrimidine would generate intermediate **2.5.9** with an entropic driving force.²⁵⁶ Iodination of this species would afford tertiary iodide **2.5.10**, which would then be able to undergo a lactonisation with loss of iodide to give **2.5.3**.

Alternatively, if the sulfone intermediate **2.5.6** undergoes nucleophilic attack by water (Scheme 60) opening of the ring could occur, along with oxidation to the aldehyde, to account for the formation of **2.5.4**.



Scheme 60. Possible deviation from the putative Kornblum oxidation, leading to the formation of **2.5.4**. Structures have been simplified for clarity.

Despite the fact that the desired lactam compound had not been synthesised, compounds **2.5.3** and **2.5.4** were unexpected and interesting chemotypes to screen against mTOR. In fact, **2.5.3** had already been reported by Genentech as a potent inhibitor of mTOR.²⁵⁷ Accordingly, compounds **2.5.3** and **2.5.4** were screened against mTOR in a chemoproteomic kinobead binding assay (Table 13), which showed a comparable potency against mTOR for **2.5.3** compared to **2.5.1**.

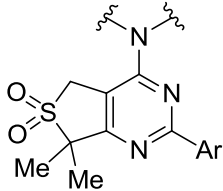
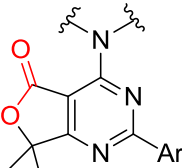
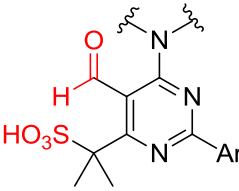
Kinase pIC_{50} (n)	Compound			
		2.5.1	2.5.3	2.5.4
mTOR		8.0 (21)	8.1 (5)	7.5 (4)
PI3Kα		5.3 (6): 560-fold	5.3 (1): 680-fold	<4.5 (1): >1100-fold
PI3Kβ		<4.8 (6): >1600-fold	4.8 (1): 1700-fold	<4.5 (1): >1100-fold
PI3Kγ		<5.1 (7): >900-fold	5.5 (1): 380-fold	<4.5 (1): >1100-fold
PI3Kδ		5.0 (6): 960-fold	5.3 (1): 600-fold	4.6 (1): 850-fold

Table 13. Comparison of compounds **2.5.3** and **2.5.4** with **2.5.1** for their ability to inhibit mTOR and their selectivity over PI3K isoforms. n = the number of times the compound was run through the assay. x-fold = the selectivity of inhibition of mTOR compared with the corresponding PI3 kinase. Structures have been simplified for clarity.

However, the selectivity over the gamma and delta PI3K isoforms, which are related kinases, decreased for **2.5.3** compared with **2.5.1**. It should be noted that the data for the inhibition of the PI3K isoforms was measured in a time-resolved fluorescence energy transfer (TR-FRET) assay, as PI3K kinobead assays were not run for **2.5.3** and

2.5.4. Whereas TR-FRET assays are biochemical assays that use recombinant protein, and often make use of protein fragments, the kinobead assays involve binding of multiple kinases from cell lysates to a bead. This then allows for better mimicry of *in vivo* conditions by testing the potency of a compound against a large portion of the kinome and related proteins on a mixed kinase-inhibitor matrix.²⁵⁸ This has the effect that pIC_{50} values are generally lower in kinobead assays (data not shown), compared with TR-FRET assays, because kinobead assays can mimic better the native conformation and activity of the target in its physiological context.

Sulfonic acid **2.5.4** recorded a lower potency for inhibition of mTOR than **2.5.1** and **2.5.3**, with a pIC_{50} value of 7.5, but the standout feature of this compound is the incredibly high selectivity over the PI3K isoforms. Affinity for the α , β and γ isoforms did not register on the assay, while inhibition of PI3K δ decreased from 5.0 for **2.5.1** to 4.6 for **2.5.4**. The reason for this significant increase in selectivity was believed to have arisen from the introduction of the ring-opened carbonyl moiety at the benzylic position of the pyrimidine, which increased steric hindrance relative to the hydrogen atoms in the parent molecule **2.5.1** and the conformationally restricted cyclic lactone in **2.5.3**. This theory had not until this point been conclusively validated due to difficulties in synthesis of tetrasubstituted monocyclic pyrimidines, such as **2.5.4**.

These fascinating results demonstrated the formation of new complex functionality in one step from a highly functionalized late-stage compound **2.5.1**, going from one potent molecule to another with completely different chemotypes. While the expected result was not achieved, the application of a late-stage chemical procedure enabled the rapid formation of a novel chemotype, which has shaped strategy and decision-making for a medicinal chemistry program. Similarly, for testing the effects of hERG reduction of **2.4.1a**, while the drop in target potency was disappointing, the compound was synthesised rapidly, hence the data could be generated quickly; this is the purpose of applying late-stage functionalisation to medicinal chemistry programmes.

2.6 Developing a Predictive Model for the Iodine-Mediated C–H Oxidation of Azacycles

The development of a predictive model would be the final aspect of analysis that would consolidate the utility of this methodology as a tool for late-stage C–H oxidation. It was initially proposed that the pK_{aH} of the azacyclic amine was the main parameter for controlling the amount of lactam formed, although comparison of the calculated pK_{aH} for the model substrates in Table 6 and Table 7 with the yield of lactam product showed poor correlation (Appendix 1, Table 16).

Another hypothesis was that the dihedral angle between the N–I bond and the α -C–H bond of the *N*-iodoammonium intermediate, such as **2.3.2a** (Figure 19), may influence the yield of lactam.

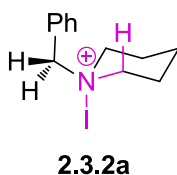


Figure 19. It was proposed that the H-C-N-I dihedral arrangement (highlighted in pink) of the *N*-iodoammonium intermediate could be used to predict the yield of the lactam product.

It would be expected that an angle close to 180° would allow for more efficient elimination of hydrogen iodide from the intermediate, as this antiperiplanar arrangement should offer better orbital overlap for elimination of the iodide. Computational conformational modelling was carried out on *N*-iodoammonium intermediates for each model substrate, and the dihedral angle of the H-C-N-I bonds was measured for the lowest energy conformation where the N-I bond was in an axial configuration. However, once again, no trend was seen between yield and dihedral angle (Appendix 2, Table 17).

In most cases, the calculated lowest energy conformation had the N-I bond equatorial, but in some instances the energy difference between the lowest state with an axial N-I bond was under 2 kcalmol⁻¹, so this conformation is likely to be accessible at room temperature. Intermediates **2.3.2d-e, h-k, m, o, s** and **u** (Figure 20) have energy differences greater than 2 kcalmol⁻¹, so the relevant high energy intermediates are unlikely to be easily accessible under the reaction conditions. These disparities mean that a direct link between dihedral angle and yield is not immediately apparent.

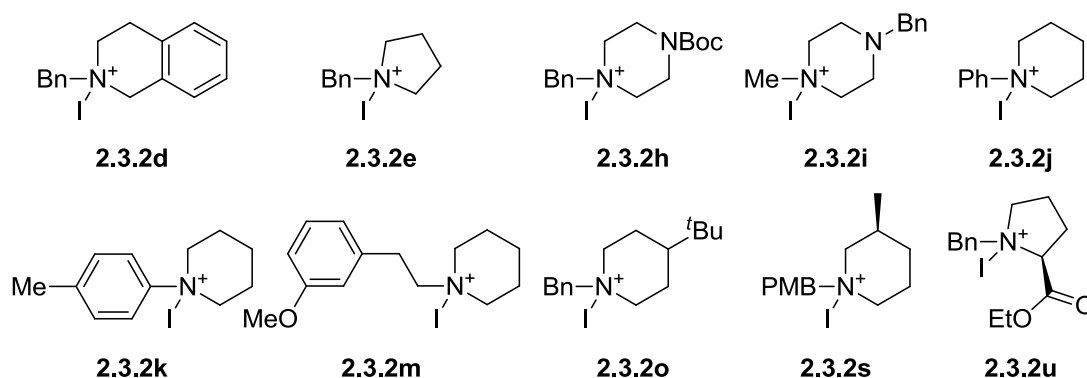
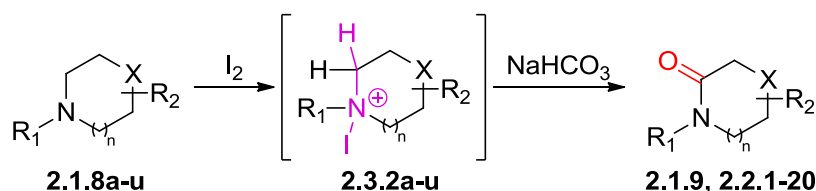


Figure 20. *N*-iodoammonium intermediates **2.3.2d-e, h-k, m, o, s** and **u** were calculated²⁴² to have an energy difference of greater than 2 kcal/mol between the lowest energy conformation and the conformation with the N-I bond and the α -C-H bond in an antiperiplanar arrangement.

On closer inspection of the data, a trend between yield of lactam product with dihedral angle can be observed for some examples, in particular the six-membered azacycles. There is also a trend with pK_aH , although not for all the same substrates, although dihedral angle appeared to be more influential on the yield of lactam product than pK_aH . As a result, it was proposed that the amount of conversion to lactam may be dictated by a combination of both pK_aH and dihedral angle of the intermediate. A comparison of yield for the six-membered ring lactams with some function (F_n) of dihedral angle of the *N*-iodoammonium intermediate and the pK_aH of the substrate amine was carried out, where F_n is defined as:

$$F_n = (\text{dihedral angle}) \times (\sqrt{pK_aH})$$

A general correlation can be observed between yield of δ -lactam product and F_n for the six-membered rings (Table 14).



Substrate	Calculated pK_aH^{250}	Dihedral angle ^[a] ($^\circ$) ²⁴²	F_n	Yield (%)
2.1.8i	8.1	171	486	45
2.1.8n	10.1	163	517	51
2.1.8r	9.7	171	533	53
2.1.8j	5.6	170	401	54
2.1.8h	6.9	169	441	56
2.1.8k	6.0	170	416	56
2.1.8m	9.1	171	517	70
2.1.8s	9.1	169	510	73 ^[b]
2.1.8t	7.2	169	454	75
2.1.8o	9.4	171	525	76
2.1.8g	7.2	172	460	78
2.1.8d	8.5	162	474	80
2.1.8l	8.8	172	508	84
2.1.8b	8.8	171	509	91
2.1.8c	8.2	171	491	95
2.1.8a	9.4	171	525	96

Table 14. Comparison of yield of lactam with F_n , a combination of pK_aH and dihedral angle, with the data sorted from lowest to highest yield of lactam product. [a] The value was measured as the dihedral angle across the H-C-N-I bonds of **2.3.2a-u** in the lowest energy state that had the N-I bond in an axial conformation. [b] Combined yield of **2.2.18a** and **2.2.18b** were used in data analysis to measure conversion of substrate to lactam product.

Substrates **2.1.8i**, **n** and **r** do not appear to follow the trend the other substrates display. The pH of the reaction mixture was measured to be 7.6, and for piperazine **2.1.8i** only 23% of the free amine was calculated to be in solution based on the calculated pK_aH . Approximately 46% of species were predicted to be protonated on the benzyl-substituted nitrogen, and 31% protonated on the methyl-substituted nitrogen. The low proportion of free amine was likely to have accounted for the low conversion of substrate, and the fact that a higher proportion of the more basic benzyl-substituted nitrogen would have been protonated at any one time in solution explains the observed

regioselectivity. Similarly, for **2.1.8n** 99% of the substrate was predicted to have been protonated in solution at the reaction pH based on the calculated pK_aH , so there would have been a very small amount of freely basic amine available to interact with iodine, accounting for the slow reactivity of this substrate. There would also not be same level of release of steric hindrance through elimination of hydrogen iodide for this secondary amine substrate as there would be for the tertiary amines. The low yield of **2.2.17** from **2.1.8r** is attributed to the increased steric hindrance imparted by the benzylic methyl group, limiting the ability for the large iodine molecule to coordinate to the nitrogen lone pair.

If these three results are considered as anomalous and excluded for the above reasons, then a graph can be plotted of F_n against isolated yield to show the positive correlation of yield of δ -lactam with F_n for the six-membered azacycles (Figure 21).

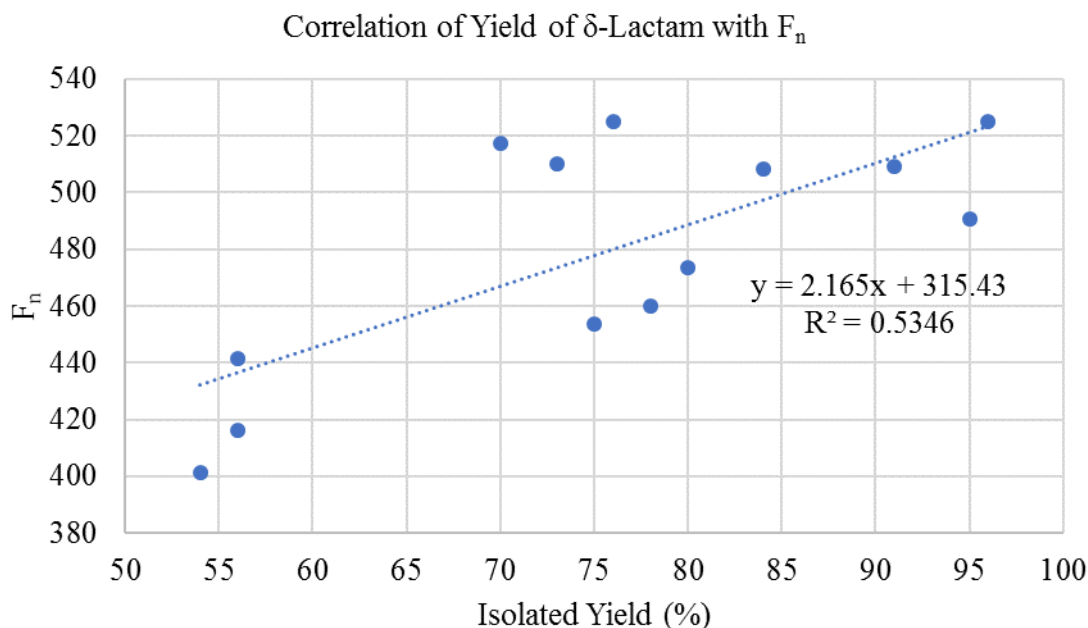
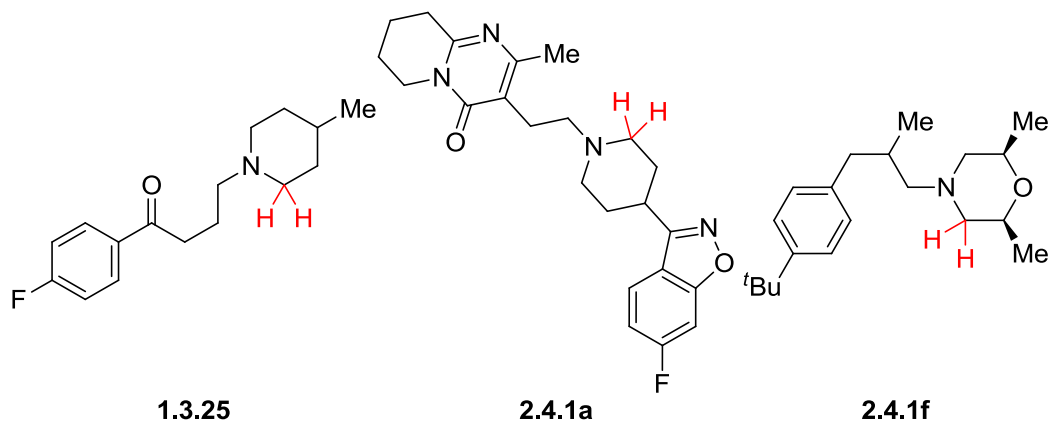


Figure 21. Graphical representation of correlation of yield with F_n for the iodine-mediated C–H oxidation of six-membered azacycles to δ -lactams.

In order to test this trend and validate it as a tool for predicting the expected outcome of late-stage oxidation of six-membered azacycles, bioactive drug substrates

melperone **1.3.25**, risperidone, **2.4.1a**, and fenpropimorph, **2.4.1f**, were resubmitted into the model (Table 15).



Substrate	Calculated pK_aH^{250}	Dihedral angle ^[a] (°) ²⁴²	F_n	Predicted Yield (%)	Isolated Yield (%)
1.3.25	8.9	170	506	88	83
2.4.1a	8.8	168	497	84	56
2.4.1f	8.5	170	495	83	55

Table 15. Resubmission of 1.3.25 to the predictive equation. [a] The value was measured as the dihedral angle across the H-C-N-I bonds of **2.3.2a-u** in the lowest energy state that had the N-I bond in an axial conformation.

The model predicts a yield for the oxidation of **1.3.25** to **2.4.11** that is in close agreement with the actual isolated yield from the reaction; for the more complex examples **2.4.1a** and **2.4.1f**, however, the model is not quite as accurate in its prediction. The deviation of **2.4.1a** from the model may arise from the fact that the lowest energy conformation of the starting material is oriented such that the pyrimidinone group attached to the piperidine nitrogen is on top of the piperidine ring, possibly blocking the availability of the nitrogen lone pair to interact with iodine (Figure 22).

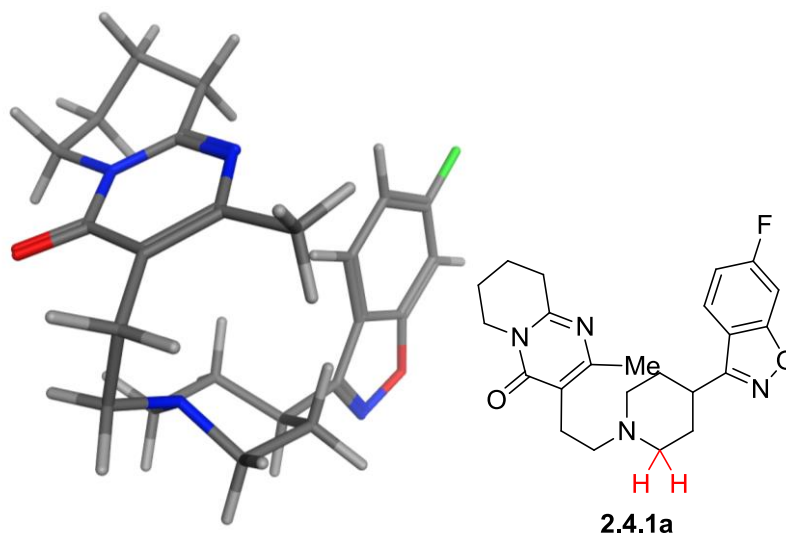


Figure 22. Calculated lowest energy conformation of **2.4.1a**,²⁴² with the pyrimidinone group blocking one face of the core piperidine ring.

The lower than predicted yield of **2.4.1f** may have resulted from by-product formation: a polar species with a m/z value of 219 (ES, negative mode) was formed during the reaction with substrate **2.4.1f**, with the by-product formed in approximately a 1:3 ratio by LCMS %area relative to the product **2.4.7**. This by-product had poor ionisation in the positive electrospray, which suggested that it was an acidic proton source. Carboxylic acid **2.6.1** was proposed as a possible structure of this by-product (Figure 23).

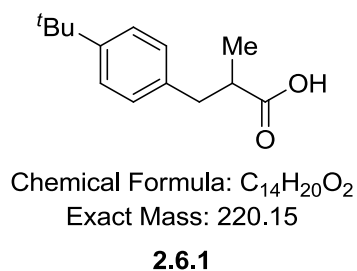


Figure 23. Putative structure of by-product in the C–H oxidation of **2.4.1f**, accounting for the lower than predicted yield of **2.4.7**.

LCMS analysis of a commercially available source of **2.6.1** exhibited the same ionisation pattern and ran on the chromatogram within 0.02 minutes of the by-product formed in the reaction. This provides further evidence that **2.6.1** formed during the

oxidation of **2.4.1f**, likely resulting from oxidative cleavage of the morpholine group. It is not currently clear, however, why **2.4.1f** would cleave in this manner, when such fragmentation was not observed in the model morpholine substrates **2.1.8g** and **2.1.8t**.

The model also predicted a cut-off F_n value of 315, below which lactam formation will not occur, which is in agreement with results to date, such as the F_n value of 81 for **2.5.1**, where no lactam was observed. Unfortunately, the five and seven-membered rings did not fit into this model, possibly because these rings have decreased or increased conformational flexibility, respectively, compared to the six-membered rings, which creates additional complications in predicting oxidation yield. In addition, the correlation of the data to the line of best fit was quite low, with a R^2 value of 0.53. This suggested that the model developed was not accurate enough to act as a predictive tool, hence why other ring sizes and some of the drug substrates fitted into the model poorly. As such, the mechanistic hypothesis would need to be revised.

Instead of an antiperiplanar elimination to form the iminium intermediate, a *syn* intramolecular elimination (E_i) is a possible pathway.^{259,260} In this type of elimination, two vicinal substituents leave simultaneously *via* a cyclic transition state. Examples of this phenomenon include the Cope elimination,^{259,261} the Chugaev elimination²⁶² and the sulfoxide elimination,^{263,264} which all proceed through either a five- or six-membered cyclic transition state, and require high temperatures to achieve thermal elimination. Another example of E_i elimination is the iodoso elimination,²⁶⁵ where alkyl iodides were observed to undergo *syn*-elimination of hypoiodous acid following oxidation of the iodine atom to an iodoso substituent.

Hypoiodous acid **2.6.2** and hypoiodite salts **2.6.3** are known to be prepared through the treatment of molecular iodine with alkali hydroxide (Scheme 61).²⁶⁶

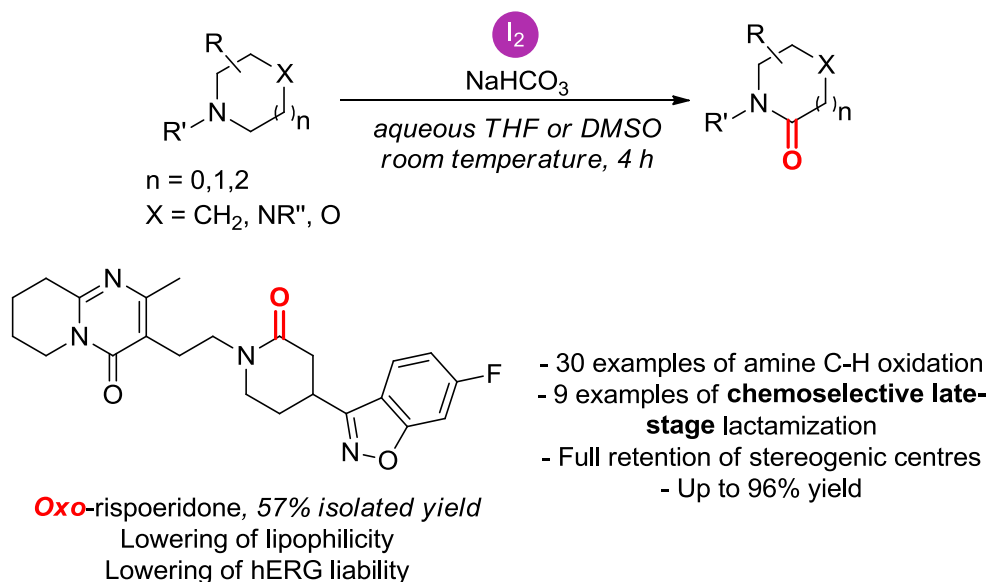
equatorial C–H bond to form the cyclic iminium **2.3.11** could lead to a removal of the unfavourable 1,3-diaxial clash between the axial hydrogens; this effect is an established rationale for regioselectivities in C–H functionalisation reactions.^{35,267–269} This proposed elimination pathway would also account for the regioselectivity for the formation of the less-substituted intermediary iminium, resulting in oxidation occurring on the less-substituted side of the azacycle, as E_i eliminations are known to follow the Hofmann rule where the less-substituted alkene is formed preferentially.^{259,270} *Syn*-elimination through a five-membered transition state reforms **2.6.2**, so, in principle, only a trace quantity has to form in the reaction for the oxidation to proceed.

Quenching of **2.3.11** with water affords **2.3.12**, and *N*-iodination to **2.3.14** and oxidation to *N*-iodoso species **2.6.6** enables a second *syn*-iodoso elimination to take place. The resulting hydroxyiminium **2.3.15** can then tautomerise to the product **2.1.9**. This revision of the mechanistic hypothesis, proceeding *via* a *syn*-iodoso elimination, serves to explain some of the selectivities and yields that were observed during the development of this methodology; the five- and seven-membered heterocycles possibly do not suffer from as much 1,3-diaxial strain, meaning strain-release is less of a driving force. Further work is needed to fully elucidate the mechanism of this reaction, and it is hoped that this would offer an improved predictive model to increase the value and application for medicinal chemistry.

2.7 Summary

This work discloses the development of a chemoselective iodine-mediated strategy for the C–H oxidation of cyclic amines under mild conditions (Scheme 62). The procedure was used to carry out late-stage C–H oxidation of a suite of high value small molecules, and preliminary correlations were established to assist in being able to predict how oxidatively susceptible a complex late-stage substrate might be under these conditions. The application of this methodology in the late-stage synthesis of novel chemotypes, as well as the implication that this has for medicinal chemistry, has

been described. Lipophilicity and hERG liability were reduced in a late-stage manner, showcasing iodine-mediated late-stage C–H oxidation as a viable tool for modulating the physical chemical and the toxicological properties of bioactive small molecules.



Scheme 62. Chemo- and regioselective C–H oxidation of cyclic amines to lactams using molecular iodine as an oxidant. This protocol was exemplified as a tool for the late-stage oxidation of several bioactive drug molecules.

It is envisaged that this approach could be generalised by medicinal chemists for creating a diverse range of compounds from a small subset of molecular scaffolds, and for providing synthetic access to drug metabolites,^{271,272} potentially accelerating the hit-to-lead process of drug discovery.

2.8 Experimental

General Experimental

Solvents and Reagents

Unless otherwise stated:

- Reactions were carried out under a standard atmosphere of air at room temperature, and glassware was not dried beforehand. Solvents used were non-anhydrous.
- Solvents and reagents were purchased from commercial suppliers or obtained from GSK's internal compound storage and used as received without further purification. All drug compounds used in transformations are commercially available.
- Reactions were monitored by Liquid Chromatography-Mass Spectrometry (LCMS) and Nuclear Magnetic Resonance (NMR).

Where substrates were synthesized in-house, literature references have been given for spectral data of these compounds.

Where products are given a defined stereochemical label, this is based upon the starting material stereochemical assignment once chiral high-performance liquid chromatography (HPLC) has determined the enantiomeric excess of the major enantiomer.

Chromatography

Thin layer chromatography (TLC) was carried out using plastic-backed 50 precoated silica plates (particle size 0.2 mm). Spots were visualized by ultraviolet (UV) light ($\lambda_{\text{max}} = 254 \text{ nm}$ or 365 nm) and then stained with potassium permanganate solution followed by gentle heating. Silica gel chromatography was carried out using the Teledyne ISCO CombiFlash[®] Rf+ apparatus with RediSep[®] silica cartridges. Reverse phase preparative HPLC was carried out using the Grace Reveleris[®] Prep apparatus

with an XTerra® Prep RP₁₈ OBD™ column. Where modifiers are used as additives in the eluent, the stated percentage value signifies percentage by volume.

Hydrophobic frit cartridges by ISOLUTE® contain a frit which is selectively permeable to organic solutions. These are separated from aqueous phase under gravity. Various cartridge sizes were used.

Reaction pH was measured using a Mettler Toledo S20 SevenEasy™ pH meter.

Melting points (M.pt.) were recorded on a Stuart SMP10 melting point apparatus.

Liquid Chromatography-Mass Spectrometry (LCMS)

LCMS analysis was carried out on an H₂O_s Acquity UPLC instrument equipped with a BEH column (50 mm x 2.1 mm, 1.7 μm packing diameter) and H₂O_s micromass ZQ MS using alternate-scan positive and negative electrospray. Analytes were detected as a summed UV wavelength of 210 – 350 nm. Two liquid phase methods were used:

Method A – High pH: 40 °C, 1 mL/min flow rate. Gradient elution with the mobile phases as (A) 10 mM aqueous ammonium bicarbonate solution, adjusted to pH 10 with 0.88 M aqueous ammonia and (B) MeCN. Gradient conditions were initially 1% B, increasing linearly to 97% B over 1.5 min, remaining at 97% B for 0.4 min then increasing to 100% B over 0.1 min.

Method B – Low pH: 40 °C, 1 mL/min flow rate. Gradient elution with the mobile phases as (A) H₂O containing 0.1% volume/volume (v/v) formic acid and (B) MeCN containing 0.1% (v/v) formic acid. Gradient conditions were initially 1% B, increasing linearly to 97% B over 1.5 min, remaining at 97% B for 0.4 min then increasing to 100% B over 0.1 min.

Nuclear Magnetic Resonance (NMR) Spectroscopy

Proton (^1H) and carbon (^{13}C) spectra were recorded in deuterated solvents at ambient temperature using standard pulse methods on any of the following spectrometers and signal frequencies: Bruker AV-400 (^1H = 400 MHz, ^{13}C = 101 MHz), Bruker AV-500 (^1H = 500 MHz, ^{13}C = 126 MHz) and Bruker AV-600 (^1H = 600 MHz, ^{13}C = 151 MHz). Chemical shifts are reported in ppm and were referenced to the following solvent peaks: CDCl_3 (^1H = 7.27 ppm, ^{13}C = 77.0 ppm), d_6 -DMSO (^1H = 2.50 ppm, ^{13}C = 39.5 ppm), and D_2O (^1H = 4.79 ppm). Where D_2O was used as the solvent, the default referencing was used based on the D_2O lock frequency for ^{13}C NMR. Peak assignments were made on the basis of chemical shifts, integrations, and coupling constants using COSY, DEPT, HSQC, HMBC, NOESY and ROESY where appropriate. Coupling constants (J) are quoted to the nearest 0.1 Hz and multiplicities are described as singlet (s), doublet (d), triplet (t), quartet (q), quintet (quin), sextet (sxt), br. (broad) and multiplet (m), and combinations therein.

Infrared (IR) Spectroscopy

IR spectra were recorded using a Perkin Elmer Spectrum 1 machine. Absorption maxima (ν_{max}) are reported in wavenumbers (cm^{-1}).

High Resolution-Mass Spectrometry (HRMS)²⁷³

High-resolution mass spectra were recorded on one of two systems:

System A: Micromass Q-ToF Ultima hybrid quadrupole time-of-flight mass spectrometer, with analytes separated on an Agilent 1100 Liquid Chromatograph equipped with a Phenomenex Luna C18 (2) reversed phase column (100 mm x 2.1 mm, 3 μm packing diameter). LC conditions were 0.5 mL/min flow rate, 35 $^\circ\text{C}$, injection volume 2–5 μL , using a gradient elution with (A) H_2O containing 0.1% (v/v) formic acid and (B) MeCN containing 0.1% (v/v) formic acid. Gradient conditions were initially 5% B, increasing linearly to 100% B over 6 min, remaining at 100% B

for 2.5 min then decreasing linearly to 5% B over 1 min followed by an equilibration period of 2.5 min prior to the next injection.

System B: Waters XEVO G2-XS quadrupole time-of-flight mass spectrometer, with analytes separated on an Acquity UPLC CSH C18 column (100mm x 2.1mm, 1.7 μ m packing diameter). LC conditions were 0.8 mL/min flow rate, 50 °C, injection volume 0.2 μ L, using a gradient elution with (A) H₂O containing 0.1% (v/v) formic acid and (B) MeCN containing 0.1% (v/v) formic acid. Gradient conditions were initially 3% B, increasing linearly to 100% B over 8.5 min, remaining at 100% B for 0.5 min then decreasing linearly to 3% B over 0.5 min followed by an equilibration period of 0.5 min prior to the next injection.

Mass to charge ratios (m/z) are reported in Daltons (Da).

Mass-Directed Automated Preparative HPLC (MDAP)

MDAP purification was carried out using an H₂O_s ZQ MS using alternate-scan positive and negative electrospray and a summed UV wavelength of 210–350 nm. The liquid phase method used was a high pH method as follows: Xbridge C18 column (100 mm x 19 mm, 5 μ m packing diameter, 20 mL/min flow rate) or Xbridge C18 column (150 mm x 30 mm, 5 μ m packing diameter, 40 mL/min flow rate). Gradient elution at ambient temperature with the mobile phases as (A) 10 mM aqueous ammonium bicarbonate solution, adjusted to pH 10 with 0.88 M aqueous ammonia and (B) MeCN. The elution gradients used were at a flow rate of 40 mL/min over 20 or 30 min depending on separation:

Method	Gradient B (%)
A	5-30
B	15-55
C	30-85
D	50-99
E	80-99

Synthetic Procedures

General Procedure for the Iodine-Mediated C–H Oxidation of Cyclic Amines A.

Iodine (7.5 eq.) was added to a mixture of cyclic amine (1.0 eq.) and solid sodium bicarbonate (10.0 eq.) in THF/H₂O (2.5:1, 0.025 M). The reaction mixture was stirred gently at room temperature for 4 h and monitored by LCMS. The reaction mixture was then pipetted into a solution of saturated aqueous sodium thiosulfate (10 mL) and saturated aqueous sodium bicarbonate (10 mL). The crude material was extracted in DCM (2 x 10 mL), and the combined organic layer was washed with saturated aqueous sodium bicarbonate (10 mL), passed through a hydrophobic frit, concentrated under reduced pressure and then purified as described.

General Procedure for the Iodine-Mediated C–H Oxidation of Cyclic Amines B.

General procedure B was the same as general procedure A, with exception that DMSO replaced THF in the solvent system.

General Procedure for the Iodine-Mediated C–H Oxidation of Cyclic Amines C.

General procedure C was the same as general procedure A, with exception that the reaction was run over a period of 20 h rather than 4 h.

Reaction Optimisation

General Procedure for the Reaction Optimisation

Iodine or NIS (equivalents indicated) was added to a mixture of 1-benzylpiperidine (amount indicated) and solid sodium bicarbonate (amount indicated) in the indicated solvent system with the indicated solvent volume. The reaction mixture was stirred gently at room temperature for 4 h and monitored by LCMS. The reaction mixture was then pipetted into a solution of saturated aqueous sodium thiosulfate (10 mL) and saturated aqueous sodium bicarbonate (10 mL). The crude material was extracted in DCM (2 x 10 mL), and the combined organic layer was washed with saturated aqueous sodium bicarbonate (10 mL), passed through a hydrophobic frit and concentrated under reduced pressure. Conversion to product was quantified *via* ¹H NMR analysis of the crude material together with a known amount of internal standard 3,4,5-trichloropyridine in CDCl₃, with the integral of the benzylic 2H singlet of the desired product (δ 4.57 ppm) compared with the integral of the aryl 2H singlet for 3,4,5-trichloropyridine (δ 8.51 ppm).

Data are reported as (a) amount of 1-benzylpiperidine substrate, (b) amount of iodine (NIS for entry 15), (c) amount of sodium bicarbonate, (d) solvent system, (e) solvent volume and concentration of substrate, (f) percentage formation of **2.1.9** determined *via* ¹H NMR analysis, and (g) amount of 3,4,5-trichloropyridine used as a standard. The entries correspond to the entries in Table 4.

Entry 1

(a) 25 mg, 0.14 mmol, (b) 363 mg, 1.43 mmol, (c) 120 mg, 1.43 mmol, (d) 2.5:1 Toluene:H₂O, (e) 5.6 mL, 0.025 M, (f) 0%, and (g) 3.4 mg, 0.019 mmol of Cl₃C₅H₂N.

Entry 2

(a) 25 mg, 0.14 mmol, (b) 363 mg, 1.43 mmol, (c) 120 mg, 1.43 mmol, (d) 2.5:1 DCM:H₂O, (e) 5.6 mL, 0.025 M, (f) 5%, and (g) 3.0 mg, 0.016 mmol of Cl₃C₅H₂N.

Entry 3

(a) 25 mg, 0.14 mmol, (b) 363 mg, 1.43 mmol, (c) 120 mg, 1.43 mmol, (d) 2.5:1 MeOH:H₂O, (e) 5.6 mL, 0.025 M, (f) 5%, and (g) 3.2 mg, 0.018 mmol of Cl₃C₅H₂N.

Entry 4

(a) 25 mg, 0.14 mmol, (b) 363 mg, 1.43 mmol, (c) 120 mg, 1.43 mmol, (d) 2.5:1 HFIP:H₂O, (e) 5.6 mL, 0.025 M, (f) 2%, and (g) 3.8 mg, 0.021 mmol of Cl₃C₅H₂N.

Entry 5

(a) 25 mg, 0.14 mmol, (b) 363 mg, 1.43 mmol, (c) 120 mg, 1.43 mmol, (d) H₂O, (e) 5.6 mL, 0.025 M, (f) 6%, and (g) 3.7 mg, 0.020 mmol of Cl₃C₅H₂N.

Entry 6

(a) 25 mg, 0.14 mmol, (b) 363 mg, 1.43 mmol, (c) 120 mg, 1.43 mmol, (d) 2.5:1 MeCN:H₂O, (e) 5.6 mL, 0.025 M, (f) 6%, and (g) 3.5 mg, 0.019 mmol of Cl₃C₅H₂N.

Entry 7

(a) 50 mg, 0.29 mmol, (b) 724 mg, 2.85 mmol, (c) 240 mg, 2.85 mmol, (d) 2.5:1 THF:H₂O, (e) 11.4 mL, 0.025 M, (f) 91% (based on a 1 mL aliquot of the reaction mixture, which was worked up, concentrated and redissolved in CDCl₃ together with the standard), and (g) 24.3 mg, 0.13 mmol of Cl₃C₅H₂N.

Entry 8

(a) 25 mg, 0.14 mmol, (b) 363 mg, 1.43 mmol, (c) 120 mg, 1.43 mmol, (d) 2.5:1 DMSO:H₂O, (e) 5.6 mL, 0.025 M, (f) 90%, and (g) 3.4 mg, 0.019 mmol of Cl₃C₅H₂N.

Entry 9

(a) 50 mg, 0.29 mmol, (b) 724 mg, 2.85 mmol, (c) 240 mg, 2.85 mmol, (d) 2.5:1 THF:H₂O, (e) 2.8 mL, 0.1 M, (f) 59% (based on a 0.5 mL aliquot of the reaction mixture, which was worked up, concentrated and redissolved in CDCl₃ together with the standard), and (g) 7.0 mg, 0.038 mmol of Cl₃C₅H₂N.

Entry 10

(a) 50 mg, 0.29 mmol, (b) 724 mg, 2.85 mmol, (c) 240 mg, 2.85 mmol, (d) 2.5:1 THF:H₂O, (e) 5.6 mL, 0.05 M, (f) 57% (based on a 0.5 mL aliquot of the reaction mixture, which was worked up, concentrated and redissolved in CDCl₃ together with the standard), and (g) 9.6 mg, 0.053 mmol of Cl₃C₅H₂N.

Entry 11

(a) 50 mg, 0.29 mmol, (b) 80 mg, 0.31 mmol, (c) 240 mg, 2.85 mmol, (d) 2.5:1 THF:H₂O, (e) 11.4 mL, 0.025 M, (f) 15%, and (g) 19.6 mg, 0.11 mmol of Cl₃C₅H₂N.

Entry 12

(a) 50 mg, 0.29 mmol, (b) 181 mg, 0.71 mmol, (c) 240 mg, 2.85 mmol, (d) 2.5:1 THF:H₂O, (e) 11.4 mL, 0.025 M, (f) 15%, and (g) 22.3 mg, 0.12 mmol of Cl₃C₅H₂N.

Entry 13

(a) 50 mg, 0.29 mmol, (b) 362 mg, 1.43 mmol, (c) 240 mg, 2.85 mmol, (d) 2.5:1 THF:H₂O, (e) 11.4 mL, 0.025 M, (f) 68%, and (g) 39.3 mg, 0.22 mmol of Cl₃C₅H₂N.

Entry 14

(a) 35 mg, 0.20 mmol, (b) 381 mg, 1.50 mmol, (c) 168 mg, 2.00 mmol, (d) 2.5:1 THF:H₂O, (e) 11.4 mL, 0.025 M, (f) NMR conversion to product was not measured – 36.3 mg (96%) of **2.1.9** was isolated (see entry in subsequent experimental section).

Entry 15 – NIS used as iodine source

(a) 50 mg, 0.29 mmol, (b) 481 mg, 2.14 mmol, (c) 240 mg, 2.85 mmol, (d) 2.5:1 THF:H₂O, (e) 11.4 mL, 0.025 M, (f) 62%, and (g) 6.5 mg, 0.036 mmol of Cl₃C₅H₂N.

Entry 16 – No sodium bicarbonate used

(a) 25 mg, 0.14 mmol, (b) 272 mg, 1.07 mmol, (c) 0 mg, (d) 2.5:1 THF:H₂O, (e) 5.6 mL, 0.025 M, (f) 0%, and (g) 5.4 mg, 0.030 mmol of Cl₃C₅H₂N.

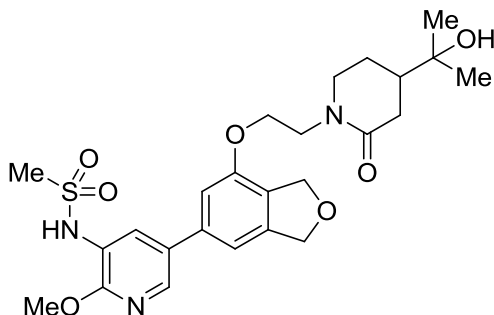
Entry 17 – Anhydrous conditions

(a) 25 mg, 0.29 mmol, (b) 272 mg, 1.07 mmol, (c) 120 mg, 1.43 mmol, (d) THF, (e) 5.7 mL, 0.025 M, (f) 0%, and (g) 7.2 mg, 0.039 mmol of $\text{Cl}_3\text{C}_5\text{H}_2\text{N}$.

Entry 18

(a) 25 mg, 0.14 mmol, (b) 272 mg, 1.07 mmol, (c) 120 mg, 1.43 mmol (d) 2.5:1 THF:H₂O, (e) 5.6 mL, 0.025 M, (f) NMR conversion to product was not measured – however no change in the reaction LCMS profile was observed, with full consumption of starting material seen. The reaction was not worked up or purified further.

5-(7-(2-(4-(2-Hydroxypropan-2-yl)-2-oxopiperidin-1-yl)ethoxy)-1,3-dihydroisobenzofuran-5-yl)-2-methoxy-N-methylpyridine-3-sulfonamide 2.1.7



Iodine (63.5 mg, 0.25 mmol) was added to a mixture of the hydrochloride salt of **2.1.1** (54.2 mg, 0.10 mmol)^{274,275} and sodium bicarbonate (84.0 mg, 1.0 mmol) in THF/H₂O (7.1 mL:2.9 mL, 0.01 M). The reaction mixture was stirred gently at room temperature for 16 h. The reaction mixture was then pipetted into a solution of saturated aqueous sodium thiosulfate (10 mL) and saturated aqueous sodium bicarbonate (10 mL). The crude material was extracted in DCM (2 x 10 mL), and the combined organic layer was washed with saturated aqueous sodium bicarbonate (10 mL), passed through a hydrophobic frit and concentrated under reduced pressure. The crude material was purified by reverse phase flash chromatography using 0-55% 0.1% aqueous formic acid/0.1% formic acid in MeCN as the eluent, affording **2.1.7** (19.4 mg, 37%) as a white solid.

LCMS (Method A, UV, ESI) R_t = 0.72 min, [M+H]⁺ 520.3

¹H NMR (DMSO-d₆, 400MHz): δ 8.32 (d, *J* = 2.4 Hz, 1H), 7.88 (d, *J* = 2.4 Hz, 1H), 7.16 (s, 1H), 7.14 (s, 1H), 5.06 (s, 2H), 5.00 (s, 2H), 4.27 (t, *J* = 5.3 Hz, 2H), 3.97 (s, 3H), 3.56-3.71 (m, 3H), 3.44 (ddd, *J* = 12.0, 5.6, 2.4 Hz, 1H), 3.35 (td, *J* = 12.0, 4.2 Hz, 2H), 3.08 (s, 3H), 2.27 (ddd, *J* = 17.1, 5.1, 2.0 Hz, 1H), 2.03 (dd, *J* = 17.6, 12.0 Hz, 1H), 1.86-1.94 (m, 1H), 1.64 (tdd, *J* = 12.1, 5.1, 2.9 Hz, 1H), 1.37 (qd, *J* = 12.3, 5.6 Hz, 1H), 1.04 ppm (s, 3H), 1.03 (s, 3H)

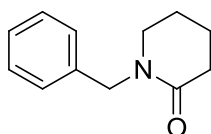
¹³C NMR (DMSO-d₆, 101MHz): δ 169.8, 156.8, 153.6, 142.4, 141.1, 138.9, 131.5, 130.3, 126.3, 121.8, 112.2, 109.3, 73.6, 71.4, 70.1, 66.0, 54.2, 49.1, 46.2, 43.8, 41.2, 34.1, 27.3, 26.9, 24.5

IR ν_{max} (cm⁻¹) (thin film): 3401 (br), 2968, 1617

HRMS: Calculated for C₂₅H₃₄N₃O₇S [M+H]⁺: 520.2112, found [M+H]⁺: 520.2107 (-0.5 ppm)

M.pt.: 195-196 °C.

1-Benzylpiperidin-2-one **2.1.9**



Iodine (381 mg, 1.50 mmol) was added to a mixture of 1-benzylpiperidine (36.9 μ L, 0.20 mmol) and sodium bicarbonate (168 mg, 2.00 mmol) in THF/H₂O (5.7/2.3 mL). The reaction mixture was stirred gently at room temperature for 4 h and monitored by LCMS. The reaction mixture was then pipetted into a solution of saturated aqueous sodium thiosulfate (10 mL) and saturated aqueous sodium bicarbonate (10 mL). The crude material was extracted in DCM (2 x 10 mL), and the combined organic layer was washed with saturated aqueous sodium bicarbonate (10 mL), passed through a hydrophobic frit, and concentrated under reduced pressure. The crude material was purified by silica gel chromatography using 35-60% TBME (with 1% triethylamine, 5% methanol modifier)/cyclohexane as the eluent, to afford **2.1.9** (36.3 mg, 96%) as a yellow oil.*

LCMS (Method A, UV, ESI) R_t = 0.85 min, [M+H]⁺ 190.1

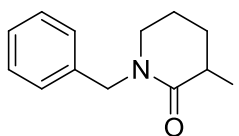
¹H NMR (CDCl₃, 400 MHz): δ 7.23-7.36 (m, 5H), 4.61 (s, 2H), 3.21 (t, *J* = 5.7 Hz, 2H), 2.48 (t, *J* = 6.5 Hz, 2H), 1.73-1.86 (m, 4H)

¹³C NMR (CDCl₃, 101 MHz): δ 169.8, 137.3, 128.5, 128.0, 127.3, 50.1, 47.3, 32.5, 23.2, 21.4

IR ν_{\max} (cm⁻¹) (thin film): 2946, 1634, 1494

HRMS: Calculated for C₁₂H₁₆NO [M+H]⁺: 190.1232, found [M+H]⁺: 190.1229 (-1.6 ppm).

*3 wt% **2.1.9b** co-eluted with product

1-Benzyl-3-iodopiperidin-2-one 2.1.9b

Iodine (543 mg, 2.10 mmol) was added to a mixture of **2.1.8a** (52.6 μ L, 0.29 mmol) and sodium bicarbonate (240 mg, 2.90 mmol) in THF/H₂O (4.1 mL/1.6 mL, 0.05 M). The reaction mixture was stirred gently at room temperature for 16 h. The reaction mixture was then pipetted into a solution of saturated aqueous sodium thiosulfate (10 mL) and saturated aqueous sodium bicarbonate (10 mL). The crude material was extracted in DCM (2 x 10 mL), and the combined organic layer was washed with saturated aqueous sodium bicarbonate (10 mL), passed through a hydrophobic frit and concentrated under reduced pressure. The crude material was purified by high pH MDAP (Method C), affording **2.1.9** (54.0 mg, 62%) as a yellow oil and **2.1.9b** (9.4 mg, 10%) as an amber coloured oil

LCMS (Method A, UV, ESI) R_t = 1.02 min, $[M+H]^+$ 316.0

¹H NMR (CDCl₃, 400MHz): δ 7.25-7.39 (m, 5H), 4.93 (m, 1H), 4.80 (d, J = 14.7 Hz, 1H), 4.37 (d, J = 14.7 Hz, 1H), 3.32-3.45 (m, 2H), 2.18-2.32 (m, 2H), 2.00-2.13 (m, 1H), 1.76-1.88 ppm (m, 1H)

¹³C NMR (CDCl₃, 101MHz): δ 167.9, 136.7, 128.7, 128.0, 127.5, 50.6, 46.9, 32.6, 23.1, 20.6

IR ν_{max} (cm⁻¹) (thin film): 2927, 1641, 1493

HRMS: Calculated for C₁₂H₁₅INO $[M+H]^+$: 316.0198, found $[M+H]^+$: 316.0199 (0.3 ppm).

Influencing Ratio of 2.1.9:2.1.9b with Substrate Concentration

Iodine (724 mg, 2.85 mmol) was added to a mixture of 1-benzylpiperidine (50 mg, 0.29 mmol) and solid sodium bicarbonate (240 mg, 2.85 mmol) in 2.5:1 THF:H₂O with the indicated solvent volume. The reaction mixture was stirred gently at room

temperature for 4 h. An aliquot (volume indicated) was taken from the reaction mixture and concentrated, and the residue redissolved in CDCl₃. The ratio of **2.1.9**:**2.1.9b** was determined *via* ¹H NMR analysis of the crude material with the integral of the benzylic 2H singlet of **2.1.9** (δ 4.57 ppm) compared with the integral of the 1H doublet for one of the benzylic hydrogens of **2.1.9b** (δ 4.37 ppm). The reactions were only monitored by LCMS and ¹H NMR, and were not worked up or purified further.

Data are reported as (a) volume of reaction solvent, (b) volume of aliquot taken from reaction mixture, and (c) integrals of appropriate signals for **2.1.9** and **2.1.9b**. In relation to Table 5, entry 1 corresponds to 0.1 M, entry 2 corresponds to 0.05 M, and entry 3 corresponds to 0.025 M.

Entry 1

(a) 1.4 mL, (b) 0.5 mL, and (c) 2.00 (2H) and 0.31 (1H) – 3:1 ratio.

Entry 2

(a) 2.8 mL, (b) 0.5 mL, and (c) 2.10 (2H) and 0.12 (1H) – 9:1 ratio.

Entry 3

(a) 5.6 mL, (b) 0.5 mL, and (c) 2.00 (2H) and 0.054 (1H) – 18:1 ratio.

Entry 4

(a) 11.4 mL, (b) 1.0 mL, and (c) 2.00 (2H) and 0.045 (1H) – >20:1 ratio.

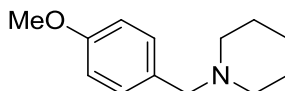
Probing Formation of 2.1.9b by Subjecting 2.1.9 to Iodine-Mediated Oxidative Conditions.

Iodine (169 mg, 0.67 mmol) was added to a mixture of **2.1.9** (13 mg, 0.067 mmol) and solid sodium bicarbonate (56 mg, 0.67 mmol) in 2.5:1 THF:H₂O (1.1 mL). The reaction mixture was stirred gently at room temperature for 4 h and monitored by LCMS. Only **2.1.9** (0.85 min, 16%UV) and iodine (0.38 min, 84%UV) were observed in the UV chromatogram of the reaction mixture. Due to there being no evidence

observed for the reaction of **2.1.9** or the formation of **2.1.9b**, the reaction was not worked up or purified further, and no material was isolated from the reaction.

Substrate Scope

1-(4-Methoxybenzyl)piperidine **2.1.8b**²⁷⁶

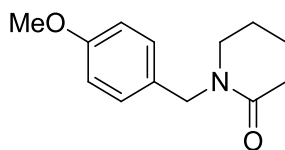


Piperidine (0.54 mL, 5.5 mmol), 4-methoxybenzyl chloride (0.68 mL, 5.0 mmol) and potassium carbonate (0.83 g, 6.0 mmol) were heated to 55 °C in MeCN (20 mL) for 42 h. The reaction mixture was cooled to RT, and then passed through a sintered funnel and the filtrate was concentrated under reduced pressure. The crude material was purified by silica gel chromatography, with 25-80% TBME (5% methanol, 2% triethylamine modifier)/cyclohexane, to afford **2.1.8b** (0.64 g, 63%) as a colourless oil.

LCMS (Method A, UV, ESI) $R_t = 1.11$ min, $[M+H]^+$ 206.1

$^1\text{H NMR}$ (CDCl_3 , 400 MHz): δ 7.23 (d, $J = 8.6$ Hz, 2H), 6.86 (d, $J = 8.8$ Hz, 2H), 3.81 (s, 3H), 3.42 (s, 2H), 2.37 (br. s., 4H), 1.58 (quin, $J = 5.6$ Hz, 4H), 1.44 (br. s, 2H).

1-(4-Methoxybenzyl)piperidin-2-one **2.2.1**



General procedure for the iodine-mediated C–H oxidation of cyclic amines **A** was followed. Iodine (381 mg, 1.50 mmol) was added to a mixture of **2.1.8b** (41 mg, 0.20 mmol) and sodium bicarbonate (168 mg, 2.00 mmol) in THF/H₂O (5.7/2.3 mL). Purification was carried out by silica gel chromatography using 50-100% TBME (with 1% triethylamine and 5% methanol modifier)/cyclohexane as the eluent, to afford **2.2.1** (39.8 mg, 91%) as a colourless oil.

LCMS (Method A, UV, ESI) $R_t = 0.85$ min, $[M+H]^+$ 220.1

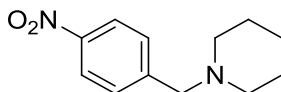
^1H NMR (CDCl_3 , 400 MHz): δ 7.19 (d, $J = 8.6$ Hz, 2H), 6.84 (d, $J = 8.6$ Hz, 2H), 4.52 (s, 2H), 3.79 (s, 3H), 3.17 (t, $J = 5.5$ Hz, 2H), 2.44 (t, $J = 6.5$ Hz, 2H), 1.68-1.84 (m, 4H)

^{13}C NMR (CDCl_3 , 101 MHz): δ 169.7, 158.9, 129.5 (2C), 113.9, 55.2, 49.5, 47.0, 32.5, 23.2, 21.4

IR ν_{max} (cm^{-1}) (thin film): 2936, 1633

HRMS: Calculated for $\text{C}_{13}\text{H}_{18}\text{NO}_2$ $[M+H]^+$: 220.1332, found $[M+H]^+$: 220.1337 (2.4 ppm).

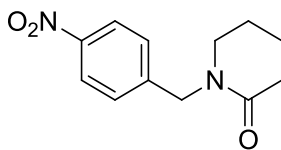
1-(4-Nitrobenzyl)piperidine **2.1.8c**²⁷⁷



4-Nitrobenzyl bromide (1.19 g, 5.5 mmol) was slowly added to a solution of piperidine (0.49 mL, 5.0 mmol) and DIPEA (1.31 mL, 7.5 mmol) in DCM (25 mL) at 0 °C. After the addition was complete, the solution was left to stir at RT for 18 h. The reaction mixture was then washed with distilled water (20 mL) and brine (20 mL), and the organic layer was passed through a hydrophobic frit and concentrated under reduced pressure. The crude material was purified by silica gel chromatography with 10-45% EtOAc/cyclohexane as the eluent, to afford **2.1.8c** (0.98 g, 89%) as a yellow oil.

LCMS (Method A, UV, ESI) $R_t = 1.22$ min, $[M+H]^+$ 221.1

^1H NMR (CDCl_3 , 400 MHz): δ 8.13 (d, $J = 8.6$ Hz, 2H), 7.48 (d, $J = 8.6$ Hz, 2H), 3.52 (s, 2H), 2.36 (t, $J = 5.3$ Hz, 4H), 1.56 (quin, $J = 5.6$ Hz, 4H), 1.41-1.46 (m, $J = 5.6$ Hz, 2H).

1-(4-Nitrobenzyl)piperidin-2-one 2.2.2

General procedure for the iodine-mediated C–H oxidation of cyclic amines **A** was followed. Iodine (432 mg, 1.70 mmol) was added to a mixture of **2.1.8c** (50 mg, 0.23 mmol) and sodium bicarbonate (191 mg, 2.27 mmol) in THF/H₂O (6.5/2.6 mL). Purification was carried out by silica gel chromatography using 40-60% (3:1 EtOAc/EtOH) (with 1% ammonia modifier)/cyclohexane as the eluent, to afford **2.2.2** (50.4 mg, 95%) as a white solid.

LCMS (Method A, UV, ESI) $R_t = 0.84$ min, $[M+H]^+$ 235.1

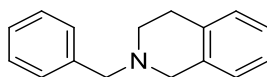
¹H NMR (CDCl₃, 400 MHz): δ 8.19 (d, $J = 8.8$ Hz, 2H), 7.43 (d, $J = 8.6$ Hz, 2H), 4.69 (s, 2H), 3.25 (t, $J = 5.4$ Hz, 2H), 2.51 (t, $J = 6.2$ Hz, 2H), 1.79-1.88 (m, 4H)

¹³C NMR (CDCl₃, 101 MHz): δ 170.1, 147.4, 145.0, 128.6, 123.9, 49.9, 47.9, 32.3, 23.2, 21.3

IR ν_{max} (cm⁻¹) (thin film): 2953, 2879, 1628

HRMS: Calculated for C₁₂H₁₅N₂O₃ $[M+H]^+$: 235.1077, found $[M+H]^+$: 235.1079 (0.6 ppm)

M.pt.: 97-100 °C.

2-Benzyl-1,2,3,4-tetrahydroisoquinoline 2.1.8d²⁷⁸

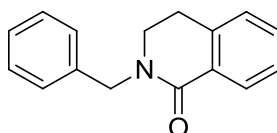
A mixture of benzaldehyde (1.0 mL, 9.8 mmol), 1,2,3,4-tetrahydroquinoline (1.2 mL, 9.8 mmol) and acetic acid (0.3 mL) was charged with 2-picoline borane (1.05 g, 9.8 mmol) over 5 min, and the reaction mixture was stirred at RT for 72 h. The reaction was quenched with 10% (w/v) aqueous HCl (10 mL) and the solution was stirred for 30 min at RT. The solution was basified to pH 9 with saturated aqueous sodium

bicarbonate. The aqueous layer was extracted with EtOAc (2 x 30 mL), and the combined organic layer was washed with brine (15 mL), passed through a hydrophobic frit and concentrated under reduced pressure. The crude product was purified by silica gel chromatography with 0-50% EtOAc (1% 4M ammonia/methanol modifier)/cyclohexane as the eluent, to afford **2.1.8d** (2.08 g, 94%) as a colourless oil.

LCMS (Method A, UV, ESI) $R_t = 1.32$ min, $[M+H]^+$ 224.1

^1H NMR (CDCl_3 , 400 MHz): δ 7.50 (d, $J = 7.1$ Hz, 2H), 7.40-7.46 (m, 2H), 7.36 (tt, $J = 7.1, 2.3$ Hz, 1H), 7.16-7.22 (m, 3H), 7.07 (s, 1H), 3.78 (s, 2H), 3.74 (s, 2H), 3.00 (t, $J = 5.8$ Hz, 2H), 2.84 (t, $J = 6.1$ Hz, 2H).

2-Benzyl-3,4-dihydroisoquinolin-1(2H)-one **2.2.3**



General procedure for the iodine-mediated C–H oxidation of cyclic amines **A** was followed. Iodine (426 mg, 1.68 mmol) was added to a mixture of **2.1.8d** (50 mg, 0.22 mmol) and sodium bicarbonate (188 mg, 2.24 mmol) in THF/ H_2O (6.4/2.6 mL). Purification was carried out by silica gel chromatography using 10-30% TBME (with 1% 4M ammonia in methanol modifier)/cyclohexane as the eluent, to afford **2.2.3** (42.6 mg, 80%) as a colourless oil.

LCMS (Method A, UV, ESI) $R_t = 1.09$ min, $[M+H]^+$ 238.2

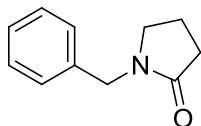
^1H NMR (CDCl_3 , 400 MHz): δ 8.16 (dd, $J = 7.6, 1.8$ Hz, 1H), 7.39-7.45 (m, 1H), 7.30-7.38 (m, 5H), 7.24-7.29 (m, 1H), 7.15 (d, $J = 7.3$ Hz, 1H), 4.80 (s, 2H), 3.48 (t, $J = 6.7$ Hz, 2H), 2.93 (t, $J = 6.7$ Hz, 2H)

^{13}C NMR (CDCl_3 , 126 MHz): δ 164.5, 138.0, 137.4, 131.6, 129.3, 128.5, 128.4, 128.0, 127.4, 127.0, 126.8, 50.4, 45.3, 28.0

IR ν_{max} (cm^{-1}) (thin film): 3030, 2935, 1644

HRMS: Calculated for C₁₆H₁₆NO [M+H]⁺: 238.1226, found [M+H]⁺: 238.1226 (0.0 ppm).

1-Benzylpyrrolidin-2-one 2.2.4



General procedure for the iodine-mediated C–H oxidation of cyclic amines A was followed. Iodine (295 mg, 1.16 mmol) was added to a mixture of **2.1.8e** (25 mg, 0.16 mmol) and sodium bicarbonate (130 mg, 1.55 mmol) in THF/H₂O (4.4/1.8 mL). Purification was carried out by silica gel chromatography using 30-85% TBME (with 1% 4M ammonia in methanol modifier)/cyclohexane as the eluent, to afford **2.2.4** (18.7 mg, 69%) as an orange oil.

LCMS (Method A, UV, ESI) R_t = 0.79 min, [M+H]⁺ 176.1

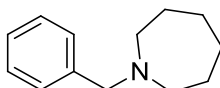
¹H NMR (CDCl₃, 400 MHz): δ 7.22-7.37 (m, 5H), 4.46 (s, 2H), 3.27 (t, *J* = 7.1 Hz, 2H), 2.45 (t, *J* = 8.1 Hz, 2H), 2.00 (quin, *J* = 7.6 Hz, 2H)

¹³C NMR (CDCl₃, 101 MHz): δ 174.9, 136.6, 128.6, 128.1, 127.5, 46.6, 30.9, 17.7

*One carbon environment was not observed, but this is consistent with literature precedent for this compound.*²⁷⁹

IR ν_{max} (cm⁻¹) (thin film): 2918, 1675

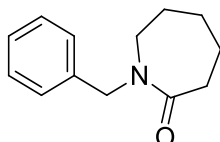
HRMS: Calculated for C₁₁H₁₄NO [M+H]⁺: 176.1070, found [M+H]⁺: 176.1069 (-0.5 ppm).

1-Benzylazepane 2.1.8f²⁸⁰

A mixture of benzaldehyde (0.85 mL, 8.3 mmol), azepane (0.94 mL, 8.3 mmol) and acetic acid (0.3 mL) was charged with 2-picoline borane (0.83 g, 8.3 mmol) over 5 min, and the reaction mixture was stirred at RT for 72 h. The reaction was quenched with 10% aqueous HCl (10 mL) and the solution was stirred for 30 min at RT. The solution was basified to pH 9 with saturated aqueous sodium bicarbonate. The aqueous layer was extracted with EtOAc (2 x 30 mL), and the combined organic layer was washed with brine (15 mL), passed through a hydrophobic frit and concentrated under reduced pressure. The crude product was purified by reverse phase preparative HPLC, with 30-85% MeCN (with 0.1% ammonia modifier)/10 mM aqueous ammonium bicarbonate as the eluent, to afford **2.1.8f** (0.91 g, 58%) as an amber coloured oil.

LCMS (Method A, UV, ESI) $R_t = 1.33$ min, $[M+H]^+$ 190.2

¹H NMR (CDCl₃, 400 MHz): δ 7.41 (d, $J = 7.3$ Hz, 2H), 7.36 (t, $J = 7.4$ Hz, 2H), 7.28 (tt, $J = 7.1, 2.5$ Hz, 1H), 3.70 (s, 2H), 2.69 (br. t, $J = 5.2$ Hz, 4H), 1.69 (br. s, 8H).

1-Benzylazepan-2-one 2.2.5

General procedure for the iodine-mediated C–H oxidation of cyclic amines A was followed. Iodine (503 mg, 1.98 mmol) was added to a mixture of **2.1.8f** (50 mg, 0.26 mmol) and sodium bicarbonate (222 mg, 2.64 mmol) in THF/H₂O (7.6/3.0 mL). Purification was carried out by silica gel chromatography using 30-65% TBME (with 1% 4M ammonia in methanol modifier)/cyclohexane as the eluent, to afford **2.2.5** (35.5 mg, 66%) as a brown oil.

LCMS (Method A, UV, ESI) $R_t = 0.95$ min, $[M+H]^+$ 204.1

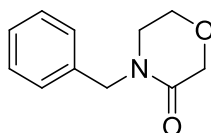
^1H NMR (CDCl_3 , 400 MHz): δ 7.22-7.35 (m, 5H), 4.59 (s, 2H), 3.24-3.35 (m, 2H), 2.57-2.64 (m, 2H), 1.64-1.75 (m, 4H), 1.45-1.54 (m, 2H)

^{13}C NMR (CDCl_3 , 101 MHz): δ 176.0, 137.9, 128.5, 128.1, 127.3, 51.1, 48.9, 37.2, 29.9, 28.1, 23.4

IR ν_{max} (cm^{-1}) (thin film): 2928, 2856, 1635

HRMS: Calculated for $\text{C}_{13}\text{H}_{18}\text{NO}$ $[\text{M}+\text{H}]^+$: 204.1383, found $[\text{M}+\text{H}]^+$: 204.1379 (-1.9 ppm).

4-Benzylmorpholin-3-one 2.2.6



General procedure for the iodine-mediated C–H oxidation of cyclic amines B was followed. Iodine (537 mg, 2.12 mmol) was added to a mixture of **2.1.8g** (48.4 μL , 0.28 mmol) and sodium bicarbonate (237 mg, 2.82 mmol) in DMSO/ H_2O (8.1/3.2 mL). Purification was carried out by silica gel chromatography using 30-80% TBME (with 2% triethylamine and 5% methanol modifier)/cyclohexane as the eluent, to afford **2.2.6** (42.0 mg, 78%) as a colourless oil.

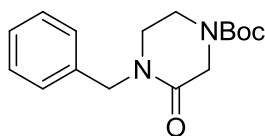
LCMS (Method A, UV, ESI) R_t = 0.71 min, $[\text{M}+\text{H}]^+$ 192.0

^1H NMR (CDCl_3 , 400 MHz): δ 7.26-7.38 (m, 5H), 4.64 (s, 2H), 4.26 (s, 2H), 3.85 (t, J = 5.3 Hz, 2H), 3.28 (t, J = 5.0 Hz, 2H)

^{13}C NMR (CDCl_3 , 101 MHz): δ 166.8, 136.1, 128.7, 128.3, 127.7, 68.2, 63.9, 49.5, 45.5

IR ν_{max} (cm^{-1}) (thin film): 2924, 2866, 1646

HRMS: Calculated for $\text{C}_{11}\text{H}_{14}\text{NO}_2$ $[\text{M}+\text{H}]^+$: 192.1019, found $[\text{M}+\text{H}]^+$: 192.1019 (-0.2 ppm).

***tert*-Butyl 4-benzyl-3-oxopiperazine-1-carboxylate 2.2.7**

General procedure for the iodine-mediated C–H oxidation of cyclic amines A was followed. Iodine (381 mg, 1.50 mmol) was added to a mixture of **2.1.8h** (55 mg, 0.20 mmol) and sodium bicarbonate (168 mg, 2.00 mmol) in THF/H₂O (5.7/2.3 mL). ¹H NMR analysis of the crude material showed 56% conversion to **2.2.7** based on the peak at 4.62 ppm, and 41% remaining starting material. Purification was carried out by silica gel chromatography using 0-35% TBME (with 1% triethylamine and 5% methanol modifier)/cyclohexane as the eluent, to afford **2.2.7** (25.6 mg, 44%) as a white solid.

LCMS (Method A, UV, ESI) R_t = 1.04 min, [M+H]⁺ 291.1

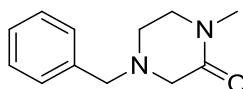
¹H NMR (CDCl₃, 400 MHz): δ 7.24-7.38 (m, 5H), 4.63 (s, 2H), 4.17 (s, 2H), 3.59 (t, *J* = 5.4 Hz, 2H), 3.23-3.29 (m, 2H), 1.46 (s, 9H)

¹³C NMR (CDCl₃, 101 MHz): δ 165.7, 153.8, 136.2, 128.8, 128.2, 127.8, 80.8, 50.0, 48.0, 45.6, 40.0, 28.3

IR ν_{max} (cm⁻¹) (thin film): 2976, 1694, 1650, 1494

HRMS: Calculated for C₁₆H₂₂N₂O₃Na [M+Na]⁺: 313.1529, found [M+Na]⁺: 313.1522 (-2.2 ppm)

M.pt.: 89-92 °C.

4-Benzyl-1-methylpiperazin-2-one 2.2.8

General procedure for the iodine-mediated C–H oxidation of cyclic amines A was followed. Iodine (381 mg, 1.50 mmol) was added to a mixture of **2.1.8i** (38 mg, 0.20 mmol) and sodium bicarbonate (168 mg, 2.00 mmol) in THF/H₂O (5.7/2.3 mL). ¹H

NMR analysis of the crude material showed 45% conversion to **2.2.8** based on the peak at 3.54 ppm, and 29% remaining starting material against 3,4,5-trichloropyridine (0.12 mmol) as a standard. Purification was carried out by silica gel chromatography using 30-100% TBME (with 1% triethylamine and 5% methanol modifier)/cyclohexane as the eluent, to afford **2.2.8** (13.8 mg, 34%) as a colourless oil.*

LCMS (Method A, UV, ESI) $R_t = 0.73$ min, $[M+H]^+$ 205.2

^1H NMR (CDCl_3 , 400 MHz): δ 7.24-7.36 (m, 5H), 3.55 (s, 2H), 3.30 (t, $J = 5.3$ Hz, 2H), 3.16 (s, 2H), 2.95 (s, 3H), 2.67 (t, $J = 5.6$ Hz, 2H)

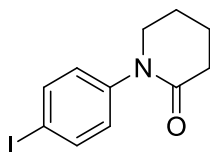
^{13}C NMR (CDCl_3 , 101 MHz): δ 167.1, 136.9, 129.0, 128.4, 127.5, 61.9, 57.4, 49.2, 48.7, 33.8

IR ν_{max} (cm^{-1}) (thin film): 2924, 2807, 1645

HRMS: Calculated for $\text{C}_{12}\text{H}_{17}\text{N}_2\text{O}$ $[M+H]^+$: 205.1335, found $[M+H]^+$: 205.1326 (-4.7 ppm).

**LCMS showed 11% area of an poorly ionising unknown artefact at 0.64 min, but no impurity was observed by NMR, so the peak was attributed to some small amount of a highly UV active impurity.*

1-(4-Iodophenyl)piperidin-2-one **2.2.9**



General procedure for the iodine-mediated C–H oxidation of cyclic amines A was followed. Iodine (381 mg, 1.50 mmol) was added to a mixture of **2.1.8j** (32.0 μL , 0.20 mmol) and sodium bicarbonate (168 mg, 2.00 mmol) in THF/ H_2O (5.7/2.3 mL). Purification was carried out by silica gel chromatography using 40-85% TBME (with 1% triethylamine and 5% methanol modifier)/cyclohexane as the eluent, to afford **2.2.9** (32.3 mg, 54%) as a white solid.

LCMS (Method A, UV, ESI) $R_t = 0.97$ min, $[M+H]^+$ 302.0

^1H NMR (CDCl_3 , 400 MHz): δ 7.70 (d, $J = 8.6$ Hz, 2H), 7.03 (d, $J = 8.6$ Hz, 2H), 3.62 (t, $J = 5.9$ Hz, 2H), 2.55 (t, $J = 6.0$ Hz, 2H), 1.88-2.00 (m, 4H)

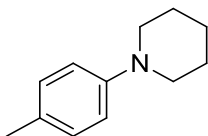
^{13}C NMR (CDCl_3 , 101 MHz): δ 169.9, 143.1, 138.2, 128.1, 91.3, 51.4, 32.9, 23.5, 21.4

IR ν_{max} (cm^{-1}) (thin film): 2940, 2863, 1630

HRMS: Calculated for $\text{C}_{11}\text{H}_{13}\text{NOI}$ $[\text{M}+\text{H}]^+$: 302.0036, found $[\text{M}+\text{H}]^+$: 302.0032 (-1.4 ppm)

M.pt.: 117-120 °C.

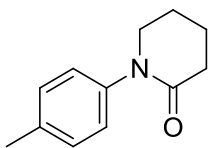
1-(*para*-Tolyl)piperidine **2.1.8k**²⁸¹



Under a nitrogen atmosphere, 4-chlorotoluene (0.59 mL, 5.0 mmol) was added to a solution of piperidine (0.59 mL, 6.0 mmol), 1,3-*bis*-(2,6-diisopropylphenyl)-1*H*-imidazol-3-ium chloride (85 mg, 0.2 mmol), potassium *tert*-butoxide (842 mg, 7.5 mmol) and $\text{Pd}_2(\text{dba})_3$ (46 mg, 0.05 mmol) in 1,4-dioxane (15 mL), and the reaction mixture was stirred at 100 °C for 24 h. The reaction mixture was allowed to cool to RT, before addition of water (20 mL) and extraction into diethyl ether (2 x 30 mL). The combined organic layer was washed with brine (25 mL), passed through a hydrophobic frit and concentrated under reduced pressure. The crude material was purified by silica gel chromatography using 0-40% (3:1 EtOAc:EtOH)/cyclohexane as the eluent, to afford **2.1.8k** (363 mg, 41%) as a yellow oil.

LCMS (Method A, UV, ESI) $R_t = 1.34$ min, $[\text{M}+\text{H}]^+$ 176.2

^1H NMR (CDCl_3 , 400 MHz): δ 7.07 (d, $J = 8.3$ Hz, 2H), 6.87 (d, $J = 8.6$ Hz, 2H), 3.11 (t, $J = 5.4$ Hz, 4H), 2.28 (s, 3H), 1.73 (quin, $J = 5.6$ Hz, 4H), 1.57 (quin, $J = 5.8$ Hz, 2H).

1-(*para*-Tolyl)piperidin-2-one 2.2.10

General procedure A was followed, except with the amendment that iodine was added to the reaction mixture in three portions of 2.5 equivalents after 0 h, 1 h and 2 h. Iodine (381 mg, 1.50 mmol) was added in three portions to a mixture of **2.1.8k** (35 mg, 0.20 mmol) and sodium bicarbonate (168 mg, 2.00 mmol) in THF/H₂O (5.7/2.3 mL). Purification was carried out by silica gel chromatography using 35-80% TBME (with 1% triethylamine, 5% methanol modifier)/cyclohexane as the eluent, to afford **2.2.10** (21.2 mg, 56%) as a white solid.

LCMS (Method A, UV, ESI) $R_t = 0.85$ min, $[M+H]^+$ 190.1

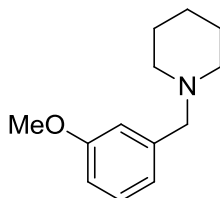
¹H NMR (CDCl₃, 400 MHz): δ 7.20 (d, $J = 8.3$ Hz, 2H), 7.13 (d, $J = 8.3$ Hz, 2H), 3.59-3.65 (m, 2H), 2.56 (t, $J = 5.6$ Hz, 2H), 2.35 (s, 3H), 1.90-1.99 (m, 4H)

¹³C NMR (CDCl₃, 101 MHz): δ 170.0, 140.9, 136.5, 129.8, 126.0, 51.8, 32.9, 23.6, 21.5, 21.0

IR ν_{max} (cm⁻¹) (thin film): 2950, 1634, 1489

HRMS: Calculated for C₁₂H₁₆NO $[M+H]^+$: 190.1232, found $[M+H]^+$: 190.1232 (0.0 ppm)

M.pt.: 88-90 °C.

1-(3-Methoxybenzyl)piperidine 2.1.8l²⁸²

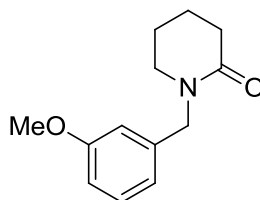
Piperidine (0.85 mL, 8.6 mmol), 3-methoxybenzyl bromide (1.00 mL, 7.1 mmol) and potassium carbonate (3.0 g, 21.4 mmol) were heated to 80 °C in MeCN (14 mL) for

96 h. The reaction mixture was cooled to RT, and then passed through a sintered funnel and the filtrate was concentrated under reduced pressure. The crude material was purified by silica gel chromatography, with 0-40% EtOAc/cyclohexane, to afford **2.1.81** (1.01 g, 69%) as a yellow oil.

LCMS (Method A, UV, ESI) $R_t = 1.16$ min, $[M+H]^+$ 206.1

^1H NMR (CDCl_3 , 400 MHz): δ 7.22 (t, $J = 8.1$ Hz, 1H), 6.89-6.93 (m, 2H), 6.79 (ddd, $J = 8.3, 2.7, 1.0$ Hz, 1H), 3.82 (s, 3H), 3.46 (s, 2H), 2.34-2.42 (m, 4H), 1.59 (quin, $J = 5.6$ Hz, 4H), 1.39-1.49 (m, 2H).

1-(3-Methoxybenzyl)piperidin-2-one **2.2.11**



General procedure for the iodine-mediated C–H oxidation of cyclic amines **A** was followed. Iodine (381 mg, 1.50 mmol) was added to a mixture of **2.1.81** (41.1 mg, 0.20 mmol) and sodium bicarbonate (168 mg, 2.00 mmol) in THF/ H_2O (5.7/2.3 mL). Purification was carried out by silica gel chromatography using 0-100% EtOAc/cyclohexane as the eluent, to afford **2.2.11** (36.9 mg, 84%) as a colourless oil.

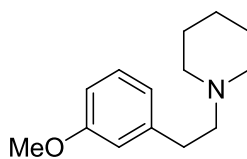
LCMS (Method A, UV, ESI) $R_t = 0.85$ min, $[M+H]^+$ 220.1

^1H NMR (CDCl_3 , 400 MHz): δ 7.18-7.25 (m, 1H), 6.76-6.85 (m, $J = 2.2$ Hz, 3H), 4.56 (s, 2H), 3.78 (s, 3H), 3.19 (t, $J = 5.5$ Hz, 2H), 2.45 (t, $J = 6.4$ Hz, 2H), 1.72-1.84 (m, 4H)

^{13}C NMR (CDCl_3 , 101 MHz): δ 169.7, 159.8, 138.9, 129.4, 120.3, 113.5, 112.6, 55.1, 49.9, 47.2, 32.3, 23.1, 21.3

IR ν_{max} (cm^{-1}) (thin film): 2943, 1634, 1489

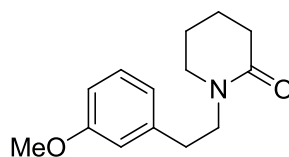
HRMS: Calculated for $\text{C}_{13}\text{H}_{18}\text{NO}_2$ $[M+H]^+$: 220.1338, found $[M+H]^+$: 220.1338 (0.0 ppm).

1-(3-Methoxyphenethyl)piperidine 2.1.8m²⁸³

Magnesium sulfate (366 mg, 3.0 mmol) was added to a solution of piperidine (0.5 mL, 5.06 mmol), 2-(3-methoxyphenyl)acetaldehyde (0.73 mL, 5.1 mmol) and DIPEA (2.7 mL, 15.2 mmol) in THF (75 mL). The resulting suspension was stirred at RT for 5 min, before addition of sodium triacetoxyborohydride (2.15 g, 10.1 mmol) and stirring was continued overnight. The solvent was removed under reduced pressure, and the residue was dissolved in DCM (20 mL). The solution was washed with saturate aqueous NaHCO₃ (20 mL), the organic layer washed with DCM (20 mL) and the combined organic layer was passed through a hydrophobic frit and concentrated under reduced pressure. The crude material was purified by silica gel chromatography, using 0-65% (3:1 EtOAc/EtOH, 1% Et₃N modifier)/cyclohexane as the eluent, to afford **2.1.8m** (932 mg, 84%) as a light yellow oil.

LCMS (Method A, UV, ESI) R_t = 1.15 min, [M+H]⁺ 220.1

¹H NMR (CDCl₃, 400 MHz): δ 7.20 (t, *J* = 7.8 Hz, 1H), 6.72-6.83 (m, 3H), 3.80 (s, 3H), 2.77-2.83 (m, 2H), 2.53-2.60 (m, 2H), 2.43-2.51 (m, 4H), 1.63 (quin, *J* = 5.6 Hz, 4H), 1.43-1.51 ppm (m, 2H).

1-(3-Methoxyphenethyl)piperidin-2-one 2.2.12

General procedure for the iodine-mediated C–H oxidation of cyclic amines A was followed. Iodine (381 mg, 1.50 mmol) was added to a mixture of **2.1.8m** (43.9 mg, 0.20 mmol) and sodium bicarbonate (168 mg, 2.00 mmol) in THF/H₂O (5.7/2.3 mL). Purification was carried out by silica gel chromatography using 0-100% EtOAc/cyclohexane as the eluent, to afford **2.2.12** (32.5 mg, 70%) as a colourless oil.

LCMS (Method A, UV, ESI) $R_t = 0.90$ min, $[M+H]^+$ 234.1

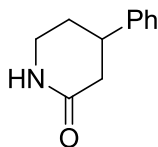
^1H NMR (CDCl_3 , 400 MHz): δ 7.20 (t, $J = 7.7$ Hz, 1H), 6.81 (d, $J = 7.6$ Hz, 1H), 6.74-6.79 (m, 2H), 3.80 (s, 3H), 3.52-3.60 (m, $J = 7.1$ Hz, 2H), 3.12 (t, $J = 5.6$ Hz, 2H), 2.83-2.88 (m, $J = 8.1, 6.8$ Hz, 2H), 2.37 (t, $J = 6.4$ Hz, 2H), 1.67-1.78 (m, $J = 4.8, 2.3$ Hz, 4H)

^{13}C NMR (CDCl_3 , 101 MHz): δ 169.6, 159.7, 140.9, 129.4, 121.2, 114.4, 111.8, 55.2, 49.3, 48.7, 33.6, 32.4, 23.2, 21.3

IR ν_{max} (cm^{-1}) (thin film): 2939, 1631, 1490

HRMS: Calculated for $\text{C}_{14}\text{H}_{20}\text{NO}_2$ $[M+H]^+$: 234.1494, found $[M+H]^+$: 234.1495 (0.4 ppm).

4-Phenylpiperidin-2-one 2.2.13



General procedure for the iodine-mediated C–H oxidation of cyclic amines **C** was followed. Iodine (590 mg, 2.33 mmol) was added to a mixture of **2.1.8n** (50 mg, 0.31 mmol) and sodium bicarbonate (260 mg, 3.10 mmol) in THF/ H_2O (8.9/3.5 mL). ^1H NMR analysis of the crude material showed 51% conversion to **2.2.13** based on the peak at 3.40 ppm, and 45% remaining starting material against 3,4,5-trichloropyridine (0.07 mmol) as a standard. Purification was carried out by reverse phase chromatography with 0-60% MeCN/10mM aqueous ammonium bicarbonate as the eluent, to afford **2.2.13** (23.6 mg, 43%) as a white solid.

LCMS (Method A, UV, ESI) $R_t = 0.75$ min, $[M+H]^+$ 176.1

^1H NMR (CDCl_3 , 400 MHz): δ 7.36 (t, $J = 7.6$ Hz, 2H), 7.20-7.31 (m, 3H), 6.64 (br. s., 1H), 3.37-3.47 (m, 2H), 3.12 (tdd, $J = 11.1, 5.4, 2.9$ Hz, 1H), 2.71 (ddd, $J = 17.6, 5.4, 2.0$ Hz, 1H), 2.51 (dd, $J = 17.9, 11.2$ Hz, 1H), 2.06-2.15 (m, 1H), 1.89-2.02 (m, 1H)

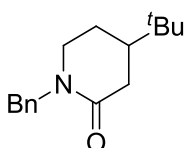
^{13}C NMR (CDCl_3 , 101 MHz): δ 172.1, 143.5, 128.8, 126.8, 126.6, 41.4, 38.7, 38.4, 29.6

IR ν_{max} (cm^{-1}) (thin film): 3178 (br), 3056 (br), 2949, 1666, 1493

HRMS: Calculated for $\text{C}_{11}\text{H}_{14}\text{NO}$ $[\text{M}+\text{H}]^+$: 176.1075, found $[\text{M}+\text{H}]^+$: 176.1071 (-2.3 ppm)

M.pt.: 140-143 °C.

1-Benzyl-4-(*tert*-butyl)piperidin-2-one **2.2.14**



General procedure for the iodine-mediated C–H oxidation of cyclic amines **A** was followed. Iodine (381 mg, 1.50 mmol) was added to a mixture of **2.1.8o** (46.3 mg, 0.20 mmol) and sodium bicarbonate (168 mg, 2.00 mmol) in THF/ H_2O (5.7/2.3 mL). Purification was carried out by silica gel chromatography using 0-100% TBME/cyclohexane as the eluent, to afford **2.2.14** (37.3 mg, 76%) as a colourless oil.

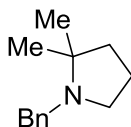
LCMS (Method A, UV, ESI) R_t = 1.19 min, $[\text{M}+\text{H}]^+$ 246.1

^1H NMR (CDCl_3 , 400 MHz): δ 7.28-7.34 (m, 2H), 7.21-7.27 (m, 3H), 4.67 (d, J = 14.7 Hz, 1H), 4.51 (d, J = 14.7 Hz, 1H), 3.23 (ddd, J = 12.0, 5.6, 2.2 Hz, 1H), 3.14 (td, J = 12.0, 4.2 Hz, 1H), 2.56 (ddd, J = 17.1, 4.9, 2.7 Hz, 1H), 2.18 (dd, J = 17.4, 12.5 Hz, 1H), 1.82-1.89 (m, 1H), 1.54 (tdd, J = 12.4, 5.0, 2.7 Hz, 1H), 1.38 (qd, J = 12.2, 5.4 Hz, 1H), 0.87 (s, 9H)

^{13}C NMR (CDCl_3 , 101 MHz): δ 170.3, 137.2, 128.5, 128.0, 127.2, 49.8, 47.1, 43.2, 34.3, 31.9, 26.7, 24.5

IR ν_{max} (cm^{-1}) (thin film): 2959, 1637, 1495

HRMS: Calculated for $\text{C}_{16}\text{H}_{24}\text{NO}$ $[\text{M}+\text{H}]^+$: 246.1858, found $[\text{M}+\text{H}]^+$: 246.1858 (0.0 ppm).

1-Benzyl-2,2-dimethylpyrrolidine 2.1.8p²⁸³

2,2-Dimethylpyrrolidine hydrochloride (753 mg, 5.6 mmol), benzyl bromide (0.60 mL, 5.0 mmol) and potassium carbonate (2.1 g, 15.1 mmol) were heated to 60 °C in MeCN (15 mL) for 20 h. The reaction mixture was cooled to RT, and then passed through a sintered funnel and the filtrate was concentrated under reduced pressure. The crude material was purified by silica gel chromatography, with 0-20% TBME/cyclohexane, to afford **2.1.8p** (706 mg, 74%) as a colourless oil.

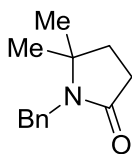
LCMS (Method A, UV, ESI) $R_t = 1.26$ min, $[M+H]^+$ 190.1

¹H NMR (CDCl₃, 400 MHz): δ 7.28-7.38 (m, 4H), 7.23 (tt, $J = 7.1, 2.4$ Hz, 1H), 3.53 (s, 2H), 2.59-2.66 (m, 2H), 1.65-1.75 (m, 4H), 1.11 (s, 6H).

1-Benzyl-5,5-dimethylpyrrolidin-2-one 2.2.15 and 1-benzyl-3-iodo-5,5-dimethylpyrrolidin-2-one 2.2.15b

General procedure for the iodine-mediated C–H oxidation of cyclic amines A was followed. Iodine (381 mg, 1.50 mmol) was added to a mixture of **2.1.8p** (37.9 mg, 0.20 mmol) and sodium bicarbonate (168 mg, 2.00 mmol) in THF/H₂O (5.7/2.3 mL). Purification was carried out by silica gel chromatography using 0-100% EtOAc/cyclohexane as the eluent, to afford **2.2.15** (29.6 mg, 73%) as an amber coloured oil, and **2.2.15b** (8.0 mg, 12%) as an amber coloured oil.

1-Benzyl-5,5-dimethylpyrrolidin-2-one 2.2.15



LCMS (Method A, UV, ESI) $R_t = 0.92$ min, $[M+H]^+$ 204.1

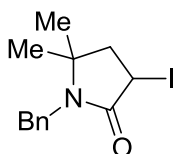
^1H NMR (CDCl_3 , 400 MHz): δ 7.29 (d, $J = 4.4$ Hz, 4H), 7.19-7.25 (m, 1H), 4.42 (s, 2H), 2.48 (t, $J = 7.9$ Hz, 2H), 1.87 (t, $J = 7.8$ Hz, 2H), 1.13 (s, 6H)

^{13}C NMR (CDCl_3 , 101 MHz): δ 174.7, 139.0, 128.3, 127.6, 126.9, 60.9, 42.7, 34.5, 29.6, 26.9

IR ν_{max} (cm^{-1}) (thin film): 2966, 1676, 1400

HRMS: Calculated for $[M+H]^+$: $\text{C}_{13}\text{H}_{18}\text{NO}$ 204.1388, found $[M+H]^+$: 204.1382 (-2.9 ppm).

1-Benzyl-3-iodo-5,5-dimethylpyrrolidin-2-one 2.2.15b



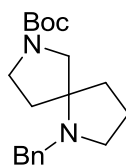
LCMS (Method A, UV, ESI) $R_t = 1.08$ min, $[M+H]^+$ 329.9

^1H NMR (CDCl_3 , 400 MHz): δ 7.23-7.37 (m, 5H), 4.78 (dd, $J = 8.6, 5.1$ Hz, 1H), 4.56 (d, $J = 15.4$ Hz, 1H), 4.42 (d, $J = 15.6$ Hz, 1H), 2.56 (dd, $J = 14.4, 8.6$ Hz, 1H), 2.41 (dd, $J = 14.2, 4.6$ Hz, 1H), 1.32 (s, 3H), 1.16 (s, 3H)

^{13}C NMR (CDCl_3 , 101 MHz): δ 172.0, 138.2, 128.5, 127.8, 127.3, 46.3, 43.7, 28.4, 26.3, 15.5

IR ν_{max} (cm^{-1}) (thin film): 2967, 1681, 1401

HRMS: Calculated for $\text{C}_{13}\text{H}_{17}\text{NOI}$ $[M+H]^+$: 330.0355, found $[M+H]^+$: 330.0348 (-2.1 ppm).

***tert*-Butyl 1-benzyl-1,7-diazaspiro[4.4]nonane-7-carboxylate 2.1.8q**

A mixture of *tert*-butyl-1,7-diazaspiro[4.4]nonane-7-carboxylate (1.0 g, 4.4 mmol), benzyl bromide (0.45 mL, 3.8 mmol) and potassium carbonate (1.6 g, 11.4 mmol) were heated to 60 °C in MeCN (11 mL) for 20 h. The reaction mixture was cooled to RT, and then passed through a sintered funnel and the filtrate was concentrated under reduced pressure. The crude material was purified by silica gel chromatography, with 30-85% TBME/cyclohexane, to afford **2.1.8q** (567 mg, 47%) as a colourless oil.

LCMS (Method A, UV, ESI) $R_t = 1.40$ min, $[M+H]^+$ 317.2

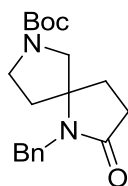
1H NMR (DMSO- d_6 , 400 MHz, 120 °C): δ 7.25-7.32 (m, 4H), 7.17-7.24 (m, 1H), 3.62-3.72 (m, 2H), 3.45 (ddd, $J = 10.9, 8.9, 3.7$ Hz, 1H), 3.35 (d, $J = 11.0$ Hz, 1H), 3.26 (dt, $J = 11.1, 8.1$ Hz, 1H), 3.13 (d, $J = 11.0$ Hz, 1H), 2.59-2.70 (m, 2H), 2.09 (dt, $J = 12.5, 8.8$ Hz, 1H), 1.80 (s, 2H), 1.64-1.78 (m, 3H), 1.43 (s, 9H)

^{13}C NMR (DMSO- d_6 , 101 MHz): δ 154.8 (2C), 154.7, 140.2, 128.3, 128.2, 126.7, 79.1, 69.9, 69.2, 53.3, 53.1, 51.8, 50.7, 44.7, 44.4, 38.0, 37.8, 31.9, 30.7, 28.5, 20.9, 20.8

More than the expected number of ^{13}C signals because restricted rotation led to formation of a mixture of rotamers at RT.

IR ν_{max} (cm $^{-1}$) (thin film): 2969, 1693, 1396

HRMS: Calculated for C $_{19}$ H $_{29}$ N $_2$ O $_2$ $[M+H]^+$: 317.2229, found $[M+H]^+$: 317.2225 (-1.2 ppm).

***tert*-Butyl 1-benzyl-2-oxo-1,7-diazaspiro[4.4]nonane-7-carboxylate 2.2.16**

General procedure for the iodine-mediated C–H oxidation of cyclic amines A was followed. Iodine (381 mg, 1.50 mmol) was added to a mixture of **2.1.8q** (63.3 mg, 0.20 mmol) and sodium bicarbonate (168 mg, 2.00 mmol) in THF/H₂O (5.7/2.3 mL). Purification was carried out by silica gel chromatography using 80-100% TBME/cyclohexane as the eluent, to afford **2.2.16** (48.1 mg, 73%) as a yellow gum.

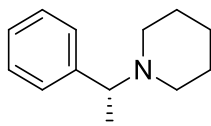
LCMS (Method A, UV, ESI) $R_t = 1.05$ min, $[M+H]^+$ 331.1

¹H NMR (DMSO-*d*₆, 400 MHz, 393 K): δ 7.19-7.33 (m, 5H), 4.42 (s, 2H), 3.34-3.42 (m, 1H), 3.11-3.29 (m, 3H), 2.38-2.45 (m, 2H), 2.03 (m, 3H), 1.69-1.78 (m, 1H), 1.40 (s, 9H)

¹³C NMR (DMSO-*d*₆, 101 MHz): δ 175.1, 154.4, 138.1, 128.6, 127.3, 126.9, 79.8, 68.2, 52.5, 43.8, 43.1, 35.0, 32.4, 29.3, 28.4

IR ν_{\max} (cm⁻¹) (thin film): 2973, 1677, 1397

HRMS: Calculated for C₁₉H₂₇N₂O₃ $[M+H]^+$: 331.2021, found $[M+H]^+$: 331.2016 (-1.6 ppm).

(*R*)-1-(1-Phenylethyl)piperidine 2.1.8r²⁸⁴

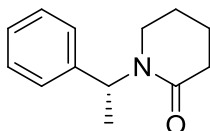
A solution of (*R*)-1-phenylethylamine (0.80 mL, 6.2 mmol) in MeCN (8.8 mL) was added to a mixture of 1,5-dibromopentane (1.05 mL, 7.4 mmol) and potassium carbonate (3.4 g, 24.8 mmol) in MeCN (16.0 mL). The reaction mixture was stirred at 50 °C for 42 h. The reaction mixture was allowed to cool to RT, and then filtered through a sintered funnel and the filtrate was concentrated under reduced pressure.

The crude material was purified by silica gel chromatography, with 35-80% TBME (5% methanol, 2% triethylamine modifier)/cyclohexane to afford **2.1.8r** (0.95 g, 81%) as a colourless oil.

LCMS (Method A, UV, ESI) $R_t = 1.23$ min, $[M+H]^+$ 190.1

^1H NMR (CDCl_3 , 400 MHz): δ 7.31 (d, $J = 4.5$ Hz, 4H), 7.21-7.26 (m, 1H), 3.41 (q, $J = 6.8$ Hz, 1H), 2.31-2.46 (m, 4H), 1.56 (quin, $J = 5.6$ Hz, 4H), 1.41 (t, $J = 5.8$ Hz, 2H), 1.38 (d, $J = 6.8$ Hz, 3H).

(R)-1-(1-Phenylethyl)piperidin-2-one 2.2.17



General procedure for the iodine-mediated C–H oxidation of cyclic amines A was followed. Iodine (381 mg, 1.50 mmol) was added to a mixture of **2.1.8r** (38 mg, 0.20 mmol) and sodium bicarbonate (168 mg, 2.00 mmol) in THF/ H_2O (5.7/2.3 mL). Purification was carried out by silica gel chromatography using 0-20% TBME (with 1% triethylamine and 5% methanol modifier)/cyclohexane as the eluent, to afford **2.2.17** (21.6 mg, 53%) as an amber coloured oil.*

LCMS (Method A, UV, ESI) $R_t = 0.93$ min, $[M+H]^+$ 204.2

^1H NMR (CDCl_3 , 400 MHz): δ 7.22-7.40 (m, 5H), 6.16 (q, $J = 7.1$ Hz, 1H), 3.11 (ddd, $J = 12.3, 7.9, 4.6$ Hz, 1H), 2.76-2.83 (m, 1H), 2.49 (t, $J = 6.7$ Hz, 2H), 1.70-1.81 (m, 3H), 1.57-1.68 (m, 1H), 1.51 (d, $J = 7.3$ Hz, 3H)

^{13}C NMR (CDCl_3 , 101 MHz): δ 169.6, 140.5, 128.4, 127.3, 127.2, 49.7, 41.4, 32.5, 23.2, 21.2, 15.3

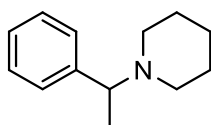
IR ν_{max} (cm^{-1}) (thin film): 2940, 1628, 1417

HRMS: Calculated for $\text{C}_{13}\text{H}_{18}\text{NO}$ $[M+H]^+$: 204.1388, found $[M+H]^+$: 204.1397 (4.3 ppm)

Chiral HPLC (25 cm Chiralpak AS, 40% EtOH/*n*-heptane, 1.0 mL/min, detection at 215 nm) $R_t = 3.9$ min (major) and 8.0 min (minor), ee = 98.8%.²⁸⁵

*LCMS showed 7% area of an unknown artefact at 1.09 min, which ionised to $m/z = 330.0$ (ES, positive mode). No impurity was observed by NMR, so the peak was proposed to be a trace amount of the corresponding highly UV-active iodo-lactam.

1-(1-Phenylethyl)piperidine 2.8.1

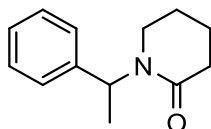


A solution of 1-phenylethanamine (0.80 mL, 6.2 mmol) in MeCN (8.8 mL) was added to a mixture of 1,5-dibromopentane (1.05 mL, 7.4 mmol) and potassium carbonate (3.4 g, 24.8 mmol) in MeCN (16.0 mL). The reaction mixture was stirred at 50 °C for 42 h. The reaction mixture was allowed to cool to RT, and then filtered through a sintered funnel and the filtrate was concentrated under reduced pressure. The crude material was purified by silica gel chromatography, with 35-80% TBME (5% methanol, 2% triethylamine modifier)/cyclohexane to afford **2.8.1** (1.02 g, 87%) as a colourless oil.

LCMS (Method A, UV, ESI) $R_t = 1.24$ min, $[M+H]^+$ 190.2

¹H NMR (CDCl₃, 400 MHz): δ 7.33 (d, $J = 4.3$ Hz, 4H), 7.22-7.28 (m, 1H), 3.42 (q, $J = 6.8$ Hz, 1H), 2.31-2.48 (m, 4H), 1.58 (quin, $J = 6.3$ Hz, 4H), 1.41-1.45 (m, 2H), 1.40 (d, $J = 6.8$ Hz, 3H).

1-(1-Phenylethyl)piperidin-2-one 2.8.2



General procedure for the iodine-mediated C–H oxidation of cyclic amines A was followed. Iodine (381 mg, 1.50 mmol) was added to a mixture of **2.8.1** (38 mg, 0.20

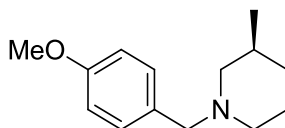
mmol) and sodium bicarbonate (168 mg, 2.00 mmol) in THF/H₂O (7.5/3.0 mL). Purification was carried out by silica gel chromatography using 10-60% TBME (with 5% MeOH, 1% triethylamine modifier)/cyclohexane as the eluent, but the resultant product was impure, so this material was re-purified by high pH MDAP (Method C) to afford **2.8.2** (11.1 mg, 27%) as an amber coloured oil.*

LCMS (Method A, UV, ESI) R_t = 0.94 min, [M+H]⁺ 204.1

¹H NMR (CDCl₃, 400 MHz): δ 7.23-7.39 (m, 5H), 6.18 (q, *J* = 7.1 Hz, 1H), 3.12 (ddd, *J* = 12.3, 8.0, 4.4 Hz, 1H), 2.76-2.86 (m, 1H), 2.50 (t, *J* = 6.7 Hz, 2H), 1.71-1.82 (m, 3H), 1.58-1.69 (m, 1H), 1.53 (d, *J* = 7.1 Hz, 3H)

**LCMS showed 13% area of a poorly ionising unknown artefact at 0.66 min, but no impurity was observed by NMR, so the peak was attributed to some small amount of a highly UV active impurity.*

(*S*)-1-(4-Methoxybenzyl)-3-methylpiperidine **2.1.8s**



A mixture of (*S*)-3-methylpiperidine (0.65 mL, 5.5 mmol), 4-methoxybenzyl chloride (0.68 mL, 5.0 mmol) and potassium carbonate (0.83 g, 6.0 mmol) were heated to 55 °C in MeCN (20 mL) for 42 h. The reaction mixture was cooled to RT, and then passed through a sintered funnel and the filtrate was concentrated under reduced pressure. The crude material was purified by silica gel chromatography, with 25-80% TBME (5% methanol, 2% triethylamine modifier)/cyclohexane, to afford **2.1.8s** (0.78 g, 71%) as a colourless oil.

LCMS (Method A, UV, ESI) R_t = 1.23 min, [M+H]⁺ 220.2

¹H NMR (CDCl₃, 400 MHz): δ 7.24 (d, *J* = 8.8 Hz, 2H), 6.86 (d, *J* = 8.6 Hz, 2H), 3.81 (s, 3H), 3.43 (s, 2H), 2.73-2.84 (m, 2H), 1.85 (td, *J* = 11.1, 3.5 Hz, 1H), 1.51-1.74 (m, 5H), 0.86-0.92 (m, 1H), 0.85 (d, *J* = 6.3 Hz, 3H)

^{13}C NMR (CDCl_3 , 101 MHz): δ 158.6, 130.7, 130.3, 113.5, 63.0, 61.9, 55.2, 53.9, 33.1, 31.1, 25.6, 19.8

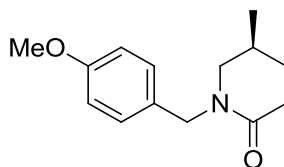
IR ν_{max} (cm^{-1}) (thin film): 2927, 1612, 1510

HRMS: Calculated for $\text{C}_{14}\text{H}_{22}\text{NO}$ $[\text{M}+\text{H}]^+$: 220.1696, found $[\text{M}+\text{H}]^+$: 220.1689 (-3.4 ppm).

(S)-1-(4-Methoxybenzyl)-5-methylpiperidin-2-one 2.2.18a and (S)-1-(4-methoxybenzyl)-3-methylpiperidin-2-one 2.2.18b

General procedure for the iodine-mediated C–H oxidation of cyclic amines A was followed. Iodine (381 mg, 1.50 mmol) was added to a mixture of **2.1.8s** (44 mg, 0.20 mmol) and sodium bicarbonate (168 mg, 2.00 mmol) in THF/ H_2O (5.7/2.3 mL). Purification was carried out by silica gel chromatography using 0-50% TBME (with 1% triethylamine and 5% methanol modifier)/cyclohexane as the eluent, with 15 min isochratically at 40% TBME (with 1% triethylamine and 5% methanol modifier)/cyclohexane to afford **2.2.18a** (24.9 mg, 53%) as a colourless oil, and **2.2.18b** (9.5 mg, 20%) as a colourless oil.

(S)-1-(4-Methoxybenzyl)-5-methylpiperidin-2-one 2.2.18a



LCMS (Method A, UV, ESI) R_t = 0.95 min, $[\text{M}+\text{H}]^+$ 234.2

^1H NMR (CDCl_3 , 400 MHz): δ 7.19 (d, J = 8.6 Hz, 2H), 6.85 (d, J = 8.6 Hz, 2H), 4.59 (d, J = 14.9 Hz, 1H), 4.44 (d, J = 14.1 Hz, 1H), 3.79 (s, 3H), 3.15 (ddd, J = 11.9, 5.1, 1.8 Hz, 1H), 2.80 (dd, J = 11.6, 10.4 Hz, 1H), 2.52 (ddd, J = 17.7, 6.1, 3.3 Hz, 1H), 2.36-2.47 (m, 1H), 1.87-1.96 (m, 1H), 1.78-1.86 (m, 1H), 1.45 (dtd, J = 13.1, 11.3, 5.9 Hz, 1H), 0.94 (d, J = 6.6 Hz, 3H)

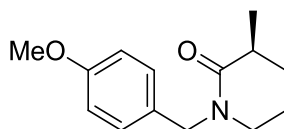
^{13}C NMR (CDCl_3 , 101 MHz): δ 169.6, 158.9, 129.4, 119.6, 113.9, 55.2, 53.9, 49.5, 31.7, 29.5, 29.0, 18.5

IR ν_{max} (cm^{-1}) (thin film): 2928, 2837, 1634

HRMS: Calculated for $\text{C}_{14}\text{H}_{20}\text{NO}_2$ $[\text{M}+\text{H}]^+$: 234.1489, found $[\text{M}+\text{H}]^+$: 234.1492 (1.6 ppm)

Chiral HPLC (25 cm Whelk-o 1, 10% EtOH/*n*-heptane, 1.0 mL/min, detection at 215 nm) $R_t = 39.6$ min, $ee > 99\%$.²⁸⁵

(S)-1-(4-Methoxybenzyl)-3-methylpiperidin-2-one 2.2.18b



LCMS (Method A, UV, ESI) $R_t = 0.97$ min, $[\text{M}+\text{H}]^+$ 234.2

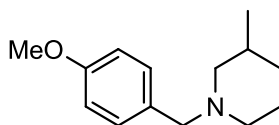
^1H NMR (CDCl_3 , 400 MHz): δ 7.19 (d, $J = 8.6$ Hz, 2H), 6.85 (d, $J = 8.6$ Hz, 2H), 4.60 (d, $J = 14.4$ Hz, 1H), 4.44 (d, $J = 14.4$ Hz, 1H), 3.80 (s, 3H), 3.19 (dd, $J = 7.3, 5.1$ Hz, 2H), 2.41-2.52 (m, 1H), 1.91-2.00 (m, 1H), 1.78-1.89 (m, 1H), 1.65-1.78 (m, 1H), 1.52 (dtd, $J = 12.9, 9.9, 3.3$ Hz, 1H), 1.29 (d, $J = 7.1$ Hz, 3H)

^{13}C NMR (CDCl_3 , 101 MHz): δ 173.2, 158.9, 129.7, 129.4, 113.9, 55.3, 49.6, 47.4, 36.7, 29.6, 21.7, 18.1

IR ν_{max} (cm^{-1}) (thin film): 2931, 2867, 1631

HRMS: Calculated for $\text{C}_{14}\text{H}_{20}\text{NO}_2$ $[\text{M}+\text{H}]^+$: 234.1489, found $[\text{M}+\text{H}]^+$: 234.1495 (2.6 ppm)

Chiral HPLC (25 cm Chiralpak AS-H, 25% EtOH/*n*-heptane, 1.0 mL/min, detection at 215 nm) $R_t = 5.3$ min (minor) and 6.4 min (major), $ee = 99.2\%$.²⁸⁵

1-(4-Methoxybenzyl)-3-methylpiperidine 2.8.3

A mixture of 3-methylpiperidine (0.65 mL, 5.5 mmol), 4-methoxybenzyl chloride (0.68 mL, 5.0 mmol) and potassium carbonate (0.83 g, 6.0 mmol) were heated to 55 °C in MeCN (20 mL) for 21 h. The reaction mixture was cooled to RT, and then passed through a sintered funnel and the filtrate was concentrated under reduced pressure. The crude material was purified by silica gel chromatography, with 0-20% (3:1 EtOAc/EtOH)/cyclohexane, to afford **2.8.3** (0.87 g, 79%) as a colourless oil.

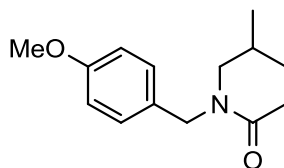
LCMS (Method A, UV, ESI) $R_t = 1.25$ min, $[M+H]^+$ 220.3

$^1\text{H NMR}$ (CDCl_3 , 400 MHz): δ 7.25 (d, $J = 8.8$ Hz, 2H), 6.87 (d, $J = 8.8$ Hz, 2H), 3.80 (s, 3H), 3.44 (s, 2H), 2.81 (t, $J = 10.7$ Hz, 2H), 1.86 (td, $J = 11.0, 3.8$ Hz, 1H), 1.53-1.75 (m, 5H), 0.88-0.94 (m, 1H), 0.87 (d, $J = 6.3$ Hz, 3H).

1-(4-Methoxybenzyl)-5-methylpiperidin-2-one 2.8.4a and 1-(4-methoxybenzyl)-3-methylpiperidin-2-one 2.8.4b

General procedure for the iodine-mediated C–H oxidation of cyclic amines A was followed. Iodine (952 mg, 3.75 mmol) was added to a mixture of **2.8.3** (110 mg, 0.50 mmol) and sodium bicarbonate (420 mg, 5.00 mmol) in THF/ H_2O (14.3/5.7 mL). Purification was carried out by silica gel chromatography using 0-50% TBME (with 1% Et_3N and 5% MeOH modifier)/cyclohexane as the eluent, with 15 min isochratically at 40% TBME (with 1% triethylamine and 5% methanol modifier)/cyclohexane to afford **2.8.4a** (21.6 mg, 19%) as a colourless oil, and **2.8.4b** (22.7 mg, 19%) as a colourless oil.*

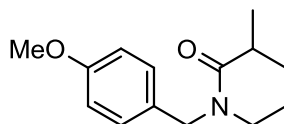
1-(4-Methoxybenzyl)-5-methylpiperidin-2-one 2.8.4a



LCMS (Method A, UV, ESI) $R_t = 0.96$ min, $[M+H]^+$ 234.1

$^1\text{H NMR}$ (CDCl_3 , 400 MHz): δ 7.19 (d, $J = 8.6$ Hz, 2H), 6.86 (d, $J = 8.6$ Hz, 2H), 4.59 (d, $J = 14.4$ Hz, 1H), 4.44 (d, $J = 14.4$ Hz, 1H), 3.80 (s, 3H), 3.16 (ddd, $J = 12.0, 5.1, 1.9$ Hz, 1H), 2.81 (dd, $J = 11.9, 10.4$ Hz, 1H), 2.53 (ddd, $J = 17.9, 5.8, 3.0$ Hz, 1H), 2.42 (ddd, $J = 17.9, 11.4, 6.6$ Hz, 1H), 1.79-1.98 (m, 2H), 1.45 (dtd, $J = 13.1, 11.3, 5.9$ Hz, 1H), 0.95 (d, $J = 6.6$ Hz, 3H).

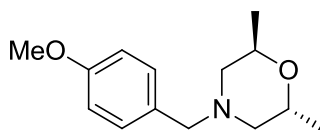
1-(4-methoxybenzyl)-3-methylpiperidin-2-one 2.8.4b



LCMS (Method A, UV, ESI) $R_t = 0.97$ min, $[M+H]^+$ 234.1

$^1\text{H NMR}$ (CDCl_3 , 400 MHz): δ 7.19 (d, $J = 8.6$ Hz, 2H), 6.86 (d, $J = 8.8$ Hz, 2H), 4.60 (d, $J = 14.4$ Hz, 1H), 4.44 (d, $J = 14.4$ Hz, 1H), 3.80 (s, 3H), 3.20 (dd, $J = 7.3, 5.1$ Hz, 2H), 2.40-2.53 (m, 1H), 1.96 (dtd, $J = 12.9, 6.3, 3.3$ Hz, 1H), 1.79-1.88 (m, 1H), 1.71 (ddd, $J = 17.2, 10.4, 6.9, 3.4$ Hz, 1H), 1.47-1.57 (m, 1H), 1.29 (d, $J = 7.3$ Hz, 3H).

*LCMS showed 13% area of an artefact at 1.12 min, which ionised with an $m/z = 359.9$ (ES, positive mode). No impurity was observed by NMR, so the peak was attributed to a trace amount of a highly UV-active iodinated lactam species.

(2*R*,6*R*)-4-(4-Methoxybenzyl)-2,6-dimethylmorpholine 2.1.8t

A mixture of (2*R*,6*R*)-2,6-dimethylmorpholine (0.70 mL, 5.5 mmol), 4-methoxybenzyl chloride (0.68 mL, 5.0 mmol) and potassium carbonate (0.83 g, 6.0 mmol) were heated to 50 °C in MeCN (20 mL) for 42 h. The reaction mixture was cooled to RT, and then passed through a sintered funnel and the filtrate was concentrated in vacuo. The crude material was purified by silica gel chromatography, with 0-20% (3:1 EtOAc:EtOH)/cyclohexane, to afford **2.1.8t** (1.03 g, 87%) as a colourless oil.

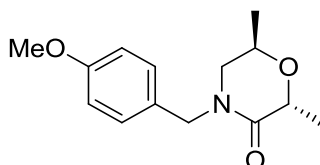
LCMS (Method A, UV, ESI) $R_t = 1.11$ min, $[M+H]^+$ 236.2

^1H NMR (CDCl_3 , 400 MHz): δ 7.25 (d, $J = 8.6$ Hz, 2H), 6.86 (d, $J = 8.6$ Hz, 2H), 4.01 (quind, $J = 6.3, 3.5$ Hz, 2H), 3.80 (s, 3H), 3.42 (d, $J = 12.6$ Hz, 1H), 3.33 (d, $J = 12.9$ Hz, 1H), 2.45 (dd, $J = 11.0, 3.2$ Hz, 2H), 2.13 (dd, $J = 11.0, 5.7$ Hz, 2H), 1.24 (d, $J = 6.3$ Hz, 6H)

^{13}C NMR (CDCl_3 , 101 MHz): δ 158.7, 130.4, 129.9, 113.6, 66.7, 62.5, 58.6, 55.2, 18.2

IR ν_{max} (cm^{-1}) (thin film): 2970, 2803, 1612, 1510

HRMS: Calculated for $\text{C}_{14}\text{H}_{22}\text{NO}_2$ $[M+H]^+$: 236.1645, found $[M+H]^+$: 236.1638 (-2.9 ppm).

(2*R*,6*R*)-4-(4-Methoxybenzyl)-2,6-dimethylmorpholin-3-one 2.2.19

General procedure for the iodine-mediated C–H oxidation of cyclic amines **B** was followed. Iodine (381 mg, 1.50 mmol) was added to a mixture of **2.1.8t** (47 mg, 0.20 mmol) and sodium bicarbonate (168 mg, 2.00 mmol) in DMSO/ H_2O (5.7/2.3 mL).

Purification was carried out by silica gel chromatography using 0-30% (3:1 EtOAc/EtOH)/cyclohexane as the eluent, to afford **2.2.19** (37.5 mg, 75%) as a colourless oil.

LCMS (Method A, UV, ESI) $R_t = 0.87$ min, $[M+H]^+$ 250.2

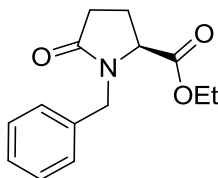
^1H NMR (CDCl_3 , 400 MHz): δ 7.19 (d, $J = 8.8$ Hz, 2H), 6.87 (d, $J = 8.6$ Hz, 2H), 4.61 (d, $J = 14.4$ Hz, 1H), 4.44 (d, $J = 14.2$ Hz, 1H), 4.44 (q, $J = 6.9$ Hz, 1H), 4.05 (sxt, $J = 6.3$ Hz, 1H), 3.81 (s, 3H), 3.05-3.11 (m, 2H), 1.52 (d, $J = 7.1$ Hz, 3H), 1.18 (d, $J = 6.4$ Hz, 3H)

^{13}C NMR (CDCl_3 , 151 MHz): δ 169.8, 159.2, 129.6, 128.5, 114.1, 71.9, 63.7, 55.3, 51.9, 49.1, 18.2, 17.7

IR ν_{max} (cm^{-1}) (thin film): 2977, 2934, 1645

HRMS: Calculated for $\text{C}_{14}\text{H}_{20}\text{NO}_3$ $[M+H]^+$: 250.1438, found $[M+H]^+$: 250.1429 (-3.6 ppm).

(S)-Ethyl 1-benzyl-5-oxopyrrolidine-2-carboxylate 2.2.20²⁸⁶



General procedure for the iodine-mediated C–H oxidation of cyclic amines A was followed. Iodine (381 mg, 1.50 mmol) was added to a mixture of *L*-**2.1.8u** (44.5 μL , 0.20 mmol) and sodium bicarbonate (168 mg, 2.00 mmol) in THF/ H_2O (5.7/2.3 mL). Purification was carried out by silica gel chromatography using 0-50% (3:1 EtOAc/EtOH) (with 1% triethylamine modifier)/cyclohexane as the eluent, to afford **2.2.20** (42.4 mg, 86%) as a colourless oil.

LCMS (Method B, UV, ESI) $R_t = 0.92$ min, $[M+H]^+$ 248.2

^1H NMR (CDCl_3 , 400 MHz): δ 7.25-7.34 (m, 3H), 7.19-7.23 (m, 2H), 5.02 (d, $J = 14.7$ Hz, 1H), 4.06-4.19 (m, 2H), 4.00 (d, $J = 14.9$ Hz, 1H), 3.96 (dd, $J = 9.0, 3.2$ Hz, 1H),

2.51-2.62 (m, 1H), 2.41 (ddd, $J = 16.9, 9.5, 3.9$ Hz, 1H), 2.18-2.30 (m, 1H), 2.07 (ddt, $J = 13.1, 9.6, 3.5$ Hz, 1H), 1.24 (t, $J = 7.2$ Hz, 3H)

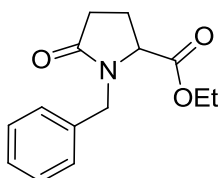
^{13}C NMR (CDCl_3 , 101 MHz): δ 175.0, 171.7, 135.9, 128.7, 128.5, 127.8, 61.4, 58.9, 45.6, 29.6, 22.8, 14.1

IR ν_{max} (cm^{-1}) (thin film): 2983, 1737, 1690

HRMS: Calculated for $\text{C}_{14}\text{H}_{18}\text{NO}_3$ $[\text{M}+\text{H}]^+$: 248.1281, found $[\text{M}+\text{H}]^+$: 248.1274 (-2.8 ppm).

Chiral HPLC (25 cm Chiralcel OD-H, 5% EtOH/*n*-heptane, 1.0 mL/min, detection at 215 nm) $R_t = 11.0$ min (minor) and 12.4 (major), $ee = 96.2\%$.²⁸⁵

Ethyl 1-benzyl-5-oxopyrrolidine-2-carboxylate 2.8.5



General procedure for the iodine-mediated C–H oxidation of cyclic amines A was followed. Iodine (761 mg, 3.00 mmol) was added to a mixture of *L*-**2.1.8u** (44.5 μL , 0.20 mmol), *D*-**2.1.8u** (44.5 μL , 0.20 mmol) and sodium bicarbonate (336 mg, 4.00 mmol) in THF/ H_2O (11.4/4.6 mL). Purification was carried out by silica gel chromatography using 0-50% (3:1 EtOAc/EtOH) (with 1% triethylamine modifier)/cyclohexane as the eluent, to afford 2.8.5 (54.7 mg, 55%) as a colourless oil.

LCMS (Method B, UV, ESI) $R_t = 0.92$ min, $[\text{M}+\text{H}]^+$ 248.2

^1H NMR (CDCl_3 , 400 MHz): δ 7.27-7.36 (m, 3H), 7.20-7.24 (m, 2H), 5.03 (d, $J = 14.7$ Hz, 1H), 4.08-4.21 (m, 2H), 4.01 (d, $J = 14.9$ Hz, 1H), 3.97 (dd, $J = 9.0, 3.2$ Hz, 1H), 2.53-2.63 (m, 1H), 2.42 (ddd, $J = 16.9, 9.5, 3.7$ Hz, 1H), 2.19-2.31 (m, 1H), 2.08 (ddt, $J = 13.1, 9.6, 3.5$ Hz, 1H), 1.25 (t, $J = 7.1$ Hz, 3H).

Mechanistic Investigations

Screen of alternative bases for isotope study – reactions were used to determine what other bases would work, and no products were isolated.

Sodium acetate:

General procedure for the iodine-mediated C–H oxidation of cyclic amines A was followed. Iodine (381 mg, 1.5 mmol) was added to a mixture of **2.1.8a** (37 μ L, 0.20 mmol) and sodium acetate (164 mg, 2.0 mmol) in THF/H₂O (5.7/2.3 mL). The reaction was monitored by high pH LCMS, which showed product formation. ¹H NMR analysis of the crude material showed 57% conversion to **2.1.9** against 1,1,1,3,3,3-hexamethyldisiloxane (3.9 mg, 0.024 mmol) as a standard, with a 2.7:1 ratio of **2.1.9** to **2.1.9b** observed.

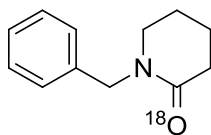
Triethylamine:

General procedure for the iodine-mediated C–H oxidation of cyclic amines A was followed. Iodine (381 mg, 1.5 mmol) was added to a mixture of **2.1.8a** (37 μ L, 0.20 mmol) and triethylamine (0.28 mL, 2.0 mmol) in THF/H₂O (5.7/2.3 mL). The reaction was monitored by high pH LCMS, which showed product no formation, thus the reaction was terminated.

DBU:

General procedure for the iodine-mediated C–H oxidation of cyclic amines A was followed. Iodine (381 mg, 1.5 mmol) was added to a mixture of **2.1.8a** (37 μ L, 0.20 mmol) and DBU (0.30 mL, 2.0 mmol) in THF/H₂O (5.7/2.3 mL). The reaction was monitored by high pH LCMS, which showed product no formation, thus the reaction was terminated.

Isotope-labelling experiments

¹⁸O-1-Benzylpiperidin-2-one **2.3.1**

General procedure for the iodine-mediated C–H oxidation of cyclic amines A was followed. Iodine (190 mg, 0.75 mmol) was added to a mixture of **2.1.8a** (18.5 μ L, 0.10 mmol) and sodium bicarbonate (84 mg, 1.00 mmol) in THF/H₂¹⁸O (2.9/1.1 mL). Purification was carried out by silica gel chromatography using 30-85% TBME (with 1% 4M ammonia in methanol modifier)/cyclohexane as the eluent, to afford **2.3.1** (19.2 mg, >99%) as a yellow oil.

LCMS (Method A, UV, ESI) R_t = 0.86 min, [M+H]⁺ 192.2 (100%), 190.2 (3%)

¹H NMR (CDCl₃, 400 MHz): δ 7.30-7.36 (m, 2H), 7.24-7.30 (m, 3H), 4.61 (s, 2H), 3.21 (t, *J* = 6.0 Hz, 2H), 2.48 (t, *J* = 6.5 Hz, 2H), 1.73-1.85 (m, 4H)

HRMS: Calculated for C₁₂H₁₆N¹⁸O [M+H]⁺: 192.1269, found [M+H]⁺: 192.1266 (-1.6 ppm).

Studies carried out with sodium acetate instead of sodium bicarbonate: otherwise general procedure A was followed for all cases, although the reaction mixtures were not purified.

- with NaOAc/H₂O

Iodine (381 mg, 1.50 mmol) was added to a mixture of **2.1.8a** (36.9 μ L, 0.20 mmol) and sodium acetate (164 mg, 2.00 mmol) in THF/H₂O (5.7/2.3 mL).

LCMS (Method A, UV, ESI) R_t = 0.86 min (**2.1.9**), [M+H]⁺ 190.1 (100%).

- with Na¹⁸OAc/H₂O

Iodine (381 mg, 1.50 mmol) was added to a mixture of **2.1.8a** (36.9 μ L, 0.20 mmol) and sodium acetate (164 mg, 2.00 mmol) in THF/H₂O (5.7/2.3 mL).

LCMS (Method A, UV, ESI) $R_t = 0.85$ min (**2.1.9**), $[M+H]^+$ 190.1 (100%).

- with $\text{Na}^{18}\text{OAc}/\text{H}_2^{18}\text{O}$

Iodine (381 mg, 1.50 mmol) was added to a mixture of **2.1.8a** (36.9 μL , 0.20 mmol) and sodium acetate (164 mg, 2.00 mmol) in THF/ H_2O (5.7/2.3 mL).

LCMS (Method A, UV, ESI) $R_t = 0.86$ min (**2.1.9b**), $[M+H]^+$ 192.1 (100%).

NMR Studies into Formation of *N*-Iodoammonium Intermediate **2.3.2**

A solution of iodine (1090 mg, 4.28 mmol) in d^8 -THF (2.85 mL) was treated with **2.1.8a** (100 mg, 0.57 mL). The reaction mixture was stirred at RT for 1.5 h, and a 0.3 mL aliquot was taken out, diluted with MeOD (0.3 mL) and analysed by ^1H NMR. A change in the chemical shift of the 2H benzylic CH_2 signal was observed from δ 3.48 for **2.1.8a** to δ 4.31 (in MeOD), proposed to be intermediate **2.3.2**. A 1 mL aliquot was taken from the reaction mixture, corresponding to 0.2 mmol of **2.1.8a**, which was diluted with d^8 -THF (4.7 mL) and D_2O (2.3 mL), providing a substrate concentration of 0.025 M in 2.5:1 d^8 -THF: D_2O . Solid sodium bicarbonate was added in portions (net amount in the reaction mixture after addition of each portion) and stirred for discrete time periods (indicated below). After each period of time a 0.3 mL aliquot of the reaction mixture was taken, which was diluted with MeOD and analysed by ^1H NMR. The ratio of species was determined by comparison of the integrals for the benzylic CH_2 signal of **2.1.8a** (δ 3.48), the benzylic CH_2 signal of **2.3.2** (δ 4.31), and the benzylic CH_2 signal of **2.1.9** (δ 4.59). After the final addition of sodium bicarbonate, and a total reaction time of 360 min, the final aliquot was taken and analysed by NMR. The reaction was not worked up or purified further, and no products were isolated.

concentrated under reduced pressure. The crude material was purified by silica gel chromatography using 0-30% TBME/cyclohexane as the eluent, to afford **2.3.3** (199.9 mg, 60%) as a yellow oil.

LCMS (Method A, UV, ESI) $R_t = 1.41$ min, $[M+H]^+$ 216.2

1H NMR (DMSO- d_6 , 400 MHz): δ 7.25-7.34 (m, 4H), 7.17-7.23 (m, 1H), 4.50 (d, $J = 13.7$ Hz, 1H), 3.02 (d, $J = 13.4$ Hz, 1H), 2.64 (dtd, $J = 11.6, 4.0, 1.5$ Hz, 1H), 1.82 (td, $J = 10.9, 3.1$ Hz, 1H), 1.71-1.78 (m, 1H), 1.66 (dquin, $J = 12.2, 4.0$ Hz, 1H), 1.39-1.47 (m, 2H), 1.28-1.39 (m, 2H), 1.22 (qt, $J = 11.0, 3.4$ Hz, 1H), 0.76 (qt, $J = 8.4, 4.9$ Hz, 1H), 0.62 (dddd, $J = 9.3, 7.9, 5.6, 4.2$ Hz, 1H), 0.37-0.46 (m, 1H), 0.27 (dt, $J = 13.4, 5.1$ Hz, 1H), 0.03 (td, $J = 9.5, 5.0$ Hz, 1H)

^{13}C NMR (DMSO- d_6 , 101 MHz): δ 140.4, 128.3, 128.0, 126.3, 67.0, 58.0, 51.6, 32.2, 25.2, 23.7, 14.5, 7.5, 1.1

IR ν_{max} (cm $^{-1}$) (thin film): 2932, 1495

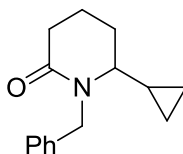
HRMS: Calculated for $C_{15}H_{22}N$ $[M+H]^+$: 216.1752, found $[M+H]^+$: 216.1753 (0.5 ppm).

1-Benzyl-6-cyclopropylpiperidin-2-one 2.3.4 and (1-Benzylpyrrolidin-2-yl)(cyclopropyl)methanone 2.3.5

Iodine (283 mg, 1.12 mmol) was added to a mixture of **2.3.3** (32 mg, 0.15 mmol) and sodium bicarbonate (125 mg, 1.49 mmol) in THF (4.3 mL) and H $_2$ O (1.7 mL). The reaction mixture was stirred at RT for 1 h. The reaction was quenched with saturated aqueous sodium thiosulfate (5 mL) and saturated aqueous sodium bicarbonate (5 mL), and extracted into DCM (3 x 15 mL). The combined organic layer was washed with water (10 mL), passed through a hydrophobic frit and concentrated in vacuo. The crude material was analysed by 1H NMR against dibromomethane (15 μ l, 0.215 mmol) as a standard, which showed 20% conversion to **2.3.4** (based on the 1H signal at 5.45 ppm, corresponding to a benzylic proton), and 54% conversion to **2.3.5** (based on the 1H signal at 3.90 ppm, corresponding to a benzylic proton). The crude product was purified initially by high pH MDAP (Method C), to afford **2.3.4** (5.0 mg, 15%) as an

orange oil. Clean purification of **2.3.5** was challenging, and this had to be purified again by low pH MDAP (Method A) to afford **2.3.5** (7.5 mg, 22%) as an orange oil.

1-Benzyl-6-cyclopropylpiperidin-2-one **2.3.4**



LCMS (Method B, UV, ESI) $R_t = 1.04$ min, $[M+H]^+$ 230.1

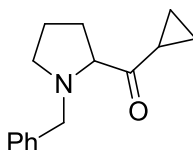
^1H NMR (CDCl_3 , 400 MHz): δ 7.27-7.33 (m, 2H), 7.17-7.26 (m, 3H), 5.45 (d, $J = 15.4$ Hz, 1H), 4.37 (d, $J = 15.4$ Hz, 1H), 2.47-2.57 (m, 3H), 1.95-2.07 (m, 1H), 1.81-1.87 (m, 2H), 1.71-1.81 (m, 1H), 0.84-0.95 (m, 1H), 0.65-0.74 (m, 1H), 0.42-0.51 (m, 1H), 0.35 (dq, $J = 9.9, 4.9$ Hz, 1H), -0.07-0.00 (m, 1H)

^{13}C NMR (CDCl_3 , 101 MHz): δ 170.3, 138.0, 128.4, 127.3, 126.9, 60.5, 46.8, 32.4, 29.4, 18.2, 15.3, 7.3, 1.0

IR ν_{max} (cm^{-1}) (thin film): 2947, 1636, 1450

HRMS: Calculated for $\text{C}_{15}\text{H}_{20}\text{NO}$ $[M+H]^+$: 230.1545, found $[M+H]^+$: 230.1540 (-2.2 ppm).

(1-Benzylpyrrolidin-2-yl)(cyclopropyl)methanone **2.3.5**



LCMS (Method B, UV, ESI) $R_t = 0.42$ min, $[M+H]^+$ 230.2 (only 82% by UV, with an impurity that ionised to 473.2 (ES, positive mode) observed).

^1H NMR (CDCl_3 , 400 MHz): δ 7.30-7.39 (m, 4H), 7.24-7.29 (m, 1H), 3.91 (d, $J = 13.0$ Hz, 1H), 3.44 (d, $J = 12.7$ Hz, 1H), 3.21 (t, $J = 8.1$ Hz, 1H), 3.11 (t, $J = 8.7$ Hz, 1H),

2.43-2.55 (m, 1H), 2.27-2.37 (m, 1H), 2.08-2.19 (m, 1H), 1.79-2.01 (m, 3H), 1.00-1.08 (m, 1H), 0.90-0.95 (m, 1H), 0.83-0.90 (m, 2H)*

^{13}C NMR (CDCl_3 , 101 MHz): δ 213.3, 138.8, 129.0, 128.2, 127.1, 73.8, 59.2, 53.6, 29.7, 29.0, 23.4, 16.1, 11.1*

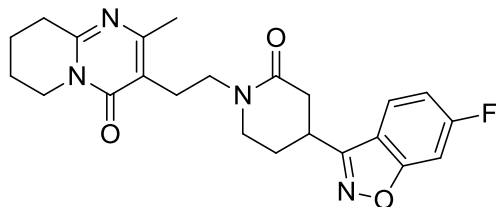
IR ν_{max} (cm^{-1}) (thin film): 2926, 1694, 1651, 1453

HRMS: Calculated for $\text{C}_{15}\text{H}_{20}\text{NO}$ $[\text{M}+\text{H}]^+$: 230.1545, found $[\text{M}+\text{H}]^+$: 230.1543 (-0.9 ppm).

**Large silyl impurity detected by NMR at 0.10 ppm in ^1H and at 1.0 ppm in ^{13}C spectra. The origin of this contaminant is unknown, but did not interfere with structural assignment.*

Late-Stage C–H Oxidation of Bioactive Small Molecules

3-(2-(4-(6-Fluorobenzo[d]isoxazol-3-yl)-2-oxopiperidin-1-yl)ethyl)-2-methyl-6,7,8,9-tetrahydro-4H-pyrido[1,2-a]pyrimidin-4-one 2.4.2



General procedure for the iodine-mediated C–H oxidation of cyclic amines **A** was followed. Iodine (190 mg, 0.75 mmol) was added to a mixture of **2.4.1a** (41 mg, 0.10 mmol) and sodium bicarbonate (84 mg, 1.00 mmol) in THF/ H_2O (2.9/1.1 mL). Purification was carried out by high pH MDAP (Method B), to afford **2.4.2** (24.1 mg, 57%) as a pale brown solid.

LCMS (Method A, UV, ESI) R_t = 0.88 min, $[\text{M}+\text{H}]^+$ 425.3

^1H NMR (DMSO-d_6 , 400 MHz): δ 8.06 (dd, J = 8.7, 5.3 Hz, 1H), 7.70 (dd, J = 9.3, 2.2 Hz, 1H), 7.30 (td, J = 9.0, 2.2 Hz, 1H), 3.76-3.81 (m, 2H), 3.69-3.76 (m, 1H), 3.46-3.55 (m, 1H), 3.33-3.42 (m, 3H), 2.76 (t, J = 6.6 Hz, 2H), 2.70 (dd, J = 5.7, 1.3 Hz,

1H), 2.62-2.68 (m, 2H), 2.55-2.62 (m, 1H), 2.26-2.34 (m, 1H), 2.23 (s, 3H), 2.02-2.13 (m, 1H), 1.81-1.89 (m, 2H), 1.72-1.80 (m, 2H)

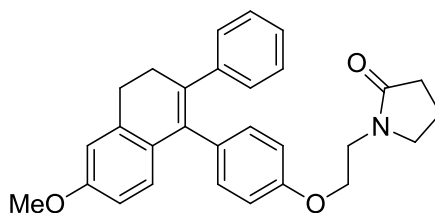
¹³C NMR (DMSO-d₆, 126 MHz): δ 167.2, 163.6 (d, ³J_{C-F} = 13.9 Hz), 163.2, 163.0, 161.2 (d, *J* = 231.2 Hz), 158.8, 158.8, 156.9, 124.3 (d, ³J_{C-F} = 12.0 Hz), 117.4 (d, ⁴J_{C-F} = 3.7 Hz), 113.1 (d, ¹J_{C-F} = 25.0 Hz), 97.9 (d, ²J_{C-F} = 27.7 Hz), 46.6, 45.4, 42.6, 36.1, 31.2, 30.8, 27.5, 24.0, 21.8, 21.3, 19.0

IR ν_{max} (cm⁻¹) (thin film): 3060, 2959, 1658, 1635

HRMS: Calculated for C₂₃H₂₆F N₄O₃ [M+H]⁺: 425.1983, found [M+H]⁺: 425.1977 (-1.6 ppm)

M.pt.: 178-180 °C.

1-(2-(4-(6-Methoxy-2-phenyl-3,4-dihydronaphthalen-1-yl)phenoxy)ethyl)pyrrolidin-2-one 2.4.3



General procedure for the iodine-mediated C–H oxidation of cyclic amines A was followed. Iodine (95 mg, 0.38 mmol) was added to a mixture of the hydrochloride salt of **2.4.1b** (23 mg, 0.05 mmol) and sodium bicarbonate (42 mg, 0.50 mmol) in THF/H₂O (1.4/0.6 mL). Purification was carried out by silica gel chromatography using 10-45% EtOAc/cyclohexane as the eluent, to afford **2.4.3** (20.2 mg, 92%) as a white solid.*

LCMS (Method A, UV, ESI) R_t = 1.42 min, [M+H]⁺ 440.2

¹H NMR (CDCl₃, 400 MHz): δ 7.09-7.14 (m, 2H), 7.00-7.07 (m, 3H), 6.97 (d, *J* = 8.8 Hz, 2H), 6.70-6.80 (m, 4H), 6.60 (dd, *J* = 8.6, 2.8 Hz, 1H), 4.09 (t, *J* = 5.2 Hz, 2H), 3.81 (s, 3H), 3.67 (t, *J* = 5.2 Hz, 2H), 3.59 (t, *J* = 7.1 Hz, 2H), 2.95 (dd, *J* = 8.6, 7.1

Hz, 2H), 2.78 (dd, $J = 8.6, 6.3$ Hz, 2H), 2.40 (t, $J = 8.1$ Hz, 2H), 2.03 (quin, $J = 7.6$ Hz, 2H)

^{13}C NMR (CDCl_3 , 101 MHz): δ 175.3, 158.5, 157.0, 143.3, 137.7, 134.6, 134.5, 132.6, 132.2, 130.4, 128.3, 127.6, 127.4, 125.7, 113.9, 113.2, 110.8, 66.5, 55.3, 49.0, 42.5, 30.8, 30.8, 29.0, 18.2

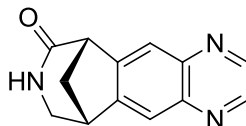
IR ν_{max} (cm^{-1}) (thin film): 2930, 2833, 1681

HRMS: Calculated for $\text{C}_{29}\text{H}_{30}\text{NO}_3$ $[\text{M}+\text{H}]^+$: 440.2220, found $[\text{M}+\text{H}]^+$: 440.2219 (-0.4 ppm)

M.pt.: 99-101 °C.

** ^1H NMR analysis showed presence of 4wt% of an unidentified species. The presence of additional signals in the aryl region relative to 2.4.3 suggest an oxidized product arising from aromatization of the fused cyclohexene ring in 2.4.3.*

(6S,10R)-9,10-Dihydro-6H-6,10-methanoazepino[4,5-g]quinoxalin-7(8H)-one
2.4.4



General procedure for the iodine-mediated C–H oxidation of cyclic amines A was followed. Iodine (190 mg, 0.75 mmol) was added to a mixture of the hydrochloride salt of **2.4.1c** (25 mg, 0.10 mmol) and sodium bicarbonate (84 mg, 1.00 mmol) in THF/ H_2O (2.9/1.1 mL). Purification was carried out by reverse phase flash chromatography using 0-30% MeCN/10 mM aqueous ammonium bicarbonate to afford **2.4.4** (11.9 mg, 53%) as a white solid.

LCMS (Method A, UV, ESI) $R_t = 0.56$ min, $[\text{M}+\text{H}]^+$ 226.2

^1H NMR (CDCl_3 , 400 MHz): δ 8.81 (dd, $J = 9.3, 2.0$ Hz, 2H), 8.04 (d, $J = 13.0$ Hz, 2H), 5.14 (br. s., 1H), 3.91 (d, $J = 3.9$ Hz, 1H), 3.84 (ddd, $J = 11.1, 4.3, 1.2$ Hz, 1H),

3.72 (t, $J = 4.3$ Hz, 1H), 3.37 (ddt, $J = 11.1, 2.4, 1.0$ Hz, 1H), 2.59-2.66 (m, 1H), 2.51 (d, $J = 11.5$ Hz, 1H)

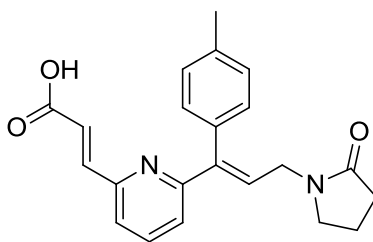
^{13}C NMR (CDCl_3 , 101 MHz): δ 171.9, 147.8, 146.8, 144.5, 144.3, 143.5, 143.3, 123.1, 122.6, 49.2, 48.2, 38.9, 37.7

IR ν_{max} (cm^{-1}) (thin film): 3228 (br), 2922, 1667, 1478

HRMS: Calculated for $\text{C}_{13}\text{H}_{12}\text{N}_3\text{O}$ $[\text{M}+\text{H}]^+$: 226.0980, found $[\text{M}+\text{H}]^+$: 226.0976 (-1.8 ppm)

M.pt.: 182-184 °C.

(*E*)-3-(6-((*E*)-3-(2-Oxopyrrolidin-1-yl)-1-(*para*-tolyl)prop-1-en-1-yl)pyridin-2-yl)acrylic acid **2.4.5**



General procedure for the iodine-mediated C–H oxidation of cyclic amines **A** was followed. Iodine (190 mg, 0.75 mmol) was added to a mixture of **2.4.1d** (35 mg, 0.10 mmol) and sodium bicarbonate (84 mg, 1.00 mmol) in THF/ H_2O (2.9/1.1 mL). ^1H NMR analysis of the crude material showed 56% conversion to **2.4.5** based on the peak at 2.21 ppm against hexamethyldisiloxane (24.0 μmol) as a standard. Purification was carried out by reverse phase preparative HPLC using 15-55% MeCN (with 0.1% ammonia modifier)/10 mM aqueous ammonium bicarbonate as the eluent, to afford **2.4.5** (5.6 mg, 15%) as a white gum.

LCMS (Method A, UV, ESI) $R_t = 0.74$ min, $[\text{M}+\text{H}]^+$ 363.2

^1H NMR (DMSO-d_6 , 400 MHz): δ 7.74 (t, $J = 7.6$ Hz, 1H), 7.58 (d, $J = 8.1$ Hz, 1H), 7.56 (d, $J = 15.7$ Hz, 1H), 7.29 (d, $J = 8.1$ Hz, 2H), 7.14 (d, $J = 8.1$ Hz, 2H), 6.91 (d, $J = 7.6$ Hz, 1H), 6.83 (d, $J = 15.7$ Hz, 1H), 6.78 (t, $J = 6.9$ Hz, 1H), 3.85 (d, $J = 7.1$ Hz,

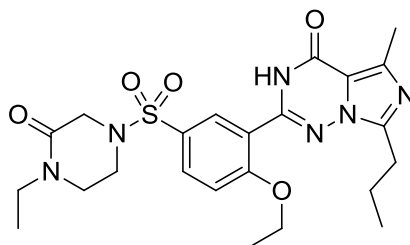
2H), 3.30 (t, $J = 7.1$ Hz, 3H), 2.38 (s, 3H), 2.21 (t, $J = 8.1$ Hz, 2H), 1.91 (quin, $J = 7.5$ Hz, 2H)

^{13}C NMR (DMSO- d_6 , 126 MHz): δ 174.1, 167.6, 157.4, 152.3, 143.3, 142.7, 138.3, 137.3, 134.5, 129.8, 129.7, 127.9, 123.3, 122.9, 55.4, 46.8, 41.5, 30.7, 21.3, 17.8

IR ν_{max} (cm^{-1}) (thin film): 3380 (br), 2923, 1678, 1643

HRMS: Calculated for $\text{C}_{22}\text{H}_{23}\text{N}_2\text{O}_3$ $[\text{M}+\text{H}]^+$: 363.1703, found $[\text{M}+\text{H}]^+$: 363.1703 (-0.1 ppm).

2-(2-Ethoxy-5-((4-ethyl-3-oxopiperazin-1-yl)sulfonyl)phenyl)-5-methyl-7-propylimidazo[5,1-*f*][1,2,4]triazin-4(3*H*)-one 2.4.6



General procedure for the iodine-mediated C–H oxidation of cyclic amines **B** was followed. Iodine (190 mg, 0.75 mmol) was added to a mixture of the hydrochloride trihydrate salt of **2.4.1e** (58 mg, 0.10 mmol) and sodium bicarbonate (84 mg, 1.00 mmol) in DMSO/ H_2O (2.9/1.1 mL). LCMS (Method A, UV, ESI) analysis of the reaction mixture showed a 3:1 ratio of **2.4.6** ($R_t = 0.92$ min, 22% area) to **2.4.1e** ($R_t = 1.03$ min, 7% area). ^1H NMR analysis of the crude material showed 57% conversion to **2.4.6** based on the peak at 3.66 ppm against hexamethyldisiloxane (24.0 μmol) as a standard. Purification was carried out by high pH MDAP (Method C), to afford **2.4.6** (13.2 mg, 26%) as a white solid. Unreacted starting material was not isolated.

LCMS (Method A, UV, ESI) $R_t = 0.93$ min, $[\text{M}+\text{H}]^+$ 503.3

^1H NMR (CDCl_3 , 400 MHz): δ 9.70 (br. s., 1H), 8.48 (d, $J = 2.4$ Hz, 1H), 7.92 (dd, $J = 8.8, 2.4$ Hz, 1H), 7.19 (d, $J = 8.8$ Hz, 1H), 4.35 (q, $J = 6.9$ Hz, 2H), 3.72 (s, 2H), 3.34-3.47 (m, 6H), 3.01 (t, $J = 7.6$ Hz, 2H), 2.64 (s, 3H), 1.89 (dq, $J = 14.9, 7.5$ Hz, 2H), 1.60 (t, $J = 7.0$ Hz, 3H), 1.09 (t, $J = 7.2$ Hz, 3H), 1.04 (t, $J = 7.3$ Hz, 3H)

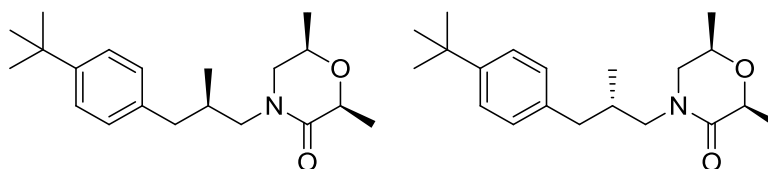
^{13}C NMR (CDCl_3 , 101 MHz): δ 163.1, 160.3, 154.5, 146.5, 144.3, 140.4, 132.5, 130.3, 128.4, 119.1, 113.6, 113.4, 66.2, 48.8, 45.5, 43.1, 41.7, 27.9, 20.9, 14.5, 14.4, 14.0, 12.0

IR ν_{max} (cm^{-1}) (thin film): 3533 (br), 3325, 2968, 1697, 1641

HRMS: Calculated for $[\text{M}+\text{H}]^+$: $\text{C}_{23}\text{H}_{31}\text{N}_6\text{O}_5\text{S}$ 503.2071, found $[\text{M}+\text{H}]^+$: 503.2073 (0.3 ppm)

M.pt.: 208-211 °C.

(2S,6R)-4-(3-(4-(*tert*-butyl)phenyl)-2-methylpropyl)-2,6-dimethylmorpholin-3-one (1.2:1 diastereomeric mixture) 2.4.7



General procedure for the iodine-mediated C–H oxidation of cyclic amines **B** was followed. Iodine (190 mg, 0.75 mmol) was added to a mixture of **2.4.1f** (30 mg, 0.10 mmol) and sodium bicarbonate (84 mg, 1.00 mmol) in DMSO/ H_2O (2.9/1.1 mL). Purification was carried out by silica gel chromatography using 0-25% TBME (with 1% triethylamine and 5% methanol modifier)/cyclohexane as the eluent, to afford **2.4.7** (17.6 mg, 55%) (dr 1.2:1) as a colourless oil.

LCMS (Method A, UV, ESI) R_t = 1.38 min, $[\text{M}+\text{H}]^+$ 318.3

^1H NMR (CDCl_3 , 400 MHz): δ 7.30 (dd, J = 8.4, 2.3 Hz, 4H) ‡,‡ , 7.09 (d, J = 8.3 Hz, 4H) ‡,‡ , 4.20 (q, J = 6.8 Hz, 1H) ‡ , 4.13 (q, J = 6.8 Hz, 1H) ‡ , 3.81 (dtd, J = 16.6, 5.9, 3.2 Hz, 1H) ‡ , 3.63 (dtd, J = 16.6, 6.1, 2.9 Hz, 1H) ‡ , 3.14-3.41 (m, 6H) ‡,‡ , 3.07 (dd, J = 12.0, 2.7 Hz, 1H) ‡ , 2.99 (dd, J = 11.7, 2.7 Hz, 1H) ‡ , 2.56-2.66 (m, 2H) ‡,‡ , 2.47 (dd, J = 7.3 Hz, 1H) ‡ , 2.39 (dd, J = 13.7, 8.6 Hz, 1H) ‡ , 2.18 (dq, J = 14.9, 7.6 Hz, 2H) ‡,‡ , 1.45 (dd, J = 6.8, 2.4 Hz, 6H) ‡,‡ , 1.32 (s, 18H) ‡,‡ , 1.23 (dd, J = 15.4, 6.1 Hz, 6H) ‡,‡ , 0.89 (t, J = 7.0 Hz, 6H) ‡,‡

‡ Major diastereomer; ‡‡ Minor diastereomer

^{13}C NMR (CDCl_3 , 151 MHz): δ 170.0, 169.9, 148.8, 148.7, 137.3, 137.2, 128.6, 128.5, 125.1, 125.1, 74.2, 74.2, 68.9, 68.6, 53.8, 53.4, 52.7, 52.3, 40.8, 40.3, 34.3, 32.9, 32.6, 31.4, 18.5, 18.4, 18.4, 18.3, 17.6, 17.5

IR ν_{max} (cm^{-1}) (thin film): 2962, 1651, 1487

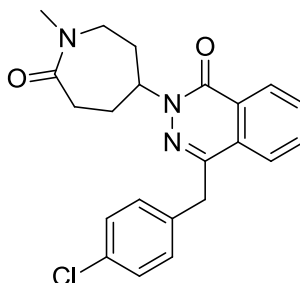
HRMS: Calculated for $\text{C}_{20}\text{H}_{32}\text{NO}_2$ $[\text{M}+\text{H}]^+$: 318.2433, found $[\text{M}+\text{H}]^+$: 318.2425 (-2.5 ppm).

4-(4-Chlorobenzyl)-2-(1-methyl-7-oxoazepan-4-yl)phthalazin-1(2H)-one 2.4.8a
and **4-(4-chlorobenzyl)-2-(1-methyl-2-oxoazepan-4-yl)phthalazin-1(2H)-one 2.4.8b**

General procedure for the iodine-mediated C–H oxidation of cyclic amines A was followed. Iodine (190 mg, 0.75 mmol) was added to a mixture of the hydrochloride salt of **2.4.1g** (42 mg, 0.10 mmol) and sodium bicarbonate (84 mg, 1.00 mmol) in THF/ H_2O (2.9/1.1 mL). Purification was carried out by silica gel chromatography using 0-25% (3:1 EtOAc/EtOH, with 1% triethylamine modifier)/cyclohexane as the eluent, to afford a co-eluting mixture of **2.4.8a** and **2.4.8b** (26.9 mg, 68%*), in 4.3:1 ratio of **2.4.8a** to **2.4.8b**, determined by ^1H NMR. The isomers were only separable by high pH MDAP (Method C) to afford **2.4.8a** (14.8 mg, 37%) as a white solid and **2.4.8b** (2.2 mg, 6%) as a white solid.

*Based on 30.6 mg isolated yield, with 12.1 wt% cyclohexane impurity by ^1H NMR.

4-(4-Chlorobenzyl)-2-(1-methyl-7-oxoazepan-4-yl)phthalazin-1(2H)-one 2.4.8a



LCMS (Method A, UV, ESI) R_t = 1.11 min, $[\text{M}+\text{H}]^+$ 396.2 (^{35}Cl), 398.2 (^{37}Cl)

^1H NMR (CDCl_3 , 400 MHz): δ 8.44-8.52 (m, 1H), 7.66-7.77 (m, 3H), 7.26-7.30 (m, 2H), 7.19 (d, $J = 8.3$ Hz, 2H), 5.27 (tt, $J = 11.4, 4.4$ Hz, 1H), 4.27 (s, 2H), 3.76 (dd, $J = 15.7, 10.3$ Hz, 1H), 3.33 (ddd, $J = 15.5, 6.2, 1.3$ Hz, 1H), 3.08 (s, 3H), 2.64-2.78 (m, 2H), 2.11-2.25 (m, 2H), 2.02-2.11 (m, 2H)

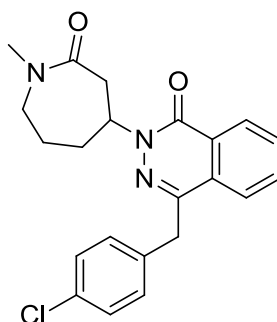
^{13}C NMR (CDCl_3 , 151 MHz): δ 174.7, 158.5, 144.8, 136.2, 133.0, 132.7, 131.3, 129.8, 128.9, 128.6, 128.1, 127.6, 124.7, 57.3, 48.5, 38.3, 35.8, 33.8, 32.4, 28.1

IR ν_{max} (cm^{-1}) (thin film): 2936, 1635

HRMS: Calculated for $\text{C}_{22}\text{H}_{23}\text{N}_3\text{O}_2\text{Cl}$ $[\text{M}+\text{H}]^+$: 396.1479, found $[\text{M}+\text{H}]^+$: 396.1475 (-1.0 ppm)

M.pt.: 242-244 °C.

4-(4-Chlorobenzyl)-2-(1-methyl-2-oxoazepan-4-yl)phthalazin-1(2H)-one 2.4.8b



LCMS (Method A, UV, ESI) $R_t = 1.16$ min, $[\text{M}+\text{H}]^+$ 396.2 (^{35}Cl), 398.2 (^{37}Cl)

^1H NMR (CDCl_3 , 400 MHz): δ 8.43-8.49 (m, 1H), 7.69-7.74 (m, 2H), 7.64-7.69 (m, 1H), 7.28 (d, $J = 8.6$ Hz, 2H),* 7.19 (d, $J = 8.6$ Hz, 2H), 5.22-5.31 (m, 1H), 4.26 (s, 2H), 3.66 (dd, $J = 14.9, 10.3$ Hz, 1H), 3.26-3.37 (m, 2H), 3.05 (s, 3H), 2.76 (dt, $J = 13.8, 1.9$ Hz, 1H), 2.15-2.23 (m, 1H), 1.95-2.11 (m, 2H), 1.74-1.87 (m, 1H)

^{13}C NMR (CDCl_3 , 101 MHz): δ 172.4, 158.2, 144.6, 136.2, 132.9, 132.6, 131.3, 129.8, 128.8, 128.6, 128.2, 127.6, 124.7, 52.3, 50.7, 42.6, 38.4, 36.0, 34.9, 26.2

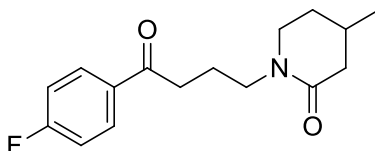
IR ν_{max} (cm^{-1}) (thin film): 2928, 1644

HRMS: Calculated for $\text{C}_{22}\text{H}_{23}\text{N}_3\text{O}_2\text{Cl}$ $[\text{M}+\text{H}]^+$: 396.1479, found $[\text{M}+\text{H}]^+$: 396.1476 (-0.8 ppm)

M.pt.: 176-178 °C.

*Chemical shift peak was obscured slightly by chloroform signal at 7.27 ppm.

1-(4-(4-Fluorophenyl)-4-oxobutyl)-4-methylpiperidin-2-one 2.4.11



General procedure for the iodine-mediated C–H oxidation of cyclic amines A was followed. Iodine (190 mg, 0.75 mmol) was added to a mixture of the hydrochloride salt of **1.3.25** (30 mg, 0.10 mmol) and sodium bicarbonate (84 mg, 1.00 mmol) in THF/H₂O (2.9/1.1 mL). Purification was carried out by silica gel chromatography using 0-60% TBME (with 1% triethylamine, 5% methanol modifier)/cyclohexane as the eluent, to afford **2.4.11** (23.0 mg, 83%) as a white solid.

LCMS (Method A, UV, ESI) R_t = 1.00 min, [M+H]⁺ 278.2

¹H NMR (CDCl₃, 400 MHz): δ 7.97 (dd, *J* = 9.0, 5.4 Hz, 2H), 7.11 (t, *J* = 8.6 Hz, 2H), 3.47-3.55 (m, 1H), 3.36-3.44 (m, 1H), 3.32 (d, *J* = 4.0 Hz, 1H), 3.29-3.31 (m, 1H), 2.97 (t, *J* = 7.1 Hz, 2H), 2.40 (dtd, *J* = 11.9, 10.1, 1.8 Hz, 1H), 1.99 (quind, *J* = 7.1, 1.8 Hz, 2H), 1.81-1.93 (m, 3H), 1.36-1.48 (m, 1H), 0.97 (d, *J* = 6.3 Hz, 3H)

¹³C NMR (CDCl₃, 101 MHz): δ 198.0, 169.7, 165.7 (d, ¹*J*_{C-F} = 258.0 Hz), 133.3 (d, ⁴*J*_{C-F} = 3.2 Hz), 130.7 (d, ³*J*_{C-F} = 9.6 Hz), 115.6 (d, ²*J*_{C-F} = 22.4 Hz), 46.8, 46.0, 40.5, 35.6, 31.0, 27.9, 21.5, 21.0

IR ν_{max} (cm⁻¹) (thin film): 2950, 2869, 1684, 1627

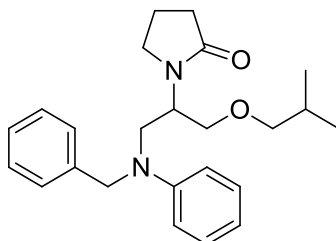
HRMS: Calculated for C₁₆H₂₁FNO₂ [M+H]⁺: 278.1551, found [M+H]⁺: 278.1553 (0.7 ppm)

M.pt.: 76-77 °C.

1-(1-(Benzyl(phenyl)amino)-3-isobutoxypropan-2-yl)pyrrolidin-2-one 2.4.12 and 1-(1-(benzyl(4-iodophenyl)amino)-3-isobutoxypropan-2-yl)pyrrolidin-2-one 2.4.12b

General procedure for the iodine-mediated C–H oxidation of cyclic amines A was followed. Iodine (190 mg, 0.75 mmol) was added to a mixture of the hydrochloride hydrate salt of **2.4.10** (42 mg, 0.10 mmol) and sodium bicarbonate (84 mg, 1.00 mmol) in THF/H₂O (2.9/1.1 mL). ¹H NMR analysis of the crude material showed 81% conversion to **2.4.12** and 17% conversion to **2.4.12b** based on peaks at 6.85 and 6.63 ppm, respectively, against hexamethyldisiloxane (24.0 μmol) as a standard. Purification was attempted initially by silica gel chromatography using 0-50% EtOAc (with 1% 4M ammonia in methanol modifier)/cyclohexane, but the products **2.4.12** and **2.4.12b** co-eluted. Separation could only be achieved by high pH MDAP (Method E), to afford **2.4.12** (11.5 mg, 30%) as a yellow oil, and **2.4.12b** (2.6 mg, 5%) as a yellow oil.

1-(1-(Benzyl(phenyl)amino)-3-isobutoxypropan-2-yl)pyrrolidin-2-one 2.4.12



LCMS (Method A, UV, ESI) $R_t = 1.40$ min, $[M+H]^+$ 381.3

¹H NMR (CDCl₃, 400 MHz): δ 7.29 (t, $J = 6.8$ Hz, 2H), 7.15-7.24 (m, 5H), 6.84 (d, $J = 8.3$ Hz, 2H), 6.71 (t, $J = 7.2$ Hz, 1H), 4.66 (d, $J = 16.7$ Hz, 1H), 4.49-4.58 (m, 2H), 3.66 (m, 2H), 3.61 (dd, $J = 10.1, 5.6$ Hz, 1H), 3.52 (dd, $J = 10.1, 4.0$ Hz, 1H), 3.40-3.47 (m, 1H), 3.34 (td, $J = 9.0, 5.2$ Hz, 1H), 3.11-3.20 (m, 2H), 2.15-2.34 (m, 2H), 1.80-1.93 (m, 2H), 1.66-1.77 (m, 1H), 0.91 (dd, $J = 6.7, 0.9$ Hz, 6H)

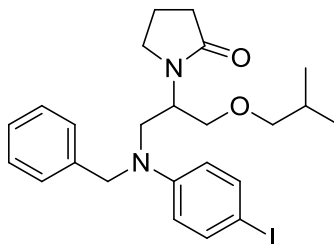
¹³C NMR (CDCl₃, 101 MHz): δ 175.4, 148.6, 138.5, 129.2, 128.5, 126.8, 126.7, 117.1, 113.4, 78.0, 69.8, 54.1, 49.9, 49.6, 45.6, 31.1, 28.6, 19.4, 18.4

IR ν_{\max} (cm⁻¹) (thin film): 2957, 2872, 1679

HRMS: Calculated for C₂₄H₃₃N₂O₂ [M+H]⁺: 381.2537, found [M+H]⁺: 381.2538 (0.4 ppm).

1-(1-(Benzyl(4-iodophenyl)amino)-3-isobutoxypropan-2-yl)pyrrolidin-2-one

2.4.12b



LCMS (Method A, UV, ESI) R_t = 1.53 min, [M+H]⁺ 507.1*

¹H NMR (CDCl₃, 400 MHz): δ 7.43 (d, J = 9.1 Hz, 2H), 7.29 (t, J = 7.6 Hz, 2H), 7.23 (t, J = 7.1 Hz, 1H), 7.16 (d, J = 7.1 Hz, 2H), 6.63 (d, J = 9.1 Hz, 2H), 4.62 (d, J = 17.2 Hz, 1H), 4.51 (d, J = 16.9 Hz, 1H), 4.44-4.49 (m, 1H), 3.64 (d, J = 7.1 Hz, 2H), 3.59 (dd, J = 10.1, 5.3 Hz, 1H), 3.51 (dd, J = 10.1, 4.0 Hz, 1H), 3.31-3.47 (m, 2H), 3.12-3.20 (m, 2H), 2.16-2.34 (m, 2H), 1.81-1.94 (m, 2H), 1.70-1.80 (m, 1H), 0.91 (d, J = 6.8 Hz, 6H)

¹³C NMR (CDCl₃, 126 MHz): δ 175.4, 147.9, 137.9, 137.8, 128.6, 127.0, 126.7, 115.6, 110.0, 78.0, 69.6, 54.1, 49.8, 49.7, 45.7, 31.0, 28.6, 19.4, 18.4

IR ν_{\max} (cm⁻¹) (thin film): 2956, 2870, 1677

HRMS: Calculated for [M+H]⁺: C₂₄H₃₂IN₂O₂ 507.1503, found [M+H]⁺: 507.1518 (3.0 ppm).

*LCMS showed 12% area of an impurity at 1.30 min, which ionised with m/z = 417.1 (ES, positive mode), corresponding to a mass loss of 90 relative to **2.4.12b**. This could have resulted from some debenzylation of **2.4.12b** in the LCMS run; no impurity was observed by NMR, so likely instability in LCMS.

Comparison to Literature Precedent

Investigating Late-Stage Oxidation Under Milstein conditions¹⁹⁷

Stock solutions of acridine Ru complex **1.4.33** (6 mg, 0.01 mmol) in 1,4-dioxane (1.5 mL) and NaOH (40 mg, 1.01 mmol) in water (1.5 mL) were prepared; 1.0 extra equivalent of NaOH was added compared to the literature conditions in order to neutralize the HCl salt of the drug substrates. A 0.15 mL aliquot of the catalyst solution and a 0.15 mL aliquot of the NaOH solution were added to either the hydrochloride salt of **1.3.25** (30 mg, 0.10 mmol) or the hydrochloride hydrate salt of **2.4.10** (42 mg, 0.10 mmol). The reaction mixture was heated to 150 °C for 48 h. The reaction mixture was then allowed to cool to room temperature, before diluting in water (1 mL) and extracting into DCM (2 x 1.5 mL). The crude solution was concentrated under flow of nitrogen, and the crude material was redissolved in CDCl₃ and analysed by ¹H NMR.

¹H NMR analysis of the crude materials showed:

- 4% conversion to **2.4.11** and 93% remaining starting material based on peaks at 3.40 ppm and 7.10 ppm, respectively, against 3,4,5-trichloropyridine (0.086 mmol) as a standard;
- 8% conversion to **2.4.12** and 91% remaining starting material based on peaks at 2.24 ppm and 6.79 ppm, respectively, against 3,4,5-trichloropyridine (0.119 mmol) as a standard.

Investigating late-stage oxidation under Emmert conditions¹⁹⁸

A stock solution of FeCl₃.6H₂O (14 mg, 0.05 mmol) in pyridine (3.60 mL) was prepared. A 0.36 mL aliquot of this solution was added to a mixture of 2-picolinic acid (0.6 mg, 5.0 μmol), *tert*-butyl peroxybenzoate (57.0 μL, 0.30 mmol), water (16.2 μL, 0.90 mmol), and either the hydrochloride salt of **1.3.25** (30 mg, 0.10 mmol) or the hydrochloride hydrate salt of **2.4.10** (42 mg, 0.10 mmol), and the reaction mixture was stirred at 50 °C for 24 h. The solvent was removed and the crude residue was redissolved in CDCl₃ and analysed by ¹H NMR.

¹H NMR analysis of the crude materials showed:

- 0% conversion to **2.4.11** against 3,4,5-trichloropyridine (0.056 mmol) as a standard;
- 0% conversion to **2.4.12** against 3,4,5-trichloropyridine (0.094 mmol) as a standard.

Investigating late-stage oxidation under classical Ru^{IV}O₂/NaIO₄ conditions¹⁹³

Either the hydrochloride salt of **1.3.25** (30 mg, 0.10 mmol) or the hydrochloride hydrate salt of **2.4.10** (42 mg, 0.10 mmol) was added to a mixture of ruthenium(IV) oxide (1.3 mg, 10.0 μmol) and sodium periodate (135.0 mg, 0.63 mmol) in ethyl acetate (0.24 mL) and water (0.94 mL), and the reaction mixture was stirred at RT for 64 h. The reaction mixture was diluted with water (10 mL) and extracted into EtOAc (3 x 10 mL). The combined organic layer was passed through a hydrophobic frit, and concentrated under reduced pressure. The crude residue was redissolved in CDCl₃ and analysed by ¹H NMR.

¹H NMR analysis of the crude materials showed:

- 0% conversion to **2.4.11** against 3,4,5-trichloropyridine (0.094 mmol) as a standard;
- 0% conversion to **2.4.12** against 3,4,5-trichloropyridine (0.066 mmol) as a standard.

Investigating late-stage oxidation under hypervalent iodine conditions²⁴³

Either the hydrochloride salt of **1.3.25** (30 mg, 0.10 mmol) or the hydrochloride hydrate salt of **2.4.10** (42 mg, 0.10 mmol) was added to a solution of iodobenzene diacetate (71 mg, 0.22 mmol) in THF (0.36 mL). Water (0.14 mL) was added, and the reaction mixture stirred at RT for 16 h. The solvent was evaporated under flow of nitrogen and the crude residue was redissolved in CDCl₃ and analysed by ¹H NMR.

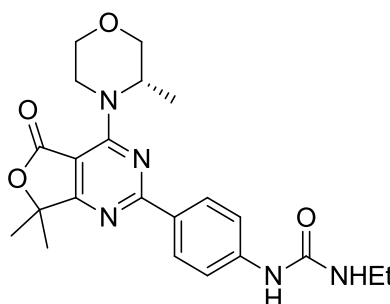
¹H NMR analysis of the crude materials showed:

- 0% conversion to **2.4.11** against 3,4,5-trichloropyridine (0.067 mmol) as a standard;
- 0% conversion to **2.4.12** against 3,4,5-trichloropyridine (0.080 mmol) as a standard.

Water was used as a co-solvent in order to try to form phenyliodosobenzene²⁸⁷ as the oxidant *in situ*. Comparative reactions were also carried out using DCM as the solvent, as was used in the route described by Waghmode,²⁴³ and also in anhydrous THF to ascertain if the presence of water was inhibiting the oxidation, but the reaction profiles were same as with the THF/H₂O system.

Application for Medicinal Chemistry

(S)-1-(4-(7,7-Dimethyl-4-(3-methylmorpholino)-5-oxo-5,7-dihydrofuro[3,4-d]pyrimidin-2-yl)phenyl)-3-ethylurea **2.5.3**



Iodine (381 mg, 1.5 mmol) was added to a mixture of **2.5.1** (92.0 mg, 0.20 mmol)²⁷⁴ and sodium bicarbonate (168 mg, 2.0 mmol) in DMSO/H₂O (5.7 mL/2.3 mL, 0.025 M). The reaction mixture was stirred at 100 °C for 48 h. The reaction mixture was allowed to cool to room temperature, and then pipetted into a solution of saturated aqueous sodium thiosulfate (10 mL) and saturated aqueous sodium bicarbonate (10 mL). The crude material was extracted in DCM (2 x 10 mL), and the combined organic layer was washed with saturated aqueous sodium bicarbonate (10 mL), passed through a hydrophobic frit and concentrated under reduced pressure. The crude material was

purified by silica gel chromatography with 0-60% (3:1 EtOAc:EtOH (with 1% Et₃N modifier)/cyclohexane as the eluent, affording **2.5.3** (23.4 mg, 28%) as an orange solid.

LCMS (Method A, UV, ESI) R_t = 1.10 min, [M+H]⁺ 426.4

¹H NMR (CDCl₃, 400MHz): δ 8.40 (d, *J* = 8.8 Hz, 2H), 7.47 (d, *J* = 8.8 Hz, 2H), 6.85 (br. s., 1H), 4.87-5.50 (m, 3H), 4.06 (dd, *J* = 11.1, 2.8 Hz, 1H), 3.83 (d, *J* = 11.2 Hz, 1H), 3.78 (dd, *J* = 12.2, 2.9 Hz, 1H), 3.68 (td, *J* = 11.7, 2.0 Hz, 1H), 3.54 (br. s., 1H), 3.34 (ddd, *J* = 14.2, 7.0, 3.8 Hz, 2H), 1.67 (d, *J* = 2.2 Hz, 6H), 1.47 (d, *J* = 6.8 Hz, 3H), 1.19 ppm (t, *J* = 7.2 Hz, 3H)

¹³C NMR (CDCl₃, 101MHz): δ 159.0, 155.0, 142.5, 131.3, 130.4, 125.0, 118.9, 97.0, 84.2, 71.1, 67.2, 35.3, 25.5, 25.4, 15.3

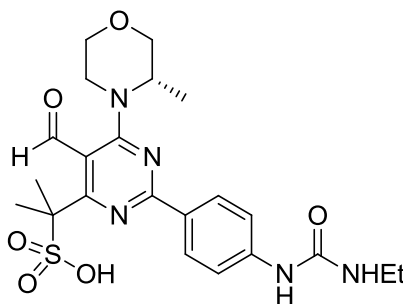
Some ¹³C chemical shifts were not observed and some ¹H signals were broadened out. This is proposed to be due to restricted rotation from the methyl group on the morpholine ring.

IR ν_{max} (cm⁻¹) (thin film): 3420, 3337, 2978, 1719

HRMS: Calculated for C₂₂H₂₈N₅O₄ [M+H]⁺: 426.2136, found [M+H]⁺: 426.2129 (-1.7 ppm)

M.pt.: 235-238 °C.

(S)-2-(2-(4-(3-Ethylureido)phenyl)-5-formyl-6-(3-methylmorpholino)pyrimidin-4-yl)propane-2-sulfonic acid 2.5.4



Iodine (190 mg, 0.75 mmol) was added to a mixture of **2.5.1** (46.0 mg, 0.10 mmol)²⁷⁴ and sodium bicarbonate (84 mg, 1.0 mmol) in DMSO/H₂O (2.9 mL/1.1 mL, 0.025 M).

The reaction mixture was stirred at 100 °C for 48 h. The reaction mixture was allowed to cool to room temperature before addition of saturated aqueous sodium thiosulfate (1 mL). The crude mixture was then transferred into 6 x 1 mL vials for purification by high pH MDAP (Method B), affording **2.5.4** (25.9 mg, 47%) as a yellow oil.*

LCMS (Method A, UV, ESI) $R_t = 0.70$ min, $[M+H]^+$ 492.3

^1H NMR (DMSO- d_6 , 400 MHz): δ 10.71 (s, 1H), 8.87 (br. s., 1H), 8.20 (d, $J = 8.8$ Hz, 2H), 7.50 (d, $J = 8.8$ Hz, 2H), 6.41 (br. s., 1H), 4.73 (q, $J = 6.8$ Hz, 1H), 3.81 (d, $J = 9.0$ Hz, 1H), 3.70 (d, $J = 11.0$ Hz, 1H), 3.63 (dd, $J = 11.5, 2.4$ Hz, 1H), 3.48 (td, $J = 11.7, 2.7$ Hz, 2H), 3.03-3.16 (m, 3H), 1.76 (d, $J = 6.6$ Hz, 6H), 1.28 (d, $J = 6.8$ Hz, 3H), 1.05 (t, $J = 7.2$ Hz, 3H)

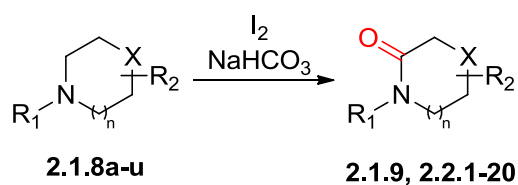
^{13}C NMR (DMSO- d_6 , 101 MHz): δ 192.1, 173.0, 162.5, 160.4, 155.3, 144.1, 129.8, 129.7, 117.3, 113.2, 70.9, 66.5, 64.8, 50.2, 46.0, 34.4, 27.9, 27.7, 15.8, 15.1

IR ν_{max} (cm^{-1}) (thin film): 2977, 1659, 1596

HRMS: Calculated for $\text{C}_{22}\text{H}_{30}\text{N}_5\text{O}_6\text{S}$ $[M+H]^+$: 492.1911, found $[M+H]^+$: 492.1898 (-2.8 ppm).

*Isolated with 5.4 wt% ammonia by ^1H NMR.

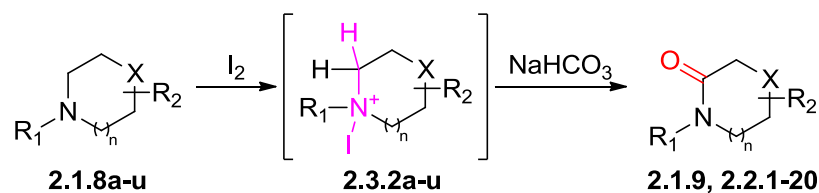
Appendix 1

Comparison of pK_aH of Substrate With Yield of Lactam

Substrate	Calculated pK_aH of Nitrogen Atom ²⁵⁰	Yield (%)
2.1.8i	8.1	45
2.1.8n	10.1	51
2.1.8r	9.7	53
2.1.8j	5.6	54
2.1.8h	6.9	56
2.1.8k	6.0	56
2.1.8f	9.9	66
2.1.8e	9.6	69
2.1.8m	9.1	70
2.1.8p	10.1	73
2.1.8q	8.8	73
2.1.8s	9.1	73 ^[a]
2.1.8t	7.2	75
2.1.8o	9.4	76
2.1.8g	7.2	78
2.1.8d	8.5	80
2.1.8l	8.8	84
2.1.8u	7.2	86
2.1.8b	8.8	91
2.1.8c	8.2	95
2.1.8a	9.4	96

Table 16. No clear trend between pK_aH of substrate and %yield of lactam. [a] Combined yield of 2.2.18a and 2.2.18b were used in data analysis to measure conversion of substrate to lactam product.

Appendix 2

Comparison of pK_a H of Substrate With Yield of Lactam

Intermediate	H-C-N-I Dihedral angle ^[a] (°) ^{242,250}	Yield (%)
2.3.2s (minor)	161	20
2.3.2i	171	45
2.3.2n	163	51
2.3.2r	171	53
2.3.2s (major)	169	53
2.3.2j	170	54
2.3.2h	169	56
2.3.2k	170	56
2.3.2f	160	66
2.3.2e	164	69
2.3.2m	171	70
2.3.2p	159	73
2.3.2q	158	73
2.3.2t	169	75
2.3.2o	171	76
2.3.2g	172	78
2.3.2d	162	80
2.3.2l	172	84
2.3.2u	163	86
2.3.2b	171	91
2.3.2c	171	95
2.3.2a	171	96

Table 17. No clear trend between dihedral angle of putative *N*-iodoammonium intermediate and %yield of lactam. [a] Dihedral angle across the H-C-N-I bonds of **2.3.2a-u** in the lowest energy state that had the N-I bond in an axial conformation. Note: **2.3.2a** here = **2.3.2** in Table 10.

Assay Protocols

hERG Potassium Ion Channel

Compounds **2.4.1a** and **2.4.2** were screening in a hERG human antagonist Barracuda assay according to the protocol described by Gillie *et al.*²⁸⁸

Serotonin_{2A} and Dopamine₂

Compounds **2.4.1a** and **2.4.2** were screening in 5-HT_{2A} and D₂ antagonist assays that were outsourced to DiscoverX.²⁸⁹

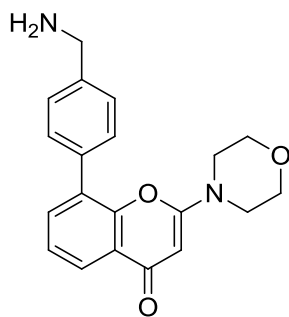
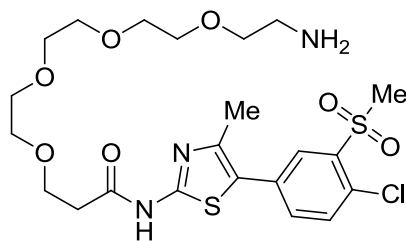
mTOR

The affinity of compounds **2.5.1**, **2.5.3** and **2.5.4** for mTOR was determined in the mTOR kinobeads assay. This is a competition-binding assay based on the capturing of endogenously expressed target proteins from cell extracts by a bead-immobilized capturing ligand in presence of the test compound.

HuT-78 cells (European Collection of Authenticated Cell Cultures, 88041901) were cultured according to vendor's instructions. Frozen cell pellets were homogenized in 3x pellet volumes lysis buffer (50 mM Tris-HCl, 0.4% (v/v) Igepal-CA630, 5% glycerol, 150 mM NaCl, 1.5 mM MgCl₂, 25 mM NaF, 1 mM sodium vanadate, 1 mM DTT, pH 7.5, supplemented with EDTA-free protease inhibitor tablet (Roche)). The sample was dispersed using a Dounce homogenizer, kept rotating for 30 min at 4 °C, and centrifuged for 10 min at 20,000g at 4°C. The supernatant was centrifuged again for 1 h at 145,000 g. The protein concentration was determined by Bradford assay (BioRad), aliquots were snap frozen in liquid nitrogen and stored at –80 °C.

The capturing matrices were generated by derivatizing N-hydroxysuccinimide (NHS) activated Sepharose 4 beads (GE Healthcare) with the functionalized ligands **2.8.6** and

2.8.7 at a ligand density of 5 mM. Remaining NHS-groups were blocked with ethanolamine.

**2.8.6****2.8.7**

For the mTOR kinobeads assay the matrices were combined in a 1:1 ratio and equilibrated in DP buffer (50 mM Tris-HCl (pH 7.5), 0.4% (v/v) Igepal-CA630, 5% (v/v) glycerol, 150 mM NaCl, 1.5 mM MgCl₂, 25 mM NaF, 1 mM Na₃VO₄, 1 mM dithiothreitol). All steps of the mTOR kinobeads assay were performed at 4 °C or on ice. The cell lysate was diluted with DP buffer to a final concentration of 5mg/mL and a final detergent concentration of 0.4% (v/v) Igepal-CA630. For the assay 250 µg cell lysate and 2.5 µL capturing matrix per well (final assay volume: 75 µL) were incubated in the presence of test compounds in a 384-well filter plate (MultiScreenHTS HV Filter Plate, 0.45 µm, MZHVN0W50, Merck Millipore). Each plate contained 16 positive (100 µM GSK1061135A) and 16 negative (2% v/v DMSO) control wells. Compounds were tested in a concentration-response applying 1:3 or 1:4 dilution steps for in total 11 data points. DMSO concentration was 2% (v/v). After 2 h incubation on an overhead shaker (Roto-Shake Genie, Scientific Industries Inc.) at 4 °C the non-bound fraction was removed by washing the beads with DP buffer. Proteins retained on the beads were eluted in SDS sample buffer (200 mM Tris (pH 7.4), 250 mM Trizma Base, 4% (w/v) SDS, 20% (v/v) glycerol, 0.01% (w/v) bromophenol blue, 50 mM dithiothreitol) into a collection plate (384 well polypropylene microplate, V-shape, Greiner, 781 280). Eluates were spotted on nitrocellulose membranes (400 nL per spot) using an automated pin-tool liquid transfer (Biomek FX, Beckman). After drying, the membranes were rehydrated in 20% (v/v) ethanol and blocked by incubation with Odyssey blocking buffer (LICOR, 927-40000) for 1 h at RT. Blocked membranes were

incubated overnight at 25 °C with Odyssey blocking buffer supplemented with a specific anti-mTOR antibody (Cell Signalling, 2972; 1:500) and 0.4% TWEEN-20. Then the membranes were washed in PBST buffer and incubated for 60 min at RT with the detection antibody (IRDye™ labelled antibody from LI-COR) diluted in Odyssey blocking buffer (LICOR 927-40000) containing 0.2% TWEEN-20. Then the membranes were washed with PBST and finally rinsed twice with PBS buffer to remove residual Tween-20. The membranes were then scanned with the Odyssey® Infrared Imaging System (LI-COR Biosciences). Fluorescence signals were recorded and analyzed according to the instructions of the manufacturer. Concentration response curves were computed with the software Activity Base. All data were normalized to the mean of 16 high (negative control) and 16 low (positive control) control wells on each plate. Concentration-response curves were fitted using a 4 parameter logistic fit using the equation: $Y = A + ((B - A)/(1 + 10^{pIC_{50}(X * D)}))$; where: Y = response, A = minimum response (positive control), B = maximum response (negative control), D = slope factor, x = log(Molar compound concentration). pIC₅₀ values are the negative logarithm of the IC₅₀ value.

PI3K α , β , γ and δ

The affinity of compounds **2.5.1**, **2.5.3** and for PI3K α , β , γ and δ was determined by homogeneous time resolved fluorescence (TR-FRET) assays according to the following protocol:

Briefly, solid compound is dissolved in 100% DMSO at a concentration of 2 mM. Dilutions are prepared in 100% DMSO using a 1 in 4 serial step dilution. The dilutions are transferred to black low volume Greiner assay plates ensuring that the DMSO concentration is constant across the plate at 1% (0.1 μ L/well).

PI3K Reaction Buffer (contains 50 mM HEPES pH 7.0 (NaOH), 150 mM NaCl, 10 mM MgCl₂, 2.3 mM sodium cholate, 10 μ M CHAPS made up in milliQ water). Fresh DTT is added at a final concentration of 1 mM on the day of use. Wortmannin at a

concentration sufficient to produce 100% inhibition (8.33×10^{-6} M) is added to column 18 of compound plates.

Enzyme solutions: 1x PI3K assay Buffer containing:

- 550 pM PI3K-Alpha enzyme (275 pM final assay concentration)
- 800 pM PI3K-Beta enzyme (400 pM final assay concentration)
- 3 nM PI3K-Delta enzyme (1.5 nM final assay concentration)
- 10 nM PI3K-Gamma enzyme (5 nM final assay concentration)

These concentrations are optimal to achieve a signal:background of between 1.5-4.5. The enzyme solution is added to columns 1-24 (3 μ L/well) and plates are incubated for 15 min at RT.

Substrate solution: 1 x PI3K assay buffer containing:

- PI3K-Alpha: 500 μ M ATP, 20 μ M PIP₂ and 120 nM biotin-PIP₃. (Final assay concentrations are 250 μ M ATP, 10 μ M PIP₂ (both at Km) and 40 nM biotin-PIP₃).
- PI3K-Beta: 800 μ M ATP, 20 μ M PIP₂ and 120 nM biotin- PIP₃. (Final assay concentrations are 400 μ M ATP, 10 μ M PIP₂ (both at Km) and 40 nM biotin-PIP₃).
- PI3K-Delta: 160 μ M ATP, 20 μ M PIP₂ and 120 nM biotin- PIP₃. (Final assay concentrations are 80 μ M ATP, 10 μ M PIP₂ (both at Km) and 40 nM biotin-PIP₃).
- PI3K-Gamma: 30 μ M ATP, 20 μ M PIP₂ and 120 nM biotin- PIP₃. (Final assay concentrations are 15 μ M ATP, 10 μ M PIP₂ (both at Km) and 40 nM biotin-PIP₃).

This is added to all wells and plates are incubated for 1 h at room temperature. Detection solution: PI3K Detection Buffer (contains 50 mM HEPES pH 7.0 (hydrochloric acid), 150 mM NaCl, 2.3 mM sodium cholate, 10 μ M CHAPS, 240 mM

KF) containing 2 mM DTT (2 x final concentration), 90 nM GRP-1 PH domain, 300 nM Streptavidin-APC and 24 nM Europium-anti-GST (6 x final concentrations).

This is mixed and left at room temperature (protected from light).

STOP solution: PI3K STOP Buffer (contains 50 mM HEPES pH 7.0 (hydrochloric acid), 150 mM NaCl, 2.3 mM sodium cholate, 10 μ M CHAPS, 150 mM EDTA).

Detection solution is diluted 1:1 with STOP solution and added to all wells (3 μ L/well). Plates are covered and incubated on the bench for 45-60 min.

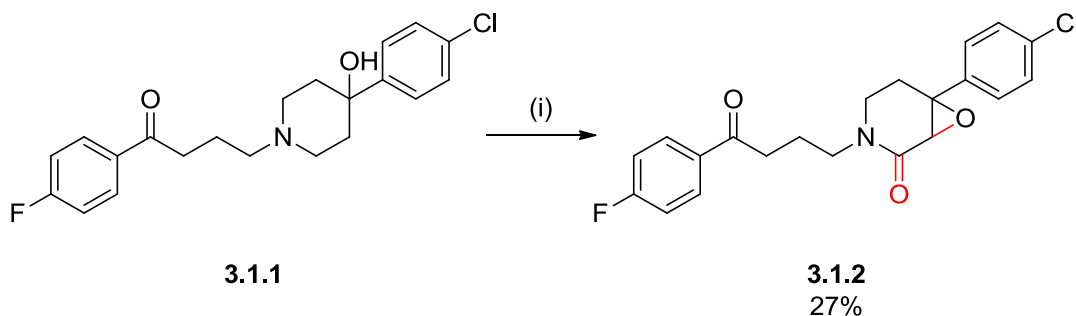
Plates are read on a PerkinElmer Envision, measuring TR-FRET between the complex formed between the GST-tagged PH domain and biotinylated PIP₃ which both recruit fluorophores (Europium-labelled anti-GST & Strep-APC respectively). In the presence of an inhibitor, this complex is disrupted by the competitive action of non-biotinylated PIP₃ (formed in the assay by the phosphorylation of PIP₂ by the kinase & ATP). From this, the ratio of acceptor/donor was calculated and used for data analysis.

Chapter 3. Elaboration of Iodine-Mediated Azacycle C–H Oxidation

3.1 Deviations from Anticipated Lactam Formation

The conditions developed and described in chapter two could be used to carry out α -C–H oxidation of azacycles predictably and selectively for most substrates. There were some instances, however, where deviation from the anticipated lactam formation was observed, which are described in this chapter.

For the antipsychotic drug haloperidol, **3.1.1**, an unexpected oxidation product was observed (Scheme 63).



Scheme 63: Oxidation of 3.1.1 to epoxy-lactam 3.1.2. Conditions: (i) I₂ (7.5 eq.), NaHCO₃ (10.0 eq.), THF:H₂O (2.5:1, 0.025 M), 4 h, RT.

Instead of mono-oxidation of the piperidine ring to the corresponding lactam, epoxy-lactam **3.1.2** was isolated in 27% yield. Starting material **3.1.1** was fully consumed in this reaction, so the low yield is likely due to a mixture of divergent oxidation pathways possible for this substrate. A mixture of close-running, more polar species were observed in the reaction LCMS profile, though these could not be isolated. These by-products did ionise cleanly to 374.2 (ES, positive mode), 388.4 (ES, negative mode) and 402.4 (ES, negative mode), maintaining the chlorine isotopic mass pattern. Based on these observed mass to charge (m/z) ratios and the structure of the isolated product, structures **3.1.3** to **3.1.5** were proposed to also form in the reaction mixture (Figure 25).

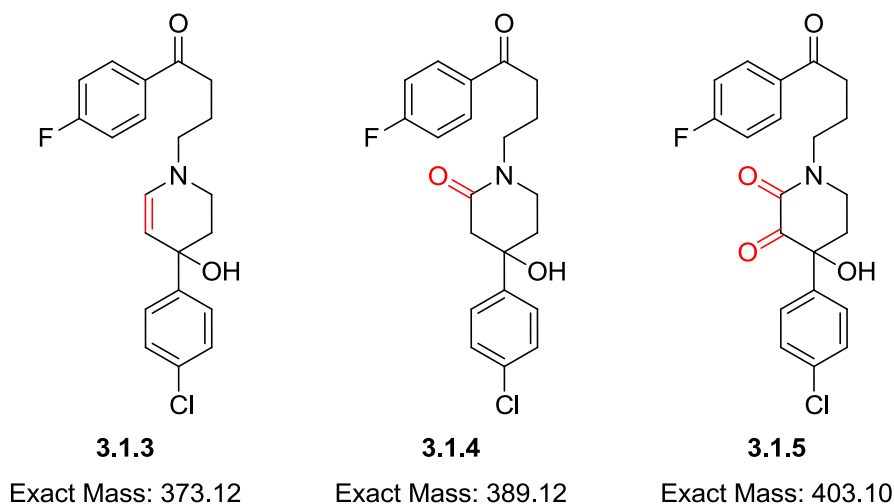
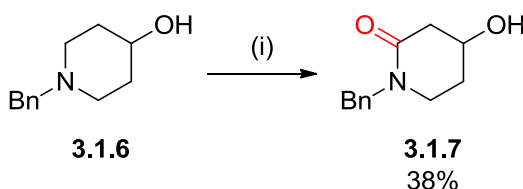


Figure 25: Putative side-products formed in the oxidation of 3.1.1.

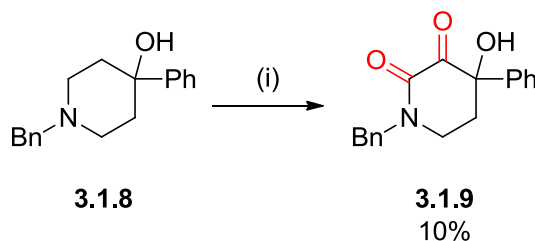
Epoxy-amides, such as **3.1.2**, are interesting motifs found in natural products^{290,291} and are useful building blocks in organic synthesis.^{292–294} Therefore, it was felt that it would be worthwhile investigating this unexpected result further by probing the oxidation of structurally similar, but less complex, model substrates. Hydroxy-piperidine **3.1.6** (Scheme 64) was subjected to the iodine-based oxidation conditions, with a similar epoxy-lactam expected to be formed.



Scheme 64: 4-Hydroxy substituted piperidine 3.1.6 was oxidised to lactam 3.1.7. Conditions: (i) I₂ (7.5 eq.), NaHCO₃ (10.0 eq.), THF:H₂O (2.5:1, 0.025 M), 16 h, RT.

However, only the direct oxidation to lactam **3.1.7** was observed, along with reaction stalling at approximately 50% conversion of starting material, by LCMS, which resulted in a 38% yield after HPLC purification. While the tolerance of secondary alcohols under the developed oxidation conditions is demonstrated, the oxidation of **3.1.6** did not, at first glance, appear to offer much insight into the oxidative behaviour of **3.1.1**. The most apparent difference between substrates **3.1.1** and **3.1.6** was the change from a benzylic tertiary alcohol to a secondary alcohol. As such, oxidation of

tertiary alcohol **3.1.8** (Scheme 65) was explored, which led to the formation of keto-lactam **3.1.9** in 10% yield, after a second purification.



Scheme 65: Oxidation of tertiary alcohol substituted piperidine 3.1.8 led to double oxidation of the azacycle. Conditions: (i) I₂ (7.5 eq.), NaHCO₃ (10.0 eq.), DMSO:H₂O (2.5:1, 0.025 M), 4 h.

Oxidation in a DMSO/water solvent system gave a reaction profile with fewer by-products than the THF/water system, hence this was studied further. The oxidation proceeded unselectively, however, with a mixture of oxidative by-products formed in approximately equal quantities, based on the LCMS profile, which were hypothesised to be compounds **3.1.10** and **3.1.11** (Figure 26) based on the ionisation (ES, positive mode) to 262.1 and 282.1.

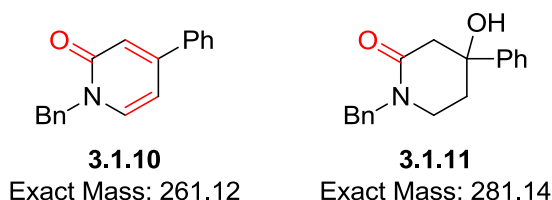


Figure 26: Putative side-products in oxidation of 3.1.8.

Additionally, incomplete consumption of starting material was observed by LCMS. Purification and isolation of all the major species formed was attempted, but silica gel chromatography did not yield clean material, so a second purification by HPLC was necessary, leading to a low recovery of **3.1.9**. Also, some of the by-products seen in the analysis of the reaction mixture were not detected following the work-up of the reaction and initial column chromatography. This suggested that these were either polar, water soluble species, or unstable on silica, and this is why **3.1.9** was the only clean product isolated from the reaction.

No desired epoxy-lactam was formed in this transformation, however the formation of keto-lactam **3.1.9** is still ostensibly a double oxidation of **3.1.8**, and therefore proceeded with similar reactivity to **3.1.1**. One possible reason for tertiary alcohols deviating from the expected oxidation to a lactam is that the alcohol group is held in the axial position on the ring, with the bulkier aromatic group in the equatorial position, unlike for secondary alcohol **3.1.6** (Figure 27).

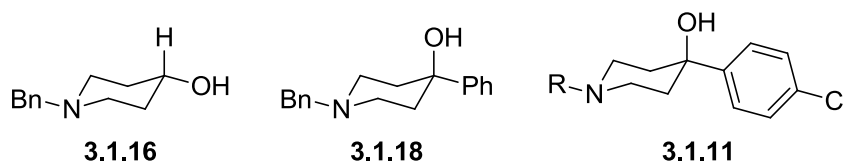


Figure 27: Chair conformations of the hydroxy-substituted substrates.

This structural arrangement means that the flipping of the ring to a boat conformation puts the hydroxyl group and the nitrogen close to one another, and allow hydrogen bonding interactions to be established, thereby stabilising a boat conformation (Figure 28).

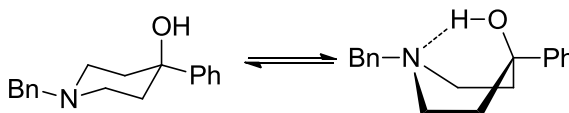
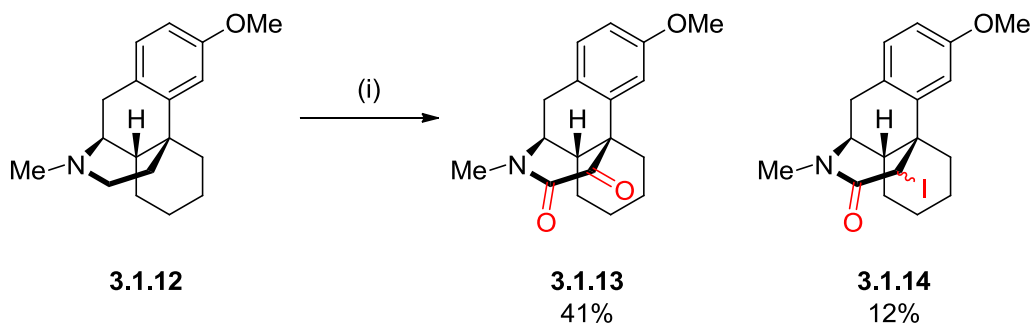


Figure 28: Hydrogen bonding between the piperidine nitrogen atom and the axial tertiary alcohol may increase the lifetime of the boat conformation.

This hydrogen bond could possibly increase the lifetime of the boat conformation, and restrict the ability to ring flip. Literature precedent for the double oxidation of a piperidine ring to a keto-lactam motif principally occurs in ring systems with restricted movement.^{91,295,296} It is therefore possible that the conformational arrangement that the ring adopts has an effect on the susceptibility to oxidation.

Dextromethorphan, **3.1.12** (Scheme 66), a serotonin reuptake antagonist of the morphinan class, was used to test this hypothesis, because the azacyclic ring is fixed into a boat configuration.



Scheme 66. Double oxidation was observed for the boat-restricted piperidine ring of dextromethorphan 3.1.12. Conditions: (i) I₂ (7.5 eq.), NaHCO₃ (10.0 eq.), THF:H₂O (2.5:1, 0.025 M), 16 h, RT.

As anticipated, the keto-lactam **3.1.13** was observed in 41% yield, in addition to the iodolactam **3.1.14** as a by-product, where the stereochemistry of the carbon-iodine bond was not determined. The double oxidation to **3.1.13** suggested that the enamine side of the iminium-enamine tautomeric mixture was favoured; it is possible that the β C–H bond of iminium **3.1.15** (Figure 29) is made more acidic by donation of electron density from the C–H σ-bonding orbital into the iminium antibonding orbital, which is promoted by the restricted conformation of the ring in **3.1.12**.

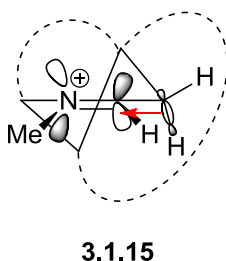
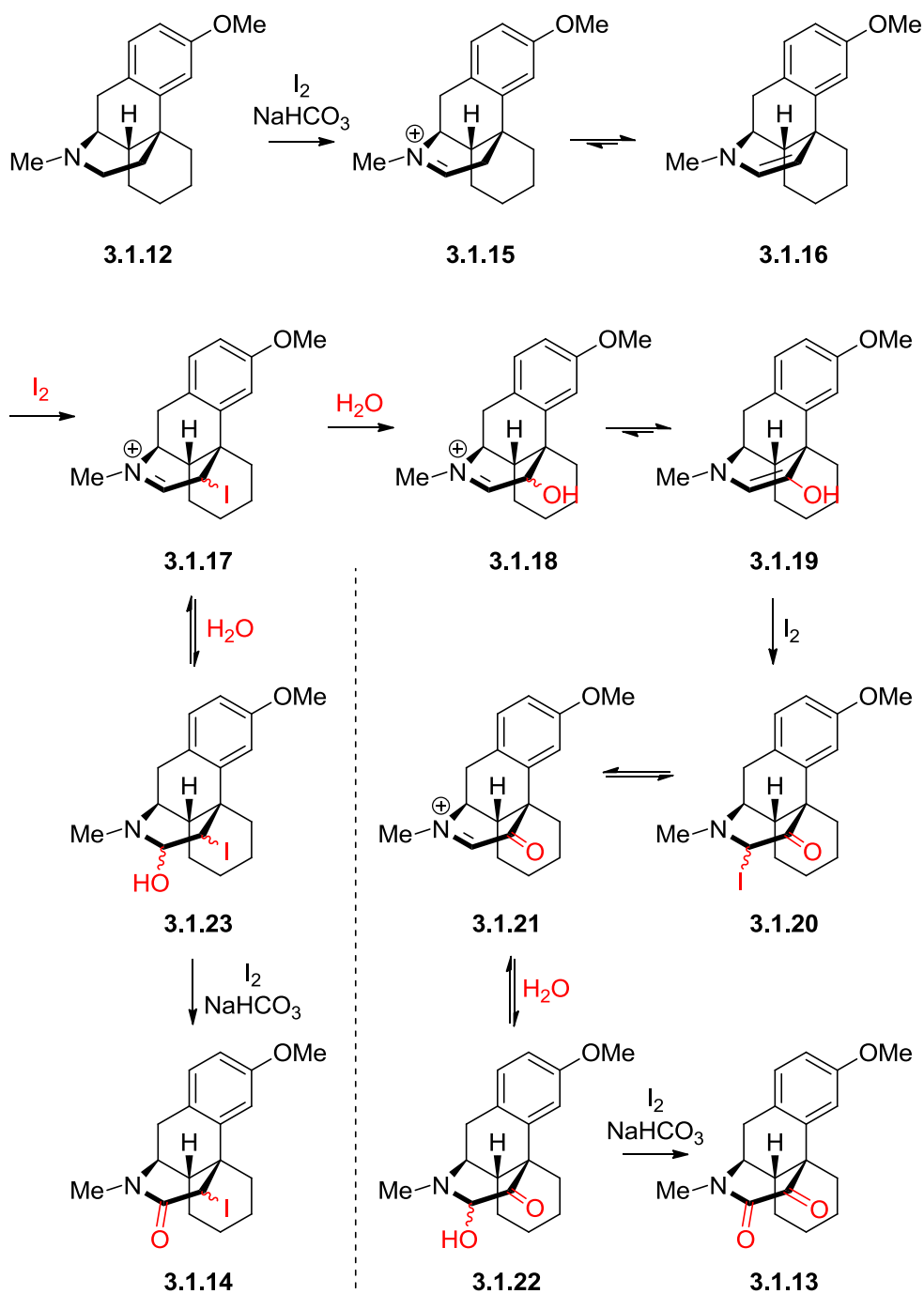


Figure 29. Donation of electron-density from the β C–H bond to the iminium antibonding orbital increases the propensity for formation of the enamine tautomer.

Accordingly, it is then feasible that an increase in the amount of enamine tautomer **3.1.16** (Scheme 67) can lead to formation of iodoiminium **3.1.17**.



Scheme 67. Proposed mechanism accounting for the increased amount of oxidation for azacycles with an increased lifetime of boat configuration.

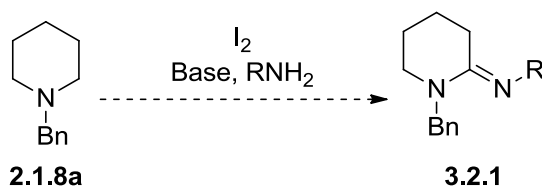
This intermediate can then undergo substitution of iodide with water to β -hydroxyiminium **3.1.18**, which can tautomerise to enamine **3.1.19** and then iodinate to α -iodinated species **3.1.20**. Elimination of iodide by the nitrogen lone pair forms ketoiminium **3.1.21**, which can undergo nucleophilic attack by water to α -hydroxyiminium

3.1.22, and can then be *N*-iodinated and oxidised to **3.1.13**. An alternative pathway from **3.1.17** could be attack by water directly into the iminium moiety to give **3.1.23**; *N*-iodination and oxidation would then form **3.1.14**.

These examples demonstrated the variation of products that can be prepared with this methodology owing to the fact that oxidation is substrate-controlled, which is potentially very interesting for drug discovery, where rapid late-stage access to structural diversity is required. So far this methodology has been limited to the transformation of C–H bonds into C–O bonds, thus elaboration of this methodology to incorporate other functionality was investigated.

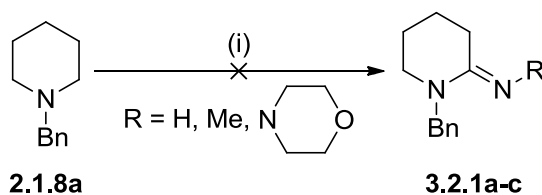
3.2 Proposed Nucleophilic Trapping of Iminium Intermediate

Using the understanding of the oxidation protocol gathered so far, and based on the proposed mechanism of oxidation, it was proposed that C–H amination of azacycles could be achieved by replacement of water in the oxidation procedure with an amine nucleophile to allow access to amidine-type structures **3.2.1** (Scheme 68).



Scheme 68. Proposed adjustment of iodine-mediated C–H oxidation procedure to allow for elaboration into a C–H amination protocol.

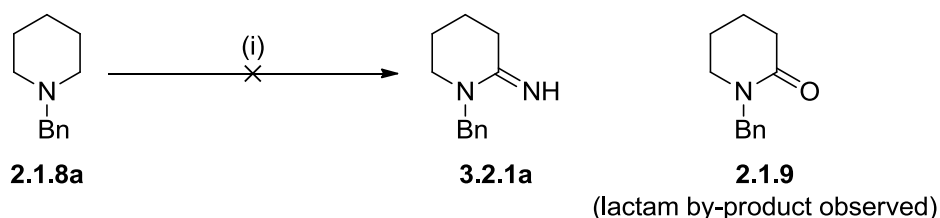
Since the water was to be removed from the solvent system, the transformation was initially investigated with the amine prospectively functioning as both a nucleophile and an organic soluble base. Three amines were screened (Scheme 69), but no desired product was isolated from any of the reactions.



Scheme 69. Attempted C–H amination via elaboration of oxidation protocol. Conditions: (i) I₂ (5.0 eq.), H₂NR (10.0 eq.), THF (0.025 M), RT, 4 h.

With ammonia (solution in THF), a lot of unreacted starting material was observed, but a mass ion that correlated with the mass of the desired amidine was detected in small quantity by LCMS. Unfortunately, no product could be observed by crude NMR or isolated using HPLC purification. Use of methylamine also showed principally unreacted starting material by LCMS and NMR analysis, and a mass ion corresponding to double addition of methylamine was observed in low quantity, although again this species could not be isolated. Hydrazine 4-aminomorpholine did not show any signs of desired product formation, instead only forming what seemed to be dimers of the aminomorpholine, based on ¹H NMR.

Since trace levels of putative product were observed with ammonia, a screen of bases was carried out to test whether these would promote product formation (Table 18).



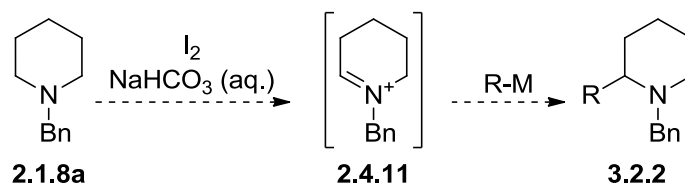
Entry	1	2	3	4	5	6
Base	NaHCO ₃ ^[a]	NaH ₂ PO ₃ ^[a]	K ₂ HPO ₃ ^[a]	(Et ₄ N)(HCO ₃)	C ₅ H ₅ N	Et ₃ N

Table 18. Bases screened to test whether base choice would have an effect on promoting C–H amination. Conditions: (i) I₂ (5.0 eq.), NH₃ (4M in THF, 10.0 eq.), Base (10.0 eq.) THF (0.025 M), RT. [a] For inorganic bases, 10:1 THF:water was used as solvent to solubilise the base.

For inorganic bases (entries 1-3), a small amount of water was added to partially solubilise the base, but this resulted in mainly formation of lactam **2.1.9**. Organic

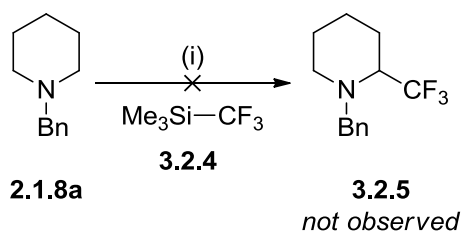
soluble tetraethylammonium carbonate (entry 4) showed poor consumption of starting material to a complex mixture of trace products. Pyridine (entry 5) appeared to show improved conversion of starting material to the proposed product species, but disappointingly material of high enough purity for analysis could not be isolated from the reaction. Triethylamine (entry 6), which was proposed to be more basic than the prospective nucleophile ammonia,^{297,298} showed an increased number of by-products than that seen for pyridine, perhaps as a result of the oxidisable alkyl groups present causing side-reactivity. Despite tentative indications of product formation with the use of pyridine, no product had been isolated to prove the concept of this C–H amination transformation. This was possibly due to the instability of the desired product towards ammonia elimination. As such, the use of nucleophiles that would not be such good leaving groups should be investigated, such as carbon-based nucleophiles.

Given the aqueous solvent system used in the iodine-mediated C–H oxidation, a Barbier reaction was proposed because conditions used in Barbier reactions involve the *in situ* formation of organometallic nucleophiles under aqueous conditions.²⁹⁹ The majority of Barbier-transformations describe the addition of organometallics into aldehydes,^{300–302} though there have been reports of quenching imines and iminium species with nucleophiles generated under Barbier conditions.^{303,304} Barbier-type functionalization of **2.1.8a** (Scheme 70) was envisaged to be possible *via* nucleophilic attack of an organometallic on the purported iminium species **2.3.11** to form the α -functionalized amine **3.2.2**.



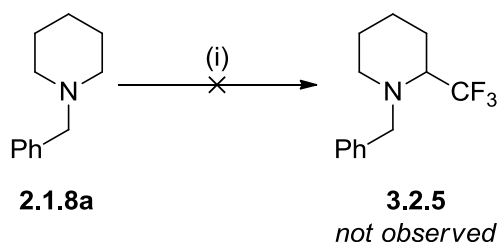
Scheme 70. Proposed interception of iminium intermediate 2.3.11 with a Barbier reaction.

As such, non-organometallic nucleophilic trapping was investigated. α -Trifluoromethylation was investigated using Ruppert's reagent **3.2.4** (Scheme 73),^{305,306} in the presence of an activating species that could generate a trifluoromethyl nucleophile *in situ*, to form **3.2.5** from **2.1.8a**. Addition of fluoro-alkyl units into iminium species has been recently demonstrated by Huang *et al.*³⁰⁷



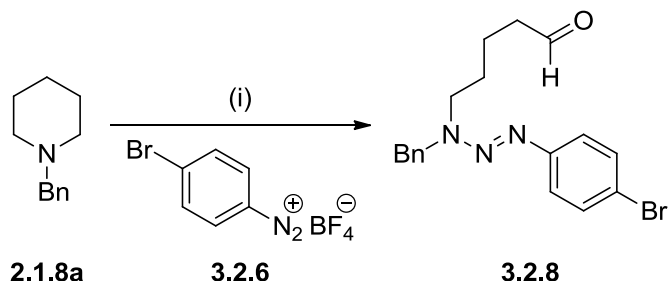
Scheme 73. Attempted trifluoromethylation using Ruppert's reagent. Conditions: (i) I₂ (1.2 eq.), **3.2.4** (2.0 eq.), activator (KF, NH₄F or NaOAc) (3.0 eq.), THF, RT, 16 h, no reaction.

However, no reaction was observed to occur between amine **2.1.8a** and **3.2.4** in the presence of iodine and potassium fluoride, ammonium fluoride or sodium acetate as potential activators. Trapping with a trifluoromethyl group generated oxidatively from a sulfinate salt was attempted, because the proposed iminium was rationalised to be ostensibly similar to the substrates used by Baran *et al.* for the C–H functionalisation of heterocycles.⁶⁸ Disappointingly, no reaction of starting material was observed when the Baran conditions were incorporated into the iodine-mediated C–H oxidation conditions (Scheme 74).



Scheme 74. Trifluoromethylation of 2.1.8a using the Langlois reagent was unsuccessful. Conditions: (i) I₂ (3.0 eq.), CF₃SO₂Na (3.0 eq.), *tert*-butylhydroperoxide (5.0 eq.), DCM:H₂O (2:1), RT, 4 h, no reaction.

investigated. Initially, a comparison of iodine with NIS was carried out (Table 19), with NIS providing a moderately increased conversion to **3.2.8** compared to iodine, from 7% to 21% conversion.



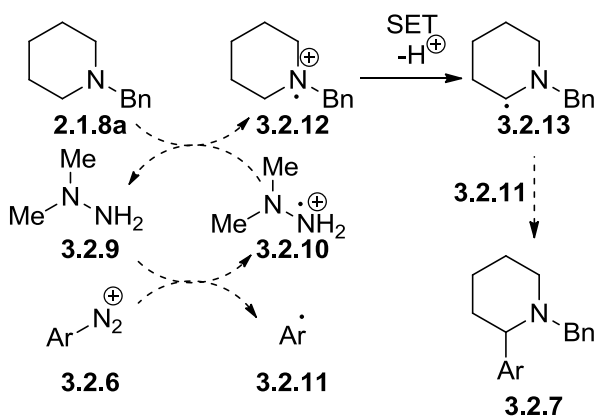
Iodine source	Stoichiometry	% conv. ^[a]
I ₂	1.0	7
	2.0	18
NIS	1.0	13
	2.0	21

Table 19. Comparison of iodine with NIS, which indicated that NIS was a better source of electrophilic iodine. Conditions: (i) Iodine source, **3.2.6** (2.0 eq.), NaHCO₃ (3.0 eq.), THF:water (2:1, 0.067 M), RT, 3 h. [a] Conversion determined by ¹H NMR analysis of crude material against an internal standard.

It was desirable to avoid the use of very high stoichiometry of the iodine source, so increasing the amount of diazonium salt in the reaction mixture was investigated. No difference in the reaction LCMS profile for two, four, six or eight equivalents of **3.2.6** was observed, which indicated that increasing the stoichiometry of **3.2.6** does not significantly affect the conversion of **2.1.8a** to **3.2.8**. Therefore, the stoichiometry of oxidant was investigated. Increasing the amount of NIS to 2.5 equivalents gave no change in the LCMS reaction profile compared to two equivalents and, while increasing the stoichiometry further resulted in consumption of starting material, a very complex mixture of poly-oxidised by-products was formed. As such, it was concluded that higher stoichiometry of NIS did not offer any beneficial change to the conversion of **2.1.8a** to **3.2.8**, and alternative strategies will need to be pursued to investigate optimisation of this transformation. Future optimisation of the ring-opening formation of triazenes through scoping different diazonium species, activating

agents and bases could benefit the scientific community due to the potential wide application of triazenes, which has not been widely explored due to limited preparative methods.

Given the issues encountered with iodination of the diazonium salt, α -arylation of **2.1.8a** was attempted in the absence of an iodine source. Maulide *et al.* recently reported the generation of aryl radicals from aryldiazonium salts using alkyl hydrazines as organocatalysts for a single-electron transfer (SET) process.^{323,324} This method has been used for the functionalisation of electron-rich heterocycles, and cyclic amides in an intramolecular fashion, although the diazonium salt is used as the limiting reagent, which is undesirable for the late-stage functionalisation of azacycles. It was hypothesised that use of a hydrazine organocatalyst **3.2.9** could instigate the generation of the aryl radical **3.2.11** from **3.2.6** (Scheme 76), and alkyl radical **3.2.13** from **2.1.8a** via a SET.

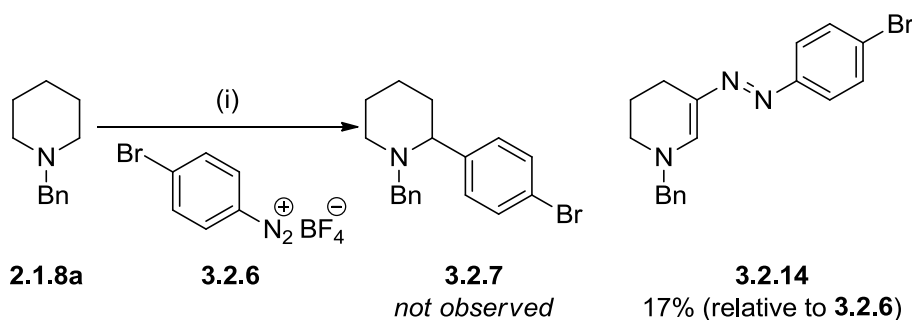


Scheme 76. Proposed mechanistic rationale for the use of a hydrazine organocatalyst to carry out α -arylation of azacycles.

The resulting primary amino radical cation **3.2.10** could then abstract a radical from tertiary amine **2.1.8a**, reforming the hydrazine and generating tertiary amino radical cation **3.2.12**. This could then undergo a SET and loss of a proton to generate the secondary carbon-centred radical **3.2.13**,^{235,236} which would be anticipated to be more stable than the nitrogen radical, due to the increased electronegativity of nitrogen

compared to carbon. This radical species could then be quenched by the aryl radical generating the desired α -arylation product **3.2.7**.

However, for the reaction of **2.1.8a** with **3.2.6** in the presence of a catalytic amount of **3.2.9**, no α -arylation product was observed (Scheme 77). Instead the enaminyldiazene **3.2.14** was isolated in 17% yield, with the limiting reagent **3.2.6** not being fully consumed.



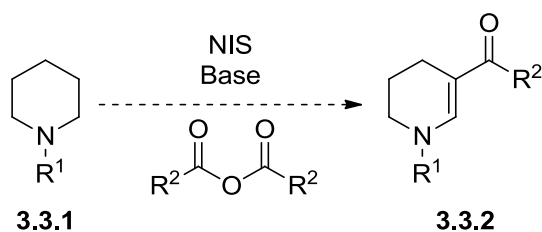
Scheme 77. Generation of enaminyldiazene 3.2.14 in the presence of an alkylhydrazine organocatalyst. Conditions: (i) **3.2.6** (1.0 eq.), **2.1.8a** (5.0 eq.), **3.2.9** (10 mol%), DMSO, RT, 60 min.

This was an unexpected, but interesting transformation, as it exemplified the interception of an enamine intermediate by the electrophilic diazonium salt **3.2.6**. Disappointingly, lowering the stoichiometry of **2.1.8a** only led to decreased consumption of **3.2.6**, and increasing the amount of organocatalyst **3.2.9** present to one equivalent resulted in increased by-product formation. Additionally, changing to 4-aminohydrazine as the organocatalyst and MeCN as the solvent, as used by Maulide *et al.*,³²³ did not provide any improvement in the reaction profile.

Given the need for a large excess of the amine, and the lack of improvement during the initial optimisation scoping, it was decided that the reactions with diazonium salts was not likely to deliver appreciable results in the short term, and would require extensive investigation. Nevertheless, this discovery did provide a proof of concept that intermediates in the oxidative functionalisation of azacycles could be intercepted by an electrophilic species.

3.3 Electrophilic Trapping of an Enamine Intermediate

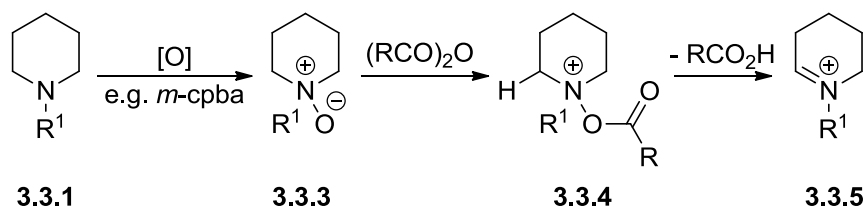
The complex reactivity and unsuccessful optimisation of the reaction of diazonium salts with azacycles may have resulted from the high reactivity and instability of the diazonium motif. As such, it was proposed that it would be more beneficial if a reactive electrophile could be generated *in situ* under the oxidation conditions. For the formation of **3.2.14** it was possible that the diazonium salt coordinated to the basic amine, activating the azacycle towards oxidation to the enamine intermediate. This is similar to the proposed initiation of the iodine-mediated C–H oxidation, hence NIS was initially to be used as the activating oxidant. To enable enamine formation, a base would need to be present, and a species that can be activated to become electrophilic during the course of the reaction would be suitable for enamine functionalisation. A carboxylic anhydride presented as an appropriate reagent since these can be activated to become more electrophilic by nucleophilic bases, such as 4-dimethylaminopyridine (DMAP). This is then complementary to the necessity for basic conditions to generate an enamine. In this regard, it was hypothesised that enaminyll ketones, such as **3.3.2** (Scheme 78), could be prepared from **3.3.1** *via* a C–H oxidative functionalisation strategy using NIS as an oxidant, and an anhydride and a nucleophilic base to generate an electrophile *in situ*.



Scheme 78. Proposed synthesis of enaminyll ketones *via* iodine-mediated C–H oxidative functionalisation.

Generation of an iminium species from a saturated amine *via* oxidative activation of the nitrogen atom can be carried out by the Polonovski reaction.^{325–327} Trapping of an *N*-oxide **3.3.3** (Scheme 79) with an electrophilic anhydride generates an acetate-substituted ammonium species **3.3.4**. The acetate group can then function as a leaving group to generate an iminium species **3.3.5**. This reaction has been used for the

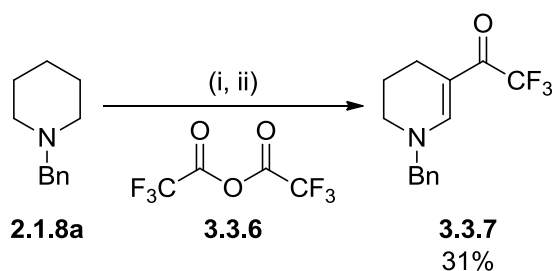
functionalisation of natural product intermediates,^{328,329} and, for cyclic systems, tautomerisation of **3.3.5** to the enamine can lead to oxidative β -functionalisation of the azacycle.³²⁹



Scheme 79. Generation of an iminium species *via* the Polonovski reaction. *m*-cpba = *meta*-chloroperbenzoic acid.

The application of this reaction is somewhat narrowed by the limited functional group tolerance associated with the formation of *N*-oxides, and the necessity to pre-form and isolate the *N*-oxide. As such, it was proposed that *in situ* transient activation of the amine with an iodine source could offer similar reactivity to generate an iminium species, which could then react with an electrophilic anhydride *via* the enamine tautomer.

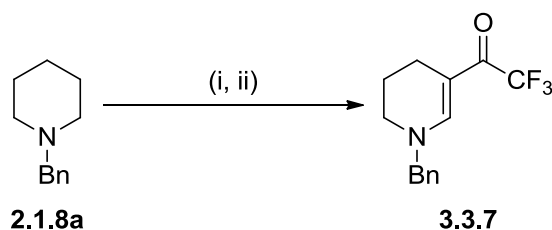
Initial studies using **2.1.8a** and NIS in the presence of pyridine and trifluoroacetic anhydride **3.3.6** (Scheme 80) showed that oxidative β -carbonylation could indeed occur to afford enaminyll ketone **3.3.7** in 31% yield.



Scheme 80. Polonovski-type oxidative carbonylation of **2.1.8a** to afford **3.3.7**. Conditions: (i) NIS (4.0 eq.), DCM, RT, 30 min; (ii) **3.3.6** (5.0 eq.), pyridine (3.0 eq.), -10 °C to RT, 2.5 h.

This was important validation of the proposition that aliphatic azacycles could be activated *in situ* with electrophilic iodine to generate an iminium species, which could then be used for β -functionalisation of the azacycle. Subsequent investigations were undertaken to optimise this transformation, and to examine the scope of the transformation to explore the utility of this reaction.

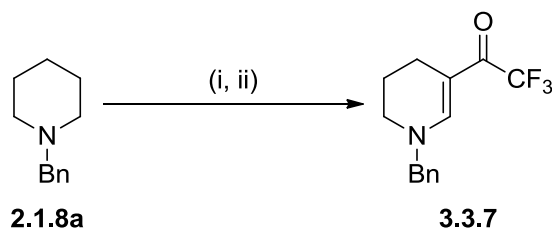
The first solvent, DCM, was selected because a great deal of literature precedent for the Polonovski reaction had been carried out in DCM.^{328,329} A comparison with THF was of interest as this was found to be the optimal solvent for the iodine-mediated C–H oxidation, however this gave a less selective reaction with a greater proportion of by-products observed by LCMS when compared with DCM (Table 20, entry 2).



Entry	Eq. of NIS	Solvent	Comments
1	4.0	DCM	31% yield (Scheme 80)
2	4.0	THF	Multiple products observed
3	1.1	DCM	No reaction
4	1.1	THF	No reaction

Table 20. Comparison of DCM and THF across two stoichiometries of NIS. Conditions: (i) NIS (1.1 or 4.0 eq.), DCM or THF, RT, 30 min; (ii) **3.3.6** (5.0 eq.), pyridine (3.0 eq.), -10 °C to RT, 2.5 h.

Additionally, lowering the stoichiometry of NIS led to no reaction of **2.1.8a** in both cases (entries 3 and 4). This may have been due to coordination of NIS with pyridine,³³⁰ rendering it unable to activate the amine substrate. To test if this was occurring, the stoichiometry of all reagents was lowered to just over one equivalent. This resulted in a low conversion to **3.3.7** of 11%, although this was an improvement on the previous use of 1.1 equivalents of NIS (Table 21, entry 1).

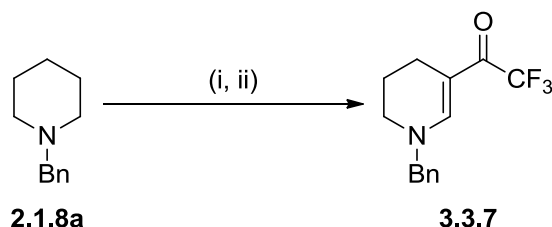


Entry	Eq. of NIS	Eq. of 3.3.6	Eq. of Pyridine	Conversion ^[a] to 3.3.7 (%)
1	1.1	1.2	1.2	11
2	1.1	1.2	2.2	16
3	2.2	5.0	6.0	0 ^[b]
4	1.1	1.2	2.2	20 ^[c]
5	1.1	1.2	2.2	2 ^[d]
6	4.0	5.0	6.0	46
7	4.0	1.2	6.0	0
8	4.0	2.5	6.0	0
9	4.0	10.0	6.0	45

Table 21. Increasing ratio of pyridine relative to NIS gave an increase in formation of 3.3.7. Conditions: (i) NIS (1.1 to 4.0 eq.), DCM, RT, 30 min; (ii) 3.3.6 (1.2 to 10.0 eq.), pyridine (1.2 to 6.0 eq.), -10 °C to RT, 2.5 h. [a] Conversion determined by ¹H NMR analysis of crude material against an internal standard. [b] 3.3.6 and pyridine not added dropwise. [c] Reaction run at RT. [d] Reaction run at 60 °C.

Increasing the amount of base further led to a comparable 16% conversion to 3.3.7 (entry 2), but increasing the ratio of pyridine and 3.3.6 to NIS further led to no product formation (entry 3). It should be pointed out that in this case the addition of 3.3.6 and pyridine was not dropwise, due to human error. The reaction mixture was observed to warm up on addition of reagents in step (ii), so it is hypothesised that for entry 3 an exotherm could have occurred, which ultimately led to degradation of the reaction. Undertaking the reaction at room temperature (entry 4) showed comparable conversion to entry 2, but at 60 °C very low product formation was observed (entry 5), which was consistent with the notion that fast addition of pyridine and 3.3.6 likely leads to an unfavourable exotherm. Formation of 3.3.7 could be pushed higher to 46% conversion by increasing the stoichiometry of all reagents relative to 2.1.8a (entry 6). Lowering the amount of 3.3.6 resulted in no product formation, while increasing to higher stoichiometry had no change on product formation (entries 7 to 9).

Acylation reactions have been well-precedented to be promoted by DMAP, including in a catalytic fashion,^{331,332} so the effect of adding DMAP to the reaction mixture was explored. Addition of a catalytic amount of DMAP led to a reduced level of product formation (Table 22, entry 1).



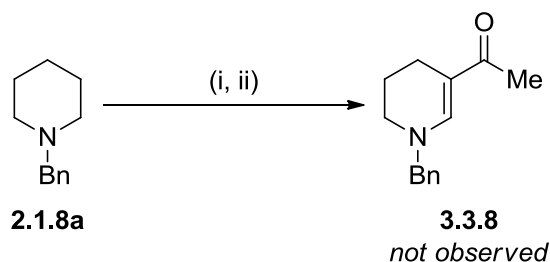
Entry	Eq. of Pyridine	Eq. of DMAP	Conversion ^[a] to 3.3.7 (%)
1	6.0	0.2	23
2	6.0	1.0	50
3	6.0	2.0	69
4	0	0.2	0
5	0	1.0	0
6	0	6.0	70 (54% isolated)

Table 22. Influence of DMAP on the oxidative C–H carbonylation of 2.1.8a. Conditions: (i) NIS (4.0 eq.), DCM, RT, 30 min; (ii) **3.3.6** (5.0 eq.), pyridine (0.0 or 6.0 eq.), DMAP (0.2 to 6.0 eq.), -10 °C to RT, 2.5 h. [a] Conversion determined by ¹H NMR analysis of crude material against an internal standard.

However, increasing the amount of DMAP to a stoichiometric amount gave a significant boost in formation of **3.3.7** to 50% conversion (entry 2), and a further increase to two equivalents of DMAP increased conversion further to 69% (entry 3). A catalytic or single equivalent of DMAP without pyridine present as a co-base resulted in no product formation (entries 4 and 5), but increasing to six equivalents of DMAP afforded **3.3.7** in 70% conversion and 54% isolated yield, a marked improvement compared with the same stoichiometry of pyridine.

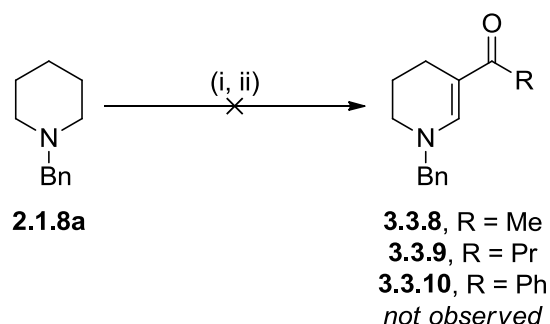
It was apparent at this stage that much more optimisation was going to be necessary in order to be able to lower the stoichiometries of the anhydride and DMAP, as it was felt

that this would be necessary to provide a valuable and scalable methodology. As a result, it was decided that it would be useful to explore the wider scope of this transformation, as it would not be worthwhile to optimise a process with limited versatility. Disappointingly, however, attempts to facilitate oxidative acylation of **2.1.8a** with acetic anhydride did not lead to formation of any desired product **3.3.8** (Scheme 81), with a mixture of oxidative products seen by LCMS.



Scheme 81. Unsuccessful oxidative acylation of 2.1.8a with acetic anhydride. Conditions: (i) NIS (4.0 eq.), DCM, RT, 30 min; (ii) Ac₂O (5.0 eq.), DMAP (6.0 eq.) -10 °C to RT, 2.5 h.

The lack of desired product formation may have resulted from the anhydride being much less electrophilic than **3.3.6**, since the trifluoromethyl groups withdraw electron density from the carbonyl units, making them more susceptible to nucleophilic attack. As such, reactivity with acyl chlorides was investigated, because these are more reactive to nucleophilic attack than the corresponding anhydride. Unfortunately, reaction with acyl, butyryl or benzoyl chloride afforded no desired oxidative carbonylation product (Scheme 82).



Scheme 82. Unanticipated oxidative acylation of 2.1.8a with acyl chlorides. Conditions: (i) NIS (4.0 eq.), DCM, RT, 30 min; (ii) RC(O)Cl (5.0 eq.), DMAP (6.0 eq.), -15 °C to RT, 2.5 h.

Formation of complex mixtures of polar oxidative by-products was observed for all cases, except for the reaction with butyryl chloride, in which the α -chloroketone **3.3.11** was isolated in 7% yield following HPLC purification (Figure 30).

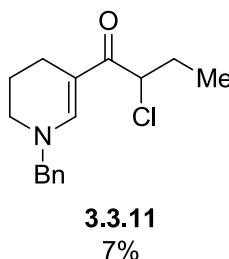


Figure 30. Unusual α -chloroketone product isolated from the attempted oxidative C–H acetylation of **2.1.8a** with butyryl chloride.

A structurally similar species is proposed to have formed with acetyl chloride as the corresponding mass ion of 250.1 (ES, positive mode) was observed by LCMS, although this product could not be isolated. However, for the reaction with benzoyl chloride the products formed did not ionise well, suggesting oligomerisation, and efforts to isolate the major product did not afford stable, pure material.

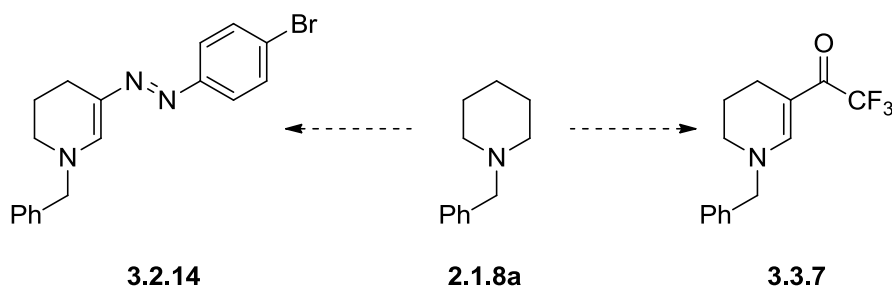
The difficulties in optimisation of this reaction could have arisen from complex cross-reactivity of the reagents used to facilitate the transformation. The nucleophilic base necessary to activate the electrophile and form the enamine could coordinate to iodine, preventing the desired reaction pathway from occurring. Despite high conversion to **3.3.7** demonstrated, the high stoichiometries of fairly expensive reagents and apparent lack of scope for this reaction is undesirable. Accordingly, it was proposed that greater success might be achieved if the electrophilic species could be generated from reaction with iodine, which shall be discussed in chapter four.

3.4 Summary

Expansion of the portfolio of C–H oxidation substrates demonstrated the subtleties and the range of transformations possible when carrying out innate C–H functionalisation

reactions. These findings could highlight points on chemical templates that are susceptible to oxidation, and, as a result, are liable to oxidative mechanisms of metabolism. Further work is required to obtain a better understanding of the mechanistic pathway of the more unexpected transformations, such as those observed for **3.1.2** and **3.1.9**, as this will improve the predictability and increase the usability of these general methodological approaches.

Attempts to carry out nucleophilic interception of the proposed iminium intermediate in the iodine-mediated C–H oxidation of azacycles were unsuccessful, and expansion of the oxidation methodology to carry out wider C–H functionalisation adjacent to the azacyclic nitrogen atom was also unsuccessful. Yet oxidative β -functionalisation was successful with electrophiles, which was consistent with the proposition that the iodine-mediated C–H oxidation proceeds with the formation of an iminium/enamine tautomeric mixture. Trapping with a diazonium salt and an electron-deficient anhydride was demonstrated (Scheme 83), although the high reactivity of those reaction systems led to complications with side reactivity and unsustainable reaction conditions required for appreciable product formation.



Scheme 83. Oxidative β -C–H functionalisation of cyclic amine 2.1.8a with electrophiles.

The findings from these studies were used to investigate more selective transformations *via* a slightly modified approach, and are discussed in the next chapter.

3.5 Experimental

General Experimental

Solvents and Reagents

Unless otherwise stated:

- Reactions were carried out under a standard atmosphere of air at room temperature, and glassware was not dried beforehand. Solvents used were non-anhydrous.
- Solvents and reagents were purchased from commercial suppliers or obtained from GSK's internal compound storage and used as received without further purification. All drug compounds used in transformations were commercially available.
- Reactions were monitored by Liquid Chromatography-Mass Spectrometry (LCMS) and Nuclear Magnetic Resonance (NMR).

Where substrates were synthesized in-house, literature references have been given for spectral data of these compounds.

Chromatography

Thin layer chromatography (TLC) was carried out using plastic-backed 50 precoated silica plates (particle size 0.2 mm). Spots were visualized by ultraviolet (UV) light ($\lambda_{\text{max}} = 254 \text{ nm}$ or 365 nm) and then stained with potassium permanganate solution followed by gentle heating. Silica gel chromatography was carried out using the Teledyne ISCO CombiFlash[®] Rf+ apparatus with RediSep[®] silica cartridges. Reverse phase preparative HPLC was carried out using the Grace Reveleris[®] Prep apparatus with an XTerra[®] Prep RP₁₈ OBD[™] column. Where modifiers are used as additives in the eluent, the stated percentage value signifies percentage by volume.

Hydrophobic frit cartridges by ISOLUTE® contain a frit which is selectively permeable to organic solutions. These are separated from aqueous phase under gravity. Various cartridge sizes were used.

Melting points (M.pt.) were recorded on a Stuart SMP10 melting point apparatus.

Liquid Chromatography-Mass Spectrometry (LCMS)

LCMS analysis was carried out on an H₂O_s Acquity UPLC instrument equipped with a BEH column (50 mm x 2.1 mm, 1.7 µm packing diameter) and H₂O_s micromass ZQ MS using alternate-scan positive and negative electrospray. Analytes were detected as a summed UV wavelength of 210 – 350 nm. Two liquid phase methods were used:

Method A – High pH: 40 °C, 1 mL/min flow rate. Gradient elution with the mobile phases as (A) 10 mM aqueous ammonium bicarbonate solution, adjusted to pH 10 with 0.88 M aqueous ammonia and (B) MeCN. Gradient conditions were initially 1% B, increasing linearly to 97% B over 1.5 min, remaining at 97% B for 0.4 min then increasing to 100% B over 0.1 min.

Method B – Low pH: 40 °C, 1 mL/min flow rate. Gradient elution with the mobile phases as (A) H₂O containing 0.1% (v/v) formic acid and (B) MeCN containing 0.1% (v/v) formic acid. Gradient conditions were initially 1% B, increasing linearly to 97% B over 1.5 min, remaining at 97% B for 0.4 min then increasing to 100% B over 0.1 min.

Nuclear Magnetic Resonance (NMR) Spectroscopy

Proton (¹H) and carbon (¹³C) spectra were recorded in deuterated solvents at ambient temperature using standard pulse methods on any of the following spectrometers and signal frequencies: Bruker AV-400 (¹H = 400 MHz, ¹³C = 101 MHz), Bruker AV-500 (¹H = 500 MHz, ¹³C = 126 MHz) and Bruker AV-600 (¹H = 600 MHz, ¹³C = 151 MHz). Chemical shifts are reported in ppm and were referenced to the following solvent peaks: CDCl₃ (¹H = 7.27 ppm, ¹³C = 77.0 ppm), *d*₆-DMSO (¹H = 2.50 ppm,

^{13}C = 39.5 ppm), and D_2O (^1H = 4.79 ppm). Where D_2O was used as the solvent, the default referencing was used based on the D_2O lock frequency for ^{13}C NMR. Peak assignments were made on the basis of chemical shifts, integrations, and coupling constants using COSY, DEPT, HSQC, HMBC, NOESY and ROESY where appropriate. Coupling constants (J) are quoted to the nearest 0.1 Hz and multiplicities are described as singlet (s), doublet (d), triplet (t), quartet (q), quintet (quin), sextet (sxt), br. (broad) and multiplet (m), and combinations therein.

Infrared (IR) Spectroscopy

IR spectra were recorded using a Perkin Elmer Spectrum 1 machine. Absorption maxima (ν_{max}) are reported in wavenumbers (cm^{-1}).

High Resolution-Mass Spectrometry (HRMS)²⁷³

High-resolution mass spectra were recorded on one of two systems:

System A: Micromass Q-ToF Ultima hybrid quadrupole time-of-flight mass spectrometer, with analytes separated on an Agilent 1100 Liquid Chromatograph equipped with a Phenomenex Luna C18 (2) reversed phase column (100 mm x 2.1 mm, 3 μm packing diameter). LC conditions were 0.5 mL/min flow rate, 35 °C, injection volume 2–5 μL , using a gradient elution with (A) H_2O containing 0.1% (v/v) formic acid and (B) MeCN containing 0.1% (v/v) formic acid. Gradient conditions were initially 5% B, increasing linearly to 100% B over 6 min, remaining at 100% B for 2.5 min then decreasing linearly to 5% B over 1 min followed by an equilibration period of 2.5 min prior to the next injection.

System B: Waters XEVO G2-XS quadrupole time-of-flight mass spectrometer, with analytes separated on an Acquity UPLC CSH C18 column (100mm x 2.1mm, 1.7 μm packing diameter). LC conditions were 0.8 mL/min flow rate, 50 °C, injection volume 0.2 μL , using a gradient elution with (A) H_2O containing 0.1% (v/v) formic acid and (B) MeCN containing 0.1% (v/v) formic acid. Gradient conditions were initially 3% B, increasing linearly to 100% B over 8.5 min, remaining at 100% B for 0.5 min then

decreasing linearly to 3% B over 0.5 min followed by an equilibration period of 0.5 min prior to the next injection.

Mass to charge ratios (m/z) are reported in Daltons.

Mass-Directed Automated Preparative HPLC (MDAP)

MDAP purification was carried out using an H₂O_s ZQ MS using alternate-scan positive and negative electrospray and a summed UV wavelength of 210–350 nm. The liquid phase method used was a high pH method as follows: Xbridge C18 column (100 mm x 19 mm, 5 µm packing diameter, 20 mL/min flow rate) or Xbridge C18 column (150 mm x 30 mm, 5 µm packing diameter, 40 mL/min flow rate). Gradient elution at ambient temperature with the mobile phases as (A) 10 mM aqueous ammonium bicarbonate solution, adjusted to pH 10 with 0.88 M aqueous ammonia and (B) MeCN. The elution gradients used were at a flow rate of 40 mL/min over 20 or 30 min depending on separation:

Method	Gradient B (%)
A	5-30
B	15-55
C	30-85
D	50-99
E	80-99

Synthetic Procedures

General Procedure for the Iodine-Mediated C–H Oxidation of Cyclic Amines A.

Iodine (7.5 eq.) was added to a mixture of cyclic amine (1.0 eq.) and sodium bicarbonate (10.0 eq.) in THF/H₂O (2.5:1, 0.025 M). The reaction mixture was stirred gently at room temperature for 4 h and monitored by LCMS. The reaction mixture was then pipetted into a solution of saturated aqueous sodium thiosulfate (10 mL) and saturated aqueous sodium bicarbonate (10 mL). The crude material was extracted in DCM (2 x 10 mL), and the combined organic layer was washed with saturated aqueous sodium bicarbonate (10 mL), passed through a hydrophobic frit, concentrated under reduced pressure and then purified as described.

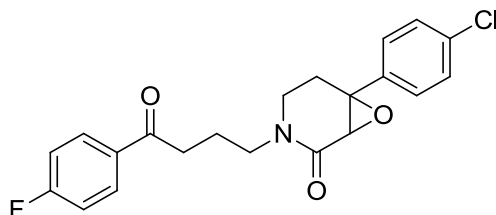
General Procedure for the Iodine-Mediated C–H Oxidation of Cyclic Amines B.

General procedure B was the same as general procedure A, with exception that DMSO replaced THF in the solvent system.

General Procedure for the Iodine-Mediated C–H Oxidation of Cyclic Amines C.

General procedure C was the same as general procedure A, with exception that the reaction was run over a period of 16 h rather than 4 h.

6-(4-Chlorophenyl)-3-(4-(4-fluorophenyl)-4-oxobutyl)-7-oxa-3-azabicyclo[4.1.0]heptan-2-one 3.1.2



General procedure for the iodine-mediated C–H oxidation of cyclic amines A was followed. Iodine (190 mg, 0.75 mmol) was added to a mixture of **3.1.1** (37.6 mg, 0.10 mmol) and sodium bicarbonate (84.0 mg, 1.0 mmol) in THF/H₂O (2.9 mL/1.1 mL, 0.025 M). Purification was carried out by high pH MDAP (Method D), affording **3.1.2** (10.4 mg, 27%) as a white gum.

LCMS (Method A, UV, ESI) $R_t = 1.24$ min, $[M+H]^+$ 388.2 (³⁵Cl), 390.2 (³⁷Cl)

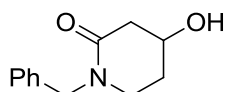
¹H NMR (CDCl₃, 400MHz): δ 7.95-8.04 (m, 2H), 7.36 (dt, $J = 8.6, 2.5$ Hz, 2H), 7.28-7.29 (m, 1H), 7.26 (br. s, 1H),* 7.14 (t, $J = 8.7$ Hz, 2H), 3.64 (td, $J = 12.6, 4.2$ Hz, 1H), 3.56 (q, $J = 6.8$ Hz, 1H), 3.48 (t, $J = 6.8$ Hz, 1H), 3.45 (s, 1H), 3.19 (ddd, $J = 12.6, 5.7, 1.6$ Hz, 1H), 3.01 (td, $J = 7.0, 4.7$ Hz, 2H), 2.59 (ddd, $J = 14.1, 12.6, 5.8$ Hz, 1H), 2.41 (dd, $J = 14.1, 3.8$ Hz, 1H), 1.94-2.14 (m, 2H)

¹³C NMR (CDCl₃, 151 MHz): δ 197.8, 166.0, 165.8 (d, $^1J_{C-F} = 255.4$ Hz), 135.8, 134.5, 133.2 (d, $^4J_{C-F} = 3.3$ Hz), 130.7 (d, $^3J_{C-F} = 10.0$ Hz), 128.9, 126.6, 115.7 (d, $^2J_{C-F} = 21.0$ Hz), 61.6, 59.9, 46.8, 41.6, 35.3, 27.5, 21.7

IR ν_{max} (cm⁻¹) (thin film): 2924, 2854, 1667, 1655

HRMS: Calculated for C₂₁H₂₀ClFNO₃ $[M+H]^+$: 388.1110, found $[M+H]^+$: 388.1107 (-1.0 ppm).

*Chemical shift peak was obscured slightly by chloroform signal at 7.27 ppm.

1-Benzyl-4-hydroxypiperidin-2-one 3.1.7

General procedure for the iodine-mediated C–H oxidation of cyclic amines C was followed. Iodine (380 mg, 1.50 mmol) was added to a mixture of **3.1.6** (38 mg, 0.20 mmol) and sodium bicarbonate (170 mg, 2.00 mmol) in THF/H₂O (5.7 mL/2.3 mL, 0.025 M). Purification was carried out by high pH MDAP (Method B) to afford **3.1.7** (15.7 mg, 38%) as a brown oil.

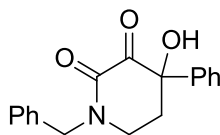
LCMS (Method A, UV, ESI) R_t = 0.64 min, [M+H]⁺ 206.1

¹H NMR (CDCl₃, 400 MHz): δ 7.16-7.38 (m, 5H), 4.64 (d, *J* = 14.7 Hz, 1H), 4.55 (d, *J* = 14.9 Hz, 1H), 4.17 (tt, *J* = 7.1, 2.9 Hz, 1H), 3.42 (ddd, *J* = 12.4, 7.6, 5.1 Hz, 1H), 3.19-3.37 (m, 1H), 3.14 (dt, *J* = 12.3, 6.1 Hz, 1H), 2.72 (dd, *J* = 17.5, 4.0 Hz, 1H), 2.49 (dd, *J* = 17.4, 5.6 Hz, 1H), 1.89-2.00 (m, 1H), 1.78-1.88 (m, 1H)

¹³C NMR (CDCl₃, 101 MHz): δ 168.6, 136.8, 128.6, 127.9, 127.3, 64.3, 49.9, 43.0, 41.0, 30.3

IR ν_{max} (cm⁻¹) (thin film): 3387 (br), 2925, 1614, 1496

HRMS: Calculated for C₁₂H₁₆NO₂ [M+H]⁺: 206.1181, found [M+H]⁺: 206.1177 (-1.9 ppm).

1-Benzyl-4-hydroxy-4-phenylpiperidine-2,3-dione 3.1.9

General procedure for the iodine-mediated C–H oxidation of cyclic amines B was followed. Iodine (380 mg, 1.50 mmol) was added to a mixture of the hydrochloride salt of **3.1.8** (61 mg, 0.20 mmol) and sodium bicarbonate (170 mg, 2.00 mmol) in DMSO/H₂O (5.7 mL/2.3 mL, 0.025 M). Purification was carried out by high pH MDAP (Method B) to afford **3.1.9** (15.7 mg, 38%) as a white solid.

LCMS (Method A, UV, ESI) $R_t = 0.88$ min, $[M+H]^+$ 296.0

^1H NMR (CDCl_3 , 400 MHz): δ 7.33-7.42 (m, 3H), 7.22-7.30 (m, 5H), 7.04-7.13 (m, 2H), 4.62 (dd, $J = 19.6, 14.7$ Hz, 2H), 3.76 (br. s., 1H), 3.28 (ddd, $J = 13.2, 5.4, 2.7$ Hz, 1H), 3.05 (td, $J = 12.5, 3.9$ Hz, 1H), 2.64-2.74 (m, $J = 14.4, 3.9, 2.6$ Hz, 1H), 2.44 (ddd, $J = 14.3, 11.9, 5.4$ Hz, 1H)

^{13}C NMR (CDCl_3 , 101 MHz): δ 223.3, 195.0, 157.8, 137.8, 135.0, 129.3, 128.8, 128.1, 128.0, 125.9, 78.6, 50.8, 42.9, 34.2

IR ν_{max} (cm^{-1}) (thin film): 3234 (br), 2928, 1739, 1646

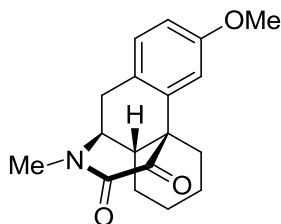
HRMS: Calculated for $\text{C}_{18}\text{H}_{18}\text{NO}_3$ $[M+H]^+$: 296.1287, found $[M+H]^+$: 296.1281 (-2.0 ppm)

M.pt.: 175-177 °C.

(4b*S*,8a*S*,9*S*)-3-Methoxy-11-methyl-6,7,8,8a,9,10-hexahydro-5*H*-9,4b-(epiminoethano) phenanthrene-12,13-dione 3.1.13, and (4b*S*,8a*S*,9*S*,13*R*)-13-iodo-3-methoxy-11-methyl-6,7,8,8a,9,10-hexahydro-5*H*-9,4b-(epiminoethano)phenanthren-12-one 3.1.14

General procedure for the iodine-mediated C–H oxidation of cyclic amines **C** was followed. Iodine (190 mg, 0.75 mmol) was added to a mixture of **3.1.12** (27.1 mg, 0.10 mmol) and sodium bicarbonate (84.0 mg, 1.0 mmol) in THF/ H_2O (2.9 mL/1.1 mL, 0.025 M). Purification was carried out by high pH MDAP (Method C), to afford **3.1.13** (12.3 mg, 41%) as a white solid, and **3.1.14** (4.8 mg, 12%) as an amber coloured gum.

(4b*S*,8a*S*,9*S*)-3-Methoxy-11-methyl-6,7,8,8a,9,10-hexahydro-5*H*-9,4b-(epiminoethano) phenanthrene-12,13-dione 3.1.13



LCMS (Method A, UV, ESI) $R_t = 1.00$ min, $[M+H]^+$ 300.2

^1H NMR (CDCl_3 , 400MHz): δ 7.04 (d, $J = 8.3$ Hz, 1H), 6.84 (d, $J = 2.4$ Hz, 1H), 6.81 (dd, $J = 8.3, 2.9$ Hz, 1H), 3.75 (s, 3H), 3.62 (td, $J = 3.9, 1.7$ Hz, 1H), 3.11-3.13 (m, 3H), 3.05-3.11 (m, 1H), 2.90-2.97 (m, 1H), 2.82-2.89 (m, 1H), 2.44 (dt, $J = 11.6, 3.3$ Hz, 1H), 1.68-1.74 (m, 2H), 1.64-1.68 (m, 1H), 1.52-1.62 (m, 1H), 1.28-1.42 (m, 2H), 1.13-1.23 ppm (m, 1H)

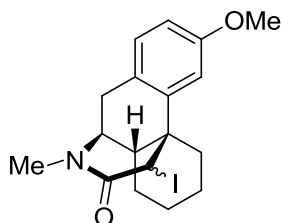
^{13}C NMR (CDCl_3 , 101MHz): δ 190.4, 159.6, 157.1, 131.5, 131.2, 125.4, 115.1, 112.3, 58.2, 55.4, 50.7, 40.1, 34.5, 29.9, 28.5, 26.4, 25.2, 21.2

IR ν_{max} (cm^{-1}) (thin film): 2932, 2859, 1726, 1664

HRMS: Calculated for $\text{C}_{18}\text{H}_{22}\text{NO}_3$ $[M+H]^+$: 300.1594, found $[M+H]^+$: 300.1589 (-1.8 ppm)

M.pt.: 190-193 °C.

(4b*S*,8a*S*,9*S*,13*R*)-13-iodo-3-methoxy-11-methyl-6,7,8,8a,9,10-hexahydro-5*H*-9,4b-(epiminoethano)phenanthren-12-one 3.1.14



LCMS (Method A, UV, ESI) $R_t = 1.24$ min, $[M+H]^+$ 412.1

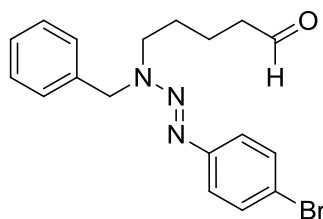
^1H NMR (CDCl_3 , 400MHz): δ 6.99 (d, $J = 8.6$ Hz, 1H), 6.88 (d, $J = 2.4$ Hz, 1H), 6.79 (dd, $J = 8.3, 2.7$ Hz, 1H), 4.66 (s, 1H), 3.78 (s, 3H), 3.57 (td, $J = 4.0, 2.0$ Hz, 1H), 2.97 (dd, $J = 17.4, 3.9$ Hz, 1H), 2.93 (s, 3H), 2.75 (d, $J = 17.4$ Hz, 1H), 2.58 (dt, $J = 12.3, 4.0$ Hz, 1H), 2.13-2.21 (m, 1H), 2.01 (td, $J = 13.6, 3.3$ Hz, 1H), 1.65-1.75 (m, 2H), 1.52-1.61 (m, 2H), 1.41 (qt, $J = 13.0, 3.5$ Hz, 1H), 1.24 (qd, $J = 13.2, 4.4$ Hz, 1H), 1.02 ppm (qt, $J = 13.2, 3.1$ Hz, 1H)

^{13}C NMR (CDCl_3 , 101MHz): δ 169.3, 159.3, 134.7, 131.5, 124.9, 113.9, 111.9, 58.6, 55.4, 43.1, 41.0, 38.9, 35.3, 34.9, 29.8, 26.1, 25.6, 22.3

IR ν_{max} (cm^{-1}) (thin film): 2934, 2857, 1646

HRMS: Calculated for $\text{C}_{18}\text{H}_{23}\text{NO}_2\text{I}$ $[\text{M}+\text{H}]^+$: 412.0773, found $[\text{M}+\text{H}]^+$: 412.0769 (-1.0 ppm).

(*E*)-5-(1-Benzyl-3-(4-bromophenyl)triaz-2-en-1-yl)pentanal 3.2.8



Iodine (51 mg, 0.20 mmol) was added to a solution of **2.1.8a** (37 μL , 0.20 mmol) in THF (2.0 mL). This solution was stirred for 30 min at RT, before sequential addition of **3.2.6** (108 mg, 0.40 mmol), sodium bicarbonate (50 mg, 0.60 mmol) and H_2O (1.0 mL). The reaction mixture was stirred at RT for 3 h, then pipetted into a solution of saturated aqueous sodium thiosulfate (10 mL) and saturated aqueous sodium bicarbonate (10 mL). The crude material was extracted in DCM (2 x 10 mL), and the combined organic layer was washed with saturated aqueous sodium bicarbonate (10 mL), passed through a hydrophobic frit and concentrated under reduced pressure. The crude material was purified by silica gel chromatography with 0-10% EtOAc/cyclohexane as the eluent, affording **3.2.8** (11.4 mg, 15%) as an orange oil.

LCMS (Method A, UV, ESI) $R_t = 1.50$ min, $[\text{M}+\text{H}]^+$ 374.1 (^{79}Br), 376.1 (^{81}Br)

^1H NMR (DMSO- d_6 , 400MHz, 343 K): δ 9.65 (t, J = 1.5 Hz, 1H), 7.50 (d, J = 8.8 Hz, 1H), 7.24-7.38 (m, 7H), 4.95 (s, 2H), 3.72 (t, J = 7.0 Hz, 2H), 2.42 (td, J = 7.0, 1.8 Hz, 2H), 1.66 (quin, J = 7.8 Hz, 2H), 1.55 (quin, J = 7.3 Hz, 2H)

^{13}C NMR (DMSO- d_6 , 101 MHz, 343 K): δ 203.4, 131.3, 128.0, 127.8, 127.6, 121.8, 53.2, 48.9, 42.2, 26.1, 18.8

^{13}C signals had to be determined by HSQC analysis since signal:noise ratio was too low in 1D ^{13}C . As such, chemical shifts for quaternary carbon centres could not be recorded at this stage.

IR ν_{max} (cm^{-1}) (thin film): 2928, 1722, 1480

HRMS: Calculated for $\text{C}_{18}\text{H}_{21}\text{N}_3\text{OBr}$ $[\text{M}+\text{H}]^+$: 374.0863, found $[\text{M}+\text{H}]^+$: 374.0848 (-3.9 ppm).

Attempted Optimisation of the Formation of **3.2.8**

Iodine or NIS (amounts indicated) was added to a solution of **2.1.8a** (37 μL , 0.20 mmol) in THF (2.0 mL). This solution was stirred for 30 min at RT, before sequential addition of **3.2.6** (108 mg, 0.40 mmol), sodium bicarbonate (50 mg, 0.60 mmol) and H_2O (1.0 mL). The reaction mixture was stirred at RT for 3 h, then pipetted into a solution of saturated aqueous sodium thiosulfate (10 mL) and saturated aqueous sodium bicarbonate (10 mL). The crude material was extracted in DCM (2 x 10 mL), and the combined organic layer was washed with saturated aqueous sodium bicarbonate (10 mL), passed through a hydrophobic frit and concentrated at 40 $^\circ\text{C}$ under flow of nitrogen gas. The crude material was dissolved in CDCl_3 , treated with dibromomethane (15 μL , 0.215 mmol) and analysed by ^1H NMR. The integral for the 1H aldehyde signal (δ 9.65) was compared with the integral for the 2H signal of dibromomethane (δ 4.92).

Data are reported, in relation to Table 19, as (a) iodine source, (b) amount of iodine source, and (c) percentage formation of **3.2.8** observed by ^1H NMR.

Entry 1

(a) Iodine, (b) 51 mg, 0.20 mmol, and (c) 7%

Entry 2

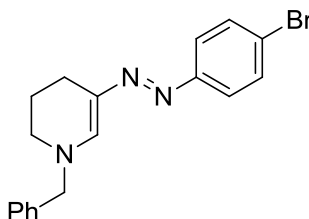
(a) Iodine, (b) 102 mg, 0.40 mmol, and (c) 18%

Entry 3

(a) NIS, (b) 45 mg, 0.20 mmol, and (c) 13%

Entry 4

(a) NIS, (b) 90 mg, 0.40 mmol, and (c) 21%

(E)-1-Benzyl-5-((4-bromophenyl)diazenyl)-1,2,3,4-tetrahydropyridine 3.2.14

A solution of 1,1-dimethylhydrazine (2.3 μL , 0.03 mmol) in DMSO (0.25 mL) was added to a solution of **2.1.8a** (277 μL , 1.50 mmol) and **3.2.6** (81.0 mg, 0.30 mmol) in DMSO (1.25 mL), and this solution was stirred under an atmosphere of nitrogen at RT for 60 min. The reaction was quenched with saturated aqueous sodium thiosulfate (3 mL) and water (3mL). The crude mixture was extracted into DCM (5 mL), passed through a hydrophobic frit, and the organic filtrate was concentrated under flow of nitrogen. The crude product was purified by high pH MDAP (Method E) to afford **3.2.14** (18.3 mg, 17%) as a dark red oil.

LCMS (Method A, UV, ESI) $R_t = 1.45$ min, $[\text{M}+\text{H}]^+$ 356.1 (^{79}Br), 358.1 (^{81}Br)

^1H NMR (CDCl_3 , 400MHz): δ 7.44-7.50 (m, 4H), 7.33-7.41 (m, 3H), 7.22-7.32 (m, 3H), 4.45 (s, 2H), 3.18-3.24 (m, 2H), 2.65 (t, $J = 6.5$ Hz, 2H), 1.95 (quin, $J = 6.1$ Hz, 2H)

^{13}C NMR (CDCl_3 , 101 MHz): δ 152.9, 150.6, 135.8, 133.5, 131.7, 129.0, 128.2, 127.6, 122.3, 119.4, 60.2, 46.8, 20.7, 19.7

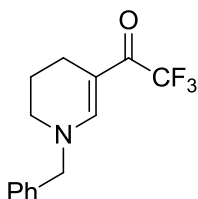
IR ν_{max} (cm^{-1}) (thin film): 3217 (br), 2929, 1666, 1612, 1486

HRMS: Calculated for $\text{C}_{18}\text{H}_{19}\text{N}_3\text{Br}$ $[\text{M}+\text{H}]^+$: 356.0762, found $[\text{M}+\text{H}]^+$: 356.0758 (-1.1 ppm).

Isolated product was approximately 77% pure by UV absorption, due to co-elution with by-products that had ionisation patterns indicative of mono and dibrominated species, suggesting degradation and dimerisation products from side-reactivity of the diazonium salt. NMR analysis demonstrated a >90% level of purity, suggesting that the by-products were highly UV active.

1-(1-Benzyl-1,4,5,6-tetrahydropyridin-3-yl)-2,2,2-trifluoroethanone 3.3.7

(Unoptimised conditions).



A solution of **2.1.8a** (37 μL , 0.20 mmol) in DCM (2.0 mL) was treated with NIS (180 mg, 0.80 mmol) under an atmosphere of nitrogen, and the reaction mixture was stirred at RT for 30 min. The reaction was cooled to $-10\text{ }^\circ\text{C}$, before dropwise addition of **3.3.6** (0.14 ml, 1.00 mmol) and pyridine (50 μL , 0.60 mmol) sequentially. The reaction was stirred at $-10\text{ }^\circ\text{C}$ for 30 min, and then allowed to warm to RT and stir for 2 h. The reaction mixture was quenched with saturated aqueous sodium thiosulfate (5 mL) and saturated aqueous sodium bicarbonate (5 mL) and extracted into DCM (3 x 15 mL). The combined organic layer was passed through a hydrophobic frit and concentrated under reduced pressure. The crude material was purified by silica gel chromatography using 0-85% TBME/cyclohexane as the eluent, to afford **3.3.7** (16.9 mg, 31%) as a colourless oil.

LCMS (Method A, UV, ESI) R_t = 1.11 min, $[\text{M}+\text{H}]^+$ 270.1

^1H NMR (400 MHz, DMSO- d_6) δ 7.90 (br. s., 1H), 7.38-7.45 (m, 2H), 7.32-7.37 (m, 1H), 7.27-7.32 (m, 2H), 4.65 (s, 2H), 3.17 (t, $J = 5.4$ Hz, 2H), 2.22 (t, $J = 6.4$ Hz, 2H), 1.73 (quin, $J = 6.1$ Hz, 2H)

For full characterisation data see more optimal conditions below.

Attempted Optimisation of the Formation of 3.3.7

A solution of **2.1.8a** (37 μL , 0.20 mmol) in DCM (1.0 mL) was treated with NIS (amounts indicated) under an atmosphere of nitrogen, and the reaction mixture was stirred at RT for 30 min. A solution of **3.3.6** (amounts indicated) and DMAP and/or pyridine (amounts indicated) in DCM (1.0 mL) was then added dropwise at the indicated reaction temperature, and the reaction was stirred at this temperature for 30 min, and then allowed to warm to the indicated temperature and stir for 2 h. The reaction mixture was quenched with saturated aqueous sodium thiosulfate (5 mL) and saturated aqueous sodium bicarbonate (5 mL) and extracted into DCM (3 x 15 mL). The combined organic layer was passed through a hydrophobic frit and concentrated at 40 $^\circ\text{C}$ under flow of nitrogen gas. The crude material was dissolved in CDCl_3 , treated with 3,4,5-trichloropyridine (amounts indicated) and analysed by ^1H NMR. The integral for the benzylic 2H singlet of the desired product (δ 4.44 ppm) was compared with the integral for the 2H signal of 3,4,5-trichloropyridine (δ 8.51).

Data are reported as (a) amount of NIS, (b) amount of **3.3.6**, (c) amount of DMAP, (d) amount of pyridine, (e) initial temperature on addition of **3.3.6**, held for 30 min, (f) subsequent reaction temperature held for 2 h, (g) percentage formation of **3.3.7** determined *via* ^1H NMR analysis, and (h) amount of 3,4,5-trichloropyridine used as a standard.

In relation to Table 21:

Entry 1

(a) 50 mg, 0.22 mmol, (b) 34 μL , 0.24 mmol, (c) 0 mg, (d) 19 μL , 0.24 mmol, (e) -10 $^\circ\text{C}$, (f) RT, (g) 11%, (h) 8 mg, 0.044 mmol

Entry 2

(a) 50 mg, 0.22 mmol, (b) 34 μ L, 0.24 mmol, (c) 0 mg, (d) 36 μ L, 0.44 mmol, (e) -10 $^{\circ}$ C, (f) RT, (g) 16%, (h) 13 mg, 0.072 mmol

Entry 3

(a) 99 mg, 0.44 mmol, (b) 140 μ L, 1.0 mmol, (c) 0 mg, (d) 97 μ L, 1.2 mmol, (e) -10 $^{\circ}$ C, (f) RT, (g) 0%, (h) 15 mg, 0.082 mmol

Entry 4

(a) 50 mg, 0.22 mmol, (b) 34 μ L, 0.24 mmol, (c) 0 mg, (d) 36 μ L, 0.44 mmol, (e) RT, (f) RT, (g) 20%, (h) 8 mg, 0.042 mmol

Entry 5

(a) 50 mg, 0.22 mmol, (b) 34 μ L, 0.24 mmol, (c) 0 mg, (d) 36 μ L, 0.44 mmol, (e) 60 $^{\circ}$ C, (f) 60 $^{\circ}$ C, (g) 2%, (h) 19 mg, 0.10 mmol

Entry 6

(a) 180 mg, 0.80 mmol, (b) 140 μ L, 1.0 mmol, (c) 0 mg, (d) 97 μ L, 1.2 mmol, (e) -10 $^{\circ}$ C, (f) RT, (g) 46%, (h) 15 mg, 0.081 mmol

Entry 7

(a) 180 mg, 0.80 mmol, (b) 34 μ L, 0.24 mmol, (c) 0 mg, (d) 97 μ L, 1.2 mmol, (e) -10 $^{\circ}$ C, (f) RT, (g) 0%, (h) 8 mg, 0.044 mmol

Entry 8

(a) 180 mg, 0.80 mmol, (b) 70 μ L, 0.50 mmol, (c) 0 mg, (d) 97 μ L, 1.2 mmol, (e) -10 $^{\circ}$ C, (f) RT, (g) 0%, (h) 13 mg, 0.072 mmol

Entry 9

(a) 180 mg, 0.80 mmol, (b) 280 μ L, 2.0 mmol, (c) 0 mg, (d) 97 μ L, 1.2 mmol, (e) -10 $^{\circ}$ C, (f) RT, (g) 45%, (h) 7 mg, 0.039 mmol

In relation to Table 22:

Entry 1

(a) 180 mg, 0.80 mmol, (b) 140 μ L, 1.0 mmol, (c) 5 mg, 0.040 mmol (d) 97 μ L, 1.2 mmol, (e) -10 $^{\circ}$ C, (f) RT, (g) 23%, (h) 8 mg, 0.044 mmol

Entry 2

(a) 180 mg, 0.80 mmol, (b) 140 μ L, 1.0 mmol, (c) 24 mg, 0.20 mmol (d) 97 μ L, 1.2 mmol, (e) -10 $^{\circ}$ C, (f) RT, (g) 50%, (h) 10 mg, 0.056 mmol

Entry 3

(a) 180 mg, 0.80 mmol, (b) 140 μ L, 1.0 mmol, (c) 49 mg, 0.40 mmol (d) 97 μ L, 1.2 mmol, (e) -10 $^{\circ}$ C, (f) RT, (g) 69%, (h) 9 mg, 0.051 mmol

Entry 4

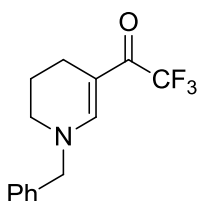
(a) 180 mg, 0.80 mmol, (b) 140 μ L, 1.0 mmol, (c) 5 mg, 0.040 mmol (d) 0 μ L, (e) -10 $^{\circ}$ C, (f) RT, (g) 0%, (h) 11 mg, 0.063 mmol

Entry 5

(a) 180 mg, 0.80 mmol, (b) 140 μ L, 1.0 mmol, (c) 24 mg, 0.20 mmol (d) 0 μ L, (e) -10 $^{\circ}$ C, (f) RT, (g) 0%, (h) 10 mg, 0.053 mmol

1-(1-Benzyl-1,4,5,6-tetrahydropyridin-3-yl)-2,2,2-trifluoroethanone 3.3.7

(Most optimised conditions developed so far).



A solution of **2.1.8a** (37 μ L, 0.20 mmol) in DCM (1.0 mL) was treated with NIS (180 mg, 0.80 mmol) under an atmosphere of nitrogen, and the reaction mixture was stirred at RT for 30 min. The reaction was cooled to -10 $^{\circ}$ C, and a solution of **3.3.6** (0.14 ml, 1.00 mmol) and DMAP (150 mg, 1.20 mmol) in DCM (1.0 ml) was then added

dropwise. The reaction was stirred at -10 °C for 30 min, and then allowed to warm to RT and stir for 2 h. The reaction mixture was quenched with saturated aqueous sodium thiosulfate (5 mL) and saturated aqueous sodium bicarbonate (5 mL) and extracted into DCM (3 x 15 mL). The combined organic layer was passed through a hydrophobic frit and concentrated under reduced pressure. ¹H NMR analysis of the crude material against 3,4,5-trichloropyridine (26.3 mg, 0.144 mmol) showed 70% conversion to **3.3.7**, based on the 2H signal at 4.40 ppm, corresponding to the benzylic protons. The crude material was purified by silica gel chromatography using 0-50% TBME/cyclohexane as the eluent, to afford **3.3.7** (29.0 mg, 54%) as an amber coloured oil.

LCMS (Method A, UV, ESI) $R_t = 1.10$ min, $[M+H]^+$ 270.2

¹H NMR (400 MHz, CDCl₃) δ 7.71 (br. s., 1H), 7.32-7.45 (m, 3H), 7.17-7.25 (m, 2H), 4.44 (s, 2H), 3.15 (t, $J = 5.6$ Hz, 2H), 2.39 (t, $J = 6.4$ Hz, 2H), 1.84 (quin, $J = 6.1$ Hz, 2H)

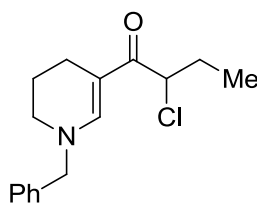
¹³C NMR (101 MHz, CDCl₃) δ 175.0 (q, $^2J_{C-F} = 30.8$), 151.5 (q, $^3J_{C-F} = 4.4$), 135.0, 129.1, 128.5, 127.5, 118.2 (q, $^1J_{C-F} = 291.2$), 102.5, 61.0, 46.2, 20.4, 18.8

¹⁹F NMR (CDCl₃, 376MHz): δ -67.12 (s, 1F)

IR ν_{max} (thin film): 2942, 1647, 1571, 1435

HRMS: Calculated for C₁₄H₁₅NOF₃ $[M+H]^+$: 270.1106, found $[M+H]^+$ 270.1103 (-1.1 ppm).

1-(1-Benzyl-1,4,5,6-tetrahydropyridin-3-yl)-2-chlorobutan-1-one **3.3.11**



A solution of **2.1.8a** (37 μ L, 0.20 mmol) in DCM (1.0 mL) was treated with NIS (180 mg, 0.80 mmol) under an atmosphere of nitrogen, and the reaction mixture was stirred

at RT for 30 min. The reaction was then cooled to -15 °C, and a solution of butyryl chloride (0.10 mL, 1.00 mmol) and DMAP (150 mg, 1.20 mmol) in DCM (1.0 mL) was then added slowly, and the reaction was stirred at -15 °C for 30 min, and then allowed to warm to RT over 2 h. The reaction mixture was quenched with saturated aqueous sodium thiosulfate (5 mL) and saturated aqueous sodium bicarbonate (5 mL) and extracted into DCM (3 x 15 mL). The combined organic layer was passed through a hydrophobic frit and concentrated under reduced pressure. The crude material was purified by low pH MDAP (Method C), to afford **3.3.11** (3.7 mg, 7%) as a brown oil.

LCMS (Method A, UV, ESI) $R_t = 1.12$ min, $[M+H]^+$ 278.3 (^{35}Cl), 280.2 (^{37}Cl)

^1H NMR (400 MHz, $\text{DMSO-}d_6$) δ 8.07 (s, 1H), 7.36-7.43 (m, 2H), 7.27-7.34 (m, 3H), 5.11 (t, $J = 7.0$ Hz, 1H), 4.50 (s, 2H), 3.03 (t, $J = 6.1$ Hz, 2H), 2.15 (td, $J = 6.4, 1.7$ Hz, 2H), 1.73-1.93 (m, 2H), 1.67 (quin, $J = 6.4$ Hz, 2H), 0.91 (t, $J = 7.3$ Hz, 3H)

^{13}C NMR (101 MHz, $\text{DMSO-}d_6$) δ 187.1, 149.4, 136.9, 129.1, 128.6, 127.5, 104.6, 58.7, 57.9, 45.1, 28.0, 20.3, 18.9, 10.9

IR ν_{max} (thin film): 2934, 1712, 1571, 1433

HRMS: Calculated for $\text{C}_{16}\text{H}_{21}\text{NOCl}$ $[M+H]^+$: 278.1312, found $[M+H]^+$ 278.1307 (-1.8 ppm).

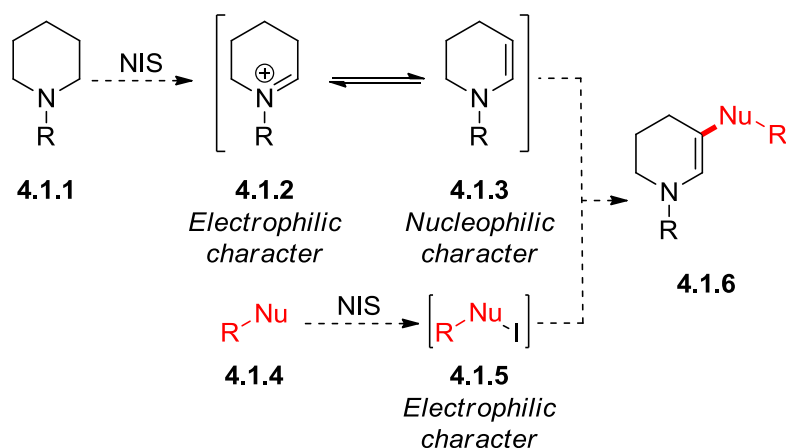
Chapter 4. Oxidative β -Sulfonylation of Azacycles

Disclaimer

The reaction optimisation investigations and the majority of the substrate scope (experimental provided in Appendix 3) were undertaken in collaboration with a Masters student, Wei Chung Kong (University of Oxford). Mr Kong was an industrial placement student based within our GSK laboratories,³³³ and was under the direct supervision of the author of this thesis, Robert Griffiths. Initial reaction discovery, preliminary optimisation and mechanistic investigations for the oxidative β -C–H sulfonylation process were carried out by Robert Griffiths, with full optimisation screening and substrate scope carried out by Wei Chung Kong. Compounds prepared by Wei Chung Kong are indicated within Table 23 and Table 24 in Section 4.2.

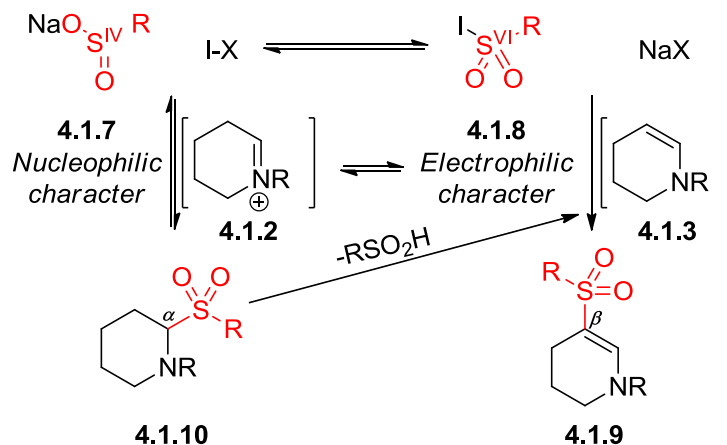
4.1 Rationale and Precedent for Oxidative β -Sulfonylation

Based on the findings described in Section 3.3 that anhydrides react with an enamine intermediate generated *in situ*, it was proposed that oxidative β -C–H functionalisation of a cyclic amine **4.1.1** could be achieved more successfully by using a nucleophile **4.1.4** (Scheme 84) that generates an electrophilic species **4.1.5** by reaction with iodine.



Scheme 84. *In situ* conversion of a nucleophile **4.1.4** into an electrophile could hypothetically enable more selective functionalisation of an enamine intermediate **4.1.3**, formed from **4.1.1**.

Sodium sulfinate salts were selected to test this hypothesis due to the variability in the oxidation state of sulfur from S(IV) to S(VI). The reaction of the nucleophilic sulfinate **4.1.7** (Scheme 85) with an iodine source should generate an electrophilic sulfonyl iodide **4.1.8** *in situ*, which could then trap the enamine intermediate **4.1.9**.



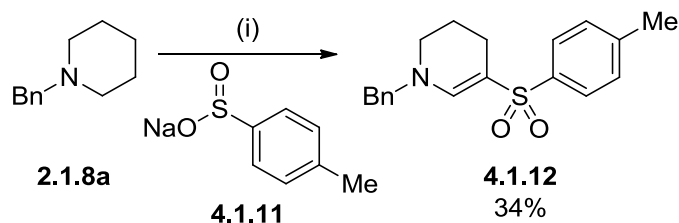
Scheme 85. Sulfinate salts such as **4.1.7** were selected as the functionalising partner due to the potential to exhibit both nucleophilic and electrophilic behaviour.

Alternatively, there is the possibility that sulfinate **4.1.7** would not be sufficiently reactive with the iodine source, and instead carry out nucleophilic functionalisation of the iminium tautomer **4.1.2** to form α -sulfonylation product **4.1.10**. In this regard, the use of a sulfinate salt **4.1.7** offered the potential for reactivity at either the α or the β position of an azacycle. Given the potential for the sulfonyl group to act as a leaving group through the reversibility of α -functionalisation,³³⁴ coupled with elimination of sulfonic acid^{335–339} to generate **4.1.3**, formation of enaminyl sulfones such as **4.1.9** was anticipated to be the more likely outcome.

The preparation of enaminyl sulfones such as **4.1.9** has been previously reported by Yuan *et al.*, with the reaction of tertiary amines with iodine and sulfinate salts in the presence of *tert*-butylhydroperoxide.³⁴⁰ The reagents react with a solvent-dependency, proceeding with either C–N bond cleavage to form sulfonamides, or *via* C–H bond cleavage to form enaminyl sulfones. But the need for a large excess of the reactive *tert*-butylhydroperoxide oxidant limits the functional group compatibility of this

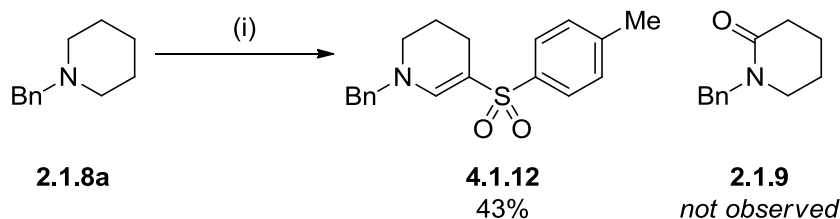
process; this is reflected by the very limited substrate scope to just triethylamine for the formation of enaminyll sulfones. A related, visible light-mediated transformation employing air-sensitive sulfonyl chlorides and at least four equivalents of amine substrate has also been reported by Zheng³⁴¹ and Zhang.³⁴² As a result of the catalytic conditions, these processes exhibit high atom economy and environmental sustainability, but the requirements for a large excess of the potentially precious substrate and the modest yields and regioselectivities limit the applicability for the β -sulfonylation of amines.

Each of the aforementioned reports focuses principally on acyclic substrates, and propose that an intermediary enamine is formed, which reacts with an electrophilic sulfonyl species. It was envisaged, therefore, that the inclusion of a sulfinate salt in the standard C–H oxidation protocol described in Chapter 2 could lead to trapping of the enamine intermediate, affording β -functionalised azacycles. Incorporation of three equivalents of sodium *para*-tolyl sulfinate **4.1.11** (Scheme 86) to the conditions for iodine-mediated C–H oxidation afforded a 34% yield of the β -sulfonylated enaminyll sulfone **4.1.12**.



Scheme 86. Inclusion of aryl sulfinate **4.1.11** in the iodine-mediated C–H oxidation conditions resulted in selective oxidative sulfonylation of azacycle **2.1.8a**. Conditions: (i) I₂ (7.0 eq.), NaHCO₃ (10.0 eq.), **4.1.11** (3.0 eq.), THF:H₂O (2:1, 0.067 M), RT, 15 h.

This result validated the hypothesis of generating an electrophile under the oxidation reaction conditions to carry out β -functionalisation of azacycles. It was subsequently found that the use of a lower excess of NIS instead of molecular iodine, along with sequential addition of reagents, resulted in the formation of fewer by-products and a marginally improved yield of 43% for **4.1.12** (Scheme 87).



Scheme 87. Using NIS instead of iodine gave slightly improved conversion to **4.1.12**. Conditions: (i) NIS (3.0 eq.), then **4.1.11** (3.0 eq.), NaHCO₃ (5.0 eq.), THF:H₂O (2:1, 0.067 M), 3.5 h, RT.

The surprising aspect of this result was the selectivity for formation of **4.1.12**, with no lactam product **2.1.9** observed to form, despite the similarity of the reaction conditions to the oxidation protocol described previously. The β -sulfonylpiperidine motif is found in a number of small molecule assets from the drug discovery industry with varying target indications, such as the ATR kinase antagonist **4.1.13**, the IL-8 antagonist **4.1.14**, and the ROR γ antagonist **4.1.15** (Figure 31).^{343–345}

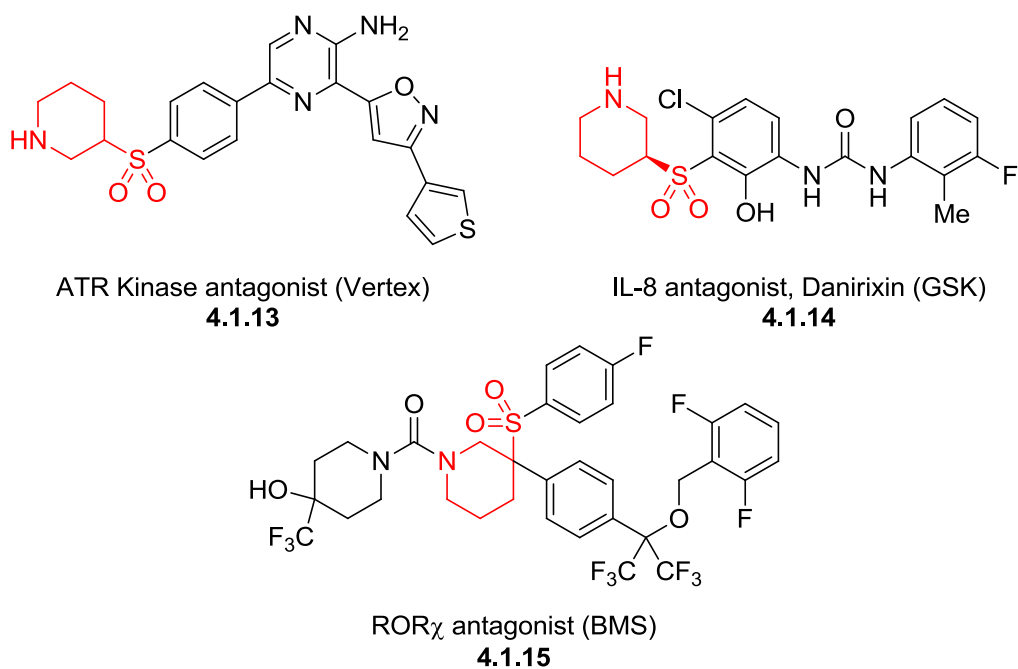
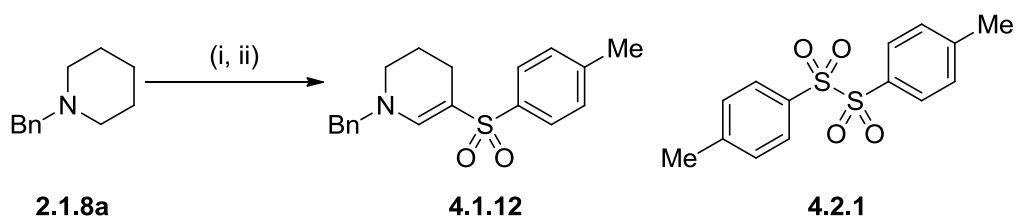


Figure 31. Examples of β -sulfonylpiperidines in recent pharmaceutical assets targeting kinases,³⁴³ GPCRs,³⁴⁴ and transcription factors.³⁴⁵ ATR = ataxia telangiectasia and Rad₃ related; IL-8 = interleukin-8; GPCR = G-protein coupled receptor; ROR γ = RAR-related orphan receptor- γ ; RAR = retinoic acid receptor; GSK = GlaxoSmithKline; BMS = Bristol-Myers-Squibb.

This remote C–H functionalisation reaction was likely to be beneficial in the drug discovery sector because the wide array of commercially available sulfinate salts could enable expedient SAR analysis.

4.2 Reaction Optimisation and Substrate Scope

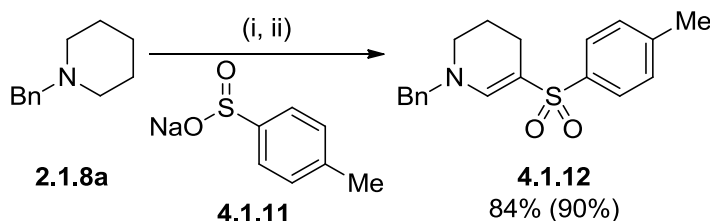
The following investigations were carried out by Wei Chung Kong and performed in order to optimise this transformation by promoting full consumption of starting material and increasing the substrate scope. These studies have been included within this thesis in order to maintain the continuity of the project described. Several sets of conditions were explored, but the generation of reproducible results was problematic. The low conversion to **4.1.12** observed by ^1H NMR, despite the appearance of very few by-products by LCMS, was a confounding result. Analysis of aqueous extractions and mass balance studies demonstrated that no product was being lost during the workup. It transpired that impurity **4.2.1** (Scheme 88) was being formed during the course of the reaction, and co-eluted with **4.1.12** in the two minute LCMS run, therefore exaggerating the initial indications of product formation.



Scheme 88. Sulfinate dimer **4.2.1 formed during the course of the oxidative sulfonylation reaction.** Conditions: (i) NIS (3.0 eq.), THF, 30 min, RT; (ii) **4.1.11** (3.0 eq.), NaHCO_3 (5.0 eq.), THF:H₂O (2:1, 0.067 M), 3 h, RT. Reaction carried out by Wei Chung Kong.³³³

Lower levels of by-product **4.2.1** were formed on removal of the base and by switching to anhydrous solvent conditions. This demonstrated that formation of an enamine species, such as **4.1.3**, was possible without the requirement of an additional base or aqueous conditions. It was also found that running the reaction under an atmosphere of nitrogen and shielded from light resulted in significantly improved reproducibility of conversion to **4.1.12**. With the optimal conditions for the oxidative β -sulfonylation

of **2.1.8a** established (Scheme 89), the scope of this reaction was studied, initially varying the sulfinate reaction component.



Scheme 89. Optimised conditions for the oxidative β -C-H sulfonation of 2.1.8a. Conditions: (i) NIS (4.0 eq.), THF, RT, 30 min; (ii) **4.1.11** (1.5 eq.), THF, RT, 2 h. Isolated yield shown; value in parentheses show conversion to product as measured by ^1H NMR analysis of crude product mixture using an internal standard. Reaction carried out by Wei Chung Kong.³³³

The reaction of **2.1.8a** with a wide range of aryl sulfinate salts proceeded with 51-84% yields, and the reaction conditions tolerated electron-rich and electron-poor arenes, halides, *ortho*- and *meta*-substituents, as well as heterocyclic systems (Table 23).

Comparable conversion to **4.1.12** was observed when the corresponding lithium sulfinate salt was used instead of the sodium sulfonate salt, providing wider applicability for sulfonates synthesised *via* a lithiation protocol. Larger scale reactions performed on 5.4 mmol and 3.75 mmol of amine substrate delivered products **4.1.12** and **4.2.7**, respectively, in 75% and 70% yields, respectively; this demonstrated the preparative utility of this method, which is important for the further diversification of the enaminyll sulfone scaffold.

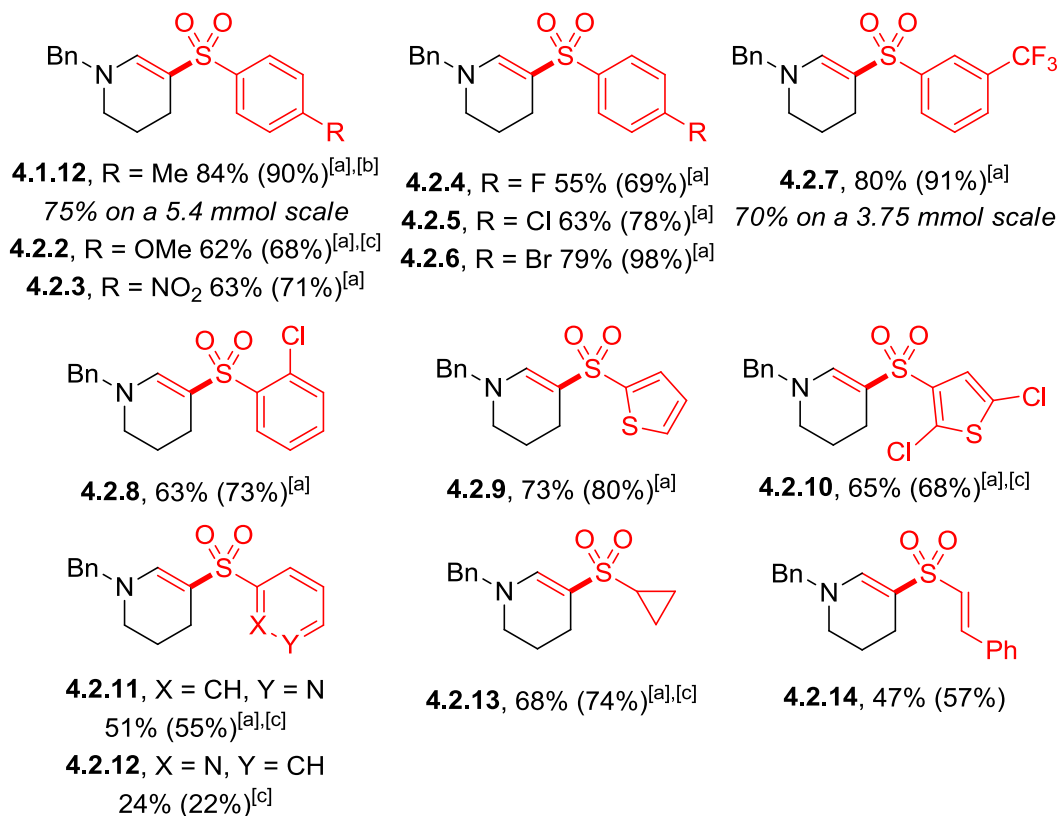
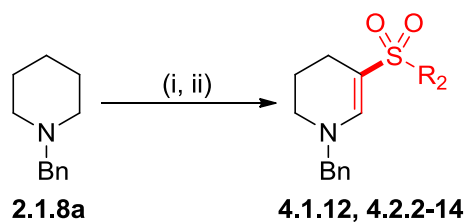
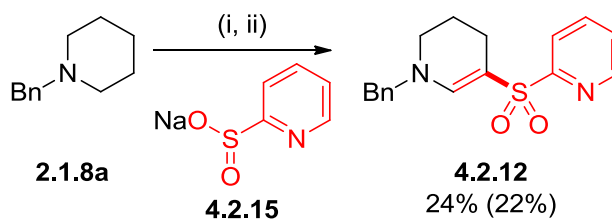


Table 23. Variation of the sulfinate reaction component. Conditions: (i) NIS (4.0 eq.), THF, RT, 30 min; (ii) RSO₂Na (1.5 eq.), THF, RT, 2 h. Isolated yields shown; values in parentheses show conversion to product as measured by ¹H NMR analysis of crude product mixture using an internal standard. Reactions carried out on 0.1-0.6 mmol scale. [a] Reaction carried out by Wei Chung Kong.³³³ [b] 71% NMR conversion observed when TolSO₂Li was used. [c] RSO₂Na (2.0 eq.) used. Tol = *para*-tolyl.

The reaction was lower yielding (24%) when 2-pyridylsulfinate³⁴⁶ **4.2.15** (Scheme 90) was used, to afford the enaminyl sulfone **4.2.12**.



Scheme 90. 2-Pyridylsulfinate led to low-yielding oxidative sulfonation. Conditions: (i) NIS (4.0 eq.), THF, RT, 30 min; (ii) **4.2.15** (2.0 eq.), THF, RT, 2 h. Isolated yield shown; value in parentheses shows conversion to product as measured by ^1H NMR analysis of crude product mixture using an internal standard.

This disappointing result may have been due to the instability of the proposed intermediary sulfonyl iodide **4.2.15b** (Figure 32).

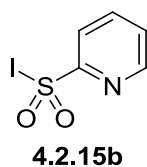
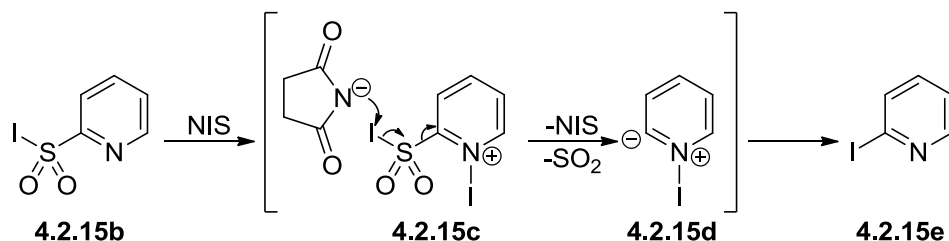


Figure 32. Sulfonyl iodide intermediate 4.2.15b proposed to form via iodination of 4.2.15.

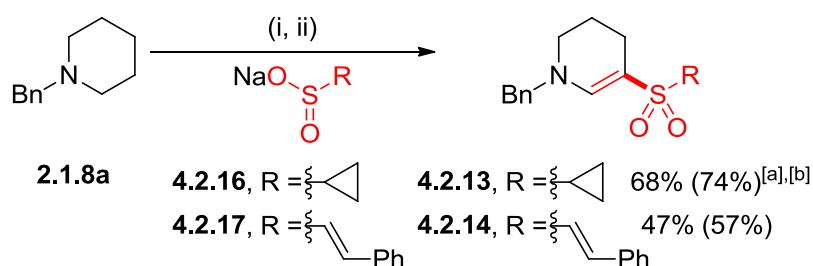
Heteroaromatic sulfonyl chlorides are known to be unstable under ambient conditions,^{347,348} while the enhanced reactivity of sulfonyl iodides compared to the lower atomic number halides makes them, in turn, more unstable.³⁴⁹ The carbon atom between the pyridyl nitrogen and the sulfonyl sulfur is electron-deficient due to the electron-withdrawing nature of the adjacent nitrogen atom and the sulfonyl group. This makes the sulfonyl iodide intermediate susceptible to C–S bond cleavage, particularly if the adjacent pyridyl nitrogen is activated to become cationic through coordination to iodine, to give iodopyridinium **4.2.15c** (Scheme 91).



Scheme 91. Proposed decomposition pathway of 4.2.15b.

The pyridinium moiety could make the sulfonyl iodide susceptible to loss of sulfur dioxide gas *via* attack by the succinimide anion to give ylid **4.2.15d**, which can then rearrange to pyridyliodide **4.2.15e**, and a mass ion of 206.1 (ES, positive mode) was observed in the reaction mixture LCMS, supporting this proposal. Additionally, this substrate instability is similar to that observed for 2-pyridylboronic acids, where facile protodeborylation is known to occur.³⁵⁰

Non-aryl sulfinates could also be used in the oxidative C–H sulfonylation reaction, although this was limited to cyclopropyl and styryl-substituted sulfinates **4.2.16** and **4.2.17**, respectively (Scheme 92), which afforded the corresponding enaminyll sulfones **4.2.13**³³³ and **4.2.14** in 74% and 57% conversion, respectively.



Scheme 92. Cyclopropyl and styryl systems were the only examples of non-aryl oxidative C–H sulfonylation of 2.1.8a. Conditions: (i) NIS (4.0 eq.), THF, RT, 30 min; (ii) **4.2.16** or **4.2.17** (1.5 eq.), THF, RT, 2 h. Isolated yields shown; values in parentheses show conversion to product as measured by ¹H NMR analysis of crude product mixture using an internal standard. [a] Reaction carried out by Wei Chung Kong.³³³ [b] **4.2.16** (2.0 eq.) used.

Other aliphatic sulfinates tested may have been ineffective at affording desired product due to the possibility of the intermediary sulfonyl iodide decomposing *via* formation of a sulfene from dehydroiodination,^{351,352} which could lead to unproductive cycloadditive side-reactivity with the purported enamine.^{353,354}

The reaction proceeded well with a wide scope of amine reaction partners **4.2.18a-m** (Table 24), and electron-rich and electron-poor benzyl groups, nitriles and α - and β -chiral centres were tolerated.

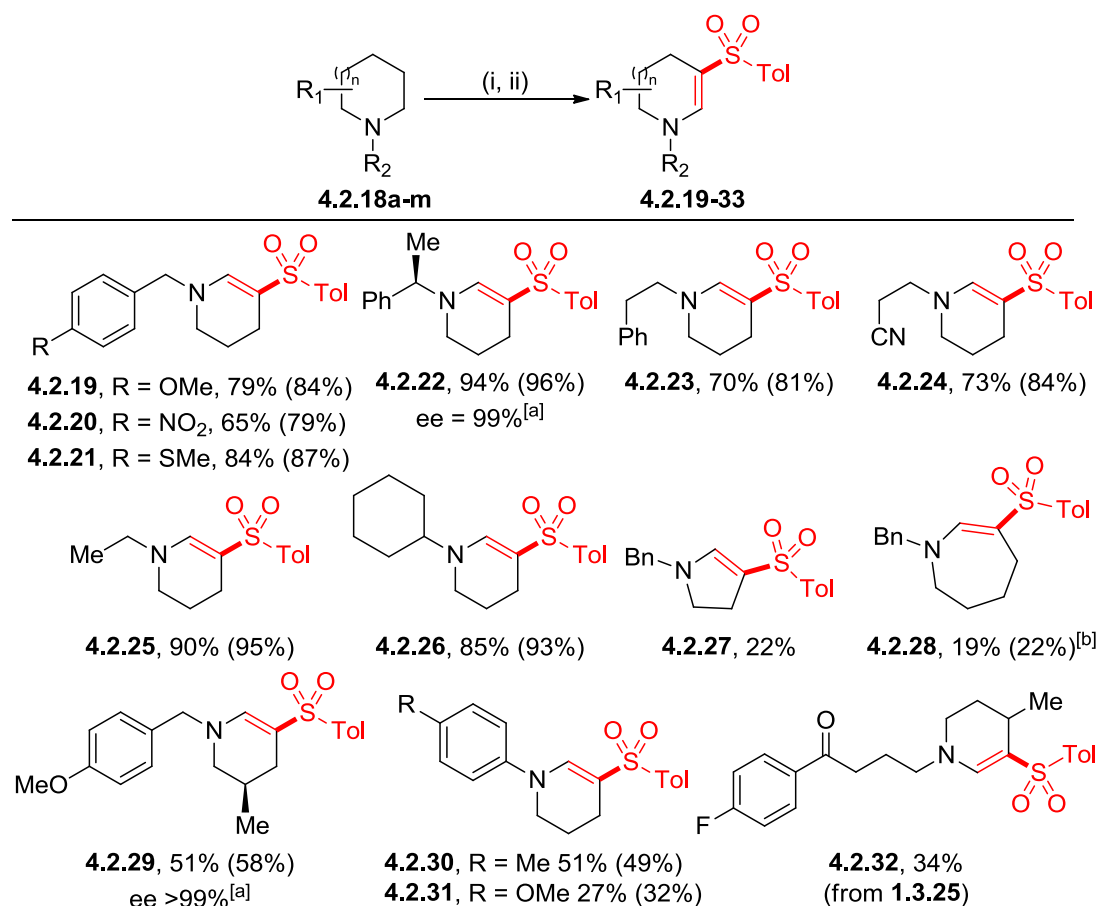
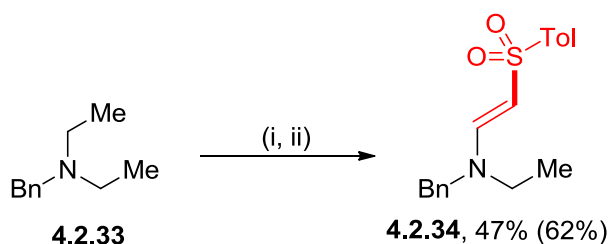


Table 24. Variation of the amine reaction component. Conditions: (i) NIS (4.0 eq.), THF, RT, 30 min; (ii) **4.1.11** (1.5 eq.), THF, RT, 2 h. Isolated yields shown; values in parentheses show conversion to product as measured by ¹H NMR analysis of crude product mixture using an internal standard. Tol = *para*-tolyl. Reactions were carried out by Wei Chung Kong.³³³ [a] ee determined by chiral HPLC analysis against the corresponding racemates **4.6.1** and **4.6.2**, respectively. [b] 3.0 equivalents of **4.1.11** was used and DMSO was used as the reaction solvent.

Oxidative sulfonation was also demonstrated on melperone, **1.3.25** to give **4.2.32**, showcasing how the developed reaction protocol could be used for the diversification of compound collections within drug discovery. The reaction proceeded with complete selectivity for endocyclic sulfonylation, although acyclic sulfonylation was demonstrated on substrate **4.2.33** (Scheme 93) where no cyclic option was available, to afford **4.2.34** in 47% yield.



Scheme 93. Oxidative C–H sulfonylation on acyclic substrate 4.2.33.³³³ Conditions: (i) NIS (4.0 eq.), THF, RT, 30 min; (ii) **4.1.11** (1.5 eq.), THF, RT, 2 h. Isolated yield shown; value in parentheses show conversion to product as measured by ¹H NMR analysis of crude product mixture using an internal standard. Tol = *para*-tolyl. Reaction carried out by Wei Chung Kong.³³³

It should also be noted that substrates **4.2.35** and **4.2.36** (Figure 33) were not reactive towards oxidative C–H sulfonylation, which indicated the requirement of a basic amine for the C–H functionalisation process to occur.

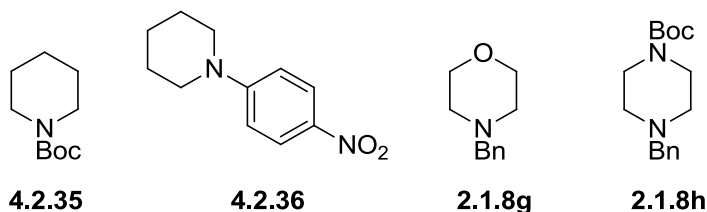
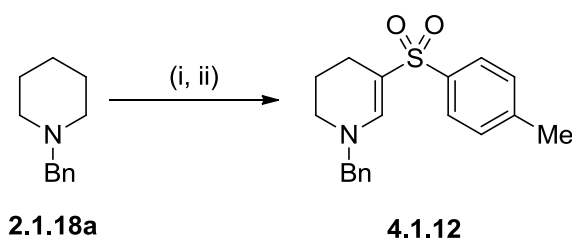


Figure 33. Substrates 4.2.35, 4.2.36, 2.1.8g and 2.1.8h did not exhibit formation of the corresponding enaminyll sulfones. Boc = *tert*-butyloxycarbonyl. Reactions carried out by Wei Chung Kong.³³³

This was consistent with the postulation from the iodine-mediated C–H oxidation work that the availability of the nitrogen lone pair was important for formation of a nitrogen-iodine interaction, which precedes oxidation of the azacycle, though the lack of product formation for morpholine **2.1.8g** and piperazine **2.1.8h** was unexpected. For these systems, unreacted starting material was seen to remain in the reaction mixture, along with the formation of a mixture of unidentifiable by-products. With these unanticipated results, investigations to probe the reaction mechanism were carried out.

4.3 Mechanistic Investigations

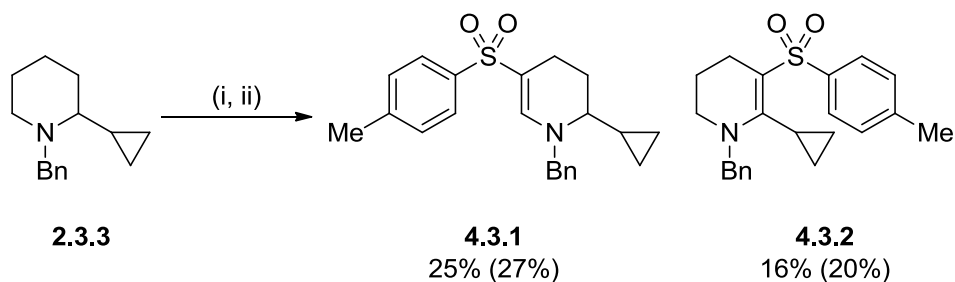
No lactam was observed to form when the sulfinate salt was added to the standard aqueous iodine-mediated C–H oxidation conditions, so a different reaction pathway to the lactam synthesis was initially hypothesised. To explore the possibility that a radical-based mechanism may be responsible for facilitating oxidative C–H sulfonylation, the reaction between **2.1.8a** and **4.1.11** was repeated with the inclusion of a selection of radical inhibitors (Table 25).



Entry	Variation from Standard Conditions	Conversion (%) ^[a]
1	None	90
2	BHT (1.1 eq.) added	70
3	Catechol (1.1 eq.) added	29
4	TEMPO (1.1 eq.) added	0

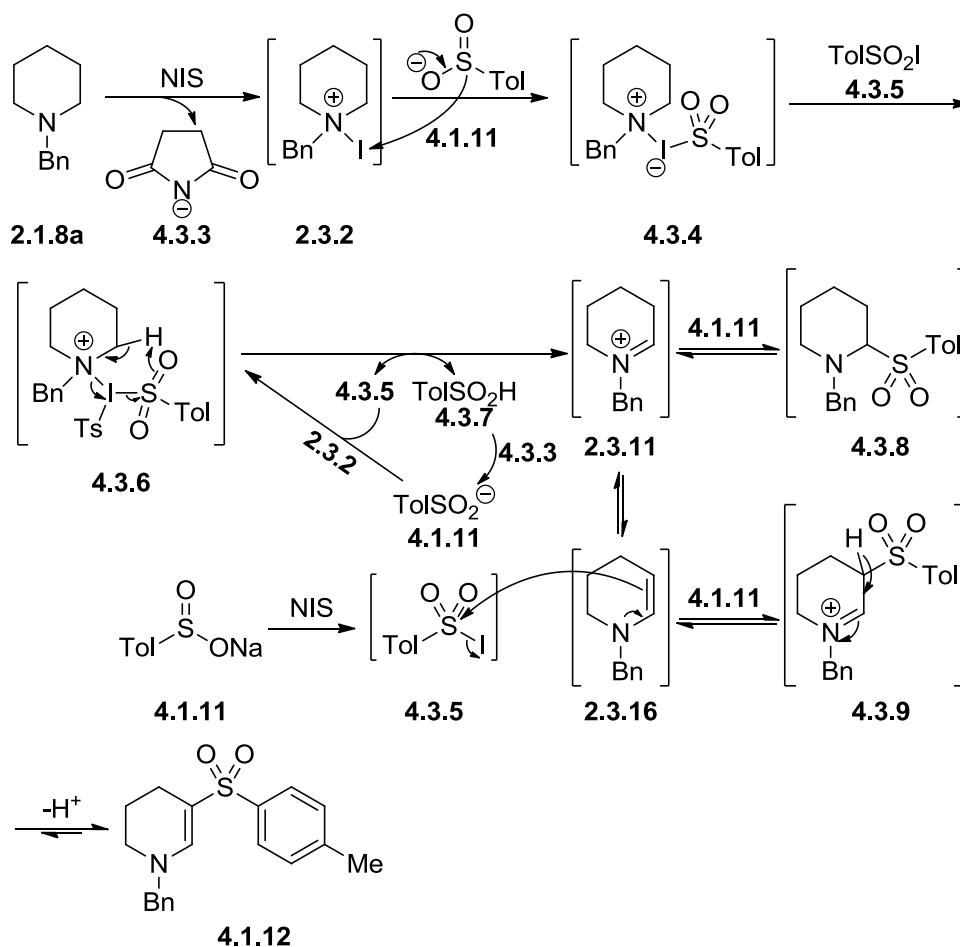
Table 25. Control experiments indicate a possible radical pathway. Conditions: (i) NIS (4.0 eq.), THF, RT, 30 min; (ii) **4.1.11** (1.5 eq.), THF, RT, 2 h. BHT = 2,6-di-*tert*-butyl-4-methylphenol. TEMPO = (2,2,6,6-Tetramethylpiperidin-1-yl)oxyl radical. [a] As measured by ¹H NMR analysis of crude product mixture using an internal standard.

It was observed during the optimisation of this protocol that using inhibitor-free THF led to slightly improved conversion to product, which suggested that the reaction might proceed *via* a radical-based mechanism. This was consistent with these radical inhibitor control experiments, whereby addition of 2,6-di-*tert*-butyl-4-methylphenol (BHT) led to a slight reduction in conversion to product **4.1.12**. Catechol lowered conversion further, and the addition of TEMPO resulted in no product formation at all. Low levels of inhibition by BHT despite inhibition by TEMPO has some precedent in related iodine/sulfinate reaction systems,³⁵⁵ hence a radical-based mechanism was a possible pathway for this reaction. To probe this further, a radical-clock experiment was carried out using **2.3.3** (Scheme 94).



Scheme 94. Radical-clock experiment investigating the possibility of a radical-based mechanism for the oxidative C–H sulfonylation of 2.3.3. Conditions: (i) NIS (4.0 eq.), THF, RT, 30 min; (ii) 4.1.11 (1.5 eq.), THF, RT, 2 h. Isolated yields shown; values in parentheses show conversion to product as measured by ^1H NMR analysis of crude product mixture using an internal standard.

No opening of the cyclopropyl ring was observed in the oxidative C–H sulfonylation of substrate **2.3.3**, with a mixture of regioisomers **4.3.1** and **4.3.2** in 25% and 16% yields, respectively. This result suggested, contrary to the radical inhibitor experiments, that the reaction did not proceed *via* a radical pathway when **2.3.3** was used. Accordingly, an alternative ionic mechanism is proposed to proceed *via* initial *N*-iodination by NIS to **2.3.2**, eliminating succinimide anion **4.3.3** (Scheme 95).

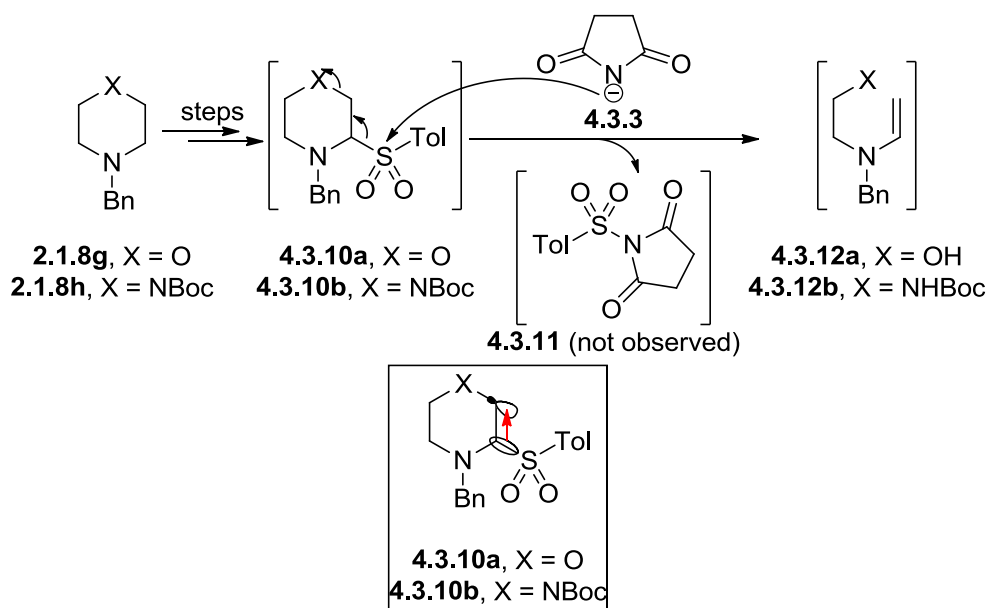


Scheme 95. Proposed ionic-based mechanism for the oxidative C–H sulfonylation of azacycles, such as 2.1.8a using NIS and sodium sulfinate salts. Tol = *para*-tolyl.

If it is assumed that the mechanism for oxidative C–H sulfonylation proceeds *via* a similar E_i mechanism to that proposed for the iodine-mediated C–H oxidation (Chapter 2.6, Scheme 61), then it is proposed that nucleophilic attack on 2.3.2 by sulfinate 4.1.11 could lead to formation of hypervalent iodine intermediate 4.3.4. This could then undergo nucleophilic attack of sulfonyl iodide 4.3.5, formed *via* iodination of 4.1.11 by NIS, to generate the *bis*-tosyl hypervalent iodoammonium species 4.3.6. This can subsequently undergo a *syn*-iodoso elimination to generate iminium 2.3.11 and eliminate sulfonamide 4.3.5 and sulfonic acid 4.3.7. The succinimide anion 4.3.3 could deprotonate 4.3.7 to form 4.1.11, which can then participate in nucleophilic attack of 2.3.2, followed by electrophilic attack of 4.3.5 to re-form 4.3.6.

When sulfinate **4.1.11** was added into the standard aqueous reaction conditions for iodine-mediated C–H oxidation, no lactam was observed. This suggested that the α -position of **2.3.11** is rapidly, but reversibly, protected by the sulfinate to give α -sulfonyl azacycle **4.3.8**, which prevents water from quenching the iminium. Ley *et al.* have reported the use of α -sulfonyl groups as formal iminium protecting groups for cyclic amines.³³⁴ This effect increases the lifetime of the iminium **2.3.11**, meaning that tautomerism to enamine **2.3.16** can occur, which can in turn attack the electrophilic sulfonyl iodide **4.3.5**. Tautomerism of the resultant β -sulfonyliminium **4.3.9** would lead to formation of the product enaminy sulfone **4.1.12**.

The formation of intermediate **4.3.8** could also account for the lack of product formation seen for morpholine **2.1.8g** and piperazine **2.1.8h**. α -Sulfonylation of an intermediary iminium species would ostensibly afford **4.3.10a** and **4.3.10b**, respectively (Scheme 96).



Scheme 96. Possible degradation pathway for azacycles with an electronegative group in the γ -position, resulting from weakening of the C–X bond by σ to σ^* donation. Tol = *para*-tolyl.

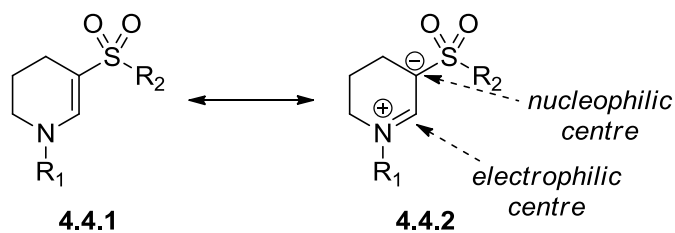
The electron-withdrawing nature of the electronegative oxygen atom or the electron-deficient carbamate would increase the overlap between the C–S σ -bonding orbital and

the antibonding orbital of the C–X bond; this would have the effect of weakening the C–X bond. This bond-weakening effect could increase the electrophilicity of the sulfonyl group, making it susceptible to nucleophilic attack by some nucleophilic species in the reaction mixture, for example the succinimide anion **4.3.3**; this pathway is subject to confirmation as no evidence of sulfonamide **4.3.11** was observed by LCMS analysis of the reaction mixture. Nucleophilic attack in this fashion would lead to fragmentation of the heterocyclic scaffold to give ring-opened products, such as **4.3.12a** and **4.3.12b**.^{356–358} While fragmentation products were not isolated from the reaction mixtures, mass ions corresponding to such species were detected in the LCMS profiles of the reaction mixtures when morpholine **2.1.8g** and piperazine **2.1.8h** substrates were used.

These investigations provided evidence for the proposed mechanism, which fulfilled the intended strategy of intercepting the intermediates formed in the α -C–H oxidation protocol, further validating the proposed mechanism for that procedure. Following completion of the substrate scope and initial mechanistic studies, the utility of the product enaminyll sulfones for organic synthesis was investigated.

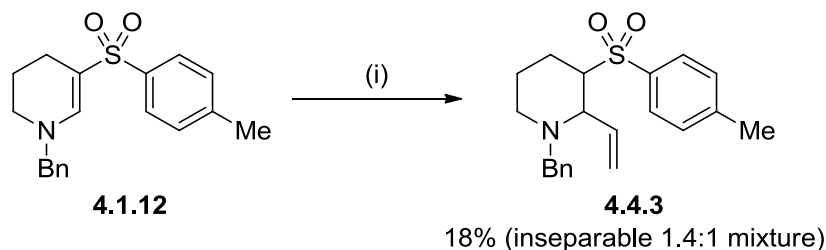
4.4 Synthetic Diversification of the Enaminyll Sulfone Scaffold

Despite the combination of synthetically useful functional groups within enaminyll sulfones, their use in synthesis has not been well explored, with a few isolated applications exemplified in the literature.^{359,360} The combination of the nucleophilic enamine with the vinyl sulfone moiety led to the proposition that enaminyll sulfones such as **4.4.1** may be able to react as either an electrophile or a nucleophile (Scheme 97).



Scheme 97. Proposed resonance form of enaminyl sulfones that possesses electrophilic and/or nucleophilic character.

Back *et al.* reported α -vinylation of cyclic enaminyl sulfones with a Grignard reagent under strongly acidic conditions, although this was only exemplified for larger nine and ten-membered rings, rather than six-membered rings.³⁶¹ These conditions were used to try to introduce α -vinylation of **4.1.12** to form **4.4.3** (Scheme 98), but 18% yield of what was proposed to be a 1.4:1 mixture, determined by ¹H NMR, of inseparable diastereomers **4.4.3** was obtained.

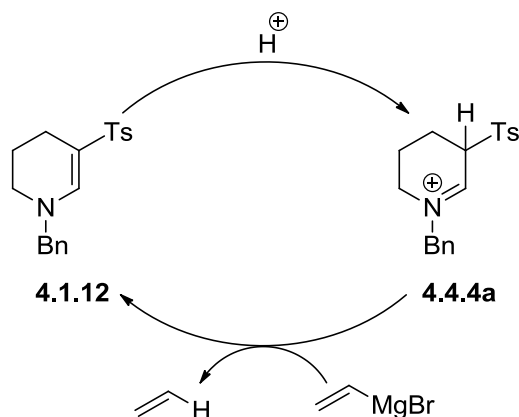


Scheme 98. α -Vinylation was achieved, but in low yield. The resulting diastereomers could not be separated for characterisation. Conditions (i) CF₃SO₃H (2.5 eq.), DCE, -10 °C, 30 min, then vinylmagnesium bromide (4.1 eq.), -10 °C to RT, 2 h.

The progress of the reaction stopped, with a lot of unreacted starting material present in the reaction mixture even after further equivalents of triflic acid and Grignard reagent were added.

It had been hypothesised that the Grignard reagent could act as a base to racemise the proton next to the sulfone, eventually leading to the preparation of one sterically preferred diastereomer. Given the low levels of product formation, it was subsequently proposed that the Grignard reagent was able to deprotonate the intermediary iminium

species **4.4.4a** (Scheme 99) to reverse iminium formation back to the starting material, and thereby quenching the Grignard.



Scheme 99. Proposed rationale for the low yield of Grignard addition to **4.1.12** by deprotonation of intermediary iminium **4.4.4a**, formed *via* protonation of **4.1.12** with triflic acid. Ts = *para*-toluenesulfonyl.

It was proposed that a Grignard reagent with increased steric bulk would be less likely to deprotonate **4.4.4a**, and would also be more likely to give one major *trans*-diastereomer, however the use of *para*-tolylmagnesium bromide only afforded unreacted starting material. The disparity between these results and the work reported by Back *et al.* could be due to the fact that, with six-membered ring **4.1.12**, a strained half-chair iminium intermediate is formed, and the nearby axial hydrogen atoms may retard the approach of the Grignard reagent for nucleophilic attack at the electrophilic iminium centre (Figure 34a).

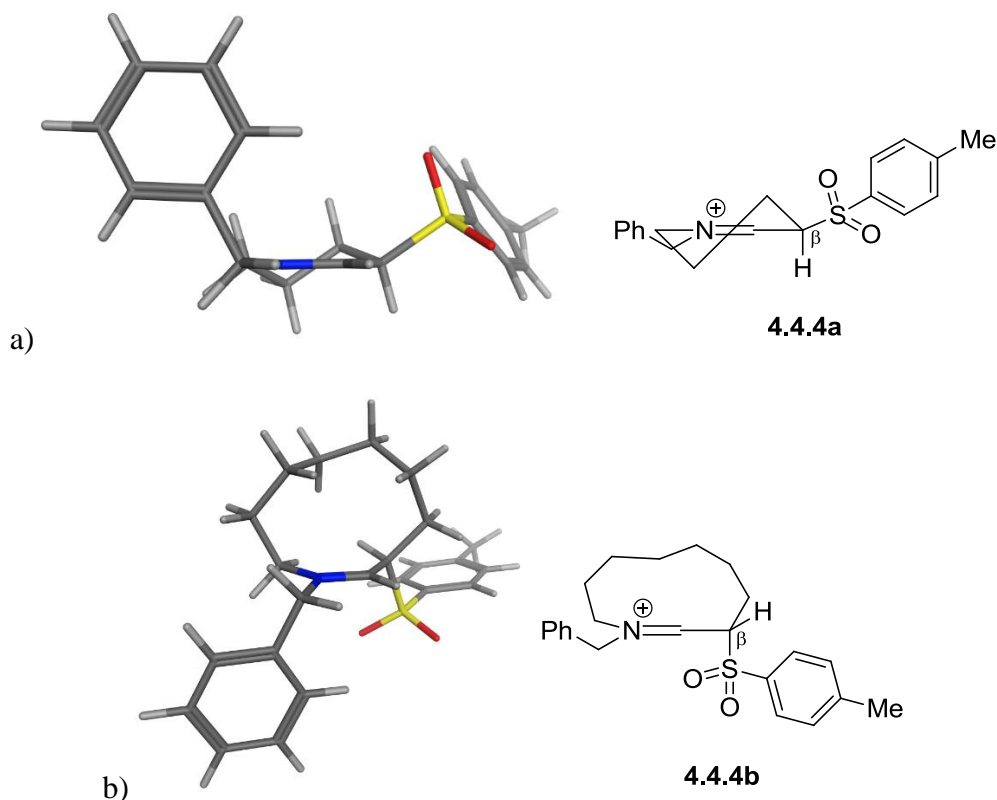
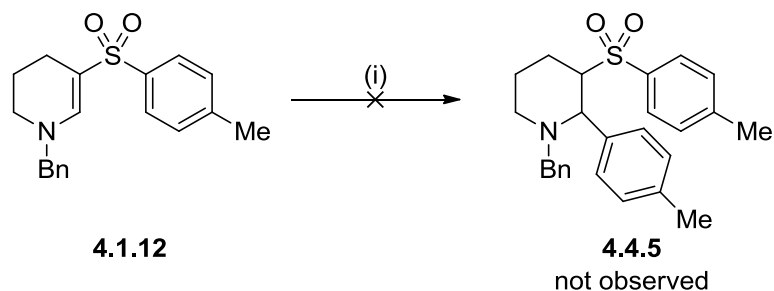


Figure 34. Calculated lowest energy states²⁴² for the iminium intermediates from the reaction of trifluoromethane sulfonic acid with a) the six-membered ring substrate 4.1.12, and b) the ten-membered ring substrate from the work reported by Back *et al.*³⁶¹

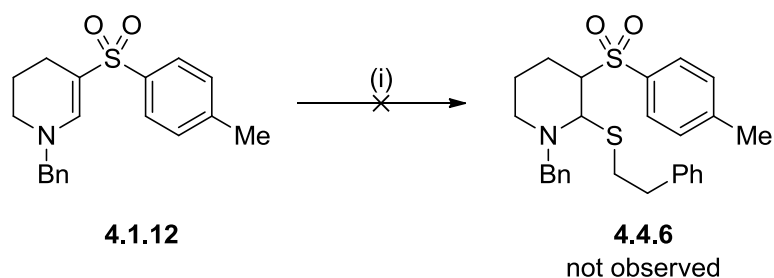
Additionally, the β -C–H bond, which was installed by reaction with triflic acid, is calculated to be in a pseudo-axial position. This puts it into an antiperiplanar arrangement with the π^* -orbitals of the iminium ion, and is therefore more prone to deprotonation by the Grignard reagent, reverting back to the starting material. In contrast, for the ten-membered ring iminium **4.4.4b** (Figure 34b) from the chemistry reported by Back *et al.*, the iminium intermediate is much more flexible, meaning that the approach of the Grignard reagent can occur more readily. The β -hydrogen is also not in an antiperiplanar arrangement with the iminium π -system, hence there was very little recovery of starting material (8%). This suggests the acidification/Grignard trapping protocol reported by Back *et al.* reaction will only work well for larger ring systems; this was reflected by the fact that when Back *et al.* carried out the reaction on a nine-membered ring 30% less product was produced than when the ten-membered ring was used.

Since this method of α -functionalisation did not appear very promising by the use of the moderately hard nucleophile vinyl magnesium bromide, the reaction of a soft nucleophile with the Michael acceptor vinyl sulfone was proposed.³⁶¹ Copper(I) and copper(II) salts were used as additives to try to facilitate conjugate addition of *para*-tolylmagnesium bromide of **4.1.12** to form the arylated sulfone **4.4.5** (Scheme 100).



Scheme 100. Conjugate addition of a Grignard reagent would not occur, even in the presence of copper(I) or copper(II) salts. Conditions (i) CuCl or CuBr₂ (20 mol%), *para*-tolylmagnesium bromide (2.2 eq.), THF, -10 °C to RT, 24 h.

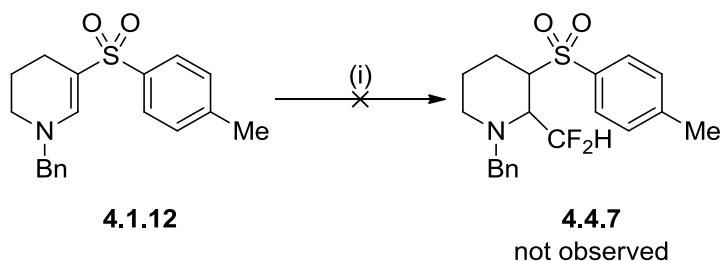
However, no reaction was observed, and a dimer of *para*-toluene was the only observed component in the reaction mixture. Similarly, no reaction was observed with the soft nucleophile phenylethanethiol (Scheme 101).³⁶²



Scheme 101. Unsuccessful conjugate addition of a soft thiol nucleophile. Conditions: (i) 2-phenylethanethiol (8.0 eq.), DCE, RT to 60 °C, 40 h.

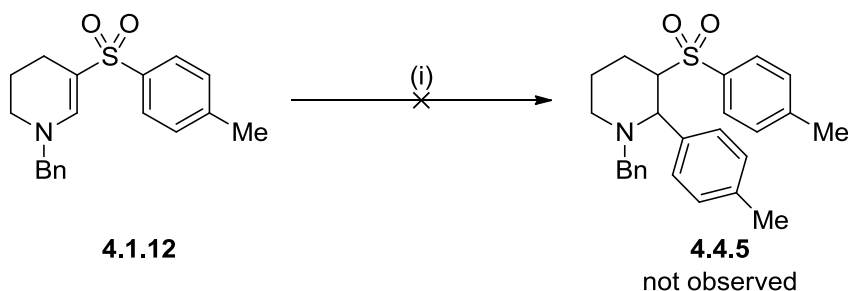
The intermediary iminium species **4.4.4a**, formed following reaction of **4.1.12** with strong acid, was proposed to be similar to the heterocyclic substrates used by Baran *et al.* for C–H functionalisation with sulfinate salts. Subjecting **4.1.12** to the acidic difluoromethylation conditions described by Baran *et al.*⁶⁹ only led to complex

degradation of the substrate and no formation of the desired product **4.4.7** (Scheme 102).



Scheme 102. Compound **4.1.12** was not susceptible to C–H difluoromethylation under the conditions of Baran *et al.* Conditions: (i) TFA (1.0 eq.), Zn(SO₂CF₂H)₂ (2.7 eq.), then *tert*-BuOOH (5.0 eq.), DCM:H₂O (2.5:1), 16 h.

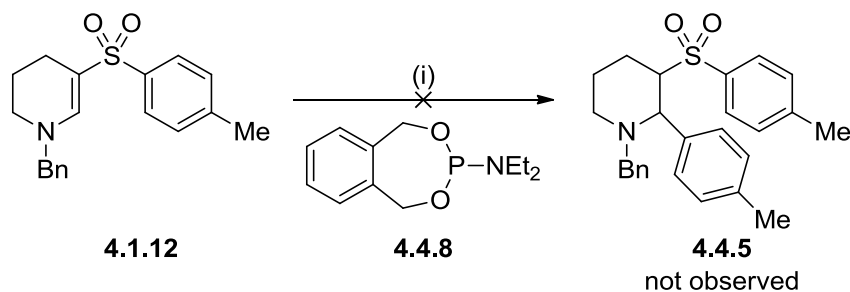
Transition metal-catalysed conjugate addition of organoboron species was subsequently pursued as an alternative strategy for nucleophilic attack of **4.1.12**, with a metal catalyst proposed as being able to activate the enaminyll sulfone towards nucleophilic attack. Palladium-mediated conjugate addition of *para*-tolylboronic acid and *para*-tolylboroxine to **4.1.12** was initially attempted (Scheme 103),³⁶³ but no reaction was observed in either case; instead a toluene dimer was observed from the boronic acid reaction.



Scheme 103. Palladium-catalysed conjugate addition of organoboron species was not successful. Conditions: (i) TolB(OH)₂ (3.0 eq.) or (TolBO)₃ (1.5 eq.), Pd(OAc)₂ (5 mol%), 2,2'-bipyridine (Bpy) (20 mol%), AcOH/THF/H₂O, 40 °C, to 100 °C, 24 h. Tol = *para*-tolyl.

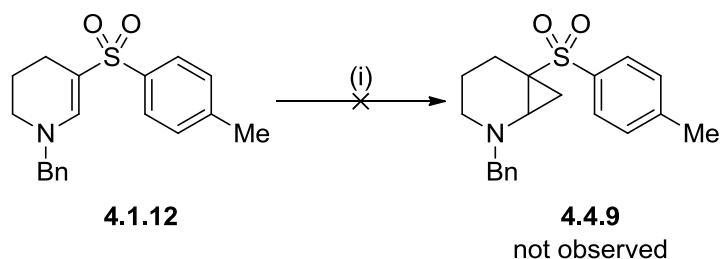
Copper-catalysis is another method for facilitating conjugate addition of boroxines into enones,³⁶⁴ but unfortunately copper-catalysed conditions in the presence of

phosphoramidite ligand **4.4.8** also did not lead to any reaction with **4.1.12** (Scheme 104).



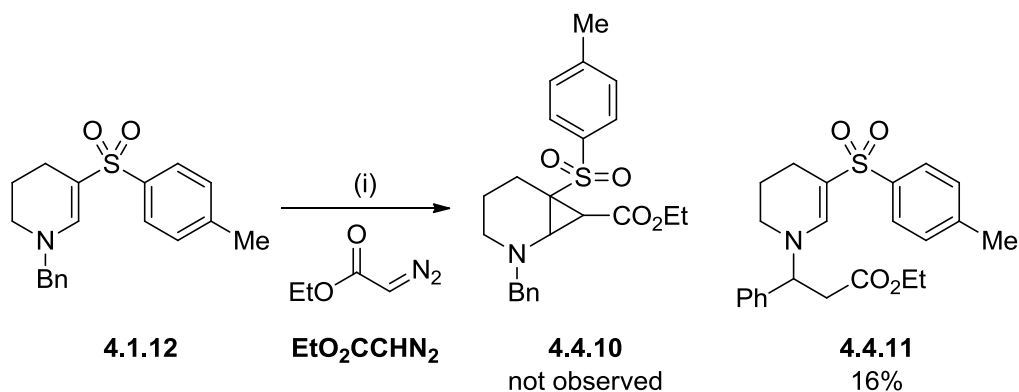
Scheme 104. Copper-catalysed conjugate addition of a boroxine was not successful. Conditions: (i) CuOTf•(0.5 toluene) (10 mol%), **4.4.8** (12 mol%), KOAc (2.0 eq.), (TolBO)₃ (0.5 eq.), toluene, 70 to 150 °C, 40 h. Tol = *para*-tolyl.

Moving away from transition metal-catalysed conjugate addition, sulfur ylides have been employed to carry out cyclopropanation of enones, such as the Corey-Chaykovsky cyclopropanation.^{365–369} However, when cyclopropanation of **4.1.12** was attempted with either a sulfonium ylide or a sulfoxonium ylide, no reaction was observed (Scheme 105).



Scheme 105. No cyclopropanation product 4.3.9 was observed in the attempted Corey-Chaykovsky cyclopropanation of 4.1.12. Conditions: (i) Me₃SI or Me₃SOI (1.3 eq.), *tert*-BuOK (1.3 eq.), DMSO, RT to 100 °C, 32 h.

Another method of cyclopropanation is *via* the addition of rhodium-carbenoids, generated from diazo-compounds, into alkene systems.^{370–374} Accordingly, **4.1.12** was subjected to conditions to attempt to carry out rhodium-catalysed cyclopropanation of the enamine bond (Scheme 106).

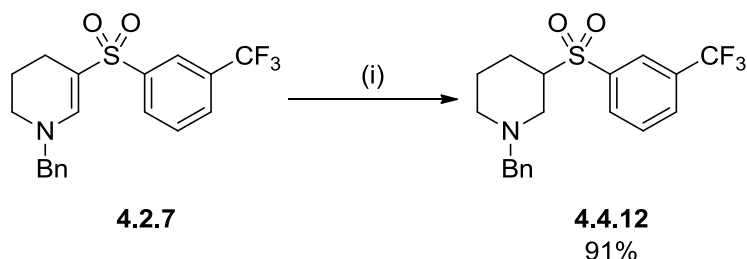


Scheme 106. Attempted rhodium-catalysed carbenoid cyclopropanation did not afford any cyclopropane product, but instead resulted in benzylic C–H functionalisation. Conditions: (i) Rh₂(OAc)₄ (1 mol%), EtO₂CCHN₂ (5.0 eq.), DCM, 60 °C, 60 h.

A large amount of unreacted starting material remained after consumption of the diazoacetate; only small amounts of product were observed to form after an extended reaction time of 60 hours, but instead of the intended cyclopropanation product **4.4.10**, benzylic C–H functionalisation was observed, whereby **4.4.11** was formed in 16% yield. While cyclopropanation of alkenes in the presence of benzylic C–H bonds is known,³⁷⁰ these have typically been in systems where the alkene reacting is activated to become more electron-rich *via* hyperconjugation. For **4.1.12**, the electron-withdrawing sulfone deactivates the alkene to electrophilic attack on the carbenoid, and while the nitrogen atom donates electron density into the alkene, it also donates into the benzylic C–H bonds *via* n to σ* hyperconjugation. This makes the benzylic position more susceptible to reaction with the rhodium-carbenoid than the enamine. A great deal of reported C–H functionalisation protocols with rhodium carbenoids are carried out in an intramolecular manner,^{375–377} with few reported cases of intermolecular processes.³⁷⁸ However, this transformation did not result in the diversification of the installed enaminyll sulfone scaffold, so it was not investigated further at this stage.

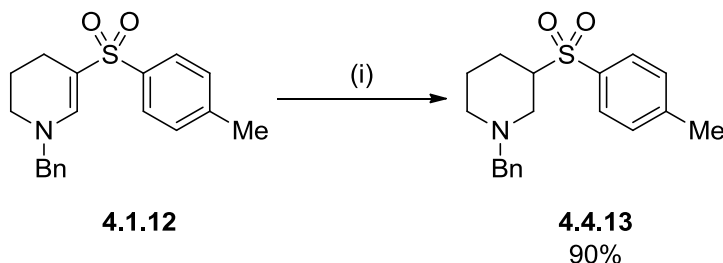
The results gathered so far indicated that the enaminyll sulfone system was in fact quite electron-rich, and therefore could behave more like a stable enamine surrogate rather than a vinyl sulfone. To test this, **4.2.7** was subjected to reducing conditions in the

presence of a silane and TFA, which led to formation of saturated amine **4.4.12** in 91% yield (Scheme 107).³⁷⁹



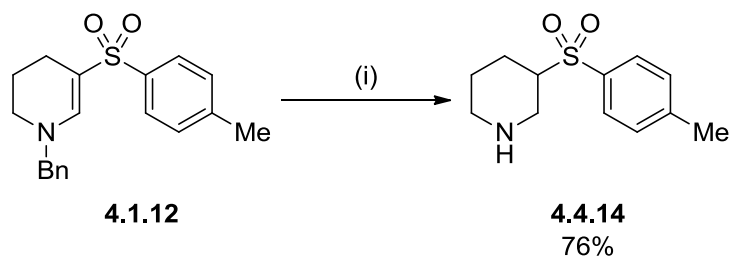
Scheme 107. Reduction of the enamine moiety of 4.2.7 under acidic silane conditions. Conditions: (i) Et₃SiH (2.0 eq.), TFA, 60 °C, 60 h.

This validated the nucleophilic nature of the enaminy sulfone through nucleophilic attack of TFA to generate an iminium tautomer that can then be reduced by triethylsilane. Alternatively, hydrogenation over a palladium catalyst, using zinc and hydrochloric acid to generate hydrogen gas in a COware reaction vessel,³⁷⁸ afforded selective reduction of **4.1.12** to the saturated system **4.4.13** in 90% yield (Scheme 108).



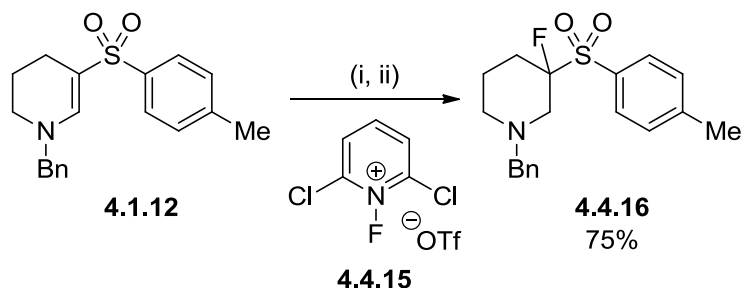
Scheme 108. Use of COware enabled selective hydrogenation of the enamine moiety of 4.1.12. Conditions: (i) 10% Pd/C (10 mol%), AcOH, (ii) Zn (s), HCl (aq.), 70 °C, 3 bar, 16 h.

Additionally, use of a H-Cube™ flow reactor allowed for straightforward small-scale hydrogenation at high temperature and pressure, with fewer safety risks that would normally be associated with batch hydrogenation. Running the reaction at 25 bar pressure led to rapid global hydrogenation of **4.1.12** to form debenzylated **4.4.14** in 76% yield (Scheme 109).

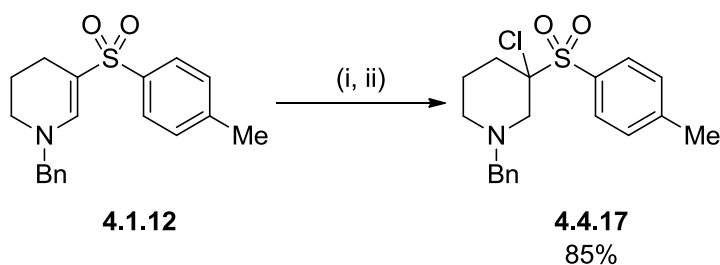


Scheme 109. Flow hydrogenation using a H-Cube™ allowed for facile access to high reaction temperature and pressure, and fast global hydrogenation to form **4.4.14**. Conditions: (i) 10% Pd/C, H₂, AcOH, 1 mL/min, 70 °C, 25 bar, 40 min.

Given reduction of the enamine proceeded well, reactivity of **4.1.12** with other electrophiles was explored. After a brief screen of conditions, fluorination with *N*-fluoropyridinium salt **4.4.15** and borane afforded β-fluorinated species **4.4.16** (Scheme 110), and a similar protocol with *N*-chlorosuccinimide (NCS) led to formation of β-chlorinated product **4.4.17** (Scheme 111).



Scheme 110. Reductive fluorination with **4.4.15** led to β-fluorination of **4.1.12**. Conditions: (i) **4.4.15** (2.1 eq.), THF, RT, 1 h; (ii) BH₃•THF (1.0 eq.), THF, RT, 2 h.



Scheme 111. Reductive chlorination with NCS led to β-chlorination of **4.1.12**. Conditions: (i) NCS (1.1 eq.), THF, RT, 15 min; (ii) BH₃•THF (1.3 eq.), THF, RT, 3 h.

These halogenation protocols gave highly efficient access to sterically hindered halo-sulfone quaternary centres, which traditionally required longer reaction sequences or greater electron-withdrawing character to prepare.^{380,381} During these studies it was observed that, following addition of the halogenation reagent, the corresponding halo-iminium intermediates **4.4.18a** and **4.4.18b** (Figure 35) were observed to be stable by LCMS analysis for over 24 hours, so were proposed to remain stable in the reaction mixture.

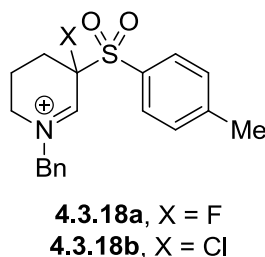
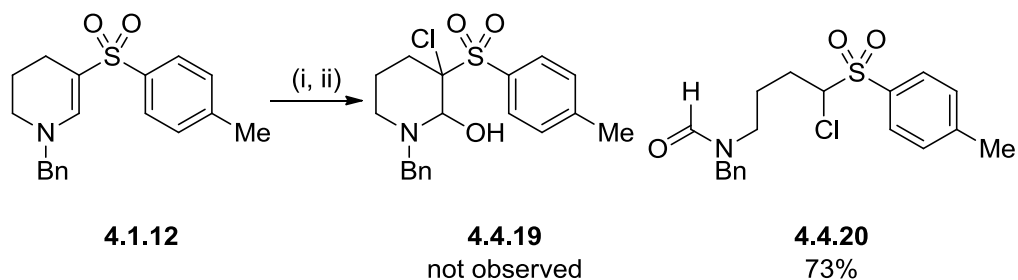
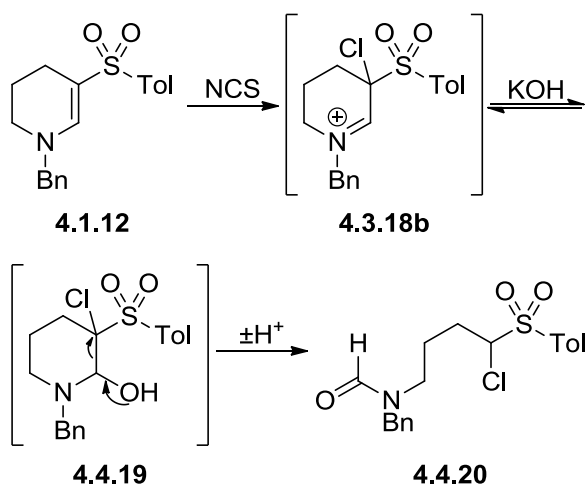


Figure 35. Halo-iminium intermediates 4.4.18a and 4.4.18b, which provided opportunity for further diversification.

This indicated that expansion of the scope of halo-functionalisation to provide access to trifunctionalised azacyclic scaffolds was likely to be possible. Analysis of the reaction mixture forming intermediates **4.4.18a** and **4.4.18b** by LCMS showed the presence of an adduct with water that was likely to have been introduced from the aqueous chromatography solvent system. Therefore, it was proposed that formation of a hemiaminal-type product may be possible by quenching **4.4.18b** with an oxyanion nucleophile, such as potassium *tert*-butoxide or potassium hydroxide. No reaction was observed with *tert*-butoxide, and quenching with potassium hydroxide did not afford any α -hydroxy product **4.4.19**, but instead led to ring-opening of the azacycle to give formamide **4.4.20** in 73% yield (Scheme 112), with the proposed mechanism of formation shown in Scheme 113.



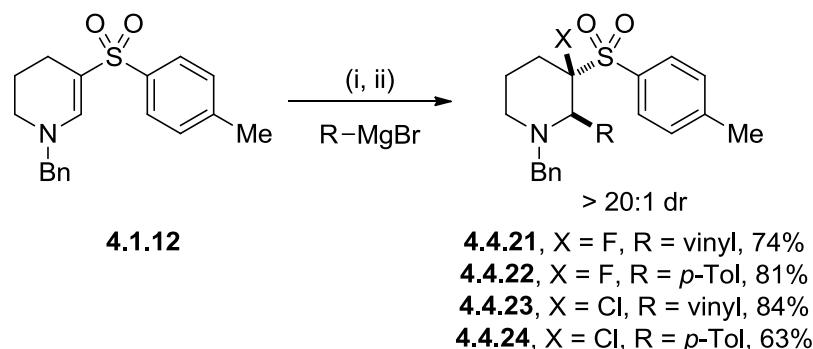
Scheme 112. Chloro-hydrative ring-opening of 4.1.12. Conditions: (i) NCS (1.5 eq.), THF, RT, 2 h; (ii) *aq.* KOH (2.0 eq.), THF, RT, 26 h.



Scheme 113. Proposed mechanism for the formation of the ring-opened product 4.4.20.

Formamides are useful functional groups in organic synthesis,^{382–384} and predictable and selective ring-opening processes offer access to interesting and novel diversification of complex scaffolds.

Functionalisation of **4.4.18a** and **4.4.18b** with organometallic nucleophiles was also investigated. Following formation of **4.4.18a** or **4.4.18b**, α -C–C bond formation was facilitated through use of vinyl and aryl Grignard reagents to afford trifunctionalised scaffolds **4.4.21** to **4.4.24** in 63–84% yields (Scheme 114).



Scheme 114. Diastereoselective halo-vinylation and halo-arylation of 4.1.12 to afford trifunctionalised scaffolds 4.4.21 to 4.4.24. Conditions: (i) **4.4.15** (X = F) or NCS (X = Cl) (1.1 eq.), THF, RT, 10 min to 1.5 h; (ii) RMgBr (1.3 eq.), RT, 1.5 to 3.0 h. Diastereomeric ratio was determined by ^1H NMR analysis of the crude material.

The reaction was observed to proceed with a very high degree of diastereoselectivity, with only a single diastereomer detected by ^1H NMR. This strongly suggested an ordered transition state controlling the approach of the nucleophile to the iminium intermediate was occurring, potentially *via* chelation of the installed halogen atom to the organometallic (Figure 36).

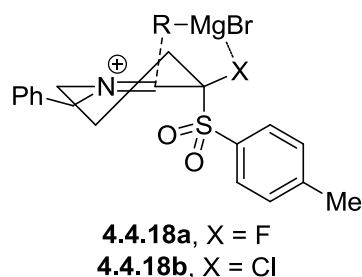


Figure 36. Proposed ordered transition state facilitating very high observed diastereoselectivity.

Despite the installed C–X and C–C bonds being positioned on the same face of the azacycle in **4.4.21** to **4.4.24**, as determined by 2D NMR analysis,³⁸⁵ there are differences in the conformational arrangement of these bonds depending on the nucleophile that had been introduced. The tolyl substituted scaffolds **4.4.22** and **4.4.24** adopted the conformation whereby the tolyl and the sulfone were in the equatorial positions (Figure 37). In contrast to this, the vinyl-substituted analogues **4.4.21** and **4.4.23** were arranged with the vinyl and the sulfone groups in axial conformations.

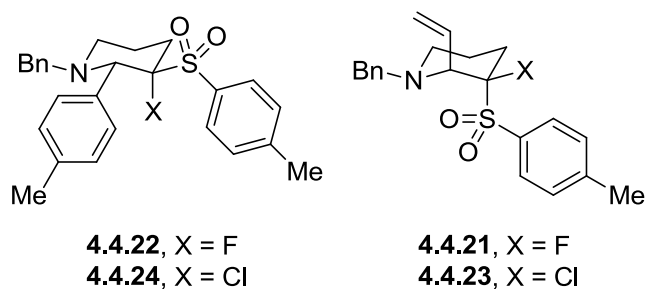


Figure 37. Rationalisation of the difference in observed conformation depending on Grignard nucleophile used. Structural assignment was carried out by NMR analysis.³⁸⁵

This observation for the vinyl analogues perhaps arises from an anomeric affect between the nitrogen atom lone pair and the vinyl group (Figure 38).

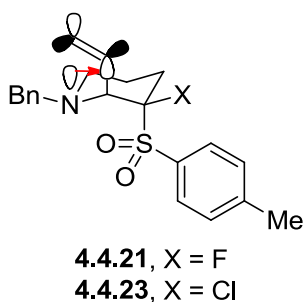


Figure 38. Proposed anomeric effect arising from n to π^* donation of the nitrogen lone pair into the alkene π^* orbitals, which causes the axial-axial arrangement of the vinyl and sulfonyl groups of 4.4.21 and 4.4.23.

For **4.4.21**, a mixture of chair conformations was seen by NMR when chloroform was used as the solvent, but the only conformer of **4.4.21** seen in DMSO was that depicted in Figure 37. The anomeric effect provides an energy benefit of only approximately 1 to 2 kcalmol⁻¹,³⁸⁶ which can be overcome by solvent effects,^{387,388} hence the difference in conformational distribution seen between the two solvents. This small energy benefit is likely to be overcome by the large steric hindrance that the α -tolyl group would induce, resulting in an equatorial arrangement for **4.4.22** and **4.4.24**. Molecular modelling of the lowest energy conformations of **4.4.21** to **4.4.24** are consistent with the structures observed by NMR (Figure 39), providing further evidence for this result.

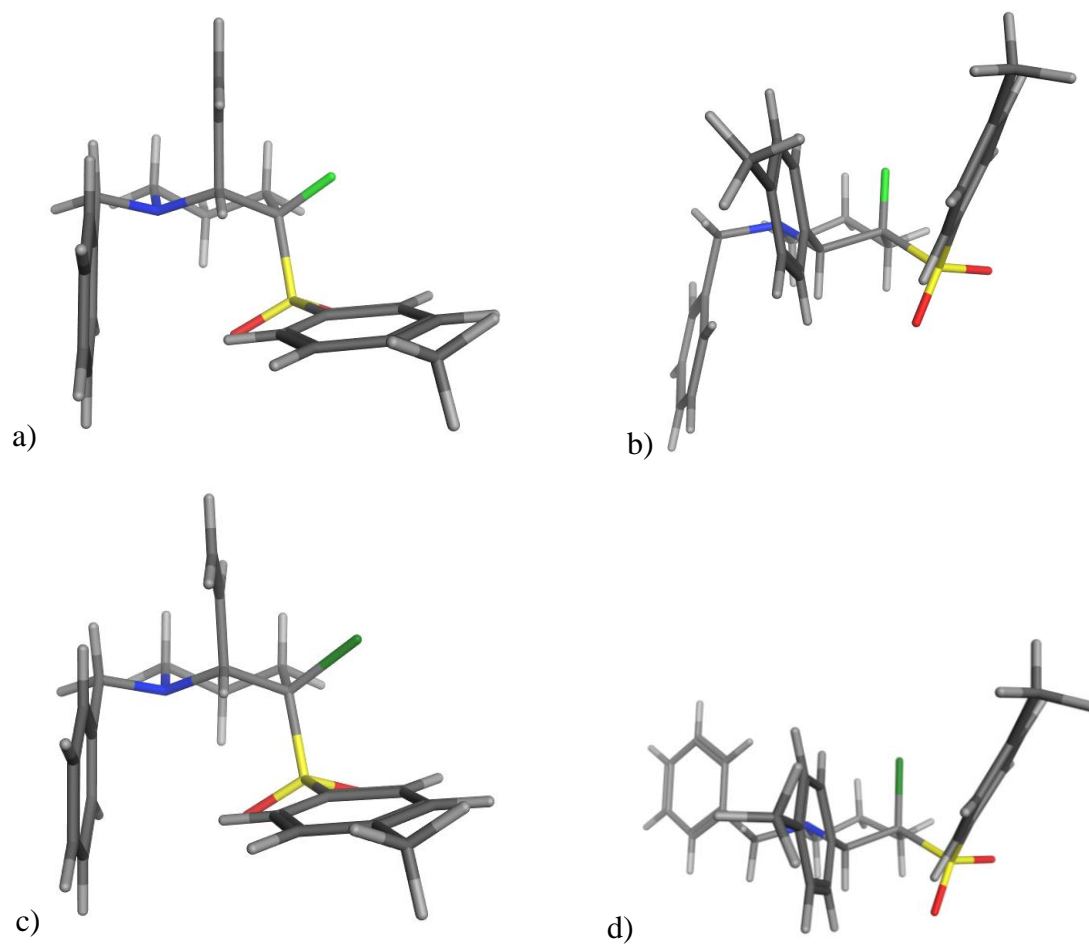
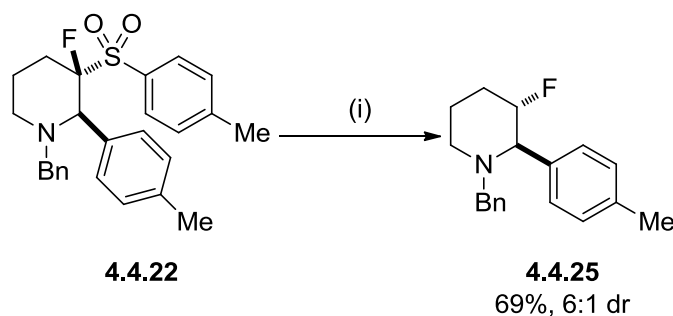


Figure 39. Calculated lowest energy states²⁴² for a) 4.4.21, b) 4.4.22, c) 4.4.23, d) 4.4.24, demonstrating the preference for axial arrangement of the vinyl groups, but equatorial arrangement of the tolyl groups.

The axial/axial arrangement of the vinyl and the sulfone groups have potential application in drug discovery, as they could provide access to novel vectors in 3D space along which to build a drug molecule.

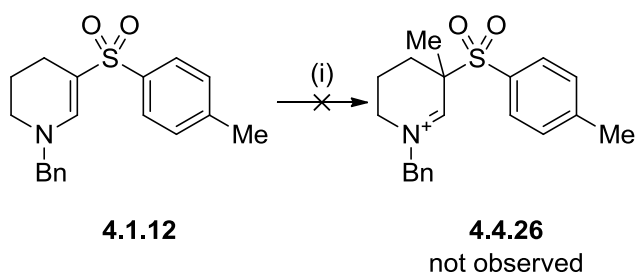
In order to demonstrate the potential transient nature of the sulfone group, reductive desulfonation of **4.4.22** was carried out using elemental magnesium,³⁸⁹ to provide the stereodefined azacycle **4.4.25** in 69% yield (Scheme 115).



Scheme 115. Reductive desulfonation led to racemisation of the β -stereocentre to give the equatorial/equatorial conformer as the major diastereomer. Conditions: (i) Mg (40.0 eq.), MeOH, RT, 16 h. Diastereomeric ratio was determined by ^{19}F NMR analysis of the crude material.

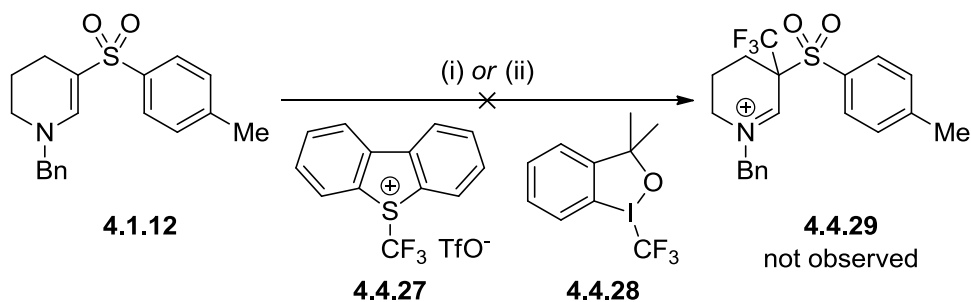
This led to racemisation of the C–F bond to give the sterically preferred equatorial conformation in 69% yield, but a 6:1 diastereoselectivity was still observed by NMR after this conversion. Scaffolds such as **4.4.25** are medicinally relevant compounds that have been shown to exhibit phosphodiesterase antagonistic behaviour,³⁹⁰ highlighting the importance that straightforward access to complex structures such as these offers to drug discovery.

Investigation into the reactivity of the enaminy sulfone with carbon-based electrophiles such as alkyl halides was explored. Alkylation of **4.1.12** with iodomethane was not achieved (Scheme 116), with only unreacted starting material observed in the reaction mixture, and no intermediate iminium ion **4.4.26**, even on addition of silver oxide as a Lewis acid additive.^{391–393}



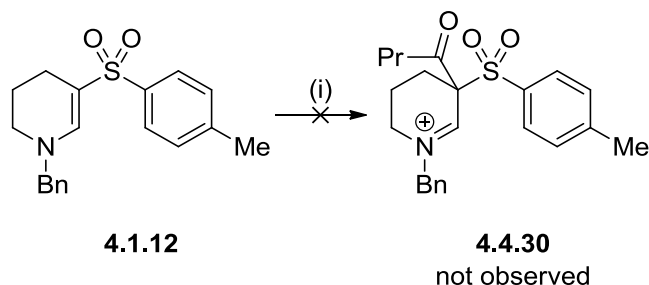
Scheme 116. Unsuccessful alkylation of the enaminy sulfone 4.1.12. Conditions: (i) MeI (13.0 eq.), Ag₂O (40 mol%), THF, RT, 36 h.

It was concluded that the electrophile used was not sufficiently electrophilic, and therefore trifluoromethylation may provide greater success. However, no reactivity was observed with either Umemoto's reagent **4.4.27**³⁹⁴ or Togni's reagent **4.4.28**³⁹⁵ (Scheme 117), with only unreacted starting material observed in the reaction mixture.



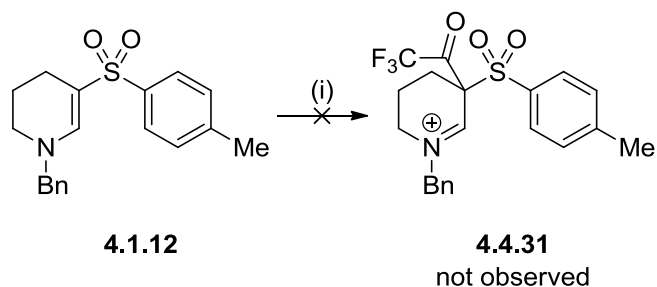
Scheme 117. Electrophilic trifluoromethylation of 4.1.12 was not successful. Conditions: (i) **4.4.27** (1.5 eq.), THF, RT to 70 °C, 40 h; (ii) **4.4.28** (2.0 eq.), 4-methylmorpholine (2.0 eq.), THF, RT to 60 °C, 36 h.

Friedel-Crafts-type acylation also proved to be unsuccessful, with no reaction observed to occur between **4.1.12** and butyryl chloride (Scheme 118).



Scheme 118. Acylation with butyryl chloride could not be achieved. Conditions: (i) butyryl chloride (26.0 eq.), AlCl₃ (1.1 eq.), THF, RT to 80 °C, 70 h.

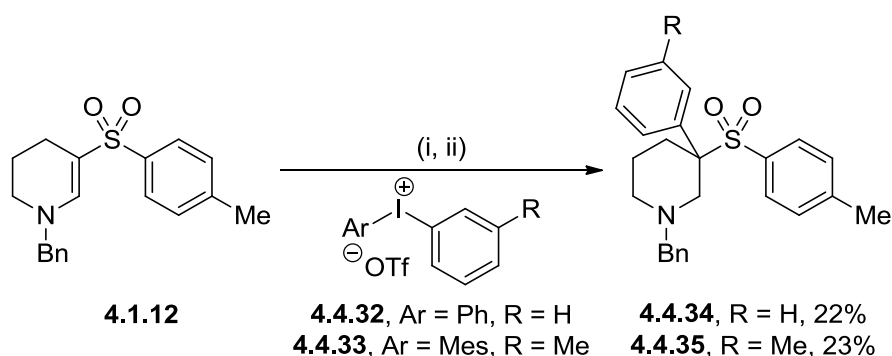
Again, despite the presence of the Lewis acid aluminium trichloride, no reactivity of the starting material was observed, so acylation of **4.1.12** with trifluoroacetic anhydride was attempted (Scheme 119).



Scheme 119. Acylation with the more electron-poor anhydride was also not observed to occur. Conditions: (i) $(\text{CF}_3\text{CO})_2\text{O}$ (1.5 eq.), DMAP (0.2 eq.), Et_3N (2.0 eq.), DCM, RT, 16 h.

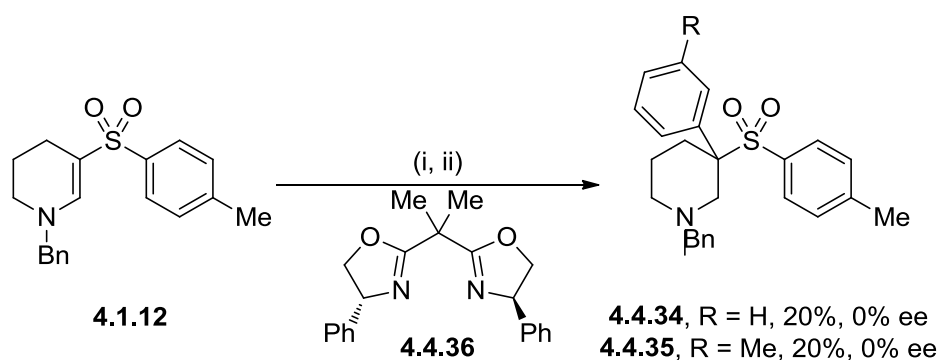
It was known that the electron-deficient anhydride reacted with an enamine moiety generated *in situ* in an oxidative acylation process, and it was anticipated that the electron-withdrawing trifluoromethyl groups would have activated the carbonyl group towards reaction with **4.1.12**, but no reaction was observed to take place.

With alkylation and acylation having proved unsuccessful to this point, focus was switched to the introduction of an aryl group at the β -position of the enaminyll sulfone. Diaryl iodonium salts have been used as sources of electrophilic aryl groups for the α -arylation of silyl enol ethers,^{396,397} and it was therefore proposed that electrophilic arylation of the enamine in **4.1.12** was feasible. Accordingly, the use of diaryliodonium salts **4.4.32** and **4.4.33** (Scheme 120) led to the formation of β -arylation products **4.4.34** and **4.4.35**, respectively, in the presence of a copper catalyst.



Scheme 120. Copper-catalysed β -arylation of 4.1.12 using arylidonium salts. Conditions: (i) **4.4.32** or **4.4.33** (2.5 eq.), $\text{Cu}(\text{OTf})_2$ (10 mol%), DCM, RT, 5 d; (ii) NaBH_4 (2.0 eq.), MeOH, RT, 1 h.

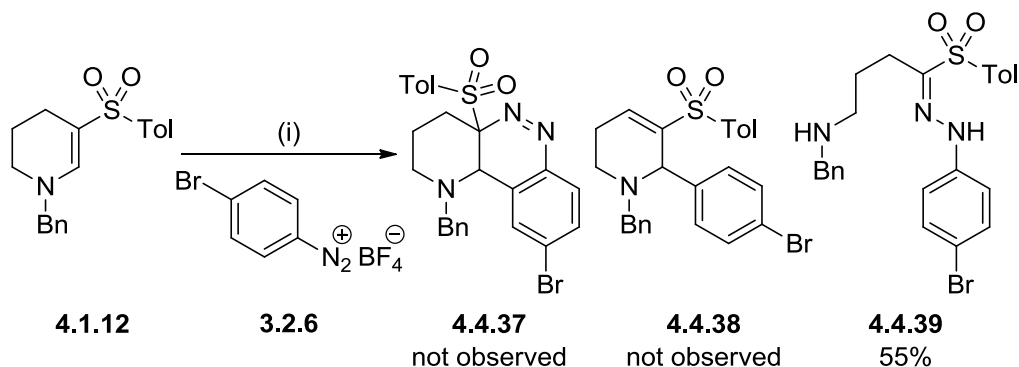
Low conversion of starting material led to yields for **4.4.34** and **4.4.35** of 22% and 23%, respectively, which is attributed to an energetically unfavourable steric clash between the large sulfonyl group and the approaching arylidonium salt. Regardless, these results demonstrate installation of a sterically crowded quaternary centre, which would be challenging to make by other means. Gaunt *et al.* have used these reaction conditions in the presence of a bisoxazoline (BOX) ligand to carry out enantioselective α -arylation of silyl enol ethers.³⁹⁷ Accordingly it was proposed that the β -arylation of enaminyll sulfone **4.1.12** could be carried out in an enantioselective manner through the use of chiral BOX ligand **4.4.36** (Scheme 121).



Scheme 121. β -Arylation of **4.1.12** in the presence of chiral BOX ligand **4.4.36**. Conditions: (i) **4.4.32** or **4.4.33** (4.0 eq.), Cu(OTf)₂ (10 mol%), **4.4.36** (11 mol%), DCM, RT to 50 °C, 40 h; (ii) NaBH₄ (2.0 eq.), MeOH, RT, 1 h. Enantioselectivity could not be achieved.

Only racemic product was isolated from the reaction, with no enantioselectivity recorded by chiral HPLC analysis.²⁸⁵ However, in contrast to the work by Gaunt *et al.*, where all the demonstrated examples are monosubstituted at the reactive centre, **4.1.12** is disubstituted at the β position. This could therefore lead to the ligand **4.4.36** detaching from the catalyst centre in order to accommodate coordination of the sterically bulky enaminyl sulfone. Further work is required to facilitate enantioselectivity for this transformation, perhaps through the use of a more tightly binding ligand, or by using a larger catalyst that can accommodate the steric bulk within its coordination sphere.

Finally, reactivity with nitrogen-based electrophiles was investigated. It was proposed that nucleophilic attack onto an aryldiazonium species could lead to formation of cinnoline-type structures, which have been shown to exhibit cytotoxic and antiplatelet activities, which could be useful for oncological and or cardiovascular applications.^{398–401} Alternatively, diazonium salts were proposed as potential coupling partners for a palladium-catalysed Heck-Matsuda reaction.^{402,403} However, under acidic conditions, reactions both with and without palladium catalyst led to formation of the same product. Instead of the anticipated cyclisation cinnoline-type species **4.4.37** or the Heck-coupling product **4.4.38**, hydrazone **4.4.39** was in fact observed to form in 52% yield when **4.1.12** was treated with *para*-bromobenzenediazonium tetrafluoroborate in the presence of TFA (Scheme 122).

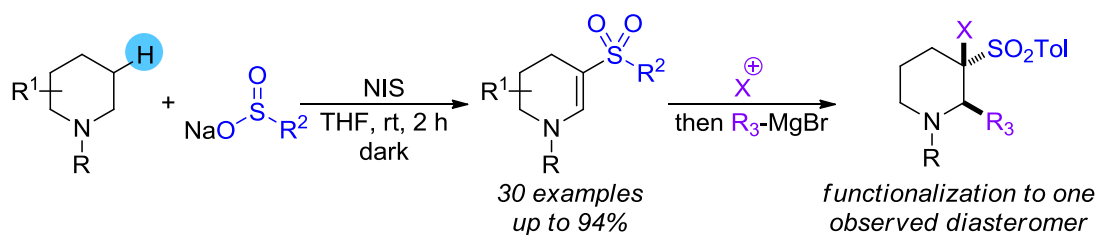


Scheme 122. Japp-Klingemann ring-opening was observed to occur following nucleophilic attack of an aryldiazonium salt by enaminyl sulfone **4.1.12.** Conditions: (i) **3.2.6** (1.1 eq.), TFA (1.0 eq.), MeOH, RT, 8 h. Tol = *para*-tolyl.

This unexpected product could have formed *via* a Japp-Klingemann ring-opening following nucleophilic attack of **4.1.12** onto the diazonium salt.^{404–407} The formation of the hydrazone unit was an interesting result because hydrazones are useful synthetic handles for iodination,⁴⁰⁸ the Shapiro reaction,⁴⁰⁹ and Wolff-Kishner reduction.⁴¹⁰ Additionally, hydrazones have also been utilised for drug delivery: conjugation to antibodies *via* the hydrazone deploys the pharmaceutical selectively to the target site, where the acid-labile hydrazone group releases the drug within the lysosome.^{411–414}

4.5 Summary

In summary, an operationally simple process for the oxidative β -C–H functionalisation of tertiary amines has been described on both cyclic and acyclic examples (Scheme 123). The reactions combined saturated amines and bench stable sulfinate salts under the action of NIS, providing access to high-value enaminyll sulfone products. The process was carried out under mild conditions, without the need for strong peroxide-based oxidants, which led to good functional group tolerance and chemoselectivity. The late-stage oxidative sulfonylation of a marketed drug has also been exemplified, demonstrating application to late-stage diversification platforms. The installed enaminyll sulfone scaffold was harnessed as a nucleophilic handle for the installation of a variety of functional groups. It is envisaged that this approach can be used to expedite the generation of diverse compound libraries for use in drug discovery.



Scheme 123. Summary of NIS-mediated oxidative C–H sulfonylation of azacycles to form enaminyll sulfones, which were subsequently used as a synthetic handle for further diversification.

4.6 Experimental

General Experimental

Solvents and Reagents

Unless otherwise stated:

- Reactions were carried out under an atmosphere of nitrogen at room temperature, and glassware was not dried beforehand. Solvents used were anhydrous.
- Solvents and reagents were purchased from commercial suppliers or obtained from GSK's internal compound storage and used as received without further purification.
- Reactions were monitored by Liquid Chromatography-Mass Spectrometry (LCMS) and Nuclear Magnetic Resonance (NMR).

Where materials were synthesized in-house, full procedures or literature references to procedures have been provided.

Chromatography

Thin layer chromatography (TLC) was carried out using plastic-backed 50 precoated silica plates (particle size 0.2 mm). Spots were visualized by ultraviolet (UV) light ($\lambda_{\text{max}} = 254 \text{ nm}$ or 365 nm) and then stained with potassium permanganate solution followed by gentle heating. Normal phase silica gel chromatography was carried out using the Teledyne ISCO CombiFlash[®] Rf+ apparatus with RediSep[®] silica cartridges. Reverse phase chromatography was carried out using Teledyne ISCO CombiFlash[®] Rf+ apparatus with Biotage[®] SNAP KP-C18-HS cartridges. Where modifiers are used as additives in the eluent, the stated percentage value signifies percentage by volume.

Hydrophobic frit cartridges by ISOLUTE[®] contain a frit which is selectively permeable to organic solutions. These are separated from aqueous phase under gravity. Various cartridge sizes were used.

Melting points (M.pt.) were recorded on a Stuart SMP10 melting point apparatus.

Liquid Chromatography Mass Spectrometry (LCMS)

LCMS analysis was carried out on an H₂O_s Acquity UPLC instrument equipped with a BEH column (50 mm x 2.1 mm, 1.7 μm packing diameter) and H₂O_s micromass ZQ MS using alternate-scan positive and negative electrospray. Analytes were detected as a summed UV wavelength of 210 – 350 nm. Two liquid phase methods were used: was a high pH method:

Method A (High pH): 40 °C, 1 mL/min flow rate. Gradient elution with the as the eluents as (A) 10 mM aqueous ammonium bicarbonate solution, adjusted to pH 10 with 0.88 M aqueous ammonia and (B) MeCN. Gradient conditions were initially 1% B, increasing linearly to 97% B over 1.5 min, remaining at 97% B for 0.4 min then increasing to 100% B over 0.1 min.

Method B (Low pH): 40 °C, 1 mL/min flow rate. Gradient elution with the as the eluents as (A) H₂O containing 0.1% (v/v) formic acid and (B) MeCN containing 0.1% (v/v) formic acid. Gradient conditions were initially 1% B, increasing linearly to 97% B over 1.5 min, remaining at 97% B for 0.4 min then increasing to 100% B over 0.1 min.

Nuclear Magnetic Resonance (NMR) Spectroscopy

Proton (¹H), carbon (¹³C) and fluorine (¹⁹F) spectra were recorded in deuterated solvents at ambient temperature using standard pulse methods on any of the following spectrometers and signal frequencies: Bruker AV-400 (¹H = 400 MHz, ¹³C = 101 MHz) and Bruker AV-600 (¹H = 600 MHz, ¹³C = 151 MHz). Chemical shifts (δ) are reported in ppm and were referenced to the following solvent peaks: CDCl₃ (¹H = 7.27 ppm, ¹³C = 77.0 ppm), DMSO-*d*₆ (¹H = 2.50 ppm, ¹³C = 39.5 ppm) and CD₂Cl₂ (¹H = 5.32 ppm, ¹³C = 53.8 ppm). Peak assignments were made on the basis of chemical shifts, integrations, and coupling constants using COSY, DEPT, HSQC, HMBC, NOESY and ROESY where appropriate. Coupling constants (*J*) are quoted to the

nearest 0.1 Hz, and multiplicities are described as singlet (s), doublet (d), triplet (t), quartet (q), quintet (quin), sextet (sxt), br. (broad) and multiplet (m), and combinations therein.

Infrared (IR) Spectroscopy

IR spectra were recorded using a Perkin Elmer Spectrum 1 machine. Absorption maxima (ν_{\max}) are reported in wavenumbers (cm^{-1}).

High Resolution Mass Spectrometry (HRMS)²⁷³

High-resolution mass spectra were recorded on one of two systems:

System A: Micromass Q-ToF Ultima hybrid quadrupole time-of-flight mass spectrometer, with analytes separated on an Agilent 1100 Liquid Chromatograph equipped with a Phenomenex Luna C18 (2) reversed phase column (100 mm x 2.1 mm, 3 μm packing diameter). LC conditions were 0.5 mL/min flow rate, 35 °C, injection volume 2–5 μL , using a gradient elution with (A) H₂O containing 0.1% (v/v) formic acid and (B) MeCN containing 0.1% (v/v) formic acid. Gradient conditions were initially 5% B, increasing linearly to 100% B over 6 min, remaining at 100% B for 2.5 min then decreasing linearly to 5% B over 1 min followed by an equilibration period of 2.5 min prior to the next injection.

System B: Waters XEVO G2-XS quadrupole time-of-flight mass spectrometer, with analytes separated on an Acquity UPLC CSH C18 column (100mm x 2.1mm, 1.7 μm packing diameter). LC conditions were 0.8 mL/min flow rate, 50 °C, injection volume 0.2 μL , using a gradient elution with (A) H₂O containing 0.1% (v/v) formic acid and (B) MeCN containing 0.1% (v/v) formic acid. Gradient conditions were initially 3% B, increasing linearly to 100% B over 8.5 min, remaining at 100% B for 0.5 min then decreasing linearly to 3% B over 0.5 min followed by an equilibration period of 0.5 min prior to the next injection.

Mass to charge ratios (m/z) are reported in Daltons.

Mass-Directed Automated Preparative HPLC (MDAP)

MDAP purification was carried out using a Waters ZQ MS, using alternate-scan positive and negative electrospray and a summed UV wavelength of 210–350 nm. Two liquid phase methods were used:

Formic – Xselect C18 column (150 mm x 30 mm, 5 µm packing diameter, 40 mL/min flow rate). Gradient elution occurred at ambient temperature with the eluents as (A) H₂O containing 0.1% volume/volume (v/v) formic acid and (B) MeCN containing 0.1% (v/v) formic acid.

High pH – Xselect C18 column (150 mm x 30 mm, 5 µm packing diameter, 40 mL/min flow rate). Gradient elution occurred at ambient temperature with the eluents as (A) 10 mM aqueous ammonium bicarbonate solution, adjusted to pH 10 with aqueous ammonia and (B) MeCN.

The elution gradients used were at a flow rate of 40 mL/min over 20 or 30 min depending on separation:

Method	Gradient B (%)
A	5-30
B	15-55
C	30-85
D	50-99
E	80-99

Synthetic Procedures

General Procedure for the Oxidative C–H Sulfonylation of Amines A.

A solution of amine substrate (1.0 eq.) in inhibitor-free THF (0.1 M), degassed with nitrogen, was added to *N*-iodosuccinimide (NIS) (4.0 eq.) shielded from light, and the resultant reaction mixture was stirred at RT under an atmosphere of nitrogen for 30 min. This reaction mixture was then transferred *via* syringe to a suspension of sodium sulfinate salt (1.5 eq.) in inhibitor-free THF (0.3 M), which had been degassed with nitrogen and shielded from light, and inhibitor-free THF was used to rinse the NIS/amine reaction vessel to ensure complete transfer to give a resulting reaction concentration of 0.06 M. The reaction was stirred at RT for 2 h. Upon completion of the reaction, the reaction mixture was quenched with saturated aqueous sodium thiosulfate (10 mL) and saturated aqueous sodium bicarbonate (10 mL). The solution was extracted into ethyl acetate (2 x 20 mL), and the combined organic layer was washed with saturated aqueous sodium bicarbonate (10 mL), passed through a hydrophobic frit and concentrated under reduced pressure. Where stated, conversion to product was quantified *via* ¹H NMR analysis of the crude material together with a known amount of internal standard 3,4,5-trichloropyridine (aryl 2H singlet at 8.51 ppm in CDCl₃) or dibromomethane (2H singlet at 4.92 ppm in CDCl₃). The crude material was then purified as described to afford the enaminyll sulfone product.

General Procedure for the Oxidative C–H Sulfonylation of Amines B

General procedure B was the same as general procedure A, with exception that 2.0 equivalents of sodium sulfinate salt were used.

General Procedure for the Oxidative C–H Sulfonylation of Amines C

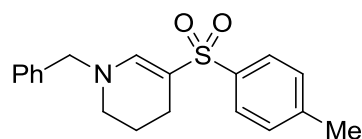
General procedure C was the same as general procedure A, with the exception that the first NIS/amine reaction solution was stirred for 60 minutes prior to addition to the sulfinate suspension.

General Procedure for the Oxidative C–H Sulfonation of Amines D.

General procedure D was the same as general procedure A, with exception that 3.0 equivalents of sodium sulfinate salt were used, and DMSO replaced THF as the reaction solvent.

1-Benzyl-5-tosyl-1,2,3,4-tetrahydropyridine 4.1.12

(Unoptimised conditions with iodine).



A mixture of **2.1.8a** (40 mg, 0.23 mmol), iodine (405 mg, 1.60 mmol) and sodium bicarbonate (192 mg, 2.28 mmol) in THF (2 mL) and H₂O (1 mL) was treated with **4.1.11** (122 mg, 0.69 mmol), and the reaction was stirred at RT for 15 h. Upon completion of the reaction, the reaction mixture was quenched with saturated aqueous sodium thiosulfate (5 mL) and saturated aqueous sodium bicarbonate (5 mL). The solution was extracted into ethyl acetate (3 x 10 mL), and the combined organic layer was passed through a hydrophobic frit and concentrated under reduced pressure. The crude material was purified by silica gel chromatography using 0-100% EtOAc/cyclohexane to afford **4.1.12** (25 mg, 34%) as an off-white solid.

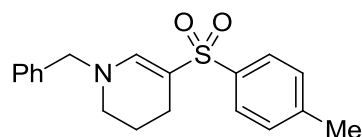
LCMS (Method B, UV, ESI) $R_t = 1.25$ min, $[M+H]^+$: 328.0

¹H NMR (400 MHz, CDCl₃) δ 7.73 (d, $J = 8.3$ Hz, 2H), 7.50 (s, 1H), 7.26-7.39 (m, 5H), 7.21 (m, 2H), 4.31 (s, 2H), 2.92-2.99 (m, $J = 5.6$ Hz, 2H), 2.42 (s, 3H), 2.17 (t, $J = 6.2$ Hz, 2H), 1.77 (quin, $J = 5.9$ Hz, 2H)

For full characterisation see Appendix 3.

1-Benzyl-5-tosyl-1,2,3,4-tetrahydropyridine 4.1.12

(Unoptimised conditions with NIS).



A solution of **2.1.8a** (35 mg, 0.20 mmol) in THF (2 mL) was treated with NIS (135 mg, 0.60 mmol), and the reaction mixture stirred for 30 min. The reaction was then charged with **4.1.11** (107 mg, 0.60 mmol), sodium bicarbonate (84 mg, 1.0 mmol) and

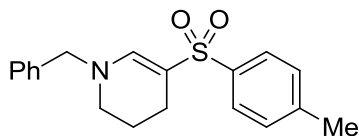
H₂O (1.0 mL), and the reaction was stirred at RT for 3 h. Upon completion of the reaction, the reaction mixture was quenched with saturated aqueous sodium thiosulfate (5 mL) and saturated aqueous sodium bicarbonate (5 mL). The solution was extracted into DCM (2 x 10 mL), and the combined organic layer was passed through a hydrophobic frit and concentrated under reduced pressure. The crude material was purified by silica gel chromatography using 0-30% 3:1 EtOAc:EtOH (1% Et₃N modifier)/cyclohexane to afford **4.1.12** (28 mg, 43%) as an off-white solid.

LCMS (Method A, UV, ESI) R_t = 1.25 min, [M+H]⁺: 328.2

¹H NMR (400 MHz, CDCl₃) δ 7.72 (d, *J* = 8.3 Hz, 2H), 7.48 (s, 1H), 7.24-7.37 (m, 5H), 7.17-7.22 (m, 2H), 4.29 (s, 2H), 2.94 (t, *J* = 5.4 Hz, 2H), 2.40 (s, 3H), 2.15 (t, *J* = 6.1 Hz, 2H), 1.75 (quin, *J* = 5.9 Hz, 2H)

For full characterisation see Appendix 3.

1-Benzyl-5-tosyl-1,2,3,4-tetrahydropyridine **4.1.12** (5.4 mmol scale)



General procedure for the oxidative C–H sulfonylation of amines **A** was followed. A solution of **2.1.8a** (0.95 g, 5.4 mmol) in THF (48 mL, 0.1 M) was added to NIS (4.88 g, 21.7 mmol) under an atmosphere of nitrogen and shielded from light. The reaction mixture was stirred at RT for 30 min, then transferred *via* syringe to a suspension of **4.1.11** (1.45 g, 8.1 mmol) in inhibitor-free THF (28 mL, 0.3 M), which had been degassed with nitrogen and shielded from light, and inhibitor-free THF (2 x 5 mL) was used to rinse the NIS/amine reaction vessel to ensure complete transfer to give a resulting reaction concentration of 0.06 M. The reaction was stirred at RT for 2 h. Upon completion of the reaction, the reaction mixture was quenched with saturated aqueous sodium thiosulfate (30 mL) and saturated aqueous sodium bicarbonate (20 mL). The solution was extracted in ethyl acetate (3 x 100 mL), and the combined organic layer was passed through a hydrophobic frit and concentrated under reduced

pressure. The crude material was purified by silica gel chromatography using 0-50% EtOAc/cyclohexane as the eluent to afford **4.1.12** (1.33 g, 75%) as an off-white solid.

LCMS (Method A, UV, ESI) $R_t = 1.22$ min, $[M+H]^+$: 328.1

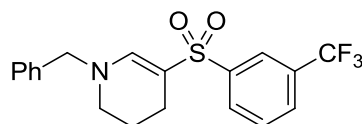
^1H NMR (400 MHz, CDCl_3) δ 7.74 (d, $J = 8.3$ Hz, 2H), 7.51 (s, 1H), 7.25-7.40 (m, 5H), 7.18-7.23 (m, 2H), 4.30 (s, 2H), 2.92-3.01 (t, $J = 5.6$ Hz, 2H), 2.41 (s, 3H), 2.17 (t, $J = 6.2$ Hz, 2H), 1.76 (quin, $J = 6.0$ Hz, 2H)

^{13}C NMR (101 MHz, CDCl_3) δ 144.2, 142.3, 139.8, 136.5, 129.4, 128.8, 127.9, 127.5, 126.9, 101.1, 59.7, 45.0, 21.5, 21.0, 19.7

For full characterisation see Appendix 3.

1-Benzyl-5-((3-(trifluoromethyl)phenyl)sulfonyl)-1,2,3,4-tetrahydropyridine

4.2.7 (3.75 mmol scale)



General procedure for the oxidative C–H sulfonylation of amines A was followed. A solution of **2.1.8a** (0.66 g, 3.75 mmol) in THF (0.1 M) was added to NIS (3.38 g, 15.0 mmol), which was stirred at RT for 30 min, then transferred *via* syringe to a suspension of sodium 3-(trifluoromethyl)benzenesulfinate (1.31 g, 5.63 mmol) in THF (0.3 M), and THF was used to rinse the NIS/amine reaction vessel to ensure complete transfer to give a resulting reaction concentration of 0.06 M. The crude material was purified by silica gel chromatography using 20-50% EtOAc/cyclohexane as the eluent to afford **4.2.7** (0.99 g, 70%) as a white solid.

LCMS (Method A, UV, ESI) $R_t = 1.29$ min, $[M+H]^+$: 382.1

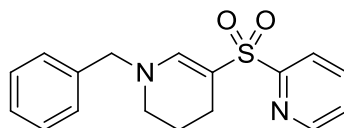
^1H NMR (400 MHz, CDCl_3) δ 8.11 (s, 1H), 8.05 (d, $J = 7.8$ Hz, 1H), 7.78 (d, $J = 8.1$ Hz, 1H), 7.60-7.67 (m, 1H), 7.56 (s, 1H), 7.30-7.42 (m, 3H), 7.21 (d, $J = 6.4$ Hz, 2H), 4.35 (s, 2H), 3.00 (t, $J = 5.7$ Hz, 2H), 2.19 (t, $J = 6.2$ Hz, 2H), 1.80 (quin, $J = 5.9$ Hz, 2H)

^{13}C NMR (101 MHz, CDCl_3) δ 145.3, 144.2, 136.1, 131.5 (q, $^2J_{\text{C-F}} = 33.0$ Hz), 130.0, 129.5, 128.9, 128.3 (q, $^3J_{\text{C-F}} = 3.7$ Hz), 128.1, 127.4, 123.8 (q, $^3J_{\text{C-F}} = \text{Hz } 3.9$ Hz), 123.4 (q, $^1J_{\text{C-F}} = 272.2$ Hz), 99.5, 59.9, 45.0, 20.9, 19.6

^{19}F NMR (CDCl_3 , 376MHz): δ -62.75 (s, 1F)

For full characterisation see Appendix 3.

2-((1-Benzyl-1,4,5,6-tetrahydropyridin-3-yl)sulfonyl)pyridine 4.2.12



General procedure for the oxidative C–H sulfonylation of amines A was followed. A solution of **2.1.8a** (100 mg, 0.57 mmol) in THF (0.1 M) was added to NIS (513 mg, 2.28 mmol), which was stirred at RT for 30 min, then transferred *via* syringe to a suspension of **4.2.15**³⁴⁶ (293 mg, 1.14 mmol) in THF (0.3 M), and THF was used to rinse the NIS/amine reaction vessel to ensure complete transfer to give a resulting reaction concentration of 0.06 M. ^1H NMR analysis of the crude material against dibromomethane (0.215 mmol) as a standard showed 22% conversion to **4.2.12**. The crude material was purified by silica gel chromatography using 0-80% 3:1 EtOAc:EtOH (with 1% Et_3N modifier)/cyclohexane as the eluent to afford **4.2.12** (43.1 mg, 24%) as an orange oil.

LCMS (Method A, UV, ESI) $R_t = 1.00$ min, $[\text{M}+\text{H}]^+$: 315.0

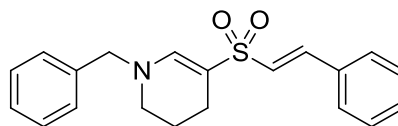
^1H NMR (400 MHz, CDCl_3) δ ppm 8.72 (ddd, $J = 4.6, 1.7, 0.7$ Hz, 1H), 8.06 (dt, $J = 7.8, 1.0$ Hz, 1H), 7.88 (td, $J = 7.7, 1.7$ Hz, 1H), 7.60 (s, 1H), 7.43 (ddd, $J = 7.6, 4.7, 1.3$ Hz, 1H), 7.29-7.39 (m, 3H), 7.21-7.25 (m, 2H), 4.34 (s, 2H), 2.97-3.01 (m, 2H), 2.31 (t, $J = 6.1$ Hz, 2H), 1.80 (dt, $J = 11.8, 6.0$ Hz, 2H)

^{13}C NMR (101 MHz, CDCl_3) δ 160.2, 150.0, 146.6, 137.6, 136.3, 128.8, 128.0, 127.7, 125.7, 121.6, 97.9, 59.9, 45.0, 21.0, 20.0

IR ν_{max} (thin film): 2931, 1616, 1315, 1110

HRMS: Calculated for $C_{17}H_{19}N_2O_2S$ $[M+H]^+$: 315.1167, found $[M+H]^+$ 315.1165 (-0.6 ppm).

(E)-1-Benzyl-5-(styrylsulfonyl)-1,2,3,4-tetrahydropyridine 4.2.14



General procedure for the oxidative C–H sulfonylation of amines A was followed. A solution of **2.1.8a** (35 mg, 0.20 mmol) in THF (0.1 M) was added to NIS (180 mg, 0.80 mmol), which was stirred at RT for 30 min, then transferred *via* syringe to a suspension of **4.2.17**⁴¹⁵ (76 wt%, 75 mg, 0.30 mmol) in THF (0.3 M), and THF was used to rinse the NIS/amine reaction vessel to ensure complete transfer to give a resulting reaction concentration of 0.06 M. ¹H NMR analysis of the crude material against 3,4,5-trichloropyridine (0.098 mmol) as a standard showed 57% conversion to **4.2.14**. The crude material was purified by silica gel chromatography using 0-30% EtOAc/cyclohexane as the eluent to afford **4.2.14** (32.0 mg, 47%) as an orange solid. LCMS (Method A, UV, ESI) $R_t = 1.23$ min, $[M+H]^+$: 340.14.

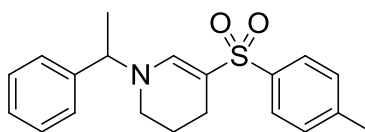
¹H NMR (400 MHz, $CDCl_3$) δ 7.47-7.52 (m, 2H), 7.29-7.46 (m, 8H), 7.22 (dd, $J = 8.1, 1.5$ Hz, 2H), 6.72 (d, $J = 15.4$ Hz, 1H), 4.32 (s, 2H), 3.02 (t, $J = 5.6$ Hz, 2H), 2.29 (t, $J = 6.2$ Hz, 2H), 1.86 (quin, $J = 5.9$ Hz, 2H)

¹³C NMR (101 MHz, $CDCl_3$) δ 144.9, 139.5, 136.4, 133.4, 130.2, 128.9, 128.9, 128.1, 128.0, 127.9, 127.5, 99.8, 59.8, 45.1, 21.1, 19.5

IR ν_{max} (thin film): 2931, 1615, 1276, 1117

HRMS: Calculated for $C_{20}H_{22}NO_2S$ $[M+H]^+$: 340.1371, found $[M+H]^+$ 340.1367 (-1.2 ppm)

M.pt.: 139-142 °C.

1-(1-Phenylethyl)-5-tosyl-1,2,3,4-tetrahydropyridine 4.6.1

General procedure for the oxidative C–H sulfonylation of amines A was followed. A solution of **2.8.1** (57 mg, 0.30 mmol) in THF (0.1 M) was added to NIS (270 mg, 1.20 mmol), which was stirred at RT for 30 min, then transferred *via* syringe to a suspension of **4.1.11** (80 mg, 0.45 mmol) in THF (0.3 M), and THF was used to rinse the NIS/amine reaction vessel to ensure complete transfer to give a resulting reaction concentration of 0.06 M. The crude material was purified by silica gel chromatography using 0-30% EtOAc/cyclohexane as the eluent to afford **4.6.1** (41.5 mg, 41%) as an orange oil.

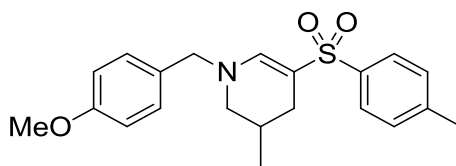
LCMS (Method A, UV, ESI) $R_t = 1.27$ min, $[M+H]^+$: 342.1

^1H NMR (400 MHz, CDCl_3) δ 7.73 (d, $J = 8.3$ Hz, 2H), 7.63 (s, 1H), 7.33-7.39 (m, 2H), 7.26-7.32 (m, 3H), 7.23 (d, $J = 7.1$ Hz, 2H), 4.45 (q, $J = 7.0$ Hz, 1H), 2.81-2.98 (m, 2H), 2.42 (s, 3H), 2.17 (t, $J = 6.2$ Hz, 2H), 1.67-1.74 (m, 2H), 1.61 (d, $J = 7.1$ Hz, 3H)

^{13}C NMR (101 MHz, CDCl_3) δ 142.2, 142.0, 140.9, 139.9, 129.4, 128.8, 127.7, 126.9, 126.4, 100.7, 62.7, 43.3, 21.5, 21.1, 20.2, 18.9

IR ν_{max} (thin film): 2932, 1611, 1277, 1131

HRMS: Calculated for $\text{C}_{20}\text{H}_{24}\text{NO}_2\text{S}$ $[M+H]^+$: 342.1528, found $[M+H]^+$ 342.1526 (-0.6 ppm).

1-(4-Methoxybenzyl)-3-methyl-5-tosyl-1,2,3,4-tetrahydropyridine 4.6.2

General procedure for the oxidative C–H sulfonylation of amines A was followed. A solution of **2.8.3** (66 mg, 0.30 mmol) in THF (0.1 M) was added to NIS (270 mg, 1.20 mmol), which was stirred at RT for 30 min, then transferred *via* syringe to a suspension of **4.1.11** (80 mg, 0.45 mmol) in THF (0.3 M), and THF was used to rinse the NIS/amine reaction vessel to ensure complete transfer to give a resulting reaction concentration of 0.06 M. The crude material was purified by silica gel chromatography using 0-30% EtOAc/cyclohexane as the eluent to afford **4.6.2** (40.6 mg, 36%) as an orange oil.

LCMS (Method A, UV, ESI) $R_t = 1.27$ min, $[M+H]^+$: 372.2

^1H NMR (400 MHz, CDCl_3) δ 7.74 (d, $J = 8.3$ Hz, 2H), 7.50 (d, $J = 1.0$ Hz, 1H), 7.28 (d, $J = 8.1$ Hz, 2H), 7.14 (d, $J = 8.8$ Hz, 2H), 6.90 (d, $J = 8.8$ Hz, 2H), 4.26 (s, 2H), 3.83 (s, 3H), 2.90 (ddd, $J = 12.2, 3.9, 2.2$ Hz, 1H), 2.55 (dd, $J = 12.5, 9.3$ Hz, 1H), 2.43 (s, 3H), 2.28 (ddd, $J = 14.9, 4.4, 2.0$ Hz, 1H), 1.81-1.91 (m, 1H), 1.74 (dd, $J = 15.7, 9.3$ Hz, 1H), 0.88 (d, $J = 6.6$ Hz, 3H)

^{13}C NMR (101 MHz, CDCl_3) δ 159.4, 143.7, 142.3, 139.8, 129.4, 128.9, 128.4, 126.9, 114.2, 100.7, 59.1, 55.3, 51.4, 27.7, 26.4, 21.5, 18.5

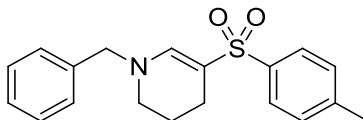
IR ν_{max} (thin film): 2924, 1617, 1512, 1132

HRMS: Calculated for $\text{C}_{21}\text{H}_{26}\text{NO}_3\text{S}$ $[M+H]^+$: 372.1633, found $[M+H]^+$ 372.1635 (0.5 ppm).

Mechanistic Investigations

General Procedure for Radical Control Additive Experiments

1-Benzyl-5-tosyl-1,2,3,4-tetrahydropyridine 4.1.12



General procedure for the oxidative C–H sulfonylation of amines A was followed. A solution of **2.1.8a** (100 mg, 0.57 mmol) in THF (0.1 M) was added to NIS (513 mg, 2.28 mmol), which was stirred at RT for 30 min, then transferred *via* syringe to a suspension of **4.1.11** (153 mg, 0.86 mmol) and radical inhibitor additive (0.63 mmol, 1.1 eq.) in THF (0.3 M), and THF was used to rinse the NIS/amine reaction vessel to ensure complete transfer to give a resulting reaction concentration of 0.06 M. The reaction mixture was stirred for 2 h at RT. The reaction was quenched and worked up as described in the general procedure for the oxidative C–H sulfonylation of amines A.

BHT as the Radical Inhibitor

The NIS/amine solution was transferred onto a suspension of **4.1.11** (153 mg, 0.86 mmol) and BHT (138 mg, 0.63 mmol). The crude material was analyzed by ¹H NMR against 3,4,5-trichloropyridine (0.125 mmol), which showed 77% conversion to **4.1.12**.

Catechol as the Radical Inhibitor

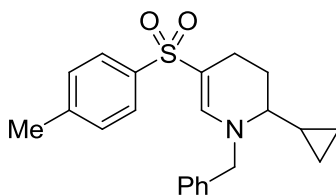
The NIS/amine solution was transferred onto a suspension of **4.1.11** (153 mg, 0.86 mmol) and catechol (69 mg, 0.63 mmol). The crude material was analyzed by ¹H NMR against 3,4,5-trichloropyridine (0.118 mmol), which showed 29% conversion to **4.1.12**.

TEMPO as the Radical Inhibitor

The NIS/amine solution was transferred onto a suspension of **4.1.11** (153 mg, 0.86 mmol) and TEMPO (98 mg, 0.63 mmol). The crude material was analyzed by ¹H NMR against 3,4,5-trichloropyridine (0.127 mmol), which showed 0% conversion to **4.1.12**.

1-Benzyl-2-cyclopropyl-5-tosyl-1,2,3,4-tetrahydropyridine 4.3.1 and 1-benzyl-6-cyclopropyl-5-tosyl-1,2,3,4-tetrahydropyridine 4.3.2

General procedure for the oxidative C–H sulfonylation of amines A was followed. A solution of **2.3.3** (43 mg, 0.20 mmol) in THF (0.1 M) was added to NIS (180 mg, 0.80 mmol), which was stirred at RT for 30 min, then transferred *via* syringe to a suspension of **4.1.11** (54 mg, 0.3 mmol) in THF (0.3 M), and THF was used to rinse the NIS/amine reaction vessel to ensure complete transfer to give a resulting reaction concentration of 0.06 M. ¹H NMR analysis of the crude material against 3,4,5-trichloropyridine as a standard (0.055 mmol) showed 27% conversion to **4.3.1** and 20% conversion to **4.3.2**. The crude material was purified by silica gel chromatography using 0-30% EtOAc/cyclohexane as the eluent, to afford **4.3.1** (18.1 mg, 25%) as a brown oil, and **4.3.2** (11.7 mg, 16%) as an orange oil.

1-Benzyl-2-cyclopropyl-5-tosyl-1,2,3,4-tetrahydropyridine 4.3.1

LCMS (Method A, UV, ESI) $R_t = 1.35$ min, $[M+H]^+$ 368.1

¹H NMR (400 MHz, CDCl₃): δ 7.74 (d, $J = 8.3$ Hz, 2H), 7.49 (s, 1H), 7.26-7.37 (m, 5H), 7.18 (d, $J = 6.8$ Hz, 2H), 4.59 (d, $J = 15.2$ Hz, 1H), 4.44 (d, $J = 15.9$ Hz, 1H), 2.42 (s, 3H), 2.18-2.35 (m, 3H), 1.84-1.92 (m, 1H), 1.52-1.64 (m, 1H), 0.73-0.84 (m,

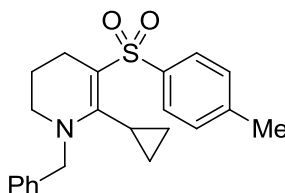
1H), 0.55-0.64 (m, 1H), 0.39 (tt, $J = 8.7, 5.2$ Hz, 1H), 0.25 (dq, $J = 9.9, 4.9$ Hz, 1H), -0.07 (dq, $J = 9.8, 5.0$ Hz, 1H)

^{13}C NMR (151 MHz, CDCl_3): δ 143.8, 142.2, 139.9, 137.1, 129.4, 128.8, 127.7, 127.2, 126.8, 100.9, 58.1, 57.7, 26.2, 21.4, 17.2, 13.4, 5.7, 0.3

IR ν_{max} (cm^{-1}) (thin film): 2923, 1614, 1132

HRMS: Calculated for $\text{C}_{22}\text{H}_{26}\text{NO}_2\text{S}$ $[\text{M}+\text{H}]^+$: 368.1684, found $[\text{M}+\text{H}]^+$ 368.1680 (-1.1 ppm).

1-Benzyl-6-cyclopropyl-5-tosyl-1,2,3,4-tetrahydropyridine 4.3.2



LCMS (Method A, UV, ESI) $R_t = 1.33$ min, $[\text{M}+\text{H}]^+$ 368.1

^1H NMR (400 MHz, CDCl_3): δ 7.78 (d, $J = 8.3$ Hz, 2H), 7.28-7.38 (m, 5H), 7.16 (d, $J = 7.1$ Hz, 2H), 4.61 (s, 2H), 2.95 (t, $J = 5.4$ Hz, 2H), 2.46 (t, $J = 6.2$ Hz, 2H), 2.42 (s, 3H), 1.69-1.79 (m, 3H), 0.89-0.95 (m, 2H), 0.63-0.72 (m, 2H)

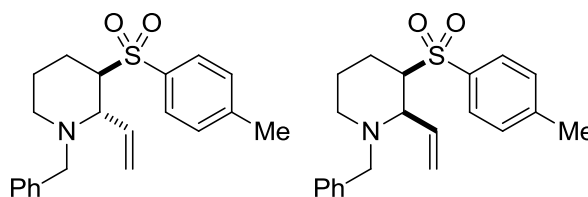
^{13}C NMR (151 MHz, CDCl_3): δ 156.8, 142.3, 141.6, 138.0, 129.2, 128.7, 127.2, 126.8, 126.7, 108.9, 55.0, 48.1, 26.0, 21.5, 21.2, 12.6, 10.0

IR ν_{max} (cm^{-1}) (thin film): 2927, 1733, 1620, 1135

HRMS: Calculated for $\text{C}_{22}\text{H}_{26}\text{NO}_2\text{S}$ $[\text{M}+\text{H}]^+$: 368.1684, found $[\text{M}+\text{H}]^+$ 368.1672 (-3.3 ppm).

Diversification of enaminyll sulfone scaffolds

1-Benzyl-3-tosyl-2-vinylpiperidine (1.4:1 diastereomeric mixture) 4.4.3



A solution of triflic acid (22 μ L, 0.25 mmol) in DCE (0.5 mL) was added to a solution of **4.1.12** (33 mg, 0.10 mmol) in DCE (0.5 mL) stirring at -10 $^{\circ}$ C. This reaction mixture was stirred for 30 min, before dropwise addition of vinylmagnesium bromide (1.0 M in THF, 0.4 mL, 0.40 mmol). The reaction mixture was then gradually warmed to 20 $^{\circ}$ C over 2 h. The reaction was cooled to 10 $^{\circ}$ C, and triflic acid (22 μ L, 0.25 mmol) was added dropwise, followed by vinylmagnesium bromide (1.0 M in THF, 0.4 mL, 0.40 mmol), and the reaction mixture was stirred at 10 $^{\circ}$ C for 16 h. Water (2 mL) and saturated aqueous sodium bicarbonate (2 mL) were added to quench the reaction, and the mixture was extracted into DCM (2 x 5 mL). The combined organic layer was washed with water (10 mL), passed through a hydrophobic frit and concentrated under reduced pressure. The crude material was purified by high pH MDAP (Method D) to afford **4.4.3** (6.3 mg, 18%) as an amber coloured residue in a 1.4:1 diastereomeric ratio, though the identity of the major diastereomer could not be determined at this stage.

LCMS (Method A, UV, ESI) $R_t = 1.37$ min, $[M+H]^+$ 356.1

^1H NMR (400 MHz, CDCl_3): δ 7.73 (d, $J = 8.1$ Hz, 3H)^{†,‡}, 7.27-7.34 (m, 8H)^{†,‡}, 7.21-7.26 (m, 4H)^{†,‡}, 6.11 (dt, $J = 16.9, 10.1$ Hz, 1H)[‡], 5.86 (dt, $J = 17.9, 8.6$ Hz, 1H)[†], 5.49 (dd, $J = 10.3, 2.2$ Hz, 1H)[‡], 5.24-5.30 (m, 2H)[†], 5.21 (dd, $J = 17.0, 2.1$ Hz, 1H)[‡], 3.95 (d, $J = 13.7$ Hz, 1H)[†], 3.65 (dd, $J = 9.9, 4.0$ Hz, 1H)[‡], 3.58 (d, $J = 13.9$ Hz, 1H)[‡], 3.36-3.49 (m, 2H)^{†,‡}, 3.12-3.21 (m, 2H)[‡], 2.71 (qd, $J = 6.2, 4.2$ Hz, 1H)[‡], 2.45 (s, 5H)^{†,‡}, 2.16 (ddd, $J = 11.7, 8.6, 3.4$ Hz, 1H)[‡], 1.90-2.02 (m, 2H)^{†,‡}, 1.74-1.89 (m, 3H)^{†,‡}, 1.41-1.50 (m, 1H)[‡]

[†]Major diastereomer; [‡]Minor diastereomer

Characteristic chemical shifts (δ) consistent with minor diastereomer indicated formation of product: 6.11 (vinyl), 5.49 (vinyl), 5.21 (vinyl), 3.65 (allylic), 3.58 (benzylic), 2.45 (tolyl methyl)

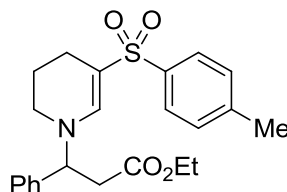
^{13}C NMR (101 MHz, CDCl_3): δ 144.4, 144.2, 139.2, 136.5, 135.6, 135.3, 135.3, 129.5, 128.9, 128.9, 128.7, 128.6, 128.4, 128.2, 128.1, 126.9, 126.8, 121.8, 120.3, 65.9, 65.7, 63.5, 60.1, 58.9, 58.5, 49.0, 45.2, 24.9, 23.3, 22.9, 21.6, 20.0

IR ν_{max} (cm^{-1}) (thin film): 2924, 1597, 1313

HRMS: Calculated for $\text{C}_{21}\text{H}_{26}\text{NO}_2\text{S}$ $[\text{M}+\text{H}]^+$: 356.1684, found $[\text{M}+\text{H}]^+$ 356.1682 (-0.6 ppm).

10 minute LCMS method of HRMS showed separation of isomeric species of identical mass, in a ratio of 57:43, providing further evidence of a mixture of diastereomers.

Ethyl 3-phenyl-3-(5-tosyl-3,4-dihydropyridin-1(2H)-yl)propanoate 4.4.11



A solution of ethyl 2-diazoacetate (15wt% DCM) (12 μL , 0.10 mmol) in DCE (3 mL) was added dropwise to a solution of **4.1.12** (33 mg, 0.10 mmol) and rhodium(II) acetate dimer (0.4 mg, 1 μmol) in DCE (3 mL), and the reaction mixture was stirred at RT for 4 h. After this time a solution of ethyl 2-diazoacetate (15wt% DCM) (49 μL , 0.40 mmol) in DCE (0.5 mL) was added dropwise to the reaction mixture. The temperature of the reaction was raised to 60 $^{\circ}\text{C}$, and the reaction mixture stirred for 60 h. The reaction was quenched with saturated aqueous sodium bicarbonate (5 mL) and extracted into DCM (2 x 10 mL). The combined organic layer was passed through a hydrophobic frit and concentrated under reduced pressure. The crude material was purified by high pH MDAP (Method D), affording **4.4.11** (6.6 mg, 16%) as an amber coloured oil.

LCMS (Method A, UV, ESI) R_t = 1.29 min, $[\text{M}+\text{H}]^+$ 414.1

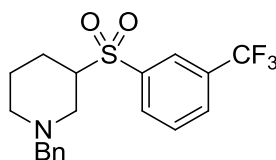
^1H NMR (400 MHz, CD_2Cl_2): δ 7.51 (d, $J = 8.1$ Hz, 2H), 7.23-7.34 (m, 5H), 7.18-7.22 (m, $J = 2.0$ Hz, 2H), 7.16 (s, 1H), 4.20 (qd, $J = 7.1, 1.6$ Hz, 2H), 4.09 (dd, $J = 10.4, 5.5$ Hz, 1H), 3.29 (dd, $J = 14.3, 5.5$ Hz, 1H), 2.94-3.13 (m, 3H), 2.41 (s, 3H), 2.04-2.13 (m, 1H), 1.90-2.00 (m, 1H), 1.63-1.70 (m, 2H), 1.26 (t, $J = 7.1$ Hz, 3H)

^{13}C NMR (151 MHz, CD_2Cl_2): δ 170.8, 144.0, 143.1, 140.3, 137.5, 129.9, 129.6, 129.2, 127.5, 127.3, 103.1, 68.7, 62.2, 44.8, 36.3, 21.7, 21.4, 20.5, 14.6

IR ν_{max} (cm^{-1}) (thin film): 2934, 1733, 1620, 1135

HRMS: Calculated for $\text{C}_{23}\text{H}_{28}\text{NO}_4\text{S}$ $[\text{M}+\text{H}]^+$: 414.1739, found $[\text{M}+\text{H}]^+$ 414.1733 (-1.4 ppm).

1-Benzyl-3-((3-(trifluoromethyl)phenyl)sulfonyl)piperidine 4.4.12



A solution of **4.2.7** (191mg, 0.50 mmol) in trifluoroacetic acid (2.5 ml) was stirred at 60 °C for 10 min. A solution of triethylsilane (160 μl , 1.00 mmol) in trifluoroacetic acid (2.5 mL) was then added dropwise to the solution of **4.2.7**, and the reaction stirred at 60 °C for 60 h. The reaction was cooled to RT, and the solvents were evaporated under reduced pressure, and the crude residue was made alkaline with aqueous sodium hydroxide (2M, 5 mL), then diluted with water (5 mL) and extracted into DCM (2 x 10 mL). The combined organic layer was passed through a hydrophobic frit and concentrated under reduced pressure. The crude material was purified by silica gel chromatography with 0-60% EtOAc/cyclohexane as the eluent, to afford **4.4.12** (174 mg, 91%) as a white solid.

LCMS (Method B, UV, ESI) $R_t = 0.74$ min, $[\text{M}+\text{H}]^+$ 384.1

^1H NMR (400 MHz, CDCl_3): δ 8.14 (s, 1H), 8.06 (d, $J = 7.8$ Hz, 1H), 7.93 (d, $J = 7.8$ Hz, 1H), 7.72 (t, $J = 7.8$ Hz, 1H), 7.19-7.34 (m, 5H), 3.54 (dd, $J = 17.9, 13.2$ Hz, 2H), 3.25 (ddt, $J = 15.1, 7.6, 3.7$ Hz, 1H), 3.12-3.19 (m, 1H), 2.83 (br. d, $J = 11.7$ Hz, 1H),

2.19 (t, $J = 10.9$, 1H), 2.03-2.10 (m, 1H), 1.93 (td, $J = 11.6$, 2.8 Hz, 1H), 1.77-1.84 (m, 1H), 1.46-1.63 (m, 2H)

^{13}C NMR (101 MHz, CDCl_3): δ 138.9, 137.3, 132.1, 132.0 (q $^2J_{\text{C-F}} = 33.7$), 130.4 (q $^3J_{\text{C-F}} = 3.7$ Hz), 129.9, 128.9, 128.3, 127.3, 125.9 (q, $^3J_{\text{C-F}} = 3.7$ Hz), 123.0 (q, $^1J_{\text{C-F}} = 272.2$ Hz), 63.0, 61.7, 52.6, 51.9, 24.2, 23.9

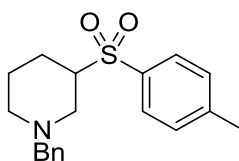
^{19}F NMR (376 MHz, CDCl_3): δ -62.82 (s, 3F)

IR ν_{max} (cm^{-1}) (thin film): 2954, 1610, 1328, 1141

HRMS: Calculated for $\text{C}_{19}\text{H}_{21}\text{NO}_2\text{SF}_3$ $[\text{M}+\text{H}]^+$: 384.1245, found $[\text{M}+\text{H}]^+$ 384.1246 (0.3 ppm)

M.pt.: 95-98 °C.

1-Benzyl-3-tosylpiperidine 4.4.13



A mixture of **4.1.12** (50 mg, 0.15 mmol), 10% Pd/C (16 mg, 0.015 mmol, 10 mol%) and acetic acid (1.5 mL) were added to one chamber of COware apparatus under a flow of nitrogen. This first reaction chamber was sealed, and granular zinc (110 mg, 1.68 mmol) and aqueous HCl (2M, 1 mL, 2.00 mmol) were added to the second chamber under flow of nitrogen. The nitrogen line was removed, the second reaction was sealed, and the first reaction chamber was heated to 70 °C for 16 h under an atmosphere of hydrogen at a pressure of approximately 2.9 atm (in addition to the 1 atm of nitrogen already in the flask). On complete conversion of starting material the reaction was cooled to RT and the pressure was released under flow of nitrogen. The reaction mixture was adsorbed onto a pad of Celite[®], which was flushed with methanol, and the filtrate was concentrated under reduced pressure. The crude product was then diluted with water and basified with aqueous sodium hydroxide (2M) and extracted into DCM (5 x 10 mL). The combined organic layer was passed through a

hydrophobic frit and concentrated under reduced pressure, affording **4.4.13** (45.5 mg, 90%) as a colourless oil.

LCMS (Method B, UV, ESI) $R_t = 0.62$ min, $[M+H]^+$ 330.1

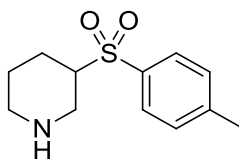
^1H NMR (400 MHz, CDCl_3): δ 7.74 (d, $J = 8.3$ Hz, 2H), 7.35 (d, $J = 8.3$ Hz, 2H), 7.22-7.33 (m, 5H), 3.57 (d, $J = 13.0$ Hz, 1H), 3.47 (d, $J = 13.7$ Hz, 1H), 3.15-3.26 (m, 2H), 2.80 (br. d, $J = 11.2$ Hz, 1H), 2.47 (s, 3H), 2.17 (t, $J = 12.5$ Hz, 1H), 2.02-2.09 (m, 1H), 1.87 (td, $J = 11.5, 2.7$ Hz, 1H), 1.71-1.79 (m, $J = 6.4$, 1H), 1.41-1.60 (m, 2H)

^{13}C NMR (101 MHz, CDCl_3): δ 144.6, 137.6, 134.5, 129.7, 128.9, 128.8, 128.2, 127.1, 63.0, 61.6, 52.5, 52.4, 24.3, 24.0, 21.6

IR ν_{max} (cm^{-1}) (thin film): 2953, 1597, 1314, 1142

HRMS: Calculated for $\text{C}_{19}\text{H}_{24}\text{NO}_2\text{S}$ $[M+H]^+$: 330.1528, found $[M+H]^+$ 330.1529 (0.3 ppm).

3-Tosylpiperidine **4.4.14**



A solution of **4.1.12** (50.4 mg, 0.15 mmol) in AcOH (5 mL) was passed through a ThalesNano H-Cube ProTM hydrogenation flow apparatus using a Pd/C (10 wt%) CatCart30TM at 70 °C, 25 bar pressure using a flow rate of 1 mL/min. The product line was fed back into the reactant solution, ensuring cycling of the reaction solution and the reaction mixture was cycled for 40 min. After full conversion of starting material the system was flushed for 10 min at 1 mL/min with 100% AcOH, and the resulting solution was concentrated under flow of nitrogen. The concentrated material was then basified with aqueous sodium hydroxide (2M, 10 mL) and extracted into DCM (5 x 15 mL). The combined organic layer was passed through a hydrophobic frit and concentrated under reduced pressure to afford **4.4.14** (28.0 mg, 76%) as a colourless oil.

LCMS (Method B, UV, ESI) $R_t = 0.43$ min, $[M+H]^+$ 240.2

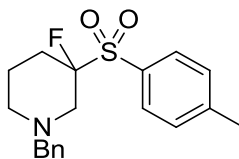
^1H NMR (400 MHz, $\text{DMSO-}d_6$): δ 7.72 (d, $J = 8.3$ Hz, 2H), 7.48 (d, $J = 8.3$ Hz, 2H), 3.02-3.15 (m, 2H), 2.75-2.84 (m, 1H), 2.45-2.48 (m, 1H), 2.42-2.44 (m, 3H), 2.28 (td, $J = 12.3, 2.8$ Hz, 1H), 1.90-1.98 (m, 1H), 1.59-1.67 (m, 1H), 1.44 (qd, $J = 12.0, 4.2$ Hz, 1H), 1.23-1.37 (m, 2H)

^{13}C NMR (101 MHz, $\text{DMSO-}d_6$): δ 144.4, 134.3, 129.8, 128.4, 60.5, 45.2, 45.0, 25.0, 23.9, 21.0

IR ν_{max} (cm^{-1}) (thin film): 3323, 2940, 1596, 1142

HRMS: Calculated for $\text{C}_{12}\text{H}_{18}\text{NO}_2\text{S}$ $[M+H]^+$: 240.1058, found $[M+H]^+$ 240.1058 (0.0 ppm).

1-Benzyl-3-fluoro-3-tosylpiperidine 4.4.16



A mixture of **4.1.12** (260 mg, 0.79 mmol) and **4.4.15** (530 mg, 1.68 mmol) were dissolved in THF (8 mL) and stirred at RT for 1 h, at which point borane tetrahydrofuranate (1 M, 0.8 mL, 0.80 mmol) was added, and the reaction mixture stirred for 2 h at RT. The reaction was quenched with water (10 mL) and diluted with sat. brine (10 mL) and extracted into DCM (3 x 30 mL). The combined organic layer was passed through a hydrophobic frit and concentrated under reduced pressure. The crude material was purified by silica gel chromatography using 0-60% TBME/cyclohexane as the eluent to afford **4.4.16** (208.1 mg, 75%) as a grey solid.

LCMS (Method A, UV, ESI) $R_t = 1.29$ min, $[M+H]^+$ 348.1

^1H NMR (400 MHz, $\text{DMSO-}d_6$): δ 7.72 (d, $J = 8.3$ Hz, 2H), 7.50 (d, $J = 8.3$ Hz, 2H), 7.28-7.34 (m, 2H), 7.23-7.28 (m, 3H), 3.55 (dd, $J = 24.0$ ($^3J_{\text{H-F}}$), 13.2 Hz, 2H), 2.86-2.96 (m, 1H), 2.73-2.80 (m, 1H), 2.60 (d, $J = 12.5$ Hz, 1H), 2.44 (s, 3H), 2.04-2.12 (m, 1H), 1.86-2.03 (m, 1H), 1.67-1.84 (m, 2H), 1.54-1.67 (m, 1H)

^{13}C NMR (101 MHz, DMSO- d_6): δ 145.9, 137.2, 130.0, 129.9, 129.9, 128.8, 128.1, 127.0, 105.4 (d, $^1J_{\text{C-F}} = 220.8$ Hz), 61.2, 52.7 (d, $^2J_{\text{C-F}} = 19.1$ Hz), 51.1, 26.6 (d, $^2J_{\text{C-F}} = 20.5$ Hz), 21.1, 20.2

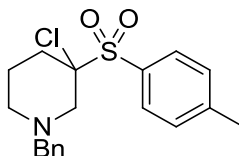
^{19}F NMR (376 MHz, DMSO- d_6): δ -156.47 (s, 1F)

IR ν_{max} (cm^{-1}) (thin film): 2966, 1596, 1321, 1154

HRMS: Calculated for $\text{C}_{19}\text{H}_{23}\text{NO}_2\text{SF}$ $[\text{M}+\text{H}]^+$: 348.1434, found $[\text{M}+\text{H}]^+$ 348.1435 (0.3 ppm)

M.pt.: 97-99 °C.

1-Benzyl-3-chloro-3-tosylpiperidine 4.4.17



A mixture of **4.1.12** (250 mg, 0.76 mmol) and *N*-chlorosuccinimide (recrystallized from water, 112 mg, 0.84 mmol) were dissolved in THF (7 mL) was stirred at RT for 15 min, at which point borane tetrahydrofuranate (1 M, 1 mL, 1.0 mmol) was added dropwise (10 min), and the reaction stirred at RT for 3 h. The reaction was quenched with water (15 mL) and stirred at RT for 5 min, and extracted into DCM (3 x 25 mL). The combined organic layer was passed through a hydrophobic frit and concentrated under reduced pressure. The crude material was purified by silica gel chromatography with 0-50% TBME/cyclohexane as the eluent. Trituration of the isolated colourless oil from Et₂O afforded **4.4.17** (236.9 mg, 85%) as a white solid.

LCMS (Method A, UV, ESI) $R_t = 1.37$ min, $[\text{M}+\text{H}]^+$ 364.1 (^{35}Cl), 366.1 (^{37}Cl)

^1H NMR (400 MHz, DMSO- d_6): δ 7.77 (d, $J = 8.3$ Hz, 2H), 7.50 (d, $J = 8.3$ Hz, 2H), 7.21-7.36 (m, 5H), 3.63 (d, $J = 13.4$ Hz, 1H), 3.53 (d, $J = 13.4$ Hz, 1H), 2.92 (dt, $J = 11.9, 2.0$ Hz, 1H), 2.79-2.85 (m, 1H), 2.64 (d, $J = 12.0$ Hz, 1H), 2.44 (s, 3H), 2.09-2.20 (m, 1H), 1.96-2.05 (m, 1H), 1.81-1.90 (m, 1H), 1.68-1.78 (m, 2H)

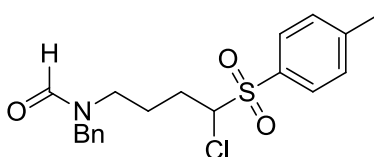
^{13}C NMR (101 MHz, DMSO- d_6): δ 145.8, 137.4, 130.8, 129.9, 129.7, 128.6, 128.1, 127.0, 85.0, 61.2, 56.4, 51.7, 31.0, 21.1, 20.8

IR ν_{max} (cm^{-1}) (thin film): 2969, 1596, 1320, 1157

HRMS: Calculated for $\text{C}_{19}\text{H}_{23}\text{NO}_2\text{S}\text{Cl}$ $[\text{M}+\text{H}]^+$: 364.1138, found $[\text{M}+\text{H}]^+$ 364.1136 (-0.5 ppm)

M.pt.: 136-138 °C.

***N*-Benzyl-*N*-(4-chloro-4-tosylbutyl)formamide 4.4.20**



A mixture of **4.1.12** (33 mg, 0.10 mmol) and *N*-chlorosuccinimide (20 mg, 0.15 mmol) were dissolved in THF (1.0 mL) and stirred at RT for 2 h, at which aqueous potassium hydroxide (1 M, 0.20 mL, 0.20 mmol) was added and the reaction stirred at RT for 24 h. The reaction mixture was diluted with water (5 mL) and extracted into DCM (3 x 10 mL). The combined organic layer was passed through a hydrophobic frit and concentrated under reduced pressure. The crude material was purified by reverse phase chromatography using 10-95% MeCN/10 mM ammonium bicarbonate as the eluent to afford **4.4.20** (27.8 mg, 73%) as a yellow gum.

LCMS (Method A, UV, ESI) R_t = 1.14 min, $[\text{M}+\text{H}]^+$ 380.1 (^{35}Cl), 382.1 (^{37}Cl)

^1H NMR (400MHz, DMSO- d_6 , 393 K): δ 8.24 (br. s., 1H), 7.80 (d, J = 8.3 Hz, 2H), 7.49 (d, J = 8.3 Hz, 2H), 7.18-7.40 (m, 5H), 5.25 (dd, J = 8.8, 3.7 Hz, 1H), 4.44 (s, 2H), 3.25 (br. s., 2H), 2.46 (s, 3H), 2.09-2.24 (m, 1H), 1.62-1.83 (m, 3H)

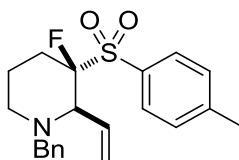
^{13}C NMR (101 MHz, DMSO- d_6): δ 163.2, 163.0, 145.6, 145.5, 137.1, 137.0, 132.0, 131.9, 129.8, 129.8, 129.4, 129.4, 128.6, 128.4, 127.6, 127.6, 127.1, 73.5, 73.4, 50.0, 45.1, 44.3, 40.2, 27.5, 27.1, 24.1, 22.8, 21.1

More than the expected number of ^{13}C signals because restricted rotation led to formation of a mixture of rotamers at RT.

IR ν_{\max} (cm⁻¹) (thin film): 3392 (br), 2923, 2257, 1663

HRMS: Calculated for C₁₉H₂₃NO₃SCl [M+H]⁺: 380.1087, found [M+H]⁺ 380.1087 (0.0 ppm).

***trans*-(2*R*,3*S*)-1-Benzyl-3-fluoro-3-tosyl-2-vinylpiperidine 4.4.21**^{416,417}



A mixture of **4.1.12** (33 mg, 0.10 mmol) and **4.4.15** (recrystallized from MeCN-Et₂O, 35 mg, 0.11 mmol) were dissolved in THF (8 mL) and stirred at RT for 10 min, at which point vinylmagnesium bromide (1M in THF, 0.13 mL, 0.13 mmol) was added dropwise and the reaction was stirred at RT for 1.5 h. The reaction mixture was then cooled over ice-water and the reaction was quenched with water (5 mL), and stirred for 10 min. The crude material was diluted with saturated aqueous sodium bicarbonate (5 mL) and brine (5 mL) and extracted into DCM (3 x 15 mL). The combined organic layer was passed through a hydrophobic frit and concentrated under reduced pressure. The crude material was purified by silica gel chromatography with 0-20% TBME/cyclohexane as the eluent affording **4.4.21** (27.9 mg, 74%) as a white solid.

LCMS (Method A, UV, ESI) R_t = 1.45 min, [M+H]⁺ 374.2

¹H NMR (400 MHz, DMSO-*d*₆): δ 7.71 (d, J = 7.6 Hz, 2H), 7.46 (d, J = 8.3 Hz, 2H), 7.30-7.38 (m, 4H), 7.23-7.28 (m, 1H), 6.02 (dt, J = 17.1, 9.8 Hz, 1H), 5.39 (dd, J = 10.3, 2.0 Hz, 1H), 5.21 (dd, J = 17.0, 2.1 Hz, 1H), 3.81 (t, J = 8.8 Hz, 1H), 3.64 (d, J = 13.9 Hz, 1H), 3.47 (d, J = 13.9 Hz, 1H), 2.59 (ddd, J = 12.2, 9.3 (³ $J_{\text{H-F}}$), 3.2 Hz, 1H), 2.43 (s, 3H), 2.32-2.40 (m, 1H), 2.03-2.15 (m, 1H), 1.83-2.03 (m, 2H), 1.59-1.68 (m, 1H)

¹³C NMR (101 MHz, DMSO-*d*₆): δ 145.8, 139.1, 132.2, 130.5 (d, ³ $J_{\text{C-F}}$ = 1.5 Hz), 130.3, 129.8 (d, ³ $J_{\text{C-F}}$ = 2.2 Hz), 128.9, 128.6, 127.3, 123.1, 106.2 (d, ¹ $J_{\text{C-F}}$ = 220.8 Hz), 64.0 (d, ² $J_{\text{C-F}}$ = 22.0 Hz), 58.0, 46.0, 27.3 (d, ² $J_{\text{C-F}}$ = 19.1 Hz), 21.6, 21.4

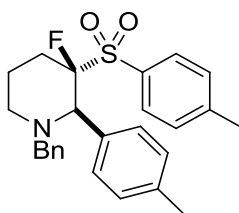
^{19}F NMR (376 MHz, DMSO-*d*₆): δ -144.52 (s, 1F)

IR ν_{max} (cm⁻¹) (thin film): 2921, 1596, 1324, 1152

HRMS: Calculated for C₂₁H₂₅NO₂SF [M+H]⁺: 374.1590, found [M+H]⁺ 374.1589 (-0.3 ppm)

M.pt.: 103-105 °C.

***trans*-(2*R*,3*S*)-1-Benzyl-3-fluoro-2-(*para*-tolyl)-3-tosylpiperidine 4.4.22**^{416,417}



A mixture of **4.1.12** (259 mg, 0.79 mmol) and **4.4.15** (recrystallized from MeCN-Et₂O, 275 mg, 0.87 mmol) were dissolved in THF (4 mL) and stirred at RT for 10 min, at which point *para*-tolylmagnesium bromide (1M in THF, 1.0 mL, 1.00 mmol) was added dropwise and the reaction was stirred at RT for 1.5 h. The reaction mixture was cooled over ice-water and the reaction was quenched with water (5 mL), and stirred for 10 min. The crude material was diluted with saturated aqueous sodium bicarbonate (5 mL) and brine (5 mL) and extracted into DCM (3 x 15 mL). The combined organic layer was passed through a hydrophobic frit and concentrated under reduced pressure. The crude material was purified by silica gel chromatography with 0-20% TBME/cyclohexane as the eluent to afford **4.4.22** (279.3 mg, 81%) as a white solid.

LCMS (Method A, UV, ESI) R_t = 1.58 min, [M+H]⁺ 438.2

^1H NMR (400 MHz, CDCl₃): δ 7.38 (dd, J = 8.3, 1.2 Hz, 2H), 7.32 (dd, J = 8.1, 2.0 Hz, 2H), 7.21-7.26 (m, 2H), 7.15-7.20 (m, 3H), 7.07 (d, J = 8.3 Hz, 2H), 6.95 (d, J = 8.3, 2H), 3.96 (d, J = 26.2 Hz ($^3J_{\text{H-F}}$), 1H), 3.57 (d, J = 13.7 Hz, 1H), 2.96 (d, J = 11.5 ($^3J_{\text{H-F}}$) Hz, 1H), 2.77 (d, J = 13.7 Hz, 1H), 2.37 (s, 3H), 2.27 (s, 3H), 2.23-2.32 (m, 1H), 1.98-2.17 (m, 2H), 1.91 (qt, J = 12.7, 3.5 Hz, 1H), 1.69-1.76 (m, 1H)

^{13}C NMR (101 MHz, CDCl_3): δ 144.0, 139.4, 138.2, 132.8, 131.9 (d, $^1J_{\text{C-F}} = 205.4$ Hz), 130.9, 129.7, 129.7, 128.8, 128.7, 128.4, 128.1, 126.7, 68.8 (d, $^2J_{\text{C-F}} = 16.1$ Hz), 58.3, 51.8, 29.9 (d, $^2J_{\text{C-F}} = 20.5$ Hz), 21.6, 21.1, 20.7

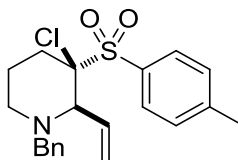
^{19}F NMR (376 MHz, CDCl_3): δ -163.05 (s, 1F)

IR ν_{max} (cm^{-1}) (thin film): 2949, 1595, 1326, 1152

HRMS: Calculated for $\text{C}_{26}\text{H}_{29}\text{NO}_2\text{SF}$ $[\text{M}+\text{H}]^+$: 438.1903, found $[\text{M}+\text{H}]^+$ 438.1904 (0.2 ppm)

M.pt.: 149-152 °C.

***cis*-(2*R*,3*R*)-1-Benzyl-3-chloro-3-tosyl-2-vinylpiperidine 4.4.23**^{416,417}



A mixture of **4.1.12** (33 mg, 0.10 mmol) and *N*-chlorosuccinimide (recrystallized from water, 15 mg, 0.11 mmol) were dissolved in THF (1 mL) and stirred at RT for 10 min, at which point vinylmagnesium bromide (1M in THF, 0.13 mL, 0.13 mmol) was added dropwise and the reaction was stirred at RT for 4.5 h. The reaction mixture was cooled over ice-water and the reaction was quenched with water (5 mL), and stirred for 10 min. The crude material was diluted with saturated aqueous sodium bicarbonate (5 mL) and brine (5 mL) and extracted into DCM (3 x 15 mL). The combined organic layer was passed through a hydrophobic frit and concentrated under reduced pressure. The crude material was purified by silica gel chromatography with 0-20% TBME/cyclohexane as the eluent to afford **4.4.23** (33.1 mg, 84%) as a white solid.

LCMS (Method A, UV, ESI) $R_t = 1.49$ min, $[\text{M}+\text{H}]^+$ 390.1 (^{35}Cl), 392.1 (^{37}Cl)

^1H NMR (400MHz, $\text{DMSO-}d_6$): δ 7.79 (d, $J = 8.6$ Hz, 2H), 7.49 (d, $J = 8.3$ Hz, 2H), 7.28-7.33 (m, 4H), 7.20-7.26 (m, 1H), 5.91 (ddd, $J = 16.9, 10.6, 8.9$ Hz, 1H), 5.43 (q, $J = 2.0$ Hz, 1H), 5.39 (dd, $J = 9.5, 1.7$ Hz, 1H), 3.92 (d, $J = 14.2$ Hz, 1H), 3.69 (d, $J =$

9.0 Hz, 1H), 3.24 (d, $J = 13.9$ Hz, 1H), 2.62-2.70 (m, 1H), 2.44 (s, 3H), 2.21-2.30 (m, 1H), 2.14 (ddd, $J = 13.2, 9.8, 2.9$ Hz, 1H), 1.57-1.78 (m, 3H)

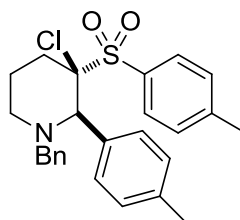
^{13}C NMR (101 MHz, DMSO- d_6): δ 145.9, 139.7, 133.7, 132.3, 131.4, 130.0, 128.7, 128.6, 127.2, 122.7, 88.4, 67.7, 57.3, 49.4, 34.6, 21.6, 21.3

IR ν_{max} (cm^{-1}) (thin film): 2924, 1597, 1325, 1151

HRMS: Calculated for $\text{C}_{21}\text{H}_{25}\text{NO}_2\text{SCl}$ $[\text{M}+\text{H}]^+$: 390.1295, found $[\text{M}+\text{H}]^+$ 390.1294 (-0.3 ppm)

M.pt.: 112-114 °C.

***cis*-(2*R*,3*R*)-1-Benzyl-3-chloro-2-(*para*-tolyl)-3-tosylpiperidine 4.4.24^{416,417}**



A mixture of **4.1.12** (33 mg, 0.10 mmol) and *N*-chlorosuccinimide (recrystallized from water, 15 mg, 0.11 mmol) were dissolved in THF (1 mL) and stirred at RT for 10 min, at which point *para*-tolylmagnesium bromide (1M in THF, 0.13 mL, 0.13 mmol) was added dropwise and the reaction was stirred at RT for 1.5 h. The reaction mixture was cooled over ice-water and the reaction was quenched with water (5 mL), and stirred for 10 min. The crude material was diluted with saturated aqueous sodium bicarbonate (5 mL) and brine (5 mL) and extracted into DCM (3 x 15 mL). The combined organic layer was passed through a hydrophobic frit and concentrated under reduced pressure. The crude material was purified by silica gel chromatography with 0-20% TBME/cyclohexane as the eluent to afford **4.4.24** (29.0 mg, 63%) as a white solid.

LCMS (Method A, UV, ESI) $R_t = 1.61$ min, $[\text{M}+\text{H}]^+$ 454.2 (^{35}Cl), 456.2 (^{37}Cl)

^1H NMR (400MHz, DMSO- d_6): δ 7.60 (d, $J = 8.6$ Hz, 2H), 7.47 (d, $J = 9.0$ Hz, 2H), 7.38 (d, $J = 8.3$, 2H), 7.25-7.32 (m, 2H), 7.17-7.24 (m, 3H), 7.12 (d, $J = 8.6$ Hz, 2H),

4.20 (s, 1H), 3.49 (d, $J = 13.9$ Hz, 1H), 2.77-2.86 (m, 2H), 2.40 (s, 3H), 2.32-2.37 (m, 1H), 2.30 (s, 3H), 2.13 (td, $J = 12.1, 3.2$ Hz, 1H), 1.60-1.82 (m, 3H)

^{13}C NMR (101 MHz, DMSO- d_6): δ 145.7, 139.4, 138.0, 133.9, 132.0, 131.2, 129.7, 128.7, 128.7, 128.5, 127.2, 125.6, 89.4, 69.0, 57.7, 52.1, 36.1, 21.6, 21.2, 21.2

IR ν_{max} (cm^{-1}) (thin film): 2922, 1597, 1315, 1144

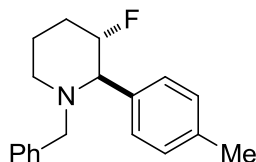
HRMS: Calculated for $\text{C}_{26}\text{H}_{29}\text{NO}_2\text{SCl}$ $[\text{M}+\text{H}]^+$: 454.1608, found $[\text{M}+\text{H}]^+$ 454.1608 (0.0 ppm)

M.pt.: 118-120 °C.

***trans*-1-Benzyl-3-fluoro-2-(*para*-tolyl)piperidine 4.4.25, and *cis*-1-benzyl-3-fluoro-2-(*para*-tolyl)piperidine 4.4.25b (dr 6:1)**

A mixture of magnesium powder (49 mg, 2.01 mmol) and **4.4.22** (22 mg, 0.05 mmol) was sonicated under an atmosphere of nitrogen for 1 min. The reaction mixture was treated with methanol (1 mL) and stirred at RT for 20 h under a positive pressure of nitrogen. The reaction mixture was filtered through a 1g Isolute NH2 SPE column and flushed with methanol. The elute was concentrated under reduced pressure, and ^{19}F NMR analysis of the crude product showed a diastereomeric ratio of 6:1 for **4.4.25:4.4.25b**, based on the peaks at 177.8 and 195.3 ppm, respectively. The crude material was purified by high pH MDAP (Method E), to afford **4.4.25** (9.8 mg, 69%) as a white solid, and **4.4.25b** (0.4 mg, 3%) as a colourless oil.

***trans*-1-Benzyl-3-fluoro-2-(*para*-tolyl)piperidine 4.4.25**



LCMS (Method A, UV, ESI) $R_t = 1.52$ min, $[\text{M}+\text{H}]^+$ 284.2

^1H NMR (400 MHz, CDCl_3): δ 7.39 (d, $J = 8.1$ Hz, 2H), 7.17-7.30 (m, 7H), 4.47 (dtd, $J = 47.7$ ($^2J_{\text{H-F}}$), 9.5, 5.1 Hz, 1H), 3.75 (d, $J = 13.7$ Hz, 1H), 3.13 (dd, $J = 8.7$ ($^3J_{\text{H-F}}$), 6.7 Hz, 1H), 2.83-2.96 (m, 2H), 2.35 (s, 3H), 2.21-2.29 (m, 1H), 1.97 (td, $J = 11.6$, 2.7 Hz, 1H), 1.69-1.77 (m, 1H), 1.57-1.62 (m, 1H), 1.52-1.57 (m, 1H)

^{13}C NMR (101 MHz, CDCl_3): δ 139.4, 137.5, 137.4, 129.3, 128.5, 128.5, 128.1, 126.7, 93.9 (d, $^1J_{\text{C-F}} = 173.9$ Hz), 72.7 (d, $^2J_{\text{C-F}} = 22.0$ Hz), 58.6, 52.0, 31.3 (d, $^2J_{\text{C-F}} = 18.3$ Hz), 22.6 (d, $^3J_{\text{C-F}} = 12.5$ Hz), 21.2

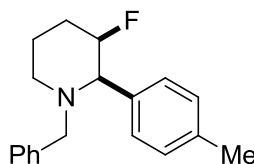
^{19}F NMR (376 MHz, CDCl_3): δ -177.79 (s, 1F)

IR ν_{max} (cm^{-1}) (thin film): 2945, 2796, 1514, 1352

HRMS: Calculated for $\text{C}_{19}\text{H}_{23}\text{NF}$ $[\text{M}+\text{H}]^+$: 284.1815, found $[\text{M}+\text{H}]^+$ 284.1814 (-0.4 ppm)

M.pt.: 78-80 °C.

***cis*-1-Benzyl-3-fluoro-2-(*para*-tolyl)piperidine 4.4.25b**



LCMS (Method A, UV, ESI) $R_t = 1.49$ min, $[\text{M}+\text{H}]^+ 284.2$

^1H NMR (600 MHz, $\text{DMSO-}d_6$): δ 7.39 (d, $J = 7.3$ Hz, 2H), 7.30 (t, $J = 7.7$ Hz, 2H), 7.20-7.26 (m, 3H), 7.17 (d, $J = 8.1$ Hz, 2H), 4.57 (d, $^2J_{\text{H-F}} = 47.3$ Hz, 1H), 3.65 (d, $J = 13.6$ Hz, 1H), 3.36 (d, $^3J_{\text{H-F}} = 31.2$ Hz, 1H), 2.86 (d, $J = 13.9$ Hz, 2H), 2.29 (s, 3H), 1.98-2.05 (m, 2H), 1.78 (qt, $J = 13.2$, 3.7 Hz, 1H), 1.67 (dtdd, $J = 45.1$, 13.9, 4.0, 1.8 Hz, 1H), 1.45-1.51 (m, 1H)

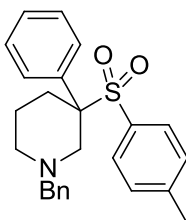
^{13}C NMR (151 MHz, $\text{DMSO-}d_6$): δ 138.7, 137.3, 136.3, 128.7, 128.5, 128.2, 128.1, 126.7, 89.9 (d, $^1J_{\text{C-F}} = 178.0$ Hz) 69.1 (d, $^2J_{\text{C-F}} = 16.6$ Hz), 58.6, 51.8, 29.2 (d, $^2J_{\text{C-F}} = 22.1$ Hz), 20.6, 19.5

^{19}F NMR (376 MHz, CDCl_3): δ -195.31 (s, 1F)

IR ν_{\max} (cm⁻¹) (thin film): 2929, 1670, 1453, 1139

HRMS: Calculated for C₁₉H₂₃NF [M+H]⁺: 284.1815, found [M+H]⁺ 284.1813 (-0.7 ppm).

1-Benzyl-3-phenyl-3-tosylpiperidine 4.4.34



Copper(II) triflate (1.8 mg, 5.0 μ mol, 10 mol%) and three 3Å molecular sieves were placed under an atmosphere of nitrogen and heated to 200 °C under vacuum for 2 h, and then cooled to RT and placed back under a nitrogen atmosphere. The catalyst solution was then treated with a solution containing **4.1.12** (16 mg, 0.05 mmol), diphenyliodonium triflate (52.6 mg, 0.12 mmol) and three 3Å molecular sieves in DCM (1.0 ml), and the reaction mixture was stirred at RT for 5 d. Sodium borohydride (3.7 mg, 0.10 mmol) and methanol (0.1 ml) were added to the reaction mixture and the reaction stirred at RT for 1 h. Water (2 mL) was added to quench the reaction, and the crude material was extracted into DCM (2 x 5 mL). The combined organic layer was passed through a hydrophobic frit and concentrated under flow of nitrogen. The crude material was purified by formic MDAP (Method B), affording **4.4.34** (4.4 mg, 22%) as a yellow oil.

LCMS (Method A, UV, ESI) R_t = 1.43 min, [M+H]⁺ 406.2

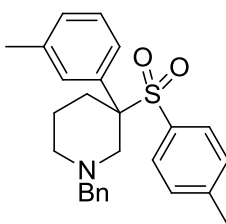
¹H NMR (400 MHz, DMSO-*d*₆): δ 7.16-7.34 (m, 10H), 7.11 (d, J = 8.3 Hz, 2H), 7.06 (d, J = 7.6 Hz, 2H), 3.49-3.54 (m, 2H), 3.42-3.49 (m, 2H), 2.64-2.71 (m, 1H), 2.57 (dd, J = 13.8, 3.1 Hz, 1H), 2.35 (s, 3H), 1.92-2.04 (m, 2H), 1.56-1.65 (m, 1H), 1.24 (qt, J = 13.4, 3.7 Hz, 1H)

¹³C NMR (101 MHz, DMSO-*d*₆): δ 144.9, 138.0, 133.3, 132.4, 130.3, 130.1, 129.7, 129.5, 128.4, 128.4, 127.9, 127.6, 69.2, 62.5, 54.6, 53.6, 28.0, 21.7, 21.5

IR ν_{\max} (cm⁻¹) (thin film): 2926, 1597, 1313, 1143

HRMS: Calculated for C₂₅H₂₈NO₂S [M+H]⁺: 406.1827, found [M+H]⁺ 406.1842 (0.5 ppm).

1-Benzyl-3-(*meta*-tolyl)-3-tosylpiperidine 4.4.35



Copper(II) triflate (1.8 mg, 5.0 μ mol, 10 mol%) and three 3 \AA molecular sieves were placed under an atmosphere of nitrogen and heated to 200 $^{\circ}$ C under vacuum for 2 h, and then cooled to RT and placed back under a nitrogen atmosphere. The catalyst solution was treated with a solution containing **4.1.12** (16 mg, 0.05 mmol), mesityl(*meta*-tolyl)iodonium triflate (59.4 mg, 0.12 mmol) and three 3 \AA molecular sieves in DCM (1.0 ml), and the reaction was stirred at RT for 5 d. Sodium borohydride (3.7 mg, 0.10 mmol) and methanol (0.1 ml) were added and the reaction stirred at RT for 1 h. Water (2 mL) was added to quench the reaction, and the crude material was extracted into DCM (2 x 5 mL). The combined organic layer was passed through a hydrophobic frit and concentrated under flow of nitrogen. The crude material was purified by formic MDAP (Method B), affording **4.4.35** (4.7 mg, 23%) as a yellow oil.

LCMS (Method A, UV, ESI) R_t = 1.47 min, [M+H]⁺ 420.3

¹H NMR (600 MHz, CDCl₃): δ 7.28-7.32 (m, 2H), 7.25 (br. s, 1H), 7.22 (d, J = 7.3 Hz, 2H), 7.02-7.12 (m, 6H), 6.86 (d, J = 7.3 Hz, 1H), 6.70 (s, 1H), 3.63 (d, J = 12.8 Hz, 1H), 3.49 (d, J = 10.6, 1H), 3.36 (d, J = 12.8 Hz, 1H), 2.81 (d, J = 11.4 Hz, 1H), 2.67 (d, J = 11.7 Hz, 1H), 2.60 (dd, J = 12.8, 2.2 Hz, 1H), 2.36 (s, 3H), 2.25 (td, J = 13.4, 4.4 Hz, 1H), 2.18 (s, 3H), 2.11-2.17 (m, 1H), 1.67 (dt, J = 13.6, 3.3 Hz, 1H), 1.46-1.52 (m, 1H)

^{13}C NMR (151 MHz, CDCl_3): δ 144.2, 137.8, 137.1, 133.0, 132.1, 130.7, 130.1, 129.4, 128.7, 128.5, 128.1, 127.6, 127.2, 126.9, 69.5, 63.3, 54.3, 54.3, 27.7, 21.7, 21.5, 21.4

IR ν_{max} (cm^{-1}) (thin film): 2924, 1597, 1313, 1143

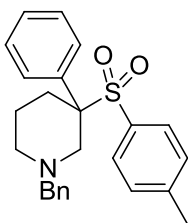
HRMS: Calculated for $\text{C}_{26}\text{H}_{30}\text{NO}_2\text{S}$ $[\text{M}+\text{H}]^+$: 420.1997, found $[\text{M}+\text{H}]^+$ 420.1997 (0.0 ppm).

Attempted Asymmetric β -Arylation of 4.1.12

Preparation of catalyst solution:

Copper(II) triflate (35 mg, 0.1 mmol) and three 3Å molecular sieves were placed under an atmosphere of nitrogen and heated to 200 °C under vacuum for 30 min, and then cooled to RT and placed back under a nitrogen atmosphere. This process was repeated twice more. The vial containing the catalyst was then charged with a degassed solution of **4.4.36** (36 mg, 0.11 mmol) in DCM (2.0 mL), and the resulting green solution was stirred under an atmosphere of nitrogen for 20 h.

1-Benzyl-3-phenyl-3-tosylpiperidine 4.4.34



An oven-dried vial containing three 3Å molecular sieves was charged with diphenyliodonium triflate (84 mg, 0.20 mmol), then sealed, placed under an atmosphere of nitrogen and suspended in DCM (2.0 mL). The reaction mixture was then charged with the preformed catalyst solution (0.1 mL, 10 mol%), followed by a solution of **4.1.12** (16 mg, 0.05 mmol) in DCM (0.3 mL). The reaction mixture was stirred under an atmosphere of nitrogen at RT for 5 h, then heated to 50 °C for 35 h. The reaction was then cooled to RT and treated with sodium borohydride (3.7 mg, 0.01 mmol) and methanol (0.1 mL). Water (2 mL) was added to quench the reaction, and the crude material was extracted into DCM (2 x 5 mL). The combined organic layer

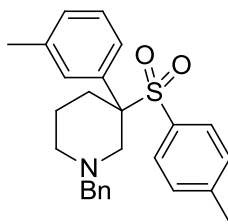
was passed through a hydrophobic frit and concentrated under flow of nitrogen. The crude material was purified by silica gel chromatography, using 0-50% TBME/cyclohexane as the eluent, to afford **4.4.34** (4.0 mg, 20%) as a white solid. Chiral HPLC demonstrated only racemic product was prepared.

LCMS (Method B, UV, ESI) $R_t = 0.86$ min, $[M+H]^+$ 406.2

^1H NMR (400 MHz, CDCl_3): δ 7.39-7.57 (m, 1H), 7.17-7.32 (m, 6H), 7.02-7.11 (m, 6H), 6.92 (d, $J = 8.8$ Hz, 1H), 3.58 (d, $J = 12.7$ Hz, 1H), 3.47-3.53 (m, 1H), 3.43 (d, $J = 13.2$ Hz, 1H), 2.71-2.83 (m, 2H), 2.57-2.67 (m, 1H), 2.36 (s, 3H), 2.23-2.33 (m, 1H), 2.07-2.17 (m, 1H), 1.67 (d, $J = 14.9$ Hz, 1H), 1.41-1.51 (m, 1H)

Chiral HPLC (25 cm Chiralcel OJ-H, 10% EtOH/*n*-heptane, 1.0 mL/min, detection at 230 nm) $R_t = 14.2$ min (49.5% area), 18.8 min (50.5% area).²⁸⁵

1-Benzyl-3-(*meta*-tolyl)-3-tosylpiperidine **4.4.35**



An oven-dried vial containing three 3Å molecular sieves was charged with mesityl(*meta*-tolyl)iodonium triflate (95 mg, 0.20 mmol), then sealed, placed under an atmosphere of nitrogen and suspended in DCM (2.0 mL). The reaction mixture was then charged with the preformed catalyst solution (0.1 mL, 10 mol%), followed by a solution of **4.1.12** (16 mg, 0.05 mmol) in DCM (0.3 mL). The reaction mixture was stirred under an atmosphere of nitrogen at RT for 5 h, then heated to 50 °C for 35 h. The reaction was then cooled to RT and treated with sodium borohydride (3.7 mg, 0.01 mmol) and methanol (0.1 mL). Water (2 mL) was added to quench the reaction, and the crude material was extracted into DCM (2 x 5 mL). The combined organic layer was passed through a hydrophobic frit and concentrated under flow of nitrogen. The crude material was purified by silica gel chromatography, using 0-50%

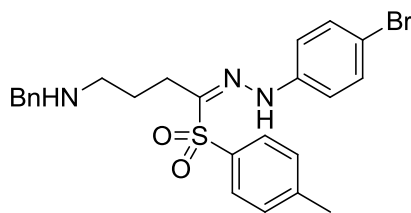
TBME/cyclohexane as the eluent, to afford **4.4.35** (4.2 mg, 20%) as a white solid. Chiral HPLC demonstrated only racemic product was prepared.

LCMS (Method B, UV, ESI) $R_t = 0.89$ min, $[M+H]^+$ 420.3

^1H NMR (400 MHz, CDCl_3): δ 7.20-7.35 (m, 5H), 7.04-7.13 (m, 6H), 6.84-6.91 (m, 1H), 6.69-6.74 (m, 1H), 3.64 (d, $J=13.0$ Hz, 1H), 3.51 (d, $J=11.2$ Hz, 1H), 3.38 (d, $J=12.7$ Hz, 1H), 2.83 (d, $J=11.7$ Hz, 1H), 2.68 (d, $J=11.7$ Hz, 1H), 2.58-2.65 (m, 1H), 2.37 (s, 3H), 2.26 (td, $J=13.4, 4.3$ Hz, 1H), 2.20 (s, 3H), 2.11-2.17 (m, 1H), 1.64-1.73 (m, 1H), 1.48-1.55 (m, 1H)

Chiral HPLC (25 cm Chiralpak AD, 20% EtOH/*n*-heptane, 1.0 mL/min, detection at 230 nm) $R_t = 5.4$ min (49.7% area), 6.6 min (50.3% area).²⁸⁵

***N*-Benzyl-4-(2-(4-bromophenyl)hydrazono)-4-tosylbutan-1-amine 4.4.39**



Trifluoroacetic acid (7.5 μL , 0.10 mmol) was added to a solution of **4.1.12** (32 mg, 0.10 mmol) and 4-bromobenzenediazonium tetrafluoroborate (29 mg, 0.11 mmol) in MeOH (1 mL). The reaction mixture was stirred at RT for 8 h, then concentrated under reduced pressure. The crude material was purified by high pH MDAP (Method E), to afford **4.4.39** (27 mg, 55%) as an orange gum.

LCMS (Method A, UV, ESI) $R_t = 1.48$ min, $[M+H]^+$ 500.1 (^{79}Br), 502.1 (^{81}Br)

^1H NMR (600 MHz, $\text{DMSO}-d_6$): δ 7.78 (d, $J = 8.1$ Hz, 2H), 7.46 (d, $J = 8.1$ Hz, 2H), 7.30-7.36 (m, 6H), 7.23-7.27 (m, 1H), 6.79 (d, $J = 8.8$ Hz, 2H), 3.66 (s, 2H), 2.72 (t, $J = 7.3$ Hz, 2H), 2.44 (t, $J = 6.4$ Hz, 2H), 2.42 (s, 3H), 1.72 (quin, $J = 7.0$ Hz, 2H)

The amine and aza protons underwent exchange in the wet deuterated solvent, therefore were not observed.

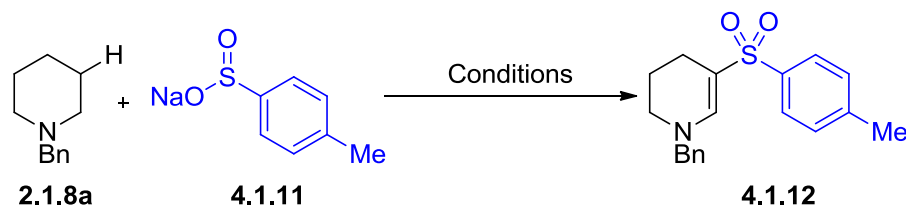
^{13}C NMR (151 MHz, DMSO- d_6): δ 145.2, 144.1, 143.3, 140.1, 136.3, 131.7, 129.8, 128.1, 128.1, 128.0, 126.6, 115.3, 112.3, 52.1, 46.4, 25.5, 22.6, 21.0

IR ν_{max} (cm^{-1}) (thin film): 3304, 2922, 1583, 1487, 1144

HRMS: Calculated for $\text{C}_{24}\text{H}_{27}\text{N}_3\text{O}_2\text{SBr}$ $[\text{M}+\text{H}]^+$: 500.1007, found $[\text{M}+\text{H}]^+$ 500.1010 (0.6 ppm).

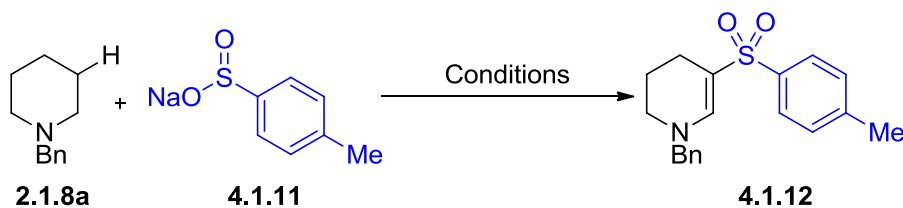
Appendix 3

Optimisation of Oxidative C–H Sulfonylation of Amines.

Reactions carried out by Wei Chung Kong.³³³

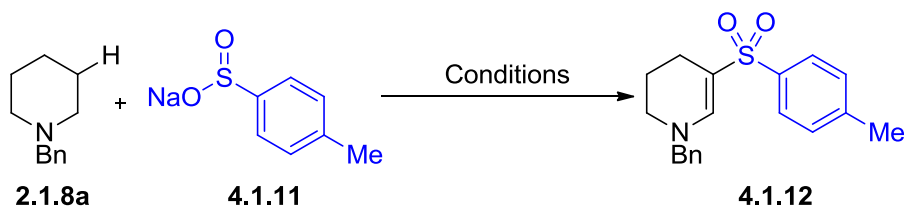
Entry	Eq. 4.1.11	Eq. Oxidant	Reaction conditions ^[a]	% conversion to 4.1.12 ^[b]
1	3	4, NIS	RT, 0.5 h actv ^[c] , 3 h, 2:1 THF ^[d] :water, 5 eq. NaHCO ₃	43
2	3	4, NIS	RT, 0.5 h actv, 3 h, 2:1 DMSO:water, 5 eq. NaHCO ₃	38
3	3	4, NIS	RT, 0.5 h actv, 3 h, 2:1 DCM:water, 5 eq. NaHCO ₃	28
4	3	4, NIS	RT, 0.5 h actv, 3 h, 2:1 EtOH:water, 5 eq. NaHCO ₃	-
5	3	4, NIS	RT, 0.5 h actv, 3 h, THF ^[d]	22

Table 26. Optimisation of the oxidative C–H sulfonylation of 2.1.8a to 4.1.12, exploring the necessity for an aqueous solvent system and an additional base. [a] Reaction conditions: **2.1.8a** (100 mg, 1.0 eq), Oxidant, solvent, 0.5 h, then **4.1.11**, solvent (0.063 M), T, 2 h. [b] % conversion to **4.1.12** measured by analysis of the crude material against 3,4,5-trichloropyridine as an internal standard. [c] “actv” refers to the pre-stirring of oxidant with **2.1.8a**. [d] THF contained 250 ppm BHT radical inhibitor.



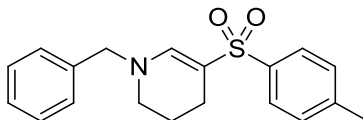
Entry	Eq. 4.1.11	Eq. Oxidant	Reaction conditions ^[a]	% conversion to 4.1.12 ^[b]
1	3	4, NIS	RT, 0.5 h actv ^[c] , 3 h, MeTHF	11
2	3	4, NIS	RT, 0.5 h actv, 3 h, DMF	27
3	3	4, NIS	RT, 0.5 h actv, 2 h, MeCN	27
4	3	4, NIS	RT, 0.5 h actv, 2 h, DCM	27
5	3	4, NIS	RT, 0.5 h actv, 2 h, DMSO	60
6	3	4, NIS	15 °C, 0.5 h actv, 24 h, DMSO	48
7	3	4, NIS	45 °C, 0.5 h actv, 2 h, DMSO	38
8	3	4, NIS	60 °C, 0.5 h actv, 2 h, DMSO	-
9	3	4, NIS	RT, 0.5 h actv, 10 min, DMSO	40
10	3	4, NIS	RT, 0.5 h actv, 2 h, DMSO, 0.025 M	33
11	3	4, NIS	RT, 0.5 h actv, 2 h, DMSO, 0.5 M	51
12	3	4, I ₂	RT, 0.5 h actv, 2 h, DMSO	trace
13	3	4, NBS	RT, 0.5 h actv, 2 h, DMSO	10
14	3	4, NCS	RT, 0.5 h actv, 2 h, DMSO	-
15	3	4, ICl	RT, 0.5 h actv, 2 h, DMSO	-
16	3	4, NIS	RT, 2 h, DMSO	trace
17	3	4, NIS	RT, 0.5 h rev-actv ^[d] , 2 h, DMSO	trace
18	3	4, NIS	RT, 0.5 h actv, 2 h, DMSO, slow addition of RSO ₂ Na	trace
19 ^[e]	3	4, NIS	RT, 0.5 h actv, 2 h, DMSO	36
20 ^[f]	3	4, NIS	RT, 0.5 h actv, 2 h, DMSO	71

Table 27. Optimisation of the oxidative C–H sulfonation of 2.1.8a to 4.1.12, screening a range of temperatures, reaction concentrations, oxidants, order of addition and scale of reaction. [a] Reaction conditions: **2.1.8a** (100 mg, 1.0 eq), Oxidant, solvent, 0.5 h, then **4.1.11**, solvent (0.063 M), T, 2 h. [b] % conversion to **4.1.12** measured by analysis of the crude material against 3,4,5-trichloropyridine as an internal standard. [c] “actv” refers to the pre-stirring of oxidant with **2.1.8a**. [d] “rev-actv” refers to the pre-stirring of oxidant with **4.1.11**. [e] Reaction carried out on a scale of 35 mg of **2.1.8a**. [f] Reaction carried out on a scale of 500 mg of **2.1.8a**.



Entry	Eq. 4.1.11	Eq. Oxidant	Reaction conditions ^[a]	% conversion to 4.1.12 ^[b]
1	3	4, NIS	RT, 0.5 h actv ^[c] , 2 h, DMSO, N ₂	76
2	3	4, NIS	RT, 0.5 h actv, 2 h, DMSO, N ₂ , dark	81
3	1.5	4, NIS	RT, 0.5 h actv, 2 h, DMSO, N ₂ , dark	31
4	3	4, NIS	RT, 0.5 h actv, 2 h, THF ^[d] , N ₂ , dark	95
5	3	4, NIS	RT, 0.5 h actv, 2 h, 2-MeTHF, N ₂ , dark	65
6	1.5	3, NIS	RT, 0.5 h actv, 2 h, THF ^[d] , N ₂ , dark	53
7	1.5	4, NIS	RT, 0.5 h actv, 2 h, THF ^[d] , N ₂ , dark	90
8	1.5 ^[e]	4, NIS	RT, 0.5 h actv, 2 h, THF ^[d] , N ₂ , dark	71

Table 28. Optimisation of the oxidative C–H sulfonylation of 2.1.8a to 4.1.12, screening the influence of light and oxygen, solvents, and stoichiometry of 4.1.11 and NIS. [a] Reaction conditions: **2.1.8a** (1.0 eq), Oxidant, solvent, 0.5 h, then **4.1.11**, solvent (0.063 M), T, 2 h. [b] % conversion to **4.1.12** measured by analysis of the crude material against 3,4,5-trichloropyridine as an internal standard. [c] “actv” refers to the pre-stirring of oxidant with **2.1.8a**. [d] THF was inhibitor-free. [e] lithium *para*-methylbenzenesulfinate was used as the sulfinate salt instead.

Substrate Scope of the Oxidative C–H Sulfonylation of Amines.Reactions carried out by Wei Chung Kong.³³³**1-Benzyl-5-tosyl-1,2,3,4-tetrahydropyridine 4.1.12**

General procedure for the oxidative C–H sulfonylation of amines A was followed. A solution of **2.1.8a** (100 mg, 0.57 mmol) in THF (0.1 M) was added to NIS (513 mg, 2.28 mmol), which was stirred at RT for 30 min, then transferred *via* syringe to a suspension of **4.1.11** (153 mg, 0.86 mmol) in THF (0.3 M), and THF was used to rinse the NIS/amine reaction vessel to ensure complete transfer to give a resulting reaction concentration of 0.06 M. ¹H NMR analysis of the crude material against 3,4,5-trichloropyridine (0.132 mmol) as a standard showed 90% conversion to **4.1.12**. The crude material was purified by silica gel chromatography using 0–30% EtOAc/cyclohexane as the eluent to afford **4.1.12** (157 mg, 84%) as an off-white solid.

LCMS (Method A, UV, ESI) $R_t = 1.23$ min, $[M+H]^+$: 328.1

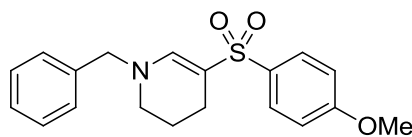
¹H NMR (400 MHz, DMSO-*d*₆) δ 7.63 (d, $J = 8.3$ Hz, 2H), 7.54 (s, 1H), 7.34–7.42 (m, 4H), 7.28–7.33 (m, 1H), 7.26 (d, $J = 8.3$ Hz, 2H), 4.43 (s, 2H), 2.94 (t, $J = 5.4$ Hz, 2H), 2.38 (s, 3H), 2.00 (t, $J = 6.0$ Hz, 2H), 1.64 (quin, $J = 5.9$ Hz, 2H)

¹³C NMR (101 MHz, DMSO-*d*₆) δ 144.4, 141.9, 140.2, 137.2, 129.5, 128.6, 127.5, 127.5, 126.1, 99.4, 58.1, 44.6, 20.9, 20.4, 19.3

IR ν_{\max} (thin film): 2936, 1618, 1280, 1134, 1094

HRMS: Calculated for C₁₉H₂₂NO₂S $[M+H]^+$: 328.1371, found $[M+H]^+$ 328.1374 (0.9 ppm)

M.pt.: 168–170 °C.

1-Benzyl-5-((4-methoxyphenyl)sulfonyl)-1,2,3,4-tetrahydropyridine 4.2.2

General procedure for the oxidative C–H sulfonylation of amines B was followed. A solution of **2.1.8a** (100 mg, 0.57 mmol) in THF (0.1 M) was added to NIS (513 mg, 2.28 mmol), which was stirred at RT for 30 min, then transferred *via* syringe to a suspension of sodium 4-methoxybenzenesulfinate (222 mg, 1.15 mmol) in THF (0.3 M), and THF was used to rinse the NIS/amine reaction vessel to ensure complete transfer to give a resulting reaction concentration of 0.06 M. ^1H NMR analysis of the crude material against 3,4,5-trichloropyridine (0.130 mmol) as a standard showed 68% conversion to **4.2.2**. The crude material was purified by silica gel chromatography using 0-30% EtOAc/cyclohexane as the eluent to afford **4.2.2** (121 mg, 62%) as a white solid.

LCMS (Method A, UV, ESI) $R_t = 1.17$ min, $[\text{M}+\text{H}]^+$: 344.1

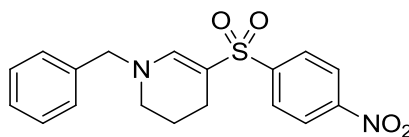
^1H NMR (400 MHz, $\text{DMSO-}d_6$) δ 7.66 (d, $J = 8.8$ Hz, 2H), 7.51 (s, 1H), 7.38 (t, $J = 7.1$ Hz, 2H), 7.30 (tt, $J = 7.3, 2.2$, 1H), 7.25 (d, $J = 8.1$ Hz, 2H), 7.07 (d, $J = 8.8$ Hz, 2H), 4.41 (s, 2H), 3.83 (s, 3H), 2.93 (t, $J = 5.4$ Hz, 2H), 1.99 (t, $J = 6.1$ Hz, 2H), 1.63 (quin, $J = 5.8$ Hz, 2H)

^{13}C NMR (101 MHz, $\text{DMSO-}d_6$) δ 161.7, 144.0, 137.3, 134.7, 128.6, 128.2, 127.5, 127.5, 114.2, 99.9, 58.1, 55.5, 44.6, 20.4, 19.3

IR ν_{max} (thin film): 2929, 1620, 1497, 1277, 1256, 1133, 1094

HRMS: Calculated for $\text{C}_{19}\text{H}_{22}\text{NO}_3\text{S}$ $[\text{M}+\text{H}]^+$: 344.1320, found $[\text{M}+\text{H}]^+$ 344.1322 (0.6 ppm)

M.pt.: 132-134 °C.

1-Benzyl-5-((4-nitrophenyl)sulfonyl)-1,2,3,4-tetrahydropyridine 4.2.3

General procedure for the oxidative C–H sulfonylation of amines A was followed. A solution of **2.1.8a** (100 mg, 0.57 mmol) in THF (0.1 M) was added to NIS (513 mg, 2.28 mmol), which was stirred at RT for 30 min, then transferred *via* syringe to a suspension of sodium 4-nitrobenzenesulfinate (179 mg, 0.86 mmol) in THF (0.3 M), and THF was used to rinse the NIS/amine reaction vessel to ensure complete transfer to give a resulting reaction concentration of 0.06 M. ¹H NMR analysis of the crude material against 3,4,5-trichloropyridine (0.136 mmol) as a standard showed 71% conversion to **4.2.3**. The crude material was purified by silica gel chromatography using 0-25% EtOAc/cyclohexane as the eluent to afford **4.2.3** (128 mg, 63%) as a yellow solid.

LCMS (Method A, UV, ESI) $R_t = 1.20$ min, $[M+H]^+$: 359.0

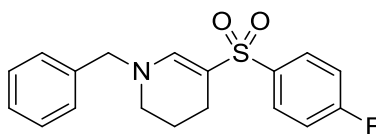
¹H NMR (400 MHz, DMSO-*d*₆) δ 8.38 (d, $J = 9.0$ Hz, 2H), 7.99 (d, $J = 9.0$ Hz, 2H), 7.68 (s, 1H), 7.35-7.41 (m, 2H), 7.31 (tt, $J = 7.3, 2.2$ Hz, 1H), 7.26 (d, $J = 8.3$ Hz, 2H), 4.47 (s, 2H), 2.97 (t, $J = 5.4$ Hz, 2H), 2.05 (t, $J = 6.1$ Hz, 2H), 1.65 (quin, $J = 5.8$ Hz, 2H)

¹³C NMR (101 MHz, DMSO-*d*₆) δ 149.1, 148.8, 146.2, 136.9, 128.6, 127.6, 127.5, 127.5, 124.5, 97.2, 58.3, 44.6, 20.2, 19.2

IR ν_{max} (thin film): 2935, 1615, 1525, 1347, 1293, 1136, 1094

HRMS: Calculated for C₁₈H₁₉N₂O₄S $[M+H]^+$: 359.1066, found $[M+H]^+$ 359.1066 (0.0 ppm)

M.pt.: 138-140 °C.

1-Benzyl-5-((4-fluorophenyl)sulfonyl)-1,2,3,4-tetrahydropyridine 4.2.4

General procedure for the oxidative C–H sulfonylation of amines A was followed. A solution of **2.1.8a** (100 mg, 0.57 mmol) in THF (0.1 M) was added to NIS (513 mg, 2.28 mmol), which was stirred at RT for 30 min, then transferred *via* syringe to a suspension of sodium 4-fluorobenzenesulfinate (156 mg, 0.86 mmol) in THF (0.3 M), and THF was used to rinse the NIS/amine reaction vessel to ensure complete transfer to give a resulting reaction concentration of 0.06 M. ¹H NMR analysis of the crude material against 3,4,5-trichloropyridine (0.136 mmol) as a standard showed 69% conversion to **4.2.4**. The crude material was purified by silica gel chromatography using 0-20% EtOAc/cyclohexane as the eluent to afford **4.2.4** (104 mg, 55%) as an off-white solid.

LCMS (Method A, UV, ESI) $R_t = 1.19$ min, $[M+H]^+$: 332.1

¹H NMR (400 MHz, DMSO-*d*₆) δ 7.77-7.83 (m, 2H), 7.58 (s, 1H), 7.35-7.42 (m, 4H), 7.30 (tt, $J = 7.3, 2.2$ Hz, 1H), 7.25 (d, $J = 8.3$ Hz, 2H), 4.43 (s, 2H), 2.94 (t, $J = 5.4$ Hz, 2H), 2.01 (t, $J = 6.1$ Hz, 2H), 1.64 (quin, $J = 5.9$ Hz, 2H)

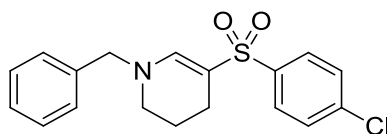
¹³C NMR (101 MHz, DMSO-*d*₆) δ 163.7 (d, $^1J_{C-F} = 253.1$ Hz), 144.8, 139.5 (d, $^4J_{C-F} = 2.9$ Hz), 137.0, 129.0 (d, $^3J_{C-F} = 9.5$ Hz), 128.6, 127.5 (2C), 116.1 (d, $^2J_{C-F} = 22.0$ Hz), 98.7, 58.1, 44.5, 20.3, 19.3

¹⁹F NMR (CDCl₃, 376MHz): δ -107.34 (s, 1F)

IR ν_{max} (thin film): 2935, 1619, 1493, 1282, 1135, 1094

HRMS: Calculated for C₁₈H₁₉FNO₂S $[M+H]^+$: 332.1121, found $[M+H]^+$ 332.1120 (-0.3 ppm)

M.pt.: 120-122 °C.

1-Benzyl-5-((4-chlorophenyl)sulfonyl)-1,2,3,4-tetrahydropyridine 4.2.5

General procedure for the oxidative C–H sulfonylation of amines A was followed. A solution of **2.1.8a** (100 mg, 0.57 mmol) in THF (0.1 M) was added to NIS (513 mg, 2.28 mmol), which was stirred at RT for 30 min, then transferred *via* syringe to a suspension of sodium 4-chlorobenzenesulfinate (170 mg, 0.86 mmol) in THF (0.3 M), and THF was used to rinse the NIS/amine reaction vessel to ensure complete transfer to give a resulting reaction concentration of 0.06 M. ¹H NMR analysis of the crude material against 3,4,5-trichloropyridine (0.112 mmol) as a standard showed 78% conversion to **4.2.5**. The crude material was purified by silica gel chromatography using 0-20% EtOAc/cyclohexane as the eluent to afford **4.2.5** (125 mg, 63%) as an off-white solid.

LCMS (Method A, UV, ESI) $R_t = 1.27$ min, $[M+H]^+$: 348.0 (³⁵Cl), 349.9 (³⁷Cl)

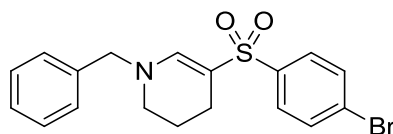
¹H NMR (400 MHz, DMSO-*d*₆) δ 7.71-7.77 (m, 2H), 7.60-7.65 (m, 2H), 7.59 (s, 1H), 7.35-7.41 (m, 2H), 7.28-7.34 (m, 1H), 7.25 (d, $J = 6.8$ Hz, 2H), 4.44 (s, 2H), 2.94 (t, $J = 5.9$ Hz, 2H), 2.01 (t, $J = 6.0$ Hz, 2H), 1.64 ppm (quin, $J = 5.9$ Hz, 2H)

¹³C NMR (101 MHz, DMSO-*d*₆) δ 145.1, 142.0, 137.1, 136.5, 129.1, 128.6, 128.0, 127.7, 127.5, 98.3, 58.2, 44.6, 20.3, 19.3

IR ν_{max} (thin film): 2940, 1616, 1273, 1171, 1136, 1093, 1010

HRMS: Calculated for C₁₈H₁₉ClNO₂S $[M+H]^+$: 348.0825, found $[M+H]^+$ 348.0827 (0.6 ppm)

M.pt.: 133-136 °C.

1-Benzyl-5-((4-bromophenyl)sulfonyl)-1,2,3,4-tetrahydropyridine 4.2.6

General procedure for the oxidative C–H sulfonylation of amines A was followed. A solution of **2.1.8a** (100 mg, 0.57 mmol) in THF (0.1 M) was added to NIS (513 mg, 2.28 mmol), which was stirred at RT for 30 min, then transferred *via* syringe to a suspension of sodium 4-bromobenzenesulfinate dihydrate (239 mg, 0.86 mmol) in THF (0.3 M), and THF was used to rinse the NIS/amine reaction vessel to ensure complete transfer to give a resulting reaction concentration of 0.06 M. ¹H NMR analysis of the crude material against 3,4,5-trichloropyridine (0.123 mmol) as a standard showed 98% conversion to **4.2.6**. The crude material was purified by silica gel chromatography using 0-15% EtOAc/cyclohexane as the eluent to afford **4.2.6** (177.6 mg, 79%) as an off-white solid.

LCMS (Method A, UV, ESI) $R_t = 1.29$ min, $[M+H]^+$: 391.9 (⁷⁹Br), 393.9 (⁸¹Br)

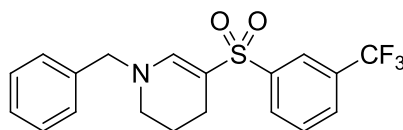
¹H NMR (400 MHz, DMSO-*d*₆) δ 7.75-7.79 (m, 2H), 7.63-7.70 (m, 2H), 7.59 (s, 1H), 7.35-7.40 (m, 2H), 7.27-7.33 (m, 1H), 7.23-7.27 (m, 2H), 4.44 (s, 2H), 2.94 (t, $J = 5.6$ Hz, 2H), 2.01 (t, $J = 6.0$ Hz, 2H), 1.64 ppm (quin, $J = 5.9$ Hz, 2H)

¹³C NMR (101 MHz, DMSO-*d*₆) δ 145.1, 142.4, 137.1, 132.1, 128.6, 128.1, 127.5, 125.4, 111.4, 98.3, 58.2, 44.5, 20.3, 19.2

IR ν_{\max} (thin film): 2935, 1616, 1172, 1133, 1093, 1008

HRMS: Calculated for C₁₈H₁₉BrNO₂S $[M+H]^+$: 392.0320, found $[M+H]^+$ 392.0317 (-0.8 ppm)

M.pt.: 135-138 °C.

1-Benzyl-5-((3-(trifluoromethyl)phenyl)sulfonyl)-1,2,3,4-tetrahydropyridine**4.2.7**

General procedure for the oxidative C–H sulfonylation of amines A was followed. A solution of **2.1.8a** (100 mg, 0.57 mmol) in THF (0.1 M) was added to NIS (513 mg, 2.28 mmol), which was stirred at RT for 30 min, then transferred *via* syringe to a suspension of sodium 3-(trifluoromethyl)benzenesulfinate (199 mg, 0.86 mmol) in THF (0.3 M), and THF was used to rinse the NIS/amine reaction vessel to ensure complete transfer to give a resulting reaction concentration of 0.06 M. ¹H NMR analysis of the crude material against 3,4,5-trichloropyridine (0.147 mmol) as a standard showed 91% conversion to **4.2.7**. The crude material was purified by silica gel chromatography using 0-20% EtOAc/cyclohexane as the eluent to afford **4.2.7** (174.5 mg, 80%) as a white solid.

LCMS (Method A, UV, ESI) $R_t = 1.29$ min, $[M+H]^+$: 382.0

¹H NMR (400 MHz, DMSO-*d*₆) δ 8.03-8.10 (m, 1H), 7.94-8.01 (m, 2H), 7.79-7.87 (m, 1H), 7.69 (s, 1H), 7.33-7.40 (m, 2H), 7.28-7.33 (m, 1H), 7.24-7.27 (m, 2H), 4.46 (s, 2H), 2.96 (t, $J = 5.4$ Hz, 2H), 2.03 (t, $J = 6.1$ Hz, 2H), 1.64 (quin, $J = 5.8$ Hz, 2H)

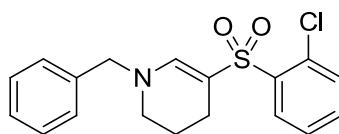
¹³C NMR (101 MHz, DMSO-*d*₆) δ 145.9, 144.6, 137.0, 130.7, 130.1, 129.7 (q, $^2J_{C-F} = 32.3$ Hz), 128.6, 128.4 (q, $^3J_{C-F} = 3.7$ Hz), 127.5, 127.5, 122.3 (q, $^3J_{C-F} = 4.2$ Hz), 122.1 (q, $^1J_{C-F} = 272.9$ Hz), 97.5, 58.2, 44.5, 20.3, 19.2

¹⁹F NMR (CDCl₃, 376MHz): δ -62.75 (s, 1F)

IR ν_{max} (thin film): 2929, 2850, 1617, 1427, 1326

HRMS: Calculated for C₁₉H₁₉F₃NO₂S $[M+H]^+$: 382.1089, found $[M+H]^+$ 382.1092 (0.8 ppm)

M.pt.: 124-126 °C.

1-Benzyl-5-((2-chlorophenyl)sulfonyl)-1,2,3,4-tetrahydropyridine 4.2.8

General procedure for the oxidative C–H sulfonylation of amines A was followed. A solution of **2.1.8a** (100 mg, 0.57 mmol) in THF (0.1 M) was added to NIS (513 mg, 2.28 mmol), which was stirred at RT for 30 min, then transferred *via* syringe to a suspension of sodium 2-chlorobenzenesulfinate (170 mg, 0.86 mmol) in THF (0.3 M), and THF was used to rinse the NIS/amine reaction vessel to ensure complete transfer to give a resulting reaction concentration of 0.06 M. ¹H NMR analysis of the crude material against 3,4,5-trichloropyridine (0.138 mmol) as a standard showed 73% conversion to **4.2.8**. The crude material was purified by silica gel chromatography using 0-30% EtOAc/cyclohexane as the eluent to afford **4.2.8** (124 mg, 63%) as a yellow solid.

LCMS (Method A, UV, ESI) $R_t = 1.23$ min, $[M+H]^+$: 348.0 (³⁵Cl), 349.8 (³⁷Cl)

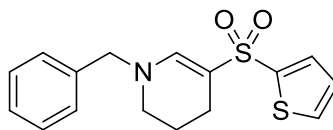
¹H NMR (400 MHz, DMSO-*d*₆) δ 8.01 (d, $J = 7.6$ Hz, 1H), 7.57-7.65 (m, 3H), 7.50-7.56 (m, 1H), 7.36-7.42 (m, 2H), 7.26-7.34 (m, 3H), 4.49 (s, 2H), 3.00 (t, $J = 5.4$ Hz, 2H), 1.94 (t, $J = 6.1$ Hz, 2H), 1.64 (quin, $J = 5.8$ Hz, 2H)

¹³C NMR (101 MHz, DMSO-*d*₆) δ 147.2, 138.7, 137.1, 133.6, 131.9, 130.7, 130.5, 128.6, 127.6, 127.5, 127.4, 95.9, 58.3, 44.7, 20.4, 19.2

IR ν_{\max} (thin film): 2919, 1618, 1453, 1296, 1139

HRMS: Calculated for C₁₈H₁₉ClNO₂S $[M+H]^+$: 348.0825, found $[M+H]^+$ 348.0825 (0 ppm)

M.pt.: 118-120 °C.

1-Benzyl-5-(thiophen-2-ylsulfonyl)-1,2,3,4-tetrahydropyridine 4.2.9

General procedure for the oxidative C–H sulfonylation of amines A was followed. A solution of **2.1.8a** (100 mg, 0.57 mmol) in THF (0.1 M) was added to NIS (513 mg, 2.28 mmol), which was stirred at RT for 30 min, then transferred *via* syringe to a suspension of sodium thiophene-2-sulfinate (146 mg, 0.86 mmol) in THF (0.3 M), and THF was used to rinse the NIS/amine reaction vessel to ensure complete transfer to give a resulting reaction concentration of 0.06 M. ¹H NMR analysis of the crude material against 3,4,5-trichloropyridine (0.153 mmol) as a standard showed 80% conversion to **4.2.9**. The crude material was purified by silica gel chromatography using 0-30% EtOAc/cyclohexane as the eluent to afford **4.2.9** (132 mg, 73%) as a colourless oil.

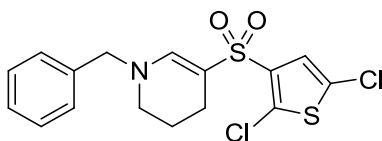
LCMS (Method A, UV, ESI) $R_t = 1.15$ min, $[M+H]^+$: 320.0

¹H NMR (400 MHz, DMSO-*d*₆) δ 7.86 (dd, $J = 5.0, 1.3$ Hz, 1H), 7.57 (s, 1H), 7.49 (dd, $J = 3.7, 1.2$ Hz, 1H), 7.35-7.40 (m, 2H), 7.28-7.33 (m, 1H), 7.23-7.27 (m, 2H), 7.13 (dd, $J = 5.1, 3.7$ Hz, 1H), 4.45 (s, 2H), 2.97 (t, $J = 5.4$ Hz, 2H), 2.10 (t, $J = 6.1$ Hz, 2H), 1.68 (quin, $J = 5.9$ Hz, 2H)

¹³C NMR (101 MHz, DMSO-*d*₆) δ 145.3, 144.6, 137.1, 131.9, 130.5, 128.6, 127.6, 127.5, 127.5, 99.5, 58.1, 44.6, 20.3, 19.3

IR ν_{\max} (thin film): 2935, 1617, 1293, 1127, 1019

HRMS: Calculated for C₁₆H₁₈NO₂S₂ $[M+H]^+$: 320.0779, found $[M+H]^+$ 320.0781 (0.6 ppm).

1-Benzyl-5-((2,5-dichlorothiophen-3-yl)sulfonyl)-1,2,3,4-tetrahydropyridine**4.2.10**

General procedure for the oxidative C–H sulfonylation of amines B was followed. A solution of **2.1.8a** (35 mg, 0.20 mmol) in THF (0.1 M) was added to NIS (180 mg, 0.80 mmol), which was stirred at RT for 30 min, then transferred *via* syringe to a suspension of sodium 2,5-dichlorothiophene-3-sulfinate (96 mg, 0.40 mmol) in THF (0.3 M), and THF was used to rinse the NIS/amine reaction vessel to ensure complete transfer to give a resulting reaction concentration of 0.06 M. ¹H NMR analysis of the crude material against 3,4,5-trichloropyridine (0.113 mmol) as a standard showed 66% conversion to **4.2.10**. The crude material was purified by silica gel chromatography using 0-40% TBME/cyclohexane as the eluent to afford **4.2.10** (50.6 mg, 65%) as an off-white solid.

LCMS (Method A, UV, ESI) $R_t = 1.37$ min, $[M+H]^+$: 388.0 (³⁵Cl³⁵Cl), 389.9 (³⁵Cl³⁷Cl), 391.9 (³⁷Cl³⁷Cl)

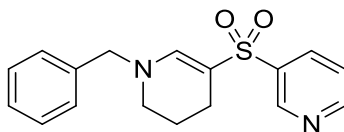
¹H NMR (400 MHz, DMSO-*d*₆) δ 7.61 (s, 1H), 7.35-7.40 (m, 2H), 7.28-7.33 (m, 1H), 7.24-7.28 (m, 3H), 4.47 (s, 2H), 3.01 (t, $J = 5.4$ Hz, 2H), 2.09 (t, $J = 6.1$ Hz, 2H), 1.69 (quin, $J = 5.9$ Hz, 2H)

¹³C NMR (101 MHz, DMSO-*d*₆) δ 146.4, 139.5, 136.9, 128.6, 127.6, 127.3, 127.0, 125.6 (2C), 97.5, 58.3, 44.7, 20.3, 19.1

IR ν_{max} (thin film): 2929, 1615, 1424, 1316, 1120, 1038

HRMS: Calculated for C₁₆H₁₆Cl₂NO₂S₂ $[M+H]^+$: 388.0000, found $[M+H]^+$ 387.9997 (-0.8 ppm)

M.pt.: 111-113 °C.

3-((1-Benzyl-1,4,5,6-tetrahydropyridin-3-yl)sulfonyl)pyridine 4.2.11

General procedure for the oxidative C–H sulfonylation of amines B was followed, with the modification that the sodium sulfinate was generated *in situ*. A solution of **2.1.8a** (35 mg, 0.20 mmol) in THF (0.1 M) was added to NIS (180 mg, 0.80 mmol), which was stirred at RT for 30 min, then transferred *via* syringe to a suspended mixture of pyridine-3-sulfinic acid hydrochloride (82 mg, 0.46 mmol) and sodium hydride (60 wt% dispersion on mineral oil, 35 mg, 0.88 mmol) in THF (0.3 M), which had been pre-stirred at RT under an atmosphere of nitrogen for 10 min, and THF was used to rinse the NIS/amine reaction vessel to ensure complete transfer to give a resulting reaction concentration of 0.06 M. ¹H NMR analysis of the crude material against 3,4,5-trichloropyridine (0.17 mmol) as a standard showed 55% conversion to **4.2.11**. The crude material was purified by silica gel chromatography, first using 0-40% (3:1 EtOAc:EtOH)/cyclohexane as the eluent, and then with 80-100% TBME/cyclohexane as the eluent, to afford **4.2.11** (32.0 mg, 51%) as a colourless oil.

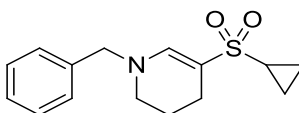
LCMS (Method A, UV, ESI) $R_t = 0.99$ min, $[M+H]^+$: 315.0

¹H NMR (400 MHz, DMSO-*d*₆) δ 8.90 (dd, $J = 2.3, 0.6$ Hz, 1H), 8.77 (dd, $J = 4.8, 1.6$ Hz, 1H), 8.12 (ddd, $J = 8.1, 2.4$ Hz, 1.6, 1H), 7.65 (s, 1H), 7.60 (ddd, $J = 8.1, 4.9, 0.7$ Hz, 1H), 7.35-7.40 (m, 2H), 7.28-7.33 (m, 1H), 7.24-7.28 (m, 2H), 4.46 (s, 2H), 2.96 (t, $J = 5.4$ Hz, 2H), 2.05 (t, $J = 6.1$ Hz, 2H), 1.65 (quin, $J = 6.1$ Hz, 2H)

¹³C NMR (101 MHz, DMSO-*d*₆) δ 152.3, 146.8, 145.7, 139.3, 137.0, 134.0, 128.6, 127.5, 124.1, 111.5, 98.0, 58.2, 44.6, 20.3, 19.2

IR ν_{\max} (thin film): 2935, 1616, 1292, 1142, 1103, 1014

HRMS: Calculated for C₁₇H₁₉N₂O₂S $[M+H]^+$: 315.1167, found $[M+H]^+$ 315.1165 (-0.6 ppm).

1-Benzyl-5-(cyclopropylsulfonyl)-1,2,3,4-tetrahydropyridine 4.2.13

General procedure for the oxidative C–H sulfonylation of amines B was followed. A solution of **2.1.8a** (100 mg, 0.57 mmol) in THF (0.1 M) was added to NIS (513 mg, 2.28 mmol), which was stirred at RT for 30 min, then transferred *via* syringe to a suspension of sodium cyclopropanesulfinate (146 mg, 1.15 mmol) in THF (0.3 M), and THF was used to rinse the NIS/amine reaction vessel to ensure complete transfer to give a resulting reaction concentration of 0.06 M. ¹H NMR analysis of the crude material against 3,4,5-trichloropyridine (0.121 mmol) as a standard showed 74% conversion to **4.2.13**. The crude material was purified by silica gel chromatography using 0-30% EtOAc/cyclohexane as the eluent to afford **4.2.13** (107 mg, 68%) as a yellow oil.

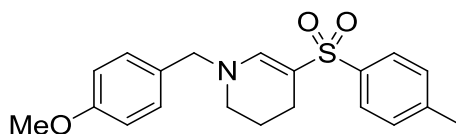
LCMS (Method A, UV, ESI) $R_t = 1.02$ min, $[M+H]^+$: 278.1

¹H NMR (400 MHz, DMSO-*d*₆) δ 7.35-7.41 (m, 2H), 7.28-7.34 (m, 1H), 7.23-7.28 (m, 3H), 4.38 (s, 2H), 2.99 (t, $J = 5.4$ Hz, 2H), 2.44-2.49 (m, $J = 2.2$ Hz, 1H), 2.25 (t, $J = 6.1$ Hz, 2H), 1.77 (quin, $J = 5.9$ Hz, 2H), 0.83-0.92 (m, 4H)

¹³C NMR (101 MHz, DMSO-*d*₆) δ 143.8, 137.4, 128.5, 127.5, 127.4, 100.0, 58.0, 44.6, 31.0, 20.6, 19.9, 4.1

IR ν_{\max} (thin film): 2929, 1621, 1275, 1118

HRMS: Calculated for C₁₅H₂₀NO₂S $[M+H]^+$: 278.1215, found $[M+H]^+$ 278.1217 (0.7 ppm).

1-(4-Methoxybenzyl)-5-tosyl-1,2,3,4-tetrahydropyridine 4.2.19

General procedure for the oxidative C–H sulfonylation of amines A was followed. A solution of **2.1.8b** (117 mg, 0.57 mmol) in THF (0.1 M) was added to NIS (513 mg, 2.28 mmol), which was stirred at RT for 30 min, then transferred *via* syringe to a suspension of **4.1.11** (153 mg, 0.86 mmol) in THF (0.3 M), and THF was used to rinse the NIS/amine reaction vessel to ensure complete transfer to give a resulting reaction concentration of 0.06 M. ¹H NMR analysis of the crude material against 3,4,5-trichloropyridine (0.159 mmol) as a standard showed 84% conversion to **4.2.19**. The crude material was purified by silica gel chromatography using 0-30% EtOAc/cyclohexane as the eluent to afford **4.2.19** (162 mg, 79%) as a white solid.

LCMS (Method A, UV, ESI) $R_t = 1.22$ min, $[M+H]^+$: 358.1

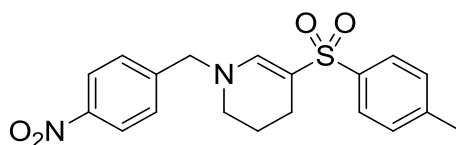
¹H NMR (400 MHz, DMSO-*d*₆) δ 7.61 (d, $J = 8.1$ Hz, 2H), 7.51 (s, 1H), 7.35 (d, $J = 8.1$ Hz, 2H), 7.19 (d, $J = 8.8$ Hz, 2H), 6.93 (d, $J = 8.8$ Hz, 2H), 4.33 (s, 2H), 3.75 (s, 3H), 2.91 (t, $J = 5.4$ Hz, 2H), 2.37 (s, 3H), 1.97 (t, $J = 6.1$ Hz, 2H), 1.61 (quin, $J = 6.1$ Hz, 2H)

¹³C NMR (101 MHz, DMSO-*d*₆) δ 158.7, 144.2, 141.8, 140.2, 129.4 (2C), 129.0, 126.1, 114.0, 99.1, 57.6, 55.0, 44.3, 20.9, 20.4, 19.4

IR ν_{max} (thin film): 2934, 1619, 1513, 1280, 1249, 1172, 1134, 1093

HRMS: Calculated for C₂₀H₂₄NO₃S $[M+H]^+$: 358.1477, found $[M+H]^+$ 358.1479 (0.6 ppm)

M.pt.: 110-112 °C.

1-(4-Nitrobenzyl)-5-tosyl-1,2,3,4-tetrahydropyridine 4.2.20

General procedure for the oxidative C–H sulfonylation of amines A was followed. A solution of **2.1.8c** (126 mg, 0.57 mmol) in THF (0.1 M) was added to NIS (513 mg, 2.28 mmol), which was stirred at RT for 30 min, then transferred *via* syringe to a suspension of **4.1.11** (153 mg, 0.86 mmol) in THF (0.3 M), and THF was used to rinse the NIS/amine reaction vessel to ensure complete transfer to give a resulting reaction concentration of 0.06 M. ¹H NMR analysis of the crude material against 3,4,5-trichloropyridine (0.217 mmol) as a standard showed 79% conversion to **4.2.20**. The crude material was purified by silica gel chromatography using 0-30% EtOAc/cyclohexane as the eluent to afford **4.2.20** (138.8 mg, 65%) as a yellow solid.

LCMS (Method A, UV, ESI) $R_t = 1.19$ min, $[M+H]^+$: 373.1

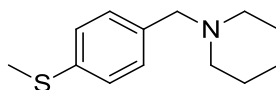
¹H NMR (400 MHz, DMSO-*d*₆) δ 8.25 (d, $J = 8.8$ Hz, 2H), 7.63 (d, $J = 8.1$ Hz, 2H), 7.58 (s, 1H), 7.53 (d, $J = 8.8$ Hz, 2H), 7.37 (d, $J = 8.1$ Hz, 2H), 4.60 (s, 2H), 2.95 (t, $J = 5.4$ Hz, 2H), 2.38 (s, 3H), 2.01 (t, $J = 6.1$ Hz, 2H), 1.66 (quin, $J = 5.8$ Hz, 2H)

¹³C NMR (101 MHz, DMSO-*d*₆) δ 146.9, 145.4, 144.3, 142.0, 140.0, 129.5, 128.6, 126.2, 123.7, 100.4, 57.2, 44.8, 20.9, 20.4, 19.3

IR ν_{\max} (thin film): 2935, 1622, 1520, 1345, 1280, 1136, 1094, 1014

HRMS: Calculated for C₁₉H₂₁N₂O₄S $[M+H]^+$: 373.1222, found $[M+H]^+$ 373.1221 (-0.3 ppm)

M.pt.: 147-150 °C.

1-(4-(Methylthio)benzyl)piperidine 4.2.18c

A solution of piperidine (1.16 mL, 11.7 mmol), 4-(methylthio)benzaldehyde (1.56 mL, 11.7 mmol) and DIPEA (6.15 ml, 35.2 mmol) in THF (30 mL) was treated with MgSO_4 (0.85 g, 7.05 mmol). The resulting suspension was stirred at RT for 5 min before addition of sodium triacetoxyborohydride (4.98 g, 23.5 mmol). The resulting reaction mixture was stirred at RT for 20 h. The reaction solvent was removed under reduced pressure, and the residue was suspended in DCM (20 mL). The solution was washed with sat. aq. NaHCO_3 (20 mL), the aqueous layer washed with DCM (20 mL). The combined organic layer was passed through a hydrophobic frit and concentrated under reduced pressure. The crude mixture was purified by silica gel chromatography using 0-20% 3:1 EtOAc:EtOH (with 1% Et_3N modifier)/cyclohexane as the eluent, to afford **4.2.18c** (1.90 g, 73%) as a yellow oil.

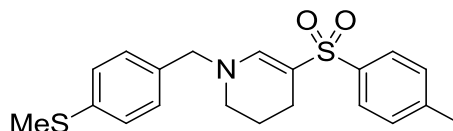
LCMS (Method A, UV, ESI) $R_t = 1.27$ min, $[\text{M}+\text{H}]^+$: 222.1

^1H NMR (400 MHz, CDCl_3) δ 7.19-7.27 (m, 4H), 3.43 (s, 2H), 2.49 (s, 3H), 2.33-2.41 (m, 4H), 1.57 (quin, $J = 5.6$ Hz, 4H), 1.39-1.48 (m, 2H)

^{13}C NMR (101 MHz, CDCl_3) δ 136.5, 135.8, 129.7, 126.7, 63.3, 54.4, 26.0, 24.4, 16.1

IR ν_{max} (thin film): 2932, 1493, 1343

HRMS: Calculated for $\text{C}_{13}\text{H}_{20}\text{NS}$ $[\text{M}+\text{H}]^+$: 222.1316, found $[\text{M}+\text{H}]^+$ 222.1318 (0.9 ppm).

1-(4-(Methylthio)benzyl)-5-tosyl-1,2,3,4-tetrahydropyridine 4.2.21

General procedure for the oxidative C–H sulfonylation of amines A was followed. A solution of **4.2.18c** (126 mg, 0.57 mmol) in THF (0.1 M) was added to NIS (513 mg,

2.28 mmol), which was stirred at RT for 30 min, then transferred *via* syringe to a suspension of **4.1.11** (153 mg, 0.86 mmol) in THF (0.3 M), and THF was used to rinse the NIS/amine reaction vessel to ensure complete transfer to give a resulting reaction concentration of 0.06 M. ¹H NMR analysis of the crude material against 3,4,5-trichloropyridine (0.121 mmol) as a standard showed 87% conversion to **4.2.21**. The crude material was purified by silica gel chromatography using 0-30% EtOAc/cyclohexane as the eluent to afford **4.2.21** (178 mg, 84%) as an off-white solid.

LCMS (Method A, UV, ESI) $R_t = 1.29$ min, $[M+H]^+$: 374.2

¹H NMR (400 MHz, DMSO-*d*₆) δ 7.61 (d, $J = 8.3$ Hz, 2H), 7.52 (s, 1H), 7.36 (d, $J = 8.1$ Hz, 2H), 7.26 (d, $J = 8.3$ Hz, 2H), 7.20 (d, $J = 8.6$ Hz, 2H), 4.37 (s, 2H), 2.91 (t, $J = 5.4$ Hz, 2H), 2.47 (s, 3H), 2.37 (s, 3H), 1.98 (t, $J = 6.1$ Hz, 2H), 1.62 (quin, $J = 5.6$ Hz, 2H)

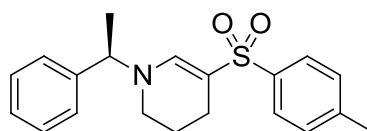
¹³C NMR (101 MHz, DMSO-*d*₆) δ 144.2, 141.9, 140.1, 137.3, 133.8, 129.5, 128.3, 126.1, 126.1, 99.4, 57.6, 44.5, 20.9, 20.4, 19.3, 14.6

IR ν_{\max} (thin film): 2919, 1619, 1280, 1135, 1093, 1013

HRMS: Calculated for C₂₀H₂₄NO₂S₂ $[M+H]^+$: 374.1248, found $[M+H]^+$ 374.1248 (0.0 ppm)

M.pt.: 128-130 °C.

(*R*)-1-(1-Phenylethyl)-5-tosyl-1,2,3,4-tetrahydropyridine **4.2.22**



General procedure for the oxidative C–H sulfonylation of amines A was followed. A solution of **2.1.8r** (108 mg, 0.57 mmol) in THF (0.1 M) was added to NIS (513 mg, 2.28 mmol), which was stirred at RT for 30 min, then transferred *via* syringe to a suspension of **4.1.11** (153 mg, 0.86 mmol) in THF (0.3 M), and THF was used to rinse the NIS/amine reaction vessel to ensure complete transfer to give a resulting reaction concentration of 0.06 M. ¹H NMR analysis of the crude material against 3,4,5-

trichloropyridine (0.158 mmol) as a standard showed 96% conversion to **4.2.22**. The crude material was purified by silica gel chromatography using 0-30% EtOAc/cyclohexane as the eluent to afford **4.2.22** (182 mg, 94%) as a white solid.

LCMS (Method A, UV, ESI) $R_t = 1.26$ min, $[M+H]^+$: 342.0

^1H NMR (400 MHz, DMSO- d_6) δ 7.62 (d, $J = 8.3$ Hz, 2H), 7.53 (s, 1H), 7.33-7.41 (m, 4H), 7.26-7.32 (m, 3H), 4.68 (q, $J = 6.8$ Hz, 1H), 2.93 (ddd, $J = 12.7, 7.6, 3.9$ Hz, 1H), 2.82 (ddd, $J = 12.7, 6.6, 3.9$ Hz, 1H), 2.36 (s, 3H), 1.99 (t, $J = 6.1$ Hz, 2H), 1.54-1.66 (m, 2H), 1.52 (d, $J = 7.1$ Hz, 3H)

^{13}C NMR (101 MHz, DMSO- d_6) δ 142.4, 141.8, 141.0, 140.1, 129.4, 128.5, 127.4, 126.4, 126.1, 99.4, 61.3, 42.4, 20.8, 20.4, 19.8, 18.1

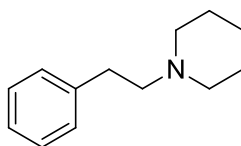
IR ν_{max} (thin film): 2929, 1615, 1280, 1134, 1092

HRMS: Calculated for $\text{C}_{20}\text{H}_{24}\text{NO}_2\text{S}$ $[M+H]^+$: 342.1528, found $[M+H]^+$ 342.1529 (0.3 ppm)

M.pt.: 83-85 °C

Chiral HPLC (25 cm Chiralpak AD, 10% EtOH/*n*-heptane, 1.0 mL/min, detection at 215 nm) $R_t = 18.7$ min (major) and 21.0 min (minor), ee = 99.4%.²⁸⁵

1-Phenethylpiperidine **4.2.18e**



A solution of piperidine (1.16 mL, 11.7 mmol), 2-phenylacetaldehyde (1.41 g, 11.7 mmol) and DIPEA (6.15 ml, 35.2 mmol) in THF (75 mL) was treated with MgSO_4 (0.85 g, 7.05 mmol). The resulting suspension was stirred at RT for 5 min before addition of sodium triacetoxyborohydride (4.98 g, 23.5 mmol). The resulting reaction mixture was stirred at RT for 20 h. The reaction solvent was removed under reduced pressure, and the residue was suspended in DCM (20 mL). The solution was washed with sat. aq. NaHCO_3 (20 mL), the aqueous layer washed with DCM (20 mL). The

combined organic layer was passed through a hydrophobic frit and concentrated under reduced pressure. The crude mixture was purified by silica gel chromatography using 0-20% 3:1 EtOAc:EtOH (with 1% Et₃N modifier)/cyclohexane as the eluent, to afford **4.2.18e** (0.31 g, 14%) as a yellow oil.

LCMS (Method A, UV, ESI) R_t = 1.12 min, [M+H]⁺: 190.2

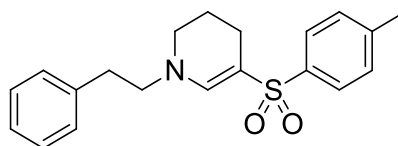
¹H NMR (400 MHz, CD₂Cl₂) δ 7.23-7.30 (m, 2H), 7.14-7.22 (m, 3H), 2.72-2.80 (m, 2H), 2.48-2.55 (m, 2H), 2.36-2.48 (m, 4H), 1.57 (dt, *J* = 11.2, 5.5 Hz, 4H), 1.39-1.48 (m, 2H)

¹³C NMR (101 MHz, CD₂Cl₂) δ 141.7, 129.3, 128.8, 126.3, 61.8, 55.1, 34.1, 26.7, 25.2

IR ν_{max} (thin film): 2932, 1452, 1154

HRMS: Calculated for C₁₃H₂₀N [M+H]⁺: 190.1596, found [M+H]⁺ 190.1601 (2.6 ppm).

1-Phenethyl-5-tosyl-1,2,3,4-tetrahydropyridine **4.2.23**



General procedure for the oxidative C–H sulfonylation of amines A was followed. A solution of **4.2.18e** (108 mg, 0.57 mmol) in THF (0.1 M) was added to NIS (513 mg, 2.28 mmol), which was stirred at RT for 30 min, then transferred *via* syringe to a suspension of **4.1.11** (153 mg, 0.86 mmol) in THF (0.3 M), and THF was used to rinse the NIS/amine reaction vessel to ensure complete transfer to give a resulting reaction concentration of 0.06 M. ¹H NMR analysis of the crude material against 3,4,5-trichloropyridine (0.155 mmol) as a standard showed 81% conversion to **4.2.23**. The crude material was purified by silica gel chromatography using 0-30% EtOAc/cyclohexane as the eluent to afford **4.2.23** (136 mg, 70%) as an orange oil.

LCMS (Method A, UV, ESI) R_t = 1.24 min, [M+H]⁺: 342.1

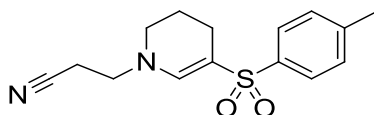
^1H NMR (400 MHz, DMSO- d_6) δ 7.41 (d, J = 8.1 Hz, 2H), 7.23-7.33 (m, 7H), 7.06 (s, 1H), 3.47 (t, J = 6.8 Hz, 2H), 3.07 (t, J = 5.4 Hz, 2H), 2.79 (t, J = 6.8 Hz, 2H), 2.37 (s, 3H), 1.90 (t, J = 6.1 Hz, 2H), 1.61 (quin, J = 6.1 Hz, 2H)

^{13}C NMR (101 MHz, DMSO- d_6) δ 144.2, 141.7, 140.1, 138.7, 129.3, 128.9, 128.3, 126.1 (2C), 97.4, 56.1, 44.5, 34.0, 20.8, 20.3, 19.3

IR ν_{max} (thin film): 2929, 1619, 1278, 1134, 1095

HRMS: Calculated for $\text{C}_{20}\text{H}_{24}\text{NO}_2\text{S}$ $[\text{M}+\text{H}]^+$: 342.1528, found $[\text{M}+\text{H}]^+$ 342.1533 (1.5 ppm).

3-(5-Tosyl-3,4-dihydropyridin-1-yl)propanenitrile **4.2.24**



General procedure for the oxidative C–H sulfonylation of amines **C** was followed. A solution of **4.2.18f** (79 mg, 0.57 mmol) in THF (0.1 M) was added to NIS (513 mg, 2.28 mmol), which was stirred at RT for 60 min, then transferred *via* syringe to a suspension of **4.1.11** (153 mg, 0.86 mmol) in THF (0.3 M), and THF was used to rinse the NIS/amine reaction vessel to ensure complete transfer to give a resulting reaction concentration of 0.06 M. ^1H NMR analysis of the crude material against 3,4,5-trichloropyridine (0.164 mmol) as a standard showed 84% conversion to **4.2.24**. The crude material was purified by reverse phase chromatography using 0-50% MeCN/10 mM ammonium bicarbonate as the eluent to afford **4.2.24** (121 mg, 73%) as a white solid.

LCMS (Method A, UV, ESI) R_t = 0.93 min, $[\text{M}+\text{H}]^+$: 291.1

^1H NMR (400 MHz, DMSO- d_6) δ 7.61 (d, J = 8.3 Hz, 2H), 7.38 (s, 1H), 7.33 (d, J = 7.8 Hz, 2H), 3.52 (t, J = 6.4 Hz, 2H), 3.09 (t, J = 5.4 Hz, 2H), 2.78 (t, J = 6.4 Hz, 2H), 2.36 (s, 3H), 1.98 (t, J = 6.1 Hz, 2H), 1.67 (quin, J = 5.9 Hz, 2H)

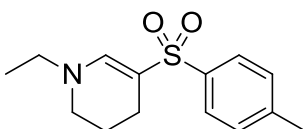
^{13}C NMR (101 MHz, DMSO- d_6) δ 144.4, 142.5, 140.5, 129.9, 126.7, 119.5, 100.5, 50.7, 44.9, 21.4, 20.9, 19.8, 17.2

IR ν_{\max} (thin film): 2936, 1621, 1277, 1135, 1095

HRMS: Calculated for $C_{15}H_{19}N_2O_2S$ $[M+H]^+$: 291.1167, found $[M+H]^+$ 291.1175 (2.7 ppm)

M.pt.: 129-131 °C.

1-Ethyl-5-tosyl-1,2,3,4-tetrahydropyridine 4.2.25



General procedure for the oxidative C–H sulfonylation of amines C was followed. A solution of **4.2.18g** (64.6 mg, 0.57 mmol) in THF (0.1 M) was added to NIS (513 mg, 2.28 mmol), which was stirred at RT for 60 min, then transferred *via* syringe to a suspension of **4.1.11** (153 mg, 0.86 mmol) in THF (0.3 M), and THF was used to rinse the NIS/amine reaction vessel to ensure complete transfer to give a resulting reaction concentration of 0.06 M. 1H NMR analysis of the crude material against 3,4,5-trichloropyridine (0.110 mmol) as a standard showed 95% conversion to **4.2.25**. The crude material was purified by silica gel chromatography using 0-20% (3:1 EtOAc-EtOH, 1% Et_3N modifier)/cyclohexane as the eluent to afford **4.2.25** (137 mg, 90%) as a white solid.

LCMS (Method A, UV, ESI) R_t = 1.07 min, $[M+H]^+$: 266.2

1H NMR (400 MHz, $DMSO-d_6$) δ 7.59 (d, J = 8.1 Hz, 2H), 7.33 (d, J = 8.1 Hz, 2H), 7.28 (s, 1H), 3.23 (q, J = 7.3 Hz, 2H), 3.03 (t, J = 5.4 Hz, 2H), 2.36 (s, 3H), 1.99 (t, J = 6.1 Hz, 2H), 1.66 (quin, J = 5.9 Hz, 2H), 1.08 (t, J = 7.1 Hz, 3H)

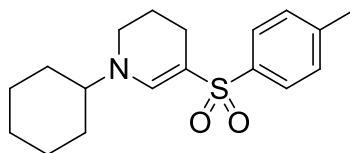
^{13}C NMR (101 MHz, $DMSO-d_6$) δ 143.7, 141.7, 140.3, 129.4, 126.1, 98.2, 49.4, 44.0, 20.8, 20.5, 19.4, 13.6

IR ν_{\max} (thin film): 2933, 1618, 1280, 1136, 1095

HRMS: Calculated for $C_{14}H_{20}NO_2S$ $[M+H]^+$: 266.1215, found $[M+H]^+$ 266.1215 (0.0 ppm)

M.pt.: 109-111 °C.

1-Cyclohexyl-5-tosyl-1,2,3,4-tetrahydropyridine 4.2.26



General procedure for the oxidative C–H sulfonylation of amines A was followed. A solution of **4.2.18h** (96 mg, 0.57 mmol) in THF (0.1 M) was added to NIS (513 mg, 2.28 mmol), which was stirred at RT for 30 min, then transferred *via* syringe to a suspension of **4.1.11** (153 mg, 0.86 mmol) in THF (0.3 M), and THF was used to rinse the NIS/amine reaction vessel to ensure complete transfer to give a resulting reaction concentration of 0.06 M. ¹H NMR analysis of the crude material against 3,4,5-trichloropyridine (0.107 mmol) as a standard showed 93% conversion to **4.2.26**. The crude material was purified by silica gel chromatography using 0-20% EtOAc/cyclohexane as the eluent to afford **4.2.26** (155.5 mg, 85%) as a white solid.

LCMS (Method A, UV, ESI) $R_t = 1.32$ min, $[M+H]^+$: 320.2

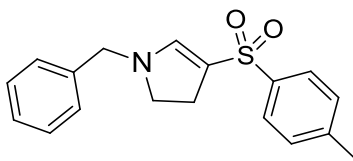
¹H NMR (400 MHz, DMSO-*d*₆) δ 7.59 (d, $J = 8.1$ Hz, 2H), 7.33 (d, $J = 8.1$ Hz, 2H), 7.29 (s, 1H), 3.12 (tt, $J = 11.5, 3.2$ Hz, 1H), 3.05 (t, $J = 5.4$ Hz, 2H), 2.36 (s, 3H), 2.00 (t, $J = 6.1$ Hz, 2H), 1.73 (t, $J = 13.6$ Hz, 4H), 1.63 (quin, $J = 6.0$ Hz, 2H), 1.58 (d, $J = 12.7$ Hz, 1H), 1.39 (qd, $J = 12.7, 3.9$ Hz, 2H), 1.26 (qt, $J = 12.7, 2.9$ Hz, 2H), 1.09 (qt, $J = 13.0, 3.2$ Hz, 1H)

¹³C NMR (101 MHz, DMSO-*d*₆) δ 142.3, 141.7, 140.3, 129.4, 126.1, 98.0, 62.7, 42.2, 30.7, 25.0, 24.8, 20.8, 20.8, 20.0

IR ν_{max} (thin film): 2930, 1615, 1280, 1132, 1093

HRMS: Calculated for C₁₈H₂₆NO₂S $[M+H]^+$: 320.1684, found $[M+H]^+$ 320.1682 (-0.6 ppm)

M.pt.: 145-147 °C.

1-Benzyl-4-tosyl-2,3-dihydro-pyrrole 4.2.27

General procedure for the oxidative C–H sulfonylation of amines **C** was followed. A solution of **2.1.8e** (100 mg, 0.62 mmol) in THF (0.1 M) was added to NIS (558 mg, 2.48 mmol), which was stirred at RT for 60 min, then transferred *via* syringe to a suspension of **4.1.11** (166 mg, 0.93 mmol) in THF (0.3 M), and THF was used to rinse the NIS/amine reaction vessel to ensure complete transfer to give a resulting reaction concentration of 0.06 M. The crude material was purified by silica gel chromatography using 0-30% EtOAc/cyclohexane as the eluent to afford **4.2.27** (43 mg, 22%) as a green gum.

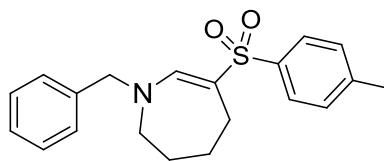
LCMS (Method A, UV, ESI) $R_t = 1.18$ min, $[M+H]^+$: 314.1

^1H NMR (400 MHz, DMSO- d_6) δ 7.62 (d, $J = 8.3$ Hz, 2H), 7.40 (s, 1H), 7.34-7.39 (m, 4H), 7.29-7.32 (m, 1H), 7.25-7.28 (m, 2H), 4.30 (s, 2H), 3.33 (t, $J = 10.3$ Hz, 2H), 2.51-2.53 (m, 2H), 2.37 (s, 3H)

^{13}C NMR (101 MHz, DMSO- d_6) δ 151.7, 142.1, 140.0, 136.6, 129.6, 128.5, 128.0, 127.5, 125.9, 104.6, 52.8, 51.0, 27.2, 20.9

IR ν_{max} (thin film): 2924, 1578, 1301, 1138, 1091

HRMS: Calculated for $\text{C}_{18}\text{H}_{20}\text{NO}_2\text{S}$ $[M+H]^+$: 314.1215, found $[M+H]^+$ 314.1213 (-0.6 ppm).

1-Benzyl-6-tosyl-2,3,4,5-tetrahydro-azepine 4.2.28

General procedure for the oxidative C–H sulfonylation of amines D was followed. A solution of **2.1.8f** (108 mg, 0.57 mmol) in DMSO (0.1 M) was added to NIS (513 mg, 2.28 mmol), which was stirred at RT for 30 min, then transferred *via* syringe to a suspension of **4.1.11** (306 mg, 1.71 mmol) in DMSO (0.3 M), and DMSO was used to rinse the NIS/amine reaction vessel to ensure complete transfer to give a resulting reaction concentration of 0.06 M. ¹H NMR analysis of the crude material against 3,4,5-trichloropyridine (0.114 mmol) as a standard showed 22% conversion to **4.2.28**. The crude material was purified by silica gel chromatography using 0-20% EtOAc/cyclohexane as the eluent to afford **4.2.28** (37 mg, 19%) as a colourless oil.

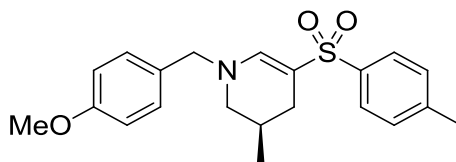
LCMS (Method A, UV, ESI) $R_t = 1.29$ min, $[M+H]^+$: 342.0

¹H NMR (400 MHz, DMSO-*d*₆) δ 7.62 (d, $J = 8.3$ Hz, 2H), 7.51 (s, 1H), 7.28-7.42 (m, 7H), 4.45 (s, 2H), 3.17 (t, $J = 5.4$ Hz, 2H), 2.38 (s, 3H), 2.19 (t, $J = 6.4$ Hz, 2H), 1.46-1.62 (m, 4H)

¹³C NMR (101 MHz, DMSO-*d*₆) δ 148.1, 142.0, 139.9, 137.9, 129.4, 128.6, 127.5, 127.4, 126.4, 104.4, 61.3, 51.6, 27.5, 26.2, 25.7, 20.9

ν_{max} (thin film): 2920, 1634, 1280, 1135, 1088

HRMS: Calculated for C₂₀H₂₄NO₂S $[M+H]^+$: 342.1528, found $[M+H]^+$ 342.1526 (-0.6 ppm).

(R)-1-(4-Methoxybenzyl)-3-methyl-5-tosyl-1,2,3,4-tetrahydropyridine 4.2.29

General procedure for the oxidative C–H sulfonylation of amines **A** was followed. A solution of **2.1.8s** (108 mg, 0.49 mmol) in THF (0.1 M) was added to NIS (513 mg, 2.28 mmol), which was stirred at RT for 30 min, then transferred *via* syringe to a suspension of **4.1.11** (151 mg, 0.85 mmol) in THF (0.3 M), and THF was used to rinse the NIS/amine reaction vessel to ensure complete transfer to give a resulting reaction concentration of 0.06 M. ¹H NMR analysis of the crude material against 3,4,5-trichloropyridine (0.165 mmol) as a standard showed 58% conversion to **4.2.29**. The crude material was purified by silica gel chromatography using 0-30% EtOAc/cyclohexane as the eluent to afford **4.2.29** (93 mg, 51%) as an off-white solid.

LCMS (Method A, UV, ESI) $R_t = 1.28$ min, $[M+H]^+$: 372.1

¹H NMR (400 MHz, DMSO-*d*₆) δ 7.61 (d, $J = 8.3$ Hz, 2H), 7.52 (s, 1H), 7.35 (d, $J = 8.1$ Hz, 2H), 7.19 (d, $J = 8.6$ Hz, 2H), 6.93 (d, $J = 8.6$ Hz, 2H), 4.37 (d, $J = 14.7$ Hz, 1H), 4.30 (d, $J = 14.7$, 1H), 3.75 (s, 3H), 2.93 (ddd, $J = 12.7, 3.7, 1.7$ Hz, 1H), 2.51-2.55 (m, 1H), 2.36 (s, 3H), 2.09 (ddd, $J = 9.8, 4.9, 1.2$ Hz, 1H), 1.65-1.77 (m, 1H), 1.58 (dd, $J = 15.2, 8.8$ Hz, 1H), 0.77 (d, $J = 6.6$ Hz, 3H)

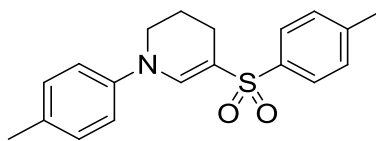
¹³C NMR (101 MHz, DMSO-*d*₆) δ 158.7, 143.8, 141.8, 140.2, 129.4, 129.1, 129.0, 126.1, 113.9, 98.9, 57.5, 55.0, 50.7, 27.3, 25.6, 20.9, 18.0

IR ν_{\max} (thin film): 2919, 1619, 1513, 1281, 1249, 1134, 1088

HRMS: Calculated for C₂₁H₂₆NO₃S $[M+H]^+$: 372.1633, found $[M+H]^+$ 372.1638 (1.3 ppm)

M.pt.: 120-122 °C

Chiral HPLC (25 cm Chiralpak AD, 40% EtOH/*n*-heptane, 1.0 mL/min, detection at 215 nm) $R_t = 8.6$ min, ee >99%.²⁸⁵

1-(*para*-Tolyl)-5-tosyl-1,2,3,4-tetrahydropyridine 4.2.30

General procedure for the oxidative C–H sulfonylation of amines A was followed. A solution of **2.1.8k** (35 mg, 0.20 mmol) in THF (0.1 M) was added to NIS (180 mg, 0.80 mmol), which was stirred at RT for 30 min, then transferred *via* syringe to a suspension of **4.1.11** (53.4 mg, 0.30 mmol) in THF (0.3 M), and THF was used to rinse the NIS/amine reaction vessel to ensure complete transfer to give a resulting reaction concentration of 0.06 M. ¹H NMR analysis of the crude material against 3,4,5-trichloropyridine (0.083 mmol) as a standard showed 49% conversion to **4.2.30**. The crude material was purified by silica gel chromatography using 0-20% EtOAc/cyclohexane as the eluent to afford **4.2.30** (33 mg, 51%) as an off-white solid.

LCMS (Method A, UV, ESI) $R_t = 1.31$ min, $[M+H]^+$: 328.1

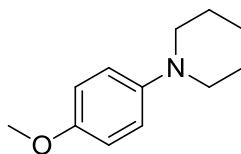
¹H NMR (400 MHz, DMSO-*d*₆) δ 7.71 (d, $J = 8.1$ Hz, 2H), 7.66 (s, 1H), 7.38 (d, $J = 8.1$ Hz, 2H), 7.19 (d, $J = 8.1$ Hz, 2H), 7.09 (d, $J = 8.6$ Hz, 2H), 3.53 (t, $J = 5.4$ Hz, 2H), 2.38 (s, 3H), 2.28 (s, 3H), 2.12 (t, $J = 6.1$ Hz, 2H), 1.84 (quin, $J = 6.1$ Hz, 2H)

¹³C NMR (101 MHz, DMSO-*d*₆) δ 142.7, 139.0, 138.7, 132.2, 131.2, 129.8, 129.6, 126.6, 117.6, 106.6, 45.3, 20.9, 20.6, 20.1, 19.6

IR ν_{max} (thin film): 2929, 1623, 1514, 1283, 1142, 1100

HRMS: Calculated for C₁₉H₂₂NO₂S $[M+H]^+$: 328.1371, found $[M+H]^+$ 328.1372 (0.3 ppm)

M.pt.: 134-136 °C.

1-(4-Methoxyphenyl)piperidine 4.2.18m

A solution of 4-methoxyaniline (1.00 g, 8.12 mmol) in MeCN (9 mL) was added to a mixture of 1,5-dibromopentane (2.28 mL, 16.2 mmol) and potassium carbonate (4.5 g, 32.5 mmol) in MeCN (16 mL), and the reaction mixture was stirred at 80 °C for 24 h. The reaction mixture was filtered through a sintered funnel, and the filtrate was concentrated under reduced pressure. The crude material was purified by silica gel chromatography using 0-30% 3:1 EtOAc:EtOH (with 1% Et₃N modifier)/cyclohexane as the eluent to afford **4.2.18m** (0.86 g, 55%) as a yellow oil.

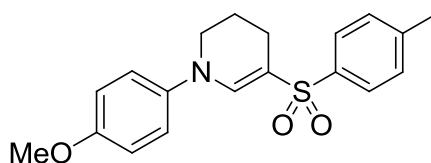
LCMS (Method A, UV, ESI) R_t = 1.17 min, [M+H]⁺: 192.1

¹H NMR (400 MHz, CD₂Cl₂) δ 6.85-6.90 (m, 2H), 6.77-6.82 (m, 2H), 3.74 (s, 3H), 3.00 (t, *J* = 5.6 Hz, 4H), 1.70 (quin, *J* = 5.7 Hz, 4H), 1.50-1.58 (m, 2H)

¹³C NMR (101 MHz, CD₂Cl₂) δ 154.1, 147.7, 119.1, 114.8, 56.0, 52.7, 26.8, 24.9

IR ν_{max} (thin film): 2929, 1508, 1231, 1039

HRMS: Calculated for C₁₂H₁₈NO [M+H]⁺: 192.1388, found [M+H]⁺ 192.1392 (2.1 ppm).

1-(4-Methoxyphenyl)-5-tosyl-1,2,3,4-tetrahydropyridine 4.2.31

General procedure for the oxidative C–H sulfonylation of amines A was followed. A solution of **4.2.18m** (109 mg, 0.57 mmol) in THF (0.1 M) was added to NIS (513 mg, 2.28 mmol), which was stirred at RT for 30 min, then transferred *via* syringe to a suspension of **4.1.11** (153 mg, 0.86 mmol) in THF (0.3 M), and THF was used to rinse the NIS/amine reaction vessel to ensure complete transfer to give a resulting reaction

concentration of 0.06 M. ^1H NMR analysis of the crude material against 3,4,5-trichloropyridine (0.177 mmol) as a standard showed 32% conversion to **4.2.31**. The crude material was purified by silica gel chromatography using 0-30% EtOAc/cyclohexane as the eluent to afford **4.2.31** (53 mg, 27%) as a white solid.

LCMS (Method A, UV, ESI) $R_t = 1.22$ min, $[\text{M}+\text{H}]^+$: 344.0

^1H NMR (400 MHz, $\text{DMSO-}d_6$) δ 7.70 (d, $J = 8.3$ Hz, 2H), 7.59 (s, 1H), 7.37 (d, $J = 8.1$ Hz, 2H), 7.14 (d, $J = 9.0$ Hz, 2H), 6.95 (d, $J = 9.0$ Hz, 2H), 3.74 (s, 3H), 3.51 (t, $J = 5.4$ Hz, 2H), 2.38 (s, 3H), 2.11 (t, $J = 6.1$ Hz, 2H), 1.83 (quin, $J = 5.7$ Hz, 2H)

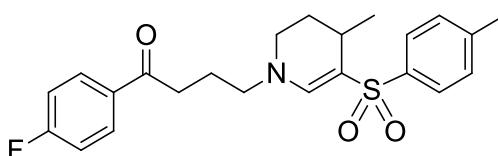
^{13}C NMR (101 MHz, $\text{DMSO-}d_6$) δ 155.6, 142.4, 139.4, 139.2, 138.8, 129.6, 126.6, 119.6, 114.6, 105.6, 55.3, 45.9, 20.9, 20.6, 19.5

IR ν_{max} (thin film): 2935, 1620, 1512, 1246, 1141, 1102

HRMS: Calculated for $\text{C}_{19}\text{H}_{22}\text{NO}_3\text{S}$ $[\text{M}+\text{H}]^+$: 344.1320, found $[\text{M}+\text{H}]^+$ 344.1322 (0.6 ppm)

M.pt.: 189-191 °C.

1-(4-Fluorophenyl)-4-(4-methyl-5-tosyl-3,4-dihydropyridin-1-yl)butan-1-one
4.2.32



General procedure for the oxidative C–H sulfonylation of amines **C** was followed. A solution of the hydrochloride salt of **1.3.25** (42 mg, 0.14 mmol) in THF (0.1 M) was added to NIS (126 mg, 0.56 mmol), which was stirred at RT for 60 min, then transferred *via* syringe to a suspension of **4.1.11** (37 mg, 0.21 mmol) in THF (0.3 M), and THF was used to rinse the NIS/amine reaction vessel to ensure complete transfer to give a resulting reaction concentration of 0.06 M. The crude material was purified by silica gel chromatography using 0-30% EtOAc/cyclohexane as the eluent to afford **4.2.32** (20 mg, 34%) as a white solid.

LCMS (Method A, UV, ESI) $R_t = 1.28$ min, $[M+H]^+$: 416.1

^1H NMR (400 MHz, DMSO- d_6) δ 8.01-8.07 (m, 2H), 7.55 (d, $J = 8.3$ Hz, 2H), 7.33-7.39 (m, 2H), 7.32 (s, 1H), 7.27 (d, $J = 8.1$ Hz, 2H), 3.31-3.41 (m, 2H), 3.09 (dd, $J = 8.8, 3.2$ Hz, 2H), 3.02 (t, $J = 7.0$ Hz, 2H), 2.34 (s, 3H), 2.26-2.32 (m, 1H), 1.81-1.94 (m, 2H), 1.53 (dq, $J = 13.0, 2.4$ Hz, 1H), 1.33-1.44 (m, 1H), 0.88 ppm (d, $J = 6.8$ Hz, 3H)

^{13}C NMR (101 MHz, DMSO- d_6) δ 198.4, 165.4 (d, $^1J_{\text{C-F}} = 250.2$ Hz), 145.0, 142.1, 141.9, 133.8 (d, $^4J_{\text{C-F}} = 2.2$ Hz), 131.3 (d, $^3J_{\text{C-F}} = 8.8$ Hz), 129.8, 129.6, 126.6, 116.2 (d, $^2J_{\text{C-F}} = 21.3$ Hz), 103.5, 54.8, 35.2, 28.0, 24.9, 22.9, 22.0, 21.4

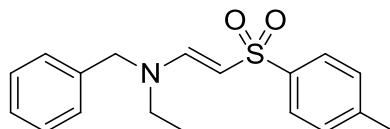
^{19}F NMR (CDCl_3 , 376 MHz): δ -104.78 (s, 1F)

IR ν_{max} (thin film): 2927, 1685, 1614, 1278, 1133, 1087, 667

HRMS: Calculated for $\text{C}_{23}\text{H}_{27}\text{NO}_3\text{FS}$ $[M+H]^+$: 416.1696, found $[M+H]^+$ 416.1694 (-0.5 ppm)

M.pt.: 180-182 °C.

(E)-N-Benzyl-N-ethyl-2-tosylethen-1-amine 4.2.34



General procedure for the oxidative C–H sulfonylation of amines **C** was followed. A solution of the hydrochloride salt of **4.2.33** (93 mg, 0.57 mmol) in THF (0.1 M) was added to NIS (513 mg, 2.28 mmol), which was stirred at RT for 60 min, then transferred *via* syringe to a suspension of **4.1.11** (153 mg, 0.86 mmol) in THF (0.3 M), and THF was used to rinse the NIS/amine reaction vessel to ensure complete transfer to give a resulting reaction concentration of 0.06 M. ^1H NMR analysis of the crude material against 3,4,5-trichloropyridine (0.169 mmol) as a standard showed 62% conversion to **4.2.34**. The crude material was purified by silica gel chromatography using 0-30% EtOAc/cyclohexane as the eluent to afford **4.2.34** monohydrate (89 mg, 47%) as a yellow gum.

LCMS (Method A, UV, ESI) $R_t = 1.19$ min, $[M+H]^+$: 316.0

^1H NMR (600 MHz, $\text{DMSO-}d_6$) δ 7.64 (br. s, 2H), 7.47 (d, $J = 12.7$ Hz, 1H), 7.17-7.40 (m, 7H), 5.17 (br. s, 1H), 4.27-4.55 (m, 2H), 3.34 (br. s, 1H), 3.05 (br. s, 1H), 2.37 (s, 3H), 0.82-1.22 (m, 3H)

^{13}C NMR (151 MHz, $\text{DMSO-}d_6$) δ 149.8, 142.9, 141.5, 137.4, 129.3, 128.5, 127.7, 127.0, 125.5, 92.1, 57.3, 42.1, 20.8, 10.4

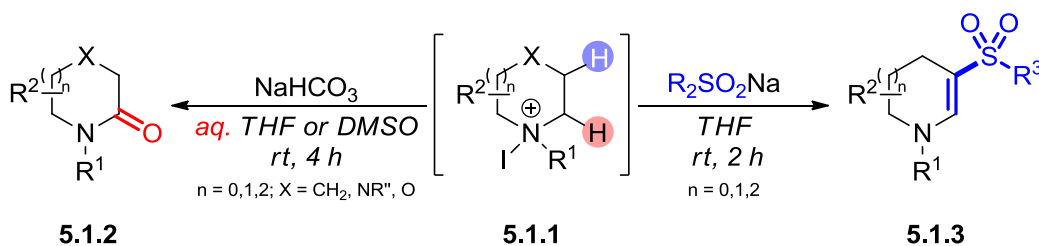
IR ν_{max} (thin film): 2976, 1613, 1280, 1134, 1081

HRMS: Calculated for $\text{C}_{18}\text{H}_{22}\text{NO}_2\text{S}$ $[M+H]^+$: 316.1371, found $[M+H]^+$ 316.1376 (1.6 ppm)

M.pt.: 118-120 °C.

Overall Conclusions

This thesis has developed two oxidative C–H functionalisation methodologies that proceed *via* activation of saturated cyclic basic amines with electrophilic iodine to *N*-iodoammonium intermediates **5.1.1** (Scheme 124).



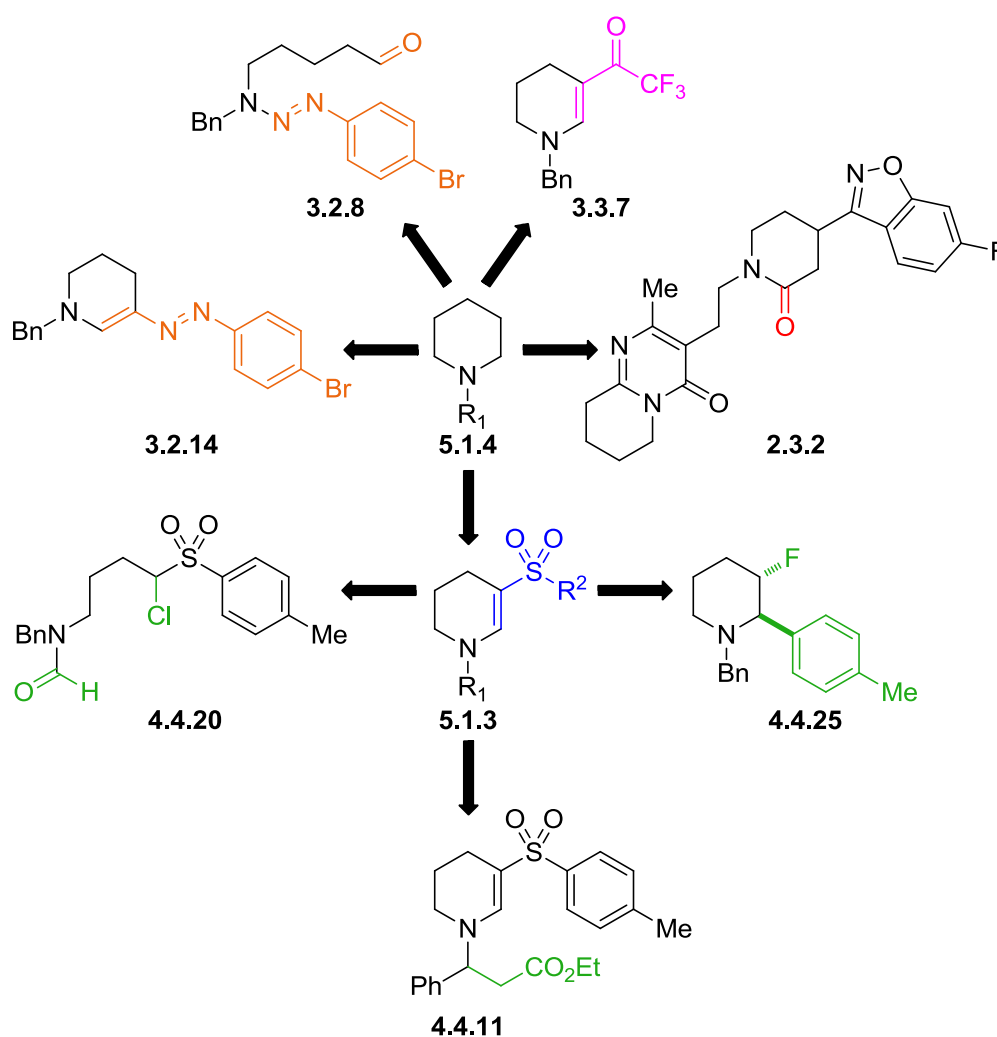
Scheme 124. Highly selective iodine-mediated oxidative C–H functionalisation of saturated *N*-heterocycles.

It was demonstrated that intermediate **5.1.1** could be used as a general intermediate to access either α or β -C–H functionalised saturated nitrogen heterocycles. Functionalisation of the α -position was achieved by α -deprotonation and interception of the resultant iminium with water, to afford lactams such as **5.1.2**. This was elaborated as a platform for late-stage oxidation of a series of high value small molecules, and modulation of physicochemical and medicinal chemistry properties of a selection of substrates was demonstrated, validating the application for drug discovery. Expansion of the portfolio of C–H oxidation substrates demonstrated the subtleties and the range of transformations possible when carrying out innate C–H functionalisation reactions. These findings could highlight points on chemical templates that are susceptible to oxidation, and, as a result, are liable to oxidative mechanisms of metabolism.

The iodine-mediated C–H oxidation protocol was subsequently expanded, with selective access to the β -functionalised enaminyl sulfones **5.1.3** achieved by trapping the intermediary enamine with an electrophilic sulfonyl iodide, which was generated *in situ*. This provided facile access to a synthetic scaffold that was used to generate a

diverse library of functionality onto the azacyclic scaffold from one common starting material.

Oxidative functionalisation provided access to a wide variety of diverse molecular frameworks. The research conducted within this thesis has described endocyclic and exocyclic C–H functionalisation, and has also afforded some novel ring-opening products, providing expedient access to complex structures, such as those described in Scheme 125.

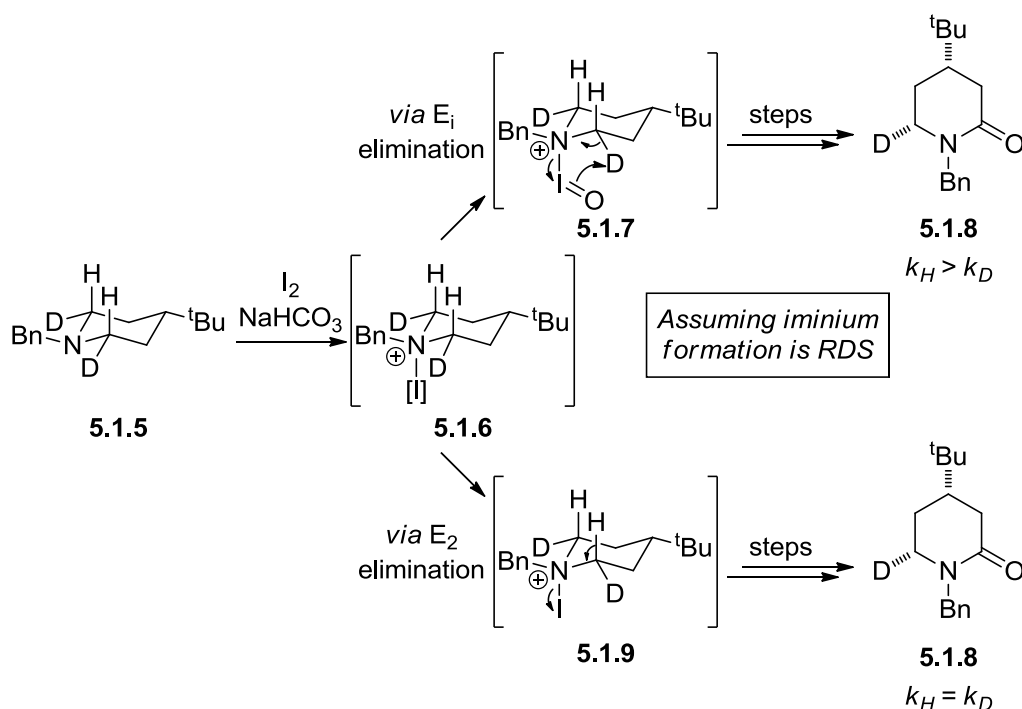


Scheme 125. Oxidative C–H functionalisation of cyclic amine scaffolds provided access to a diverse array of molecular scaffolds.

This validates the concept of C–H functionalisation to facilitate the rapid and selective diversification of molecular frameworks. It is envisaged that these techniques can be applied to the late-stage functionalisation and diversification of late-stage molecules to expedite the drug discovery.

Future Work

Future work required for the C–H oxidation of azacycles such as **5.1.4** to lactams such as **5.1.2** would involve increasing the mechanistic understanding of the reaction, which could help to improve the yields and the functional group tolerance of this process, and increase the scope of the protocol to other forms of C–H functionalisation. An improved understanding could be achieved through the use of deuterium-labelled substrate **5.1.5**⁴¹⁸ (Scheme 126) and investigating a kinetic isotope effect (KIE) to examine the effect of axial or equatorial deuteration on the rate of reaction.



Scheme 126. Possible kinetic isotope effect experiment to test the possibility of either an E_1 or an E_2 elimination occurring in the deprotonation of intermediate **5.1.6**. If an E_1 mechanism is followed, then a slower rate would be observed for the deuterated substrate compared to hydrogenated substrate, due to the increased bond strength of the C–D bond compared to the C–H bond.

A bulky substituent, such as a *tert*-butyl group, in the γ -position would provide a ring-locking effect to the azacycle, holding the deuterium atoms in the equatorial position. If iminium ion formation is the rate-determining step (RDS), then it may be possible to elucidate whether equatorial deprotonation occurs through an E_i mechanism *via* *N*-iodoso intermediate **5.1.7**, driven by release of 1,3-diaxial strain, or if iminium formation occurs as a result of a *trans*-diaxial arrangement of the C–H and N–I bonds in *N*-iodoammonium intermediate **5.1.9**. KIE analysis would only provide mechanistic information if the iminium formation is the rate-determining step, and as such ^{127}I NMR could be used to provide evidence of the formation of a *N*-iodoso-intermediate, which would suggest an E_i mechanism. The addition of functional groups onto the ring of the azacycle, such as **5.1.10** (Figure 40), could also provide insight into the nature of iminium formation.

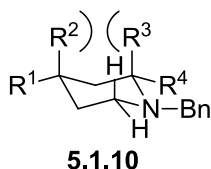


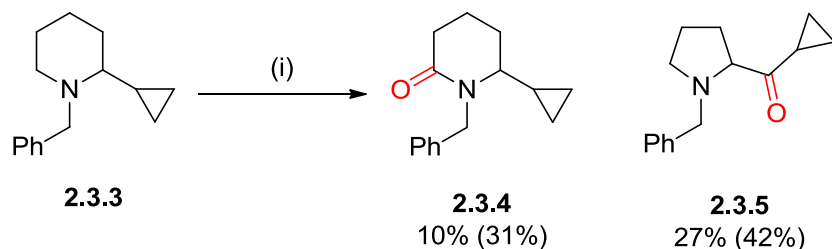
Figure 40. Modulating the nature of substituents R^1 to R^4 may lead to an increase in reaction rate or reaction yield with increased steric bulk, which would indicate an E_i mechanism.

The effect of changing the steric hindrance created by substituents R^1 to R^4 on the rate of oxidation can be examined by *in situ* infrared analysis, for example. If an increased reaction rate or yield of lactam is observed with increasing 1,3-diaxial strain, then this would be indicative of release of strain being a driving force in the rate-determining step, which would suggest an E_i mechanism.

More robust computational analysis of the reaction process, using density functional theory calculations, could allow for the development of predictive models for the mechanistic pathway taking place. This could provide an improved ability to predict the outcome of different substrates to oxidative functionalisation, which would add value for medicinal chemistry groups interesting in carrying out late-stage transformations on precious intermediates. It may also allow for the optimisation of

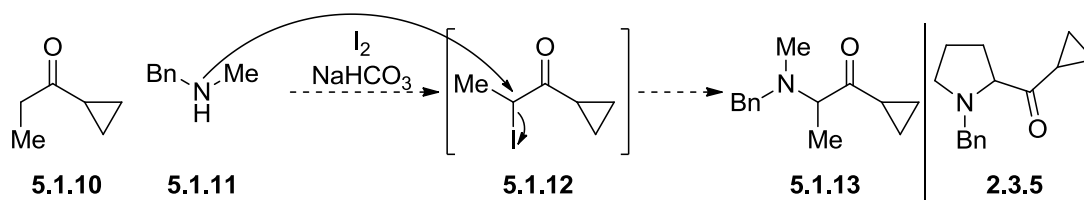
the reaction process, making it more sustainable and more tolerant of highly electron-rich systems.

The ring contraction of cyclopropyl-substituted substrate **2.3.3** to **2.3.5** was an unexpected transformation (Scheme 127).



Scheme 127. Radical-clock investigation using 2.3.3. Conditions: (i) I₂ (7.5 eq.), NaHCO₃ (10.0 eq.), THF:H₂O (2.5:1, 0.025 M), RT, 4 h. Isolated yields shown; values in parentheses show conversion to product determined by ¹H NMR analysis of the crude material against an internal standard.

Probing how this transformation occurred could enable similar ring contraction processes to be carried out predictably and selectively within complex and late-stage systems. This could be carried out by the reaction of fragment molecules **5.1.10** and **5.1.11** in the presence of iodine (Scheme 128).



Scheme 128. The mechanism of formation of 2.3.5 could be probed by the reaction of 5.1.10 and 5.1.11 in the presence of iodine.

Condensation of amine **5.1.11** onto ketone **5.1.10** would be reversible under the aqueous reaction conditions, meaning that α -iodoketone **5.1.12** could be formed. This can then undergo nucleophilic attack by **5.1.11** to afford α -aminoketone **5.1.13**. With this insight into the likely intermediates in the formation of **2.3.5**, the protocol could feasibly be explored further by examining the effect of varying the α -substituent to

groups other than a cyclopropyl ring: vinyl, aryl, alkoxy, for example. These, in turn, would provide information on the electronic and steric factors that cause this rearrangement to occur.

The potential to generalise the oxidative C–H sulfonylation to incorporate a wider array of electrophiles has already been evidenced with formation of enaminyll diazene **3.2.14** and enaminyll ketone **3.3.7** (Figure 41).

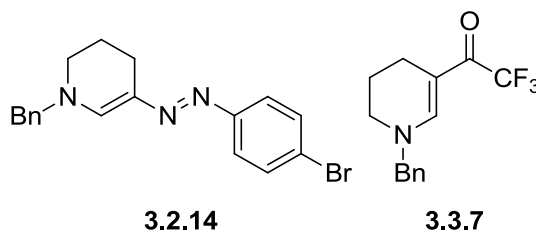
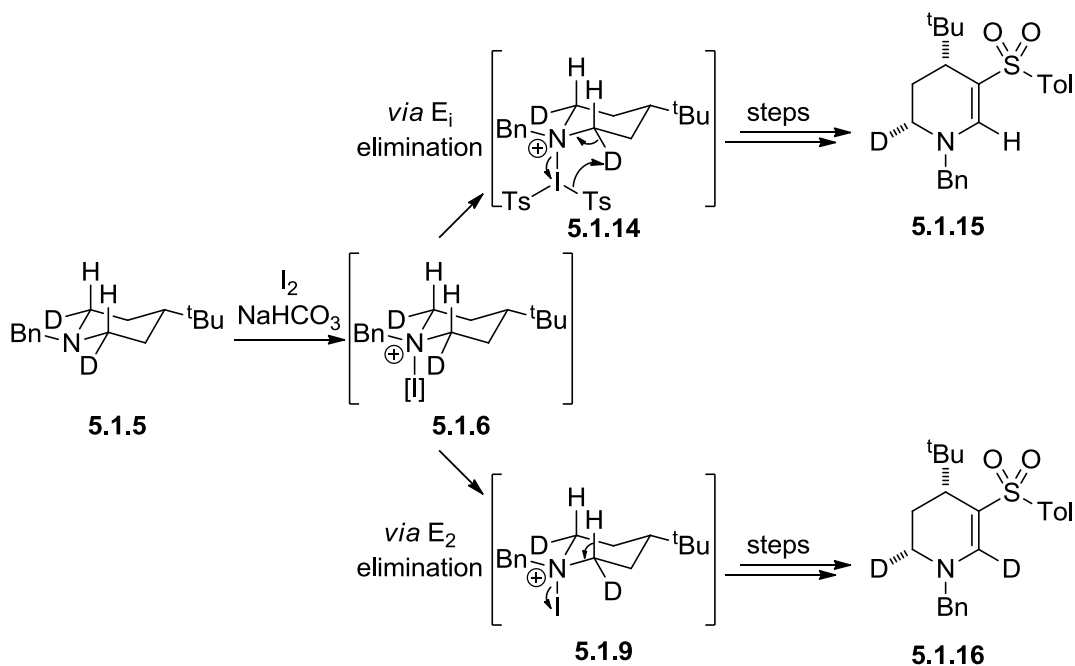


Figure 41. β -C–H functionalisation of azacycles with alternative electrophiles.

Further research into increasing the understanding of the mechanistic pathway of the sulfonylation reaction could enable a more logical and systematic elaboration to other oxidative C–H functionalisation protocols, thereby widening the scope of this protocol. Isotopic-enrichment studies could be carried out to examine the possibility of an E_i mechanism in this system, with isotopic enrichment of products **5.1.15** and **5.1.16** providing insight into the reaction mechanism (Scheme 129).



Scheme 129. Possible kinetic isotope effect experiment to test the possibility of either an E₁ or an E₂ elimination occurring in the oxidative C–H sulfonation of azacycles. Ts = *p*-toluenesulfonyl. Tol = *p*-tolyl.

These investigations could also be useful for expanding the scope of the oxidative C–H sulfonation to allow for re-optimisation of the conditions to accommodate substrates that previously did not work well, such as piperazine **2.1.8h**. It was proposed that this substrate was not compatible with the oxidative C–H sulfonation protocol due to decomposition of an intermediate, promoted by the electron-withdrawing nature of the heteroatom in the γ -position. This could be remedied by exploration and removal of the source of this decomposition. Additionally, the use of different substituents on the piperazine ring that are less electron-withdrawing than a Boc group, such as a *tert*-butyl group or a methyl group (Figure 42) may promote less weakening of the C–S bond in the purported α -sulfonyl intermediate.

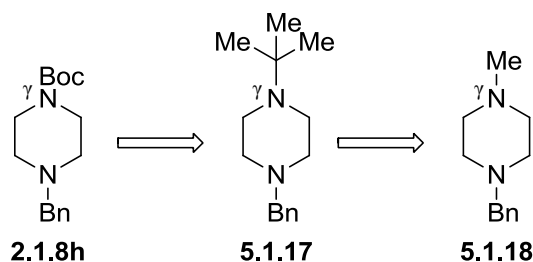
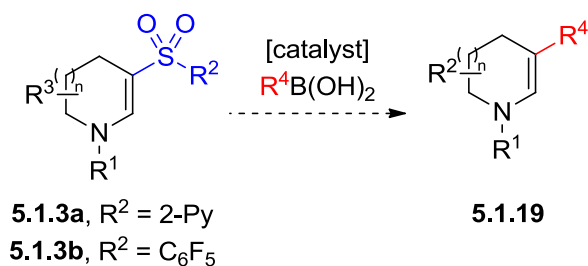


Figure 42. Modulation of the electronics of the piperazine nitrogen (N_γ) may lead to a piperazine substrate that is more compatible with the oxidative C–H sulfonylation conditions.

Future studies would also involve expanding the profile of synthetic application of the enaminyll sulfone motif. Electron-deficient sulfones have been exemplified as electrophiles in cross-coupling reactions,^{419–422} therefore it would be of interest to explore whether the oxidative C–H sulfonylation procedure could be a useful precursor to a wider array of β -functionalised motifs, such as **5.1.19** (Scheme 130).



Scheme 130. Use of the sulfone group in enaminyll sulfones as a handle for cross-coupling to access a wider array of β -functionalised products.

However, in order to achieve this, the oxidative sulfonylation protocol may need to be optimised further to allow for more efficient installation of pyridyl-sulfones, which could be achieved by avoiding the intermediary sulfonyl iodide by using alternative halogen sources. Alternatively, oxidative addition may be possible by using fluoroarene-substituted sulfones, as these would mimic the electron-deficient nature of pyridyl-substituents, but without the basic nature of the pyridyl nitrogen destabilising the sulfonyl iodide. Oxidative addition across more electron-rich carbon-sulfone bonds may be achieved through the thorough screening of metal catalysts and the exploration of photochemical conditions.⁴²³ This could be initiated by carrying out high-throughput catalyst screens in a 96-well plate format, to cover as much chemical space in as short a time as possible. In addition, measuring or modelling the bond

enthalpy or reduction potential of the C–S bond could allow for reaction design, and the use of electrochemical or photoredox conditions to match this energy, which could lead to C–S bond cleavage in cross coupling reactions.

The enaminyll sulfone motif has been exemplified to be highly amenable to selective asymmetric reduction conditions. Halogenation with electrophilic reagents was also shown, which gave access to trisubstituted manifolds *via* interception of the fluoroiminium intermediates with a high degree of diastereoselectivity. The use of asymmetric hydrogenation conditions could lead to the formation of enantiomerically-enriched β -sulfonylpiperidine scaffolds,^{424–429} such as that found in the Danirixin **4.1.14** (Figure 43).³⁴⁴

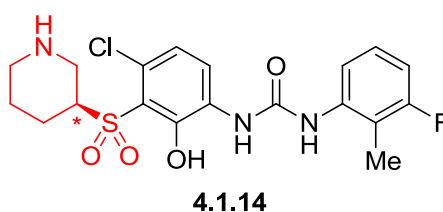
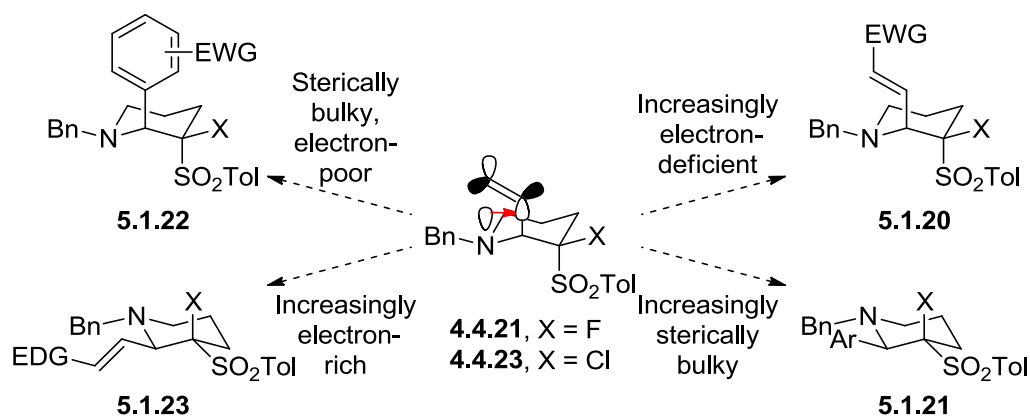


Figure 43. Asymmetric hydrogenation of the enaminyll sulfone scaffold could allow access to enantiomerically-enriched sulfones, such as **4.1.14**.

Complementarily, given the high degree of diastereomeric control observed for the halo-vinylation and halo-arylation protocols, an asymmetric halogenation step^{430–433} could lead to the preparation of enantiomerically-enriched trisubstituted azacyclic scaffolds. This could, therefore, provide straightforward access to azacyclic substrates with a high degree of three-dimensional character, which has been linked to improved physical properties and reduced promiscuity of pharmaceutical compounds.^{434,435}

Finally, stereochemical configuration and apparent anomeric effects for compounds **4.4.21** and **4.4.23** (Scheme 131) could be studied.



Scheme 131. Studying the apparent anomeric effect in compounds 4.4.21 and 4.4.23 would be interesting to explore in the future. Tol = *p*-tolyl. EWG = electron-withdrawing group. EDG = electron-donating group.

Altering the electronic and steric constraints on the vinyl group may lead to changes in the extent of this effect. Potentially, increasing the ability of the group adjacent to the nitrogen to accept electron density could increase the stability of the axial-axial arrangement **5.1.20**, while increasing the steric bulk may gradually cause a change in the conformation to give the equatorial-equatorial conformation **5.1.21**, as observed previously. Further investigations would examine whether electronic-factors could be used to overcome the energetically unfavourable axial-axial arrangement by reducing the electron-density of the aryl group in **5.1.22**. Similarly, increasing the electron-richness of the adjacent group may reduce to anomeric-type interaction, causing the more sterically favoured conformation to form sterically less-hindered substrates such as **5.1.23**. These investigations would be of interest in lead optimisation, either by providing access to novel vectors for drug molecules to grow into, or for providing rationales as to why certain ligands do not interact biologically as expected.

Bibliography

- (1) Vitaku, E.; Smith, D. T.; Njardarson, J. T. *J. Med. Chem.* **2014**, *57*, 10257–10274.
- (2) Reprinted with permission from Vitaku, E.; Smith, D. T.; Njardarson, J. T. *J. Med. Chem.* **2014**, *57*, 10257–10274. Copyright 2014 American Chemical Society.
- (3) Ritchie, T. J.; Macdonald, S. J. F.; Peace, S.; Pickett, S. D.; Luscombe, C. N. *MedChemComm* **2012**, *3*, 1062.
- (4) Petukhov, P. A.; Zhang, J.; Wang, C. Z.; Ye, Y. P.; Johnson, K. M.; Kozikowski, A. P. *J. Med. Chem.* **2004**, *47*, 3009–3018.
- (5) Nakanishi, M.; Tashiro, C.; Munakata, T.; Araki, K.; Tsumagari, T.; Imamura, H. *J. Med. Chem.* **1970**, *13*, 644–648.
- (6) Pati, B.; Banerjee, S. *J. Pharm. Res.* **2012**, *5*, 5493–5509.
- (7) Cernak, T.; Dykstra, K. D.; Tyagarajan, S.; Vachal, P.; Krska, S. W. *Chem. Soc. Rev.* **2016**, *45*, 546–576.
- (8) Dolle, R. E.; Le Bourdonnec, B.; Worm, K.; Morales, G. A.; Thomas, C. J.; Zhang, W. *J. Comb. Chem.* **2010**, *12*, 765–806.
- (9) Schreiber, S. L. *Nature* **2009**, *457*, 153–154.
- (10) Hann, M. M.; Keserü, G. M. *Nat. Rev. Drug Discov.* **2012**, *11*, 355–365.
- (11) Leung, C. S.; Leung, S. S. F.; Tirado-Rives, J.; Jorgensen, W. L. *J. Med. Chem.* **2012**, *55*, 4489–4500.
- (12) Hale, J. J.; Mills, S. G.; MacCoss, M.; Shah, S. K.; Qi, H.; Mathre, D. J.; Cascieri, M. A.; Sadowski, S.; Strader, C. D.; MacIntyre, D. E.; Metzger, J. M. *J. Med. Chem.* **1996**, *39*, 1760–1762.
- (13) Swain, C. J.; Williams, B. J.; Baker, R.; Cascieri, M. A.; Chicchi, G.; Forrest, M.; Herbert, R.; Keown, L.; Ladduwahetty, T.; Luell, S.; Macintyre, D. E.; Metzger, J.; Morton, S.; Owens, A. P.; Sadowski, S.; Watt, A. P. *Bioorg. Med. Chem. Lett.* **1997**, *7*, 2959–2962.

- (14) Lemal, D. M. *J. Org. Chem.* **2004**, *69*, 1–11.
- (15) Hale, J. J.; Mills, S. G.; MacCoss, M.; Finke, P. E.; Cascieri, M. A.; Sadowski, S.; Ber, E.; Chicchi, G. G.; Kurtz, M.; Metzger, J.; Eiermann, G.; Tsou, N. N.; Tattersall, F. D.; Rupniak, N. M. J.; Williams, A. R.; Rycroft, W.; Hargreaves, R.; MacIntyre, D. E. *J. Med. Chem.* **1998**, *41*, 4607–4614.
- (16) Pinto, D. J. P.; Orwat, M. J.; Koch, S.; Rossi, K. A.; Alexander, R. S.; Smallwood, A.; Wong, P. C.; Rendina, A. R.; Luetzgen, J. M.; Knabb, R. M.; He, K.; Xin, B.; Wexler, R. R.; Lam, P. Y. S. *J. Med. Chem.* **2007**, *50*, 5339–5356.
- (17) Gillis, E. P.; Eastman, K. J.; Hill, M. D.; Donnelly, D. J.; Meanwell, N. A. *J. Med. Chem.* **2015**, *58*, 8315–8359.
- (18) Fier, P. S.; Luo, J.; Hartwig, J. F. *J. Am. Chem. Soc.* **2013**, *135*, 2552–2559.
- (19) Tang, P.; Wang, W.; Ritter, T. *J. Am. Chem. Soc.* **2011**, *133*, 11482–11484.
- (20) Fujimoto, T.; Ritter, T. *Org. Lett.* **2015**, *17*, 544–547.
- (21) Neumann, C. N.; Hooker, J. M.; Ritter, T. *Nature* **2016**, *534*, 369–373.
- (22) Tang, P.; Furuya, T.; Ritter, T. *J. Am. Chem. Soc.* **2010**, *132*, 12150–12154.
- (23) Hollingworth, C.; Gouverneur, V. *Chem. Commun.* **2012**, *48*, 2929.
- (24) Neumann, C. N.; Ritter, T. *Angew. Chem. Int. Ed.* **2015**, *54*, 3216–3221.
- (25) Fujimoto, T.; Becker, F.; Ritter, T. *Org. Process Res. Dev.* **2014**, *18*, 1041–1044.
- (26) Tang, P.; Wang, W.; Ritter, T. *J. Am. Chem. Soc.* **2011**, *133*, 11482–11484.
- (27) Goldberg, N. W.; Shen, X.; Li, J.; Ritter, T. *Org. Lett.* **2016**, *18*, 6102–6104.
- (28) Furuya, T.; Kaiser, H. M.; Ritter, T. *Angew. Chem. Int. Ed.* **2008**, *47*, 5993–5996.
- (29) Sladojevich, F.; Arlow, S. I.; Tang, P.; Ritter, T. *J. Am. Chem. Soc.* **2013**, *135*, 2470–2473.
- (30) Lal, G. S.; Pez, G. P.; Pesaresi, R. J.; Prozonc, F. M.; Cheng, H. *J. Org. Chem.*

1999, 64, 7048–7054.

- (31) Finch, N.; Gemenden, C. W. *J. Org. Chem.* **1975**, 40, 569–574.
- (32) Hayashi, H.; Sonoda, H.; Fukumura, K.; Nagata, T. *Chem. Commun.* **2002**, 1618–1619.
- (33) Beaulieu, F.; Beauregard, L.-P.; Courchesne, G.; Couturier, M.; LaFlamme, F.; L'Heureux, A. *Org. Lett.* **2009**, 11, 5050–5053.
- (34) Zhang, X.; Guo, S.; Tang, P. *Org. Chem. Front.* **2015**, 2, 806–810.
- (35) Chen, K.; Eschenmoser, A.; Baran, P. S. *Angew. Chem. Int. Ed.* **2009**, 48, 9705–9708.
- (36) Zhu, C.; Falck, J. R. *Adv. Synth. Catal.* **2014**, 356, 2395–2410.
- (37) Sandford, C.; Aggarwal, V. K. *Chem. Commun.* **2017**, 53, 5481–5494.
- (38) Starkov, P. Applications of Boronic Acids in Organic Synthesis, University College London, 2011.
- (39) Mkhaliid, I. A. I.; Barnard, J. H.; Marder, T. B.; Murphy, J. M.; Hartwig, J. F. *Chem. Rev.* **2010**, 110, 890–931.
- (40) Saito, Y.; Segawa, Y.; Itami, K. *J. Am. Chem. Soc.* **2015**, 137, 5193–5198.
- (41) Coleman, I. W.; Little, P. E.; Bannard, R. A. B. *Can. J. Biochem. Physiol.* **1962**, 40, 815–826.
- (42) Hili, R.; Yudin, A. K. *Nat. Chem. Biol.* **2006**, 2, 284–287.
- (43) Espino, C. G.; Du Bois, J. *Angew. Chem. Int. Ed.* **2001**, 40, 598–600.
- (44) Kim, M.; Mulcahy, J. V.; Espino, C. G.; Du Bois, J. *Org. Lett.* **2006**, 8, 1073–1076.
- (45) Fiori, K. W.; Du Bois, J. *J. Am. Chem. Soc.* **2007**, 129, 562–568.
- (46) Kurokawa, T.; Kim, M.; Du Bois, J. *Angew. Chem. Int. Ed.* **2009**, 48, 2777–2779.
- (47) Roizen, J. L.; Zalatan, D. N.; Du Bois, J. *Angew. Chem. Int. Ed.* **2013**, 52, 11343–11346.

- (48) Williams Fiori, K.; Fleming, J. J.; Du Bois, J. *Angew. Chem. Int. Ed.* **2004**, *43*, 4349–4352.
- (49) Zalatan, D. N.; Du Bois, J. *J. Am. Chem. Soc.* **2008**, *130*, 9220–9221.
- (50) Roizen, J. L.; Harvey, M. E.; Du Bois, J. *Acc. Chem. Res.* **2012**, *45*, 911–922.
- (51) Paradine, S. M.; Griffin, J. R.; Zhao, J.; Petronico, A. L.; Miller, S. M.; White, M. C. *Nat. Chem.* **2015**, *7*, 987–994.
- (52) Reed, S. A.; White, M. C. *J. Am. Chem. Soc.* **2008**, *130*, 3316–3318.
- (53) Reed, S. A.; Mazzotti, A. R.; White, M. C. *J. Am. Chem. Soc.* **2009**, *131*, 11701–11706.
- (54) Paradine, S. M.; White, M. C. *J. Am. Chem. Soc.* **2012**, *134*, 2036–2039.
- (55) Rice, G. T.; White, M. C. *J. Am. Chem. Soc.* **2009**, *131*, 11707–11711.
- (56) Pattillo, C. C.; Strambeanu, I. I.; Calleja, P.; Vermeulen, N. A.; Mizuno, T.; White, M. C. *J. Am. Chem. Soc.* **2016**, *138*, 1265–1272.
- (57) Bräse, S.; Gil, C.; Knepper, K.; Zimmermann, V. *Angew. Chem. Int. Ed.* **2005**, *44*, 5188–5240.
- (58) Schilling, C. I.; Jung, N.; Biskup, M.; Schepers, U.; Bräse, S. *Chem. Soc. Rev.* **2011**, *40*, 4840–4871.
- (59) Lallana, E.; Riguera, R.; Fernandez-Megia, E. *Angew. Chem. Int. Ed.* **2011**, *50*, 8794–8804.
- (60) Hennessy, E. T.; Betley, T. A. *Science* **2013**, *340*, 591–595.
- (61) Sharma, A.; Hartwig, J. F. *Nature* **2014**, *517*, 600–604.
- (62) Huang, X.; Liu, W.; Ren, H.; Neelamegam, R.; Hooker, J. M.; Groves, J. T. *J. Am. Chem. Soc.* **2014**, *136*, 6842–6845.
- (63) Liu, W.; Huang, X.; Cheng, M.-J.; Nielsen, R. J.; Goddard, W. A.; Groves, J. T. *Science* **2012**, *337*, 1322–1325.
- (64) Huang, X.; Bergsten, T. M.; Groves, J. T. *J. Am. Chem. Soc.* **2015**, *137*, 5300–5303.

- (65) He, J.; Wasa, M.; Chan, K. S. L.; Shao, Q.; Yu, J.-Q. *Chem. Rev.* **2017**, *117*, 8754–8786.
- (66) Seiple, I. B.; Su, S.; Rodriguez, R. A.; Gianatassio, R.; Fujiwara, Y.; Sobel, A. L.; Baran, P. S. *J. Am. Chem. Soc.* **2010**, *132*, 13194–13196.
- (67) Langlois, B. R.; Laurent, E.; Roidot, N. *Tetrahedron Lett.* **1991**, *32*, 7525–7528.
- (68) Ji, Y.; Brueckl, T.; Baxter, R. D.; Fujiwara, Y.; Seiple, I. B.; Su, S.; Blackmond, D. G.; Baran, P. S. *Proc. Natl. Acad. Sci.* **2011**, *108*, 14411–14415.
- (69) Fujiwara, Y.; Dixon, J. A.; Rodriguez, R. A.; Baxter, R. D.; Dixon, D. D.; Collins, M. R.; Blackmond, D. G.; Baran, P. S. *J. Am. Chem. Soc.* **2012**, *134*, 1494–1497.
- (70) Zhou, Q.; Gui, J.; Pan, C.-M.; Albone, E.; Cheng, X.; Suh, E. M.; Grasso, L.; Ishihara, Y.; Baran, P. S. *J. Am. Chem. Soc.* **2013**, *135*, 12994–12997.
- (71) O’Hara, F.; Blackmond, D. G.; Baran, P. S. *J. Am. Chem. Soc.* **2013**, *135*, 12122–12134.
- (72) Gianatassio, R.; Kawamura, S.; Eprile, C. L.; Foo, K.; Ge, J.; Burns, A. C.; Collins, M. R.; Baran, P. S. *Angew. Chem. Int. Ed.* **2014**, *53*, 9851–9855.
- (73) Gui, J.; Zhou, Q.; Pan, C.-M.; Yabe, Y.; Burns, A. C.; Collins, M. R.; Ornelas, M. A.; Ishihara, Y.; Baran, P. S. *J. Am. Chem. Soc.* **2014**, *136*, 4853–4856.
- (74) Baskin, J. M.; Prescher, J. A.; Laughlin, S. T.; Agard, N. J.; Chang, P. V; Miller, I. A.; Lo, A.; Codelli, J. A.; Bertozzi, C. R. *Proc. Natl. Acad. Sci.* **2007**, *104*, 16793–16797.
- (75) Sassoon, I.; Blanc, V. In *Antibody-Drug Conjugates. Methods in Molecular Biology (Methods and Protocols)*; Ducry, L., Ed.; Humana Press: Totawa, NJ, 2013; pp. 1–27.
- (76) Beck, A.; Goetsch, L.; Dumontet, C.; Corvaia, N. *Nat. Rev. Drug Discov.* **2017**, *16*, 315–337.
- (77) Evans, M. J.; Cravatt, B. F. *Chem. Rev.* **2006**, *106*, 3279–3301.
- (78) Koppel, G. A. *Bioconjug. Chem.* **1990**, *1*, 13–23.

- (79) Li, G.-C.; Wang, P.; Farmer, M. E.; Yu, J.-Q. *Angew. Chem. Int. Ed.* **2017**, *56*, 6874–6877.
- (80) Hong, K.; Park, H.; Yu, J.-Q. *ACS Catal.* **2017**, *7*, 6938–6941.
- (81) Xiao, K.-J.; Chu, L.; Yu, J.-Q. *Angew. Chem. Int. Ed.* **2016**, *55*, 2856–2860.
- (82) Bedell, T. A.; Hone, G. A. B.; Valette, D.; Yu, J.-Q.; Davies, H. M. L.; Sorensen, E. J. *Angew. Chem. Int. Ed.* **2016**, *55*, 8270–8274.
- (83) Shang, M.; Wang, M.-M.; Saint-Denis, T. G.; Li, M.-H.; Dai, H.-X.; Yu, J.-Q. *Angew. Chem. Int. Ed.* **2017**, *56*, 5317–5321.
- (84) Dai, H. X.; Stepan, A. F.; Plummer, M. S.; Zhang, Y. H.; Yu, J. Q. *J. Am. Chem. Soc.* **2011**, *133*, 7222–7228.
- (85) Baillie, T. A. *Angew. Chem. Int. Ed.* **2016**, *55*, 13408–13421.
- (86) Pei, Q.-L.; Che, G.-D.; Zhu, R.-Y.; He, J.; Yu, J.-Q. *Org. Lett.* **2017**, *19*, 5860–5863.
- (87) Kola, I.; Landis, J. *Nat. Rev. Drug Discov.* **2004**, *3*, 711–716.
- (88) Hay, M.; Thomas, D. W.; Craighead, J. L.; Economides, C.; Rosenthal, J. *Nat. Biotechnol.* **2014**, *32*, 40–51.
- (89) Paul, S. M.; Mytelka, D. S.; Dunwiddie, C. T.; Persinger, C. C.; Munos, B. H.; Lindborg, S. R.; Schacht, A. L. *Nat. Rev. Drug Discov.* **2010**, *9*, 203–214.
- (90) Meanwell, N. A. *Chem. Res. Toxicol.* **2011**, *24*, 1420–1456.
- (91) Genovino, J.; Lütz, S.; Sames, D.; Touré, B. B. *J. Am. Chem. Soc.* **2013**, *135*, 12346–12352.
- (92) McNeill, E.; Du Bois, J. *J. Am. Chem. Soc.* **2010**, *132*, 10202–10204.
- (93) Clardy, J.; Walsh, C. *Nature* **2004**, *432*, 829–837.
- (94) Jennewein, S.; Long, R. M.; Williams, R. M.; Croteau, R. *Chem. Biol.* **2004**, *11*, 379–387.
- (95) Schoendorf, A.; Rithner, C. D.; Williams, R. M.; Croteau, R. B. *Proc. Natl. Acad. Sci.* **2001**, *98*, 1501–1506.

- (96) Jennewein, S.; Rithner, C. D.; Williams, R. M.; Croteau, R. B. *Proc. Natl. Acad. Sci.* **2001**, *98*, 13595–13600.
- (97) Chau, M.; Jennewein, S.; Walker, K.; Croteau, R. *Chem. Biol.* **2004**, *11*, 663–672.
- (98) Koeppe, A. E.; Hezari, M.; Zajicek, J.; Vogel, B. S.; LaFever, R. E.; Lewis, N. G.; Croteau, R. *J. Biol. Chem.* **1995**, *270*, 8686–8690.
- (99) Jennewein, S.; Wildung, M. R.; Chau, M.; Walker, K.; Croteau, R. *Proc. Natl. Acad. Sci.* **2004**, *101*, 9149–9154.
- (100) Meunier, B.; de Visser, S. P.; Shaik, S. *Chem. Rev.* **2004**, *104*, 3947–3980.
- (101) Newhouse, T.; Baran, P. S. *Angew. Chem. Int. Ed.* **2011**, *50*, 3362–3374.
- (102) Blanksby, S. J.; Ellison, G. B. *Acc. Chem. Res.* **2003**, *36*, 255–263.
- (103) Asensio, G.; Castellano, G.; Mello, R.; González Núñez, M. E. *J. Org. Chem.* **1996**, *61*, 5564–5566.
- (104) Brodsky, B. H.; Du Bois, J. *J. Am. Chem. Soc.* **2005**, *127*, 15391–15393.
- (105) Proksch, E.; de Meijere, A. *Angew. Chem. Int. Ed.* **1976**, *15*, 761–762.
- (106) Hehre, W. J. *Acc. Chem. Res.* **1975**, *8*, 369–376.
- (107) Harris, B.; Savage, G. P.; White, J. M. *Org. Biomol. Chem.* **2013**, *11*, 3151.
- (108) de Meijere, A. *Angew. Chem. Int. Ed.* **1979**, *18*, 809–826.
- (109) D'Accolti, L.; Dinoi, A.; Fusco, C.; Russo, A.; Curci, R. *J. Org. Chem.* **2003**, *68*, 7806–7810.
- (110) Vinković, V.; Mlinarić-Majerski, K.; Marinić, Ž. *Tetrahedron Lett.* **1992**, *33*, 7441–7444.
- (111) Curci, R.; D'Accolti, L.; Fiorentino, M.; Fusco, C.; Adam, W.; González-Núñez, M. E.; Mello, R. *Tetrahedron Lett.* **1992**, *33*, 4225–4228.
- (112) Díaz-Requejo, M. M.; Belderraín, T. R.; Nicasio, M. C.; Trofimenko, S.; Pérez, P. J. *J. Am. Chem. Soc.* **2002**, *124*, 896–897.
- (113) Davies, H. M. L.; Jin, Q. *Org. Lett.* **2004**, *6*, 1769–1772.

- (114) Doyle, M. P.; Kalinin, A. V. *Synlett* **1995**, 1995, 1075–1076.
- (115) Liang, C.; Robert-Peillard, F.; Fruit, C.; Müller, P.; Dodd, R. H.; Dauban, P. *Angew. Chem. Int. Ed.* **2006**, 45, 4641–4644.
- (116) Umbreit, M. A.; Sharpless, K. B. *J. Am. Chem. Soc.* **1977**, 99, 5526–5528.
- (117) Dick, A. R.; Hull, K. L.; Sanford, M. S. *J. Am. Chem. Soc.* **2004**, 126, 2300–2301.
- (118) Tenaglia, A.; Terranova, E.; Waegell, B. *J. Org. Chem.* **1992**, 57, 5523–5528.
- (119) Mbofana, C. T.; Chong, E.; Lawniczak, J.; Sanford, M. S. *Org. Lett.* **2016**, 18, 4258–4261.
- (120) Lee, M.; Sanford, M. S. *J. Am. Chem. Soc.* **2015**, 137, 12796–12799.
- (121) Lee, M.; Sanford, M. S. *Org. Lett.* **2017**, 19, 572–575.
- (122) Nakamura, A.; Nakada, M. *Synthesis (Stuttg.)* **2013**, 45, 1421–1451.
- (123) Weidmann, V.; Maison, W. *Synthesis (Stuttg.)* **2013**, 45, 2201–2221.
- (124) Moeller, K. D. *Tetrahedron* **2000**, 56, 9527–9554.
- (125) Horn, E. J.; Rosen, B. R.; Chen, Y.; Tang, J.; Chen, K.; Eastgate, M. D.; Baran, P. S. *Nature* **2016**, 533, 77–81.
- (126) Marwah, P.; Lardy, H. A. Process for effecting allylic oxidation using dicarboxylic acid imides and chromium reagents. US6384251 B1, 2002.
- (127) Litvinas, N. D.; Brodsky, B. H.; Du Bois, J. *Angew. Chem. Int. Ed.* **2009**, 48, 4513–4516.
- (128) Adams, A. M.; Du Bois, J. *Chem. Sci.* **2014**, 5, 656–659.
- (129) Adams, A. M.; Du Bois, J. *Chem. Sci.* **2014**, 5, 656–659.
- (130) Bovicelli, P.; Lupattelli, P.; Mincione, E.; Prencipe, T.; Curci, R. *J. Org. Chem.* **1992**, 57, 2182–2184.
- (131) Michaudel, Q.; Journot, G.; Regueiro-Ren, A.; Goswami, A.; Guo, Z.; Tully, T. P.; Zou, L.; Ramabhadran, R. O.; Houk, K. N.; Baran, P. S. *Angew. Chem. Int. Ed.* **2014**, 53, 12091–12096.

- (132) Sejbal, J.; Klinot, J.; Buděšínský, M.; Protiva, J. *Collect. Czechoslov. Chem. Commun.* **1991**, *56*, 2936–2949.
- (133) Sejbal, J.; Klinot, J.; Buděšínský, M.; Protiva, J. *Collect. Czechoslov. Chem. Commun.* **1997**, *62*, 1905–1918.
- (134) Zou, L.; Paton, R. S.; Eschenmoser, A.; Newhouse, T. R.; Baran, P. S.; Houk, K. N. *J. Org. Chem.* **2013**, *78*, 4037–4048.
- (135) Fagerberg, J. H.; Tsinman, O.; Sun, N.; Tsinman, K.; Avdeef, A.; Bergström, C. A. S. *Mol. Pharm.* **2010**, *7*, 1419–1430.
- (136) Chen, M. S.; White, M. C. *Science* **2007**, *318*, 783–787.
- (137) Chen, M. S.; White, M. C. *Science* **2010**, *327*, 566–571.
- (138) Gormisky, P. E.; White, M. C. *J. Am. Chem. Soc.* **2013**, *135*, 14052–14055.
- (139) Giri, R.; Liang, J.; Lei, J.-G.; Li, J.-J.; Wang, D.-H.; Chen, X.; Naggar, I. C.; Guo, C.; Foxman, B. M.; Yu, J.-Q. *Angew. Chem. Int. Ed.* **2005**, *44*, 7420–7424.
- (140) Desai, L. V.; Hull, K. L.; Sanford, M. S. *J. Am. Chem. Soc.* **2004**, *126*, 9542–9543.
- (141) Neufeldt, S. R.; Sanford, M. S. *Org. Lett.* **2010**, *12*, 532–535.
- (142) Reddy, B. V. S.; Reddy, L. R.; Corey, E. J. *Org. Lett.* **2006**, *8*, 3391–3394.
- (143) Sharpe, R. J.; Johnson, J. S. *J. Am. Chem. Soc.* **2015**, *137*, 4968–4971.
- (144) Breslow, R.; Dale, J. A.; Kalicky, P.; Liu, S. Y.; Washburn, W. N. *J. Am. Chem. Soc.* **1972**, *94*, 3276–3278.
- (145) Breslow, R.; Heyer, D. *J. Am. Chem. Soc.* **1982**, *104*, 2045–2046.
- (146) Breslow, R.; Corcoran, R. J.; Snider, B. B.; Doll, R. J.; Khanna, P. L.; Kaleya, R. *J. Am. Chem. Soc.* **1977**, *99*, 905–915.
- (147) Norrish, R. G. W.; Bamford, C. H. *Nature* **1937**, *140*, 195–196.
- (148) Breslow, R.; Baldwin, S.; Flechtner, T.; Kalicky, P.; Liu, S.; Washburn, W. J. *J. Am. Chem. Soc.* **1973**, *95*, 3251–3262.
- (149) Kasuya, S.; Kamijo, S.; Inoue, M. *Org. Lett.* **2009**, *11*, 3630–3632.

- (150) Lyons, T. W.; Sanford, M. S. *Chem. Rev.* **2010**, *110*, 1147–1169.
- (151) Neufeldt, S. R.; Sanford, M. S. *Acc. Chem. Res.* **2012**, *45*, 936–946.
- (152) Engle, K. M.; Mei, T.-S.; Wasa, M.; Yu, J.-Q. *Acc. Chem. Res.* **2012**, *45*, 788–802.
- (153) Zhang, Y. H.; Yu, J. Q. *J. Am. Chem. Soc.* **2009**, *131*, 14654–14655.
- (154) Sun, S.-Z.; Shang, M.; Wang, H.-L.; Lin, H.-X.; Dai, H.-X.; Yu, J.-Q. *J. Org. Chem.* **2015**, *80*, 8843–8848.
- (155) Shang, M.; Shao, Q.; Sun, S.-Z.; Chen, Y.-Q.; Xu, H.; Dai, H.-X.; Yu, J.-Q. *Chem. Sci.* **2017**, *8*, 1469–1473.
- (156) Fasan, R. *ACS Catal.* **2012**, *2*, 647–666.
- (157) Lewis, J. C.; Coelho, P. S.; Arnold, F. H. *Chem. Soc. Rev.* **2011**, *40*, 2003–2021.
- (158) Landwehr, M.; Hochrein, L.; Otey, C. R.; Kasrayan, A.; Bäckvall, J.-E.; Arnold, F. H. *J. Am. Chem. Soc.* **2006**, *128*, 6058–6059.
- (159) Durak, L. J.; Payne, J. T.; Lewis, J. C. *ACS Catal.* **2016**, *6*, 1451–1454.
- (160) Lee, M.; Sanford, M. S. *J. Am. Chem. Soc.* **2015**, *137*, 12796–12799.
- (161) Howell, J. M.; Feng, K.; Clark, J. R.; Trzepkowski, L. J.; White, M. C. *J. Am. Chem. Soc.* **2015**, *137*, 14590–14593.
- (162) Adams, A. M.; Du Bois, J.; Malik, H. A. *Org. Lett.* **2015**, *17*, 6066–6069.
- (163) Mack, J. B. C.; Gipson, J. D.; Du Bois, J.; Sigman, M. S. *J. Am. Chem. Soc.* **2017**, *139*, 9503–9506.
- (164) Osberger, T. J.; Rogness, D. C.; Kohrt, J. T.; Stepan, A. F.; White, M. C. *Nature* **2016**, *537*, 214–219.
- (165) Beak, P.; Basu, A.; Gallagher, D. J.; Park, Y. S.; Thayumanavan, S. *Acc. Chem. Res.* **1996**, *29*, 552–560.
- (166) Hoppe, D.; Hense, T. *Angew. Chem. Int. Ed.* **1997**, *36*, 2282–2316.
- (167) O'Brien, P. *Chem. Commun.* **2008**, 655–667.

- (168) Firth, J. D.; O'Brien, P.; Ferris, L. *J. Am. Chem. Soc.* **2016**, *138*, 651–659.
- (169) Dearden, M. J.; Firkin, C. R.; Hermet, J.-P. R.; O'Brien, P. *J. Am. Chem. Soc.* **2002**, *124*, 11870–11871.
- (170) Mitchell, E. A.; Peschiulli, A.; Lefevre, N.; Meerpoel, L.; Maes, B. U. W. *Chem. Eur. J.* **2012**, *18*, 10092–10142.
- (171) Spangler, J. E.; Kobayashi, Y.; Verma, P.; Wang, D.-H.; Yu, J.-Q. *J. Am. Chem. Soc.* **2015**, *137*, 11876–11879.
- (172) Pastine, S. J.; Gribkov, D. V.; Sames, D. *J. Am. Chem. Soc.* **2006**, *128*, 14220–14221.
- (173) He, J.; Hamann, L. G.; Davies, H. M. L.; Beckwith, R. E. J. *Nat. Commun.* **2015**, *6*, 5943–5951.
- (174) Shi, L.; Xia, W. *Chem. Soc. Rev.* **2012**, *41*, 7687.
- (175) McNally, A.; Prier, C. K.; MacMillan, D. W. C. *Science* **2011**, *334*, 1114–1117.
- (176) Affron, D. P.; Davis, O. A.; Bull, J. A. *Org. Lett.* **2014**, *16*, 4956–4959.
- (177) Topczewski, J. J.; Cabrera, P. J.; Saper, N. I.; Sanford, M. S. *Nature* **2016**, *531*, 220–224.
- (178) Drawz, S. M.; Bonomo, R. A. *Clin. Microbiol. Rev.* **2010**, *23*, 160–201.
- (179) Kazmierski, W. M.; Andrews, W.; Furfine, E.; Spaltenstein, A.; Wright, L. *Bioorg. Med. Chem. Lett.* **2004**, *14*, 5689–5692.
- (180) Enz, A.; Feuerbach, D.; Frederiksen, M. U.; Gentsch, C.; Hurth, K.; Müller, W.; Nozulak, J.; Roy, B. L. *Bioorg. Med. Chem. Lett.* **2009**, *19*, 1287–1291.
- (181) Shorvon, S. *Lancet* **2001**, *358*, 1885–1892.
- (182) Hari, Y.; Osawa, T.; Kotobuki, Y.; Yahara, A.; Shrestha, A. R.; Obika, S. *Bioorg. Med. Chem.* **2013**, *21*, 4405–4412.
- (183) Bailey, P. D.; Collier, I. D.; Morgan, K. M. In *Comprehensive Organic Functional Group Transformations*; Moody, C. J., Ed.; Pergamon: Oxford, 1995; pp. 257–307.

- (184) Naota, T.; Murahashi, S.-I. *Synlett* **1991**, 693–694.
- (185) Gunanathan, C.; Ben-David, Y.; Milstein, D. *Science* **2007**, *317*, 790–792.
- (186) Al-Subu, M. M.; Jondi, W. J.; Amer, A. A.; Hannoun, M.; Musmar, M. J. *Chem. Heterocycl. Compd.* **2003**, *39*, 478–484.
- (187) Wenkert, E.; Angell, E. C. *Synth. Commun.* **1988**, *18*, 1331–1337.
- (188) Wei, Y.; Ding, H.; Lin, S.; Liang, F. *Org. Lett.* **2011**, *13*, 1674–1677.
- (189) Rao, G.; Periasamy, M. *Synlett* **2015**, *26*, 2231–2236.
- (190) Yan, X.; Fang, K.; Liu, H.; Xi, C. *Chem. Commun.* **2013**, *49*, 10650.
- (191) Tanaka, K.-I.; Yoshifuji, S.; Nitta, Y. *Chem. Pharm. Bull.* **1988**, *36*, 3125–3129.
- (192) Sheehan, J. C.; Tulis, R. W. *J. Org. Chem.* **1974**, *39*, 2264–2267.
- (193) Breault, G.; Eyermann, C. J.; Geng, B.; Morningstar, M.; Reck, F. Compounds for the Treatment of Multi-Drug Resistant Bacterial Infections. WO2006134378 (A1), 2006.
- (194) Gunanathan, C.; Shimon, L. J. W.; Milstein, D. *J. Am. Chem. Soc.* **2009**, *131*, 3146–3147.
- (195) Gunanathan, C.; Milstein, D. *Angew. Chem. Int. Ed.* **2008**, *47*, 8661–8664.
- (196) Gunanathan, C.; Gnanaprakasam, B.; Iron, M. A.; Shimon, L. J. W.; Milstein, D. *J. Am. Chem. Soc.* **2010**, *132*, 14763–14765.
- (197) Khusnutdinova, J. R.; Ben-David, Y.; Milstein, D. *J. Am. Chem. Soc.* **2014**, *136*, 2998–3001.
- (198) Legacy, C. J.; Wang, A.; O'Day, B. J.; Emmert, M. H. *Angew. Chem. Int. Ed.* **2015**, *54*, 14907–14910.
- (199) Jin, X.; Kataoka, K.; Yatabe, T.; Yamaguchi, K.; Mizuno, N. *Angew. Chem.* **2016**, *128*, 7328–7333.
- (200) Fuentes, L.; Osorio, U.; Quintero, L.; Höpfl, H.; Vázquez-Cabrera, N.; Sartillo-Piscil, F. *J. Org. Chem.* **2012**, *77*, 5515–5524.
- (201) Osorio-Nieto, U.; Chamorro-Arenas, D.; Quintero, L.; Höpfl, H.; Sartillo-Piscil,

- F. *J. Org. Chem.* **2016**, *81*, 8625–8632.
- (202) Galloway, J. D.; Mai, D. N.; Baxter, R. D. *Org. Lett.* **2017**, *19*, 5772–5775.
- (203) He, B.; Xiao, Z.; Wu, H.; Guo, Y.; Chen, Q.-Y.; Liu, C. *RSC Adv.* **2017**, *7*, 880–883.
- (204) Ponikvar-Svet, M.; Zeiger, D. N.; Liebman, J. F. *Struct. Chem.* **2015**, *26*, 1621–1628.
- (205) Castro -C., A.; Juárez -P., J.; Gnecco, D.; Terán, J. L.; Galindo, A.; Bernès, S.; Enríquez, R. G. *Tetrahedron: Asymm.* **2005**, *16*, 949–952.
- (206) R. Juárez, J.; Castro, A.; Romero, O.; L. Terán, J.; Gnecco, D.; Orea, L.; Mendoza, A. *Heterocycles* **2014**, *89*, 725–729.
- (207) Yusubov, M. S.; Zhdankin, V. V. *Resour. Technol.* **2015**, *1*, 49–67.
- (208) Li, J.; Lear, M. J.; Kawamoto, Y.; Umemiya, S.; Wong, A. R.; Kwon, E.; Sato, I.; Hayashi, Y. *Angew. Chem. Int. Ed.* **2015**, *54*, 12986–12990.
- (209) Li, J.; Lear, M. J.; Kwon, E.; Hayashi, Y. *Chem. Eur. J.* **2016**, *22*, 5538–5542.
- (210) Liang, Y.-F.; Li, X.; Wang, X.; Zou, M.; Tang, C.; Liang, Y.; Song, S.; Jiao, N. *J. Am. Chem. Soc.* **2016**, *138*, 12271–12277.
- (211) Kutney, J. P.; Balsevich, J.; Honda, T.; Liao, P.-H.; Thiellier, H. P. M.; Worth, B. R. *Can. J. Chem.* **1978**, *56*, 2560–2566.
- (212) Langlois, N.; Andriamialisoa, R. Z.; Neuss, N. *Helv. Chim. Acta* **1980**, *63*, 793–805.
- (213) Lee, B. H.; Clothier, M. F. **1997**, *38*, 4009–4012.
- (214) Zhao, G.; Xie, X.; Sun, H.; Yuan, Z.; Zhong, Z.; Tang, S.; She, X. *Org. Lett.* **2016**, *18*, 2447–2450.
- (215) Bartlett, M. F.; Dickel, D. F.; Taylor, W. I. *J. Am. Chem. Soc.* **1958**, *80*, 126–136.
- (216) Tsubomura, H.; Nagakura, S. *J. Chem. Phys.* **1957**, *27*, 819–820.
- (217) Nagakura, S. *J. Am. Chem. Soc.* **1958**, *80*, 520–524.

- (218) Yada, H.; Tanaka, J.; Nagakura, S. *Bull. Chem. Soc. Jpn.* **1960**, *33*, 1660–1667.
- (219) Jaber, N.; Zong, W.-X. *Ann. N. Y. Acad. Sci.* **2013**, *1280*, 48–51.
- (220) Ratnikov, M. O.; Farkas, L. E.; McLaughlin, E. C.; Chiou, G.; Choi, H.; El-Khalafy, S. H.; Doyle, M. P. *J. Org. Chem.* **2011**, *76*, 2585–2593.
- (221) Watanabe, Y.; Ishimaru, M.; Ozaki, S. *Chem. Lett.* **1994**, 2163–2166.
- (222) Tetrahydrofuran Physical Properties <http://www.sigmaaldrich.com/chemistry/solvents/tetrahydrofuran-center.html> (accessed Nov 5, 2017).
- (223) Dimethyl Sulfoxide Physical Properties <http://www.sigmaaldrich.com/chemistry/solvents/dimethyl-sulfoxide-center.html> (accessed Nov 5, 2017).
- (224) Bachrach, S. M. *J. Org. Chem.* **2008**, *73*, 2466–2468.
- (225) Ringer, A. L.; Magers, D. H. *J. Org. Chem.* **2007**, *72*, 2533–2537.
- (226) Levine, M. N.; Raines, R. T. *Chem. Sci.* **2012**, *3*, 2412.
- (227) Beesley, R. M.; Ingold, C. K.; Thorpe, J. F. *J. Chem. Soc., Trans.* **1915**, *107*, 1080–1106.
- (228) Zheng, Y.; Tice, C. M.; Singh, S. B. *Bioorg. Med. Chem. Lett.* **2014**, *24*, 3673–3682.
- (229) Bettoni, G.; Franchini, C.; Morlacchi, F.; Tangari, N.; Tortorella, V. *J. Org. Chem.* **1976**, *41*, 2780–2782.
- (230) Bischoff, C. A.; Nastvogel, O. *Berichte der Dtsch. Chem. Gesellschaft* **1890**, *23*, 2026–2030.
- (231) Yan, X.; Fang, K.; Liu, H.; Xi, C. *Chem. Commun.* **2013**, *49*, 10650.
- (232) Bettoni, G.; Carbonara, G.; Franchini, C.; Tortorella, V. *Tetrahedron* **1981**, *37*, 4159–4164.
- (233) Sorribes, I.; Cabrero-Antonino, J. R.; Vicent, C.; Junge, K.; Beller, M. *J. Am. Chem. Soc.* **2015**, *137*, 13580–13587.
- (234) Roiser, L.; Robiette, R.; Waser, M. *Synlett* **2016**, *27*, 1963–1968.
- (235) Cuppoletti, A.; Dagostin, C.; Florea, C.; Galli, C.; Gentili, P.; Lanzalunga, O.;

- Petride, A.; Petride, H. *Chem. Eur. J.* **1999**, *5*, 2993–2999.
- (236) Căproiu, M.; Florea, C.; Galli, C.; Petride, A.; Petride, H. *Eur. J. Org. Chem.* **2000**, *2000*, 1037–1043.
- (237) Liu, K. E.; Johnson, C. C.; Newcomb, M.; Lippard, S. J. *J. Am. Chem. Soc.* **1993**, *115*, 939–947.
- (238) Griller, D.; Ingold, K. U. *Acc. Chem. Res.* **1980**, *13*, 317–323.
- (239) Maillard, B.; Forrest, D.; Ingold, K. U. *J. Am. Chem. Soc.* **1976**, *98*, 7024–7026.
- (240) Housecroft, C.; Sharpe, A. G. *Inorganic Chemistry*; 2nd ed.; Prentice Hall, 2004.
- (241) Greenwood, N. N.; Earnshaw, A. *Chemistry of the Elements*; 2nd ed.; Elsevier, 1997.
- (242) Conformational modelling and energy state calculations were carried out using Molecular Operating Environment (MOE) 2016 under Amber10:Extended Huckel Theory (EHT) parameters for proteins and small molecules.
- (243) Waghmode, N. A.; Kalbandhe, A. H.; Thorat, P. B.; Karade, N. N. *Tetrahedron Lett.* **2016**, *57*, 680–683.
- (244) Aronov, A. M.; Goldman, B. B. *Bioorg. Med. Chem.* **2004**, *12*, 2307–2315.
- (245) Mitcheson, J. S.; Chen, J.; Lin, M.; Culbertson, C.; Sanguinetti, M. C. *Proc. Natl. Acad. Sci.* **2000**, *97*, 12329–12333.
- (246) Sanguinetti, M. C.; Tristani-Firouzi, M. *Nature* **2006**, *440*, 463–469.
- (247) Garg, D.; Gandhi, T.; Gopi Mohan, C. *J. Mol. Graph. Model.* **2008**, *26*, 966–976.
- (248) Grant, S.; Fitton, A. *Drugs* **1994**, *48*, 253–273.
- (249) Lee, H. J.; Choi, J.-S.; Choi, B. H.; Hahn, S. J. *Naunyn. Schmiedeberg's Arch. Pharmacol.* **2017**, *390*, 633–642.
- (250) pK_aH was calculated using JChem for Excel, version 16.12.1900.1402, copyright 2008-2016 ChemAxon Ltd.

- (251) clogP was calculated using PCModels by Daylight/BioByte, integrated into JChem for Excel, version 16.12.1900.1402, copyright 2008-2016 Daylight Chemical Information Systems Inc.
- (252) Ertl, P.; Rohde, B.; Selzer, P. *J. Med. Chem.* **2000**, *43*, 3714–3717.
- (253) Cansfield, A. D.; Ladduwahetty, T.; Sunose, M.; Ellard, K.; Lynch, R.; Newton, A. L.; Lewis, A.; Bennett, G.; Zinn, N.; Thomson, D. W.; Rüger, A. J.; Feutrill, J. T.; Rausch, O.; Watt, A. P.; Bergamini, G. *ACS Med. Chem. Lett.* **2016**, *7*, 768–773.
- (254) Kornblum, N.; Jones, W. J.; Anderson, G. J. *J. Am. Chem. Soc.* **1959**, *81*, 4113–4114.
- (255) Xu, G.; Wu, J. P.; Ai, X. M.; Yang, L. R. *Chinese Chem. Lett.* **2007**, *18*, 643–646.
- (256) *Encyclopedia of Reagents for Organic Synthesis*; Paquette, L. A., Ed.; John Wiley & Sons, Ltd: Chichester, UK, 2001.
- (257) Cohen, F.; Bergeron, P.; Blackwood, E.; Bowman, K. K.; Chen, H.; DiPasquale, A. G.; Epler, J. A.; Koehler, M. F. T.; Lau, K.; Lewis, C.; Liu, L.; Ly, C. Q.; Malek, S.; Nonomiya, J.; Ortwine, D. F.; Pei, Z.; Robarge, K. D.; Sideris, S.; Trinh, L.; Truong, T.; Wu, J.; Zhao, X.; Lyssikatos, J. P. *J. Med. Chem.* **2011**, *54*, 3426–3435.
- (258) Bantscheff, M.; Eberhard, D.; Abraham, Y.; Bastuck, S.; Boesche, M.; Hobson, S.; Mathieson, T.; Perrin, J.; Raida, M.; Rau, C.; Reader, V.; Sweetman, G.; Bauer, A.; Bouwmeester, T.; Hopf, C.; Kruse, U.; Neubauer, G.; Ramsden, N.; Rick, J.; Kuster, B.; Drewes, G. *Nat. Biotechnol.* **2007**, *25*, 1035–1044.
- (259) Smith, M. B.; March, J. *Advanced Organic Chemistry*; 6th ed.; Wiley: New York, 2007.
- (260) Bruckner, R. *Organic Mechanisms*; Harmata, M., Ed.; 3rd ed.; Springer Science & Business Media: Berlin, 2010.
- (261) Cope, A. C.; Ciganek, E. *Org. Synth.* **1959**, *39*, 40.

- (262) Wang, Z. In *Comprehensive Organic Name Reactions and Reagents*; John Wiley & Sons, Inc.: Hoboken, NJ, USA, 2010; pp. 642–645.
- (263) Nokami, J.; Ueta, K.; Okawara, R. *Tetrahedron Lett.* **1978**, *19*, 4903–4904.
- (264) Nokami, J.; Kunieda, N.; Kinoshita, M. *Tetrahedron Lett.* **1975**, *16*, 2841–2844.
- (265) Reich, H. J.; Peake, S. L. *J. Am. Chem. Soc.* **1978**, *100*, 4888–4889.
- (266) Holleman, A. F.; Wiberg, E. *Inorganic Chemistry*; Wiberg, N., Ed.; 1st ed.; Academic Press: San Diego, 2001.
- (267) Roček, J.; Westheimer, F. H.; Eschenmoser, A.; Moldoványi, L.; Schreiber, J. *Helv. Chim. Acta* **1962**, *45*, 2554–2567.
- (268) Schreiber, J.; Eschenmoser, A. *Helv. Chim. Acta* **1955**, *38*, 1529–1536.
- (269) Wilcox, C. F.; Sexton, M.; Wilcox, M. F. *J. Org. Chem.* **1963**, *28*, 1079–1082.
- (270) Wang, Z. In *Comprehensive Organic Name Reactions and Reagents*; John Wiley & Sons, Inc.: Hoboken, NJ, USA, 2010; pp. 1460–1463.
- (271) Genovino, J.; Sames, D.; Touré, B. B. *Tetrahedron Lett.* **2015**, *56*, 3066–3069.
- (272) Genovino, J.; Sames, D.; Hamann, L. G.; Touré, B. B. *Angew. Chem. Int. Ed.* **2016**, *55*, 14218–14238.
- (273) Clarke, E.; Brinded, K.; Cook, T. GSK colleagues who carried out HRMS analysis.
- (274) Henley, Z. Identification of Vps34 as a key off-target activity in the search for an oral PI3Kinase delta inhibitor for the treatment of respiratory disease. *1st RSC Anglo-Nordic Medicinal Chemistry Symposium*, 2017.
- (275) Down, K.; Amour, A.; Baldwin, I. R.; Cooper, A. W. J.; Deakin, A. M.; Felton, L. M.; Guntrip, S. B.; Hardy, C.; Harrison, Z. A.; Jones, K. L.; Jones, P.; Keeling, S. E.; Le, J.; Livia, S.; Lucas, F.; Lunniss, C. J.; Parr, N. J.; Robinson, E.; Rowland, P.; Smith, S.; Thomas, D. A.; Vitulli, G.; Washio, Y.; Hamblin, J. *N. J. Med. Chem.* **2015**, *58*, 7381–7399.
- (276) Tan, P. W.; Haughey, M.; Dixon, D. J. *Chem. Commun.* **2015**, *51*, 4406–4409.

- (277) Kovalenko, O. O.; Volkov, A.; Adolfsson, H. *Org. Lett.* **2015**, *17*, 446–449.
- (278) Zou, Q.; Wang, C.; Smith, J.; Xue, D.; Xiao, J. *Chem. Eur. J.* **2015**, *21*, 9656–9661.
- (279) Smith, A. M. R.; Billen, D.; Hii, K. K. *Chem. Commun.* **2009**, 3925.
- (280) Sunada, Y.; Kawakami, H.; Imaoka, T.; Motoyama, Y.; Nagashima, H. *Angew. Chem. Int. Ed.* **2009**, *48*, 9511–9514.
- (281) Grasa, G. A.; Viciu, M. S.; Huang, J.; Nolan, S. P. *J. Org. Chem.* **2001**, *66*, 7729–7737.
- (282) Kovalenko, O. O.; Volkov, A.; Adolfsson, H. *Org. Lett.* **2015**, *17*, 446–449.
- (283) Mustazza, C.; Borioni, A.; Giudice, M.; Gatta, F.; Ferretti, R.; Meneguz, A.; Volpe, M.; Lorenzini, P. *Eur. J. Med. Chem.* **2002**, *37*, 91–109.
- (284) Asami, M.; Miyairi, N.; Sasahara, Y.; Ichikawa, K.; Hosoda, N.; Ito, S. *Tetrahedron* **2015**, *71*, 6796–6802.
- (285) Hortense, E. GSK colleague who carried out chiral HPLC analysis.
- (286) Deskus, J.; Fan, D.; Smith, M. B. *Synth. Commun.* **1998**, *28*, 1649–1659.
- (287) Moriarty, R. M.; Vaid, R. K.; Duncan, M. P.; Ochiai, M.; Inenaga, M.; Nagao, Y. *Tetrahedron Lett.* **1988**, *29*, 6913–6916.
- (288) Gillie, D. J.; Novick, S. J.; Donovan, B. T.; Payne, L. A.; Townsend, C. J. *Pharmacol. Toxicol. Methods* **2013**, *67*, 33–44.
- (289) Eurofins DiscoverX, 42501 Albrae Street, Fremont, CA 94538, U.S.A.
- (290) Hanada, K.; Tamai, M.; Yamagishi, M.; Ohmura, S.; Sawada, J.; Tanaka, I. *Agric. Biol. Chem.* **1978**, *42*, 523–528.
- (291) Milner, P. H.; Coates, N. J.; Gilpin, M. L.; Spear, S. R.; Eggleston, D. S. *J. Nat. Prod.* **1996**, *59*, 400–402.
- (292) Sarabia, F.; Vivar-García, C.; García-Castro, M.; Martín-Ortiz, J. *J. Org. Chem.* **2011**, *76*, 3139–3150.
- (293) Liu, W.-J.; Lv, B.-D.; Gong, L.-Z. *Angew. Chem. Int. Ed.* **2009**, *48*, 6503–6506.

- (294) Sarabia, F.; Vivar-García, C.; García-Ruiz, C.; Martín-Ortiz, L.; Romero-Carrasco, A. *J. Org. Chem.* **2012**, *77*, 1328–1339.
- (295) Lancefield, C. S.; Zhou, L.; Tomas, L.; Slawin, A. M. Z.; Westwood, N. *J. Org. Lett.* **2012**, *14*, 6166–6169.
- (296) Yoshifuji, S.; Arakawa, Y. *Chem. Pharm. Bull.* **1989**, *37*, 3380–3381.
- (297) Ripin, D. H.; Evans, D. A. Evans pKa Table http://evans.rc.fas.harvard.edu/pdf/evans_pKa_table.pdf (accessed Nov 21, 2017).
- (298) March, J. *Advanced Organic Chemistry: Reactions, Mechanisms, and Structure*; 3rd ed.; Wiley: New York, 1985.
- (299) Jögi, A.; Mäeorg, U. *Molecules* **2001**, *6*, 964–968.
- (300) Li, C.-J.; Chan, T. *Tetrahedron* **1999**, *55*, 11149–11176.
- (301) Isaac, M. B.; Chan, T.-H. *J. Chem. Soc., Chem. Commun.* **1995**, 1003.
- (302) Chan, T. H.; Yang, Y. *J. Am. Chem. Soc.* **1999**, *121*, 3228–3229.
- (303) Keinicke, L.; Fristrup, P.; Norrby, P.-O.; Madsen, R. *J. Am. Chem. Soc.* **2005**, *127*, 15756–15761.
- (304) Estevam, I. H. S.; Bieber, L. W. *Tetrahedron Lett.* **2003**, *44*, 667–670.
- (305) Liu, X.; Xu, C.; Wang, M.; Liu, Q. *Chem. Rev.* **2015**, *115*, 683–730.
- (306) Prakash, G. K. S.; Yudin, A. K. *Chem. Rev.* **1997**, *97*, 757–786.
- (307) Huang, W.; Ni, C.; Zhao, Y.; Zhang, W.; Dilman, A. D.; Hu, J. *Tetrahedron* **2012**, *68*, 5137–5144.
- (308) Beletskaya, I.; Sigeev, A.; Peregudov, A.; Petrovskii, P. *Synthesis (Stuttg.)* **2007**, 2534–2538.
- (309) Molinaro, C.; Mowat, J.; Gosselin, F.; O’Shea, P. D.; Marcoux, J.-F.; Angelaud, R.; Davies, I. W. *J. Org. Chem.* **2007**, *72*, 1856–1858.
- (310) Honraedt, A.; Raux, M.-A.; Le Grogneq, E.; Jacquemin, D.; Felpin, F.-X. *Chem. Commun. (Camb.)* **2014**, *50*, 5236–5238.

- (311) Crisóstomo, F. P.; Martín, T.; Carrillo, R. *Angew. Chem. Int. Ed.* **2014**, *53*, 2181–2185.
- (312) Hari, D. P.; Schroll, P.; König, B. *J. Am. Chem. Soc.* **2012**, *134*, 2958–2961.
- (313) Iakobson, G.; Du, J.; Slawin, A. M. Z.; Beier, P. *Beilstein J. Org. Chem.* **2015**, *11*, 1494–1502.
- (314) Okazaki, T.; Laali, K. K.; Bunge, S. D.; Adas, S. K. *Eur. J. Org. Chem.* **2014**, *2014*, 1630–1644.
- (315) Kimball, D. B.; Haley, M. M. *Angew. Chem. Int. Ed.* **2002**, *41*, 3338–3351.
- (316) Bräse, S.; Dahmen, S.; Pfefferkorn, M. *J. Comb. Chem.* **2000**, *2*, 710–715.
- (317) Nicolaou, K. C.; Boddy, C. N. C.; Li, H.; Koumbis, A. E.; Hughes, R.; Natarajan, S.; Jain, N. F.; Ramanjulu, J. M.; Bräse, S.; Solomon, M. E. *Chem. Eur. J.* **1999**, *5*, 2602–2621.
- (318) Connors, T. A.; Goddard, P. M.; Merai, K.; Ross, W. C. J.; Wilman, D. E. V. *Biochem. Pharmacol.* **1976**, *25*, 241–246.
- (319) Rouzer, C. A.; Sabourin, M.; Skinner, T. L.; Thompson, E. J.; Wood, T. O.; Chmurny, G. N.; Klose, J. R.; Roman, J. M.; Smith, R. H.; Michejda, C. J. *Chem. Res. Toxicol.* **1996**, *9*, 172–178.
- (320) Wirschun, W.; Winkler, M.; Lutz, K.; Jochims, J. C. *J. Chem. Soc., Perkin Trans. 1* **1998**, 1755–1762.
- (321) Gross, M. L.; Blank, D. H.; Welch, W. M. *J. Org. Chem.* **1993**, *58*, 2104–2109.
- (322) Khazaei, A.; Kazem-Rostami, M.; Moosavi-Zare, A.; Bayat, M.; Saednia, S. *Synlett* **2012**, *23*, 1893–1896.
- (323) Shaaban, S.; Oh, J.; Maulide, N. *Org. Lett.* **2016**, *18*, 345–347.
- (324) Shaaban, S.; Jolit, A.; Petkova, D.; Maulide, N. *Chem. Commun.* **2015**, *51*, 13902–13905.
- (325) Grierson, D. In *Organic Reactions*; John Wiley & Sons, Inc.: Hoboken, NJ, USA, 1990; pp. 85–295.

- (326) Grierson, D. S.; Husson, H.-P. In *Comprehensive Organic Synthesis*; Elsevier, 1991; pp. 909–947.
- (327) Cave, A.; Kan-Fan, C.; Potier, P.; Le Men, J. *Tetrahedron* **1967**, *23*, 4681–4689.
- (328) Langlois, N.; Gueritte, F.; Langlois, Y.; Potier, P. *J. Am. Chem. Soc.* **1976**, *98*, 7017–7024.
- (329) Kende, A. S.; Liu, K.; Jos Brands, K. M. *J. Am. Chem. Soc.* **1995**, *117*, 10597–10598.
- (330) Stilinović, V.; Horvat, G.; Hrenar, T.; Nemeč, V.; Cinčić, D. *Chem. Eur. J.* **2017**, *23*, 5244–5257.
- (331) Sakakura, A.; Kawajiri, K.; Ohkubo, T.; Kosugi, Y.; Ishihara, K. *J. Am. Chem. Soc.* **2007**, *129*, 14775–14779.
- (332) Xu, S.; Held, I.; Kempf, B.; Mayr, H.; Steglich, W.; Zipse, H. *Chem. Eur. J.* **2005**, *11*, 4751–4757.
- (333) Kong, W.-C. Dehydrogenative β -sulfonylation of aliphatic amines using sulfinate salts, GlaxoSmithKline/University of Oxford, 2017.
- (334) Brown, D. S.; Charreau, P.; Hansson, T.; Ley, S. V. *Tetrahedron* **1991**, *47*, 1311–1328.
- (335) Anaya, J.; Barton, D. H. R.; Gero, S. D.; Grande, M.; Martin, N.; Tachdjian, C. *Angew. Chem.* **1993**, *105*, 911–913.
- (336) Padwa, A.; Norman, B. H. *J. Org. Chem.* **1990**, *55*, 4801–4807.
- (337) Auvray, P.; Knochel, P.; Normant, J. F. *Tetrahedron Lett.* **1985**, *26*, 2329–2332.
- (338) Baker-Glenn, C. A. G.; Barrett, A. G. M.; Gray, A. A.; Procopiou, P. A.; Ruston, M. *Tetrahedron Lett.* **2005**, *46*, 7427–7430.
- (339) Koprowski, M.; Skowrońska, A.; Główska, M. L.; Fruziński, A. *Tetrahedron* **2007**, *63*, 1211–1228.
- (340) Lai, J.; Chang, L.; Yuan, G. *Org. Lett.* **2016**, *18*, 3194–3197.
- (341) Chen, M.; Huang, Z.-T.; Zheng, Q.-Y. *Org. Biomol. Chem.* **2014**, *12*, 9337–

9340.

- (342) Cai, Y.; Zhang, R.; Sun, D.; Xu, S.; Zhou, Q. *Synlett* **2017**, 28, 1630–1635.
- (343) Charrier, J.-D.; Durrant, S. J.; Knegt, R. Compounds Useful as Inhibitors of ATR Kinase. US2013115310, 2013.
- (344) Busch-Petersen, J. IL-8 Receptor Antagonists. US2007249672, 2007.
- (345) Duan, J.; Dhar, T. G. M.; Jiang, B.; Karmakar, A.; Gupta, A. K.; Lu, Z. Heterocyclic Sulfone as ROR-Gamma Modulators. WO2015103510, 2015.
- (346) Markovic, T.; Rocke, B. N.; Blakemore, D. C.; Mascitti, V.; Willis, M. C. *Chem. Sci.* **2017**, 8, 4437–4442.
- (347) Wright, S. W.; Hallstrom, K. N. *J. Org. Chem.* **2006**, 71, 1080–1084.
- (348) García-Rubia, A.; Urones, B.; Gómez Arrayás, R.; Carretero, J. C. *Angew. Chem. Int. Ed.* **2011**, 50, 10927–10931.
- (349) Liu, L. K.; Chi, Y.; Jen, K.-Y. *J. Org. Chem.* **1980**, 45, 406–410.
- (350) Blakemore, D. In *Synthetic Methods in Drug Discovery*; Blakemore, D. C.; Doyle, P. M.; Fobian, Y. M., Eds.; RSC, 2016; pp. 1–69.
- (351) Wedekind, E.; Schenk, D. *Berichte der Dtsch. Chem. Gesellschaft* **1911**, 44, 198–202.
- (352) King, J. F. *Acc. Chem. Res.* **1975**, 8, 10–17.
- (353) Stork, G.; Borowitz, I. J. *J. Am. Chem. Soc.* **1962**, 84, 313–313.
- (354) Opitz, G.; Adolph, H. *Angew. Chem. Int. Ed.* **1962**, 1, 113–114.
- (355) Sun, Y.; Abdukader, A.; Lu, D.; Zhang, H.; Liu, C. *Green Chem.* **2017**, 19, 1255–1258.
- (356) Babudri, F.; Florio, S.; Reho, A.; Trapani, G. *J. Chem. Soc., Perkin Trans. 1* **1984**, 1949–1955.
- (357) Lu, Y. J.; Hu, B.; Prashad, M.; Kabadi, S.; Repič, O.; Blacklock, T. J. *J. Heterocycl. Chem.* **2006**, 43, 1125–1127.
- (358) Lautens, M.; Fillion, E.; Sampat, M. *J. Org. Chem.* **1997**, 62, 7080–7081.

- (359) Zhu, W.; Cai, G.; Ma, D. *Org. Lett.* **2005**, *7*, 5545–5548.
- (360) Zhang, D.-J.; Xie, M.-S.; Qu, G.-R.; Gao, Y.-W.; Guo, H.-M. *Org. Lett.* **2016**, *18*, 820–823.
- (361) Weston, M. H.; Nakajima, K.; Back, T. G. *J. Org. Chem.* **2008**, *73*, 4630–4637.
- (362) Schneider, T. H.; Rieger, M.; Ansorg, K.; Sobolev, A. N.; Schirmeister, T.; Engels, B.; Grabowsky, S. *New J. Chem.* **2015**, *39*, 5841–5853.
- (363) Lu, X.; Lin, S. *J. Org. Chem.* **2005**, *70*, 9651–9653.
- (364) Wu, C.; Yue, G.; Nielsen, C. D.-T.; Xu, K.; Hirao, H.; Zhou, J. *J. Am. Chem. Soc.* **2016**, *138*, 742–745.
- (365) Allen, J. R.; Amegadzie, A.; Bourbeau, M. P.; Brown, J. A.; Chen, J. J.; Cheng, Y.; Frohn, M. J.; Guzman-Perez, A.; Harrington, P. E.; Liu, L.; Liu, Q.; Low, J. D.; Ma, V. Van; Manning, J.; Minatti, A. E.; Nguyen, T. T.; Nishimura, N.; Norman, M. H.; Pettus, L. H.; Pickrell, A. J.; Qian, W.; Rumfelt, S.; Rzasa, R. M.; Siegmund, A. C.; Stec, M. M.; White, R.; Xue, Q. Cyclopropyl fused thiazin-2-amine compounds as beta-secretase inhibitors and methods of use. WO2016022724, 2016.
- (366) Pettersson, M.; Johnson, D. S.; Rankic, D. A.; Kauffman, G. W.; am Ende, C. W.; Butler, T. W.; Boscoe, B.; Evrard, E.; Helal, C. J.; Humphrey, J. M.; Stepan, A. F.; Stiff, C. M.; Yang, E.; Xie, L.; Bales, K. R.; Hajos-Korcsok, E.; Jenkinson, S.; Pettersen, B.; Pustilnik, L. R.; Ramirez, D. S.; Steyn, S. J.; Wood, K. M.; Verhoest, P. R. *Med. Chem. Commun.* **2017**, *8*, 730–743.
- (367) Appel, R.; Hartmann, N.; Mayr, H. *J. Am. Chem. Soc.* **2010**, *132*, 17894–17900.
- (368) Corey, E. J.; Chaykovsky, M. *J. Am. Chem. Soc.* **1965**, *87*, 1353–1364.
- (369) Gololobov, Y. G.; Nesmeyanov, A. N.; Lysenko, V. P.; Boldeskul, I. E. *Tetrahedron* **1987**, *43*, 2609–2651.
- (370) Suárez del Villar, I.; Gradillas, A.; Pérez-Castells, J. *Eur. J. Org. Chem.* **2010**, *2010*, 5850–5862.
- (371) Ashtekar, K. D.; Staples, R. J.; Borhan, B. *Org. Lett.* **2011**, *13*, 5732–5735.

- (372) Doyle, M. P.; Loh, K.-L.; DeVries, K. M.; Chinn, M. S. *Tetrahedron Lett.* **1987**, 28, 833–836.
- (373) Barluenga, J.; Martínez, S.; Suárez-Sobrino, A. L.; Tomás, M. *J. Am. Chem. Soc.* **2002**, 124, 5948–5949.
- (374) Anciaux, A. J.; Hubert, A. J.; Noels, A. F.; Petiniot, N.; Teyssie, P. *J. Org. Chem.* **1980**, 45, 695–702.
- (375) Swain, N. A.; Brown, R. C. D.; Bruton, G. *J. Org. Chem.* **2004**, 69, 122–129.
- (376) Flanigan, D. L.; Yoon, C. H.; Jung, K. W. *Tetrahedron Lett.* **2005**, 46, 143–146.
- (377) Wolckenhauer, S. A.; Devlin, A. S.; Du Bois, J. *Org. Lett.* **2007**, 9, 4363–4366.
- (378) Huang, X.; Webster, R. D.; Harms, K.; Meggers, E. *J. Am. Chem. Soc.* **2016**, 138, 12636–12642.
- (379) Lanzilotti, A. E.; Littell, R.; Fanshawe, W. J.; McKenzie, T. C.; Lovell, F. M. *J. Org. Chem.* **1979**, 44, 4809–4813.
- (380) Chang, M.-Y.; Tai, H.-M.; Lin, C.-H.; Chang, N.-C. *Heterocycles* **2005**, 65, 395.
- (381) Back, T. G.; Hamilton, M. D.; Lim, V. J. J.; Parvez, M. *J. Org. Chem.* **2005**, 70, 967–972.
- (382) Ugi, I.; Fetzer, U.; Eholzer, U.; Knupfer, H.; Offermann, K. *Angew. Chem. Int. Ed.* **1965**, 4, 472–484.
- (383) Downie, I. M.; Earle, M. J.; Heaney, H.; Shuhaibar, K. F. *Tetrahedron* **1993**, 49, 4015–4034.
- (384) Kobayashi, S.; Nishio, K. *J. Org. Chem.* **1994**, 59, 6620–6628.
- (385) Richards, S. GSK colleague who assisted with structural assignment by NMR analysis.
- (386) Lemieux, R. U. *Explorations with Sugar: How Sweet It Was (Profiles, Pathways, and Dreams)*; Seeman, J. I., Ed.; American Chemical Society: Washington D.C., 1990.

- (387) Wang, C.; Ying, F.; Wu, W.; Mo, Y. *J. Org. Chem.* **2014**, *79*, 1571–1581.
- (388) Lemieux, R. U.; Pavia, A. A.; Martin, J. C.; Watanabe, K. A. *Can. J. Chem.* **1969**, *47*, 4427–4439.
- (389) Shibue, T.; Fukuda, Y. *J. Org. Chem.* **2014**, *79*, 7226–7231.
- (390) Giacoboni, J.; Clausen, R.; Marigo, M. *Synlett* **2016**, *27*, 2803–2806.
- (391) Parrilli, M.; Barone, G.; Adinolfi, M.; Mangoni, L. *Tetrahedron Lett.* **1976**, *17*, 207–208.
- (392) Nace, H. R.; Crosby, G. A. *J. Org. Chem.* **1979**, *44*, 3105–3109.
- (393) Tanabe, M.; Peters, R. H. *Org. Synth.* **1981**, *60*, 92.
- (394) Cheng, Y.; Yuan, X.; Ma, J.; Yu, S. *Chem. Eur. J.* **2015**, *21*, 8355–8359.
- (395) Cheng, Y.; Yu, S. *Org. Lett.* **2016**, *18*, 2962–2965.
- (396) Chen, K.; Koser, G. F. *J. Org. Chem.* **1991**, *56*, 5764–5767.
- (397) Bigot, A.; Williamson, A. E.; Gaunt, M. J. *J. Am. Chem. Soc.* **2011**, *133*, 13778–13781.
- (398) Bearss, D. J.; Vankayalapati, H.; Grand, C. L. Inhibitors of Polo-like Kinase-1. WO2006124996, 2006.
- (399) Rehse, K.; Gonska, H. *Arch. Pharm. (Weinheim)*. **2005**, *338*, 590–597.
- (400) Yu, Y.; Singh, S. K.; Liu, A.; Li, T.-K.; Liu, L. F.; LaVoie, E. J. *Bioorg. Med. Chem.* **2003**, *11*, 1475–1491.
- (401) Ruchelman, A. *Bioorg. Med. Chem.* **2004**, *12*, 795–806.
- (402) Machado, A. H. L.; de Sousa, M. A.; Patto, D. C. S.; Azevedo, L. F. S.; Bombonato, F. I.; Correia, C. R. D. *Tetrahedron Lett.* **2009**, *50*, 1222–1225.
- (403) Schmidt, B. *Chem. Commun.* **2003**, 1656.
- (404) Laue, T.; Plagens, A. *Named Organic Reactions*; 2nd ed.; Wiley: Chichester, UK, 2005.
- (405) Japp, F. R.; Klingemann, F. *Justus Liebig's Ann. der Chemie* **1888**, *247*, 190–

225.

- (406) Japp, F. R.; Klingemann, F. *Berichte der Dtsch. Chem. Gesellschaft* **1887**, *20*, 2942–2944.
- (407) Japp, F. R.; Klingemann, F. *Berichte der Dtsch. Chem. Gesellschaft* **1887**, *20*, 3284–3286.
- (408) Barton, D. H. R.; O'Brien, R. E.; Sternhell, S. *J. Chem. Soc.* **1962**, 470.
- (409) Adlington, R. M.; Barrett, A. G. M. *Acc. Chem. Res.* **1983**, *16*, 55–59.
- (410) Cranwell, P.; Russell, A.; Smith, C. *Synlett* **2015**, *27*, 131–135.
- (411) Trail, P.; Willner, D.; Lasch, S.; Henderson, A.; Hofstead, S.; Casazza, A.; Firestone, R.; Hellstrom, I.; Hellstrom, K. *Science* **1993**, *261*, 212–215.
- (412) Damle, N. K. *Expert Opin. Biol. Ther.* **2004**, *4*, 1445–1452.
- (413) Damle, N. *Curr. Opin. Pharmacol.* **2003**, *3*, 386–390.
- (414) Wu, A. M.; Senter, P. D. *Nat. Biotechnol.* **2005**, *23*.
- (415) Prepared by stirring (*E*)-styrylsulfinic acid (1.0 eq) and sodium hydroxide (1.0 eq) in 1:1 EtOH:H₂O (6 mL) and stirring at RT for 3 h. The EtOH was evaporated, and the crude material was diluted with water (15 mL), washed with EtOAc (3 x 15 mL) and the aqueous layer was concentrated *in vacuo* and dried in a vacuum oven overnight to afford sodium (*E*)-styrylsulfinate as an off-white solid (76 wt%).
- (416) Compound naming based on Cahn-Ingold-Prelog rules for functional group priorities., Compound naming based on Cahn-Ingold-Prelog rules.
- (417) Cahn, R. S.; Ingold, C.; Prelog, V. *Angew. Chem. Int. Ed.* **1966**, *5*, 385–415.
- (418) Blough, B. E.; Carroll, F. I. *Tetrahedron Lett.* **1993**, *34*, 7239–7242.
- (419) Beng, T. K.; Bassler, D. P. *Tetrahedron Lett.* **2014**, *55*, 6662–6664.
- (420) Denmark, S. E.; Cresswell, A. J. *J. Org. Chem.* **2013**, *78*, 12593–12628.
- (421) Nambo, M.; Keske, E. C.; Rygus, J. P. G.; Yim, J. C.-H.; Crudden, C. M. *ACS Catal.* **2017**, *7*, 1108–1112.

- (422) Nambo, M.; Crudden, C. M. *Angew. Chem. Int. Ed.* **2014**, *53*, 742–746.
- (423) Sumino, S.; Uno, M.; Huang, H.-J.; Wu, Y.-K.; Ryu, I. *Org. Lett.* **2018**, *20*, 1078–1081.
- (424) Lim, S. H.; Ma, S.; Beak, P. *J. Org. Chem.* **2001**, *66*, 9056–9062.
- (425) Wilkinson, T. J.; Stehle, N. W.; Beak, P. *Org. Lett.* **2000**, *2*, 155–158.
- (426) Lei, A.; Chen, M.; He, M.; Zhang, X. *Eur. J. Org. Chem.* **2006**, *2006*, 4343–4347.
- (427) Yamagata, T.; Tadaoka, H.; Nagata, M.; Hirao, T.; Kataoka, Y.; Ratovelomanana-Vidal, V.; Genet, J. P.; Mashima, K. *Organometallics* **2006**, *25*, 2505–2513.
- (428) Couture, A.; Deniau, E.; Lebrun, S.; Grandclaoudon, P.; Carpentier, J.-F. *J. Chem. Soc., Perkin Trans. 1* **1998**, 1403–1408.
- (429) Tang, W.; Zhang, X. *Angew. Chem. Int. Ed.* **2002**, *41*, 1612–1614.
- (430) Differding, E.; Lang, R. W. *Tetrahedron Lett.* **1988**, *29*, 6087–6090.
- (431) Shibata, N.; Suzuki, E.; Asahi, T.; Shiro, M. *J. Am. Chem. Soc.* **2001**, *123*, 7001–7009.
- (432) Mohar, B.; Baudoux, J.; Plaquevent, J.-C.; Cahard, D. *Angew. Chem. Int. Ed.* **2001**, *40*, 4214–4216.
- (433) Ibrahim, H.; Togni, A. *Chem. Commun.* **2004**, 1147.
- (434) Lovering, F.; Bikker, J.; Humblet, C. *J. Med. Chem.* **2009**, *52*, 6752–6756.
- (435) Lovering, F. *MedChemComm* **2013**, *4*, 515–519.

Appendix 4. Publications List

1. Griffiths, R. J.; Burley, G. A.; Talbot, E. P. A. *Org. Lett.* **2017**, *19*, 870–873
2. Griffiths, R. J.; Kong, W. C.; Richards, S. A.; Burley, G. A.; Willis, M. C.; Talbot, E. P. A. *Chem. Sci.* **2018**, *9*, 2295–2300.